

https://dspace.org/

PI3K in human oesophageal squamous carcinoma cells : a critical modulator in the PKB signalling pathway

Shaw, Nicolene

2013-03-05
http://hdl.handle.net/10539/12485

Downloaded from a DSpace repository. https://dspace.org/

PI3K in Human Oesophageal Squamous Cell Carcinoma: A critical modulator in the PKB signalling pathway



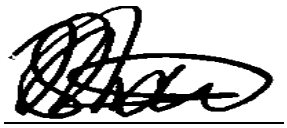
Nicolene Shaw

A thesis submitted to the Faculty of Science, University of the Witwatersrand, in fulfilment of the requirements for the degree of Doctor of Philosophy

Johannesburg, 2011

Declaration

I declare that this thesis is my own, unaided work. It is being submitted for the Degree of Doctor of Philosophy at the University of the Witwatersrand, Johannesburg. It has not been submitted before for any degree or examination in any other University.



Nicolene Shaw

13 day of December 2011

True Success comes from taking risks,

Failing horribly,

Picking yourself up and doing it differently.

~Author Unknown

Abstract

The phosphotidylinositide-3-kinase (PI3K) pro-survival signalling pathway is critical in the development of cancer. Major contributors to the proliferative and/or anti-proliferative signalling in human oesophageal squamous cell carcinoma (HOSCC) are currently unknown. Based on the Ser473 phosphorylation state of PKB (pPKB), this study dissects the overall activation status of the PI3K/PKB pathway. Despite the prevalent membrane expression of PI3K determined through western blotting and immunofluorescence, pPKB levels were shown to be surprisingly low. Activation of EGFR did not produce a hyperactivation of the PI3K/PKB pathway. Neither PI3K nor PKB sequence isolated from the 5 HOSCC cell lines possessed any of the "hotspot" mutations described previously for other tumours. Inhibiting phosphatase protein 2A (PP2A), an integral antagonist of PKB, indicated that its activity in respect of PKB is diminished in HOSCC cells. Despite the low concentration of pPKB, the reciprocal relationship with PTEN expression was not evident in the WHCO and SNO HOSCC series. Moreover, reversible oxidization and inhibition of PTEN served to augment the activation of the PI3K/PKB pathway. Since oxidation of PTEN is imperative for effective signal propagation from activated EGFR and PI3K, these data reveal an aberrant EGFR-PI3K-H_2O_2 mediated PTEN inhibition in HOSCC. Allied to this discovery, was the finding that HOSCC cells are highly susceptible to oxidative stress induced by H_2O_2. This was suggested to play an essential part in maintaining the low PI3K/PKB activation status. Although the decrease in PTEN activity was required for the induction of pPKB, PTEN may not be the only limiting component for the activation of the PI3K/PKB pathway in HOSCC. In addition to its overexpressed EGFR status, the WHCO and SNO HOSCC series have the propensity to appropriate nuclear β-catenin. Interruption of the PI3K/PKB signalling pathway caused a small, yet significant, depression in the nuclear localization of β-catenin in 3 of the HOSCC cell lines. Together, this work greatly expands our understanding of the major influences behind the proliferative and/or anti-proliferative signalling in HOSCC, primarily that, the EGFR overexpression status does not propagate these transforming capabilities via activation of the PI3K/PKB pathway, and that this may be a reflection of its transformation potential. The findings derived from this study are likely to have a profound impact on future therapeutic targets for this disease.

List of associated Publications

Local Conferences

The expression of Phosphatidylinositol 3-kinase (PI3K) in Human Oesophageal Squamous Carcinoma Cell Lines. *Accepted for poster presentation at the Bio08 conference at the 1820 Settlers' Monument, Graghamstown, South Africa, 2008.*

PI3K Signalling in Human Oesophageal Squamous Carcinoma: does it direct the nuclear localization of β-catenin. *Accepted for oral presentation at the SASBMB Conference, Bloemfontein, Ilanga Estate, 2010.*

Acknowledgements

First and foremost I would like to extend my eternal gratitude to my supervisor, Professor Rob Veale, for his resounding advice and valuable input throughout the acquisition of my PhD, which enabled me to develop the knowledge and skills I have in this subject. Furthermore, I would also like to thank him for believing in me and knowing the best way to bring out my full potential. Despite his busy schedule, he managed to set time aside to assist me, and for that I am very grateful. Lastly, if it was not for his patience, there is no doubt that this PhD would have been possible. It was a real honour to be a part of his lab. Thank you.

Secondly, I would like to thank Mrs. Elsabe' Scott for always ensuring that cells for tissue culture were readily available, and for placing the necessary orders. Thank you for always putting a smile on my face and for going the extra mile to assist me.

Additionally, to all the previous and current members of the Cell Biology Lab: Yael, Lindsay, Glenn, Ciara, Catherine, Belinda, Stephanie, Cassandra, Sindisiwe, Sandile, and Ari – thank you all for making this journey more jovial, and making sure that I always had a good cup of coffee and good company to go with it. A special thank you to Yael for encouraging me through the challenging times and for always lending a helping hand.

I would like to personally thank my family and close friends – Dad, Gail, Lee-Anne, Michalea, Dillon, Kalinka, Lerato, and Zwide - for their continual love, support and encouragement. Additionally, I would like to thank Zwide Mhlongo, specifically, for always believing in my ability and encouraging me to push through, especially when I did not have the strength. A special thanks to my father, David Shaw, for all his financial assistance and to my sister, Gail Shaw, for always believing in me.

A special thank you to David Shaw and Dr. Stephen Meddows-Taylor for proof-reading this dissertation.

Last, but not least, I would like to thank my late mother – Patricia Shaw – without her love and support, I would never have managed. Thank you.

Table of Contents

Declaration ... **II**
Abstract ... **IV**
List of associated Publications ... **V**
Acknowledgements ... **VI**
List of Tables ... **XVIII**
List of Abbreviations: ... **XIX**
Chapter 1 ... **1**
General Introduction ... **1**
The road to understanding the role of PI3K in HOSCC ... **1**
1.1 The non-linearity of signal transduction in cells. ... 1
1.2 The concept of "Oncogene Addiction". ... 3
1.3 Phosphatidylinositol-3-kinase (PI3K) ... 5
1.3.1 Structure and Inter-subunit interactions of p85α and p110α. ... 6
1.3.2 PI3K activation ... 7
1.3.2.1 Stimuli from Cell-Cell Adhesion ... 8
1.3.2.2 Stimuli from Cell-ECM Adhesion ... 11
1.3.2.3 Receptor Tyrosine Kinases ... 13
1.4 The PI3K pathway - navigating downstream. ... 15
1.4.1 Major PI3K effector protein: PKB ... 15
1.4.1.1 Activation of PKBα (PKB) ... 15
1.4.1.2 Major PI3K and PKB-mediated cellular effects. ... 17
1.5 Termination of PI3K signalling. ... 18
1.6 Deregulation of PI3K pathway in cancer. ... 21
1.6.1 The influence of the EGFR ... 21
1.6.2 Genetic variations in the PI3K pathway. ... 21
1.7 Human Oesophageal Squamous Cell Carcinoma - The model ... 24
1.8 Gaps in the characterization of HOSCC: a role for PI3K? ... 26
1.9Aims ... 27
Chapter 2 ... **28**
The PI3K pathway is active in HOSCC cells ... **28**
2.1 Introduction ... 28
2.1 Materials and Methods ... 32
2.2.1 Cell lines and their Culture ... 32
2.2.2 Total RNA Extraction ... 32

2.2.3 Amplification of p85α by Reverse Transcription Polymerase Chain Reaction 33
2.2.3.1 Reverse Transcription 33
2.2.3.2 PCR 34
2.2.3.3 Analysis of RNA, cDNA and PCR fragments by agarose gel electrophoresis 35
2.2.4 Antibodies 35
2.2.5 Whole Cell Protein Extraction 35
2.2.6 Nuclear Extraction 35
2.2.7 Plasma Membrane Extraction 36
2.2.8 Protein Estimation 36
2.2.9 Polypeptide Resolution and Western Immunolotting 37
2.2.9.1 PI3K (p85α), c-Jun, β-actin 37
2.2.9.2 pPKB (Ser473), anti-pGSK3β (Ser9) and PTEN 38
2.2.10 Indirect Immunoflourescence Microscopy 38
2.2.11 Inhibition of PI3K through LY294002 (LY29) Exposure 39
2.2.12 Densitometry 40
2.2.13 Image Capturing 40
2.2.14 Statistical Analysis 40
2.3 Results 41
2.3.1 p85α is unaltered in HOSCC cells. 41
2.3.2 HOSCC cells express high levels of PI3K (p85α). 41
2.3.3 Cellular localization of PI3K (p85α) in HOSCC cells. 43
A) PI3K (p85α) localizes to the membrane 43
B) PI3K (p85α) is present in the nucleus of HOSCC cells. 46
C) PI3K (p85α) is targeted to the membrane in HOSCC cells. 46
2.3.4 PI3K and PKB are active in the HOSCC cell lines. 49
2.3.5. Cellular distribution of active PI3K (pPKB) within HOSCC cell lines. 49
2.3.6 PKB is active in HOSCC cells. 52
2.3.7 The activation of PKB is primarily mediated by PI3K in HOSCC cells. 54
2.4 Discussion 58
Chapter 3 ..... **66**
PI3K activation in relation to the status of EGFR expression **66**
3.1 Introduction 66
3.2 Materials and Methods 71
3.2.1 Cell lines and Culture 71

3.2.2 Antibodies 71
3.2.3 EGFR Activation through EGF Treatment 71
3.2.4 Whole cell protein extraction 71
3.2.5 Nuclear Extraction 72
3.2.6 Plasma Membrane Extraction 72
3.2.7 Plasma membrane enriched extraction used for Immunoprecipitation reactions 72
3.2.8 Protein Estimation 72
3.2.9 Polypeptide Resolution and Western Immunoblotting 72
3.2.10 Indirect Immunoflourescence Microscopy 73
3.2.11 Co-immunoprecipitation analysis of EGFR and PI3K 73
3.2.12 Co-immunoprecipitation analysis of serine phosphorylated PI3K 74
3.2.13 Genomic DNA Extraction 74
3.2.14 PCR 74
3.2.15 Total RNA extraction 75
3.2.16 Amplification of PKB1 by RT-PCR 75
3.2.16.1 Reverse Transcription 75
3.2.16.2 PCR 75
3.2.17 Densitometry 76
3.2.18 Image Capturing 76
3.2.19 Statistical Analysis 76
3.2.20 Figure Design 76
3.3 Results 77
3.3.1 EGFR activation effects the expression of PI3K (p85α) in HOSCC cells. 77
3.3.2 PI3K (p85α) localizes to the membrane in response to EGFR activation. 77
3.3.3 Nuclear and membrane levels of PI3K (p85α) as a result of EGFR activation. 78
3.3.4 The state of PI3K (p85α) serine phosphorylation and its association with ErbB2. 86
3.3.5 Activation of the PI3K/PKB signalling pathway in relation to the EGFR expression status in HOSCC cells. 88
3.3.6 Wild-type PIK3CA is expressed in HOSCC cells. 89
3.3.7 Native PKB is present within HOSCC cells. 92
3.4 Discussion 94
Chapter 4 100
Suppression of the PI3K/PKB pathway 100
4.1 Introduction 100
4.2 Materials and Methods 104

4.2.1 Cell Lines and their Culture 104
4.2.2 Antibodies 104
4.2.3 Treatment with the PP2A Inhibitor, Okadaic Acid (OA) 104
4.2.4 Whole Cell Protein Extraction 105
4.2.5 Nuclear Extraction 105
4.2.6 Membrane Extraction 105
4.2.7 Protein Estimation 105
4.2.8 Polypeptide Resolution and Western Immunolotting 105
4.2.9 Indirect Immunoflourescence Microscopy for PTEN Staining 105
4.2.10 Exposure to Hydrogen Peroxide (H_2O_2) 106
4.2.11 Non-reducing extraction for detection of reduced PTEN 106
4.2.12 Densitometry 106
4.2.13 Image Capturing 106
4.2.14 Statistical Analysis 107
4.2.15 Figure Design 107
4.3 Results 108
4.3.1 The PI3K/PKB pathway is not regulated by PP2A in HOSCC cells. 108
4.3.2 HOSCC cells express relatively low PTEN protein levels. 112
4.3.3 PTEN localization in HOSCC cells 114
A) Cytoplasmic Localization 114
B) Nuclear Localization 114
4.3.4 PTEN is active in HOSCC cells 116
4.4 Discussion 126
Chapter 5 133
The role of the 26S proteasome in the regulation of PTEN in HOSCC cells 133
5.1 Introduction 133
5.2 Materials and Methods 136
5.2.1 Cell lines and their Culture 136
5.2.2 Antibodies 136
5.2.3 Whole cell protein extraction 136
5.2.4 Protein Estimation 136
5.2.5 Polypeptide Resolution and Western Immunolotting 136
5.2.6 Colorimetric MTT (tetrazolium) assay 137
5.2.7 Proteasome Inhibition through exposure to Bortezomib (Bzb). 137

5.2.8 Whole cell protein extraction of attached versus detached Bzb-treated cells. 138
5.2.9 Densitometry..... 138
5.2.10 Image Capturing..... 138
5.2.11 Statistical Analysis..... 138
5.2.12 Figure Design..... 139
5.3 Results 141
5.3.1 Relative expression of PI3K (p85α) levels in the panel of cells used as controls. 141
5.3.2 Comparative analysis of PTEN protein levels in HOSCC cells with respect to the control cells. 141
5.3.3 Inhibition of the 26S proteasome in HOSCC cells. 144
5.3.3a Evaluation of the proliferation rate of HOSCC cells..... 144
5.3.3b Bortezomib (Bzb) utilizes p53-independent mechanisms in HOSCC cells. 146
5.3.3c The expression of PTEN is upregulated in response to proteasome inhibition. 151
5.3.3d Levels of pPKB and PI3K (p85α) are sensitive to PI in HOSCC cell lines. 154
5.4 Discussion..... 165
5.4.1 HOSCC cells express unique levels of PI3K (p85α) and PTEN. 165
5.4.2 The 26S proteasome is active and regulates PTEN protein levels in HOSCC cells.. 166
5.4.3 Is the increase in PTEN following PI linked to its action? 171
5.4.4 HOSCC cells are highly susceptible to proteasome inhibition mediated by Bzb..... 174
5.4.5 Concluding Remarks..... 175
Chapter 6 176
Crosstalk between the PI3K and Wnt signalling pathways in HOSCC cells 176
6.1 Introduction 176
6.2 Materials and Methods..... 180
6.2.1 Cell lines and Culture..... 180
6.2.2 Antibodies..... 180
6.2.3 Nuclear Extraction 180
6.2.4 Protein Estimation..... 180
6.2.5 Polypeptide Resolution and Western Immunolotting 180
6.2.6 Whole Cell protein extraction..... 181
6.2.7 Plasma membrane enriched extraction used for Immunoprecipitation reactions 181
6.2.8 Co-immunoprecipitation analysis of β-catenin and its cell adhesive counterparts.... 181
6.2.9 Activation of Wnt Signalling through Lithium Chloride (LiCl) Exposure 181
6.2.10 Inhibition of PI3K through LY294002 (LY29) Exposure..... 181
6.2.11 Densitometry..... 182

6.2.12 Image Capturing 182
6.2.13 Statistical Analysis 182
6.2.14 Figure Design 182
6.3 Results 183
6.3.1 β-catenin is present at high levels in the nucleus of HOSCC cells. 183
6.3.2 Nuclear β-catenin is transcriptionally active in HOSCC cells. 183
6.3.3 The transcriptionally active β-catenin in relation to its cell adhesive roles in HOSCC cells. 187
6.3.4 The PI3K/PKB and Wnt signalling pathway in HOSCC cells. 187
6.3.5 PI3K variously influences the nuclear translocation of β-catenin. 189
6.4 Discussion 197
Chapter 7 201
General Discussion and Conclusion 201
7.1 The significance of p85α expression in HOSCC. 201
7.2 Activation of PI3K in the WHCO and SNO HOSCC series. 203
7.3 PTEN - a significant player in PI3K/PKB signalling in HOSCC. 208
7.4 Degradation of PKB by the 26S proteasome. 213
7.5 Has the importance of PP2A been overlooked in the PI3K/PKB pathway? 215
7.6 The WHCO and SNO HOSCC series – a model for crosstalk between the Wnt and PI3K pathways. 217
7.7 A case for the regulation of the PI3K/PKB pro-survival signalling pathway in HOSCC. 220
7.8 The PI3K/PKB pathway in HOSCC - novel insights into potential targets for therapy. 221
7.9 Conclusion 223
Appendix A 225
1.1 Tissue Culture Medium 225
1.1.1 DMEM Medium Solution 225
1.1.2 Hams F12 Medium Solution 225
1.1.3 1X Phosphate-buffered saline (PBS) 225
1.1.4 Trypsin: EDTA Solution 225
1.2 Reverse Transcription 226
1.2.1 MMLV-RT Buffer (5X) 226
1.2.2 Nucleotide Mix (dNTPs) 226
1.2.3 MMLV-RT 226

1.2.4 3 M Sodium Acetate pH 5.2 226
1.3 PCR 226
1.3.1 p85α Sequence and Primer Information 226
1.3.2 PCR Reaction Buffer (10X) 227
1.4 Agarose Gel Electrophoresis 228
1.4.1 1% Agarose Gel 228
1.4.2 1X Tris Acetic Acid EDTA (TAE) Buffer 228
1.4.3 Loading Buffer 228
1.5 Sample Preparation 228
1.5.1 Lysis Buffer 228
1.5.2 Nuclear Extraction Buffer 229
1.5.2.1 Nuclear Wash Buffer 229
1.5.2.2 Sucrose Solution 229
1.5.2.3 Nuclear Lysis Buffer 229
1.5.3 Plasma Membrane Extraction 229
1.5.3.2 Membrane Hypotonic Buffer 230
1.6 Protein Estimation 230
1.6.1 Bovine Serum Albumin (BSA) Solution 230
1.6.2 7.5% Trichloracetic Acid (TCA) 230
1.6.3 Coomassie Brillian Blue Stain 230
1.6.4 Destain 230
1.6.5 Elution Solution 230
1.6.6 Example of Standard curve for protein estimation 231
1.7 Electrophoresis 231
1.7.1 Separating Gel (10%) 231
1.7.2 Stacking Gel 232
1.7.3 Electrophoresis Running Buffer 232
1.7.4 Destain for SDS-PAGE 232
1.8 Western Blotting 233
1.8.1 Western Blot Transfer Buffer 233
1.8.2 Blocking Buffer (BLOTTO) 233
1.8.3 Developer 233
1.8.4 Fixer 234
1.8.5 10X Tris Buffered Saline (TBS) 234

1.8.6 Blocking Buffer 234
1.8.7 Primary Antibody Dilution Buffer 234
1.9 Indirect Immunoflourescence 234
1.9.1 4% Paraformaldehyde Solution 234
1.9.2 0.25 % Triton-X-100 234
1.9.3 Mounting Solution (Elvanol) 235
1.10 LY294002 Stock 235
1.11 Optimization of LY294002 exposure in HOSCC cells. 235
1.12 Sequencing results for the PCR amplified N-terminal SH2 domain of the p85α gene transcript. 237
Appendix B **239**
2.1 Co-immunoprecipitation Analysis 239
2.1.1 Membrane Extraction Buffer 239
2.1.2 Immunoprecipitation (IP) Buffer 239
2.2 PIK3CA Primer and Sequence Information 241
2.2.1 Sequence amplifying the p85-binding domain (exon 1) and Helical Domain (exon 9) of the PIK3CA gene: 241
2.2.2 Sequence amplifying the C2 domain (exon 4) and Kinase Domain (exon 20) of the PIK3CA gene: 242
2.3 PKB1 Primer and Sequence Information 244
2.4 PCR amplification of exon 4A, exon 4B and exon 20 of the PIK3CA gene. 247
2.5 Representative chromatogram of sequencing results for PIK3CA. 248
2.6 PCR amplification of PKB1 gene. 249
2.7 Representative chromatogram of sequencing results for PKB1. 250
Appendix C **252**
3.1 Optimization for ideal Okadaic Acid (OA) concentration and time exposure. 252
3.2 Okadaic Acid (OA) Stock 253
3.3 Non-reducing Buffer 253
Appendix D **257**
4.1 Seperating Gel (12%) 257
4.2 MTT (3-[4,5-Dimethylthiazol-2-yl]-2,5-diphenyltetrazoliumbromide) 257
4.3 Velcade®/Bortezomib (Bzb) 257
4.4 MTT Assay Results 258
4.4.1 WHCO1 258
4.4.2 MCF7 258

4.4.3 HEK293 259
4.4.4 NIH3T3 259
Appendix E 262
5.1 Lithium Chloride (LiCl) 262
5.2 Nuclear levels of β-catenin in HOSCC and the significance thereof: 262
5.3 The mean optical density values and statistical analysis of c-Jun levels in HOSCC: 263
References: 265

LIST OF FIGURES

FIGURE 2.1: DOMAIN STRUCTURE OF THE P85A REGULATORY AND P110A CATALYTIC SUBUNIT OF CLASS 1A PI3K. 28
FIGURE 2.2: PI3K SIGNALLINGILDER TOOL. 2.0. 30
FIGURE 2.3: RNA EXTRACTS AND CDNA TRANSCRIPTS. 42
FIGURE 2.4: GENE AMPLIFICATION OF THE P85 TRANSCRIPT (PIK3R1). 43
FIGURE 2.5: PI3K (P85) IS EXPRESSED AT VARIABLE LEVELS IN HOSCC CELLS. 44
FIGURE 2.6: PI3K (P85) IS PREDOMINANTLY LOCALIZED TO THE MEMBRANE AND CYTOPLASM IN HOSCC CELLS. 46
FIGURE 2.7: RELATIVELY LOW LEVELS OF PI3K (P85) ARE EXPRESSED IN THE NUCLEUS OF HOSCC CELLS. 47
FIGURE 2.8: PI3K (P85) IS TARGETED TO THE MEMBRANE OF HOSCC CELLS. 48
FIGURE 2.9: PI3K IS ACTIVE IN 4 OF THE HOSCC CELL LINES. 50
FIGURE 2.10: UNIQUE STAINING PATTERNS OF PPKB IDENTIFYING ACTIVE PI3K IN EACH OF THE HOSCC CELL LINES 52
FIGURE 2.11: THE ACTIVITY OF GSK3 APPEARS TO BE CONSTITUTIVELY INHIBITED IN 3 OF THE HOSCC CELL LINES 53
FIGURE 2.12: DISRUPTION OF THE PI3K PATHWAY IN HOSCC CELLS THROUGH LY29. 55
FIGURE 2.13: DENSITOMETRIC ANALYSIS AFFIRMS THE DEPENDENCY PPKB LEVELS HAVE ON PI3K ACTIVITY 56
FIGURE 2.14: SCHEMATIC DIAGRAM SHOWING THE POSSIBLE REASONS FOR ACQUIRING LY29 RESISTANCE 63
FIGURE 2.15: SCHEMATIC DIAGRAM ILLUSTRATING THE ROLE OF WT AND MTP53 IN THE CONTRIBUTION OF ACQUIRING LY29 RESISTANCE AND SUSCEPTIBILITY.. 64
FIGURE 3.1: EGFR SIGNALLING THROUGH ACTIVATION OF THE PI3K PATHWAY 67
FIGURE 3.2: SCHEMATIC REPRESENTATION OF THE DOMAIN STRUCTURE AND ACTIVATION MECHANISM OF PKB. 69
FIGURE 3.3: A) EGF MODULATES THE PROTEIN EXPRESSION OF PI3K (P85) SUBSEQUENT TO EGFR ACTIVATION 79
FIGURE 3.4: THREE OF THE HOSCC CELL LINES DISPLAY A MORE PRONOUNCED PI3K (P85) MEMBRANE AND NUCLEAR LOCALIZATION SUBSEQUENT TO EGFR ACTIVATION. 84
FIGURE 3.5: ACTIVE EGFR MODULATES THE NUCLEAR AND MEMBRANE EXPRESSION OF PI3K (P85). 85
FIGURE 3.6: EGFR ACTIVATION HAS A MINIMAL EFFECT ON ITS ASSOCIATION TO PI3K (P85) IN HOSCC CELLS. 87
FIGURE 3.7: EGFR ACTIVATION DOES NOT REDUCE THE OVERALL SERINE PHOSPHORYLATION STATUS OF PI3K (P85) 88
FIGURE 3.8: ACTIVATION OF THE EGFR THROUGH EGF EXPOSURE TRIGGERS ACTIVATION OF THE PI3K/PKB SIGNALLING PATHWAY 90
FIGURE 3.9: GENOMIC DNA WAS SUCCESSFULLY EXTRACTED FROM THE 5 HOSCC CELL LINES. 92
FIGURE 3.10: THE E454K (G1633A) "HOTSPOT" MUTATION IS ABSENT IN HOSCC CELLS. 93
FIGURE 4.1: PP2A SIGNALLING. 102
FIGURE 4.2: REGULATION OF PTEN THROUGH OXIDATION 103
FIGURE 4.3: PP2A IS NOT A MAJOR REGULATOR OF THE PI3K/PKB PATHWAY IN HOSCC CELLS. 109
FIGURE 4.4 A AND B: DENSITOMTERIC ANALYSIS OF THE WESTERN BLOT DETECTION OF PPKB AND PGSK3 CONSEQUENT TO PP2A 110
FIGURE 4.5: PTEN IS EXPRESSED AT LOW LEVELS WITHIN HOSCC CELLS. 113
FIGURE 4.6: PTEN IS PREDOMINANTLY LOCALIZED TO THE CYTOPLASM IN HOSCC CELLS. 116
FIGURE 4.7: PTEN IS HIGHLY EXPRESSED IN THE NUCLUES OF HOSCC CELLS 117
FIGURE 4.8 A AND B: CELLULAR PTEN IS INACTIVATED IN RESPONSE TO OXIDATIVE STRESS 118
FIGURE 4.9:THE PI3K/PKB PATHWAY IS ACTIVATED IN RESPONSE TO PTEN INHIBITION 121
FIGURE 4.10: CACO-2 CELLS EXPOSED TO 20 UM H2O2 INDUCES PPKB EXPRESSION 123
FIGURE 4.11: THE LEVELS OF PI3K AND B-CATENIN ARE NOT SIGNIFICANTLY ALTERED IN RESPONSE TO H2O2 IN HOSCC CELLS 124
FIGURE 4.12: OXIDATION OF PKB. 132
FIGURE 5.1: THE MECHANISMS KNOWN TO REGULATE PTEN EXPRESSION 134

FIGURE 5.2: PI3K (P85) IS HIGHLY EXPRESSED IN HOSCC CELLS IN COMPARISON WITH THE CONTROLS.....142
FIGURE 5.3: WITHIN A PANEL OF CELL LINES, HOSCC CELLS EXPRESS LOW LEVELS OF PTEN. 143
FIGURE 5.4: HOSCC CELLS PROLIFERATE WITHIN 24 HOURS.....145
FIGURE 5.5: INHIBITION OF THE 26S PROTEASOME ATTENUATES PI3K/PKB SIGNALLING AND STABILIZES PTEN VIA CASPASE-3-DEPENDENT MECHANISMS. 150
FIGURE 5.6: INHIBITION OF THE 26S PROTEASOME ATTENUATES THE STABILITY OF B-CATENIN IN HOSCC. 154
FIGURE 5.7: THE PROTEASOME IS INHIBITED FOLLOWING EXPOSURE TO BZB, EVIDENCED BY ELEVATION IN B-CATENIN LEVELS 156
FIGURE 5. 8: THE 26S PROTEASOME PLAYS A MAJOR ROLE IN THE DEGRADATION OF PTEN IN HOSCC CELLS.....159
FIGURE 5. 9: THE 26S PROTEASOME PLAYSA MAJOR ROLE IN THE REGULATION OF PPKB LEVELS IN HOSCC CELLS.....162
FIGURE 5.10: THE PROTEIN EXPRESSION OF PI3K (P85) DECREASES IN RESPONSE TO HIGH CONCENTRATIONS OF BZB IN HOSCC CELLS. 164
FIGURE 5.11: DIAGRAM ILLUSTRATING THE MOLECULAR MECHANISMS UNDERLYING THE EFFECTS OF BZB IN THE WHCO3 CELL LINE 169
FIGURE 5.12: DIAGRAM ILLUSTRATING THE MOLECULAR MECHANISMS UNDERLYING THE EFFECTS OF BZB IN THE SNO CELL LINE. 170
FIGURE 5.13: DIAGRAM ILLUSTRATING THE MOLECULAR MECHANISMS UNDERLYING THE EFFECTS OF BZB IN THE WHCO1, WHCO5, AND WHCO6 CELL LINES.....174
FIGURE 6.1: CANONICAL WNT SIGNALLING PATHWAY. 179
FIGURE 6.2: HOSCC CELLS EXPRESS HIGH LEVELS OF B-CATENIN IN THE NUCLUE. 184
FIGURE 6.3: NUCLEAR B-CATENIN IS ACTIVE IN HOSCC CELL LINES 185
FIGURE 6.4: C-JUN IS HIGHLY EXPRESSED IN HOSCC CELL LINES 186
FIGURE 6.5: B-CATENIN INTERACTS WITH E-CADHERIN AND A-CATENIN AT THE PLASMA MEMBRANE 188
FIGURE 6.6: THE WNT SIGNALLING PATHWAY SELECTIVELY INHIBITS GSK3B IN HOSCC CELLS. 190
FIGURE 6.7: ACTIVATION OF THE WNT SIGNALLING PATHWAY HAS A NEGLIGIBLE IMPACT ON THE TOTAL CELLULAR LEVELS OF PTEN AND B-CATENIN.....192
FIGURE 6.8: PI3K MODULATES THE NUCLEAR EXPRESSION OF B-CATENIN IN THREE HOSCC CELL LINES.....194
FIGURE 6.9: TOTAL CELLULAR LEVELS OF B-CATENIN CONSEQUENT TO PI3K INHIBITION. 196
FIGURE 7.1: PROPOSED MECHANISM FOR THE ACTIVATION AND REGULATION OF THE PI3K/PKB PATHWAY IN HOSCC. .221
FIGURE A1: SCHEMATIC DIAGRAM OF THE PIK3R1/P85A GENE TRANSCRIPT 227
FIGURE A2: THE VARIOUS ABSORBANCE READINGS (595 NM) OF 1, 3, 6, 9, 12, 16, AND 20 MG BSA USED TO CONSTRUCT A STANDARD CURVE FOR THE PROTEIN ESTIMATION OF VARIOUS PROTEIN EXTRACTS. 231
FIGURE A3: 20 μG OF PROTEIN LYSATES FROM THE SPECIFIC EXTRACTIONS PERFORMED WERE ANALYSED FROM A SEPARATION ON A 10 % SDS-PAGE. 233
FIGURE A4: OPTIMUM EXPOSURE TO LY294002 IN HOSCC CELLS.....236
FIGURE A5: NO MUTATIONS DETECTED IN THE NSH2 DOMAIN OF P85A BASED ON ITS SEQUENCE OUTPUT AND ALIGNMENT 237
FIGURE B1: PIK3CA PRIMER AND SEQUENCE INFORMATION (EXON1 AND EXON9). 241
FIGURE B2: PIK3CA PRIMER AND SEQUENCE INFORMATION (EXON4 AND EXON20). 243
FIGURE B3: PKB1 PRIMER AND SEQUENCE INFORMATION. 246
FIGURE B4: AMPLIFICATION OF EXON 4 (C2 DOMAIN) AND EXON 20 (KINASE DOMAIN) OF THE PIK3CA GENE IN HOSCC CELLS. 247
FIGURE B5: PIK3CA CHROMATOGRAM TRACES. 248
FIGURE B6: THE PKB1 TRANSCRIPT IS NOT IMPAIRED IN HOSCC CELLS. 249
FIGURE B7: PKB SEQUENCING TRACES. 251
FIGURE C1: OPTIMIZATION OF EXPOSURE TO OKADAIC ACID (OA) IN HOSCC CELLS. 252

List of Tables

TABLE 1.1: RECENT RESULTS DEMONSTRATING THE FREQUENCY OF GENETIC VARIATIONS WITHIN THE PI3K/PKB PATHWAY FOUND IN DIFFERENT TUMOUR TYPES. 23

TABLE 5.1: BRIEF SUMMARY OF PROTEINS KNOWN TO INTERACT WITH AND REGULATE PTEN IN THE VARIOUS CELL LINES USED AS POSITIVE CONTROLS FOR COMPARATIVE PURPOSES. 140

TABLE A1: OPTICAL DENSITY VALUES (MEAN) OF THE BANDS REPRESENTING WHOLE CELL PROTEIN EXPRESSION OF PI3K (P85α).....238

TABLE A2:OPTICAL DENSITY VALUES (MEAN) OF THE BANDS REPRESENTING TOTAL CELLULAR LEVELS OF PPKB AND PGSK3B. 238

TABLE A3:STUDENT'S *T* TEST RESULTS FOR PPKB EXPRESSION FOLLOWING 1 HR EXPOSURE TO 20 MM OF LY29. 238

TABLE A4: STUDENT'S *T* TEST RESULTS FOR PGSK3B EXPRESSION FOLLOWING 1 HR EXPOSURE TO 20 MM OF LY29.....238

TABLE A5:STUDENT'S *T* TEST RESULTS FOR PTEN EXPRESSION FOLLOWING 1 HR EXPOSURE TO 20 MM OF LY29. 239

TABLE A6: PEARSON'S CORRELATION COEFFICIENT RESULTS FOR VALUES NEGATIVELY CORRELATING BETWEEN PPKB AND PTEN EXPRESSION FOLLOWING 1 HR EXPOSURE TO 20 MM OF LY29.....239

TABLE B1:ONE WAY RM ANOVA1 TEST RESULTS FOR PI3K (P85A) FOLLOWING EGFR ACTIVATION. 240

TABLE B2:TUDENT'S T-TEST FOR THE NUCLEAR AND MEMBRANE EXPRESSION OF PI3K (P85A) PROTEIN FOLLOWING EGFR.....240

TABLE B3:P-VALUES OBTAINED FROM STUDENT'S T-TEST FOR THE EXPRESSION OF PPKB FOLLOWING EGFR ACTIVATION.....240

TABLE C1:STUDENT'S *T* TEST RESULTS FOR PPKB EXPRESSION FOLLOWING 1 HR EXPOSURE TO 100 NM OF OA. 253

TABLE C2:STUDENT'S *T* TEST RESULTS FOR PGSK3B EXPRESSION FOLLOWING 1 HR EXPOSURE TO 100 NM OF OA.....253

TABLE C3:STUDENT'S *T* TEST RESULTS FOR PTEN EXPRESSION FOLLOWING 1 HR EXPOSURE TO 100 NM OF OA. 254

TABLE C4: STUDENT'S *T* TEST RESULTS FOR PI3K (P85A) EXPRESSION FOLLOWING 1 HR EXPOSURE TO 100 NM OF OA. 254

TABLE C5: STUDENT'S *T* TEST RESULTS FOR B-CATENIN EXPRESSION FOLLOWING 1 HR EXPOSURE TO 100 NM OF OA.....254

TABLE C6: OPTICAL DENSITY VALUES (MEAN) OF THE BANDS REPRESENTING WHOLE CELL AND NUCLEAR PROTEIN EXPRESSION OF PTEN. 255

TABLE C7: ONE WAY RM ANOVA RESULTS FOR PTEN, PPKB, PGSK3B, PI3K (P85A) AND B-CATENIN EXPRESSION FOLLOWING PTEN OXIDATION INDUCED BY 10, 30, AND 60 MINS EXPOSURE TO 1 MM H_2O_2. 255

TABLE C8: ONE WAY RM ANOVA RESULTS FOR PPKB EXPRESSION FOLLOWING PTEN OXIDATION INDUCED BY 10, 30, AND 60 MINS EXPOSURE TO 1 MM AND 20 μM H_2O_2 IN THE CACO2 CELL LINE. 256

TABLE C9: PEARSON'S CORRELATION COEFFICIENT VALUES FOR THE INVERSE CORRELATION BETWEEN PTEN AND PPKB FOLLOWING PTEN OXIDATION INDUCED BY 10, 30, AND 60 MINS EXPOSURE TO 1 MM H_2O_2. 256

TABLE D1: OPTICAL DENSITY VALUES (MEAN) OF THE BANDS REPRESENTING WHOLE CELL PROTEIN EXPRESSION OF PI3K (P85α) AND PTEN.....257

TABLE D2: ONE WAY ANOVA STATISTICAL RESULTS FOR THE EXPRESSION OF B-CATENIN FOLLOWING BZB EXPOSURE 260

TABLE D3: P VALUES OF ONE WAY ANOVA STATISTICAL RESULTS FOR THE EXPRESSION OF PTEN FOLLOWING BZB EXPOSURE.....260

TABLE D4: 4P VALUES OF ONE WAY ANOVA STATISTICAL RESULTS FOR THE EXPRESSION OF PPKB FOLLOWING BZB EXPOSURE 261

TABLE D5: 5 P VALUES OF ONE WAY ANOVA STATISTICAL RESULTS FOR THE EXPRESSION OF PI3K (P85A) FOLLOWING BZB EXPOSURE .261

List of Abbreviations:

ANOVA	analysis of variance
APC	adenomatous polyposis coli
APS	ammonium persulphate
ATP	adenosine triphosphate
BH	Bcl-2 homology domain
BSA	bovine serum albumin
bp	base pair
Bzb	Bortezomib (Velcade)
CAMs	cell adhesion molecule
Ca2+	calcium
CIP2A	cancerous inhibitor of protein phosphatase 2A
CK2	casien kinase 2
COX-2	cyclooxygenase-2
dH2O	distilled water
DMSO	dimethyl sulfoxide
DMEM	Dulbecco‟s Modified Eagles Medium
DNA/cDNA	deoxyribonucleic acid/complimentary DNA
Dvl	dishevelled
ECACC	european collection of cell cultures
ECM	extracellular matrix
EDTA	ethylenediamine tetra-acetic acid
EGF	epidermal growth factor
EGFR	epidermal growth factor receptor
EGR-1	early growth response-1
EMT	epithelial-to-mesenchymal transition

ER	endoplasmic reticulum
ERK	extracellular-signal-regulated kinase
EtBr	ethidium bromide
FAK	focal adhesion kinase
FB_1	fumonisin B1
FCS	foetal calf serum
Fig.	Figure
FITC	fluoroscine isothiocyanate
FOXO	forkhead box O
g	gram(s)
Gab1	Grb2-associated binder-1
GF	growth factor (s)
GSK3β	glycogen synthase kinase-3β
HAUSP-7	herpesvirus-associated ubiquitin-specific protease-7
HEK293	human embryonic kidney 293
HCl	hydrochloric acid
HM	hydrophobic motif
hnRNPs	heterogenous nuclear ribonucleoproteins
HOSCC	human oesophageal squamous cell carcinoma
H_2O_2	hydrogen peroxide
HPV	human papillomavirus
hr	hour (s)
HRP	horseradish peroxidase
IB	immunoblot
IP	immunoprecipation
ILK	integrin-linked kinase

JNK	c-Jun NH2-terminal kinase/just another kinase
kDa	kilodalton
LEF-1	lymphoid enhancer factor
LiCl	lithium chloride
LY29	LY294002
mA	milliampere(s)
MAPK	mitogen activated protein kinase
$MgCl^{2+}$	magnesium chloride
min	minute(s)
mt	mutant
ml	millilitre(s)
mM	millimolar
MMLV	Moloney Murine Leukemia Virus
MMP-7	metalloproteinase-7
mRNA	messenger ribonucleic acid
mTOR	mammalian target of rapamycin
NaAc	sodium acetate
NaCl	sodium chloride
NaOH	sodium hydroxide
NEDD4-1	neural precursor cell expressed, developmentally downregulated 4-1
NF-γB	nuclear factor of kappa light chain gene enhancer in B-cells
NFAT	nuclear factor of activated cells
nM	nanomolar
Nox	NADPH oxidase
OA	okadaic acid
PAGE	polyacrylamide gel electrophoresis

PBS	phosphate buffered saline
PCR	polymerase chain reaction
PDGF	platelet derived growth factor
PDK1	phosphoinositide-dependent protein kinase 1
pGSK3β	Ser9 phosphorylated GSK3β
PH	pleckstrin homology
PI3K	phosphoinositide-3-OH-kinase
PIP2	PtdIns (4, 5) P2
PIP3	PtdIns (3,4,5) P3
PKB/AKT	protein kinase B
PMSF	phenylmethanesulphonylflouride
Prdx	peroxiredoxin
PtdIns	phosphotidylinositols
PTEN	phosphatase and tensin homologue deleted on chromosome ten
pPKB	Ser473 phosphorylated PKB
p-p53	Ser46 phosphorylated p53
USA	United States of America
RTK	Receptor tyrosine kinase
RT	Room temperature
RT-PCR	Reverse transcription PCR
RNA	ribonucleic acid
ROS	reactive oxygen species
SA	South Africa
sec	second (s)
SDS	sodium dodecyl sulphate
SH2	Src homology domain

Std Dev	standard deviation
TBS	tris buffered saline
TEMED	N,N,N',N'-tetramethylethylene-diamine
TCA	trichloro-acetic acid
TCF	T-cell factor
TF	Transcription factor (s)
TGF-β	transforming growth factor β1
Tris	tris(hydroxymethyl)aminomethane
TSP	Tumour suppressor protein (s)
µl	microliter
V	volts
WHCO-	Wits Human Carcinoma of the Oesophagus-
wt	wildtype
XIAP	X-linked Inhibitor of Apoptosis Protein

Chapter 1
General Introduction
The road to understanding the role of PI3K in HOSCC

1.1 The non-linearity of signal transduction in cells.

Constant communication between cells and their environment is imperative in multicellular organisms, in order to balance important biological processes such as cell proliferation, differentiation, cell motility, survival, apoptosis and cell adhesion[1]. Cells are highly sensitive, and responsive to changes in their external environment or extracellular matrix (ECM). These changes are communicated by various molecules within the ECM which bind to, and activate, specific transmembrane receptors located within the plasma membrane of cells[2]. Typically, these signals are acquired through direct communication between cells by the cell adhesion molecules (CAMs), and an indirect communication through signals that are transmitted by ligand-activated cell-surface receptor tyrosine kinases (RTKs) and non-receptor tyrosine kinases (see Fig. 1.1 for an overview). The latter includes growth factors (GFs), hormones, neurotransmitters, chemokines, extracellular matrix components, and cytokines, which activate secondary messengers in the cytoplasm of the cell. In turn, these are able to control which signals should be integrated and amplified in order to solicit an appropriate cellular response[1-3]. Cells responding to such stimuli undergo a variety of changes in one or more of the above mentioned biological parameters[4]. Overall, this process is referred to as signal transduction[5], which is represented in Fig. 1.1.

The various signalling ligands are too large and polar to pass through the plasma membrane and therefore bind to the extracellular domains of receptor proteins, which induce a conformational change in their cytoplasmic domains, resulting in their consequent activation[1-5]. All signalling pathways within a cell are activated as a result of ligand binding either to a RTK (GF receptor)[6,7]; G-protein coupled receptors (GPCRs)[8] or a non-RTK (the CAMs)[9]. Receptor stimuli are short-lived and must be transduced into a longer lived signal as second messengers[10]. The most common of these include cyclic AMP, inositol 1,4,5-triphosphate (IP3), diacylglycerol (DAG), phosphatidylinositol bisphosphate (PIP2), and phosphatidylinositol triphosphate

(PIP3)[11, 12, 13]. Through a series of protein phosphorylations and dephosphorylations, protein recruitment, allosteric activation or inhibition and protein binding induced by these secondary messengers across the cytoplasm, leads to either the amplification, or suppression, of signal transduction pathways through the transcription of target genes (see Fig. 1.1)[14].

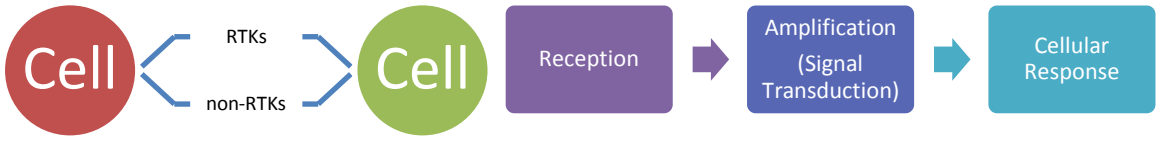


Figure 1.1: General overview of signal transduction. This figure demonstrates communication between cells through the ECM, RTKs, and non-RTKs. These signals are received, and amplified through signal transduction that induces a cellular response.

Additionally, these pathways are activated by the associated recruitment of adaptor proteins to the sites of activation at the plasma membranes[15]. Classically, these include; Grb2, Grb2-associated binder-1 (Gab1), Src, Nck2, Sos, and Shc adaptor molecules[1, 15]. The major signal transduction pathways activated as a result of these second messengers, are the Ras-mitogen-activated protein kinase (MAPK) cascade which further includes four separate signalling cascades (ERK, JNK, p38 and BMK)[16]; the phosphatidylinositol 3-kinase (PI3K) pathway, the JNK/STAT (Just another kinase) pathway, the protein kinase C (PKC) and Wnt intracellular signalling pathways[17]. A long standing question is what determines the specific activation of each of these signal transduction pathways? The answer to this is both simple and complex, in that no signal transduction pathway operates in isolation but instead, each pathway interacts with an allied pathway and function in synergy with each other (see Fig. 1.2 for an illustration)[18]. This phenomenon is known as "crosstalk"[19, 20, 21]. Cells are exposed to a multitude of external or incoming stimuli that trigger the simultaneous activation of various signalling pathways, resulting in major biochemical responses that are interpreted through a complex network activation of different signal transduction pathways (see Fig. 1.2)[22]. The negative and positive input from the diverse signalling pathways is what allows the cell to regulate its activity more effectively, than rather through a single isolated pathway[23]. Miscommunication between these pathways has severe effects on the cell that eventually lead to the current ten hallmarks of cancer such as, uncontrolled growth and proliferation, migration and invasion, and evasion of cell death (apoptosis)[24], as depicted in Fig. 1.3.

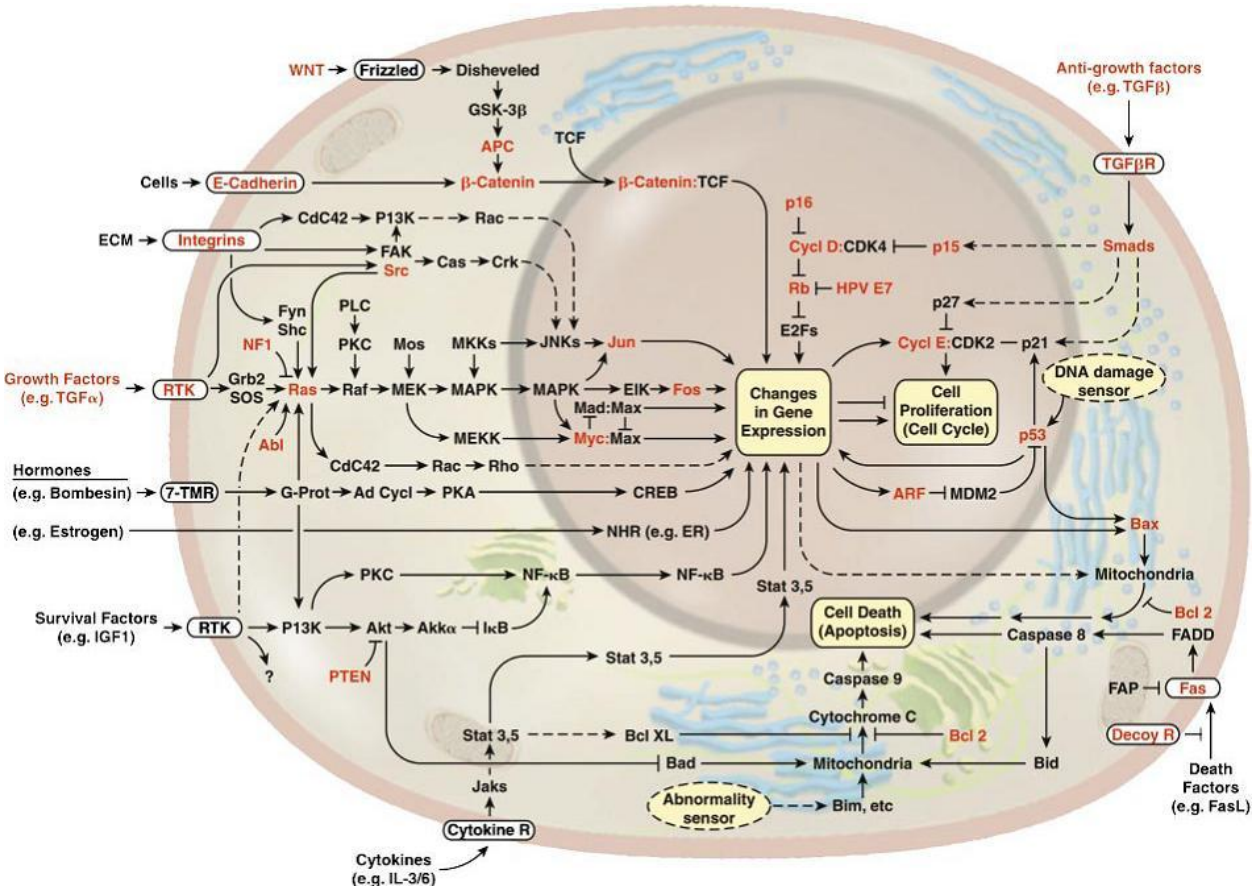


Figure 1. 2: Representation of crosstalk that takes place between the signalling pathways within the cell, showing the localization of the several receptors at the plasma membrane, adaptor molecules, signalling pathways within the cytoplasm and transcription factors in the nucleus, arrows exhibiting a positive influence[24].

1.2 The concept of "Oncogene Addiction".

Signalling miscommunication can be caused by a combination of genetic and epigenetic changes in genes and proteins, which result in aberrant cell behaviour (as represented in Fig. 1.3). Once a cancer cell reaches this stage, it is often irreversible[25, 26]. Despite the various efforts to depict the molecular intricacies that govern such aberrant intracellular circuits, a complete understanding is still lacking. Cancer is a multi-step process[27, 28, 29], and therefore it is surprising to realize that this irreversibility is commonly linked to a reliance that these cancer cells have on specific signalling pathways for their survival. This type of dependency is frequently defined as "oncogene addiction" [30, 31, 32]. In the literature, this term is used to describe the unexplained dependency or "addiction" that cancer cells have on a particular signal transduction pathway for their survival and proliferation. The general understanding behind this phenomenon is linked to the fact that mutations present within specific proteins (oncogenes) act as focal points for pathway interplay, and in turn, form the element of "addiction" that creates a self-perpetuating

state which drives the transformation process[30, 33]. Although this phenomenon has attracted considerable criticism[34], the pattern of oncogene "addiction" has been extensively studied in mice and human cancer cell lines, and shown to form a relevant part in the transformation of breast, leukemia, multiple myeloma, non-small cell lung and glial cancers[35, 36, 37, 38, 39]. One of the major signal transduction pathways forming the basis to the cancer cell "addiction", is the PI3K pro-survival signalling pathway[40, 41, 42, 43].

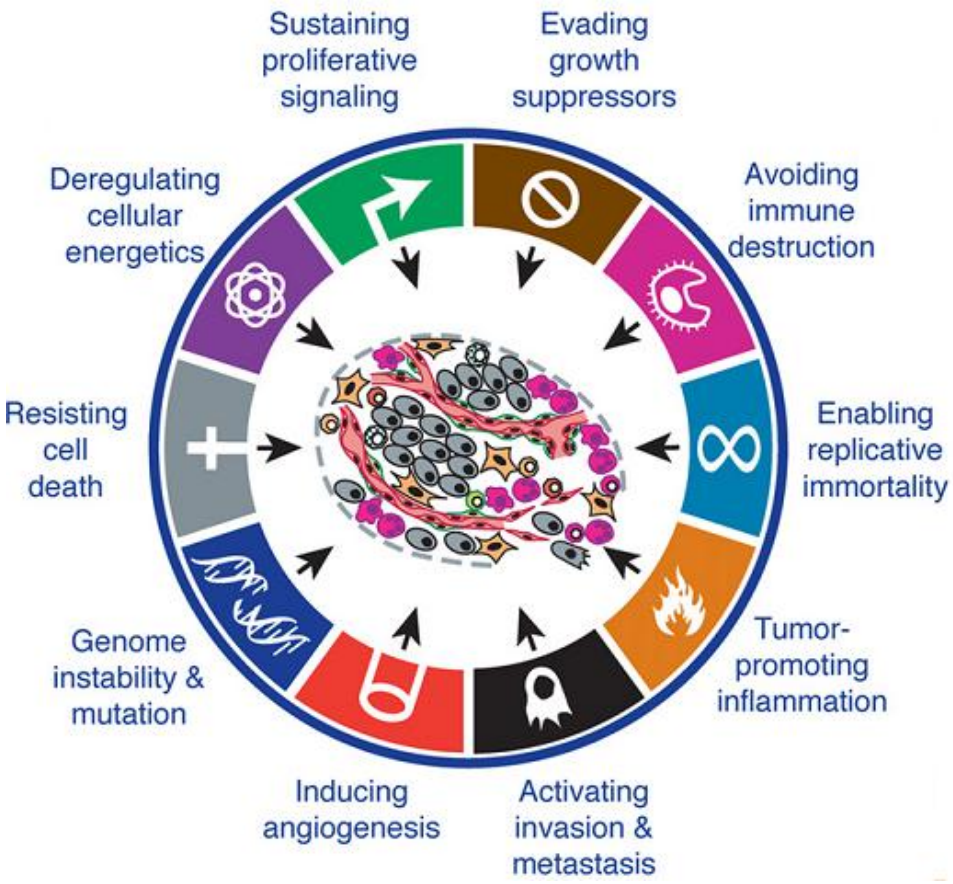


Figure 1.3: The ten hallmarks of cancer. Miscommunication between the various intracellular signal transduction pathways leads to the ten hallmarks of cancer, such as uncontrolled growth, resistance to cell death, highlighted in the figure. Figure adapted from Hanahan[26].

1.3 Phosphatidylinositol-3-kinase (PI3K)

Phosphatidylinositol (PtdIn)-3-kinase/PI3K (initially termed, type I PtdIns kinase) was originally classified as a lipid kinase, based on its ability to phosphorylate the 3'-inositol ring of membrane lipids in cells embedded with viral oncogenes, such as v-src or v-ros[44]. These substrates include; phosphotidylinositols (PtdIns); PtdIns4P, and PtdIns (4, 5) P_2[45]. To date, eight distinct classes of mammalian PI3Ks have been isolated and identified into three unique classes on the bases of their sequence homology, substrate specificity and discrete regulation[46]. Class I is subdivided into two respective groups; Class I_A and Class I_B (see Fig. 1.4). Class I_A PI3Ks are heterodimers consisting of a p85α adaptor/regulatory subunit and a p110α catalytic subunit, whereas Class I_B PI3Ks are associated with a unique family of adaptor subunits that are distinguished from the Class I_A adaptor subunits (as shown in Fig. 1.4). Class I_B shares over 90% sequence and structure homology to Class I_A except that instead of the p110α subunit, it expresses a p101 subunit and lacks an N-terminal p85 binding site, which makes it incapable of performing protein: protein interactions[47] (see Fig. 1.4).

Class II PI3Ks are mainly involved in insulin signalling and although still a matter of debate, they preferentially phosphorylate PtdIns, but are also able to phosphorylate PtdIns(4)P[48]. Little is known about their mode of activation and primary cellular functions, but has been suggested to also occur via the RTKs[49]. Class III PI3Ks are restricted in using PtdIns as their substrate. This class is not known to fulfil any purpose in the regulation of signalling pathways activated by receptor stimulation and functions primarily in membrane trafficking and vacuole sorting[50, 51]. Class I_A PI3Ks are one of the most crucial regulatory proteins within a cell and therefore commonly gains oncogenic potential in a wide variety of cancers[52, 53], and hence, forms the focus of this study.

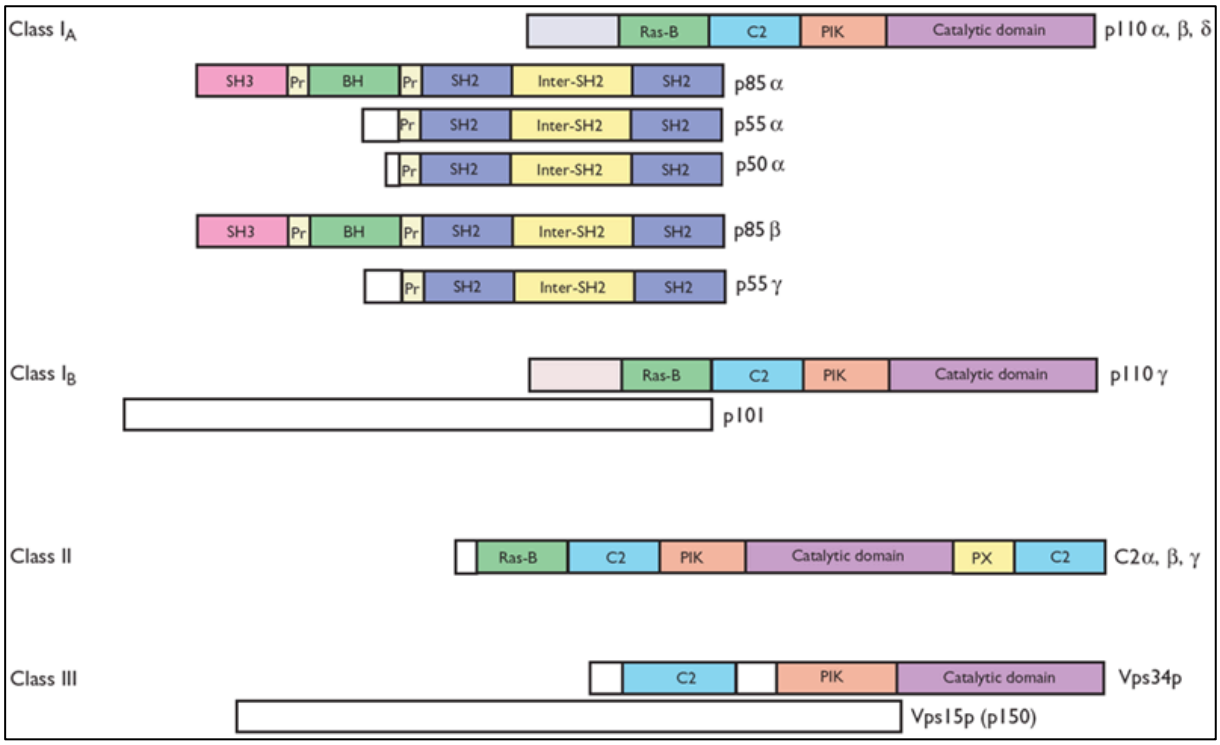


Figure 1.4: The multiple isoforms of mammalian PI3-Ks divided into three classes, according to their structure similarities, binding specificities and mode of activation in response to different stimuli[54]. Shown in the figure are Class I_A and $_B$, Class II and Class III. See text for more information.

1.3.1 Structure and Inter-subunit interactions of p85α and p110α.

The Class I_A PI3Kα isoforms are ubiquitously expressed[55, 56] and comprise of an 85 kDa regulatory subunit (p85α) that is associated with a 110 kDa catalytic subunit (p110α)[57]. The p85α protein contains two (N-and C-terminal) Src homology 2 (SH2) domains, two proline-rich domains, a single SH3 domain, a breakpoint cluster region (BCR/BH) homology domain, and an inter-SH2 (iSH2) domain[58]. Alternative splicing of the p85α PI3K gene (PIK3R1) generates three isoforms, the 85 kDa (p85α), a 55 kDa (p55α), and a 50 kDa (p50α), of which p85α is most ubiquitous acting as the major discriminator of various external stimuli (see illustration in Fig. 1.4)[59]. The iSH2 domain, aided by the N-terminal SH2 domain, sufficiently binds to the adaptor-binding domain (ABD) of the p110α subunit, forming an irreversible linkage[60, 61]. Additionally, the p110α subunit contains a Ras-binding domain, a C2 domain, followed by a helical and catalytic domain[62]. Although p110α is renowned for its lipid kinase activity by catalyzing the formation of PIP3 through its substrate, PIP2, it also has serine/threonine protein kinase activity[63]. This serine/threonine kinase activity can lead to

autophosphorylation and phosphorylation of p85α, resulting in the overall inhibition of PI3K that is only alleviated upon its membrane translocation[64].

The strong dependency p110α has for p85α, is both beneficial and unfavourable, in that, p85α inhibits its lipid kinase activity, while offering stability. This paradoxical relationship was confirmed through i*n vivo* experiments demonstrating that p85α/p110α dimerization resulted in an instant 80% reduction in its catalytic activity[65]. Monomeric p110α is also considered unstable at body temperature (37 ˚C), and it is therefore the balance between p85α mediated inhibition and stabilization that determines the overall PI3K activation status[66]. In contrast, others have shown that normal cells possess copious amounts of monomeric p85α[67], and compete with the p85α/p110α heterodimer for binding to tyrosine phosphorylated residues on activated receptors, thus acting as an antagonist for PI3K activity[68]. This theory is known as the 'free p85' hypothesis, with evidence showing that both monomeric p85α and p110α are unstable, and loss in p110α concomitantly reduces p85α expression[68].

1.3.2 PI3K activation

The mutual inhibitory relationship between the p85α (through the N-terminal and iSH2/p85ni), and the p110α (through serine/threonine p85α phosphorylation) subunits[69], is abrogated by favourable conformational changes that take place upon the p85α SH2 domain binding to membrane proteins comprising of intrinsic phosphorylated tyrosine residues[70]. This activates the lipid kinase activity of p110α without diminished p85α association[71]. As a result, the p110α catalytic subunit is in proximity with its membrane bedded lipid substrates (predominantly PtdIns (4,5) P_2) or PIP2. At the membrane, p110α catalyzes the transfer of the γ-phosphate group of adenosine triphosphate (ATP) to the 3' position of the PIP2 inositol ring, giving rise to the primary secondary messenger, PtdIns (3,4,5) P_3 or PIP3 (as depicted in Fig. 1.5)[72, 73]. PIP3 transmits the incoming signal through the activation of various PI3K effector molecules; such as the integrin linked kinase (ILK), and the phosphoinositide-dependent protein kinase 1 (PDK1) [74, 75]. This ultimately leads to protein kinase B (PKB)/Akt activation, which is pertinent for the induction of cell survival and proliferation[76, 77].

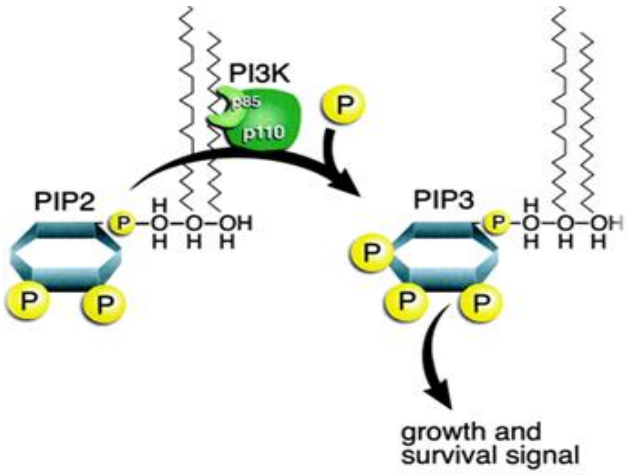


Figure 1.5: p110α-mediated conversion of PIP2 to PIP3 important for the downstream activation of growth and proliferation. Adapted from Sansel and Sellers[78].

1.3.2.1 Stimuli from Cell-Cell Adhesion

The cadherins mediate Ca^{2+}-dependant homophilic cell-cell (C-C) adhesion in a zipper-like fashion associated with the adherens junction[79, 80]. The cadherins are further divided into four subfamilies consisting of: (1) the classical cadherins; (2) desmosomal cadherins; (3) proto-cadherins and (4) cadherin-related proteins, of which the classical cadherins are most prominent[81]. The classical cadherins contain four members, all of which are structurally similar and are intimately linked by their cytoplasmic domain to the actin cytoskeleton of neighbouring cells through their direct interaction with α-, β- and γ- catenins, vinculin and α-actinin[82]. The cadherins are named according to the tissues in which they are predominantly found. These are the E-cadherins (found in epithelia), N-cadherins (found in neurons), P-cadherins (found in placenta) and VE-cadherins (found in endothelial cells)[81, 82]. E-cadherin is the best characterized and relevant to the activation of the Class I_A PI3K[83, 84].

During embryonic development and tissue repair, the expression of E-cadherin is relatively low[85, 86], to enable the movement of epithelial cells to their specified organs or for wound healing. In either process, cells need to lose their polarity and C-C adhesion and adopt what is called a mesenchymal (migratory) phenotype[87]. The overall process is formally known as the epithelial-to-mesenchymal transition/EMT[88]. Notably, this feature is generally associated with the invasion of epithelial cancer cells possessing a decreased E-cadherin expression[89, 90].

E-cadherin activates PI3K by two distinct mechanisms. Firstly, the ligation of E-cadherin molecules between neighbouring epithelial cells, recruits the c-src adaptor protein to the plasma membrane E-cadherin adhesion complex (E-cadherin, α- and β-catenins). As the cytoplasmic tail of E-cadherin does not contain any catalytic activity[91, 92], the presence of c-src concomitantly leads to the membrane recruitment of PI3K to the E-cadherin adhesion complex[93, 94] (as shown in Fig. 1.6). It is unknown whether PI3K interacts directly with E-cadherin or via c-src. Irrespective of the mechanism used for the membrane recruitment of PI3K through E-cadherin, this recruitment still results in the production of PIP3 through PI3K activation (see demonstration in Fig. 1.6). Co-immunoprecipitation experiments have verified the association between PI3K and E-cadherin at sites of C-C adhesion, as well as the co-accumulation of E-cadherin and phosphoinositides[95]. Furthermore, research also demonstrates that PI3K promotes the assembly and integrity of the E-cadherin adhesion complex, and as such, through its p85α regulatory subunit, plays a role in cellular differentiation[96, 97, 98, 99, 100]. Secondly, E-cadherin incidentally activates PI3K through its direct activation of EGFR, prompting ligand-independent activation of EGFR[101, 102, 103]. Additionally, recent evidence has shown that E-cadherin also up-regulates the transcription of EGFR, shown in head and neck cancer specifically[104].

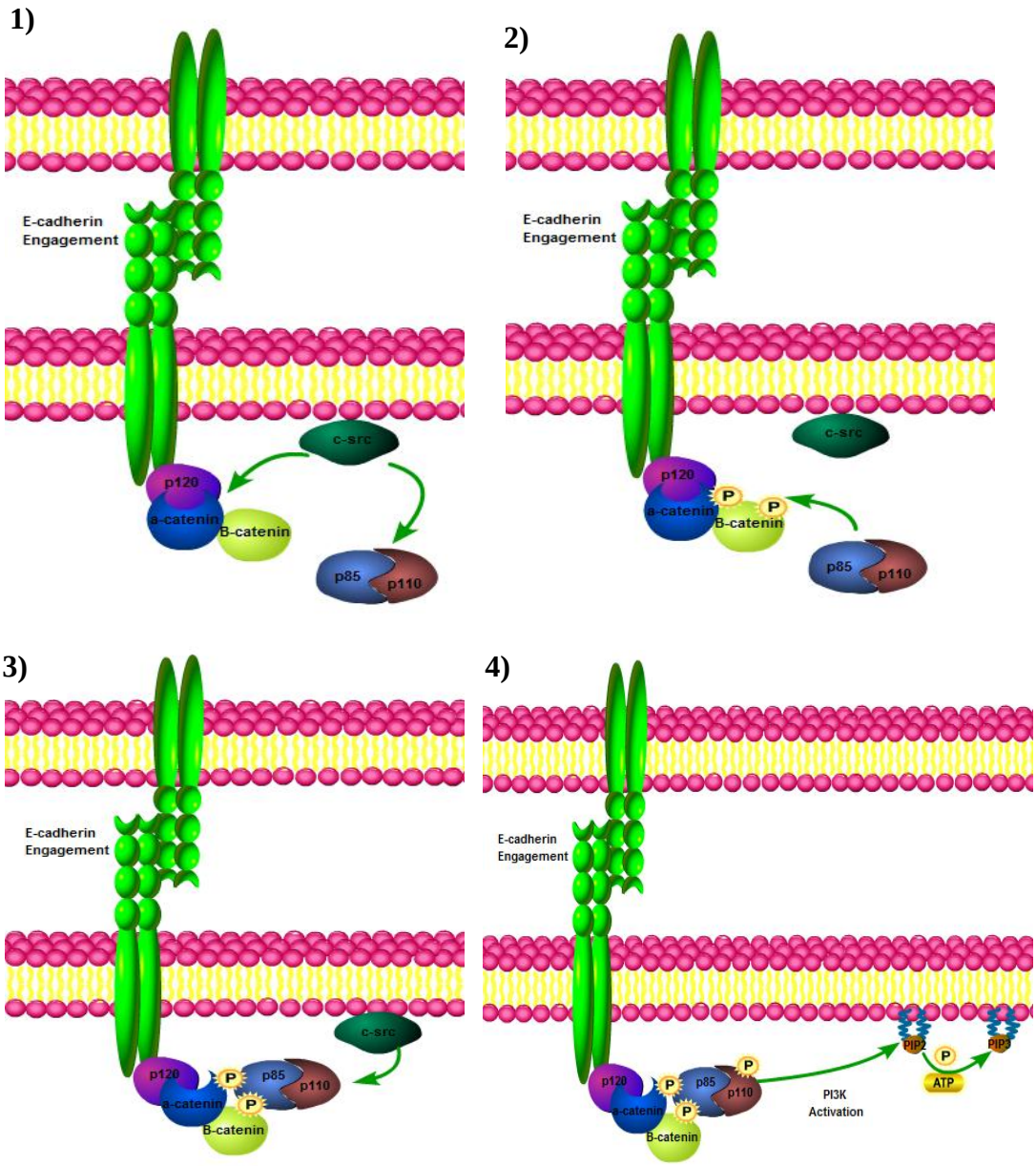


Figure 1.6: Cell adhesion mediated activation of PI3K. Cell-cell adhesion through the E-cadherin adhesion complex (E-cadherin/α/β-catenin/γ-vinculin) **(1)** leads to the membrane recruitment of c-src **(2)** which is proposed to be essential for the membrane recruitment of PI3K **(3)**, leading to the production of PIP3 at the membrane **(4)**. Figure generated using Pathway Builder Tool.2.0.

1.3.2.2 Stimuli from Cell-ECM Adhesion

During the EMT process described, cells need to migrate whilst maintaining an interaction with their ECM[105, 106]. This is achieved by the heterodimeric cell surface receptors called the integrins[107]. Integrins are CAMs made up of two non-covalent glycoprotein type-I transmembrane α and β subunits[108]. These CAMs are linked by their cytoplasmic β tail to the actin cytoskeleton through adaptor (i.e. Grb2, ILK) and anchor proteins (i.e. α-actinin and filament) that provide the essential cell-extracellular matrix (C-ECM) linkages, enabling cells to migrate across the ECM, and in the case of cancer cells, to invade[109, 110]. Each cell expresses unique subtypes of integrins on their surfaces that are categorized by distinct α and β subunit associations, which bind to different ECM protein components, leading to their subsequent activation[108,111, 112]. These associations include the $\alpha_5\beta_1$ and $\alpha_v\beta_3$ integrin that specifically binds fibronectin[113], the $\alpha_2\beta_1$ integrin that binds fibrillar collagen[114], and $\alpha_6\beta_4$ integrin binds laminin[115].

In addition to regulating migration, integrin clustering also positively influences cell growth, proliferation, survival, and differentiation by actively engaging in intracellular signalling cascades[116, 117, 118]. The integrins do not contain any enzymatic activity themselves, but instead, trigger the activation of downstream signalling molecules like the focal adhesion kinase (FAK)[119], paxillin[120], and ILK[121]. Integrin clustering triggers the α5β1 subunit-dependent autophosphorylation of FAK at Tyr397, creating a binding site for c-src, subsequently leading to the activation of the PI3K[122, 123] (see diagrammatic representation in Fig. 1.7). The signalling roles of the integrins was substantiated in the formation of lamellae (which are dynamic sites of motility in invasive carcinoma cells), through the $\alpha_6\beta_4$ integrin mediated activation of PI3K[124].

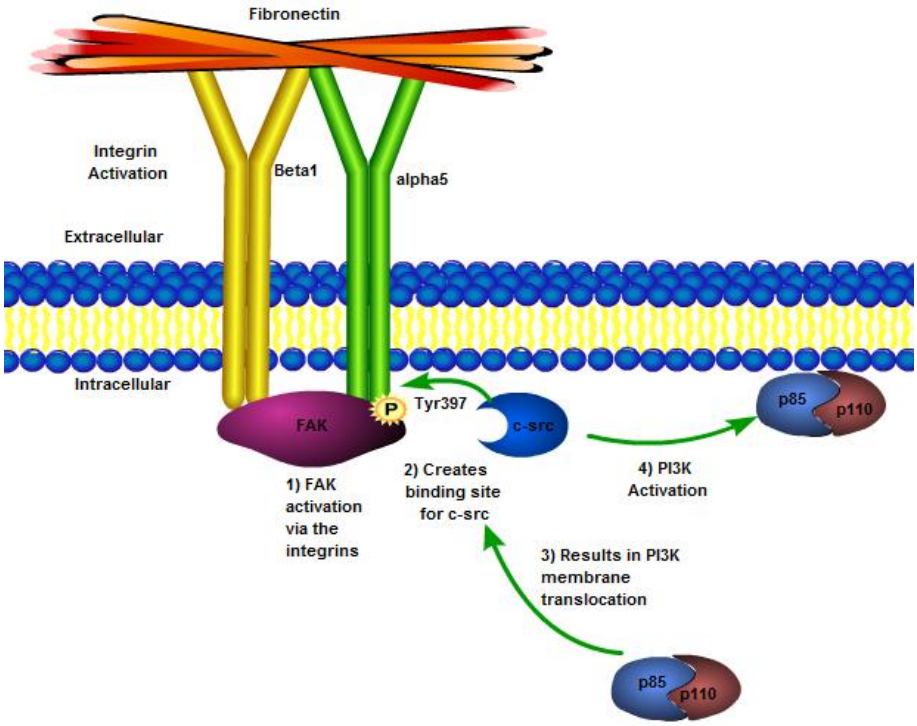


Figure 1.7: Integrin mediated activation of PI3K. The α5β1 integrin becomes activated by binding to its substrate, fibronectin resulting in its activation that induces the Tyr397 phosphorylation and activation of FAK **(1)**, which creates a binding site for c-src **(2)** which leads to the membrane recruitment of PI3K **(3)** and subsequently its activation **(4)**. Diagram created using the Pathway Builder Tool 2.0.

Furthermore, the role of the integrins in cancer is commonly linked to its downstream activation of PI3K through FAK[125, 126, 127] as illustrated in Fig. 1.8. In addition to this mechanism, coupled activation of the RTKs via the integrins can also activate PI3K, termed "inside-out" signalling[128, 129] (see Fig. 1.8). It is well defined that RTK-dependent signalling is reliant upon the simultaneous activation of the integrins for effective signal propagation[130, 131, 132]. Following C-ECM interactions, which lead to the membrane recruitment of the c-src and p130 adaptor proteins, trigger the Tyr416, Tyr845, Tyr1068, and Tyr1173 phosphorylation and activation of EGFR in an EGF-independent manner[133]. Specifically, the α5β1 integrin/EGFR interaction was shown to contribute to the invasive potential of prostate cancer cells[134] (see Fig. 1.8).

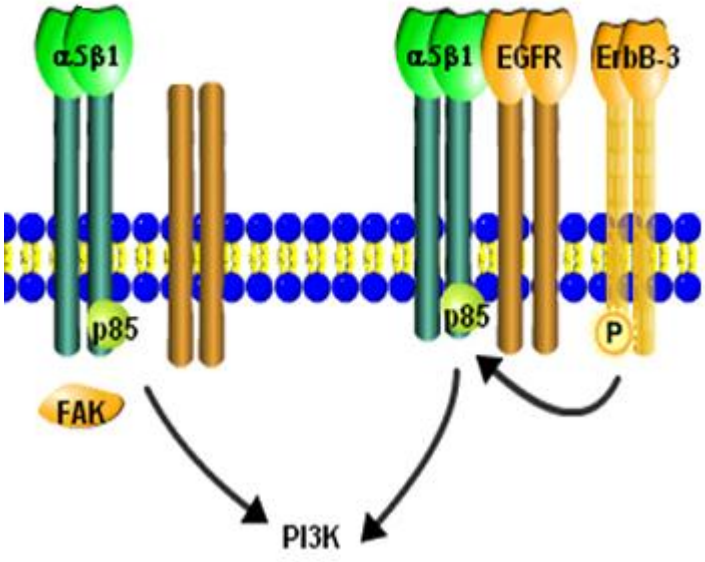


Figure 1.8: PI3K activation through crosstalk between the integrins and EGFR. The α5β1 integrin forms a complex with the EGFR that leads to p85 membrane recruitment and cross-activation through ErbB3, resulting in PI3K activation. Figure adapted from Souny, *et al.*[133]

1.3.2.3 Receptor Tyrosine Kinases

The epidermal growth factor receptor (EGFR) is one of the major ubiquitous receptor tyrosine kinases belonging to the ErbB family comprising of four members; EGFR (also known as ErbB1/HER1), ErbB2 (also known as Neu/HER2), ErbB3/HER3, and ErbB4/HER4 (see Fig. 1.9 for visualization)[135, 136]. Members of the EGFR family are often (43-89%) expressed as oncogenes in various cancers, especially in breast and oesophageal cancer[137, 138, 139, 140]. Currently, six known ligands bind to and activate the EGFR; the transforming growth factor-α (TGF-α), epidermal growth factor (EGF), amphiregulin (AR), heparin-binding EGF-like growth factor (HB-EGF), betacellulin (BTC), and epiregulin (EPR) [141]. These ligands do not appear to bind to the ErbB2, as its direct ligands remains to be determined, and instead acts as a co-receptor (see Fig. 1.9)[142, 143]. In addition to the ligand-induced ErbB receptor activation, they can also be activated in the absence of ligands[144], such as osmotic stress caused by ultraviolet (UV) radiation exposure or any other toxin and carcinogen[145, 146, 147].

Ligand binding to the N-terminal cysteine-rich ErbB receptor extracellular domain induces receptor homo-and heterodimerization, and subsequent autophosphorylation of specific tyrosine residues on its cytoplasmic tail (highlighted in Fig. 1.9)[148]. These phosphorylation

residues serve as docking sites for adaptor and kinase proteins in possession of Src homology 2 (SH2) and phosphotyrosine binding (PH) domains[149]. Phosphorylation of Tyr1086 and Tyr1068 residues on the EGFR have been shown to be specific for the binding of the Gab1 adaptor protein[150]. The activation of Gab1 serves as a docking site for the distinct membrane recruitment and activation of the p85α regulatory subunit of PI3K (shown in Fig. 1.9)[151]. The biochemical signal specificity and duration thereof are reliant upon ligand bivalency and their respective binding to low or high affinity ErbB receptors [152, 153, 154]. Low affinity receptors constitute the majority (90%) of the receptor pool, while high-affinity receptors make up the residual[155]. One of the major differences between these types of receptors lies in their particular ligand affinities[156]. It has long been thought that the small group of high-affinity receptors were the major contributors to cell fate[155]. However, recent evidence suggests that low concentrations of EGF (<2 nM) are specific for the activation of the PI3K pathway via the low-affinity receptors, whereas the STAT pathway is predominantly stimulated at higher EGF concentrations[157]. Although less frequently, PI3K can also be activated by the platelet-derived growth factor (PDGF) in specific cell types and shown to be primarily induced during cell migration[158, 159, 160].

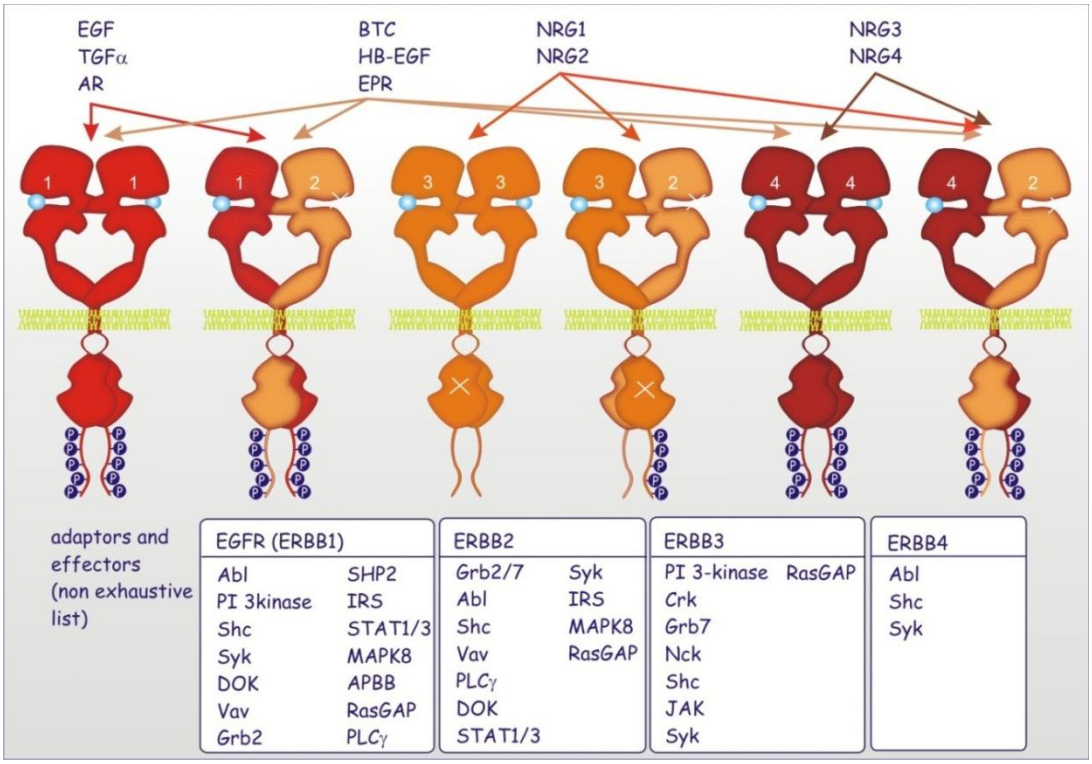


Figure 1.9: Summary of the ErbB family of receptors, their respective ligands and specific signal transduction pathways they activate[161].

1.4 The PI3K pathway - navigating downstream.

In quiescent cells, PI3K is found in the cytosol, where upon activation by one of the mechanisms described above, results in its plasma membrane recruitment where it converts PIP2 into PIP3. It is well recognized that the localization, conformation and activity of kinases is significantly affected upon binding to membrane phospholipids[162, 163, 164]. Thus, accumulation of PIP3 at these PI3K activation sites, is responsible for the membrane recruitment of numerous kinases that harbour PH-domains that enables them to efficiently bind to PIP3, resulting in their consequent activation[165, 166, 167]. Although many kinases are triggered as a consequence, recent evidence highlights that the major intracellular responses controlled by PI3K activation are through the protein serine/threonine kinase protein kinase B/PKB (commonly referred to as Akt)[168], and hence was included in the focus of this study.

1.4.1 Major PI3K effector protein: PKB

PKB is a cellular homologue of the murine transforming retrovirus oncoprotein, v-Akt, and hence its alternative name; Akt[169]. In mammalian cells, PKB has three closely related isoforms; Akt1/PKBα, Akt2/PKBβ, and Akt3/PKBγ, all of which comprise a N-terminal PH-domain, central kinase domain, and a carboxyl/C-terminal domain that contains the hydrophobic motif (HM)[170, 171, 172]. It is due to the high sequence homology within the kinase domain and HM of PKB that it is characterized as an AGC kinase, similar to protein kinase A (PKA), protein kinase C (PKC), p70 ribosomal S6 kinase (S6K1), and serum-and glucocorticoid-inducible kinase (SGK)[173, 174]. Of interest, studies on mice lacking either one of the PKB isoforms demonstrated that Akt1/PKBα plays a fundamental role in embryogenesis, cell growth and proliferation, whereas the function of Akt2/ PKBβ and Akt3/ PKBγ is directed to glucose metabolism[175, 176].

1.4.1.1 Activation of PKBα (PKB)

Inactive PKB is largely localized in the cytoplasm, whereby its activation is stimulated by membrane translocation and PH-domain-PIP3 interactions[177] (outlined above). The membrane and PH-domain associations formed, induce favourable conformational changes within PKB that set the scene for its consequent activation[178] (see representation in Fig. 1.10). Several studies reveal that its full activation requires an additional two steps[179, 180]. First, the Thr308 residue in the activation loop of PKB is phosphorylated by the PIP3-

dependent PDK1 that induces a conformational change within PKB[181], resulting in its partial activation and membrane detachment through its PH-domain (see Fig. 1.10). This "semi-active" PKB is then phosphorylated on its Ser473 residue within the hydrophobic motif by the "Ser473 kinase", resulting in its full activation[182]. The role of the "Ser473" kinase has been given to several candidates including the DNA-dependent protein kinase (DNA-PK)[183, 184] and ILK[185]. Recently however, the mTOR complex 2 (mTORC2) is widely accepted as the "Ser473 kinase" required for PKB full activation[186, 187, 188,189, 190, 191] (shown in Fig. 1.10) . Active PKB translocates to the cytoplasm and nucleus where it is in proximity to its substrates in order to affect cell survival and proliferation.

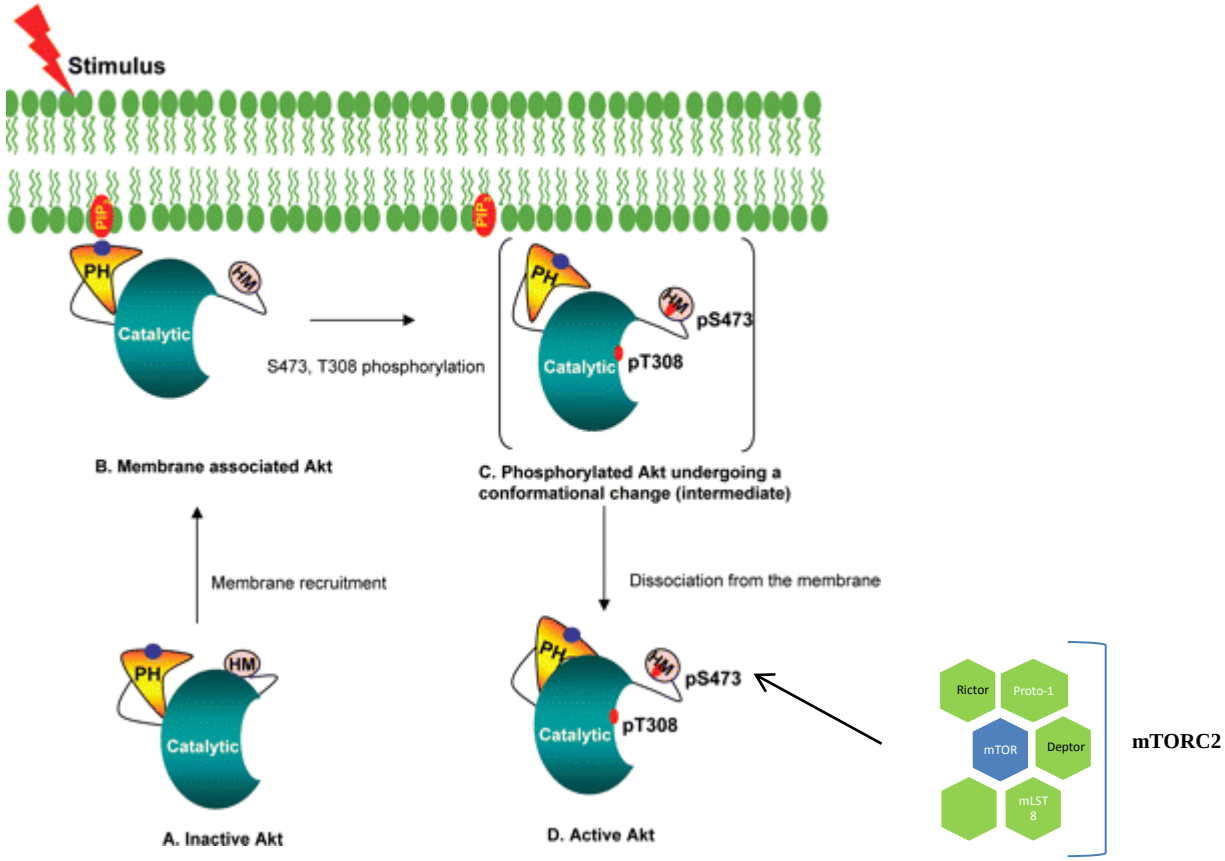


Figure 1.10: Model for PKB activation. Briefly, when PKB is localized within the cytoplasm it is inactive **(A)**. However upon PI3K-dependent production of PIP3, PKB is recruited to the plasma membrane where its PH domain interacts with PIP3 **(B)**. Upon membrane binding, PDK1 mediates the Thr308 phosphorylation of PKB that induces a conformational change, essential for its cytoplasmic relocation **(C)** and mTORC2-mediated Ser473 phosphorylation leading to its full activation **(D)**. See text for more details. Figure adapted from Ananthanarayanan, *et al.*[182]

1.4.1.2 Major PI3K and PKB-mediated cellular effects.

Studies focusing on the gene encoding the p110α isoform, known as PIK3CA[192], showed that mice carrying a deleted form of this gene (PI3CA$^{del/del}$ embryos) survived to embryonic day (ED) 8.5 with great difficulty, progressively dying at ED 9.5, and eventually dead on ED 10.5[193]. No increase in apoptosis was observed in any of these embryos, suggesting that apoptosis was not responsible for the death observed. These studies underpinned the significant role played by PI3K in tissue development and cellular proliferation. Activation of PKB through PI3K modulates a myriad of substrates through phosphorylation of specific residues that eventually affect cell growth, metabolism, proliferation, angiogenesis and survival (depicted in Fig. 1.11).

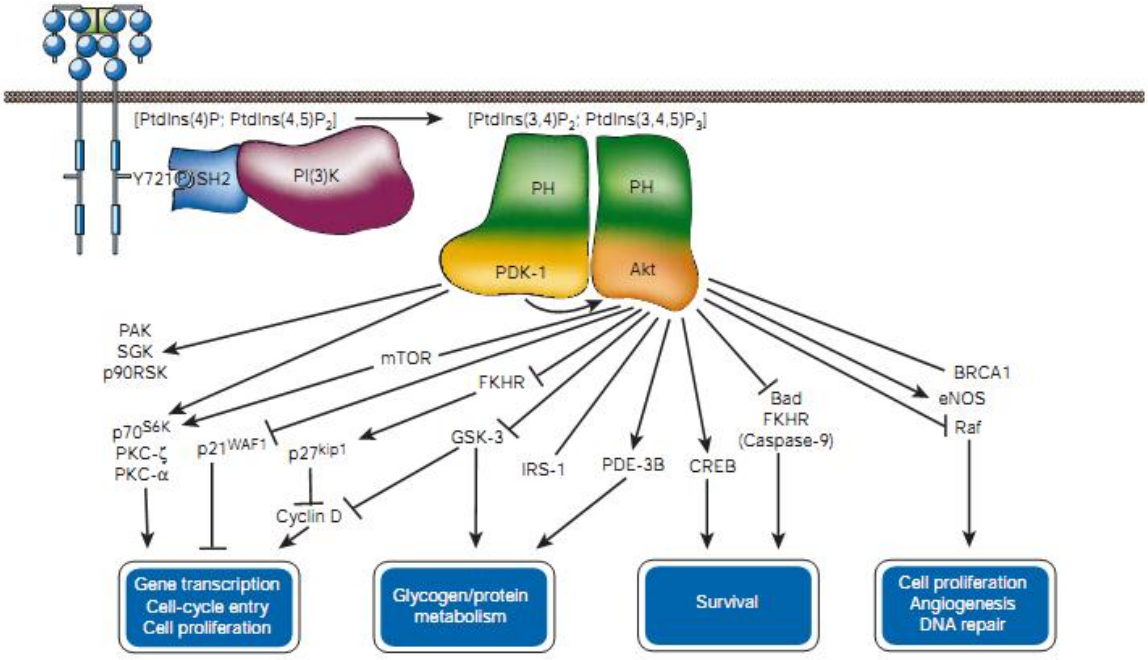


Figure 1.11: The many intracellular targets of the PI3K pathway through PKB. It is clear from the diagram above that the PI3K-dependent activation of PKB (Akt) results in the specific phosphorylation of numerous downstream target proteins involved in cell survival and apoptosis, cell proliferation, invasion, and angiogenesis that result in their respective activation or inhibition[194].

As highlighted in Fig.1.11, PKB phosphorylates an array of proteins that play a fundamental role in growth, metabolism and proliferation. Most notably are; glycogen-3-kinase (GSK3), mammalian target of rapamycin (mTOR), the insulin receptor substrate-1 (IRS-1), Bad, and the forkhead transcription factors (FKHR)[194]. One of the well-

recognized targets of PKB that regulates cellular growth, proliferation, metabolism and apoptosis is the glycogen synthase kinase (GSK3)[195, 196, 197]. GSK3 has two distinct isoforms; the α and the β isoforms. Deletion of the β isoform in mice demonstrated complete embryonic lethality[198], whereas GSK3α knock-out mice were viable[199]. PKB phosphorylates GSK3α at Ser21, and GSK3β at Ser9, both of which, lead to the significant reduction in their cellular activity[200]. GSK3β is a major component of the canonical Wnt pro-survival signalling pathway[201], and therefore represents the best example of its cellular function. In quiescent cells, GSK3β is active, and through its association with adenomatous polyposis coli (APC), Axin and protein phosphatase 2A (PP2A), it promotes the degradation of β-catenin (see demonstration in Fig. 1.12). In so doing, it abrogates the transcriptional activities of β-catenin, which are enhanced by its nuclear association to the LEF (lymphoid enhancerfactor)/TCF (T-cell factor) transcription factors, which would otherwise up-regulate the expression of growth and cell proliferation by promoting genes such as c-myc, and c-jun[202, 203] (as highlighted in Fig. 1.12). Therefore, through PKB, PI3K augments cell growth and proliferation by stimulating the up-regulation of these growth promoting genes through inhibition of GSK3β.

1.5 Termination of PI3K signalling.

It is clear from the above, that the synthesis of PIP3 by PI3K is the key step leading to the downstream activation of cell survival and proliferation. Once synthesized, PIP3 is rapidly converted back to PIP2 by the removal of the phosphate group from position 3. This removal is catalysed by the lipid phosphatase and tumour suppressor PTEN (phosphatase and Tensin homolog deleted on chromosome 10)[204] (illustrated in Fig. 1.13). Hence, lost expression of PIP3 at the membrane will prevent the membrane translocation and activation of PDK1 and PKB, terminating signalling through the PI3K/PKB pathway. As its name suggests, PTEN was originally identified as a candidate tumour suppressor gene mutatated in brain, breast and prostate cancers mapped to a frequent loss of heterozygosity (LOH) on the 10q23 chromosome[205, 206]. Since then, accumulating evidence has demonstrated that the tumour suppressive capability of PTEN is reliant on its ability to generate PIP2 from PIP3[207, 208].

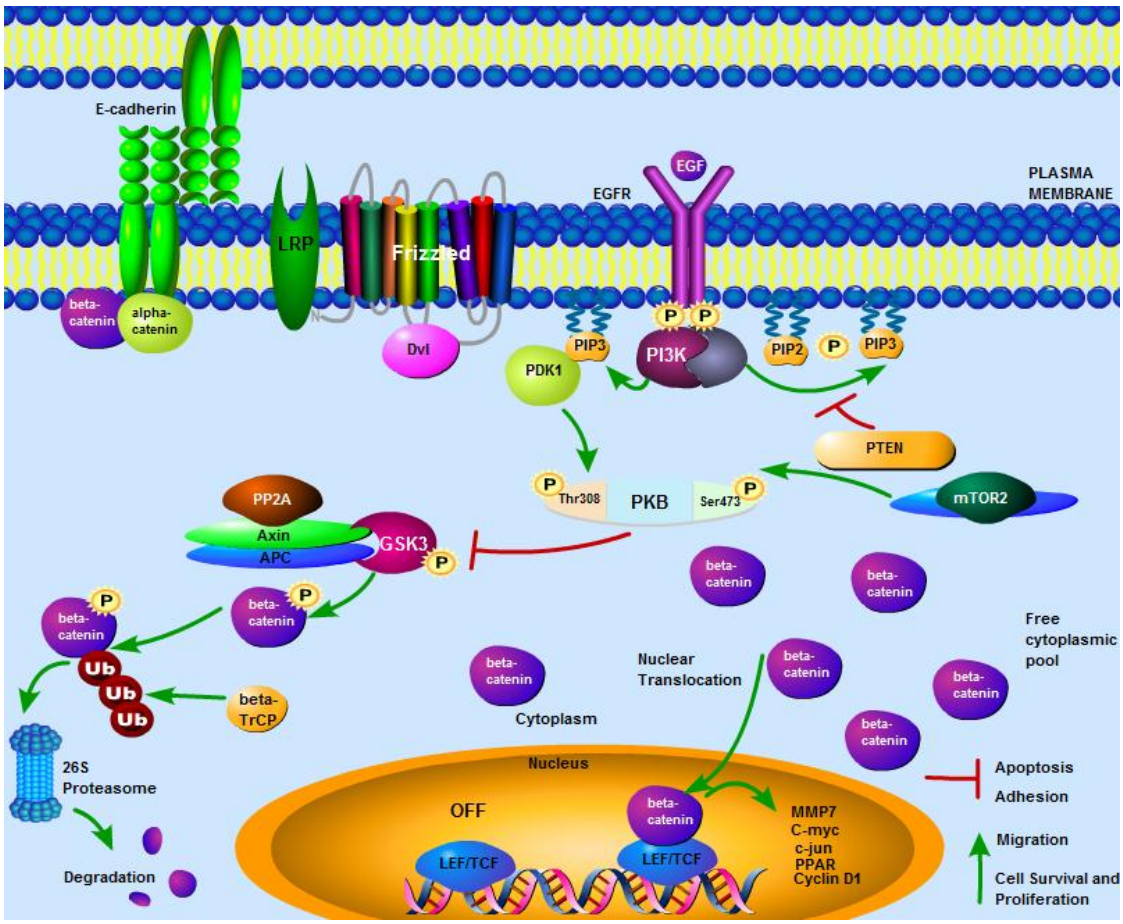


Figure 1.12: PI3K/PKB mediated activation of cell growth and proliferation through GSK3β regulation. As described within the text, although GSK3β plays an active role in the Wnt signalling pathway, PKB inhibits GSK3β by phosphorylating its Ser9 residue. This results in the up-regulation of growth promoting genes (c-myc, c-jun) through the β-catenin/LEF-1/TCF nuclear complex. Figure generated using Pathway Builder Tool.2.0.

PTEN is the major PIP3-dephosphorylating enzyme, and thus inhibitor for the PI3K/PKB pathway[209, 210]. However, under conditions where PTEN is inactive or absent, PIP3 can also be dephosphorylated by the phosphoinositide phosphatase, SHIP2 (SH2-containing inositide 5'-phosphate)[211, 212, 213]. While PTEN targets the 3' phosphatase group of PIP3, SHIP2 primarily targets the 5' position of the inositol ring (shown in Fig. 1.13). Furthermore, it has become known that type I and II inositolpolyphosphate 4-phosphatases (INPP4A and INPP4B) are also able to dephosphorylate PIP3, but specifically at the 4' position of the inositol ring[214, 215] (see Fig. 1.13). Alternatively, PIP3 can contribute to attenuated PI3K activation, by masking its SH2 domain that is essential for binding to the tyrosine phosphorylation residues on the EGFR[216]. Further, binding to the EGFR can be also be abrogated by the PI3K Interacting Protein 1 (PIK3IP1)[217], that mimics the iSH2 domain of p85α and binds to the p110α subunit.

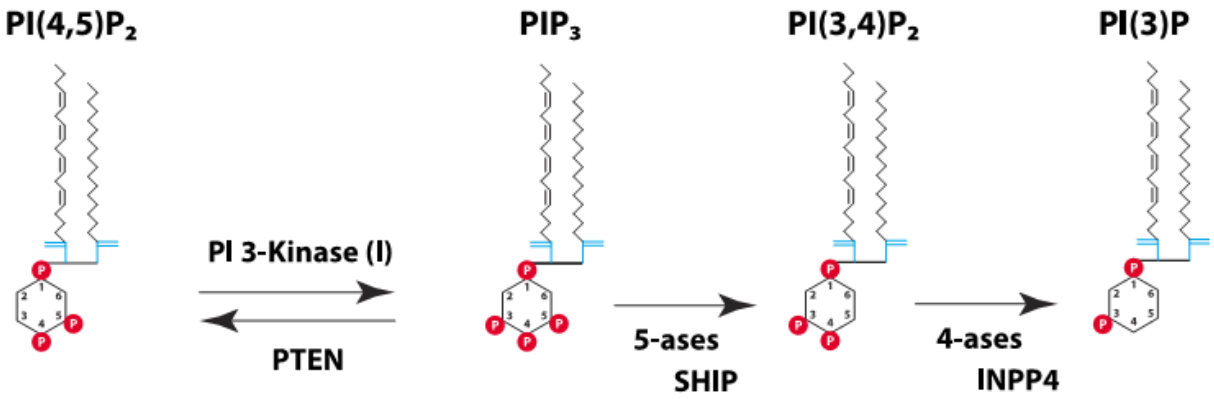


Figure 1.13: Various mechanisms for the dephosphorylation of PIP3. Figure adapted from Leslie, *et al.*[218] See text for details.

Although these phosphatases lead to termination of PI3K signalling, and indirectly PKB activity, this pathway can also be inactivated via mechanisms downstream of PI3K. The Ser473 activation and phosphorylation site of PKB is subject to dephosphorylation, and thus inactivation, by at least four enzymes (see summary in Fig. 1.14). These are; the rictor/mTORC1 complex[219], the protein phosphatase2A (PP2A)[220], the carboxyl-terminal modulator protein (CTMP)[221], and PH domain leucine-rich repeat protein phosphase (PHLPP)[222].

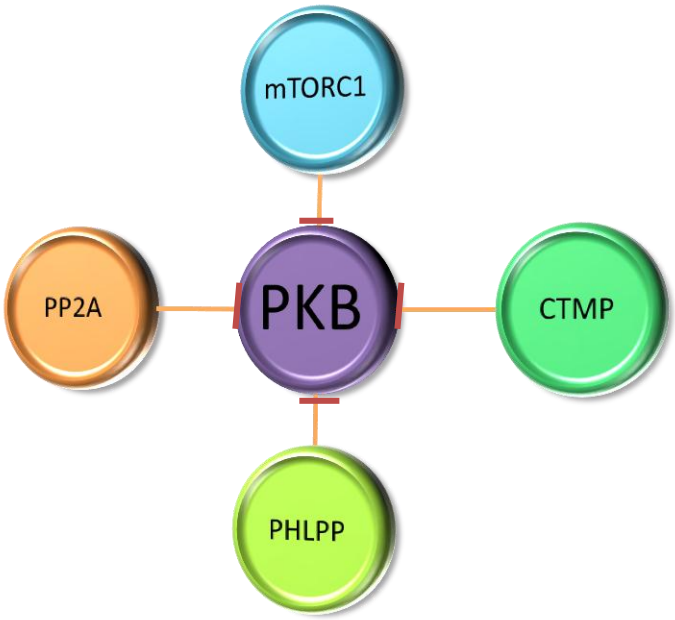


Figure 1.14: Termination of the PI3K/PKB signalling pathway through PKB inactivation. mTORC1, CTMP, PP2A and PHLPP are able to dephosphorylate the Ser473 residue of PKB.

1.6 Deregulation of PI3K pathway in cancer.

To date, the PI3K/PKB pathway is frequently found aberrant in cancer[223, 224]. There are two widely accepted mechanisms that lead to the constitutive activation of this pathway in cancer, i) mutations within EGFR and ii) mutations within the major components of the PI3K/PKB pathway (shown in Fig. 1.15) [225, 226, 227].

1.6.1 The influence of the EGFR

Since it is the membrane localization of PI3K that sets the scene for its activation and PIP3 production[228], the relentless membrane presence of PI3K is commonly allied to EGFR deregulation (see Fig. 1.15). The EGFR can be deregulated by multiple mechanisms that include its overexpression, activating mutations within its kinase and extracellular domains, stimulation of autocrine growth factor loops, augmented receptor dimerization, and accelerated receptor endocytosis and turnover[229, 230, 231]. Of these, EGFR overexpression and amplification are most frequently implicated in the initiation and progression of over 50% of epithelial cancers such as breast[232], colon[233], and cervix[234]. Essentially, and as highlighted in Fig. 1.15, the overexpression and/or mutated status of EGFR in cells will create an environment conducive for constitutive activation of the PI3K/PKB pathway, whereas normal cells still rely on external stimuli for this activation[235, 236].

1.6.2 Genetic variations in the PI3K pathway.

There are a number of genetic perturbations within PI3K, PKB, and PTEN that contribute to the initiation and maintenance of transformation in various tumours (see Table 1.1). Most commonly involved are oncogenic mutants within the gene coding for the p110α catalytic subunit (PIK3CA)[237]. Expression of p110α mutants uncontrollably activate the PI3K/PKB pro-survival pathway, which has been observed in gastric adenocarcinoma[238], breast and ovarian cancer[239, 240], human mammary epithelial cells[241], head and neck squamous cell carcinoma[242], and cervical cancer[243] (see Fig. 1.15 and Table 1.1). Importantly, three "hotspot" mutations exist within the PIK3CA (E542K, E545K and H1047R) in over 80% of these susceptible cancers (Table 1.1). These mutations, in turn, elicit constitutive activation of PI3K by inducing augmented membrane affinity and growth factor-independent activation (see Fig. 1.15). In addition to these mutations, PIK3CA is reportedly amplified in certain cancers (see Table 1.1).

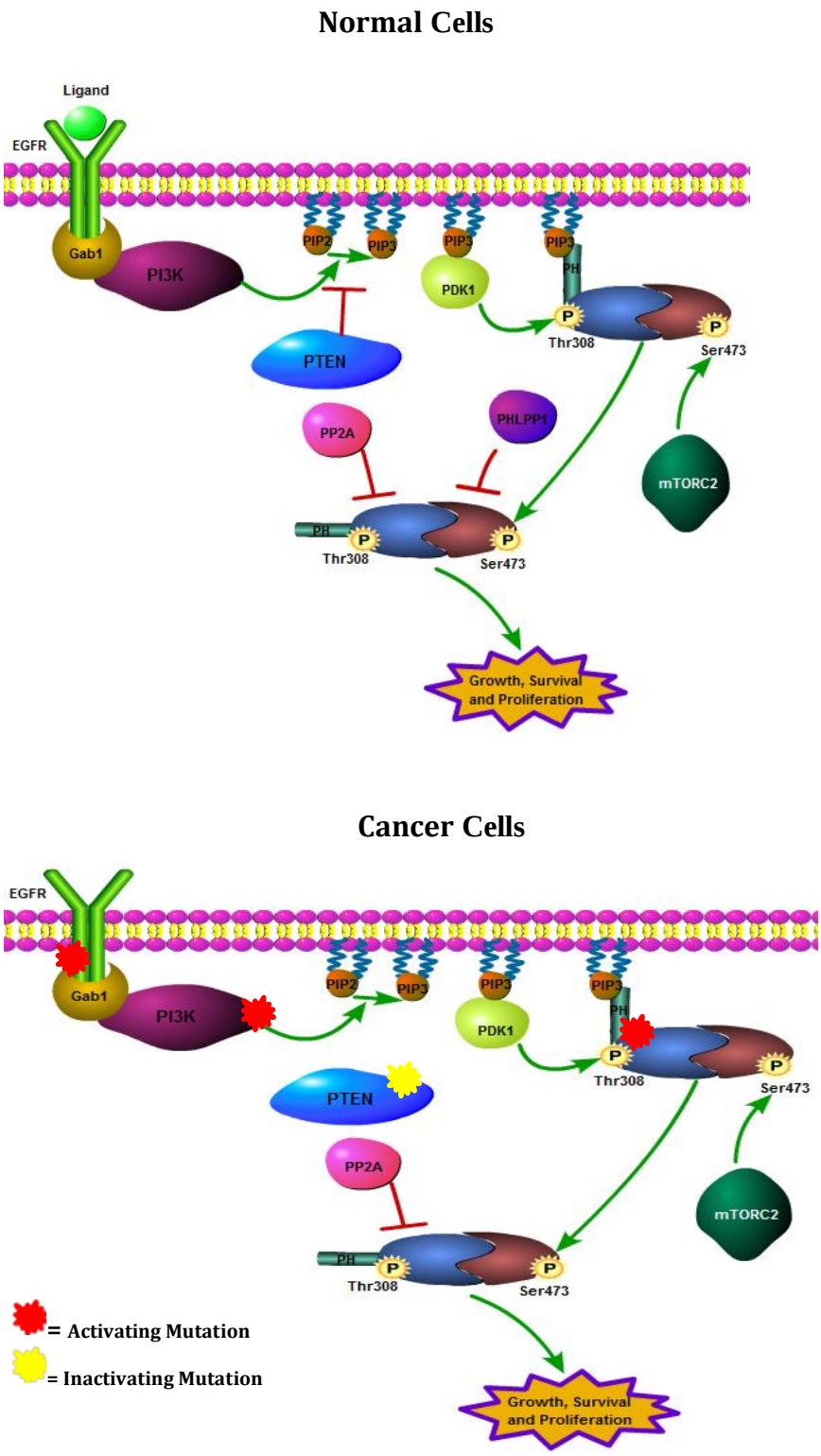


Figure 1.15: Common activation mechanisms for the PI3K/PKB pathway in cancer. Showing the contrast between normal cells and cancer cells with respect to controlled (normal cells) and aberrant (cancer cells) activation of the PI3K/PKB pathway. Figure generated using Pathway Builder Tool. 2.0.

Table 1.1:Recent results demonstrating the frequency of genetic variations within the PI3K/PKB pathway found in different tumour types. Table modified from Markman, *et al*.[244]

Generic Variation	Tumour Type	Frequency (%)
PIK3CA mutations	Breast	21-40
	Colorectal	13-32
	Glioblastoma	5-8
	Endometrial	24-32
	Hepatocellular	6-36
PIK3CA amplification	Cervix	69
	Gastric	36
	Lung (squamous)	60
	Head & Neck (H&N)	37
	Ovary	25
p85α mutation	Colorectal	<5
	Ovary	<5
PKB amplification	H&N	30
	Gastric	20
	Pancreas	20
	Ovary	12
PKB1 mutation	Breast	1.8-8
	Colorectal	6
	Ovary	2
PTEN mutation	Glioblastoma	17-44
	Endometrial	36-50
	Colorectal	7
	Prostate	12
	Breast	0-4
	Melanoma	7
PTEN LOH	Glioblastoma	54-74
	Endometrial	32-83
	Gastric	47
	Prostate	29
	Breast	39
	Melanoma	44-37

Although less common, the p85α regulatory subunit (transcribed by PIK3R1) has likewise been observed as an oncogene in human ovarian and colon cancers[245] (see Table 1.1). This mutation is considered less potent than those in PIK3CA, as they necessarily require EGFR-mediated activation of PI3K[246].

Since its initial detection in gastric carcinoma[247], PKB is recurrently found amplified in a large variety of tumours[248] (see Table 1.1). Recently, a single somatic activating mutation within the PH domain (G49A/E17K) has been identified in a subset of breast[249], lung[250], ovarian and bladder cancers[251]. The characteristic of this Lys17 mutation modifies the electrostatic interactions that PKB has for the plasma membrane by the formation of new hydrogen bonds with membrane phospholipids (see Fig. 1.15)[252, 253]. This results in the membrane recruitment of PKB despite the absence of active PI3K and has been verified through *in vitro* and *in vivo* studies[254, 255].

However, not all perturbations within the PI3K/PKB pathway are attributable to these activating mutations. Inactivation of PTEN is highly associated with the advanced stages of metastasis in cancers either through mutations or epigenetic mechanisms[78]. These inactivating mutations are primarily confined to its phosphatase domain as shown in non-small lung cell cancer[256] and certain colorectal cancers[257], causing diminished antagonistic activity towards the PI3K/PKB pathway (see illustration in Fig. 1.15). Moreover, complete loss of PTEN expression has been found in cancers, especially prevalent in prostate cancer[258]. Of note, mutations within PTEN are not commonly found, but instead the PTEN gene loci in cancer frequently display LOH, that generates a less functional and active PTEN (see Table 1.1)[259, 260, 261]. The attenuated PTEN activity leads to constitutive activation of the PI3K/PKB pathway through up-regulated PIP3 levels (see Fig. 1.15)[262].

1.7 Human Oesophageal Squamous Cell Carcinoma - The model

Human Oesophageal squamous cell carcinoma (HOSCC) is a malignancy of the oesophagus and has been ranked as the ninth most frequent cancer to occur worldwide and fifth common cancer in developing countries[263, 264]. It is one of the most widespread diseases with a variable global distribution; but areas of exceptional incidence and relevance to this study is in South Africa[265, 266]. On both an international and national scale, HOSCC is recognized as a highly aggressive

(metastatic) and drug resistant disease with a five-year survival in patients undergoing chemotherapy[267,268,269, 270, 271]. The fate of patients with this disease is greatly dependent upon coupled environmental and genetic factors over a period of time[272, 273]. According to numerous clinical observations and pathological reports, these include excessive alcohol and tobacco consumption[274, 275, 276], drinking large amounts of hot beverages (tea and coffee)[277], poor oral health and nutrition[278], bile reflux caused by high intake of pickled vegetables or spicy food[279, 280], exposure to N-nitroso compounds (from multiple sources)[281], mycotoxins (fumonisins) and human papillomavirus (HPV)[282]. Recurrent exposure of these factors has adverse effects on the stratified squamous epithelial lining of the oesophagus, predisposing them to cancer of the oesophagus. Hot beverages induce thermal injury to the peripheral oesophageal keratinocytes, bile acids have been shown to disrupt the cell membranes[283], whereas the infectious and more toxic factors cause direct toxic acinar cell necrosis[284]. These toxic effects cause an increase in the rate of cell proliferation in the intermediate layers of the oesophageal epithelium that eventually lead to cellular invasion. Characteristic of HOSCC invasion is the breakdown of the oesophageal wall into adjacent structures, and commonly metastatic to the lymph nodes[285]. As a result, tumours are graded according to their invasive or keratinizing capability. Poorly differentiated tumours are thought to possess distinguishable keratinizing potential, whereas well differentiated tumours display an overwhelming keratinization and have lost all their squamous epithelial phenotype[286]. Certain tumours are hard to categorize as they display keratinizing potential similar to well- and poorly differentiated tumours, and are thus classified as moderately differentiated[287].

Research has likened the initiation and progression of HOSCC to the presence of p53 mutations, EGFR overexpression and/or amplification, Cyclin D1 and COX-2 overexpression, elevated nuclear β-catenin levels, c-myc amplification, and high (metalloproteinase) MMP expression[288, 289, 290, 291, 292, 293, 294]. Irrespective of these molecular signatures for HOSCC, much remains to be determined regarding the specific molecular mechanisms that govern and/or contribute to such transformation. It is pertinent to note that oesophageal cancer does not feature in reports regarding "oncogene addiction". Considering the vast number of aetiological factors, and the highly metastatic and drug resistant nature of this disease[267], it becomes increasingly important to gain a firm understanding of the cellular mechanisms involved in the maintenance of the transformed state of HOSCC. This knowledge will, in turn, bear direct relationship to the discovery and design of better diagnostic and therapeutic tools.

1.8 Gaps in the characterization of HOSCC: a role for PI3K?

As mentioned above, the dominant transforming event in most cancers of epithelial origin, like HOSCC appears to include constitutive activation of PI3K. Hence, the large gaps in our understanding of the molecular mechanisms ascribed to the transformation of HOSCC have sparked an interest in exploring the role of the PI3K/PKB pathway in this disease. Of interest, the PI3K/PKB pathway has been shown to contribute to resistance of chemotherapy observed in a subset of HOSCC patients[295, 296], further substantiating the need to characterize its contribution to HOSCC transformation.

Moreover, certain of the aetiological causes of HOSCC described have been shown to transform cells by specifically targeting the PI3K/PKB pathway through various mechanisms. As an example, the mycotoxin found in maize, FB_1 was found to induce PKB overexpression in hepatocarcinoma cells[297]. Likewise, nitrosamines found in tobacco were shown to transform bronchial[298] and normal and transformed human airway epithelial cells[299] by activating the PI3K/PKB pathway. Importantly, and as highlighted above, EGFR is able to activate an array of downstream signalling pathways, one of which is the PI3K/PKB pathway. On this basis, the specific pathways stimulated by EGFR overexpression in numerous cancers appear to be somewhat cell-type specific and as a result, the molecular tools utilized by EGFR overexpression is rather controversial[300, 301]. Hence, a better understanding of the downstream effects elicited by the EGFR overexpression status is also crucial for better therapeutic targeting of HOSCC. In addition, the factors that regulate the propensity for HOSCC to accumulate nuclear β-catenin levels are cryptic. The above leaves little doubt that in-depth investigation of the specific signalling character of the PI3K/PKB pathway will ultimately benefit therapeutic strategies for HOSCC in particular, and squamous cell carcinoma in general.

1.9Aims

Although the basics of the PI3K/PKB pathway are understood, there are differences across various tissues and tumours. With oesophageal carcinoma representing a disease of both local and international importance, its status in respect of this pathway would undoubtedly augment the understanding of cellular signalling in general and PI3K/PKB in particular. Of critical value to this vision is the lineage of moderately differentiated WHCO and SNO HOSCC series of cell lines and thus the focus became to:

I. Explore the functional status of the PI3K pathway in HOSCC by assessing its cellular distribution and activation in order to establish the foreground for further analysis.
II. Determine the growth factor based activation of PI3K.
III. Establish which signalling intermediates have an impact on the PI3K/PKB pathway in HOSCC.
IV. Compare the intermediates arising out of the analyses in III with their role in the PI3K/PKB pathway in known tumour cell lineages.
V. Examine the relationship of the PI3K/PKB pathway may have with related cellular signalling pathways of significance.

Chapter 2
The PI3K pathway is active in HOSCC cells

2.1 Introduction

Mammalian Class 1_A PI3K are ubiquitous lipid and tyrosine kinases that comprise of a p85α regulatory subunit and a p110α catalytic subunit[57]. Prototypical p85α protein contains a single SH3 domain, two (N-and C-terminal) Src homology 2 (SH2) domains separated by an inter-SH2 (iSH2) domain, and a Breakpoint Cluster Region (BCR) homology domain flanked by two proline-rich domains (see demonstration in Fig. 2.1)[58]. The iSH2 domain aided by the N-terminal SH2 domain, sufficiently binds to the adaptor-binding domain (ABD) or p85α-binding domain of the p110α subunit, forming an irreversible linkage between the p85α and p110α subunits as illustrated in Fig. 2.1[60, 61].

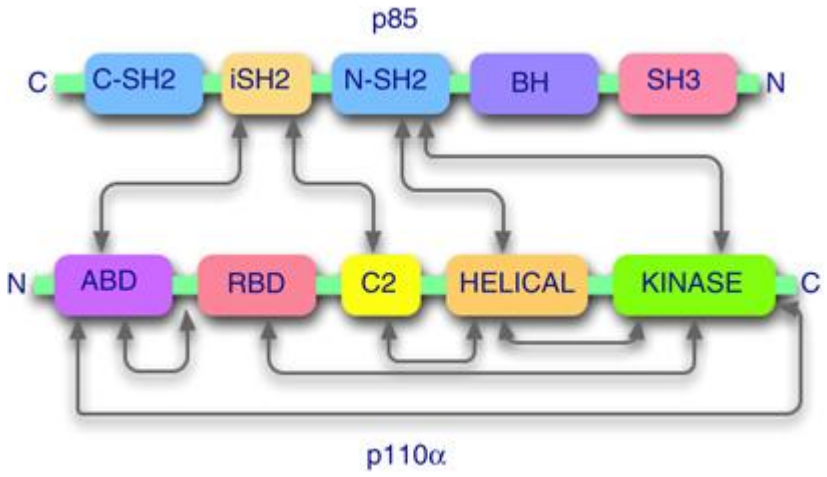


Figure 2. 1: Domain structure of the p85α regulatory and p110α catalytic subunit of class 1A PI3K, demonstrating the essential associations between the two subunits[302].

In quiescent or unstimulated epithelial cells, PI3K is primarily localized within the cytoplasm[303, 304]. However, upon receptor tyrosine (RTK) activation, PI3K translocates to the membrane to be in proximity of its substrate, phosphatidylinositol 4,5-bisphosphate (PIP2) where it catalyzes the

phosphorylation of its position 3' phosphoinositide ring, generating the secondary messenger, phosphatidylinositol 3,4,5-triphosphate (PIP3)[72, 73, 305] (see demonstration in Fig. 2.2). PIP3 concomitantly results in the membrane recruitment and activation of various PH domain-harbouring proteins, such as phosphoinositide-dependent kinase-1 (PDK1) and protein kinase B (PKB), that are central for the mediation of PI3K signal propagation [74, 165, 306] (see Fig. 2.2). PKB is a major effector of PI3K signalling[307], that is activated at the membrane by phosphorylation of two key residues, Thr308 mediated by PDK1[308], and Ser473 through the mTORC2 complex (mTORC2) (see Fig. 2.2 for an illustration)[189]. One of the mechanisms used to impact cell survival and proliferation is created through the phosphorylation of several PKB downstream kinases, for example GSK3β, MDM2 and various others, which result in their inhibition, enabling the effective transmission of PI3K signalling[309]. The activity of PI3K and its downstream effectors are terminated by dephosphosphorylation of PIP3 mediated by PTEN (phosphatase and tensin homolog deleted on chromosome 10)[204], summary shown in Fig. 2.2.

Since it is the membrane localization of PI3K that is imperative for its activation[228], it is not surprising that transformed epithelial cells are inclined to develop a membrane-bound PI3K that results in its constitutive activation[310, 311, 312]. In resting conditions, the cytoplasmic localization of inactive PI3K, is for the most part, maintained by the mutual inhibitory and obligate association that exists between the p85α regulatory and the p110α catalytic subunits that are only alleviated upon it's binding to activated membrane RTKs as depicted in Fig. 2.2 [313, 314]. Once associated with the RTKs, the lipid kinase activity of p110α is activated and p85α-mediated inhibition is prevented[315]. Monomeric p110α is unstable[71, 316], and thus it is the balance between the p85α-mediated inhibition and stabilization that determines the overall activation status of PI3K in cells.

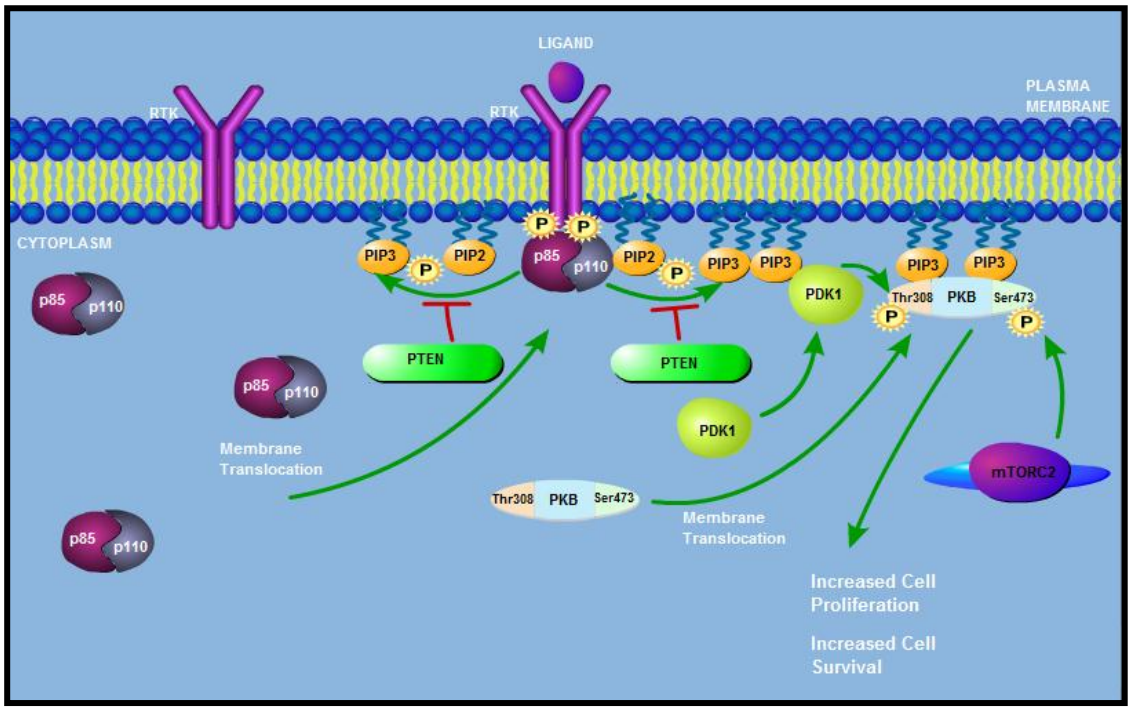


Figure 2. 2: PI3K signalling. PI3K is a central regulator of cellular survival and proliferation upon RTK activation that is essential for PIP3 production and the consequent membrane recruitment and activation of numerous PH domain-containing kinases, such as PDK1 and PKB illustrated. See text for a detailed description. Figure generated using Pathway Builder Tool. 2.0.

The p85α protein is encoded by the PIK3R1 gene[317] that frequently gains oncogenic potential in ovarian and colon cancers specifically[245, 318]. This is linked to a truncation within its nSH2 domain. A similar truncated version of p85 (amino acids 572-724 deletion coding for the C-terminal SH2 and iSH2 domain), referred to as p65, has been reported in murine transformed cells and in a Hodgkin's lymphoma-derived cell line (CO)[319]. As indicated in Fig. 2.1, the nSH2 domain acts as a tethering site for p110α activation, and therefore, absence of this domain gives rise to uninhibited PI3K[320].

The contribution made by PI3K to the cellular differentiation state is regulated through p85α[321]. The extent to which this occurs is attributed to the significantly increased cellular migration and poor differentiation in cells with elevated p85α protein levels[322, 323, 324, 325]. Based on the fact that others have shown a negative contribution made by p85α in the migration and differentiation state of cancer cells, causing these cells to adopt lower p85α protein levels to counteract such adverse effects[326, 327, 328], makes the role played by p85α in assisting the metastatic potential of cells rather controversial.

Here we explore the involvement of the PI3K pro-survival signalling pathway in five HOSCC cell lines derived from moderately differentiated tumours[329]. To achieve this, it was first necessary to determine the expression, cellular localization and activational state of p85α. Pertinent to this investigation was the known PI3K (p110α/PIK3CA) mutational state in the breast MCF7 and colon HT29 control cell lines[330], that were used as a measure of comparison for the unknown p85α status in HOSCC. In addition to the PI3K mutational state in the HT29 cell line, elevated levels of p85α protein were also reported[331], and thus used as an additional control to which p85α expression levels in HOSCC cells can be compared. The 5 HOSCC cells were previously demonstrated to possess up-regulate levels of the RTK, EGFR[332]. Therefore, it was hypothesized that a correspondingly high level of PI3K (p85α) expression and activation may have an influence on the maintenance of the transformed state of this disease.

2.1 Materials and Methods

2.2.1 Cell lines and their Culture

Five South African oesophageal squamous cell lines derived from moderately differentiated and metastatic tumours were obtained from the Cell Biology Laboratory, School of Molecular and Cell Biology, University of the Witwatersrand. The cell lines are designated as the WHCO (Wits Human Carcinoma of the Oesophagus) series consisting of WHCO1, WHCO3, WHCO5 and WHCO6, and the SNO cell line[333]. The human breast cell line, MCF7 and the HT29 colon control cancer cell lines were used (European Collection of Cell Cultures/ECACC). The cells were cultured in a monolayer and maintained in a humidified incubator at 37 °C in an established 5% CO_2 atmosphere and supplemented with Dulbecco's Modified Eagles Medium (DMEM)/Hams F12 (3:1) complemented with 10% Foetal Calf Serum/FCS (Highveld Biologicals) at a pH of 7.2-7.5 (see Appendix A 1.1).

Cells were harvested once reaching a confluence of 80%. This was done by an initial wash with phosphate buffered saline (PBS) (Appendix A 1.1.3) after the medium was appropriately dispensed. Cells were routinely detached by a 5 minute (min) incubation at 37 °C in 2 ml of trypsin (GibcoBRL) and ethylenediaminetetra-acetic acid (EDTA) (see Appendix A 1.1.4). Thereafter, medium with 10% FCS was added to the trypsinized cells and grown as above. Studies were standardly performed on cultures approaching 80% confluency (5 x 10^6 cells), as this is their exponential growth phase, and at this cell density no contact inhibition of growth is detected.

2.2.2 Total RNA Extraction

Total RNA was extracted from cells grown as described in 2.2.1, by adding 1 ml of the TRIzol® (GibcoBRL) reagent, which maintains RNA integrity while simultaneously disrupting cellular components. Cells were washed three times in PBS pH 7.6 (Appendix A 1.1.3), transferred into a sterile 1.5 ml Eppendorf tube and centrifuged at 1145 X g in a HF-120 TOMY for 3 mins to remove the excess PBS. The resultant supernatant was vortexed briefly after the 1 ml of the TRIzol® reagent was added. The homogenized samples were allowed to stand for 5 mins at room temperature (RT). 200 µl of Chloroform was added into the tubes, and vigorously hand-shaken for 15 seconds (secs). The samples were then left at

RT for an additional 3 mins to allow phase separation and centrifuged in the Sorvall® MC 12 V at 12 000 X *g* for 15 mins at -4 ºC. The aqueous phase (containing RNA) was removed, and 500 µl of isopropyl alcohol was added to the aqueous phase and allowed to precipitate for 10 min at RT. The resultant precipitate was centrifuged in the Sorvall® MC 12 V at 12 000 X *g* for 10 mins at -4 ºC, giving rise to an RNA concentrated pellet. The RNA was purified in 1 ml of 75% ethanol and centrifuged at 7500 X *g* in the SORVAL®MC (12V) for 5 mins at RT. The supernatant was decanted and after air-drying, the RNA pellet was resuspended in 50 µl of sterile nuclease free dH_2O by incubation at 60 ºC for 10 mins. Due to RNA instability, the samples were immediately stored at -70 ºC.

2.2.3 Amplification of p85α by Reverse Transcription Polymerase Chain Reaction (RT-PCR)

2.2.3.1 Reverse Transcription

It should be noted that RT-PCR is carried out in two steps, reverse transcription and polymerase chain reaction (PCR). This protocol was demonstrated to be the most efficient and sensitive in total RNA (RNA) fragment amplification[334]. 2 µl of RNA extracted from each cell line as described above, accompanied with 2 µl of random primers (oligoT/random hexamers) were incubated in an Eppendorf tube for 5 mins at 70 ºC to ensure that the random primers and the RNA remain unbound. Thereafter, 5 µl of the Moloney Murine Leukemia Virus Reverse Transcriptase (MMLV-RT) buffer (Appendix A 1.2.1), 0.6 µl RNasin® Ribonuclease inhibitor, 2 µl dNTPs (Appendix A 1.2.2), 1 µl MMLV-RT (Appendix A 1.2.3) and 12.4 µl sdH_2O was added to the mixture and incubated for 1.5 hrs at 37 ºC. The reaction was stopped by incubating the samples for 5 mins at 90 ºC. The DNA was purified by vortexing for 10 secs in 50 µl of phenol: chloroform (25:24), 25 µl of dH_2O, and centrifuged for 5 mins at RT in the SORVAL®MC (12V). The aqueous phase (50 µl) was removed and transferred into a new sterile tube containing three times the measured aqueous phase volume of 100% ethanol (150 µl), and 10% of the total volume (20 µl) was filled with 3 M sodium acetate at pH 5.2 (Appendix A 1.2.4). The cDNA was allowed to precipitate overnight at -20 ºC, and centrifuged the following day in a Sorvall® MC 12 V at 12 000 X *g* for 20 mins at 4 ºC. The supernatant was eliminated and the pellet (DNA) was left to air-dry before its resuspension overnight in 10 µl of dH_2O. The cDNA products were stored at -20 ºC.

2.2.3.2 PCR

RT-PCR can be a one-step procedure; here it has been carried out separately. The cDNA propagated from the reverse transcription reaction was utilized to amplify a region on the p85α regulatory subunit gene (PIK3R1, Accession number: NM_181523) transcribing a region of the nSH2 domain, which is partly responsible for its binding to the EGFR and to the p110α catalytic subunit (see Fig. A1, Appendix A 1.3.1). Published primers[305] were used to identify whether a truncation is present within the nSH2 domain of p85α in all the cell lines (HOSCC, MCF7 and HT29) (see Appendix A 1.3.1 for amplified sequence information and primer parameters):

Forward Primer: 5'-GCTCTCTCAAACCTCCAGCAAAA-3' (p85α-F)
Reverse Primer: 5'-GAAGCCATATTTCCCATCTCGATG-3' (p85α-R)

In a 50 µl PCR tube, 1 µl of template (cDNA) from each cell line was added to 39 µl of the PCR master mix, made-up of 5 µl 10X PCR buffer (Appendix A 1.3.2), 1 µl dNTP (Appendix A 1.2.2), and 33 µl of dH_2O. Thereafter, 1 µl of each primer (p85α-F and p85α-R, Inqaba Biotechnical Industries (Pty) Ltd.) at a concentration of 33.3 pmoles/µl was added and spun briefly in HF-120 TOMY for 5 secs before adding 5 µl of the Taq polymerase.

The cDNA was amplified using the PCRSprint Thermal Cycler (Hybaid) for 30 cycles: initial heating at 94 °C for 45 secs, denaturing at 94 °C for 1 min, annealing at 56 °C for 1 min, extension at 72 °C for 1 min, and a final extension at 72 °C for 10 mins with a holding temperature of 20 °C. A PCR tube containing primers, Taq polymerase and PCR buffer, but no template cDNA served as the negative control. The resultant PCR fragments were subject to sequencing at Inqaba Biotechnical Industries (Pty) Ltd. by the bi-directional dye-terminator method under the same conditions used during the PCR amplification (see Appendix A 1.12 for representative sequence trace). Standard procedures were performed in a laminar flow cabinet.

2.2.3.3 Analysis of RNA, cDNA and PCR fragments by agarose gel electrophoresis

A 1% agarose gel was prepared for the validation of the RNA extracts, cDNA production and PCR fragments (see Appendix A 1.4.1). Once the gel had set, the comb was removed and the gel was fully submerged in the Sigma-Aldrich Electrophoresis Unit containing 1X TAE (Tris acetic acid EDTA) buffer (Appendix A 1.4.2) and the comb gently removed. Thereafter, all samples were loaded into the wells accompanied by loading buffer (Appendix A 1.4.3) in a 2:1 ratio. A 1 Kb DNA ladder was also loaded in a 1:1 ratio with loading buffer. The gel was electrophoresed at 72 V and 400 milliamperes (mA) until the samples migrated half way across the gel (1 hr), and viewed on an UV transilluminator.

2.2.4 Antibodies

Rabbit polyclonal antibodies were used for the specific detection of PI3K (p85α) (Upstate Biotechnology), c-Jun (Santa Cruz Biotechnology), and β-actin (Sigma). Rabbit monoclonal antibodies directed against anti-Phospho-Akt (Ser473), and anti-Phospho-GSK-3β (Ser9), were used to specifically detect PKB and GSK3β when phosphorylated at Ser473 and Ser9 residues respectively (Cell Signalling Technology). PTEN were detected using the rabbit polyclonal anti-PTEN antibody (Cell Signalling Technology). Specific immunodection of immunoblot and immunoflourescent primary antibodies was done using the goat anti-rabbit IgG hydrogen peroxide (HRP) conjugate (Sigma), and the fluoroscine isothiocyanate (FITC)-conjugated-goat-anti-rabbit (Chappel, USA) respectively. **Note:** All antibodies were diluted in PBS, unless otherwise stipulated.

2.2.5 Whole Cell Protein Extraction

Cells were washed 3 times with 1 ml of PBS (4 °C), scraped off the dish into an Eppendorf tube and pelleted for 5 mins in the HF-120 TOMY (1200 X *g*). The resultant pellet was resuspended in 80 µl single Laemmli Lysis buffer[335] (Appendix A 1.5.1) by brief vortexing. Thereafter, each sample was boiled for 5 mins, and centrifuged for 20 mins at -4 °C at 12500 X *g* in an Eppendorf Centrifuge 5413; the subsequent extracts were stored at -20 °C.

2.2.6 Nuclear Extraction

Nuclear extracts were prepared as previously described by Chartier, *et al.*[336], but modified according to a reputable nuclear extraction protocol by Dignam, *et al.*[337] Briefly, cells were washed 3 times at 4 °C in PBS (excluding Ca^{2+} and Mg^{2+}), collected and centrifuged for 3 mins at 1200 X *g* using the TOMY Capsule HF-120. The cells were resuspended in 400 µl

nuclear extraction buffer (Appendix A 1.5.2) and left to swell on ice for 5 mins. Swollen cells were sheared by six passages through a 22 gauge needle fitted to a 30 ml plastic syringe. The Mg^{2+} levels were brought to an overall concentration of 5 mM, and the nuclei sedimented for 6 mins at 400 X *g* at 4 °C in the Eppendorf Centrifuge 5413. The supernatant (comprising the cytosol and plasma membrane fraction) was decanted, and the nuclear pellet was washed in nuclear wash buffer (Appendix A 1.5.2.1). To remove cytoplasmic contamination, the nuclear pellet was brought to a final concentration of 2 mg DNA/ml in 500 µl sucrose solution (Appendix A 1.5.2.2) by centrifugation at 200 X *g* at 4 °C in the Eppendorf Centrifuge 5413 for 6 mins. The resultant cytoplasmic-free nuclei pellet was resuspended in nuclear lysis buffer (Appendix A 1.5.2.3). To reduce the sample viscosity and to shear the DNA, nuclear lysates were briefly sonicated using the Misonix, Ultrasonic Liquid processor, XL2000 series, boiled for 5 mins to solubilize the protein and stored at -70 °C.

2.2.7 Plasma Membrane Extraction

Membrane extracts (comprising both integral and peripheral membrane proteins) from cells were obtained using a formerly described protocol by Chen, *et al.*[338] In brief, cells were washed twice with PBS and centrifuged in 1 ml PBS/Trazylol/PMSF (Phenylmethanesulphonylflouride, see Appendix A 1.5.3.1) at 1200 X *g* in the TOMY Capsule HF-120 for 3 mins. The pellet was resuspended in 500 µl membrane hyptonic buffer (Appendix A 1.5.3.2), and allowed to precipitate overnight at -20 °C. Samples were then thawed on ice, followed by 30 passages in a Dounce homogenizer. The homogenates were membrane pelleted by centrifugation at 100, 000 X *g* (39 000 RPM Beckman L7-65 Ultracentrifuge) for 30 mins at 4 °C, and resuspended overnight at 4 °C in 0.1% SDS.20 mM Tris-HCL (pH 7.4). The cytoplasmic fraction was decanted and membrane extracts resuspended in Laemmli lysis buffer and stored at -70 °C.

2.2.8 Protein Estimation

The approximate protein concentration within each of the whole cell, nuclear and plasma membrane proteins extracts was conducted using the Bradford assay[339], according to the method described by Bramhall, *et al.*[340] A disc of Whatmann filter paper was rinsed in dH_2O for 20 mins, and dehydrated for 5 mins each in 95% ethanol, 99.9% ethanol and 100% acetone respectively. Six bovine serum albumin (BSA) samples of known concentrations (1 µg/µl) corresponding to 1 µg; 3 µg; 6 µg; 12 µg 16 µg, and 20 µg, each of which were solubilized in the relevant buffers matching the extracted samples, were spotted onto the air-

dried filter paper (see Appendix A 1.6.1). These were left under the fume hood until completely dry. Once dried the protein samples were fixed onto the filter paper by incubation in 7.5% trichloracetic acid (TCA) (see Appendix A 1.6.2) for 40 mins accompanied by gentle agitation. The filter paper was stained with Coomassie Brilliant Blue Stain (Appendix A 1.6.3) for an initial 5 mins to remove residual TCA, followed by additional 60 min in the dark to prevent photooxidation of the Coomassie solution. Thereafter, the developed protein-dye spots (circles) were destained for 60 mins in destain (Appendix A 1.6.4) and left to air-dry. The dried stained circles were excised, and the protein was drawn from the filter paper by overnight incubation in the dark in a 5 ml elution solution (Appendix A 1.6.5). The following day the absorbance of each sample was determined using a ΛBBOTΛ SV-1100 spectrophotometer at a wavelength of 595 nm. A standard curve was formulated using the BSA readings, from which the concentration of protein present in each cell line was elucidated. This procedure was repeated three times for each extraction and graphs were plotted using Microsoft® Excel; see Appendix A 1.6.6 (Fig. A2) for representative standard curve.

2.2.9 Polypeptide Resolution and Western Immunolotting

Equal amounts of the various proteins extracted were resolved on a 10% sodium dodecyl sulphate polyacrylamide gel electrophoresis (SDS-PAGE), prepared according to Laemmli (1970)[335] (Appendix A 1.7.1 and 1.7.2). Endogenous levels of protein concentrations may vary, and therefore all lysates were followed up with β-actin (loading control) analysis. The respective samples were resolved on the polyacrylamide gels using the Mighty Small™ Electrophoresis Unit filled with electrophoresis running buffer pH 8.3 (Appendix A 1.7.3) at constant current of 20 mA and visualised with Coomassie Blue (Appendix 1.6.3). Stained gels were destained (Appendix A 1.7.4) and scanned (see Appendix A 1.7.5, Fig. A3). Unstained gels were transferred onto a Nitrobind nitrocellulose transfer membrane (MSI, USA), in a BioRad Trans-Blot™ Cell at 400 mA for 2.5 hrs in Western Blot Transfer Buffer (4 °C) (Appendix A 1.8.1), and immunoblotted as follows:

2.2.9.1 PI3K (p85α), c-Jun, β-actin

Subsequent to the above, the nitrocellulose membranes were rinsed 3 times in PBS and stored overnight at 4 °C. The following day, the membrane was blocked in casein-based blocking buffer (BLOTTO) (Appendix A 1.8.2) for 30 mins (p85α), and 1hr (c-Jun and β-actin), to prevent non-specific binding of the antibody. Six quick washes in PBS were achieved to remove the BLOTTO from the membrane, and thereafter incubated with the

appropriate antibody for 1 hr (c-Jun), and 2 hrs for PI3K (p85α) and β-actin. Rabbit polyclonal anti-p85α primary anti-body (1:6000) was used to detect PI3K (p85α), rabbit polyclonal anti-c-Jun (1:700) for c-Jun detection, and rabbit polyclonal anti- β-actin (1:1000). Following incubation with the corresponding primary antibodies, the membrane was washed 6 times at 5 min intervals with PBS, and incubated in the dark for 1 hr in a suitable secondary antibody. Immunodetection of PI3K (p85α), c-Jun and β-actin was done using the HRP-conjugated monoclonal goat-anti-rabbit anti-body, at 1:20 000 (p85α), 1:7500 (c-Jun) and 1:10 000 (β-actin) dilutions respectively. For a second time, membranes were washed 6 times with PBS at 5 min intervals. Band visualization was made possible by exposing the membrane in the dark for 5 mins in luminol:peroxide (1:1) obtained from the Supersignal® West Pico Chemiluminescent Kit (Pierce, USA). The membrane was drained from excess developing solution (West Pico) and exposed for an initial 10 mins and then overnight to Hyperfilm^{TM} MP Autoradiography film (Amersham). The film was developed in developer (Appendix A 1.8.3) for 5 mins, rinsed in H_2O and fixed for 5 mins in fixer (Appendix A 1.8.4).

2.2.9.2 pPKB (Ser473), anti-pGSK3β (Ser9) and PTEN

After the transfer was complete, the respective membranes were rinsed in 1X Tris Buffered Saline (TBS) (see Appendix A 1.8.5) and non-specific binding was prevented by incubation for 1 hr in blocking buffer (Appendix 1.8.6). After 1 hr, membranes were rinsed twice in TBS containing 0,1% Tween-20 (TBS/T), and incubated overnight at 4 °C with gentle agitation in their respective antibodies. All antibodies were diluted in primary antibody dilution buffer (see Appendix A 1.8.7) at a concentration of 1:1000. The following day, blots were washed 3 times at 5 min intervals in TBS/T, to remove residual antibody. Membranes were incubated in the dark for 1 hr in goat-anti-rabbit antibody (1:1000) diluted in 2.5% BLOTTO in TBS/T. Once again, membranes were washed 3 times with TBS/T at 5 min intervals, and band visualization was made possible as detailed above (2.2.9.1). (**Note:** Unless otherwise stipulated, all antibody incubations were done at RT and with gentle agitation)

2.2.10 Indirect Immunoflourescence Microscopy

All immunological reactions (immunoflourescent images) produced during this experiment are not the atypical staining in the strict histological sense, but is colloquially referred to here as “staining”. Cells were grown to a confluence of 50% as described above, washed 3 times in

PBS (4 °C), and fixed for 30 mins in 4% paraformaldehyde (see Appendix A 1.9.1). After 6 washes in PBS they were permeabilized in 0,25% Triton-X-100 (see Appendix A 1.9.2) for 10 mins, and washed for an additional 5 times with PBS. The cells were briefly air-dried to ensure optimum adhesion of the DAKO® pen, which was used to create an appropriate number of fluid barriers or "wells", and thereafter rehydrated in PBS for 30 mins. Each "well" was incubated for 1 hr in the primary rabbit polyclonal anti-PI 3-kinase p85α (Santa Cruz Biotechnology) (1:50), or overnight at 4℃ in the polyclonal anti-pPKB (Ser473) (1:100) diluted in TBS/T, while each reaction contained their respective negative control "well" that only contained PBS (p85α) or TBS (pPKB) respectively. Unbound primary was washed off every 1 min in PBS (p85α) or TBS (pPKB) for 5 mins. Next, the cells were incubated in the dark in monoclonal FITC-conjugated-goat-anti-rabbit (1:100) diluted in PBS (p85α) or TBS (pPKB) for 1 hr. Staining controls were done simultaneously, these exposed only to the secondary antibody incubation. Cells were subsequently washed in PBS or TBS as described, and mounted in 10 µl anti-fade medium/elvanol (see Appendix A 1.9.3). The cells were sealed with glass coverslips, and viewed immediately under a Zeiss LSM-410 confocal microscope at an eyepiece of 40X magnification (excitation wavelength of 488 nm, emission 525). All immunoflourescent reactions were done in triplicate, and negative controls were performed for each cell line. Where necessary, immunofluorescent microscopy images were sharpened using Adobe Photoshop to enhance their clarity. (**Note:** Cells were kept in a moist environment during primary and secondary antibody incubations, and unless otherwise stipulated, all antibody incubations were done at RT).

2.2.11 Inhibition of PI3K through LY294002 (LY29) Exposure

Different concentrations of the reversible PI3K inhibitor, LY294002 (IC_{50}=1.4µM) have been used within the literature, and for unique periods of time[341, 342, 343]. Therefore, for the purpose of this experiment a concentration of 20 µM of LY294002 exposed for 1 hr was found optimal (see Appendix A 1.11 for optimization).

Cells were cultured as previously described, until a confluence of 60% was reached, after which, each cell line was incubated for 1 hr with 20 µM of LY294002 diluted in Dimethyl Sulfoxide (DMSO) under serum conditions, while the control or untreated cells were exposed to DMSO only. Whole cell protein extractions were performed on all the treated and untreated cell lines as outlined above (2.2.5). **Note:** The experiment was repeated three times.

2.2.12 Densitometry

Optical density values of the bands representing concentration levels of PI3K (p85α), pPKB, pGSK3β and PTEN detected through western blot analysis were obtained using Labworks TM Image Acquisition and Analysis software (Labworks version 4.5). This program is ideal for such quantification as it is able to diminish the adverse effects created by high background and non-specific smears around the bands of interest. **Note:** the densitometric analysis results are an average of 3 separate repeated experiments and represented as a percentage of the maximum concentration.

2.2.13 Image Capturing

All western blot and SDS-PAGE images were captured using a Hewlard Packard Scanjet 4400c series scanner at 300dpi, contrast and brightness of all images were standardised using CorelDRAW version 12®.

2.2.14 Statistical Analysis

Statistical analysis results are inclusive of at least three independent experiments (mean ± S.D), and was performed using Student's *t* test and One Way Repeated Measures Analysis of Variance (Holm-Sidak method). Inverse correlations between pPKB and PTEN expression levels were calculated using Pearson's correlation coefficient represented as r. All calculations of statistical computations were carried out using the SigmaPlot Release 11.0® statistical software. P-values are provided in the respective appendices, and values of $P > 0.05$ were considered insignificant. **Note:** Based on the fact that statistical analysis requires a minimum of three independent experiments, an example of the three blots for the figures in this chapter was chosen (i.e. nothing is gained by showing all three).

2.3 Results

2.3.1 p85α is unaltered in HOSCC cells.

Transcriptional analysis of the p85α gene transcript (PIK3R1) was achieved through RT-PCR. The presence of a small (28S) and larger (18S) ribosomal RNA subunits indicated by the bands at 650 bp and 1500 bp through agarose electrophoresis, confirmed the integrity of the RNA extracts (shown in Fig. 2.3A). The intact RNA was successfully reverse transcribed into cDNA, evidenced by smears that are representative of different sized cDNA transcripts[344] (see Fig. 2.3B). The presence of a 430 bp PCR fragment confirmed that HOSCC cells, along with the MCF7 and HT29 control cell lines, positively express the full transcript encoding the nSH2 domain of p85α (presented in Fig. 2.4). The specificity of the primers were confirmed by the absence of the target fragment in lane 8 that contained no template. Sequence analysis of the PCR fragments confirmed that the 430 bp bands detected are indeed the nSH2 domain of p85α and that no alterations were evident (see Appendix A 1.12, Fig. A5 for sequence trace).

2.3.2 HOSCC cells express high levels of PI3K (p85α).

A single band at 85 kDa in all cell lines under investigation confirmed the presence of PI3K (p85α) (see Fig. 2.5A). The densitometric analysis of the concentration of p85α affirmed that its levels vary considerably across the WHCO and SNO HOSCC series, with respect to the high p85α protein levels in the HT29 cell line[331] (see Fig. 2.5B). The WHCO6 (55%) and SNO (82%) cell lines exhibited the highest PI3K (p85α) expression, and the WHCO1 (23%), WHCO3 (24%) and WHCO5 (22%) HOSCC cell lines, the lowest (Fig. 2.5B). The relatively low PI3K (p85α) protein levels observed in the mtPIK3CA HT29 and MCF7 controls[330] suggests that its protein expression is not a result of its mutated PIK3CA sequence.

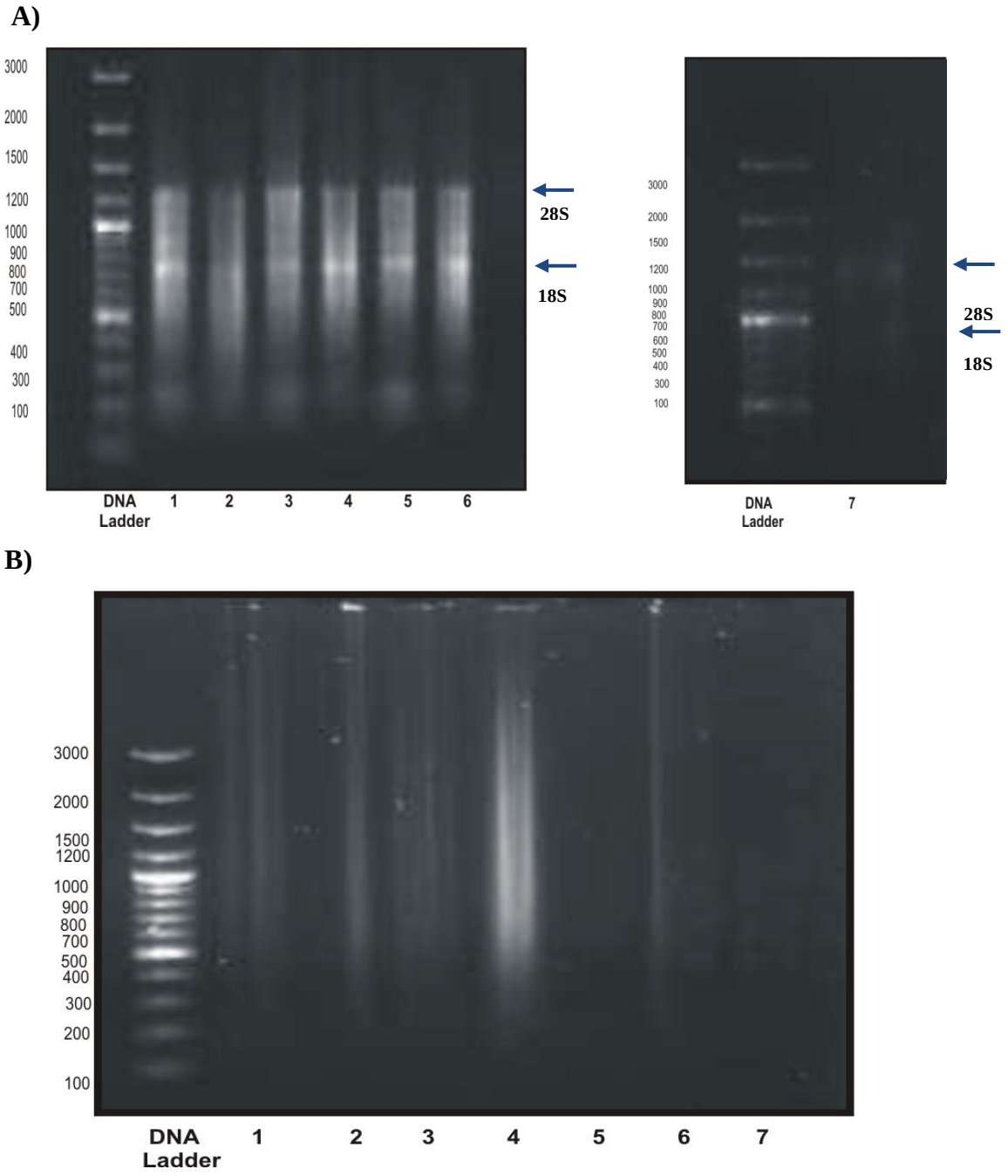


Figure 2.3: RNA extracts and cDNA transcripts from the 5 HOSCC, HT29 and MCF7 cell lines. A) Total RNA was extracted from HOSCC, MCF7 and HT29 cell lines, and thereafter electrophoresed on a 1% agarose gel. The two bands (indicated by blue arrows) represent the big 28S (1500 bp) and small 18S (650 bp) ribosomal subunits, indicative of a successful RNA extraction[345]. **B)** mRNA was effectively reverse transcribed into complimentary DNA/cDNA shown in the form of smears when resolved on a 1% agarose gel, exhibitive of variable transcript lengths. Lane's 1-WHCO1, 2-WHCO3, 3-WHCO5, 4-WHCO6, 5-SNO, 6-MCF7, 7-HT29, and DNA ladder-100 bp PLUS Marker.

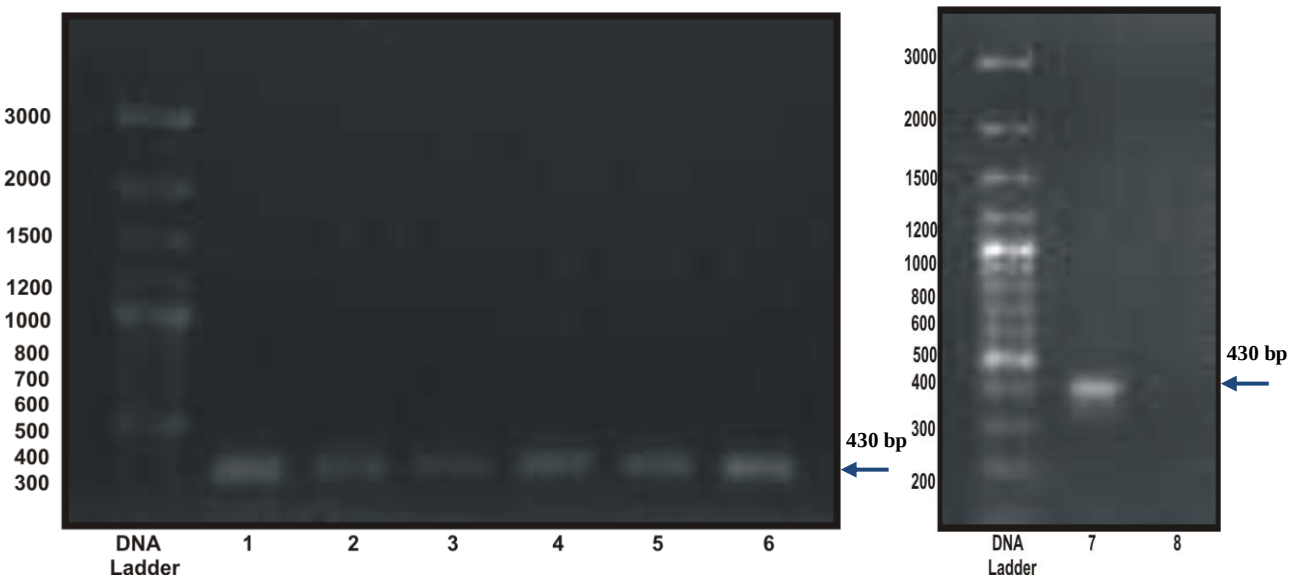


Figure 2.4: Gene amplification of the p85α transcript (PIK3R1) confirms intact p85α present in HOSCC cells. The presence of a 430 bp PCR fragment is indicative of a positive expression of the N-SH2 domain of PIK3R1/p85α in HOSCC cells (indicated by the blue arrow), resolved on two separate 1% agarose gels. The absence of a band in lane 8 (template-free) confirms the specificity of the PCR reaction. Lanes 1-8 represents the WHCO1, WHCO3, WHCO5, WHCO6, SNO, MCF7, HT29, and template-free control respectively. See Appendix A 1.12 for sequence and primer analysis.

2.3.3 Cellular localization of PI3K (p85α) in HOSCC cells.

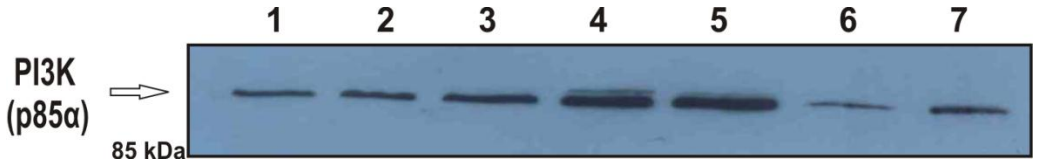
A) PI3K (p85α) localizes to the membrane

Having established its protein expression in HOSCC cell lines, it was important to determine whether it is expressed in the appropriate cellular location. Since it exclusively translocates to the membrane upon RTK activation[346,347] quiescent cells express high levels of PI3K (p85α) in the cytoplasm[57, 348] . Due to their PI3K mutational status, the HT29 and MCF7 cell lines served as ideal controls for the assessment of PI3K cellular localization relative to the HOSCC cells. Since these HOSCC lines overexpress the EGFR, we hypothesized an associated membrane localization of PI3K (p85α).

A large proportion of p85α protein was localized to the cytoplasm in all the HOSCC cell lines examined (shown in Fig. 2.6, *orange arrows*). Strong membrane staining was observed in the WHCO1 and WHCO6 HOSCC cell lines alongside the MCF7 and HT29

controls (Fig. 2.6, *purple arrows*). Additionally, the WHCO6 and MCF7 cell lines displayed diffuse p85α nuclear staining, whereas marked exclusion of p85α from the nucleus was detected within the WHCO1, SNO, and WHCO3 cell lines. Outstandingly, the WHCO5 cell line exhibited distinct nuclear and limited cytoplasmic staining for p85α, similar to that observed in the HT29 control (Fig. 2.6, *red arrows*). Moreover, the SNO, WHCO1, and the WHCO3 possessed strong perinuclear p85α localization.

A)



B)

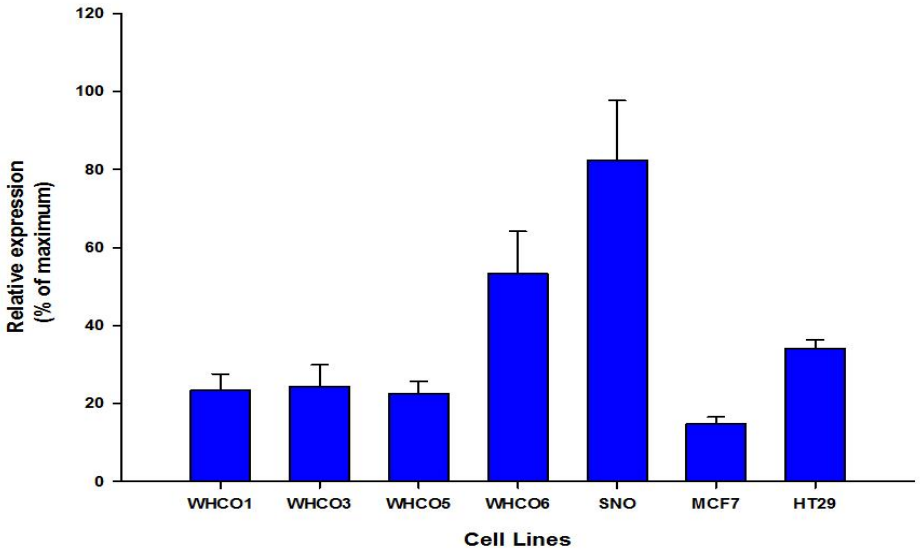
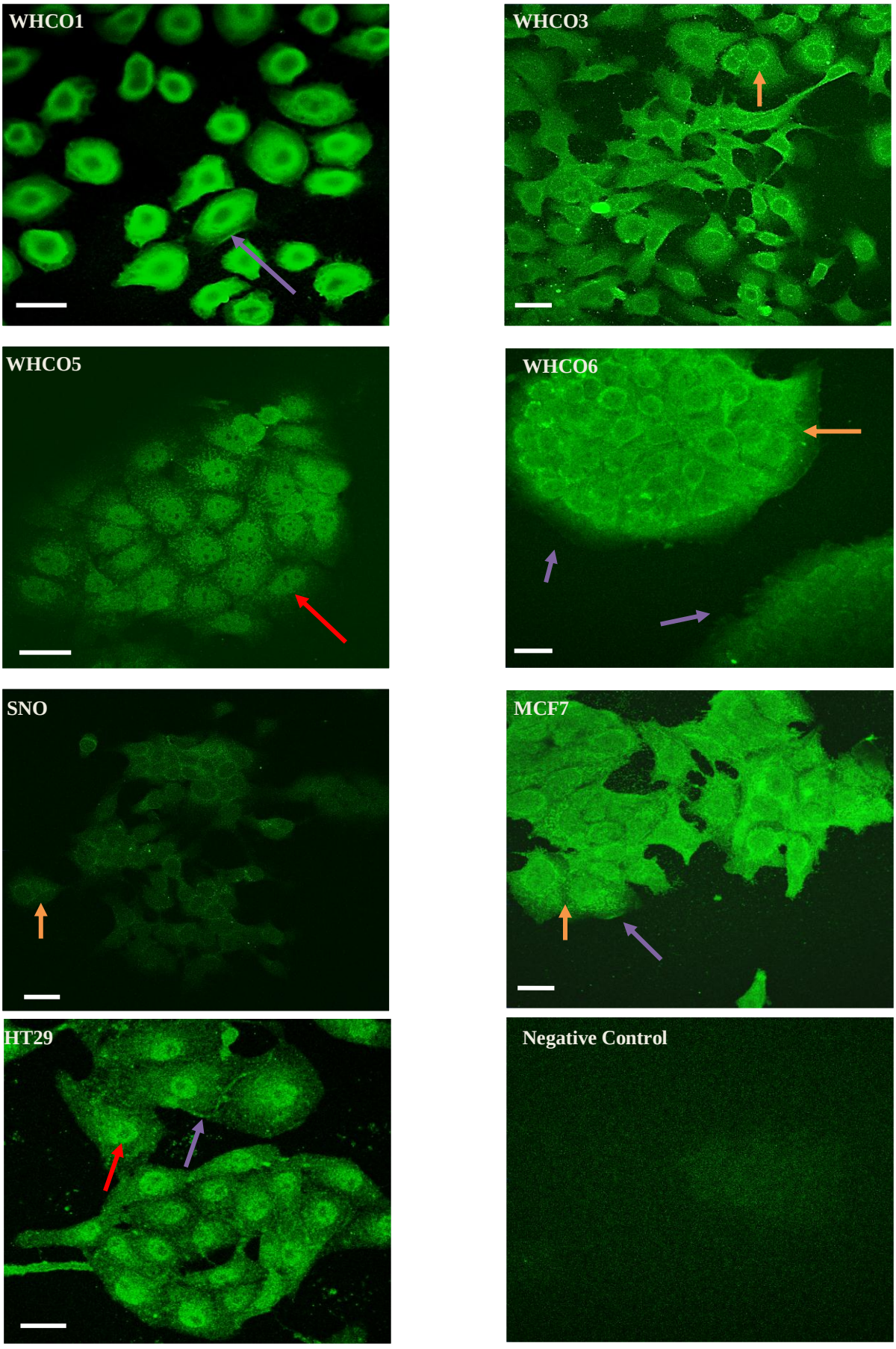


Figure 2.5: PI3K (p85α) is expressed at variable levels in HOSCC cells. **A)** Western blot analysis of PI3K (p85α) from whole cell protein extracts of HOSCC, MCF7, and HT29 cells (see Appendix A 1.6.6 and 1.7.5 for representative standard curve and 10% SDS-PAGE). Arrow indicates the p85α subunit at its defined molecular weight of 85 kDa. Lanes 1-7 represents the WHCO1, WHCO3, WHCO5, WHCO6, SNO, MCF7 and HT29 respectively. **B)** Densitometric analysis of the p85α detected through western blotting (mean ±s.d. of triplicate experiments), showing strongest expression in the WHCO6 and SNO HOSCC cell lines. See Appendix A, Table A1 for mean optical density values.



See next page for legend.

Figure 2.6: PI3K (p85α) is predominantly localized to the membrane and cytoplasm in HOSCC cells. Indirect immunoflourescence microscopy displaying PI3K (p85α) cellular localization in the 5 HOSCC cell lines and HT29 and MCF7 control cell lines. All HOSCC cells display largely cytoplasmic p85α localization (*orange arrows*). The WHCO1 and WHCO5 cell lines showing nuclear p85α staining (*red arrows*), whereas the WHCO1 and WHCO6 cell lines demonstrate cytoplasmic, which included membrane staining (*purple arrows*). Under equivalent conditions, little or no staining was detected in the negative control, indicative of staining specificity. Bar represents 25 μm.

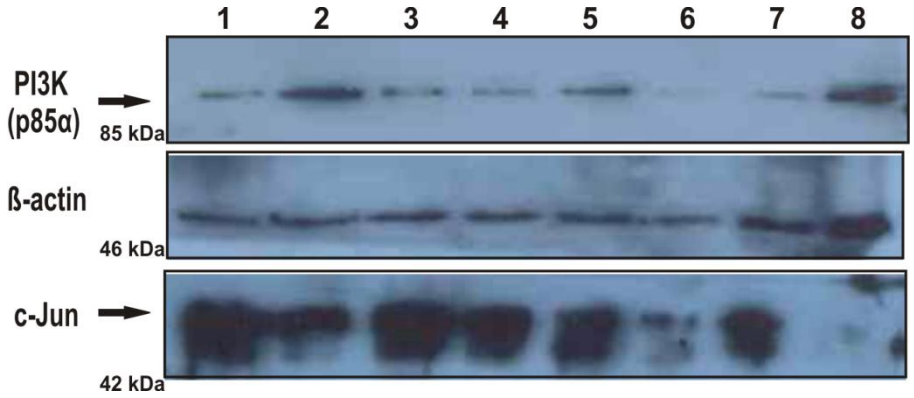
B) PI3K (p85α) is present in the nucleus of HOSCC cells.

To ensure that the nuclear localization of PI3K (p85α) was a true representation of its intracellular distribution; we performed western blot analysis from nuclear extracts. Correspondingly, relative to its immunoflourescent detection, the levels of p85α in the nucleus were indeed low, with the highest expression detected in the WHCO3 cell line (demonstrated in Fig. 2.7). No nuclear PI3K (p85α) was detected in the MCF7 cell line. This result fits with its mtPIK3CA status that ensures stabilized membrane PI3K (p85α) localization.

C) PI3K (p85α) is targeted to the membrane in HOSCC cells.

To provide a quantitative support for the PI3K (p85α) staining at the membrane, its membrane expression through western blot analysis of plasma membrane-specific protein extractions was evaluated. As can be seen in Fig. 2.8, PI3K (p85α) is expressed at the membrane in the WHCO and SNO HOSCC series. The WHCO5 (60%) WHCO6 (80%) and SNO (80%) cell lines showed the highest expression, while the WHCO1 (40%) and WHCO3 (20%) cell lines displayed the lowest levels. Under these conditions, the membrane expression of PI3K (p85α) in the HOSCC cells is validated by its detection in the mtPIK3CA control cell line (HT29) that was previously demonstrated to possess strong membrane binding[349]. Furthermore, the purity of the membrane extract was confirmed by the presence of the largely plasma-membrane associated adhesive protein, E-cadherin[350]. This was clearly detectable in all the membrane extracts performed, excluding the HT29 cell line (Fig. 2.8), which inherently express low E-cadherin membrane levels[351]. Therefore, the specificity of the membrane extraction is further strengthened against the positive detection of E-cadherin in the MCF7 and the negative detection in the HT29 controls.

A)



B)

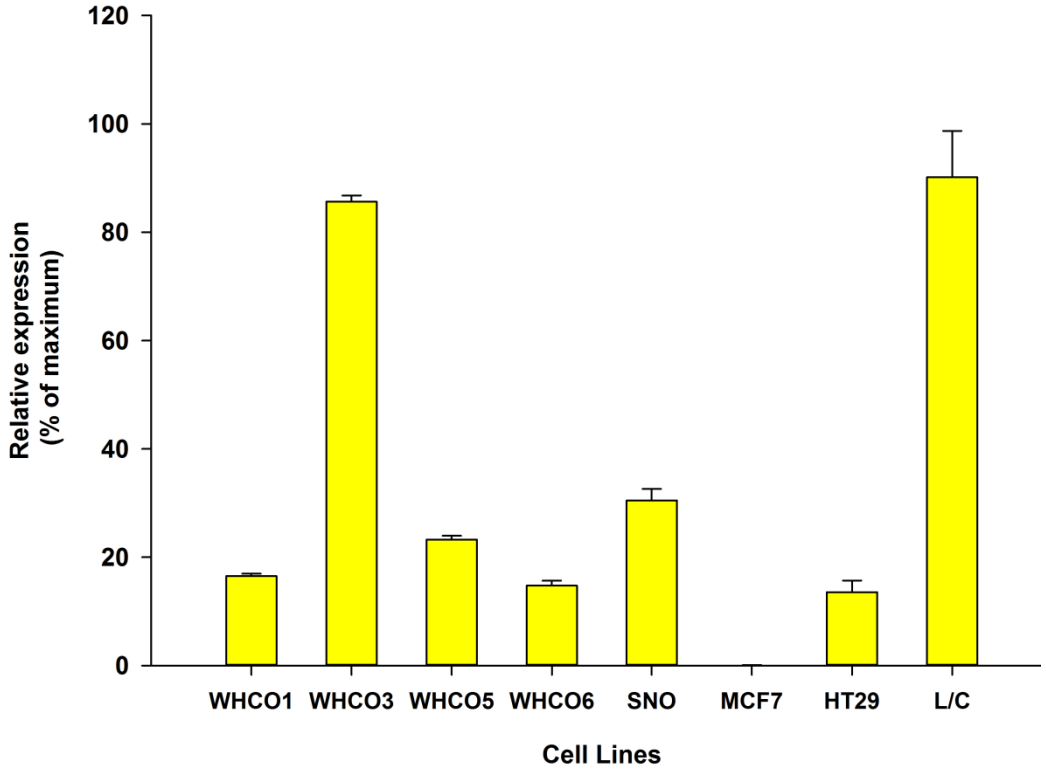


Figure 2.7: Relatively low levels of PI3K (p85α) are expressed in the nucleus of HOSCC cells. A) 30 µg of nuclear extracts (as described in Materials and Methods) taken from HOSCC, MCF7 and HT29 cell lines were immunoblotted for the detection of PI3K (p85α) (see Appendix A 1.6.6 and 1.7.5 for representative standard curve and 10% SDS-PAGE. Arrows show the positive PI3K (p85α) detection at 85 kDa. The integrity of the nuclear extracts was verified through the positive detection of the c-Jun transcription factor at 42 kDa, which is predominantly expressed within the nucleus[352]. Lanes 1-8: WHCO1, WHCO3, WHCO5, WHCO6, SNO, MCF7, HT29, and WHCO6 whole cell lysate as the loading control (L/C). **B)** Densitometric analysis of the nuclear western blot detection of PI3K (p85α), (mean ±s.d. of triplicate experiments), revealing the highest expression in the WHCO3 cell line (>80%), see Appendix A, Table A1 for mean optical density values.

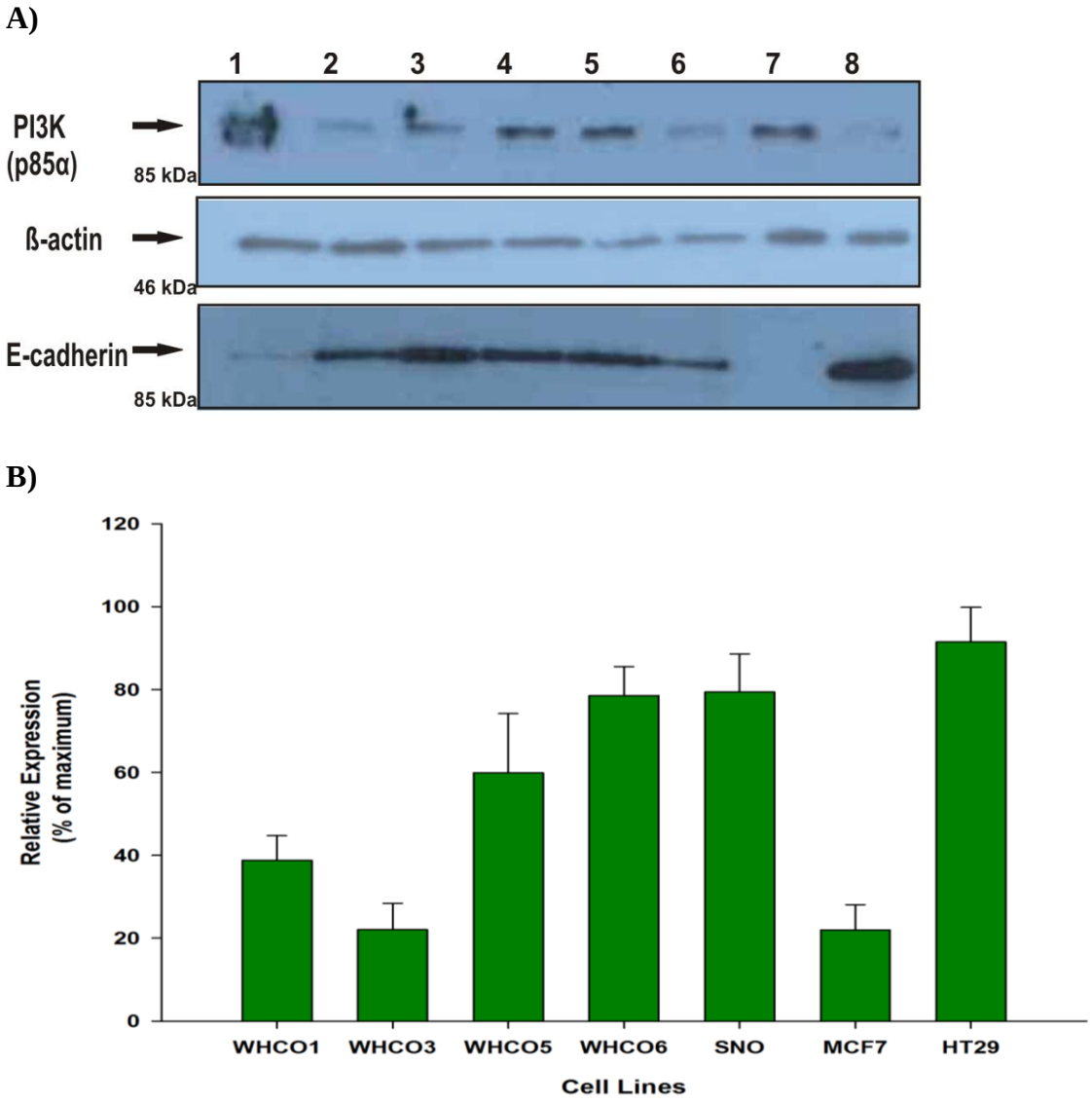


Figure 2.8: PI3K (p85α) is targeted to the membrane of HOSCC cells. A) 20 μg of plasma membrane extracts derived from HOSCC, MCF7 and HT29 cell lines were subjected to western immunublotting for the detection of PI3K (p85α), see Appendix A 1.6.6 and 1.7.5 for representative standard curve and 10% SDS-PAGE. The success and specificity of the membrane extraction was verified through the detection of the transmembrane E-cadherin protein at 85 kDa. Lanes 1-8 represent the WHCO1, WHCO3, WHCO5, WHCO6, SNO, MCF7, HT29 and the WHCO6 whole cell protein lysate loading control. **B)** The experiment was performed three times and PI3K (p85α) detection in the form of bands was quantified through densitometry (mean ±s.d. of triplicate experiments), revealing that the WHCO6 and SNO cell lines possess the highest amount of PI3K (p85α) at the membrane. See Appendix A, Table A1 for mean optical density values.

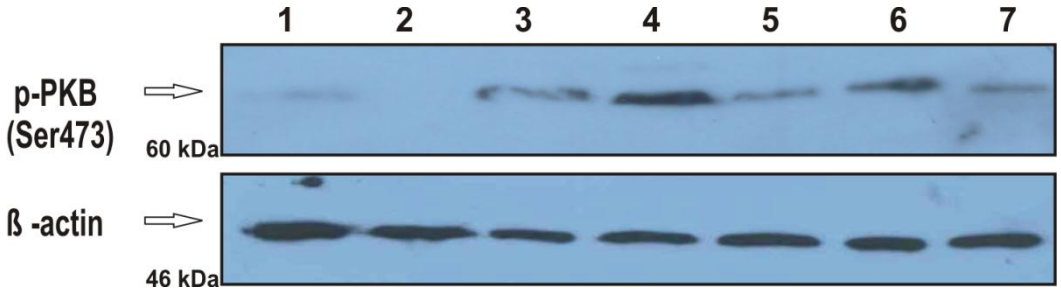
2.3.4 PI3K and PKB are active in the HOSCC cell lines.

The Ser473 phosphorylation state of one the major downstream targets of PI3K, PKB, is specifically used as a marker for the presence of active PI3K[353, 354]. In an attempt to determine whether PI3K is active, as suggested by its membrane localization, the Ser473 phosphorylation state of PKB was used as a measure for its level of activity, albeit indirect. To varying degrees, western blot analysis revealed a positive pPKB (Ser473) reaction in all the HOSCC cell lines, except the WHCO3 cell line (shown in Fig. 2.9A). This experiment was repeated with increasing protein concentrations (60, 80 and 100 μg) to ensure the lack of pPKB (Ser473) levels in the WHCO3 cell line (see Appendix A, Table A2).With respect to the HT29 and MCF7 controls, this was taken as evidence of an active PI3K. Since PKB Ser473 phosphorylation is required for its full activation[355], these data equivalently point to an active PKB in 4 of the HOSCC cell lines. Densitometric analysis revealed that the WHCO6 cell line exhibited the strongest pPKB (Ser473) expression (100%), hereafter referred to as pPKB, whereas marginally lower expression levels were displayed in the WHCO5 (50%) which was similar to the levels displayed in the MCF7 (60%) control (see Fig. 2.9B). The WHCO1 (10%), SNO (22%) and HT29 (30%) cell line possessed the least amount of pPKB respectively (Fig. 2.9B). These results clearly point to an active PI3K and PKB present within 4 HOSCC cell lines, albeit to unique concentrations and an obvious departure being the WHCO3 cell line.

2.3.5. Cellular distribution of active PI3K (pPKB) within HOSCC cell lines.

Protein kinase B (PKB) plays multiple roles in the regulation and activation of various cellular processes, such as, apoptosis and proliferation[356, 357]. Similar to PI3K, its membrane localization and cytoplasmic distribution serves as a good indicator of its functional and activational state[358, 359]. Immunoflouresent images of the 5 HOSCC, MCF7 and HT29 cells portray distinct staining patterns (illustrated in Fig. 2.10). The WHCO1, WHCO5, WHCO6, and SNO cell lines demonstrated apparent nucleolar pPKB localization, with the WHCO1 and SNO displaying a less obvious cytoplasmic staining (Fig. 2.10, *red arrows*). The WHCO5 cell line, on the other hand, possessed a more pronounced cytoplasmic and membrane pPKB staining pattern. In accordance with its western blot detection (see Fig. 2.9), immunoflourescence of pPKB in the WHCO3 cell line showed only background levels. Strong membrane localization of pPKB, alongside a faint cytoplasmic staining and nuclear exclusion, was observed in the mtPIK3CA MCF7 and HT29 controls.

A)



B)

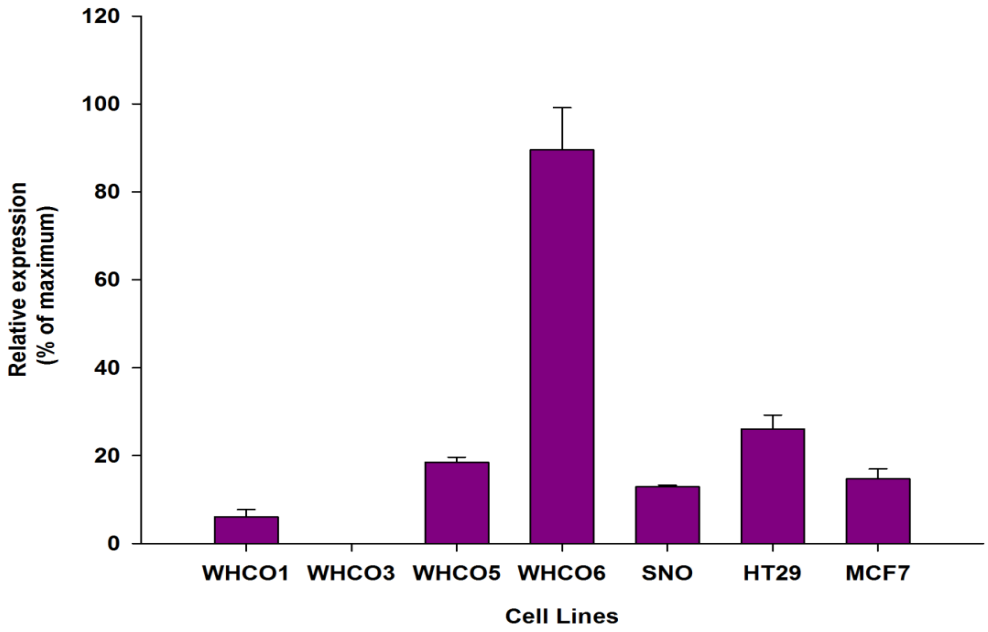
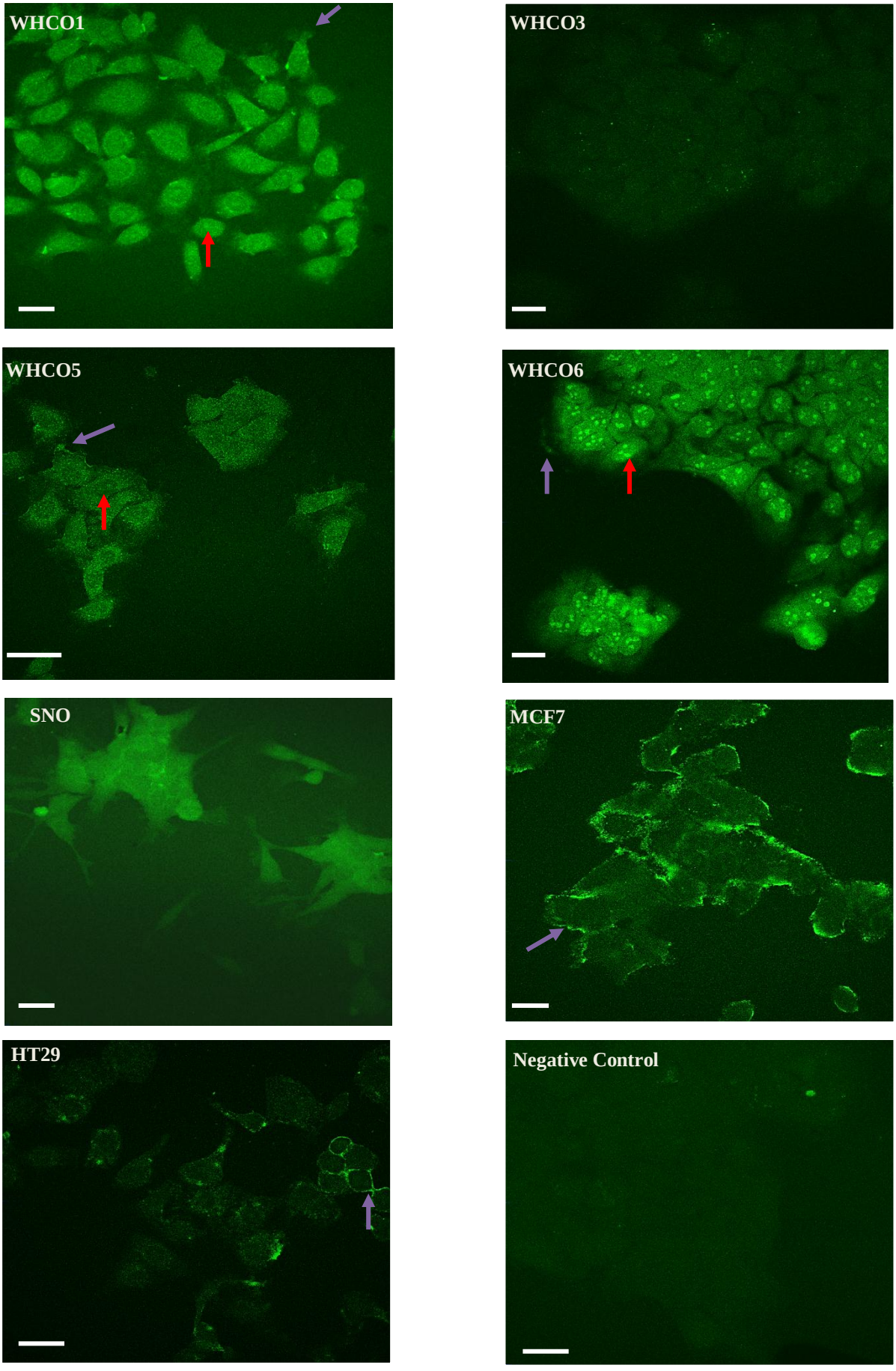


Figure 2.9: PI3K is active in 4 of the HOSCC cell lines. A) Western blot analysis of 80 µg total phospho-PKB/p-PKB (Ser473) from resolved HOSCC, MCF7 and HT29 whole cell protein lysates (see Appendix A 1.6.6 and 1.7.5 for representative standard curve and 10% SDS-PAGE generated during the protein estimation) detected at 60 kDa. Lanes 1-7 represent the WHCO1, WHCO3, WHCO5, WHCO6, SNO, HT29, MCF7 cell lines respectively. **B)** The identified western blot band was quantified by densometric analysis (mean ±s.d. of triplicate experiments), confirming that PI3K (pPKB) is active in four of the HOSCC cell lines, with the highest pPKB present in the WHCO6 cell line, and the lowest in the WHCO1 cell line. Note: The experiment was repeated with increasing protein concentrations (60, 80 and 100 µg) to ensure the lack of Phospho-PKB (Ser473) expression in the WHCO3 cell line. See Appendix A, Table A2 for mean optical density values.



See next page for legend.

Figure 2.10: Unique staining patterns of pPKB identifying active PI3K in each of the HOSCC cell lines. Immunoflourescence microscopy affirmed membrane pPKB staining in the WHCO5, WHCO6, SNO and the HT29 and MCF7 control cell lines (*purple arrows*). Apparent nucleolar pPKB detected in the WHCO1, WHCO5, and WHCO6 HOSCC cell lines (*red arrows*). The lack of a similar staining pattern in the negative control is an indication that the cellular localization of phospho-PKB (Ser473) detected is unambiguous. Bar represents 25µm.

2.3.6 PKB is active in HOSCC cells.

The Ser9 phosphorylation status of one of PKBs major downstream effectors, GSK3β, is commonly used as a marker for the presence of active PKB in various cellular milieu[360, 361, 362]. Therefore, to further confirm the activational state of PKB, as its cellular localization suggests in the 5 HOSCC cell lines, we used the detection of phospho-GSK3 (Ser9), herein referred to pGSK3β. In addition to their PIK3CA mutational status, the HT29 and MCF7 cell lines served as ideal controls for the Ser9 phosphorylation state of GSK3β previously established to be active (dephosphorylated)[363], and highly inactive (phosphorylated) [364] respectively.

According to its Ser9 phosphorylation status, these results reveal that GSK3β is inactive in the WHCO5, WHCO6, SNO HOSCC, and MCF7 cell lines (shown in Fig. 2.11). This suggests that the membrane localization of pPKB demonstrated above (Fig. 2.10) is linked to its active state in these cell lines. In keeping with its low and absent pPKB levels in the WHCO1 and WHCO3 cell lines respectively, a weaker pGSK3β expression, indicative of an active GSKβ and less active PKB was demonstrated.

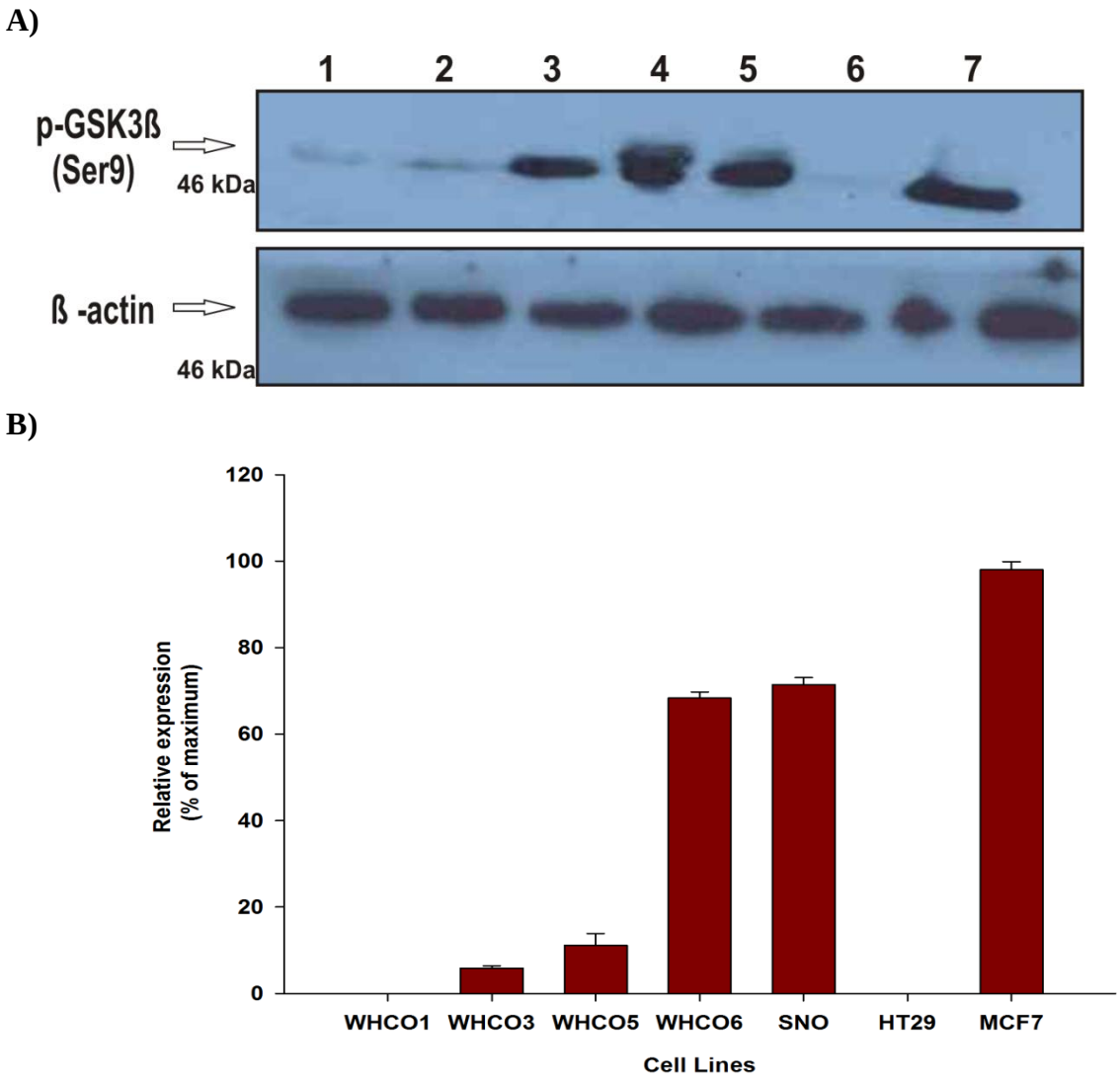


Figure 2.11: The activity of GSK3β appears to be constitutively inhibited in three of the HOSCC cell lines. A) Western blot analysis of active PKB (pGSK3β) in 10 µg of whole cell protein extracts from HOSCC, HT29 and MCF7 cell lines detected at 46 kDa (see Appendix A 1.6.6 and 1.7.5 for representative standard curve and 10% SDS-PAGE). β-actin was used as a measure for equal loading. Lanes 1-7 represent the WHCO1, WHCO3, WHCO5, WHCO6, SNO, HT29, and MCF7 cell lines respectively. **B)** The identified western blot band at 46 kDa was quantified by densitometric analysis (mean ±s.d. of triplicate experiments), illustrating that the WHCO6 and SNO HOSCC cell lines are in possession of the strongest active PKB (pGSK3β). See Appendix A, Table A2 for optical density values.

2.3.7 The activation of PKB is primarily mediated by PI3K in HOSCC cells.

Due to the importance of PI3K in the Ser473 phosphorylation and activation of PKB[184], it was further investigated whether the activity of PI3K is indeed required for PKB activation through its Ser473 phosphorylation. To reveal the contribution made by PI3K, its activational state was manipulated by using the PI3K-specific inhibitor, LY294002 (hereafter referred to as LY29). LY29 is said to mimic the activity of PTEN in cells[365]. Since the activity of PI3K and PKB are constantly attenuated by PTEN, the expression of PTEN was also evaluated subsequent to PI3K inhibition as a control for the influence of LY29. The wild-type and overexpressed state of functional PTEN in the HT29 and MCF7 cell lines respectively[366, 367], were used as additional controls for this influence.

Blocking the PI3K pathway confirmed the dependency that PKB has on PI3K for its full activation, with the WHCO1, WHCO5, WHCO6 and HT29 cell line ($P<0.001$) possessing the highest and the WHCO3, SNO and MCF7 cell lines ($P<0.001$) demonstrating the least dependency thereof (shown in Fig. 2.12 and 2.13). A reduction in pPKB corresponded to dissuaded pGSK3β phosphorylation in the WHCO1, SNO, HT29 and MCF7 cell lines exclusively (Fig. 2.12 and 2.13). Although significantly affected ($P<0.05$), the decreases observed in levels of pGSK3β in the remaining cell lines, did not correspond to the changes in pPKB.

These results also demonstrate that although PKB is active, deduced by its Ser473 phosphorylation status, it plays a relatively small role in the Ser9 phosphorylation, and thus inhibition of GSK3β, in all of the cell lines examined (see in Fig. 2.12 and 2.13). This is especially noted in the WHCO3 cell line, where pPKB is absent, yet the Ser9 phosphorylation of GSK3β was significantly attenuated ($P<0.05$) as a result of PI3K inhibition. These data strongly suggest that PKB-independent mechanisms are used to regulate the Ser9 phosphorylation, and hence activity of GSK3β in HOSCC cells.

It is well established that the expression of pPKB and its antagonist, PTEN are inversely proportional[368, 369, 370, 371, 372]. However, this relationship was not observed in the WHCO and SNO HOSCC series (see Fig. 2.12 and 2.13). Even though the WHCO1, WHCO3 and SNO HOSCC cell lines demonstrated a noticeable drop in the protein concentration of PTEN (Fig. 2.12 and 2.13), it was not inversely correlated to pPKB (see Appendix A, Table A6). Likewise, no inverse correlation between PTEN and pPKB levels was found in the two cell

(HT29 and MCF7) lines that have been shown to harbour functional PTEN, suggesting that despite the lack of this relationship between PTEN and pPKB in HOSCC cells, PTEN may still be functional.

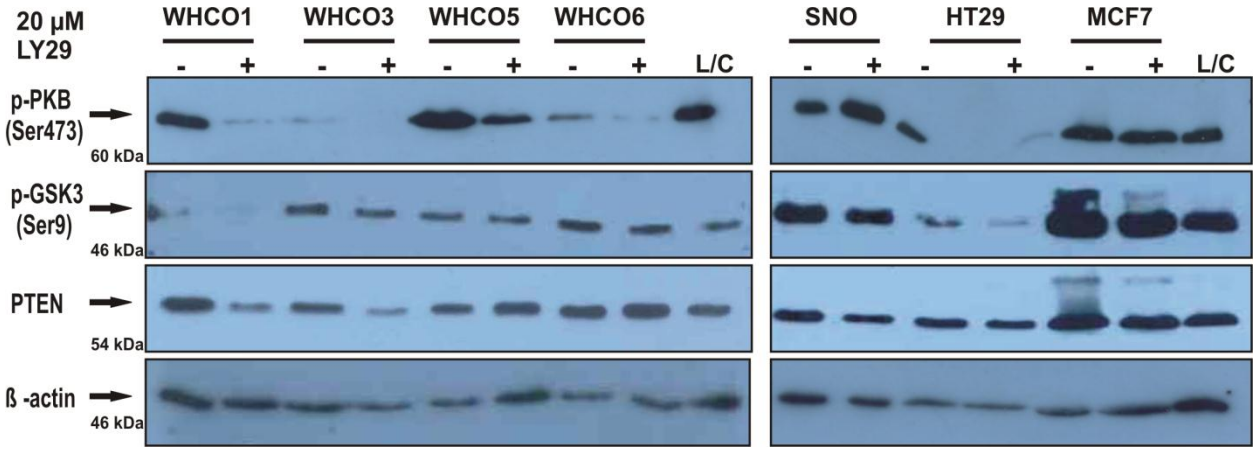
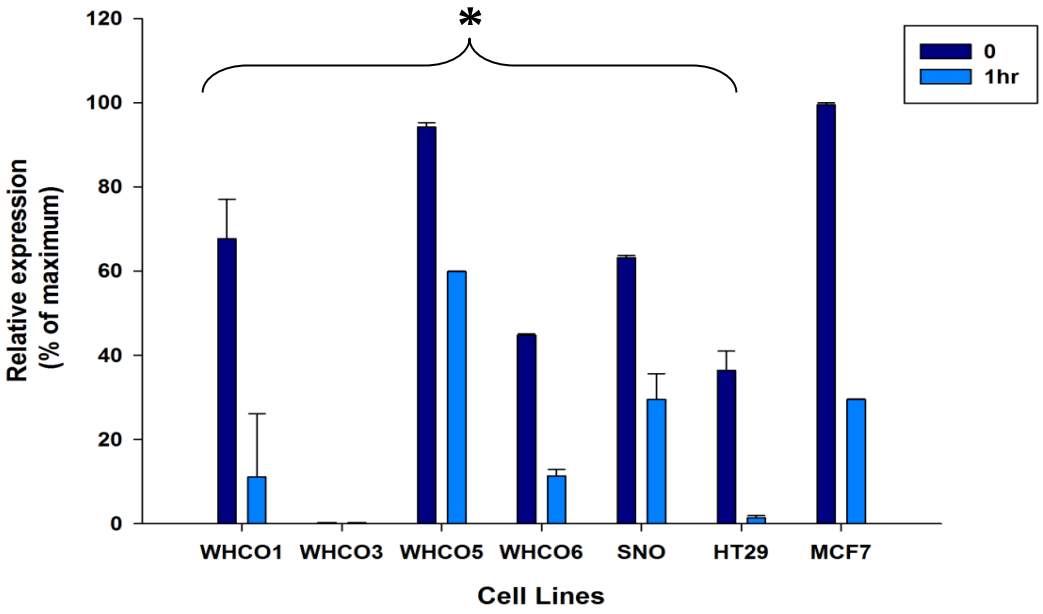


Figure 2. 12: Disruption of the PI3K pathway in HOSCC cells through LY29 confirms the dependency that PKB has on PI3K for its Ser473 phosphorylation, and thus full activation. HOSCC, HT29 and MCF7 cells were treated for 1 hour with (+) or without (-) 20 µM of the PI3K inhibitor, LY294002 (LY29). Western blotting was used to determine the consequent effect PI3K inhibition had on the overall protein levels of p-PKB (Ser473), its downstream effector, p-GSK3β (Ser9), PTEN, and PI3K (p85α) (see AppndiX A 1.6.6 and 1.7.5 for representative standard curve and 10% SDS-PAGE). Untreated cells (-) were exposed to the LY29 vehicle control, DMSO. The loading control (L/C) is representative of the WHCO6 whole cell lysate used for comparison between the different blots. Equal loading of treated versus untreated proteins was detected with β-actin. Note: Experiments were performed three times.

A)



B)

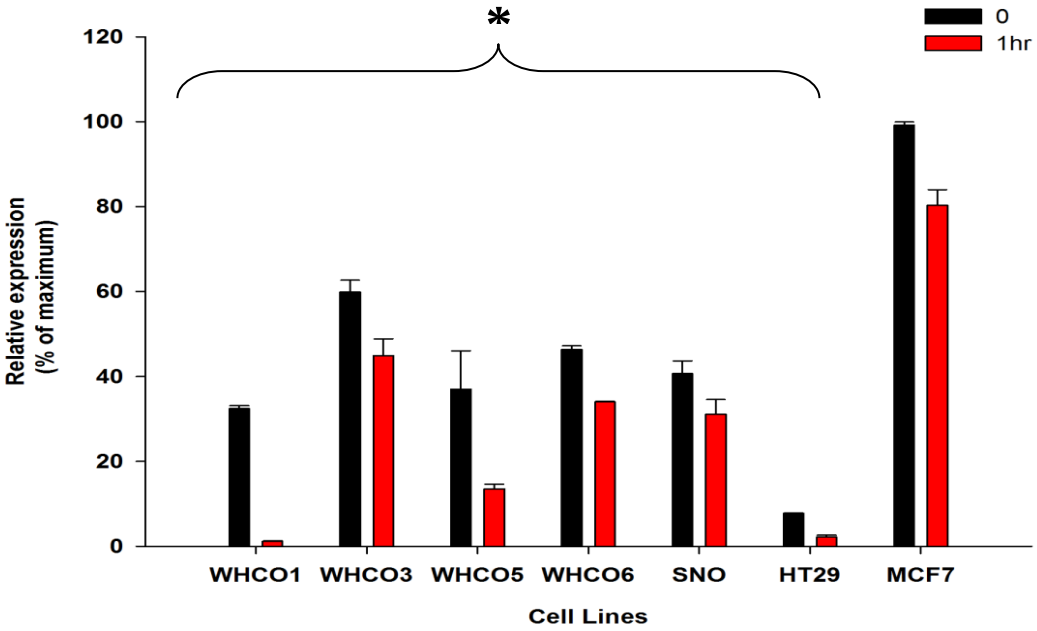


Figure 2.13: Densitometric analysis affirms the dependency pPKB levels have on PI3K activityependency pPKB levels have on PI3K activity in HOSCC cells. A) Densitometric analysis revealing the attenuated p-PKB (Ser473) levels following PI3K inhibition mediated by exposure to LY29, with the WHCO1 showing the highest, and the SNO the least sensitivity. **B)** Densitometric analysis of p-GSK3β (Ser9), subsequent to PI3K inhibition, demonstrating strong inhibition in the WHCO1, WHCO3, SNO, HT29 and MCF7 cell lines respectively. pPKB and pGSK3β results represent mean ± S.D. obtained from the three separate experiments, *P significantly different from control, P<0.05. See Appendix A, Table A3 and A4 for statistical analysis.

C)

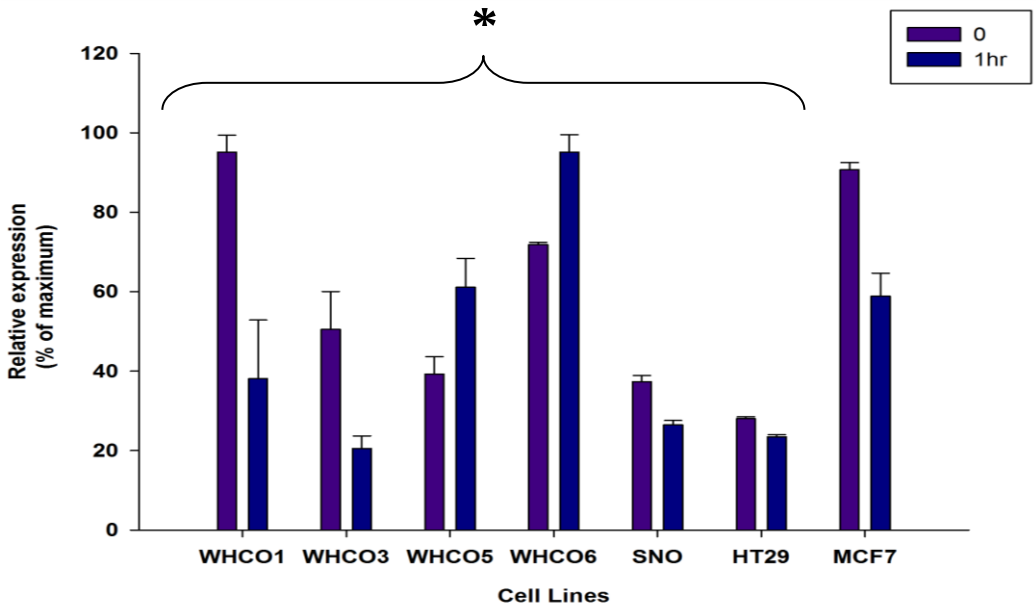


Figure 2.13: C) PTEN responded differentially to PI3K inhibition in the cell lines examined, affirmed by densitometric analysis. PTEN results represent mean ± S.D. obtained from the three separate experiments, *P significantly different from control, P<0.05. See Appendix A, Table A5 for statistical analysis.

2.4 Discussion

Even though genetic variations of the major components within the PI3K/PKB pathway have recently been shown to offer resistance to chemotherapy in HOSCC patients[295], much remains to be determined regarding a specific role for this pro-survival signalling pathway in HOSCC[140]. Of particular interest, is the p85α regulatory subunit of PI3K that acts as an oncogene in epithelial-derived cancers like HOSCC[373, 374, 375]. This oncogenicity has been linked to a truncation in the nSH2 domain of the p85α protein transcribed by PIK3R1 that normally prevents PI3K activation through its constant inhibition of the p110α catalytic subunit[318].

In the present study, transcription of p85α was verified and revealed that the 5 HOSCC cell lines are free of p85α nSH2 domain truncations or mutations (Appendix A 1.12). The 400 bp PCR fragment amplified here is consistent with the 425 bp fragment acquired by Krymskaya, *et al.*[305] who used the same set of primers on human airway smooth muscle cells. Moreover, each of the HOSCC lines were shown to express unique levels of PI3K (p85α) protein (see Fig. 2.5). Ostensibly, one would expect an enhanced protein expression in cells possessing activating PI3K mutations[42, 376, 377]. Surprisingly, the mtPIK3CA (E454K) MCF7 cell line expressed only weak PI3K (p85α) protein concentrations, in comparison to the WHCO and SNO HOSCC series. As highlighted previously, the need for p85α protein during tumour metastasis and differentiation is highly controversial. The HT29 colon cell line was shown previously to possess high protein concentrations of p85α, that was strongly associated with its poor differentiation state[331, 378]. Furthermore, based on their keratinizing capability, the 5 HOSCC lines were established as poor differentiating and highly metastatic cells[329]. PI3K (p85α) protein appears to be highly expressed in HOSCC lines, relative to the strong p85α expression in the HT29 control, with the WHCO6 and SNO cell lines being the atypical examples of this. Therefore, an elevation in p85α protein levels may in fact serve as an ideal pathological grading marker for HOSCC cells.

Although the possibility that monomeric p85α expression exists, it is for the most part dimerized to the p110α catalytic subunit in a 2:1 ratio[69]. On this basis, the p85α immunoblot detection here may represent the mutually favourable, yet obligate p85α-p110α dimer. This interpretation is corroborated by a number of studies illustrating that intracellular levels of p110α are completely saturated by p85α, and that p110α expression is not possible otherwise[68, 72, 379]. Additionally, human embryonic kidney cells, HEK293T[65] and COS-7 cells[66] transfected with monomeric

p110α consequently displayed negligible frequencies of PI3K activity that was strikingly reinstated when co-expressed with the p85α subunit.

As part of improving the understanding of the functional role played by PI3K in HOSCC pathology, we sought to explore its cellular compartmentalization. Inactive PI3K (p85α) is predominantly localized to the cytoplasm[380, 381]. Given the context in which PI3K finds itself at the membrane[382, 383], many are of the view that membrane biased PI3K is sufficient to confer constitutive activation of the PI3K pathway in cancer[40, 384, 385, 386, 387, 388, 389]. PI3K (p85α) was found localized to the membrane only in the WHCO1 and WHCO6 HOSCC cell lines respectively (see Fig. 2.6). As expected, the two PIK3CA mutant cell lines, MCF7 (E454K) and HT29 (P449T)[330] positively displayed membrane localized PI3K (p85α). This membrane localization strongly points to the existence of constitutively activated PI3K in two of the HOSCC lines.

In addition to their known membrane localization, inositol lipids have reportedly been found in the nucleus, demonstrating functionality similar to those at the plasma membrane[390, 391, 392, 393]. These authors also reported that the propensity of a cell to acquire a nuclear PI3K signalling network, is cell-type specific. Nuclear staining supported by western blot analysis found PI3K (p85α) present within the nucleus of all HOSCC cell lines, with the WHCO3 cell line demonstrating the highest concentration (see Fig. 2.6 and 2.7). It should be noted that the apparent difference between the nuclear localization of PI3K, and that in the western blot of the nuclear extraction, is likely a result of the nuclear extracts not containing the cytoplasmic fraction (see Fig. 2.6), which is therefore more prominent in the immunoflourescent detection (see Fig 2.7). Consistent with this result, electron microscope immunocytochemistry confirmed nuclear localization of PI3K in rat liver nuclei[394], rat pheoctomocytoma PC 12 cells[395], and human HL-60 leukemia cells[396]. Interestingly, human osteosarcoma Saos-2 cells treated with drugs commonly used for cancer chemotherapy, like the anthracycline antibiotic and doxorubicin, reduced the nuclear and cytoplasmic localization of PI3K[397]. This is highly suggestive of a role played by PI3K in the nucleus in the promotion of cellular transformation. Accordingly, the PI3K antagonist, PTEN[398], and its derivative, pPKB[399], were also found localized in the nucleus of in HL-60 cells that was directly linked to cellular transformation.

In support of an oncogenic role for PI3K in the nucleus, evidence derived from HepG2 human hepato-carcinoma cells[400], osteosarcoma Saos-2 cells[401], osteoblast-like clonal cell line, and

osteoblast-like MC3T3-E1 cells[402], demonstrated rapid nuclear sequestration of PI3K in response to various stimuli such as insulin, PDGF, and nerve growth factor (NGF) respectively. Thus, these studies indicate that the nuclear localization of PI3K is not constitutively present but sequential to its activation by exogenous stimulation. Hence, it would appear that a separate PI3K nuclear signalling network may exist in HOSCC cells in the absence of exogenous stimulation.

In keeping with its membrane and nuclear cellular localization, both of which are characteristic of a constitutively active PI3K, led us to question whether it is indeed active in the 5 HOSCC lines. Given that the Ser473 phosphorylation status of its downstream target, PKB, is the classic, yet indirect method used to ascertain the intracellular levels of PI3K activity[403, 404, 405], it became necessary to determine whether pPKB is present in the HOSCC lines. Based on the overexpressed EGFR status in these HOSCC cell lines[332], as well as the established membrane localized PI3K (demonstrated in Fig. 2.6), we anticipated a correspondingly high level of PI3K activation[150]. It was shown that PI3K is indeed active at dissimilar levels in four of the HOSCC ines, with respect to the known positive HT29 and MCF7 controls. Since PIP3 production is PI3K-dependent, and PKB activation is PIP3-dependent[406, 407, 408], these results also provide a good indication that PIP3 is present in these four HOSCC lines. Furthermore, western blot detection of pPKB has been previously linked to potentiated PKB activity through high concentrations of PIP3[177 and 409], and therefore the data presented here suggest that both basal levels of PI3K and PKB are active. On the other hand, our data also demonstrated that the membrane localization of PI3K does not always correspond to its activational state of PI3K (pPKB) in HOSCC cell lines. This has especially been noted for the WHCO1 and WHCO6 cell lines, both of which possessed strong membrane localized PI3K, yet only the WHCO6 cell line possessed a high concentration of pPKB (see Fig. 2.6 and Fig. 2.9). Furthermore, a strong relationship between p85α protein and pPKB levels was shown to exist within the HT29 and MCF7 control cell lines, whereas no such relationship was evident within either of the HOSCC lines.

The WHCO3 cell line was notable for its absent pPKB expression. The undetectable pPKB in this cell line could be attributed to a number of factors. Firstly, since PI3K activity determines the Ser473 phosphorylation and hence, activation of PKB[355], this result implies that basal levels of PI3K, and consequently PKB, are greatly suppressed in this cell line. Ironically, the WHCO3 cell line was shown to possess the highest concentration of EGFR[332], yet no corresponding levels of pPKB exists. A particular study illustrated that at high temperatures, pPKB was undetectable

through western blot analysis[410]. However, this would seem as an unlikely explanation for the absent pPKB in the WHCO3 cell line, as all the cell line extractions were performed under the same temperature conditions (see Materials and Methods), yet its lack of detection was limited to the WHCO3 cell line.

The specific function and regulation of many kinases is largely determined by their cellular localization, and PKB is no exception[359]. Bearing in mind that its membrane translocation is essential for its activation, and its substrates are situated in both the cytoplasm and nucleus[182, 411, 412], it was no surprise to discover staining in all three cellular compartments in the four HOSCC cell lines (WHCO1, WHCO5, WHCO6, and SNO) (see Fig. 2.10). In accordance with its western blot detection, no specific staining for pPKB was evident in the WHCO3 cell line. The propensity for PKB to become phosphorylated on its Ser473 residue is mediated by the catalytic Lys179 that enables the phosphate transfer from ATP to the Ser473 residue[413]. Interestingly, the specificity of the anti-pPKB (Ser473) antibody was tested on HEK293 cells transfected with a "kinase-dead" version of PKB created by converting the catalytic Lys179 residue to an alanine[414]. Bearing this in mind, it seems plausible to suggest that a similar mutation may be present within the WHCO3 cell line, giving rise to the undetectable pPKB clearly observed in this chapter.

Even though the Ser9 phosphorylation and thus inactivation of GSK3β can be regulated by various other kinases, such as PKA and PKC[415, 416], it is for the most part under the regulation of PKB[197]. Therefore the Ser9 phosphorylation of GSK3β has become the method of choice for discovering and confirming the intracellular activity of PKB[417]. Using this method, and as its Ser473 phosphorylation status suggests, PKB is indeed active in HOSCC cells. The data presented in this study show that basal concentrations of GSK3β are inactive in the HOSCC cells (see Fig. 2.11). This was determined with respect to the known active, and hence Ser9 dephosphorylated state of GSK3β previously established in the HT29 control[363]. Despite the absence of pPKB in the WHCO3 cell line, pGSK3β levels were still detectable, suggesting that PKB may not be the primary regulator of this site in the WHCO and SNO HOSCC series. An earlier report indicated that although dephosphorylated on its Ser473 residue, PKB still maintains a minimal level of activity[418], and therefore this possibility cannot be excluded.

To fully confirm the influence played by PI3K in the regulation of PKB in HOSCC cells, it became necessary to manipulate its activational state. PI3K inhibition by LY294002 (LY29) is

one of the most commonly used methods for elucidating its intracellular activity[419, 420]. It was demonstrated by using LY29, that the Ser473 phosphorylation, and thus activation of PKB, is highly dependent on PI3K in the WHCO1, WHCO5, WHCO6 and SNO HOSCC cell lines exclusively (see Fig. 2.12 and 2.13). Despite recent evidence bringing to question the use of LY29 as a specific inhibitor for PI3K[421], the concentration of 20 μM used here has been utilized by numerous other studies and demonstrated to be specific towards the ATP-binding site of PI3K[342, 343, 422,423, 424, 425]. Therefore, these data explicitly underscores the importance of PI3K in the Ser473 phosphorylation of PKB in these four HOSCC lines.

Culminating from the significant, yet small reduction obtained in pPKB in the WHCO5 and SNO cell lines, as opposed to the stronger attenuation displayed in the WHCO1 and WHCO6 cell lines as a result of PI3K inhibition (see Fig. 2.13A), suggests that the former cell lines are more resistant to LY29. Notably, tumour cells harbouring PI3K or PTEN mutations are considered to be more sensitive to LY29 exposure[426, 427], whereas those possessing p53 mutations confer resistance[428]. The SNO HOSCC cell line was shown to harbour the R175H "hotspot" p53 mutation[429]. Although the mutant (mt) PI3K status in the control cell lines (HT29 and MCF7) may explain their significant sensitivity to LY29 and the mtp53 status in the SNO cell line, the resistance to LY29 respectively, it does not account for the resistance depicted in the wtp53 WHCO5 cell line[429]. Consequently, it would appear that the resistance to LY29 in the WHCO5 and SNO HOSCC cell lines is independent of their p53 status.

Consistent with this resistance presented in the WHCO5 and SNO cell lines, Matsumoto, *et al.*[430] showed that based on the unaffected concentration of pPKB, certain pancreatic cancer cell lines were also resistant to LY29. As a result, the authors questioned the importance of PI3K in the downstream activation of PKB. Since LY29 is a competitive inhibitor for the ATP binding site of PI3K, these results may imply that the resistance encountered in these two HOSCC cell lines may be due to the presence of higher intracellular levels of ATP, that out-competes LY29 binding on the PI3K ATP-binding site[431], leading to the resistance observed (see illustration in Fig. 2.14). This suggestion is not impractical, since ATP was shown to maintain an active state of PI3K by keeping its antagonist, PTEN, in the nucleus of breast, colorectal and thryroid carcinoma cells[432]. Indeed, EGFR overexpression has been shown to constitutively activate PI3K and PKB[433] leading to LY29 resistance[434, 435]. The resistance observed here is more than likely achieved by maintaining high levels of ATP at the PI3K active site (shown in Fig. 2.14). On the other hand, there were no detectable levels of pPKB in the WHCO3 cell line despite its overt EGFR frequency. Therefore, it seems logical to suggest that although EGFR overexpression

may contribute to the resistance acquired in the WHCO5 and SNO cell lines, another key player, that possibly counteracts the effects induced by EGFR; may be more pronounced in the WHCO1, WHCO3, and WHCO6 HOSCC cell lines; causing these cells to develop greater susceptibility towards LY29.

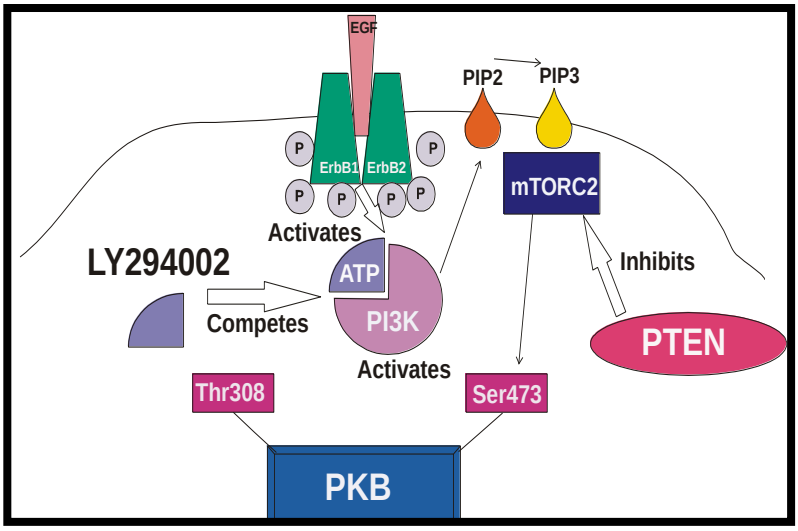


Figure 2.13: Schematic diagram showing the possible reasons for acquiring LY29 resistanceram showing the possible reasons for acquiring LY29 resistance in the WHCO5 and SNO HOSCC cell lines. The competitive relationship between ATP and LY294002 binding to the PI3K active site is shown, inevitably reversing cellular activation of PI3K. Figure generated using Microsoft Powerpoint®

A study revealed that the p53-R175H mutant present within the SNO cell line, up-regulates the EGFR-PI3K-PKB pathway by activating the EGFR promoter[436]. In contrast, an earlier study showed that both wild-type (wt) and mutant (mt) p53 are able to activate the EGFR promoter, albeit via distinct mechanisms[437]. Thus, strengthening the above suggestion, a contribution made by p53 in this light can be overlooked. Weak Ser473 phosphorylation of PKB is commonly observed in cells where casein kinase 2 (CK2) is down-regulated[438, 439]. The protein kinase CK2 is a highly ubiquitous serine/threonine kinase that up-regulates and maintains the activation of PKB by positively regulating its Ser473 phosphorylation state[440]. Furthermore, cells harbouring wtp53 were shown to suppress the kinase activity of CK2[441], while mtp53-containing cells were severely lacking in this regard. Although LY29 has been reported to also directly inhibit CK2[421], there is no evidence supporting this action at the concentration (20 μM) used here. Thus, even though p53 may not contribute to the LY29 resistance or susceptibility by up-regulating EGFR highlighted above, it may aid in the cellular response to LY29 via its negative regulation on CK2. Therefore, the resistance observed in the mtp53 SNO cell line may incorporate the up-

regulated and sustained levels of pPKB through its inability to suppress CK2 via p53, as shown in Fig. 2.15. This interpretation raises the intriguing possibility that the absence of pPKB in the WHCO3 cell line could be resulting from the wtp53-mediated suppression of CK2, that antagonizes its ability to activate PKB. Consistent with this view, Jurkat cells treated with CK2 inhibitors resulted in severely reduced concentrations of pPKB, similar to those detected in the WHCO3 cell line[439].



Figure 2.14: Schematic diagram illustrating the role of wt and mtp53chematic diagram illustrating the role of wt and mtp53 in the contribution of acquiring LY29 resistance and susceptibility. Cells with wtp53 are still able to attenuate the positive regulation CK2 has on PKB, whereas this attenuation is abrogated in cells harbouring mtp53.

These results also reveal that PKB plays a small role in the Ser9 phosphorylation, and thus inhibition of GSK3β (see Fig. 2.13). This is especially noted in the WHCO3 cell line, where pPKB is undetectable, yet a significant drop in Ser9 phosphorylation levels of GSK3β following PI3K inhibition was observed. Our interpretation is on par with recent work by Maher, *et al.*[442], who were unable to link the activity of PKB to the Ser9 phosphorylation of GSK3β. In addition to PKB, the Ser9 phosphorylation of GSK3β has been shown to be under the regulation of another PI3K-dependent kinase, the integrin-linked kinase (ILK)[443]. However, there appears to be insufficient data to support this view, and so it is suggested to occur in certain cells only[444]. Since GSK3β can also be negatively regulated by the Wnt signalling pathway[201], it was suggested that ILK inhibits the "Wnt-regulated" and not the "PKB-regulated" pools of GSK3β[445]. Evidence is emerging, that under conditions of low PKB activity, the S6 kinase is responsible for the Ser9 phosphorylation of GSK3β[361]. Nonetheless, seeing as great discrepancy exists on the regulation of GSK3β Ser9 phosphorylation, and even though the scope of this study does not include GSK3β, the data presented in this study indicate that HOSCC represents a perfect model for studying novel mechanisms for such a regulation.

The PI3K and PKB antagonist, PTEN, is regarded as a quasi-sufficient protein, and therefore any small change in its concentration is sufficient to elicit a cellular response[446]. Negative regulation of PTEN stability, and thus expression, by cellular PIP3 levels is well documented[447, 448]. Since the down-regulation in pPKB could easily be attributable to a rise in the concentration of PTEN, the levels of PTEN following PI3K inhibition was included as a measure of control for this. Here, it was shown that PTEN increased only in the WHCO5 and WHCO6 HOSCC cell lines (see Fig. 2.13C). The fact that the concentration of pPKB was not completely down-regulated despite the rise in PTEN levels in the WHCO5 cell line, verifies that LY29, and not PTEN, contributed to the down-regulation in pPKB observed.

Together, the role played by PI3K in the activation of PKB and GSK3β in 5 moderately differentiated HOSCC cell lines was compared to the mtPIK3CA status in the MCF7 (E454K) and HT29 (P449T) cell lines. A positive relationship between the membrane localization and activation of PI3K (pPKB levels) was disclosed in the WHCO1 and WHCO6 HOSCC cell lines. The results presented in this chapter also point to a role for CK2 in the regulation of PI3K activity through its regulation and maintenance of PKB Ser473 phosphorylation in the SNO cell line specifically. An important feature of these observations is the potential implications for an abrogated levels of pPKB in the WHCO3 cell line. The observations in this chapter were devoid of any mutations within the p85α transcript. Furthermore, our study also shows that levels of p85α protein are high in HOSCC cells. Finally, these data unveil that PKB-independent but PI3K-dependent is the preferred mechanism for the Ser9 phosphorylation of GSK3β in HOSCC cells.

This data has set the precedence for further exploring the role played by the PI3K signalling pathway in HOSCC. Accordingly, the following chapters will attempt to understand a number of underlining mechanisms that are central for a part played by this pathway in cancer, but are unknown in the WHCO and SNO HOSCC series.

Chapter 3
PI3K activation in relation to the status of EGFR expression

3.1 Introduction

Inappropriate activation of the PI3K pro-survival signalling pathway is one of the hallmarks of a deregulated intracellular signalling network that enables the survival of many cancer cells[449]. The EGFR and PTEN are major upstream activators, and inhibitors, of the PI3K signalling pathway respectively[450, 451]. Evidence in the literature has clearly linked this unscheduled activation to mutations and/or overexpression within PI3K, PTEN, EGFR, or the downstream effector, PKB[452, 453, 454, 455]. This is of particular significance to the up-regulated levels of EGFR exhibited by the 5 HOSCC cell lines under investigation in this study[332]. The focus here will be on the EGFR levels with respect to the PI3K signalling pathway, since aberrations within the PTEN gene have been demonstrated to be an extremely rare event in HOSCC[456, 457].

EGFR is an ubiquitous RTK belonging to the ErbB family[17, 136], which are frequently (43-89%) expressed as oncogenes in oesophageal cancer[137]. The signal transducing capability of the ErbB family is inactive when receptors are in isolation, and therefore it is the dimerization that enables effective signal transmission[138]. The EGFR/HER2 heterodimer is most well-studied in terms of their contributions towards cell proliferation and tumorigenesis[458, 459]. Ligand binding to the N-terminal cyteine-rich extracellular domain of EGFR induces receptor homo-and hetero-dimerization, activation of its kinase domain and subsequent autophosphorylation of specific tyrosine residues on its cytoplasmic tail, resulting in the downstream activation of the MAPK, JNK, JAK/STAT, and PI3K signalling pathways. Cellular transformation in breast and oesophageal carcinoma is frequently coupled to mutations within the extracellular/intracellular domain of the EGFR, gene amplifications or protein overexpression[232, 460, 461]. Although these indicators for oncogenic transformation through the EGFR are consistent; based on the initiation and consequent maintenance of the transformed phenotype, which is limited to the tissue from whence it originates; the proclivity for distinct pathway activation by the EGFR in these tumours is still a matter of grave uncertainty. The ligand affinities of EGFR determine the particular downstream pathway scheduled for activation[155]. Relevantly, it was recently shown that

stimulation of the low affinity receptors is specific for the activation of the PI3K pathway[157]. In fact, it is the low-affinity EGFRs that were found overexpressed in the WHCO and SNO HOSCC series[332] suggesting that activation of the PI3K pathway in HOSCC cells should be highly responsive to EGFR activation.

In the absence of EGFR overexpression or activation, a mutual inhibitory relationship exists between the p85α regulatory and p110α catalytic subunits of PI3K, ensuring that its activation exclusively occurs in the presence of external stimuli. While the nSH2 domain of p85α acts as a tethering site for p110α activation by allosteric binding interactions with its C2 and p85α-binding or ABD, p110α phosphorylates p85α on its Ser608 residue, preventing its binding to the EGFR[60, 65] (see Fig. 3.1 for an illustration). It is only upon tyrosine phosphorylation of p85α induced by EGFR activation at the membrane, that this mutual inhibition between these two subunits is alleviated, resulting in PI3K activation (Fig. 3.1).

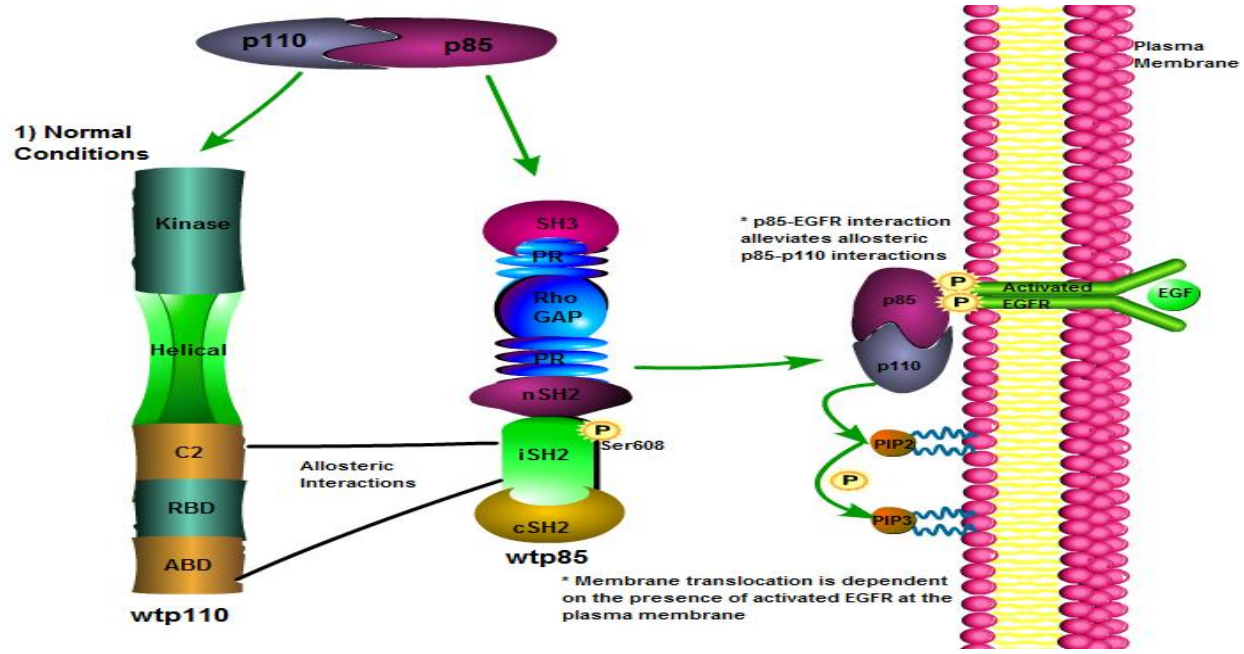
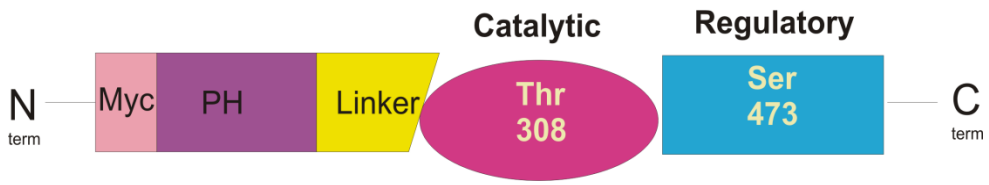


Figure 3.1: EGFR signalling through activation of the PI3K pathway. As highlighted within the text and shown in the figure, when EGFR is inactive, the PI3K heterodimer (p85α/p110α) is localized within the cytoplasm. However, ligand binding (EGF) to the EGFR, induces its homo/heterodimerization to EGFR or HER/ErbB2, resulting in the phosphorylation of its cytoplasmic tail, leading to its activation. This in turn, induces the concomitant membrane recruitment and activation of PI3K by alleviating the mutual inhibitory association that exists between the p85α and p110α PI3K subunits.

In addition to the p85α truncation (addressed in the former Chapter 2, Section 2.1), constitutive activation of PI3K is known to arise from somatic mutations within the gene transcribing the p110α catalytic subunit (PIK3CA)[462]. There are two mutational "hotspots" and two weak PI3K-activating mutations within PIK3CA that are commonly associated with the oncogenic state of a wide variety of cancers[463, 464, 465, 466]. These are primarily found within the p85α-binding domain (R38H, E53K), C2 domain (V344M, C420R), helical domain (E454K, E542K), and the kinase domain (H1047R), each transcribed by exon 1, exon 4, exon 9, and exon 20 respectively.

Generally, cells that overexpress EGFR are known to possess a membrane-biased localization, tyrosine phosphorylation, and thus activation of its downstream proteins[467]. As detailed in the previous chapter (Chapter 2, Section 2.3.3), PI3K is indeed active in four (WHCO1, WHCO5, WHCO6, and SNO) of the HOSCC cell lines, evidenced by its membrane localization and pPKB detection. Furthermore, it was also disclosed that levels of pPKB are negligible in the WHCO3 cell line, and was therefore suggested that this could be a product of mutations within PKB. The PKB protein is comprised of a PH and catalytic domain flanked by a linker and regulatory domain (see Fig. 3.2A). As highlighted previously, the PH domain is central to the activation of PKB via PIP3 at the membrane[355]. Once localized to the membrane, the active confirmation of PKB is now free to be phosphorylated by PDK1 on its Thr308 residue that eventually leads to its full activation via the mTORC2-mediated phosphorylation on its Ser473 residue (see demonstration in Fig. 3.2B). Central to the Ser473 phosphorylation, and activation of PKB, is the Lys179 residue, situated in the Linker domain, in close proximity to the ATP-binding site. The importance of this residue was confirmed by a study performed by Polakiewicz, *et al.*[414], who demonstrated that, when Lys179 was mutated to Alanine, the Ser473 phosphorylation of PKB was prohibited, giving rise to a "kinase-dead" PKB. Amplification of PKB has been discovered in a subset of breast and ovarian cancers[468, 469], also, a novel PKB oncogenic mutation in its PH domain (E17K) has been identified, and suggested to enhance PKB-membrane interactions, conducive for its activation[253, 250, 464, 470]. Since pPKB was found localized to the membrane in the WHCO5, WHCO6, and SNO HOSCC cell lines in the absence of exogenous stimulation (Chapter 2, Section 2.3.6), obviated the need to explore the existence of such a mutation.

A)



B)

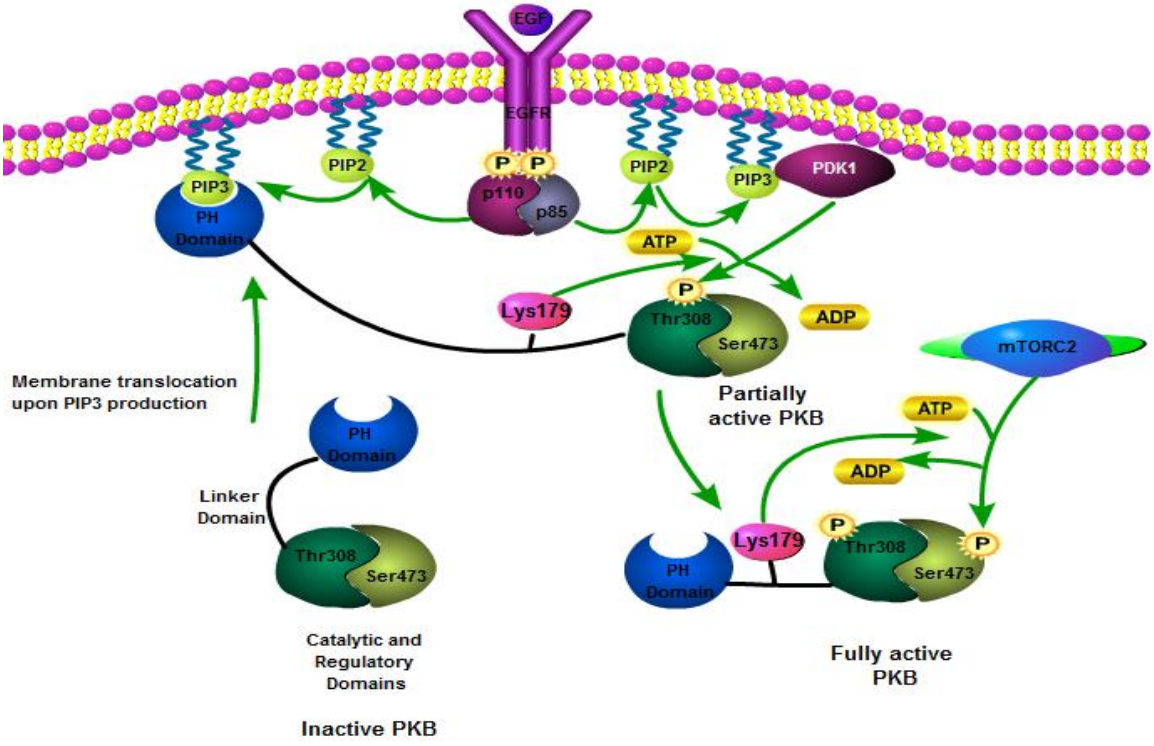


Figure 3.2: Schematic representation of the domain structure and activation mechanism of PKB. A) Domain structure of PKB highlighting the essential catalytic residues and "hotspot" mutations. The PH domain responsible for phosphoinositide-binding contains the "hotspot" E17K mutation, enabling constitutive PKB membrane-binding and activation, and is situated at the N-terminal. The Linker domain, which is part of the catalytic domain, contains the essential Lys179 that catalyzes the phosphate transfer from ATP to the Thr308 and Ser473 residues situated in the catalytic (Thr308), and regulatory or hydrophobic motif (Ser473)[174]. **B)** EGFR activation at the membrane by its ligand activates PI3K which produces PIP3, needed for PDK1 activation, and PKB membrane recruitment. The PH domain of PKB binds to PIP3, inducing an active conformation that makes Thr308 more available for phosphorylation by PDK1. Thr308 phosphorylation of PKB in turn primes it for its Ser473 phosphorylation by the mTORC2 complex, resulting in its full activation. Images created using CorelDRAW version 12® (A), and Pathway Builder Tool Version 2.0 (B) respectively.

The aim for this component of this study was to provide some rationale for the low and absent levels of pPKB established in the previous chapter. First we considered the possibility of mutations within PIK3CA and PKB that could account for the membrane localized and active PI3K in the four HOSCC cell lines, and the lack thereof in the WHCO3 cell line. As the specific downstream events governed by up-regulated EGFR levels in cancer are still a major anomaly[471,472]; our second goal was also to understand how this overexpressed EGFR status within these 5 HOSCC cell lines impacts the PI3K signalling pathway. Previous studies that have reported resistance to LY29; similar to what was observed in the WHCO5 and SNO HOSCC cell lines (Chapter 2, Section 2.3.8), strongly linked this acquired resistance to overexpressed ErbB2[434, 435]. Finally, this chapter sought to clarify the relationship between the overexpressed EGFR and resistance to LY29 featured in the respective HOSCC cell lines.

3.2 Materials and Methods

3.2.1 Cell lines and Culture

As previously described, see Chapter 2, Section 2.2.1.

3.2.2 Antibodies

Rabbit polyclonal antibodies used for immunoblot analysis; anti-PI3 Kinase (p85α) antibody (Upstate Biotechnology), anti-β-Actin (Sigma), and anti-c-Jun (Santa Cruz Biotechnology). Mouse monoclonal antibodies used for immunoblot analysis were the anti-E-cadherin (RD science), anti-phosphoserine (Sigma) and the anti-ErbB2, also referred to as anti-Neu (Santa Cruz Biotechnology). The rabbit polyclonal anti-Phospho-Akt (Ser473) (Cell Signalling Technology), was used to detect PKB/AKT when phosphorylated at Ser473 specifically. The rabbit polyclonal anti-rabbit PI 3-kinase p85α (Santa Cruz Biotechnology), directed against the N-terminal of p85α, was used for immunofluorescent detection. The secondary antibody, HRP-bound goat- anti-rabbit IgG (Sigma), was used for the specific detection of all rabbit polyclonal antibodies for immunoblotting, whereas detection of all monoclonal primary antibodies were specifically detected using the anti-mouse IgG (Fab Specific) peroxidase conjugate secondary antibody. The fluoroscine isothiocyanate FITC-conjugated-goat-anti-rabbit (Chappel, USA) antibody was used for the specific detection of rabbit polyclonal antibodies used during immunoflourescent reactions.

3.2.3 EGFR Activation through EGF Treatment

Cells reaching 60% confluence (see Chapter 2, Section 2.2.1), were incubated under serum conditions in 10 ng/ml EGF (Sigma) for periods of 0.5, 1, 3, 6, 9, and 12 hours (hrs) at 37 ºC at the appropriate CO_2 level. This was done alongside an untreated dish, serving as a control. The 10 ng/ml EGF concentration used in this study was chosen on the basis of four factors; the EGFR is known to be active for a maximum of 24 hrs[473, 474]; and low concentrations of EGF is specific for the activation of the PI3K pathway[157].

3.2.4 Whole cell protein extraction

Following exposure to EGF as outlined above, whole cell protein extractions were carried out as detailed in Chapter 2, Section 2.2.5.

3.2.5 Nuclear Extraction

Following the optimum EGF exposure obtained from an average of three independent experiments, nuclear protein extractions were performed as described in Chapter 2, Section 2.2.6.

3.2.6 Plasma Membrane Extraction

Following the optimum EGF exposure obtained from an average of three independent experiments, nuclear protein extractions were performed as described in Chapter 2, Section 2.2.7.

3.2.7 Plasma membrane enriched extraction used for Immunoprecipitation reactions

A Triton X-100 extraction protocol was performed specifically for the immunoprecipitation reactions; as it has been shown previously to preserve protein-protein interactions, as well as membrane and cytoplasmic associated proteins[475]. Following the optimum EGF exposure obtained from an average of the three independent experiments, tissue culture medium obtained from both EGF-treated and untreated cells reaching was aspirated, and the cells were washed twice in PBS and once in PBS/Trazylol/PMSF (Appendix A 1.5.3.1), before transferring them to a fresh Eppendorf tube. Sequentially, the cells were centrifuged at 1200 X *g* for 3 mins in the TOMY Capsule HF-120 bench top centrifuge. The supernatant was discarded, and the pellet was allowed to resuspend on ice for 2 hrs in 100 µl membrane extraction buffer (see Appendix B 2.1.1), accompanied by gentle tapping every 15 mins. Thereafter, samples were centrifuged at 12 000 X *g* at 4 °C in the Eppendorf Centrifuge 5413, for 10 mins and the consequent supernatant (membrane fraction), was transferred into a fresh Eppendorf and stored at -20 °C prior to investigation.

3.2.8 Protein Estimation

The protein concentration was estimated as detailed in Chapter 2 (Section 2.2.8) on whole cell, nuclear, membrane and Triton-X-100 based extractions described above; see Appendix A 1.6.6 for a representative standard curve.

3.2.9 Polypeptide Resolution and Western Immunoblotting

25 µg of EGF-treated and untreated protein from each cell line obtained from the various extractions (whole cell, nuclear, and membrane) was prepared and separated by 10% SDS-PAGE, and immunoblotted for PI3K (p85α), β-actin, c-Jun, and pPKB as detailed in Chapter 2, Section 2.2.9. Following the procedure described in Chapter 2, Section 2.2.9, the bands

from the treated and untreated membrane extracts were probed with the mouse monoclonal anti-E-cadherin antibody (1:100) for 3 hrs, and thereafter incubated for 1 hr in the HRP-bound anti-mouse IgG for the specific detection of E-cadherin. **Note:** The membrane lysates were denatured before loading by adding an equal amount of single lysis buffer, boiled for 5 mins and centrifuged for 3 secs in the TOMY Capsule HF-120 bench top centrifuge.

3.2.10 Indirect Immunoflourescence Microscopy

Both EGF-treated and untreated cells were grown to 60% confluence, prepared and stained for PI3K (p85α) according to the procedure outlined in Chapter 2, Section 2.2.10.

In addition to PI3K (p85α), the cellular distribution of β-actin in the presence of EGF was used as a comparison against PI3K (p85α) localization, ensuring the specificity of the changes induced by EGFR activation. Similar to p85α, staining for β-actin entailed 1 hour incubation in primary anti- β-actin rabbit polyclonal antibody (Sigma) at 1:100 dilutions, while its detection was made possible through 1 hour incubation in the FITC-goat-anti-rabbit antibody (Chappel, USA) at 1:100 dilutions. Where necessary, immunofluorescent microscopy images were sharpened using Adobe Photoshop to enhance their clarity. **Note:** All immunofluorescence assays were repeated three times, and a negative control was performed for each cell line.

3.2.11 Co-immunoprecipitation analysis of EGFR and PI3K

Following the optimum EGF exposure obtained; membrane-associated protein extractions were performed as described above (3.2.7) on both EGF-treated and untreated cells. Lysates containing 300 μg of protein from each cell line were incubated in 4 μl (1:125) of the mouse monoclonal anti-ErbB2/Neu primary anti-body (Santa Cruz Biotechnology) made up to a total volume of 500 μl with IP (immunoprecipitation) buffer (Appendix B 2.1.2) on a rotor at 4 °C overnight, enabling the formation of antigen (and proteins it interacts with)-antibody complexes. The following day, these complexes were captured by Protein G sepharose beads (Amersham, SA) that were initially washed in 1 ml IP buffer and centrifuged at 12 000 X *g* for 30 secs in the SORVALL® MC 12V centrifuge. The supernatant was aspirated and procedure repeated twice. After the final wash, 30 μl of the Protein G sepharose beads was transferred to each of the protein-antibody complexes and incubated overnight on a rotor at 4 °C. Thereafter, the samples were centrifuged at 12 000 X *g* in the SORVAL for 30 secs and the supernatant removed. 700 μl of IP buffer was added to the pellet (containing EGFR and

associated proteins complexed to the Protein G sepharose beads) and centrifuged as described. The washing procedure was done twice and after the final wash, 50 μl of single lysis buffer (Appendix A 1.5.1) was gently mixed with the beads and boiled for 5 mins, allowing cleavage of ErbB2 and its associated proteins from the agarose beads. Subsequently, the samples were centrifuged at 12 000 X *g* at 4 °C for 10 mins and the supernatants reserved for western blot analysis described above.

3.2.12 Co-immunoprecipitation analysis of serine phosphorylated PI3K

Similarly, 300 μg (from each cell line) of EGF-treated and untreated membrane-associated protein lysates, was incubated on a rotor at 4 °C overnight in 4 μl (1:125) of the mouse monoclonal anti-phosphoserine antibody (Sigma) diluted in 500 μl IP buffer. Thereafter the protocol was carried out as detailed above (see 3.2.11).

3.2.13 Genomic DNA Extraction

According to Samuels, *et al.*[465], genomic DNA is used to detect mutations within the PIK3CA gene. Genomic DNA was extracted from 5 x 10^6 cells using the DNeasy Tissue Kit (50) (Qiagen), according to the manufacturer's instructions. The DNeasy extraction is a simple procedure that enables the extraction of high-quality DNA without organic extraction or ethanol precipitation, by direct DNA binding to the DNeasy membrane. The recovery of DNA was assessed on a 0.5% agarose gel.

3.2.14 PCR

The presence of "hotspot" mutations present within the PIK3CA gene (NM_006218.2 for mRNA and NW_001838884 for genomic DNA) was evaluated using the following universally used and published primers[476]: see Appendix B 2.3 for detailed description of region amplified for each exon.

Region Amplified:	FW:	RW:
EXON 1	5'- CTCCACGACCATCATCAGG -3'	5'-GATTACGAAGGTATTGGTTTAGACAG-3'
EXON 9	5'-GATTGGTTCTTTCCTGTCTCTG-3'	5'-CCACAAATATCAATTTACAACCATTG-3'
EXON 4A	5'-TCTTGTGCTTCAACGTAAATCC-3'	5'-CGGAGATTTGGATGTTCTCC-3'
EXON 4B	5'-TCTCAACTGCCAATGGACTG-3'	5'-CGGAGATTTGGATGTTCTCC-3'
EXON 20	5'-TGGGGTAAAGGGAATCAAAAG-3'	5'-CCTATGCAATCGGTCTTTGC-3'

The same PCR conditions were used for all five exons. Thermal cycle conditions included an initial heating at 95 °C for 10 mins, followed by 32 cycles of; denaturation at 95 °C for 10 mins, annealing at 54 °C for 1 min, extension at 72 °C for 1 min, followed by a final

elongation at 72 °C for 10 mins. The breast MCF7 and colon HT29 cell lines bear the common exon 9 (E454K) and exon 20 (P337T) mutations, and thus served as controls for sequencing analysis of these two regions specifically. Two forwards primers were used for the PCR amplification of the C2 domain (exon 4), as there is a splice site within the genomic sequence of exon 4[465]. PCR fragments were visualized on a 1% agarose gel, and sent to Inqaba Biotech® for sequencing. Representative sequence traces can be viewed in Appendix B 2.6.

3.2.15 Total RNA extraction

As detailed in Chapter 2, Section 2.2.2.

3.2.16 Amplification of PKB1 by RT-PCR

3.2.16.1 Reverse Transcription

As detailed in Chapter 2, Section 2.2.3.1

3.2.16.2 PCR

PCR was carried out as detailed in Chapter 2, Section 2.2.3.2. Primers for PKB (NM_005163.2) were designed to specifically amplify the PH domain, Linker domain, and two regions on the Catalytic domain (Thr308 and Ser473), using the web-based interactive primer design program, Primer3 (see Appendix B 2.3 for primer design and sequence analysis). The primers used were as follows:

Region Amplified:	FW:	RW:
PH Domain	5'-GGCTCTGGACTCCCGTTT-3'	5'-AAGGTGCGTTCGATGACAGT-3'
Linker Domain	5'-ATCCAGACTGTGGCTGACG-3'	5'-TTGGCGTACTCCATGACAAA-3'
Ser473	5’-GACGCCAAGGAGATCATGCAG-3’	5’-GGCTTCTCTCAAATGCACCCG-3’
Thr308	5'-CGAGCTGTTCTTCCACCTGT-3'	5'-CTTCTTGAGCAGCCCTGAAA-3'

The same PCR conditions were used for all four exons. Thermal cycle conditions included an initial heating at 95 °C for 5 mins, followed by 32 cycles of; denaturation at 95 °C for 45 secs, annealing at 56 °C for 1 min, extension at 72 °C for 1 min, followed by a final elongation at 72 °C for 10 mins. PCR fragments were visualized on a 1% agarose gel, and sent to Inqaba Biotech® for sequencing. Representative sequence traces can be viewed in Appendix B 2.8.

3.2.17 Densitometry

Labworks TM Image Acquisition and Analysis software (Labworks version 4.5) was used for densitometric analysis to semi-quantitatively determine the concentration level of PI3K (p85α), and pPKB detected through western blotting. **Note:** The densitometric results are an average of three independent experiments and expressed as a percentage relative to the maximum.

3.2.18 Image Capturing

All western blot and SDS-PAGE images were captured on a Hewlard Packard Scanjet 4400c series scanner at 300dpi, contrast and brightness of all images were standardised using CorelDRAW version 12®.

3.2.19 Statistical Analysis

Statistical analysis results are inclusive of at least three independent experiments (mean ± S.D). P-values are given in the figure legends, and values of $P > 0.05$ were considered not to be significant. Statistical analyses were performed using Student's paired *t* test and One Way Repeated Measures Analysis of Variance (Holm-Sidak Method). All calculations of statistical computations were carried out using the SigmaPlot Release 11.0® statistical software. **Note:** Based on the fact that statistical analysis requires a minimum of three independent experiments, an example of the three blots for the figures in this chapter was chosen (i.e. nothing is gained by showing all three).

3.2.20 Figure Design

All schematic diagrams were designed using the Pathway Builder Tool version 2.0, unless otherwise stipulated.

3.3 Results

3.3.1 EGFR activation effects the expression of PI3K (p85α) in HOSCC cells.

The activational state of the PI3K/PKB signalling pathway in HOSCC has been established in the previous chapter. These cell lines all overexpress the EGFR, albeit to unique levels[332]. The influence of these overexpressed EGFR levels on the PI3K/PKB pathway was investigated by activating the EGFR through exposure to EGF. Under standard tissue culture conditions, PI3K (p85α) protein levels were increased significantly ($P<0.001$) in response to EGFR activation at 0.5 and 1 hr in the WHCO1, WHCO6, and SNO HOSCC cell lines respectively (shown in Fig. 3.3). This result is consistent with the significant increase in the concentration of PI3K (p85α) protein illustrated in the control MCF7 ($P<0.001$) and HT29 ($P<0.004$) cell lines following EGFR activation at 0.5 hrs. For the sake of clarity two line graphs are provided. The first allows us to unequivocally analyse the statistical significance of PI3K (p85α) expression (Fig. 3.3B), and the second merely mimics the graphical representation of these changes to ensure visual simplicity (Fig. 3.3C). No significant change in PI3K (p85α) was demonstrated in the WHCO3 cell line, while the WHCO1, WHCO5, and SNO cell lines showed a significant ($P<0.001$) drop in the concentration of PI3K (p85α) consequent to EGFR activation at 12 hrs (Fig. 3.3).

3.3.2 PI3K (p85α) localizes to the membrane in response to EGFR activation.

To elucidate whether the membrane localization of PI3K (p85α) was influenced by EGFR activation; the activation of EGFR was induced by exposing cells to EGF for 0.5 hrs. Consistent with the increase observed following EGFR activation above (see Fig. 3.3), PI3K (p85α) staining conferred a more prominent membrane distribution in the WHCO1, WHCO5, WHCO6 and SNO HOSCC cell lines exclusively (shown in Fig. 3.4, *blue arrows*). This was identified by PI3K (p85α) differentiating from a faint peri-nuclear, limited cytoplasmic and nuclear localization to a highly membranous location. Interestingly, PI3K (p85α) exhibited a greater cytoplasmic staining upon EGFR activation in the WHCO6 and SNO cell lines as opposed to the more diffuse cytoplasmic localization in the remaining cell lines. Whereas this increase was evident, membrane localization of PI3K (p85α) was still found in the HOSCC cell lines in the absence of EGFR activation (Fig. 3.4). This is consistent with the HT29 and MCF7 cell lines, that maintained their membrane and nuclear PI3K (p85α) localization

following EGFR activation (Fig. 3.4), suggesting that the EGFR overexpressed state in these HOSCC cell lines is insufficient to maintain the observed membrane-biased PI3K.

3.3.3 Nuclear and membrane levels of PI3K (p85α) as a result of EGFR activation.

To quantify the observed nuclear and membrane staining for PI3K (p85α) following EGFR activation (Fig. 3.4), western blot analysis was performed on plasma membrane-specific and nuclear-specific extracts consequent to a 0.5 hr EGF exposure. Western blot analysis confirmed a significant ($P<0.05$) increase in the plasma membrane expression of PI3K (p85α) subsequent to EGFR activation in the WHCO1, WHCO5, and SNO HOSCC cell lines respectively (demonstrated in Fig. 3.5). PI3K (p85α) at the plasma membrane in the remaining two cell lines (WHCO3 and WHCO5) were unchanged post EGFR activation. Furthermore, most of the HOSCC cell lines, excluding the WHCO5 cell line, displayed a clear drop in the nuclear levels of PI3K (p85α) as a result of EGFR stimulation. As indicated in Fig. 3.5, the concentration of PI3K (p85α) increased in the nucleus of the WHCO5 cell line; corroborating with the visual evidence shown above (Fig. 3.4).

A)

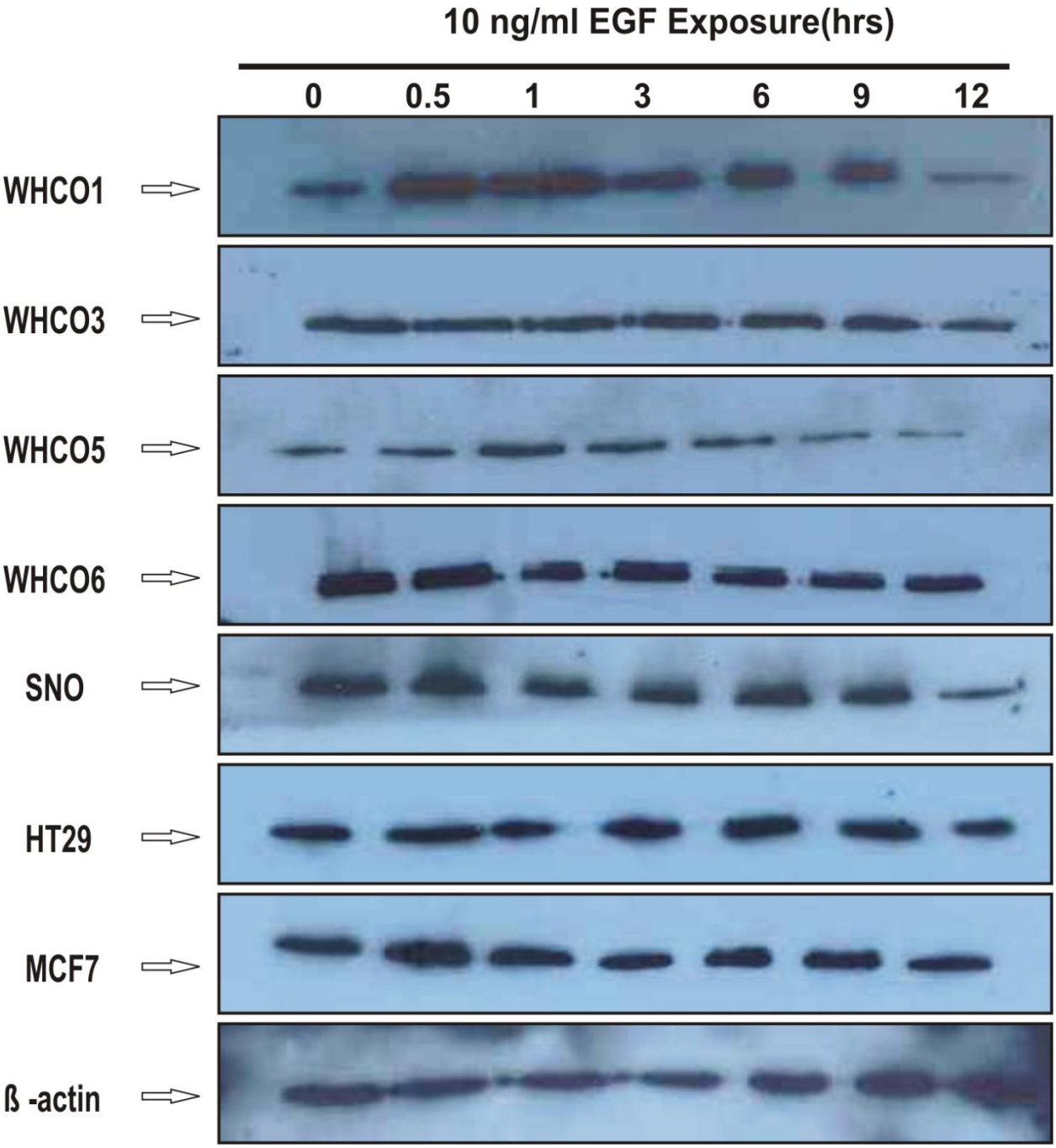
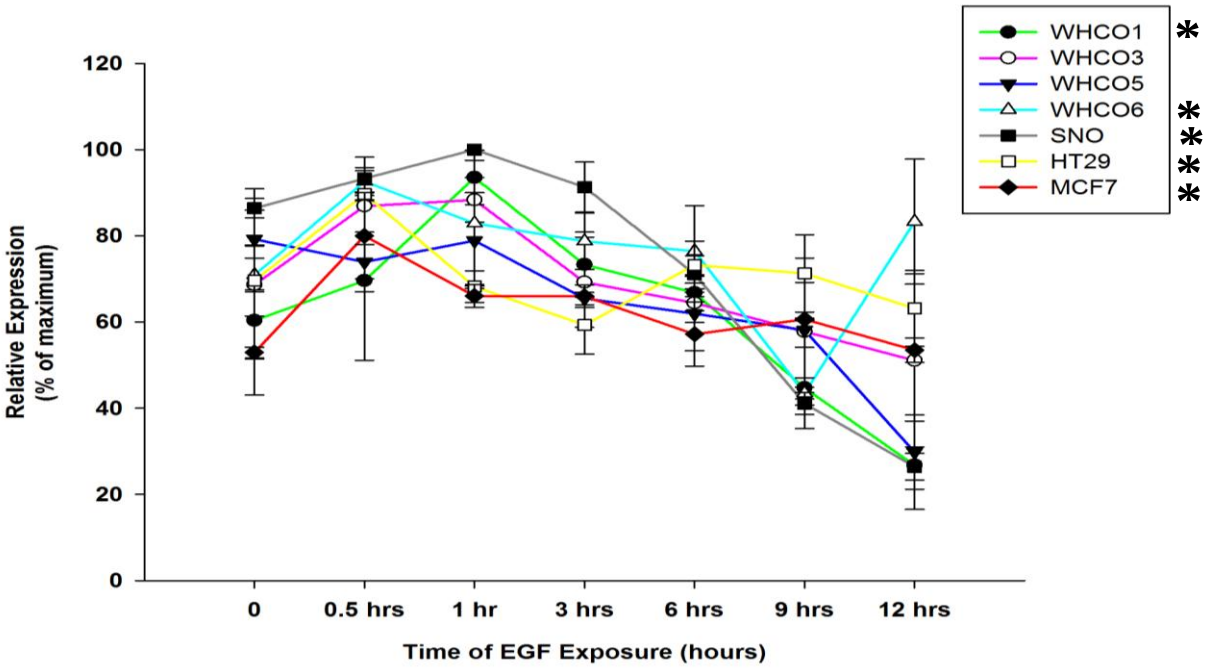


Figure 3. 3 A): EGF modulates the protein expression of PI3K (p85α) subsequent to activation of the EGFR. The 5 HOSCC cell lines, along with the MCF7 and HT29 control cells were treated with 10 ng/ml of EGF for intervals of 0.5, 1, 3, 6, 9, and 12 hrs (see Appendix A 1.6.6 and 1.7.5 for standard curve and 10% SDS-PAGE). Western blot analysis revealed the protein expression of PI3K (p85α) consequent to EGF exposure, detected at 85kDa. β-actin was used as a loading control. Results shown are representative of three independent experiments.

B)



C)

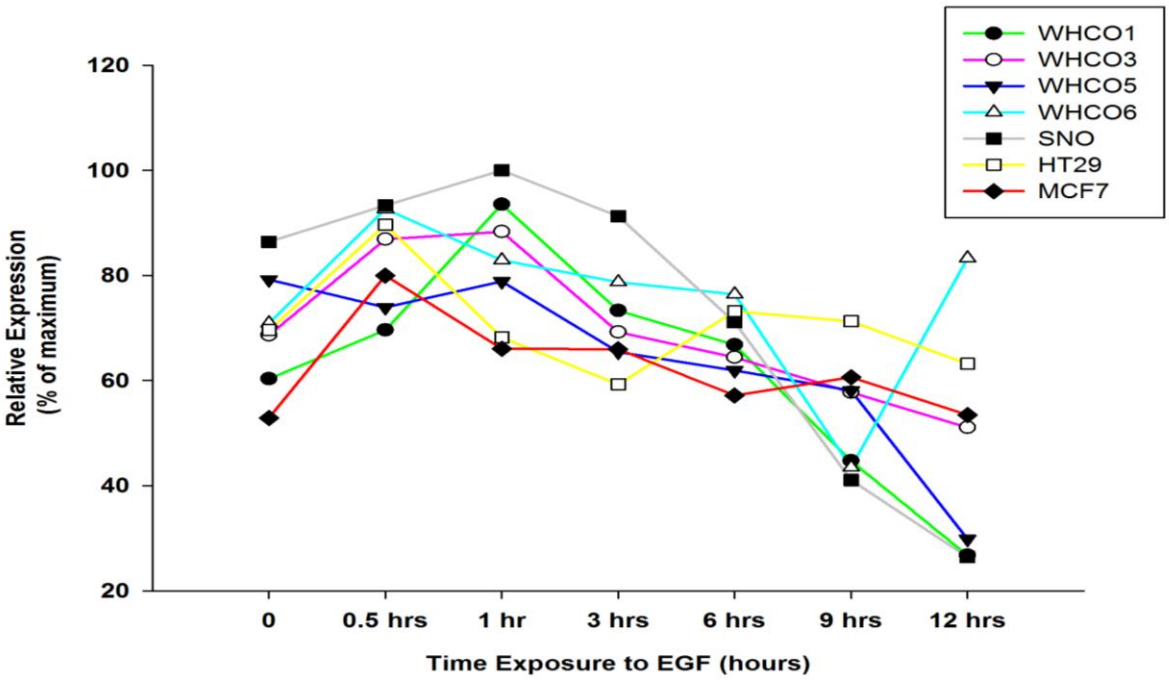
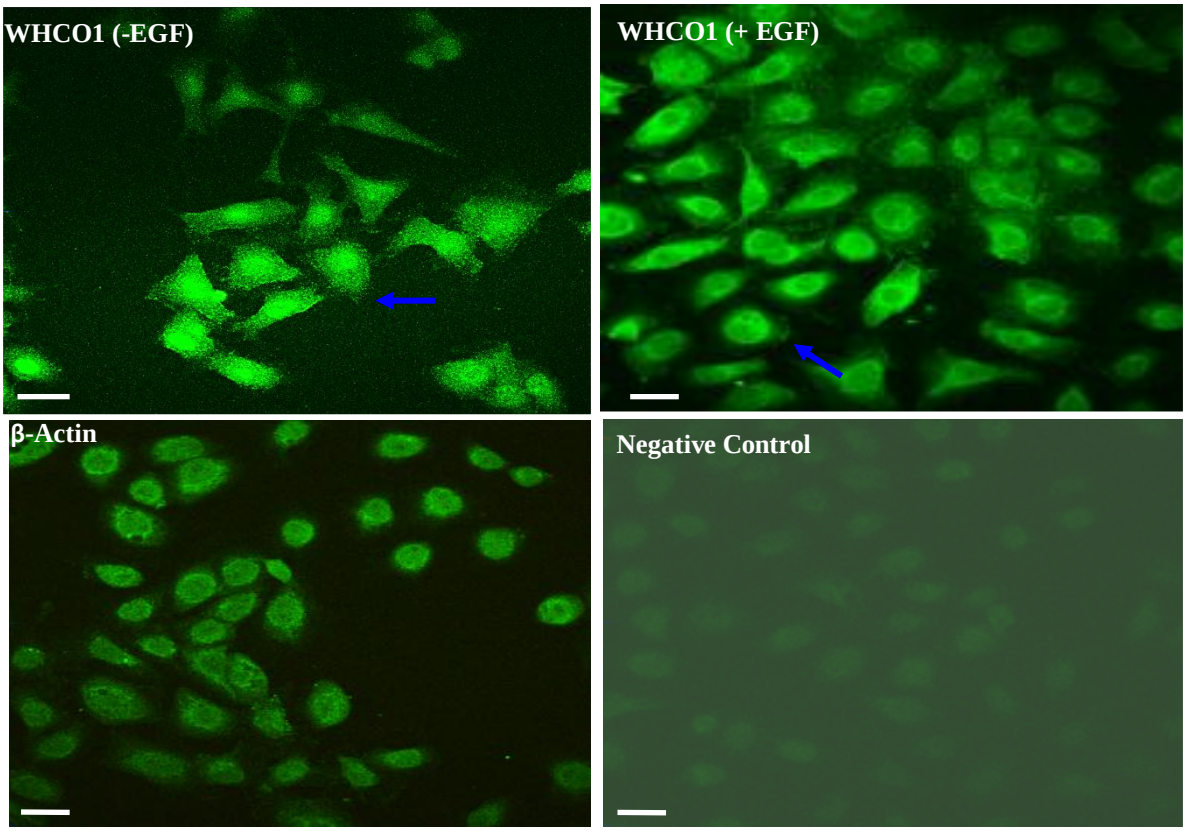
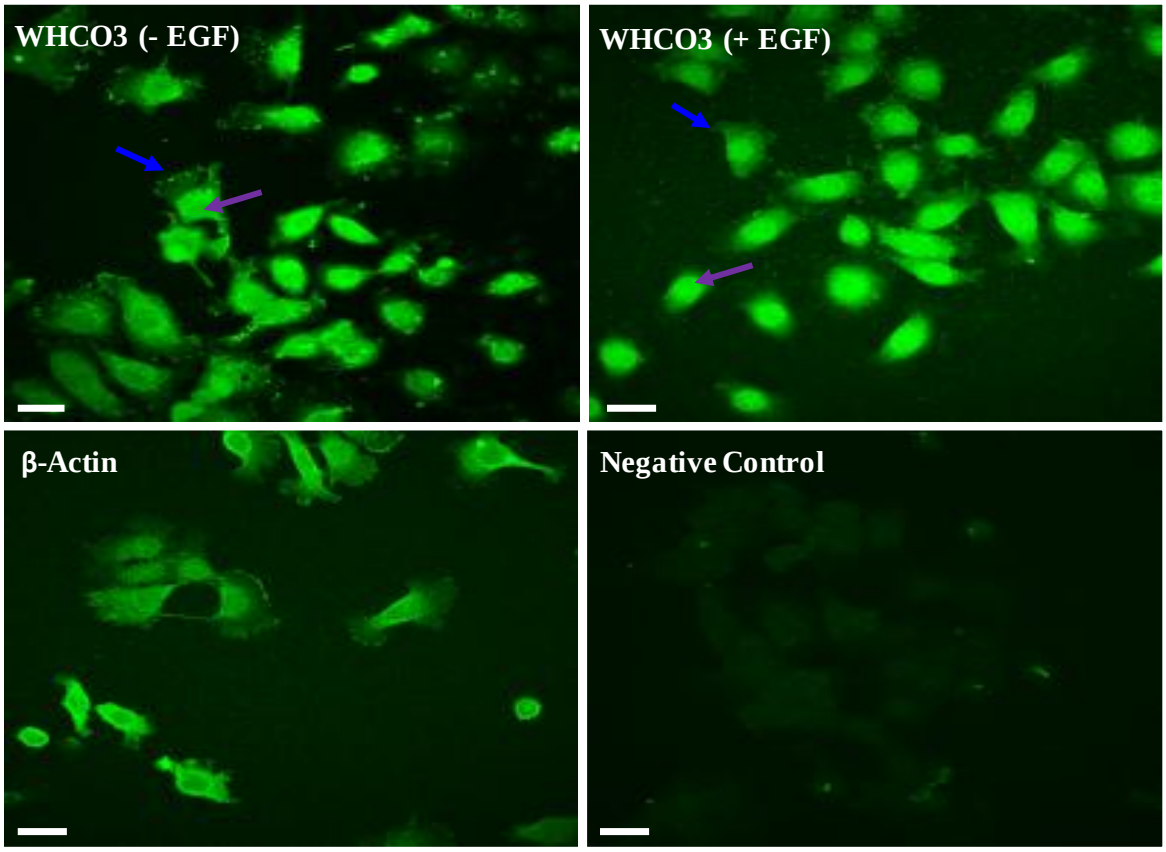


Figure 3.3 B) and C): Line graph of densitometric analysis of the western blot detection of PI3K (p85α), showing statistical analysis of the significant increase in its levels following 0.5 and 1 hr activation of EGFR **(B)**. Note: Results represent mean ± S.D. from the three separate experiments, *significantly different from control, $P<0.05$. **C)** Bar graph, excluding the statistical analysis used for the biological comparison of PI3K (p85α) expression following EGFR activation. See Appendix B 2.2, Table B1 for statistical analysis.

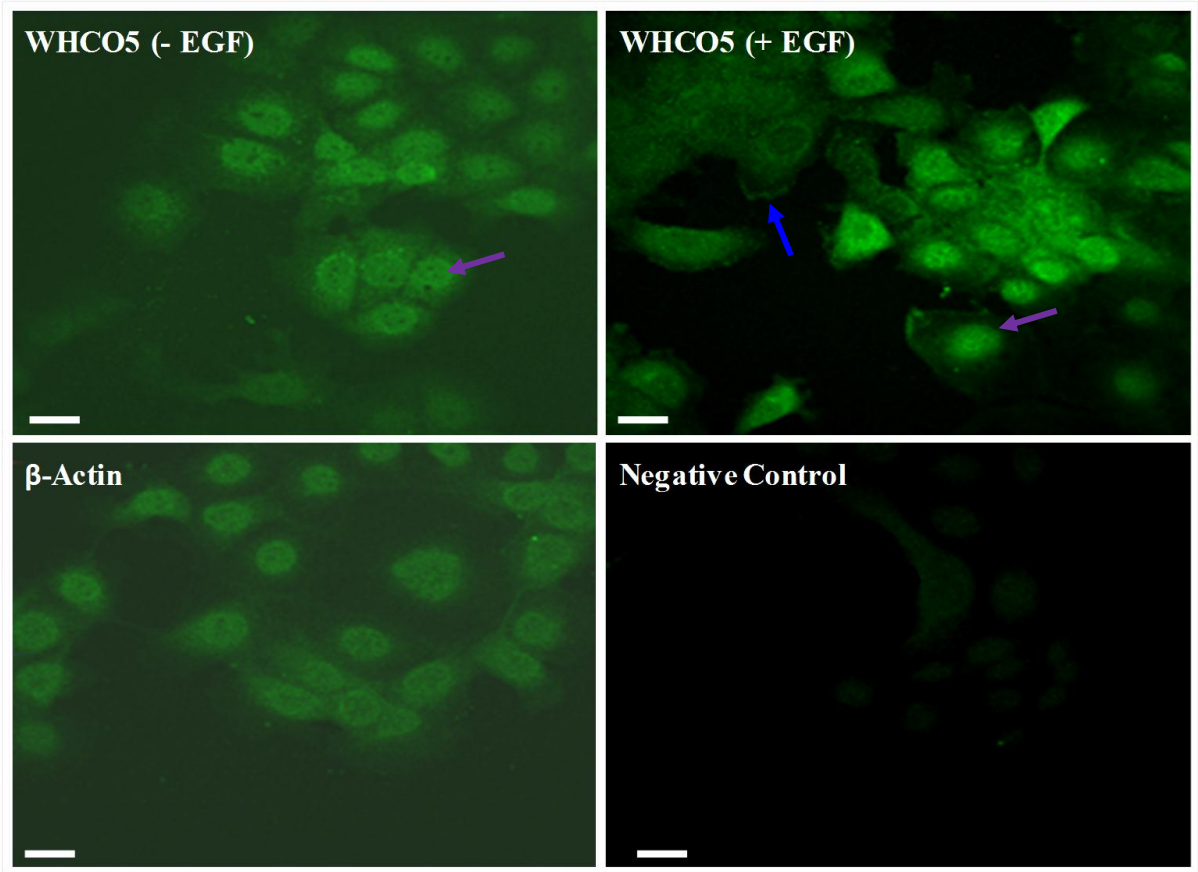
A)


WHCO1 (-EGF)
WHCO1 (+ EGF)
β-Actin
Negative Control

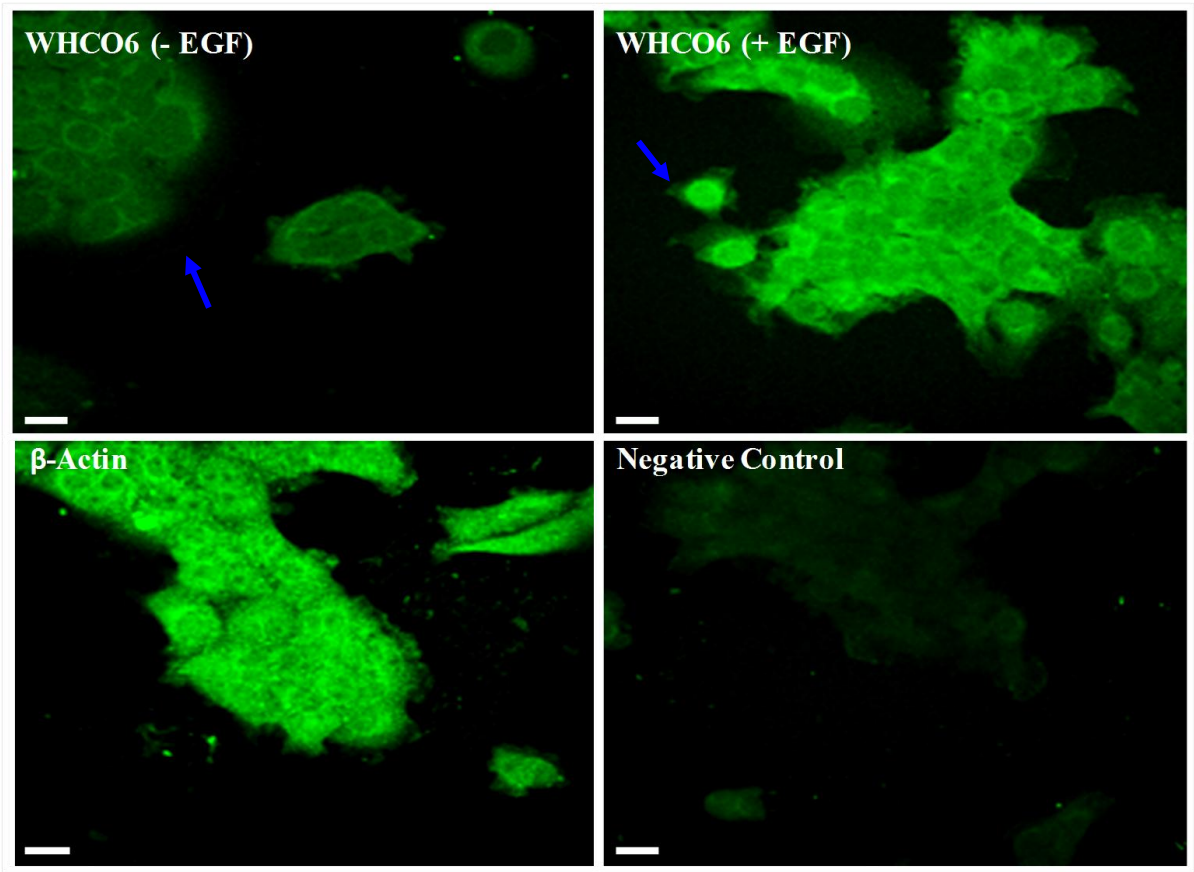
B)


WHCO3 (- EGF)
WHCO3 (+ EGF)
β-Actin
Negative Control

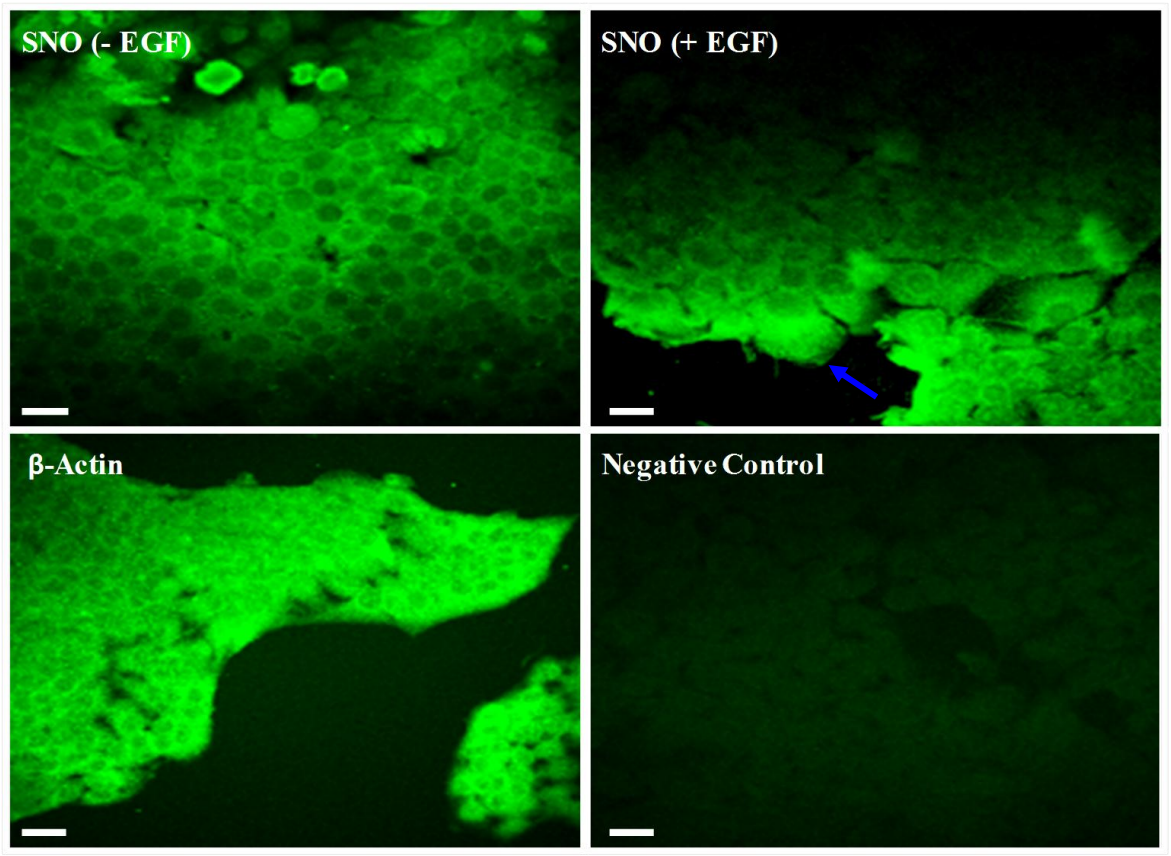
C)


WHCO5 (- EGF)
WHCO5 (+ EGF)
β-Actin
Negative Control

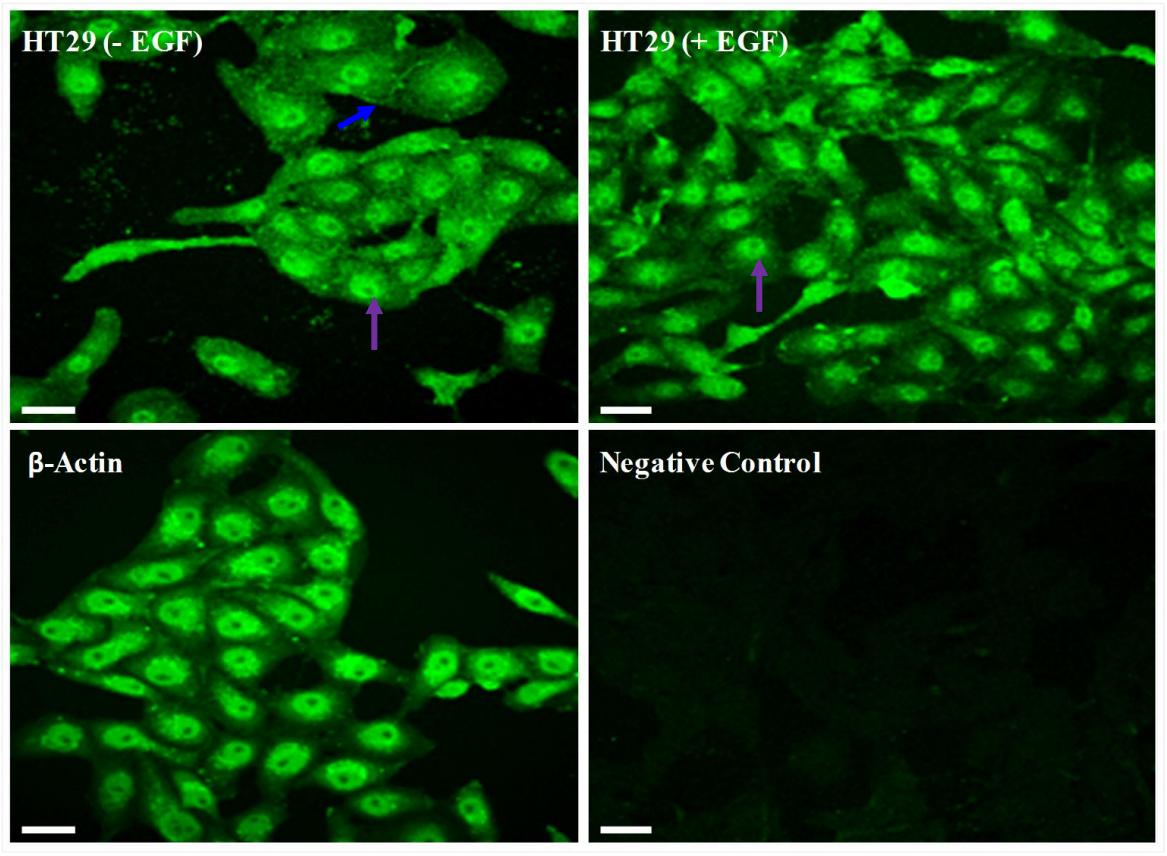
D)


WHCO6 (- EGF)
WHCO6 (+ EGF)
β-Actin
Negative Control

E)


SNO (- EGF)
SNO (+ EGF)
β-Actin
Negative Control

F)


HT29 (- EGF)
HT29 (+ EGF)
β-Actin
Negative Control

G)

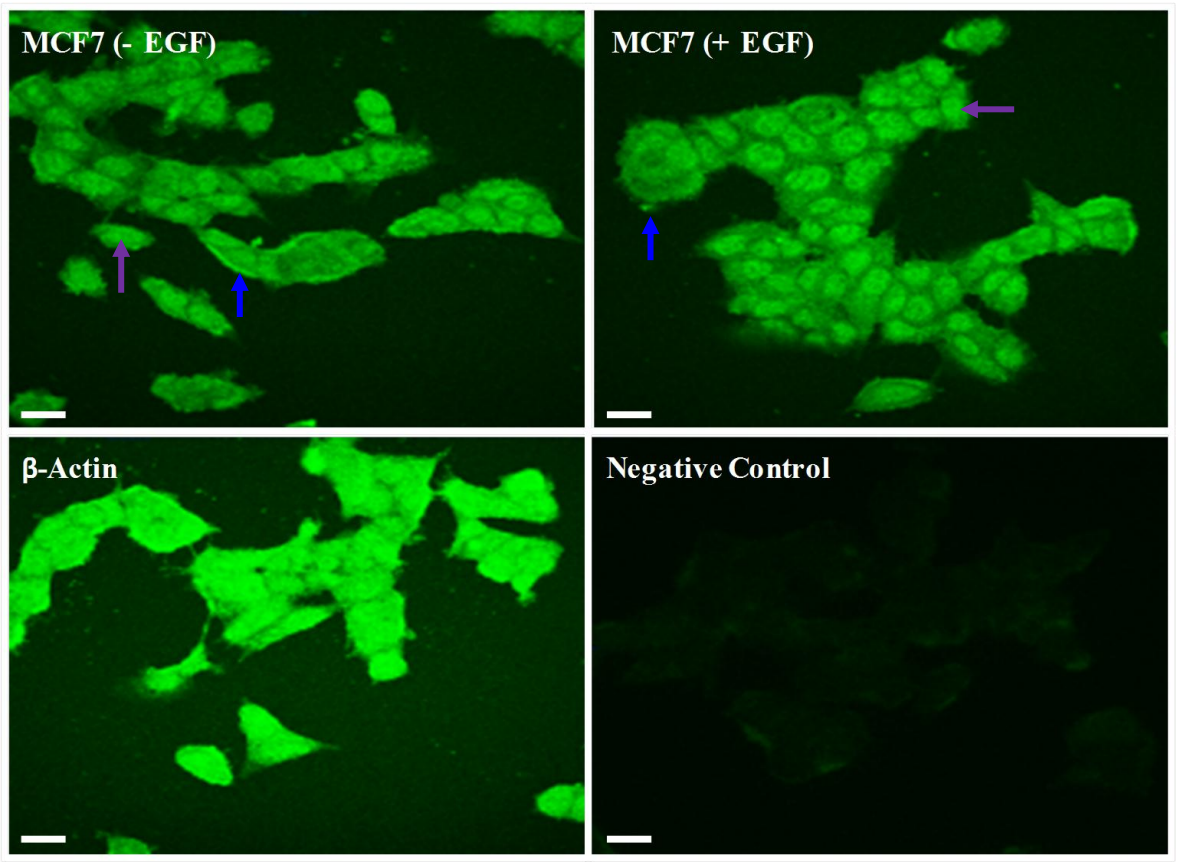


Figure 3.4: Three of the HOSCC cell lines display a more pronounced PI3K (p85α) membrane and nuclear localization subsequent to EGFR activation post 0.5 hr EGF stimulation. Immunoflourescent detection of the cellular localization of p85α in EGF-treated (+EGF) and untreated (-EGF) HOSCC cells (A-E), and the MCF7 (F) and HT29 (G) control cell lines. Membrane-specific (blue arrow) and possible nuclear staining (purple arrow) highlighted, and to a lesser degree, cytoplasmic staining can also be observed. Similarly, β-actin expression was detected to ensure that any changes in p85α localization consequent to EGF treatment are unique. Under equivalent conditions, little or no staining was detected in the negative control, indicative of staining specificity. Bar column=25µm.

A)

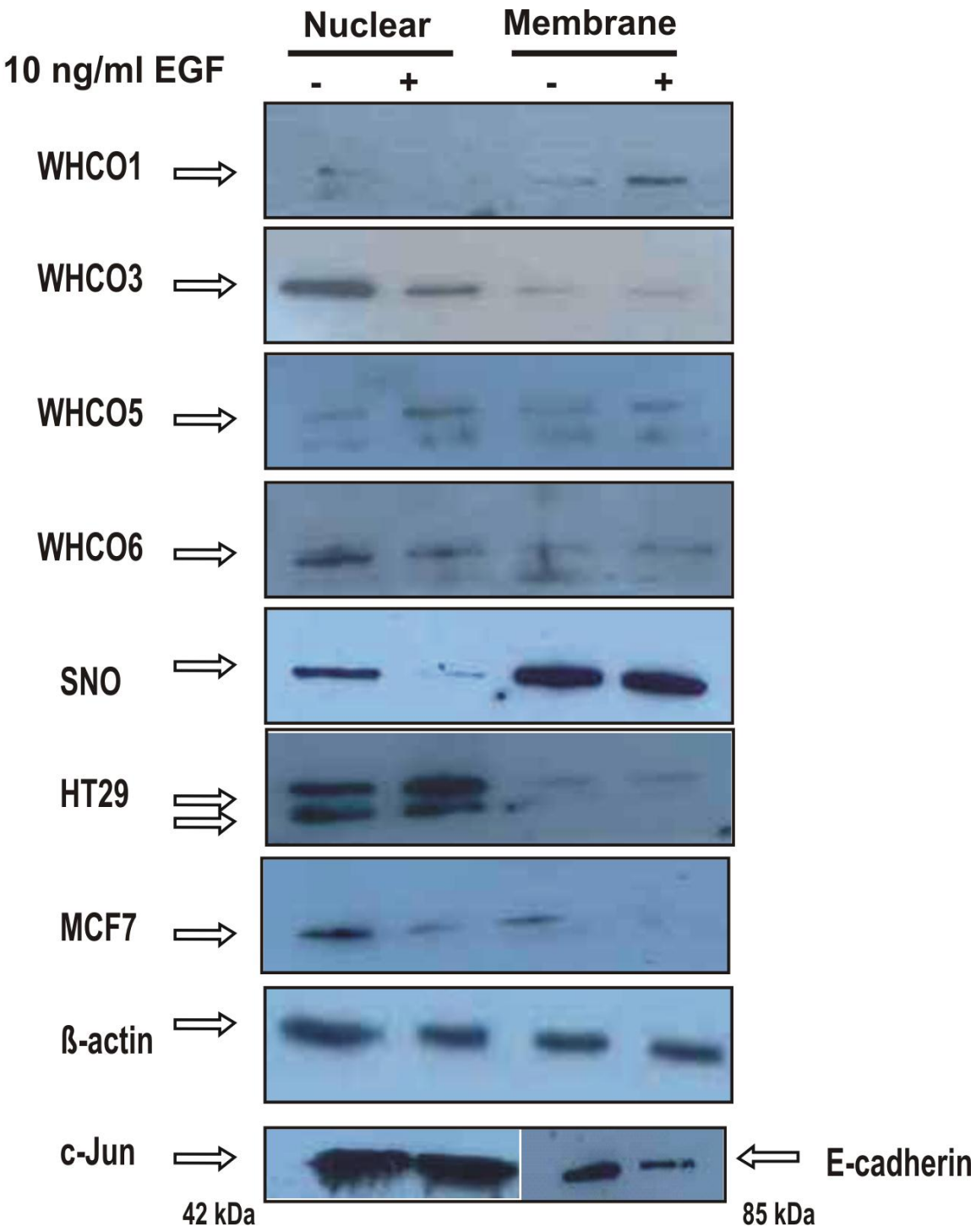


Figure3. 5: Active EGFR modulates the nuclear and membrane expression of PI3K (p85α). A) EGFR activation influenced the membrane expression of p85α, whereas the overall nuclear levels of p85α were down-regulated (see Appendix A 1.6.6 and 1.7.5 for standard curve and 10% SDS-PAGE). β-actin was used as a loading control. The integrity of the nuclear and membrane extracts were assessed through the western blot detection of c-Jun and E-cadherin respectively.

B)

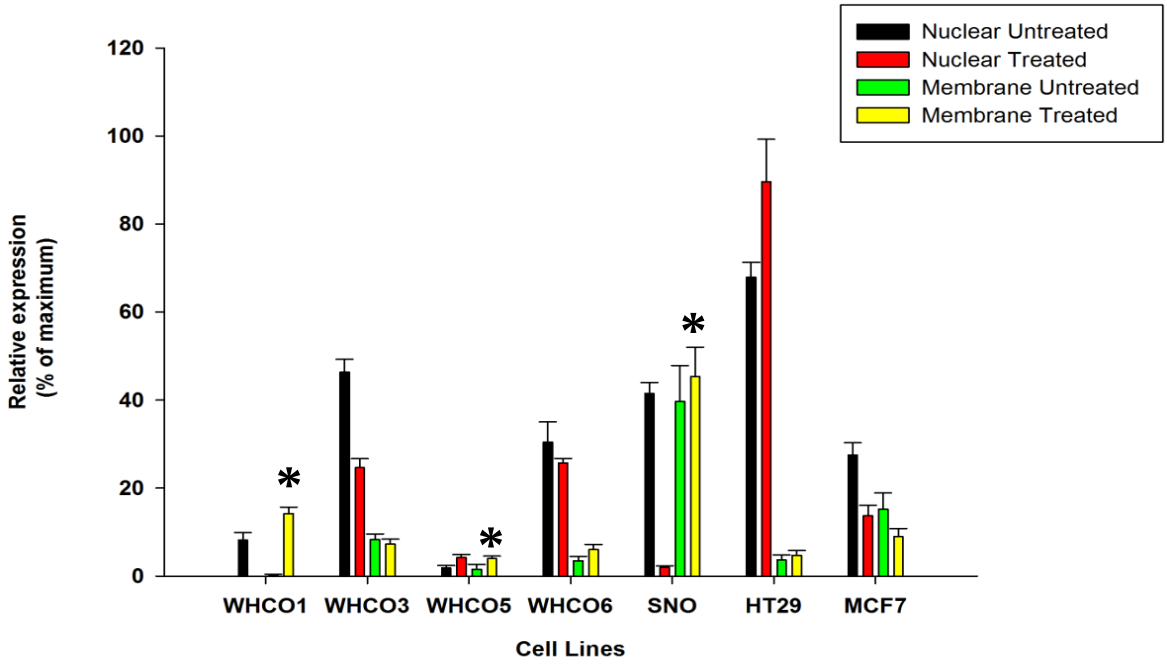


Figure 3.5 B): Bar graph of densitometric analysis of the nuclear and membrane western blot detection of PI3K (p85α), showing a significant increase in its membrane levels in the WHCO1 (P=0.005), WHCO5 (P=0.035), and SNO (P=0.036) HOSCC cell lines following a 0.5 hr activation of EGFR. Note: Experiments were performed three times for PI3K (p85α) detection mean ± S.D. from the three separate experiments, *significantly different from control, P<0.05. Therefore results represent mean S.E. from the three separate experiments. See Appendix B, Table B2 for statistical analysis.

3.3.4 The state of PI3K (p85α) serine phosphorylation and its association with ErbB2.

In quiescent or unstimulated cells, little or no association exists between p85α and the EGFR[70]. Additionally, the Ser608 phosphorylation of p85α mediated by the catalytic p110α subunit of PI3K keeps it in an inactive state, which is only alleviated upon binding to the EGFR[61]. On the basis that PI3K (p85α) was shown localized to the plasma membrane, which was also significantly enhanced in response to EGFR activation (see Fig. 3.4 and Fig. 3.5), the effect that EGFR activation has on the plasma membrane activities of PI3K (p85α) in HOSCC cells was investigated through assessment of its overall serine phosphorylation status and association to the EGFR. The affinity between PI3K (p85α) and ErbB2 was used as a marker for its corresponding association to the EGFR, since complete activation of the EGFR is not possible without ErbB2[477].

As can be seen in Fig. 3.6, in the absence of EGF stimulation, PI3K (p85α) is weakly associated to the ErbB2 in the majority of the HOSCC cell lines, while a strong association was evident in the WHCO6 cell line. This association was augmented upon EGFR activation in the WHCO5 and SNO cell lines. No increase in the association between PI3K (p85α) and ErbB2 was seen post EGFR activation in the WHCO1 and WHCO3 HOSCC cell lines. Consistent with their ErbB2-null status, PI3K (p85α) was not found associated with ErbB2 in the MCF7[478] and HT29[479] cell lines (Fig. 3.6), confirming the specificity of this reaction.

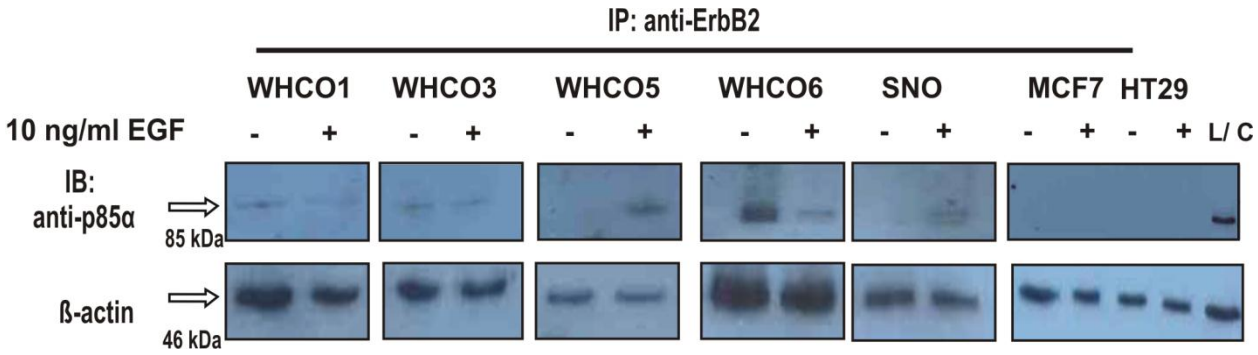


Figure 3. 6: EGFR activation has a minimal effect on its association to PI3K (p85α) in HOSCC cells. Immunoblot detection (IB) of PI3K (p85α) was identified in the ErbB2 immunoprecipitates (IP) in the WHCO1, WHCO3, and WHCO6 HOSCC cell lines. This association was enhanced post EGFR activation in the WHCO5 and SNO HOSCC cell lines exclusively, while a decreased affiliation was detected in the WHCO1, WHCO3, and WHCO6 HOSCC cell lines. An equal amount of protein was immunoprecipiated and loaded (See Appendix A 1.6.6 for representative standard curve). No association between PI3K (p85α) and ErbB2 was identified in the ErbB2-null MCF7 and HT29 control cell lines, affirming the specificity of the reaction. The presence of a band in the positive WHCO6 whole cell protein extract (C) confirms that the band detected at 85 kDa is indeed the p85α subunit of PI3K. These experiments were executed purely for the detection and not strength of an ErbB2-p85α association, and therefore no quantifiable data was required.

Corresponding to its low ErbB2 association, stimulation of EGFR had no significant impact on the overall serine phosphorylation state of PI3K (p85α) (shown in Fig. 3.7). Consistent with its weakened association to the ErbB2 post EGFR activation in the WHCO3 cell line (see Fig. 3.6), PI3K (p85α) serine phosphorylation increased accordingly (Fig. 3.7). Surprisingly, no PI3K (p85α) serine phosphorylation was detected prior or subsequent to EGFR activation in the WHCO1 cell line (Fig. 3.7).

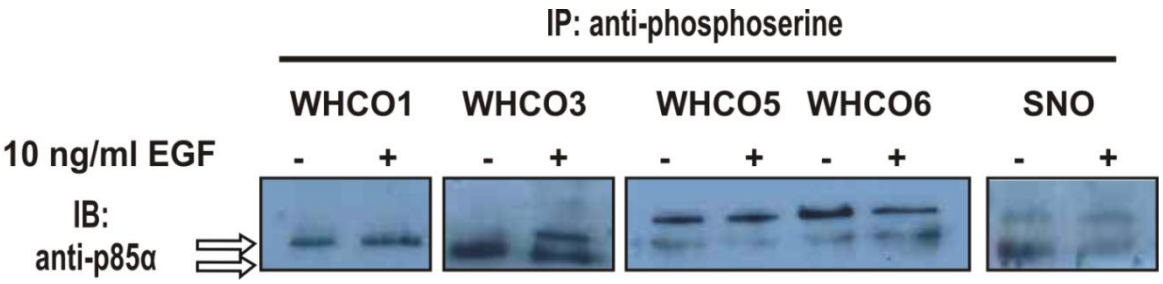


Figure 3. 7: EGFR activation does not reduce the overall serine phosphorylation status of PI3K (p85). Western immunoblot (IB) analysis of anti-phosphoserine immunoprecipitates (IP) verifies an uninterrupted overall serine phosphorylation state of PI3K (p85α) in the WHCO5, WHCO6, and SNO HOSCC cell lines post EGFR activation. Activation of EGFR enhanced p85α serine phosphorylation in the WHCO3 cell line exclusively. No serine phosphorylation was detected in the WHCO1 cell line. p85α was detected at 85 kDa with an IgG present at 60 kDa.

3.3.5 Activation of the PI3K/PKB signalling pathway in relation to the EGFR expression status in HOSCC cells.

The importance of PI3K in the Ser473 phosphorylation and activation of its downstream target, PKB, was established in the previous chapter (see Chapter 2, Section 2.3.7). It was also revealed that pPKB is greatly reduced in the WHCO3 cell line. Since these HOSCC cell lines are known to overexpress the EGFR, it became necessary to evaluate its influence on the pPKB status. To study the effect of EGFR overexpression, cells were exposed to EGF at various time intervals. EGFR activation induced a significant up-regulation in pPKB at unique intervals in the WHCO1 (75%) and WHCO5 (85%) cell lines respectively ($P<0.0001$, shown in Fig. 3.8), whereas its expression appeared to be unaltered in the WHCO6 and SNO HOSCC cell lines. For the sake of clarity, the results are presented in two line graphs. The first highlights the statistical analysis of pPKB expression levels and includes error bars (Fig.

3.8B). The second merely mimics the first such that changes and trends are highlighted (Fig. 3.8C). Up-regulation in pPKB resulting from EGFR activation at 0.5, 1 and 3 hrs was obtained in the MCF7 and HT29 cell lines ($P<0.0001$, Fig. 3.8), even though low levels of EGFR are present within these lines[480, 481]. Surprisingly, no apparent increase in levels of pPKB following EGFR stimulation was evident in the WHCO3 cell line, despite it possessing an overexpressed EGFR and membrane localized PI3K (p85α) (see Fig. 3.2).

3.3.6 Wild-type PIK3CA is expressed in HOSCC cells.

Mutations within the gene transcribing the PI3K p110α catalytic subunit (PIK3CA) have been shown to abrogate the activation of PKB through EGFR, leading to its constitutive activation[239 and 245]. As highlighted previously, these activating mutations in the PIK3CA gene are clustered around exon 1 (p85α-binding domain), exon 4 (C2 Domain) exon 9 (helical domain), and exon 20 (kinase domain)[482]. We have demonstrated augmentation of the PI3K/PKB pathway following EGFR activation in the WHCO1 and WHCO5 HOSCC cell lines (see Fig. 3.8), whereas the remaining cell lines showed no apparent changes. These data prompted the investigation of the mutational status of PIK3CA. Furthermore, and although it has not been reported, this investigation should shed some light on whether the undetectable levels of pPKB in the WHCO3 cell line are attributable to inactivating mutations within the PIK3CA gene. To amplify the four mutational "hotspot" regions, genomic DNA (Fig. 3.9) was used as a template for the PCR amplification. The presence of band at 420 bp and 450 bp are indicative of the successfully amplified fragments representing exon 1 and exon 9 respectively (seen in Fig. 3.10). No mutations were found within exon 1 in all the 5 HOSCC cell lines (see Appendix B 2.5 for representative sequence trace). Making use of the known G1633A (E454K) mutation present in the MCF7 cell line[330], absence of this mutation in the 5 HOSCC cell lines was affirmed through sequence analysis; see Fig. 3.10C for a representative sequence trace. Amplification of exon 20 and the two splice variants from exon 4 (exon4 A and B) produced PCR fragment sizes of 550 bp, 350 bp, and 500 bp accordingly (see Appendix B 2.4, Fig. B4 for PCR gels). The absence of these "hotspot" mutations in the 5 HOSCC cell lines was confirmed through sequence analysis using the mutational-free state of both these exons present in the MCF7 cell line as a control; see Appendix B 2.5 for representative sequence traces.

A)

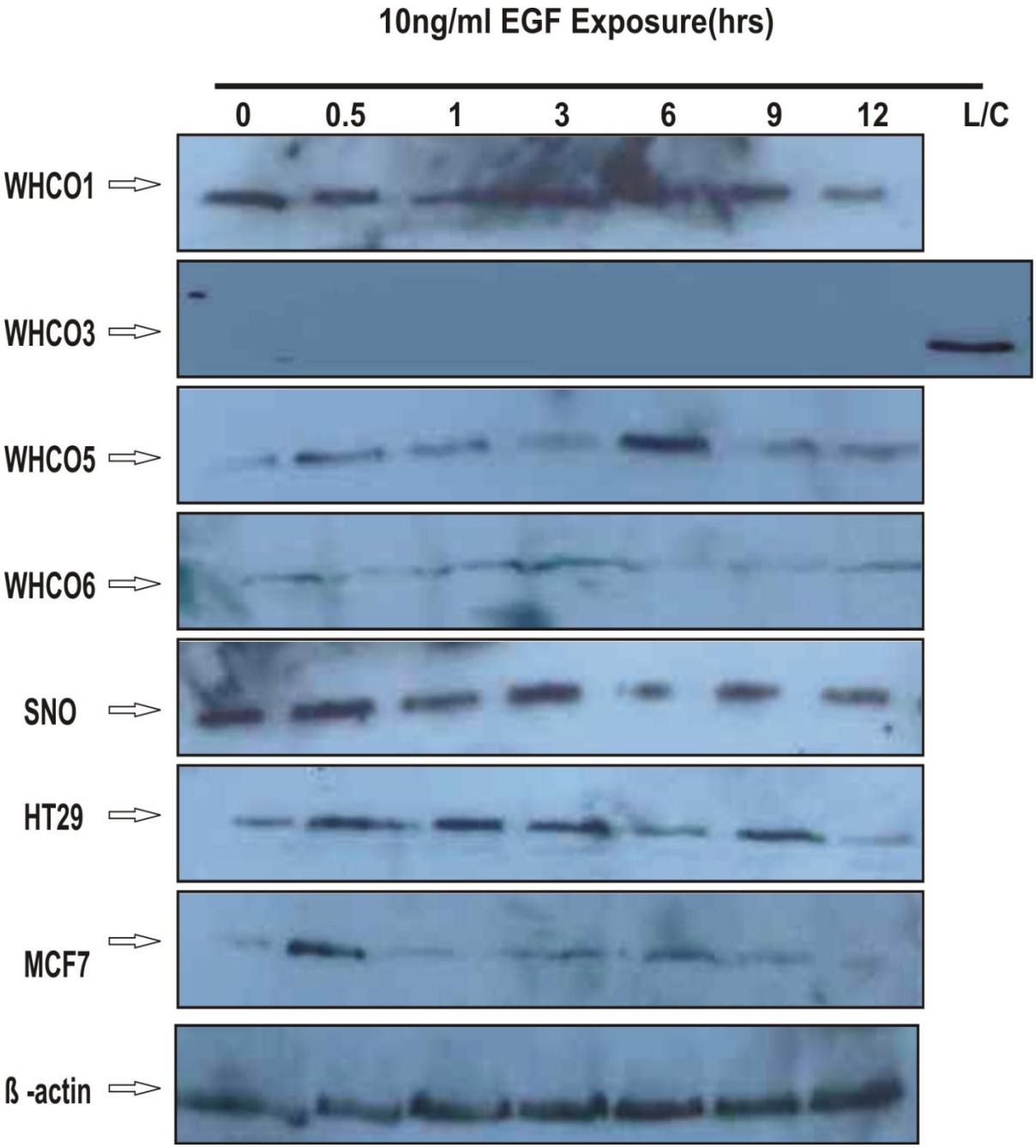
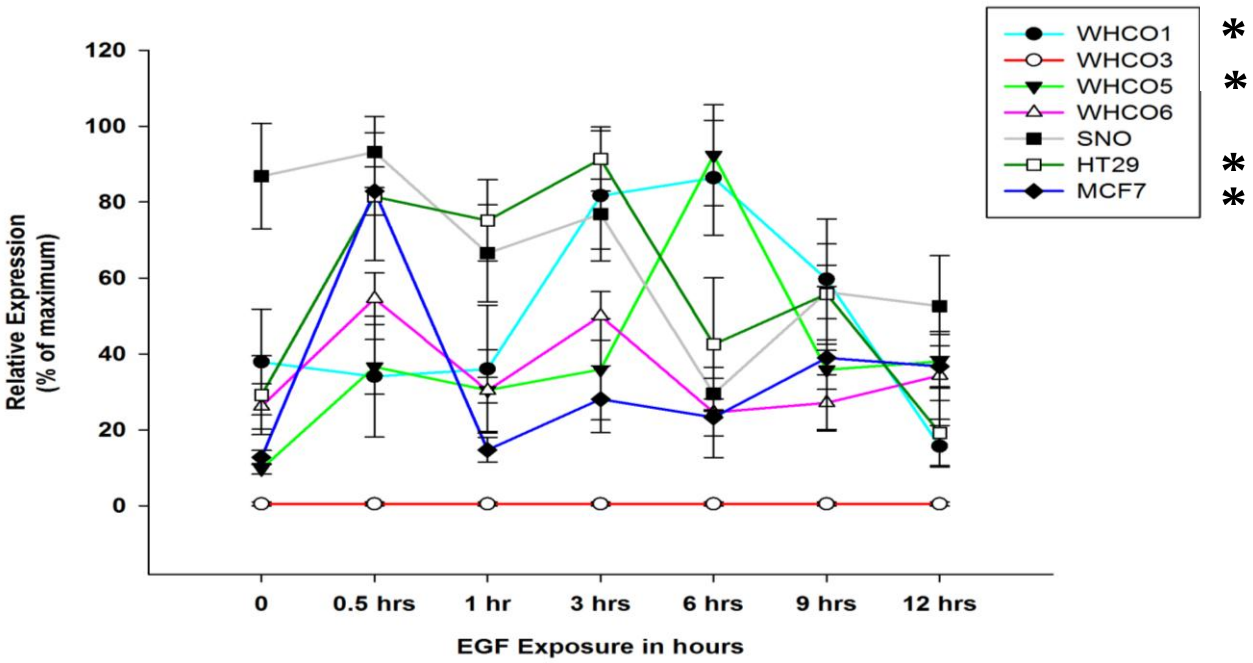


Figure 3. 8: Activation of the EGFR through EGF exposure triggers activation of the PI3K/PKB signalling pathway in two of the HOSCC cell lines. A) HOSCC, HT29 and MCF7 cells were treated with and without EGF for 0.5, 1, 3, 6, 9, and 12 hrs (see Appendix A 1.6.6 and 1.7.5 for standard curve and 10% SDS-PAGE). Western blotting was used to detect the Ser473 phosphorylation status of PKB (pPKB). β-actin levels were used as a loading control. C is representative of the WHCO6 whole cell lysate, used as a control for pPKB western blot detection in the WHCO3 cell line.

B)



C)

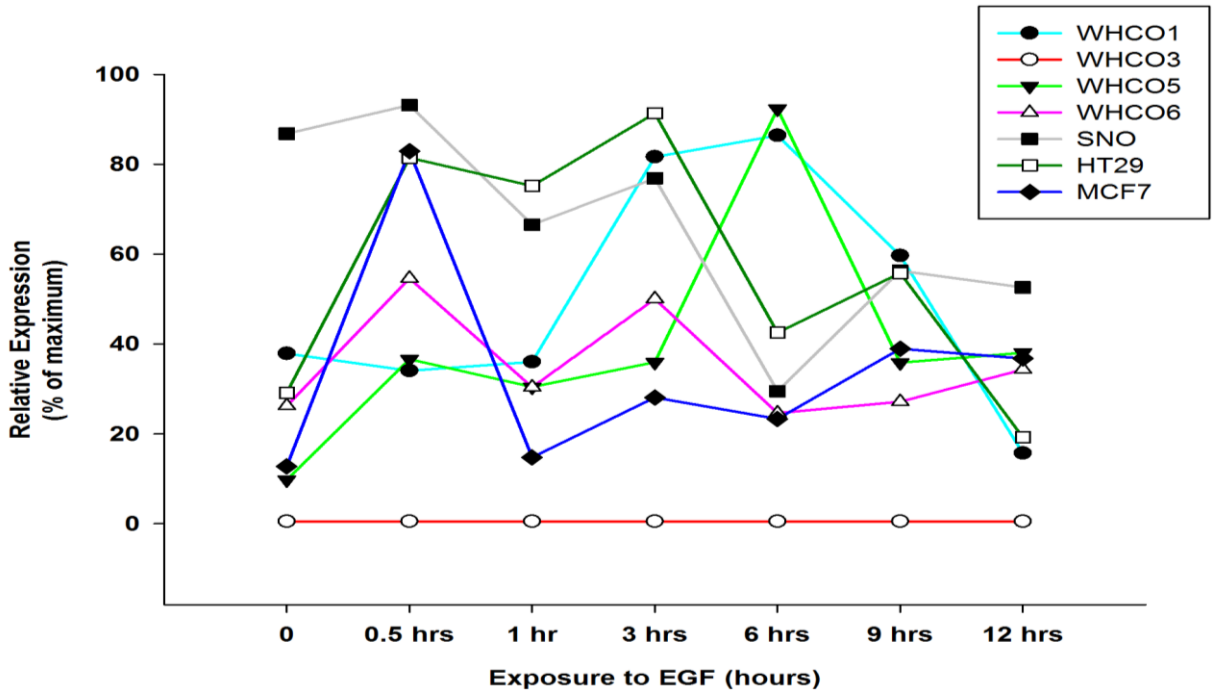


Figure 3.8 B) and C): The band representing pPKB in the western blot analysis was quantified through densitometry; see Appendix 2, Table 3.3 for statistical analysis **(B)**. Activation of EGFR significantly upregulates pPKB levels in the WHCO1 (3 hrs and 9 hrs), WHCO5 (at each interval), HT29 (0.5-3 hrs), and the MCF7 (0.5 hrs) cell lines respectively. Results represent mean ± S.D. from the three separate experiments, *significantly different from control, $P<0.05$. **C)** Bar graph, excluding the statistical analysis used for the biological comparison of pPKB levels following EGFR activation. See Appendix B, Table B3 for statistical analysis.

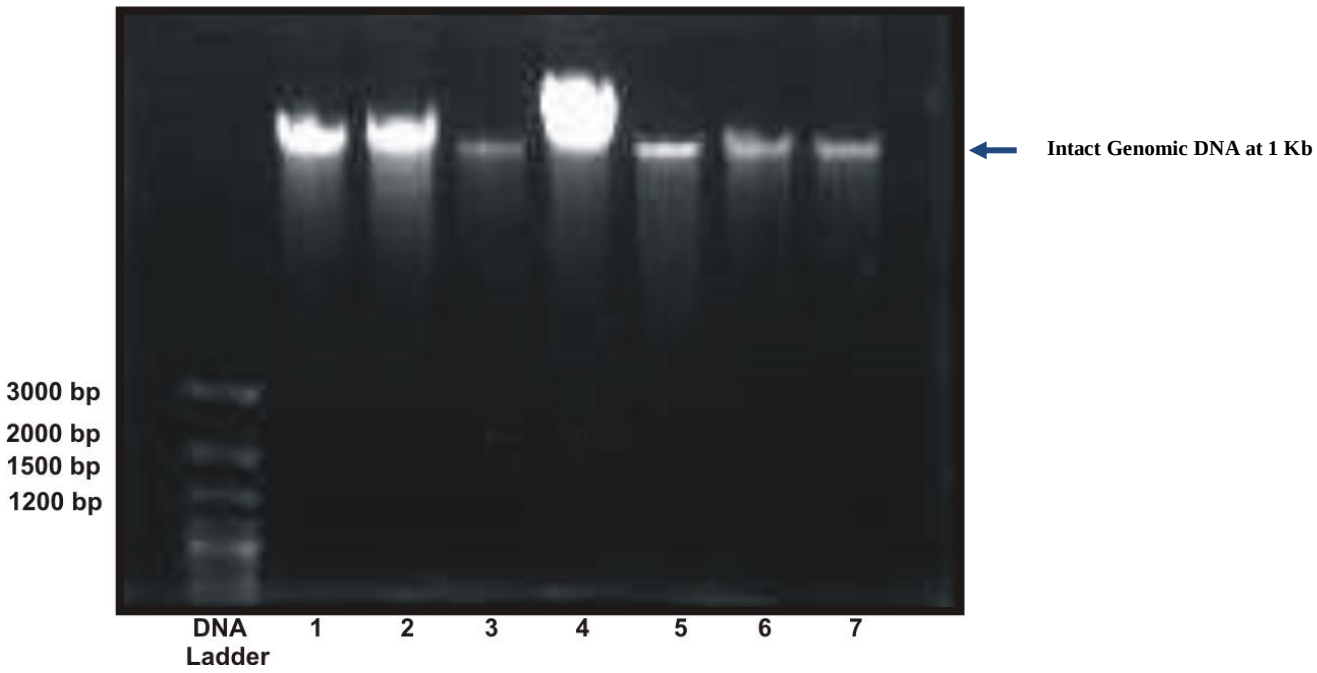


Figure 3. 9: Genomic DNA was successfully extracted from the 5 HOSCC cell lines. Genomic DNA was extracted from HOSCC, MCF7 and HT29 cell lines as described under materials and methods. The presence of an intact, sheared-free band is indicative of a pure genomic DNA extraction at a molecular weight of 1 Kb (blue arrow). DNA Ladder= 100 bp Plus. Lanes1-7: WHCO1, WHCO3, WHCO5, WHCO6, SNO, MCF7 and HT29 respectively.

3.3.7 Native PKB is present within HOSCC cells.

Recent reports have identified transforming mutations present within the PKB gene (PKB1/AKT1) in particular types of cancers[255,483, 484, 485]. Since the 5 HOSCC cell lines express wtPIK3CA (see Section 3.3.6), it became a necessity to elucidate whether mutations within the gene transcribing its downstream effector, PKB1 are present. Unlike PIK3CA, no "hotspot" genetic mutations have been reported within the PKB1 gene. The four sites that are considered imperative for PKB activation and function were thus scrutinized. These are; the region transcribing the Ser473 and Thr308 active sites, combined with the essential Linker and PH domains that mediate the activation of the Ser473 and Thr308 sites[174, 179]. Moreover, the inability to detect pPKB has been linked to an alanine substitution at Ser473[486]. Therefore inspection of these sites may provide answers to the undetectable pPKB levels in the WHCO3 cell line.

The four regions of the PKB transcript were successfully amplified via RT-PCR (see Chapter 2, Fig. 2.3). Amplicons give rise to PCR fragments sized 319 bp (Ser473), 450 bp (Thr308), 650 bp (PH domain), and 450 bp (Linker domain) respectively (see Appendix B 2.6 for PCR gels). Using the wtPKB1 status previously established in the MCF7 cell line[487], sequence analysis of these fragments confirmed that no mutations are present within the PKB1 transcript in the 5 HOSCC cell lines (see Appendix B 2.7, Fig. B7 for representative sequence traces).

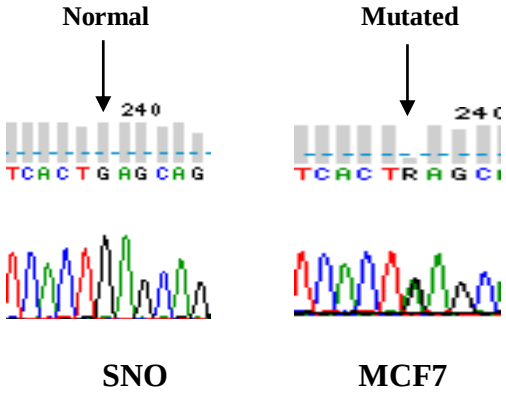


Figure 3. 10: The E454K (G1633A) "hotspot" mutation is absent in HOSCC cells. Sequence chromatogram of exon 9 (helical domain) from the SNO and MCF7 cell lines, confirming the base change (G to A/R) previously shown within MCF7[330], while demonstrating a mutant-free SNO, indicative of all the HOSCC cell lines examined through sequencing. Detection of the E454K (G1633R) mutation present within the MCF7 cell line confirms the specificity of the sequencing results in the representative chromatogram traces for exon 1, exon 4 and exon 20 (see Appendix B 2.6).

3.4 Discussion

Signal transduction is a complex intracellular communication network enabling cells to respond effectively and specifically to various external stimuli that will ultimately determine their fate[488]. Unscheduled initiation of this intracellular communication network gives rise to unwanted cellular activity[489]. Spontaneous activation of the EGFR signalling network is a well-defined event that is pertinent to such catastrophic events in oesophageal cancer[490, 491, 492]. The level of EGFR expression is commonly associated with its transforming capabilities and has been correlated to the poor prognosis of numerous types of tumours[493, 494]. Based on its inherent complexity, in HOSCC and most cancers, less is known regarding the downstream effects of EGFR overexpression, and in particular, its effects on the PI3K/PKB pathway. As aberrancies in the EGFR network are often found specific to tumour lineages[495], a tumour specific analysis is required to understand them in different cell types. This is borne by the fact that depending on which ErbB receptors are associated at the time of initiation of the disease; the downstream activation of specific pathways will vary[496]. In this regard, the ErbB2/ErbB3 heterodimer was shown to be relevant for the maintenance of transformed head and neck squamous cell carcinoma cells (HNSCC) via activation of both the ERK and PI3K pathways[497]. Whereas prostate cancer (PC) cells are not reliant on signalling propagated from the ErbB1/ErbB2 heterodimer[498]. Further, normal breast cells were demonstrated to maintain low levels of pPKB through the ErbB1/ErbB2 heterodimer[499]. Therefore, the specific effect that the EGFR overexpression status has on the PI3K/PKB pathway in the WHCO and SNO HOSCC series needs to be established.

In several experimental systems, PKB has been shown to be the major mediator of PI3K signalling that is activated by Ser473 phosphorylation respectively[500, 501, 502]. Given the membrane p85α localization and the concentration of pPKB in the absence of EGFR stimulation in four of the HOSCC lines (Chapter 2, Section 2.3.3 and Section 2.3.5), strongly implicates the presence of a constitutively active PI3K in these lines. One of the factors that remain to be determined, is how activation of this pathway is maintained in the four HOSCC cell lines (WHCO1, WHCO5, WHCO6, and SNO), and how it is dismissed in the WHCO3 HOSCC cell line. The results produced, demonstrate that although EGFR activation had no major impact on the total cellular levels of PI3K (p85α), it modulates its activity, evidenced by the responsive pPKB levels. Now it is well established that PI3K (p85α) only translocates to the plasma membrane upon receptor stimulation, leading to its activation[72, 228]. Bearing in mind the

relatively strong to moderate PI3K (p85α) membrane expression already established in the HOSCC lines (Chapter 2, Section 2.3.3), indirect immunoflourescence revealed that the membrane localization of PI3K (p85α) was more prominent following EGFR activation in the WHCO5, WHCO6, and SNO HOSCC cell lines explicitly (see Fig. 3.4). These data strongly suggest that the overexpressed EGFR in these cell lines is indispensable for the affinity PI3K (p85α) has for the plasma membrane. Hence, no significant changes were observed in the presence of exogenous stimulation. These findings are corroborated by Yang, *et al.*[503] who similarly showed no difference in the membrane; and in their case a combined cytoplasmic levels of p85α, subsequent to ligand stimulation in SKBR3 breast cancer cells. They understood this to be the result of an inherently membrane bound PI3K (p85α).

In addition to ErbB tyrosine receptor activation, the membrane localization of p85α could be consequential to at least three alternative mechanisms. One such a mechanism would be through its association with α-actinin for cytoskeletal reorganization via its SH3 domain[504]. This membrane role of p85α was demonstrated in confluent NIH3T3 fibroblasts, which may be particularly relevant for the p85α localization observed here in the WHCO1, WHCO5, WHCO6, SNO, and MCF7 cell lines respectively (see Fig. 3.4). A second alternative could be a result of its active role in cell-cell adhesion through its association with E-cadherin and β-catenin at the membrane, which was demonstrated to be independent of its membrane recruitment in response to RTK activation[505]. Observations made by Laprise *et al.*[506], suggested that this localization contributed to the structural integrity of the E-cadherin cell adherens junctions in epithelial cells, confirmed by a lack thereof when treated with the PI3K inhibitor, LY29. Lastly, p85α may be localized to the membrane via its association with the integrins, through its regulation of cell-extracellular matrix (C-ECM) adhesion[507]. Its role in C-ECM adhesion was particularly evident in AtT20 mesenchymal cells, where the membrane recruitment of p85α was influenced upon ligation of the α8β1 integrin to its ligand, fibronectin[508]. During C-ECM adhesion, it was shown that the autophosphorylation of the focal adhesion kinase (FAK) at Tyr397 influenced by the integrins, is essential for the membrane recruitment and activation of PI3K through its p85α regulatory subunit[509]. Recently it was shown that elevated levels of Tyr397 phosphorylated FAK (pFAK) are present in the WHCO6 cell line, whereas no pFAK was evident in the WHCO1, WHCO3, WHCO5, and SNO HOSCC cell lines[510]. Therefore, the high pFAK in the WHCO6 cell line is particularly relevant to its high pPKB levels established (see Chapter 2, Section 2.3.5), and its p85α membrane localization.

The nuclear detection of PI3K (p85α) demonstrated in the 5 HOSCC cell lines (Chapter 2, Section 3.3.3 B), was suggested to be part of an autonomous nuclear inositol system distinct from the well-established membrane activated PI3K pathway[511, 512], that may be relevant for the maintenance of their transformed state. Due to the extremely limited body of experimental evidence characterizing the nuclear levels of p85α in cells of epithelial origin[513], it is not known whether these levels are EGF dependent, and/or acts in concert with or independently of the membrane stimulated p85α. Therefore, the illustration that the nuclear levels of p85α were negatively affected in response to EGFR activation; predominantly observed in the WHCO1, WHCO3, WHCO6, and SNO HOSCC cell lines was of particular interest. Inconsistent with these data was the demonstration of enhanced nuclear levels of PI3K (p85α) in response to various exogenous stimulation in Hep2G, Saos-2 and MC3T3-E1 cells[400-402] and in ErbB-transfected NIH3T3 fibroblasts[514]. Here, only the WHCO5 cell line and HT29 control illustrated an up-regulation in nuclear p85α levels following EGFR activation. On the other hand, activation of the EGFR appears to completely abolish the nuclear p85α in the WHCO1 and SNO cell lines. Even though a separate nuclear PI3K pathway has been proposed by others[393], the data presented here shows that it is largely influenced by its membrane activation status through the EGFR.

Tyrosine phosphorylation of p85α is one of the well-known regulatory tools used to prepare PI3K for activation; through alleviation of its inhibition on p110α[515]. Additionally, Ser608 phosphorylation of p85α by p110α maintains a low activational state of PI3K that is simultaneously reduced upon tyrosine phosphorylation of p85α[61]. Once PI3K localizes to the membrane, this mutual inhibitory relationship is diminished through p85α binding to the activated EGFR. In this study, the PI3K (p85α) membrane expression was positively linked to its association with the EGFR via ErbB2, which was shown to be more pronounced in the presence of exogenous stimuli in the WHCO5 and SNO HOSCC cell lines specifically. The low intensities between the p85α-ErbB2 interactions detected across the 5 HOSCC cell lines; may be indicative of the numbers and/or availability of the ErbB receptors expressed within each cell line[332]. Based on these weak p85α-ErbB2 interactions, it was not surprising to note that the overall serine phosphorylation status of p85α was detected within the WHCO5, WHCO6, and SNO HOSCC cell lines specifically; since the p110α-mediated Ser608 phosphorylation on p85α abrogates it's binding to the EGFR. As the major Serine phosphorylation site on p85α is its Ser608 residue[64], assessment of its overall serine phosphorylated state thus still offers the same level of confirmation, even though the specific Ser608 phosphorylation site of p85α was not evaluated here. This conclusion is consistent with a previous study that similarly illustrated enhancement in the overall serine phosphorylation levels of p85α following PDGF stimulation in

T cells[516]. The seemingly constant state of serine phorphorylation of p85α may explain the weak association between the p85α and ErbB2 shown in this study. Consistent with this explanation, is work performed by Kobayashi *et al.*[517] who revealed that even though the PI3K pathway is activated by ErbB2, it is in fact, predominantly activated by the ErbB3 receptor. This influence was linked to the fact that even though adaptor proteins, such as Gab1, aid the affinity p85α acquires towards ErbB2, the ErbB2 still lacks the specific Tyr docking site imperative for a more efficient p85α-EGFR interaction[230]. Therefore, activation of PI3K by specific members of the ErbB family of receptors appears to be cell-type specific, and in the case of HOSCC cells, ErbB2 weakly associates with PI3K (p85α).

Following its membrane recruitment and EGFR association, PI3K induces the Ser473 phosphorylation and activation of PKB via PIP3-mediated activation of PDK1 and the mTORC2 complex[180, 189]. Here, it was illustrated that pPKB, and hence activation of PI3K, are indeed influenced by EGFR in the WHCO1, WHCO5, WHCO6, and SNO HOSCC cell lines, albeit to a small degree. These findings are on par with work performed on the TE HOSCC cell line series, whereby EGF induced-pPKB was both PI3K- and EGFR-dependent[518]. Since the pPKB levels in the low EGFR-expressing MCF7 control[480] were similarly triggered as a result of EGFR activation (see Fig. 3.7), suggests that the intracellular events triggered by the EGFR overexpression status in the HOSCC cell lines is not preferential to the PI3K/PKB pathway. This notion that the EGFR status in HOSCC cells is dispensable for the activation of the PI3K/PKB pathway is further supported by the highly significant elevation in pPKB observed in the EGFR-positive HT29 cell line[481].

Having established the membrane localized PI3K (p85α) in the WHCO3 cell line (Chapter 2, Section 2.3.3); that was also responsive to EGFR activation (see Fig. 3.4); it was surprising to note, that despite this cell line possessing the highest EGFR levels; the sequential activation of PKB was not observed (see Fig. 3.8). Therefore, an inability for PI3K to produce PIP3 at the membrane that would impair the Ser473 phosphorylation of PKB seems highly unlikely. It should be noted, than in addition to PKB, PI3K is responsible for the activation of yet another PH-domain harbouring protein, the integrin-linked kinase (ILK)[519]. Furthermore ILK activity was previously demonstrated in all the 5 HOSCC cell lines[520]. Hence, diminished levels of active PI3K cannot explain the non-responsive pPKB in the WHCO3 cell line.

The combined data presented thus far point to the existence of PI3K (p85α) which has a high membrane affinity accompanied by weak interactions with ErbB2, presumably caused by the

serine phosphorylated state of p85α that leads to its overall low and unresponsive downstream activity (pPKB) in HOSCC cells. Exogenous EGF has been reported to have no significant impact on the activity of PI3K when mutations within PI3K (p110α) or PKB exist[140, 239]. Logically, this prompted the assessment of the mutational status of PKB and the catalytic subunit of p110α. Research has linked the oncogenic activity of PI3K to weak-activating and "hotspot" mutations within the gene transcribing the p110α catalytic subunit (PIK3CA) [237,521, 522, 523, 524]. These are situated within the p85α-binding domain (R38H, E53K), C2 domain (V344M, C420R), helical domain (E454K, E542K), and the kinase domain (H1047R), each transcribed by exon 1, exon 4, exon 9, and exon 20 respectively[522]. Here, even though the low concentration of pPKB in HOSCC cells was similar to the low levels shown in the mtPI3K3CA MCF7 cell line (see Fig. 2.9), neither of these proteins, when isolated from the 5 HOSCC cell lines possessed any of the "hotspot" mutations described previously for other tumours. These findings are in agreement with a previous report that also demonstrated absence of mutations within exon 1, exon 9, and exon 20 specifically in adenocarcinomas of the oesophagus and Barrett's oesophagus[525]. Even though the same study; along with a separate report[526] found mutations within exon 4 in oesophageal samples, the data presented here were inconsistent with these studies, in that, no mutations were found. Of note, our findings are complimented by a study performed on pharyngeal cancer[527], which similarly demonstrated an absence in exon 4 mutations. Since part of the aim was to discover whether the resistance to LY29 acquired in the WHCO5 and SNO HOSCC cell lines (Chapter 2, Section 2.3.8) was a result of PIK3CA mutations; we can exclude this as an explanation, since none of the major functional domains of PIK3CA were found to be mutated.

Although infrequent, the presence of pPKB, combined with its recognized cytoplasmic and membrane localization (Chapter 2, Section 2.3.5 and 2.3.6) is indicative of an overexpressed or mutated PKB gene transcript, and thus its expression serves as a prognostic marker for many cancers[484,528, 529, 530]. Therefore, on this basis, it was thought that the presence of activating and inactivating mutations in at least one of the central domains of PKB is responsible for the overt pPKB levels in four of the HOSCC cell lines and the lack thereof in the WHCO3 cell line. Several studies focus on a particular domain on the PKB gene transcript, here; all four of the potential hotspot sites, namely; the hydrophobic, catalytic, PH and linker domains, which included the well-studied E17K mutation within the PH domain[250], were examined. Similar to the wild-type PKB status in the MCF7 cell line[487], no mutations in either one of these central domains was found in the 5 HOSCC cell lines. These data complements previous studies that correspondingly did not discover PKB alterations in cancers of epithelial and non-epithelial

origin[531, 532, 533]. Although overexpression of PKB was not the focus of this study, it has been reported to occur in many squamous epithelial-based cancers[534, 535, 536], and thus cannot be completely ignored as an explanation when extrapolating these results. The data described in this chapter also showed that the undetectable concentrations of pPKB within the WHCO3 cell line are not attributable to mutations. On the basis that the major functional domains of PKB were analyzed and shown to affect its kinase activity, PKB is indeed functional in HOSCC cells, despite the possible existence of alternative mutations.

As briefly outlined in the previous chapter, PTEN antagonizes the activation of PKB by counteracting the levels of PIP3 produced through PI3K at the membrane[537]. As such, it is highly uncertain how cells with active PI3K and PKB manage to sustain a pro-survival state amidst a functional PTEN[487, 538]. To this end, there are at least two alternative explanations for the lack of pPKB detection within the WHCO3 cell line. One possibility could be the outcome of hyperactive PTEN that disallows the Ser473 phosphorylation and activation of PKB. In addition to PTEN, the Ser473 phosphorylation of PKB is subject to dephosphorylation by yet another serine/threonine phosphatase and tumour suppressor, the phosphatase protein 2 (PP2A)[220]. Hence, a role for PP2A in the WHCO3 cell line, and perhaps a lack thereof in the other HOSCC cell lines, can provide the second alternative explanation for the pPKB levels in these cell lines respectively.

In this chapter it was shown that HOSCC cells express wtPIK3CA and wtPKB. Hence, mutations within these proteins cannot account for the response to LY29 observed in the previous chapter (Chapter 2, Section 2.3.7). By the same token, deactivating mutations in PIK3CA or PKB are similarly not associated with the absence of pPKB in the WHCO3 cell line. Pertinently, based on the more responsive pPKB levels in the EGFR-low expressing MCF7 control, it appears that the EGFR overexpression status in the 5 HOSCC cell lines plays a small role in the activation of the PI3K/PKB pathway. As a result, these data strongly support the presence of alternative routes for the membrane targeting of PI3K (p85α) in these 5 HOSCC cell lines (Chapter 2, Section 2.3.3). Consequentially, these results strongly suggests that the major pro-survival signalling components of the PI3K/PKB pathway are deviant in the WHCO3 cell line, causing an unusual, but extraordinary setting, that leaves room to explore other equally imperative, yet compensatory pro-survival mechanisms. The functionality of the PI3K/PKB pathway is measured by the fine balance between the positive and negative influences it is subjected to, therefore it is necessary to include an understanding of the negative regulators of this pathway in HOSCC.

Chapter 4
Suppression of the PI3K/PKB pathway

4.1 Introduction

A key role for the involvement of PI3K and PKB in the development of cancer is necessitated by activating mutations within their respective genes[539,540, 541, 542, 543]. Importantly, it was shown that these mutations are not present within the 5 HOSCC cell lines (Chapter 3, Section 3.3.6 and 3.3.7). In epithelial cells, the complex mechanisms that govern the dephosphorylation and thus inactivation of PKB on its Ser473 residue have become evident[219]. As noted previously, the activation of PI3K and PKB is for the most part antagonized by PTEN[544, 545]. Yet another negative regulator of the PKB Ser473 site, is the tumour suppressor and protein phosphatase, the protein phosphatase 2A (PP2A)[220]. This chapter addresses the influence of these phosphatases on the low activation status of PI3K/PKB signalling in these 5 HOSCC cells.

PP2A is a ubiquitous serine/threonine phosphatase and tumour suppressor protein (TSP) that is responsible for regulating a broad range of protein kinases, the specificity of which has been shown to be uniquely orchestrated for each cell type[546]. The tumor suppressive function of PP2A is well-known, despite the fact that its role is largely limited to the tissue in which it is expressed[547, 548, 549]. The cell-permeable marine-sponge toxin; okadaic acid (OA) specifically targets and inhibits PP2A[550], and this is widely used in studies of the activity of PP2A within cells[551, 552, 553, 554]. The importance of PP2A was demonstrated through exposure of embryonic stem cells to OA that resulted in lethal embryonic development[555, 556, 557]. Two of the major etiological factors for HOSCC; namely the mycotoxin, fumonisin B_1 (FB_1) [558], and HPV-16,-17[559] are known to specifically target and inhibit PP2A. This enhanced our need to explore a role for this phosphatase in HOSCC, and sets the precedence for evaluating the part played by PP2A on the PI3K/PKB pathway.

Once active, PP2A impinges upon the activity of PI3K and PKB on several fronts. One such mechanism is through its direct dephosphorylation of PKB on its Thr308 residue[560], thus making its activity antagonistic to that of PDK1 (depicted in Fig. 4.1). It is uncertain whether PP2A can also directly dephosphorylate PKB on its Ser473 residue, or if this is, in part, a consequence of its Thr308 dephosphorylation, which is recognized as a prerequisite for its Ser473

phosphorylation[355, 561]. Nonetheless, either mechanism will give rise to dephosphorylation and inhibition of PKB on its Ser473 residue (see Fig. 4.1). PP2A also plays an active role in the Wnt signalling pathway by regulating cellular β-catenin levels[562]. One such mechanism is through its direct dephosphorylation, and activation of GSK3β on its Ser9 residue, when bound to APC and Axin[563] (as shown in Fig. 4.1).

The PTEN TSP is a lipid phosphatase that is responsible for the bulk of the antagonism on the PI3K/PKB pathway[438, 538]. This is primarily achieved by reversing the action of PI3K on its physiological substrate, PIP3, through removal of a phosphate attached to its 3'-hydroxyl group[564]. Irrespective of its expression levels, PTEN is known to be quasi-sufficient. Therefore, its presence alone permits its appropriate function on PIP3 [565, 566]. Based on the fact that the expression of PTEN inhibits growth[567], it is still largely undetermined how cancer cells that retain their expression of PTEN manage to sustain their tumorigenic state[568,569,570]. According to the PTEN prostate cancer (PC) model[571]; cancer cells that retain PTEN possess lower levels; and the mechanisms used to maintain such low concentrations and the downstream effects thereof, are restricted to the type of tissue[572,573]. In addition to expressing lower levels, the pathogenic role of PTEN was also linked to its cytoplasmic localization[446, 574, 575, 576]. This has been shown to be the result of an inability to transport PTEN into the nucleus, where it can contribute to tumour suppression[577]. Conversely, a recent report linked PTEN nuclear localization to the pathological state of colon cancers[578]. Therefore the role played by the cellular compartmentalization of PTEN in the neoplastic condition remains a conundrum.

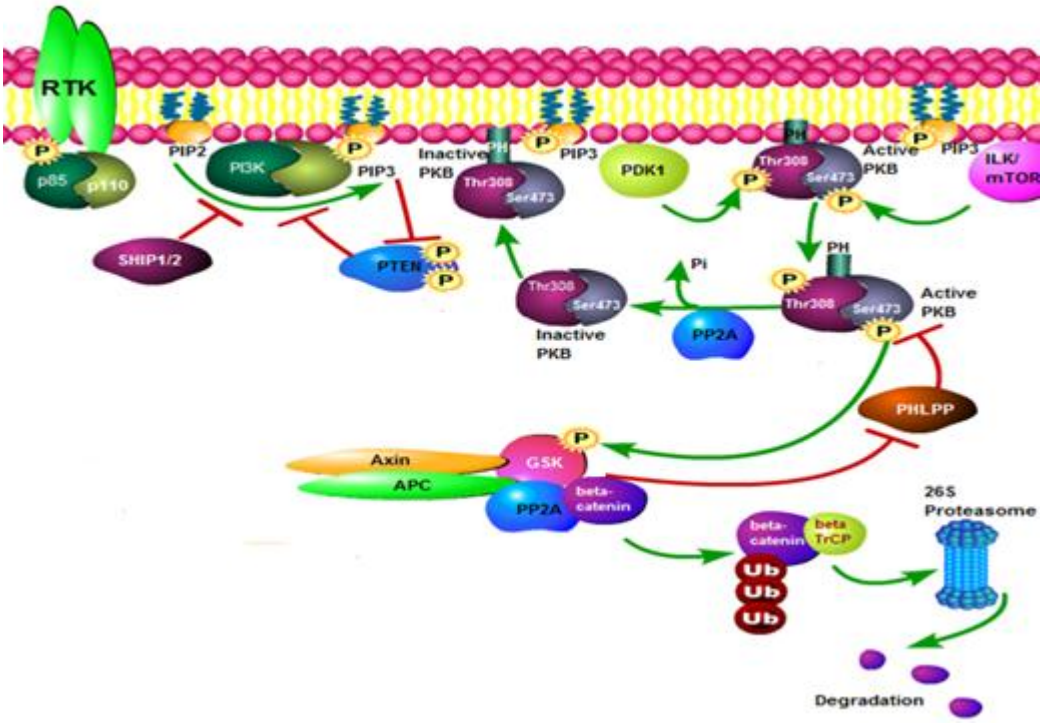


Figure 4. 1: PP2A signalling. As highlighted within the text, PP2A antagonizes the activation of PKB by dephosphorylating its Thr308 residue that is phosphorylated by PDK1. This dephosphorylation, in turn, leads to the dephosphorylation of PKB on its Ser473 residue, or alternatively, can be directly dephosphorylated by PP2A, leading to its inactivation. PP2A also enhances the stabilization of the β-catenin degradation complex (GSK3β-Axin-APC) by regulating the Ser9 phosphorylation status of GSK3β. Figure generated using the Pathway Builder Tool. 2.0.

The regulation of PTEN activity in specific cell-types is extremely complex, as its stability and activity are currently known to be modulated by over 20 kinases and phosphatases[579]. Unlike PP2A described above, a specific PTEN inhibitor is yet to be discovered. Importantly, PTEN is highly susceptible to oxidation[580], which presents a way of manipulating PTEN regulation. At the plasma membrane, activation of PI3K upon RTK stimulation activates the NADPH oxidase (Nox) essential for the generation of the hydrogen peroxide (H_2O_2) reaction oxygen species (ROS) (see demonstration in Fig. 4.2). Subsequently, the membrane recruitment of PTEN leads to the oxidation of its catalytically active cysteine residues by H_2O_2, resulting in its reversible inactivation and augmentation of the PI3K/PKB pathway (Fig. 4.2). Compelling data implicates a role for H_2O_2 in intracellular signalling pathways through the oxidization of and hence the reversible inhibition of PTEN[581, 582, 583].

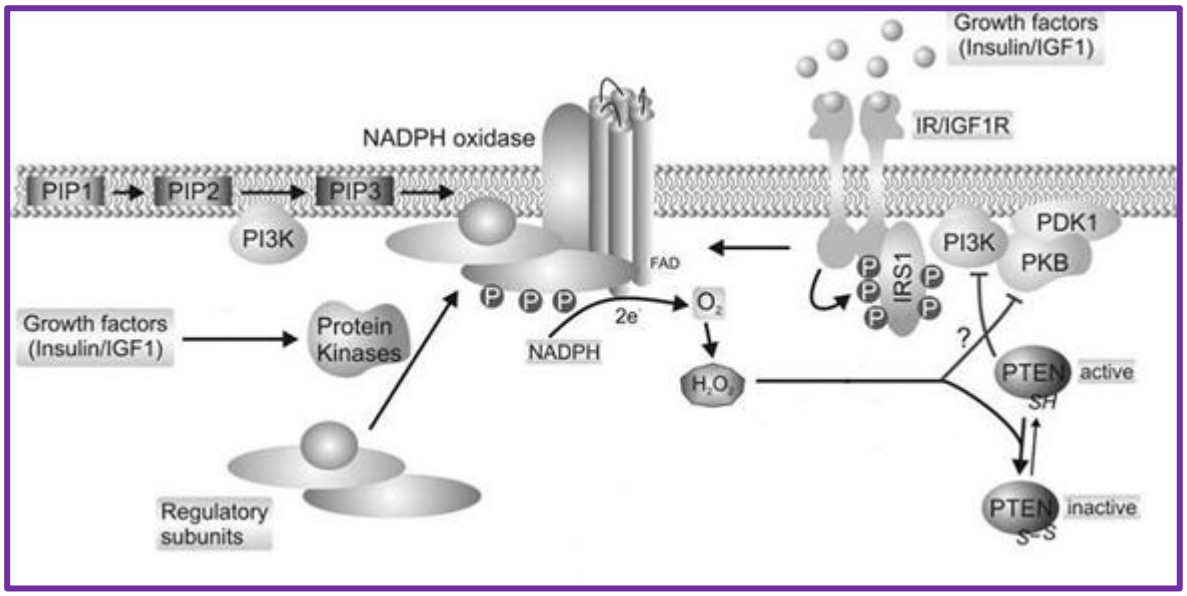


Figure 4. 2: Regulation of PTEN through Oxidation. RTK activation (illustrated here as the Insulin Tyrosine Receptor/IR), leads to the production of H_2O_2 through the membrane-bound NADPH oxidase. The recruitment of PTEN to the membrane, results in the H_2O_2-mediated oxidation of its catalytic cysteine residues, leading to its reversible inhibition. See test for further details. Figure adapted from Szypowska[584].

Pertinent to the active state of PKB within the WHCO1, WHCO5, WHCO6, and SNO cell lines, and its inactive state in the WHCO3 HOSCC cell line respectively (Chapter 2, Section 2.3.5, and Chapter 3, Section 3.3.5), may point to a part played by PP2A or PTEN. Hence, in order to gain insight into the mechanism behind the pPKB regulation in these HOSCC cells, and since PP2A plays a more direct role in the Ser473 dephosphorylation of PKB (see above), we explored the influence of PP2A by manipulating its activity through OA. This was followed by examining the active state of PTEN through H_2O_2 exposure.

4.2 Materials and Methods

4.2.1 Cell Lines and their Culture

The 5 HOSCC cell lines including the HT29, MCF7 and Caco-2 control cell lines were cultured as previously described in Chapter 2, Section 2.2.1.

4.2.2 Antibodies

PI3K (p85α) was specifically detected with the rabbit polyclonal anti-PI3 Kinase (p85α) antibody (Upstate Biotechnology), while the rabbit polyclonal anti-β-Actin, anti-β-catenin (Sigma), and anti-c-Jun (Santa Cruz Biotechnology) were specific for the detection of β-Actin, β-catenin and c-Jun accordingly. The Ser473 and Ser9 phosphorylation of PKB and GSK3β respectively, as well as endogenous PTEN levels were specifically detected with the rabbit polyclonal anti-Phospho-Akt (Ser473), anti-Phospho-GSK-3β (Ser9), and anti-PTEN antibodies all of which were obtained from Cell Signalling Technology. E-cadherin was specifically detected with the mouse monoclonal anti-E-cadherin antibody (RD science), which was then detected using the goat-anti-mouse IgG (Fab Specific) peroxidase conjugate secondary antibody, while detection of all rabbit polyclonal antibodies was detected using the goat-anti-rabbit IgG (Sigma). Immunoflourescence staining of PTEN was specifically detected using the rabbit polyclonal anti-PTEN antibody (Sigma), and was detected using the fluoroscine isothiocyanate FITC-conjugated-goat-anti-rabbit antibody (Chappel, USA).

4.2.3 Treatment with the PP2A Inhibitor, Okadaic Acid (OA)

OA is used to investigate the intracellular roles of PP2A[585] in HOSCC cells. According to crystal structure studies, OA specifically inhibits (ID_{50}) PP2A at 0.1 nM concentrations, whereas this specificity is lost at > 10 nM concentrations[586]. Based on the fact that specific inhibition of PP2A in cellular systems requires higher concentrations of OA, that have been demonstrated to be specific for each cell type, we found a concentration of 100 nM for 1 hour (hr) optimum (see Appendix C 3.1). The previously established active state of PP2A[587, 588] and functional PTEN[589, 590] present within the MCF7 and HT29 cell lines served as ideal controls. Cells were cultured as previously described, until they reached 60% confluency, after which, each cell line was incubated for 1 hr with 100 nM of OA diluted in DMSO (see Appendix C 3.2) under serum conditions, while the control or untreated cells were exposed to DMSO only. Whole cell protein extractions were performed on all the treated and untreated cell lines. **Note:** Three independent experiments were performed.

4.2.4 Whole Cell Protein Extraction

Subsequent to exposure of OA, whole cell protein extractions were performed as detailed in Chapter 2, Section 2.2.5.

4.2.5 Nuclear Extraction

As detailed in Chapter 2, Section 2.2.6.

4.2.6 Membrane Extraction

As detailed in Chapter 2, Section 2.2.7.

4.2.7 Protein Estimation

As detailed in Chapter 2, Section 2.2.8.

4.2.8 Polypeptide Resolution and Western Immunolotting

30 μg of whole cell, nuclear, and membrane protein extracts were resolved on a 10% SDS-PAGE as detailed in Chapter 2, Section 2.2.9. Non-specific binding sites on the nitrocellulose membrane were blocked by incubation in BLOTTO (Appendix A 1.8.2) for 1 hr at RT. Following 6 quick washes in PBS, blots were incubated for 1 hr at RT in the primary anti-β-catenin antibody (1:5000). Unbound primary from the blots were removed by six 5 min PBS washes that preceded 1 hr incubation at RT in the secondary HRP-conjugated goat-anti-rabbit (1:30000). Thereafter, membranes were exposed to Supersignal West Pico Chemiluminescent working solution and film as described in Chapter 2, Section 2.2.9. Immunoblot detection for PI3K (p85α), β-actin, c-Jun, E-cadherin, pPKB, pGSK3β, and PTEN were carried out as detailed in Chapter 2 (Section 2.2.9) and Chapter 3 (Section 3.2.9) respectively.

4.2.9 Indirect Immunoflourescence Microscopy for PTEN Staining

Notably, because the nuclear localization of PTEN in the HT29 cell line has recently been linked to its pathological state[578], it was chosen as a comparison against the unknown PTEN cellular distribution in the HOSCC lines. As documented in Chapter 2, Section 2.2.10, cells were grown to 50% confluence, fixed and permeabilized for 10 mins onto glass slides using 4% paraformaldehyde and 0.25% Triton-X-100 respectively. Non-specific binding in the respective "wells" created with the DAKO® pen was prevented by 30 min incubation in PBS, followed by 1 hr incubation in the primary anti-PTEN antibody (Sigma), at a 1:1000 dilution. Subsequent to five 1 min PBS washes, the cells were incubated in the dark for 1 hr in the FITC-conjugated secondary anti-rabbit antibody (1:1000). Thereafter, the procedure was

performed as described in Chapter 2, Section 2.2.10. Where necessary, immunofluorescent microscopy images were sharpened using Adobe Photoshop to enhance their clarity. **Note:** Each immunofluorescence microscopy was repeated three times, and a negative control was performed for each cell line.

4.2.10 Exposure to Hydrogen Peroxide (H_2O_2)

Cells grown to 60% confluence as previously documented (Chapter 2, Section 2.2.1) were exposed to 1 mM H_2O_2 (Unilab®/SAARCHEM (Pty) Ltd) for time intervals of 10, 30, and 60 minutes (mins) under serum conditions at 37 ºC at the appropriate CO_2 level. This concentration and time intervals were chosen based on the fact that H_2O_2 is a representative oxidant at 1 mM, and has been shown to sufficiently induce PTEN oxidation[581, 591]. Following exposure to H_2O_2, whole cell and non-reducing protein extractions were conducted.

4.2.11 Non-reducing extraction for detection of reduced PTEN

Consequent to H_2O_2 exposure detailed above, a non-reducing protein extraction was performed on selected cell lines (WHCO3, WHCO6, SNO, and HT29) in order to verify the oxidative state of PTEN. This protocol was adapted from Meng, *et al.*[592] Briefly, cells were washed three times in PBS, scraped off the dish into an Eppendorf tube and pelleted for 3 mins in the HF-120 TOMY (1200 X *g*). The resultant supernatant was resuspended in non-reducing buffer (Appendix C 3.3), and immediately allowed to extract on ice for 10 mins. Thereafter, nitrogen (N_2) gas was injected into each Eppendorf, vortexed, exposed to N_2 gas for an additional 3 secs, and centrifuged for 10 mins at -4 °C at 13000 X *g* in an Eppendorf Centrifuge 5413; the resultant extracts were stored at -70 °C.

4.2.12 Densitometry

Labworks TM Image Acquisition and Analysis software (Labworks version 4.5) was used for densitometric analysis to semi-quantitatively determine the concentration level of PI3K (p85α), pPKB, pGSK3β, PTEN, and β-catenin detected through western blotting. **Note:** The densitometric results are an average of three independent experiments and expressed as a percentage relative to the maximum.

4.2.13 Image Capturing

All western blot and SDS-PAGE images were captured on a Hewlard Packard Scanjet 4400c series scanner at 300dpi, contrast and brightness of all images were standardised using CorelDRAW version 12®.

4.2.14 Statistical Analysis

Statistical analysis results are inclusive of three independent experiments (mean ± S.D). P-values are given in the figure legends, and only $P < 0.05$ was considered significant. Statistical analyses were performed using Student's *t* test and One Way Repeated Measures Analysis of Variance. Inverse correlations between pPKB, pGSK3β, and PTEN levels were calculated using Pearson's correlation coefficient, where values of $P<0.05$ were set as the cut-off for statistical significance. All calculations of statistical computations were carried out using the SigmaPlot Release 11.0® statistical software. **Note:** Based on the fact that statistical analysis requires a minimum of three independent experiments, an example of the three blots for the figures in this chapter was chosen (i.e. nothing is gained by showing all three).

4.2.15 Figure Design

All schematic diagrams were designed using the Pathway Builder Tool version 2.0, unless otherwise stipulated.

4.3 Results

4.3.1 The PI3K/PKB pathway is not regulated by PP2A in HOSCC cells.

In response to EGFR activation, levels of pPKB was not affected significantly (Chapter 3, Section 3.3.5). Furthermore, pPKB levels did not correlate to those of its downstream effector, pGSK3β (Chapter 2, Section 2.3.8). As PP2A has been shown to attenuate pPKB and augment pGSK3β levels in specific cells[219, 593], we examined its influence on pGSK3β and pPKB in the 5 HOSCC cell lines. As OA has been shown to effectively and specifically inhibit PP2A[554], it was used as a tool to evaluate the contribution made by PP2A in the regulation of pPKB and pGSK3β levels. Furthermore, because PP2A is a major regulator of Wnt signalling[594], we included an assessment of the expression levels of β-catenin following PP2A inhibition.

On the understanding that pPKB and caspase-3 were activated in response to PP2A inhibition (see Appendix C, Fig. C1), PP2A plays a significant (P=0.001) role in regulating the Ser473 phosphorylation of PKB in the WHCO1 and WHCO6 HOSCC cell lines exclusively (as shown in Fig. 4.3 and 4.4A), while no significant changes in pPKB levels was evident in the WHCO3, WHCO5 and SNO HOSCC cell lines. In comparison to the significant up-regulation in pPKB in the WHCO6 and cell line, PP2A inhibition appears to have a negative impact on pPKB levels in the WHCO1 cell line. This is in line with the significant decrease in pPKB following PP2A inhibition in the two PP2A positive controls (HT29 and MCF7). We clearly show that PP2A has a significantly negative (P=0.03) impact on the Ser9 phosphorylation of GSK3β in the SNO HOSCC cell line (Fig. 4.3 and 4.4B). This was substantiated by the equally significant (P=0.03) effect PP2A inhibition had on pGSK3β levels in the PP2A positive control (MCF7) (Fig. 4.3 and 4.4). The concentration of pGSK3β was not significantly altered in the WHCO1, WHCO3 and WHCO5 HOSCC cell lines.

Detection of PTEN was included as a control for the changes in pPKB obtained, and as can be seen in Fig. 4.3 and 4.4C, the significant changes ($P<0.05$) in PTEN expression obtained in the WHCO1, WHCO5, and SNO cell lines do not correspond to changes in pPKB. Protein levels of PTEN were affected in response to PP2A inhibition in the WHCO1, WHCO5 and SNO cell lines, albeit to different degrees (Fig. 4.3 and 4.4C). This result was similar to that demonstrated in the MCF7 control. The expression of PI3K (p85α) was only

significantly altered in the WHCO3 and WHCO6 cell lines (Fig. 4.3 and 4.4D). Furthermore, based on the extent to which levels of β-catenin were affected in the WHCO1 (P=0.01) and WHCO3 (P=0.01) cell lines, provides evidence for an active PP2A in these cell lines (Fig. 4.3 and 4.4E). This is consistent with the significant down-regulation in β-catenin obtained in the control (HT29) cell line (P=0.03), that is known to possess constitutively active Wnt signalling[595].

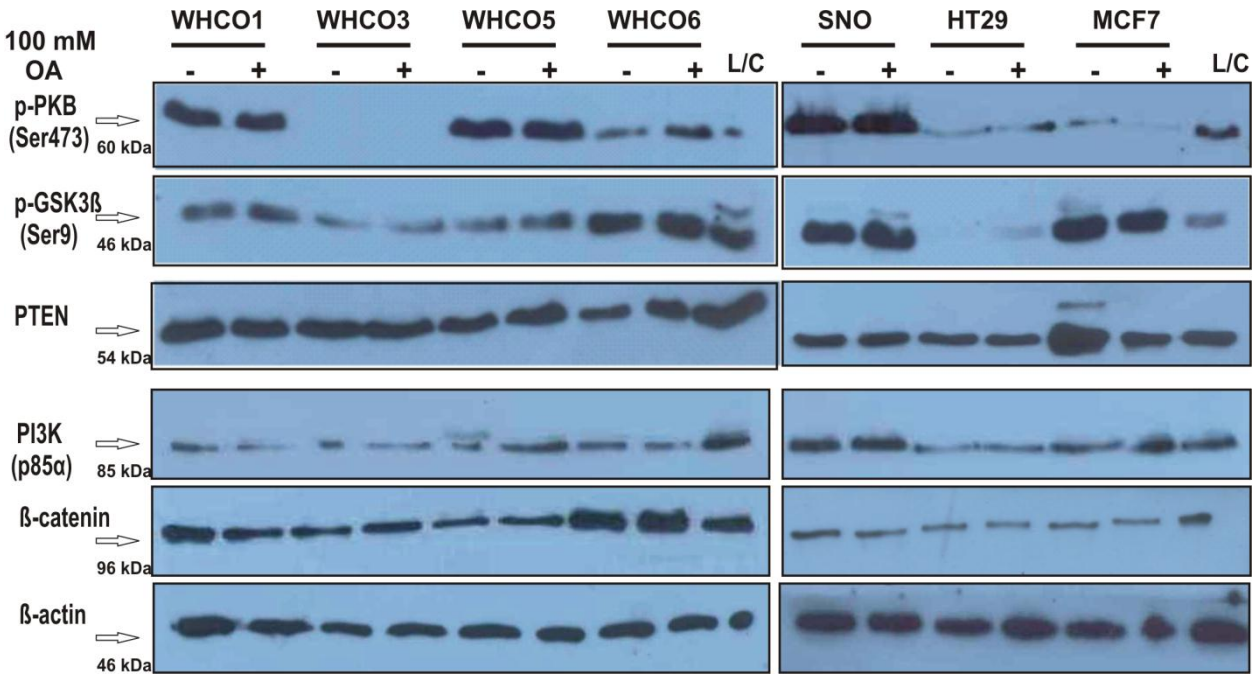
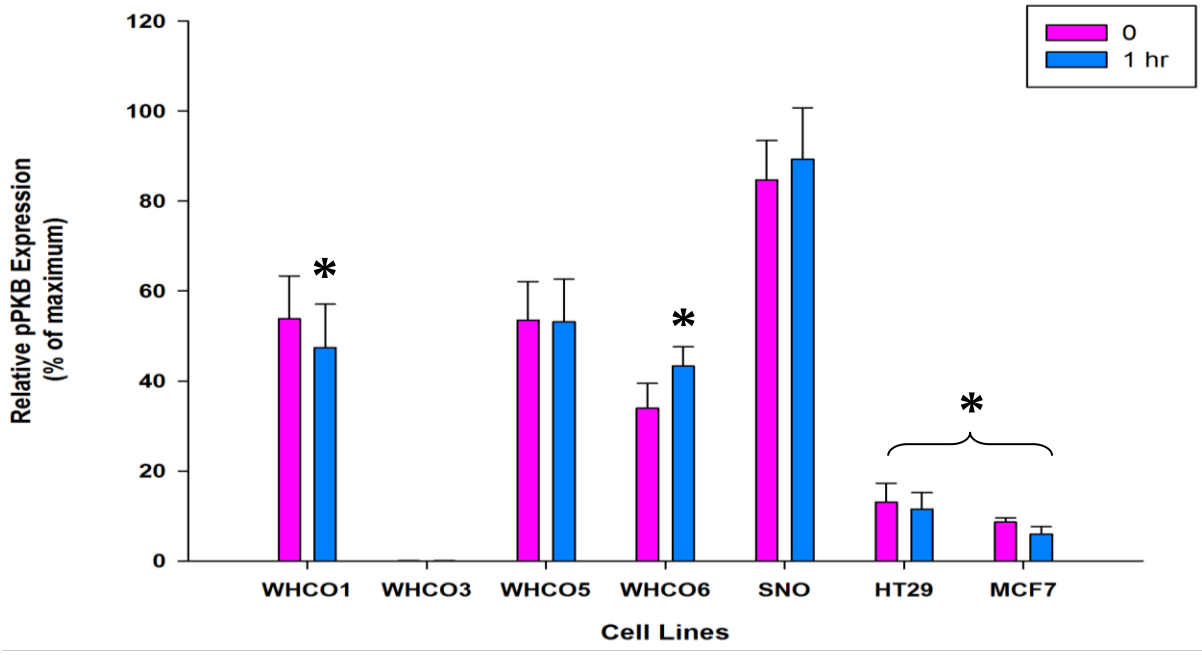


Figure 4. 3: PP2A is not a major regulator of the PI3K/PKB pathway in HOSCC cells. HOSCC, MCF7 and HT29 cell lines were treated with (+) and without (-) 100 nM of the PP2A inhibitor, Okadaic acid (OA), for 1 hr. Western blot analysis was used to determine the consequent effect OA had on the overall protein levels of p-PKB (Ser473)/pPKB, its downstream effector, p-GSK3β (Ser9)/pGSK3β, PTEN, PI3K (p85α), and β-catenin (see Appendix A 1.6.6 and 1.7.5 for representative standard curve and 10% SDS-PAGE). The loading control (L/C) is representative of the WHCO6 whole cell lysate used for comparison between the different blots. Equal loading of treated versus untreated proteins was detected with β-actin.

A)



B)

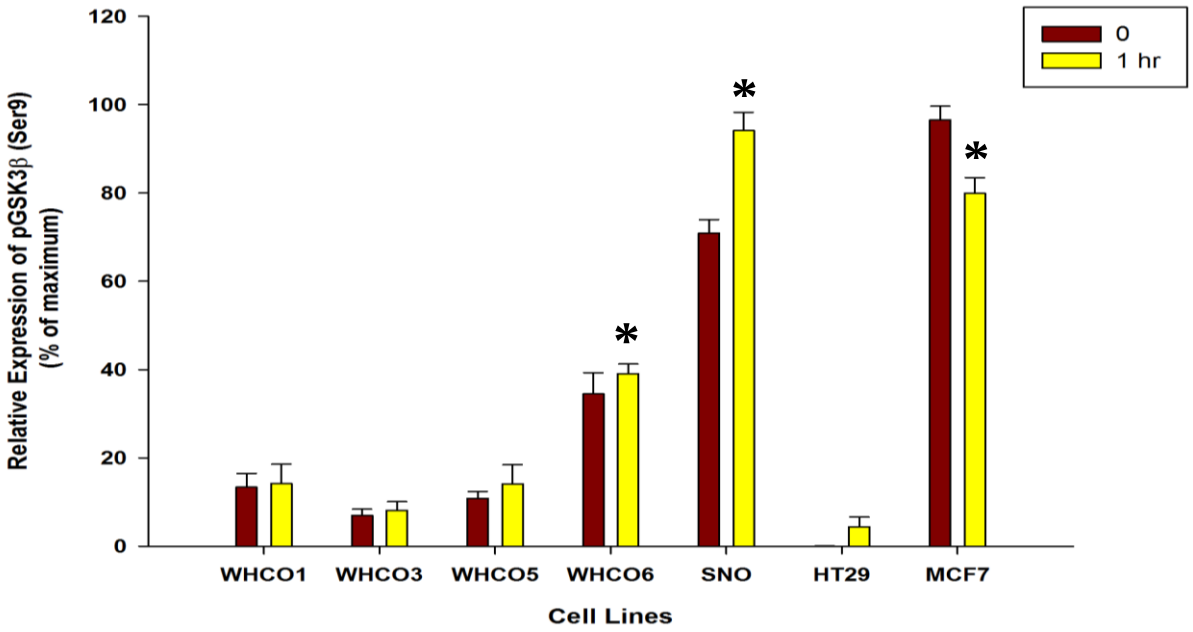
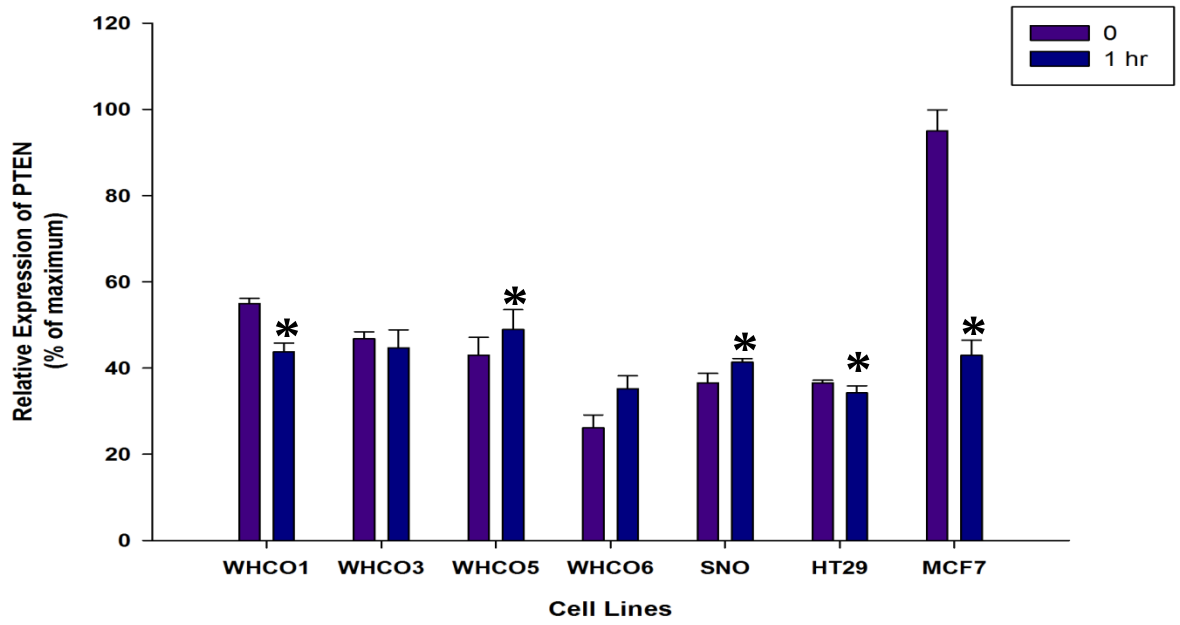


Figure 4. 4 A and B: Densitometric analysis of the western blot detection of pPKB and pGSK3β consequent to PP2A inhibition. A) Statistical analysis revealed PP2A inhibition significantly affected pPKB levels in the WHCO1 (P=0.001), HT29 (P=0.007), and MCF7 (P=0.027) respectively. **B)** Statistical analysis showing the significant effect PP2A inhibition had on pGSK3 levels in the SNO (P=0.031) and MCF7 (P=0.031) cell lines. Data are representative of mean ± S.D. obtained from the three separate experiments, *P significantly different from control, P<0.05. See Appendix C, Table C1 and C2 for statistical analysis and mean optical density values.

C)



D)

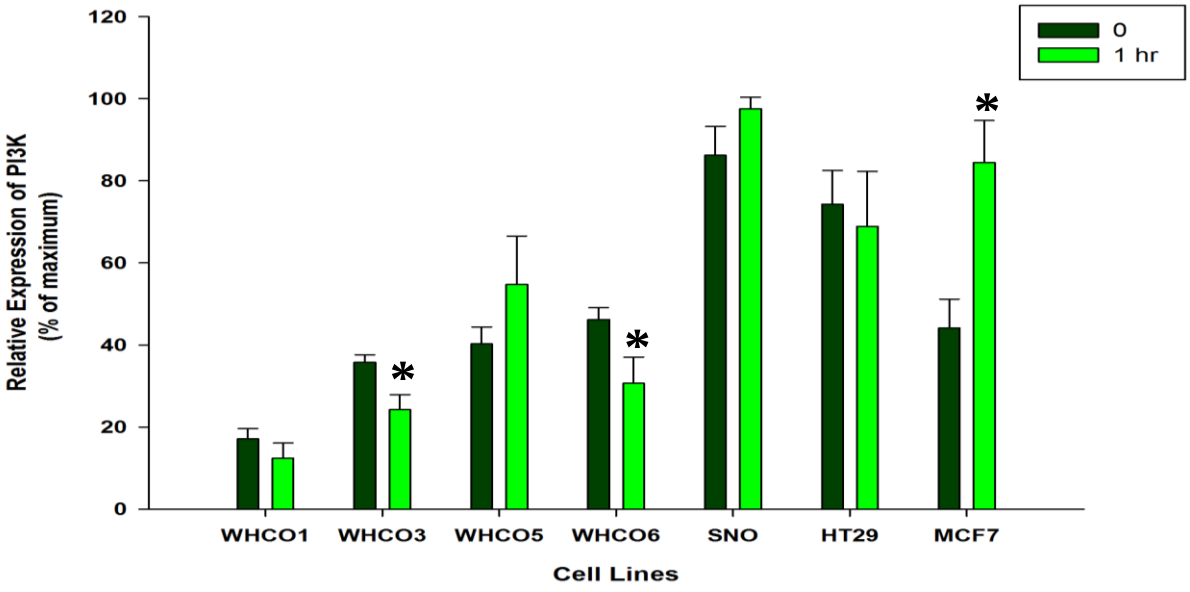


Figure 4.4 C and D: Densitometric analysis of the western blot detection of PTEN and PI3K (p85α) consequent to PP2A inhibition. A) Statistical analysis revealed PP2A inhibition significantly affected PTEN protein levels in the WHCO1 (P=0.027), WHCO5 (P=0.044), SNO (P=0.032), and MCF7 (P=0.008) respectively. **B)** Statistical analysis showing the significant effect PP2A inhibition had on PI3K (p85α) protein levels in the WHCO1 (P=0.017), WHCO6 (P=0.039) and MCF7 (P=0.003) cell lines. Data are representative of mean ± S.D. obtained from the three separate experiments, *P significantly different from control, P<0.05. See Appendix C, Table C3 and C4 for statistical analysis and mean optical density values.

E)

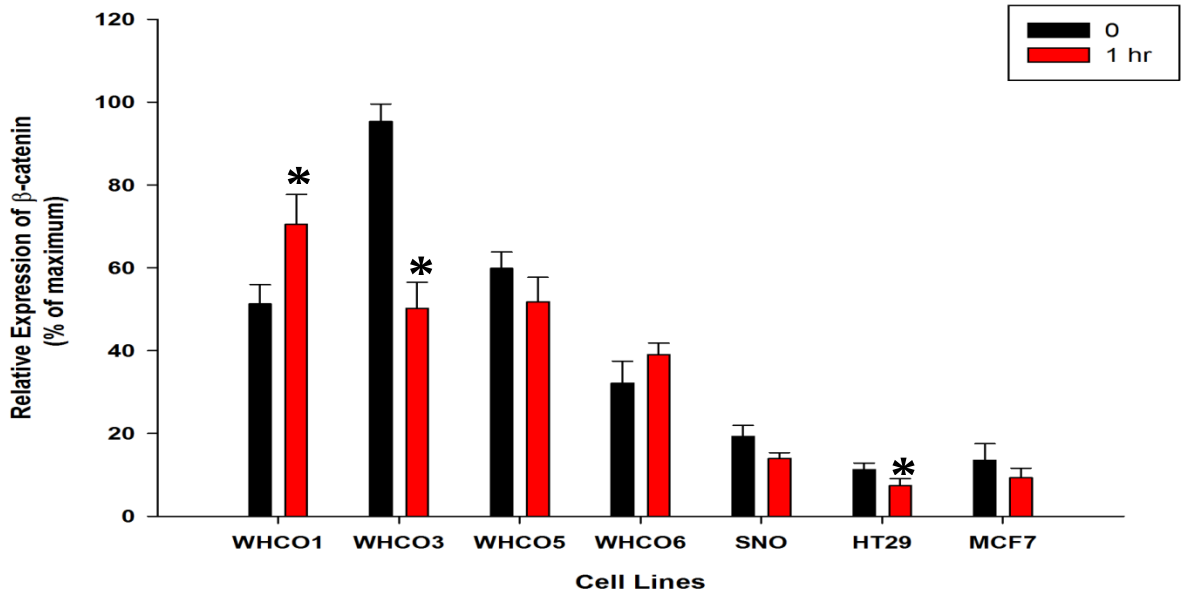
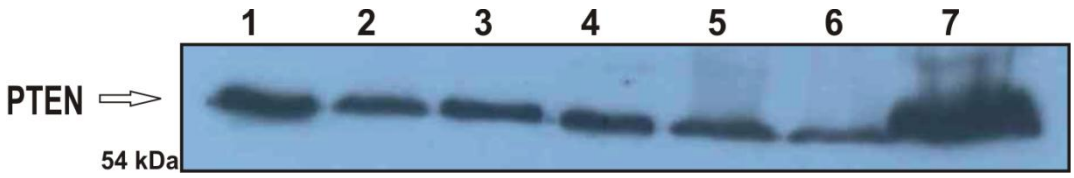


Figure 4.4 E: Densitometric analysis of the western blot detection of β-catenin consequent to PP2A inhibition. A) Statistical analysis revealed that PP2A inhibition significantly affected levels of β-catenin in the WHCO1 (P=0.01), WHCO3 (P=0.018) and HT29 (P=0.032) respectively. Data are representative of mean ± S.D. obtained from the three separate experiments, *P significantly different from control, P<0.05. See Appendix C, Table C5 for statistical analysis and mean optical values.

4.3.2 HOSCC cells express relatively low PTEN protein levels.

Since PTEN is a quasi-sufficient protein, its expression is often found to be low or absent in cancer cells[446, 596]. Despite the fact that the protein expression of PTEN was used as a control against the changes in pPKB induced by EGFR activation (Chapter 3, Section 3.3.5), PI3K inhibition (Chapter 2, Section 2.3.7), and PP2A inhibition (Chapter 4, Section 4.3.1), the basal concentration of PTEN expression in HOSCC cells still requires examination. Levels of PTEN protein are low in the 5 HOSCC lines, albeit to different degrees (shown in Fig. 4.5). Relative to the high and low PTEN previously determined within the MCF7[589] and HT29[597] controls, these data indicate that HOSCC cells are low PTEN-expressing cells. Furthermore, it is clear from these results that higher protein concentrations of PTEN in the WHCO3 cell line do account for its undetectable pPKB.

A)



B)

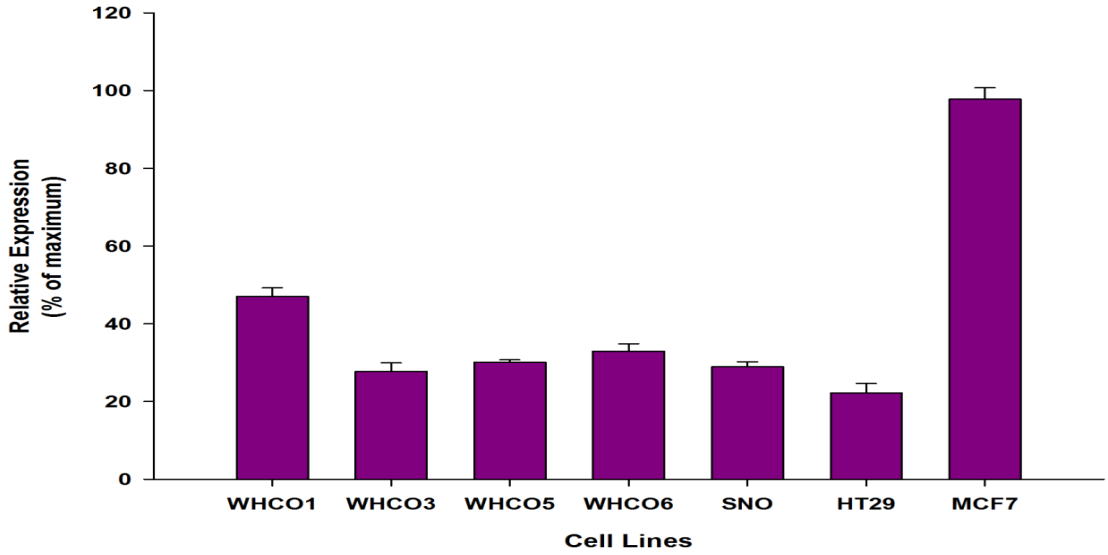


Figure 4. 5: PTEN is expressed at low levels within HOSCC cells. A) 10 μg of whole cell protein lysates derived from HOSCC, HT29 and MCF7 cell lines showing positive western blot detection for PTEN at 54 kDa (see Appendix A 1.6.6 and 1.7.5 for representative standard curve and 10% SDS-PAGE). Lanes 1-7 represent the WHCO1, WHCO3, WHCO5, WHCO6, SNO, HT29 and MCF7 cell lines accordingly. **B)** The bands representing PTEN were quantified through densitometry (mean ± s.d. of triplicate experiments), showing the highest PTEN expression in the MCF7 cell line, and the lowest in the HT29 cell line. See Appendix C, Table C6 for mean optical values.

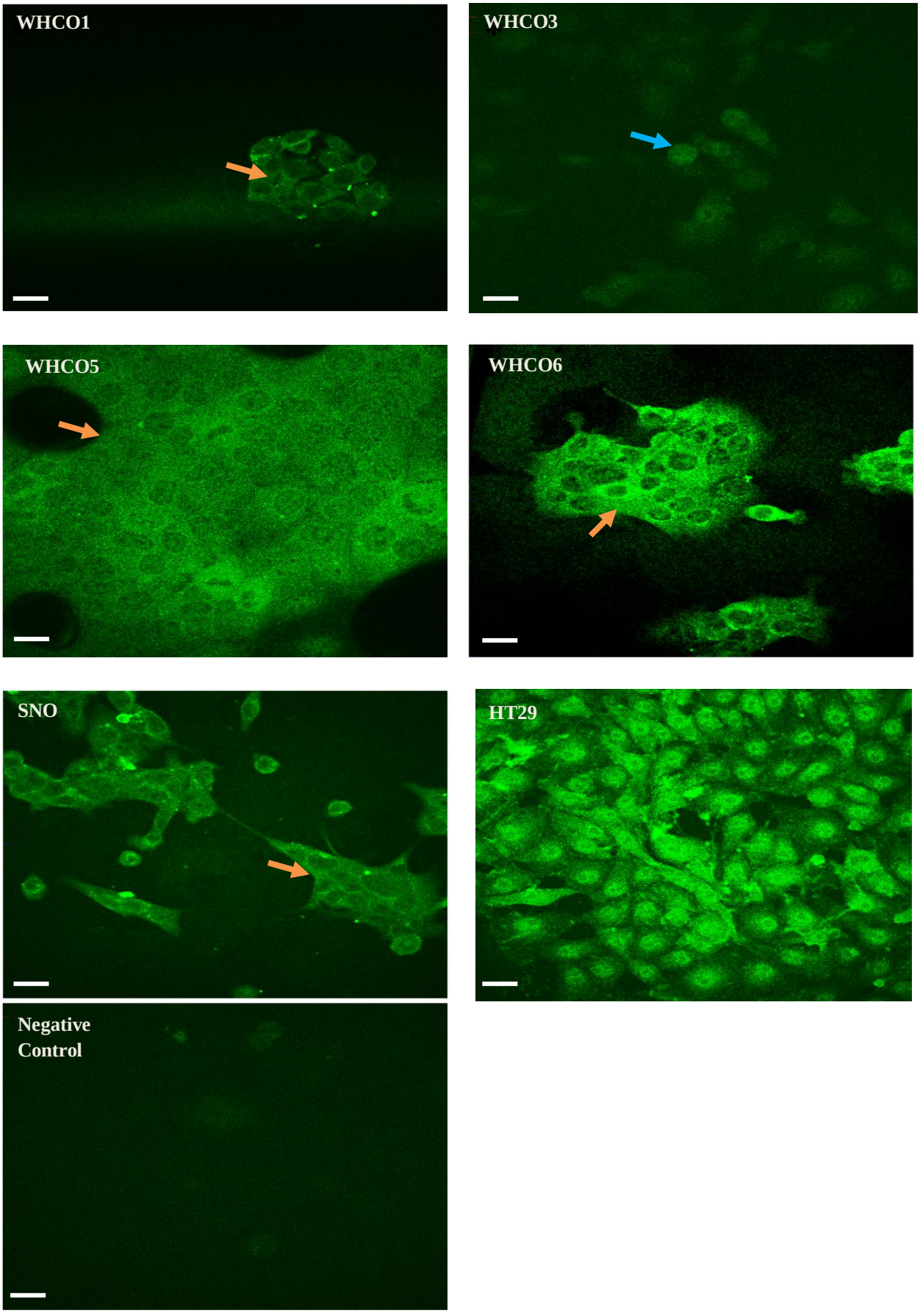
4.3.3 PTEN localization in HOSCC cells

A) Cytoplasmic Localization

The inability of a cell to transport PTEN into the nucleus is considered as one of the hallmarks of the neoplastic state, which is indicated by the accumulation of PTEN in the cytoplasm[577]. PTEN is excluded from the nucleus and localised primarily to the cytoplasm in the WHCO1, WHCO5, WHCO6, and SNO cell lines; as indicated in Fig. 4.6 (yellow arrows). The WHCO3 cell line illustrated a similar distribution pattern to that observed in the control (HT29) cell line, which included a strong PTEN nuclear localization, with a diffuse cytoplasmic distribution (indicated by the blue arrow in Fig. 4.6).

B) Nuclear Localization

As highlighted previously, the function of PTEN in the nucleus is a highly controversial issue[577, 598]. Hence, it became necessary to verify its nuclear status through western blot analysis of nuclear-specific extracts. Relative to the high nuclear levels of PTEN established for the control (HT29) cell line[578], we found that PTEN was expressed in the nucleus of four HOSCC cell lines, with the WHCO1, WHCO3, and WHCO5 in possession of the highest (> 75%) and the SNO cell line the least (20%) (see Fig. 4.7). Consistent with its cellular distribution above (Fig. 4.6), PTEN was completely absent from the nucleus in the WHCO6 cell line (Fig. 4.7).



See next page for legend.

Figure 4. 6: PTEN is predominantly localized to the cytoplasm in HOSCC cells. HOSCC and HT29 cell lines were stained for PTEN. The cytoplasmic and nuclear localization is indicated by the orange and blue arrows respectively, highlighting that the majority of PTEN was localized to the cytoplasm in the HOSCC cell lines are largely excluded from the nucleus. Under equivalent conditions, little or no staining was detected in the negative control, indicative of staining specificity. Bar column=25µm.

4.3.4 PTEN is active in HOSCC cells

We have previously shown that the down-regulation in pPKB following PI3K (Chapter 2, Section 2.3.8) and PP2A inhibition (Chapter 4, Section 4.3.1) was not induced by the relative augmented levels of PTEN[570]. Since PTEN is the major intracellular suppressor of the PI3K/PKB pathway, we examined whether PTEN is active in these HOSCC cell lines through the H_2O_2-mediated oxidation and reversible inhibition of PTEN. Elucidating its active state is of particular relevance to the greatly reduced pPKB levels within the WHCO3 cell line (Chapter 2, Section 2.3.4, and Chapter 3, Section 3.3.5).

As demonstrated in Fig. 4.8A, exposing HOSCC cells to H_2O_2 induced the oxidation, and thus inhibition, of PTEN specifically represented in the WHCO3, SNO, and HT29 cell lines. This inhibited state was symptomatic of a significant elevation in PTEN protein levels in the WHCO3 ($P<0.001$), WHCO5 ($P<0.001$), and WHCO6 ($P=0.005$) HOSCC cell lines (Fig. 4.8B). Exposure to H_2O_2 for only 10 mins was sufficient to attenuate the protein expression of PTEN significantly in the WHCO1 ($P<0.001$) and SNO ($P<0.001$) HOSCC cell lines (Fig. 4.8B). The changes in PTEN in the HOSCC cells are consistent with the levels of PTEN that were affected following exposure to H_2O_2 in the control HT29 and MCF7 cell lines that possess functional PTEN (Fig. 4.8B).

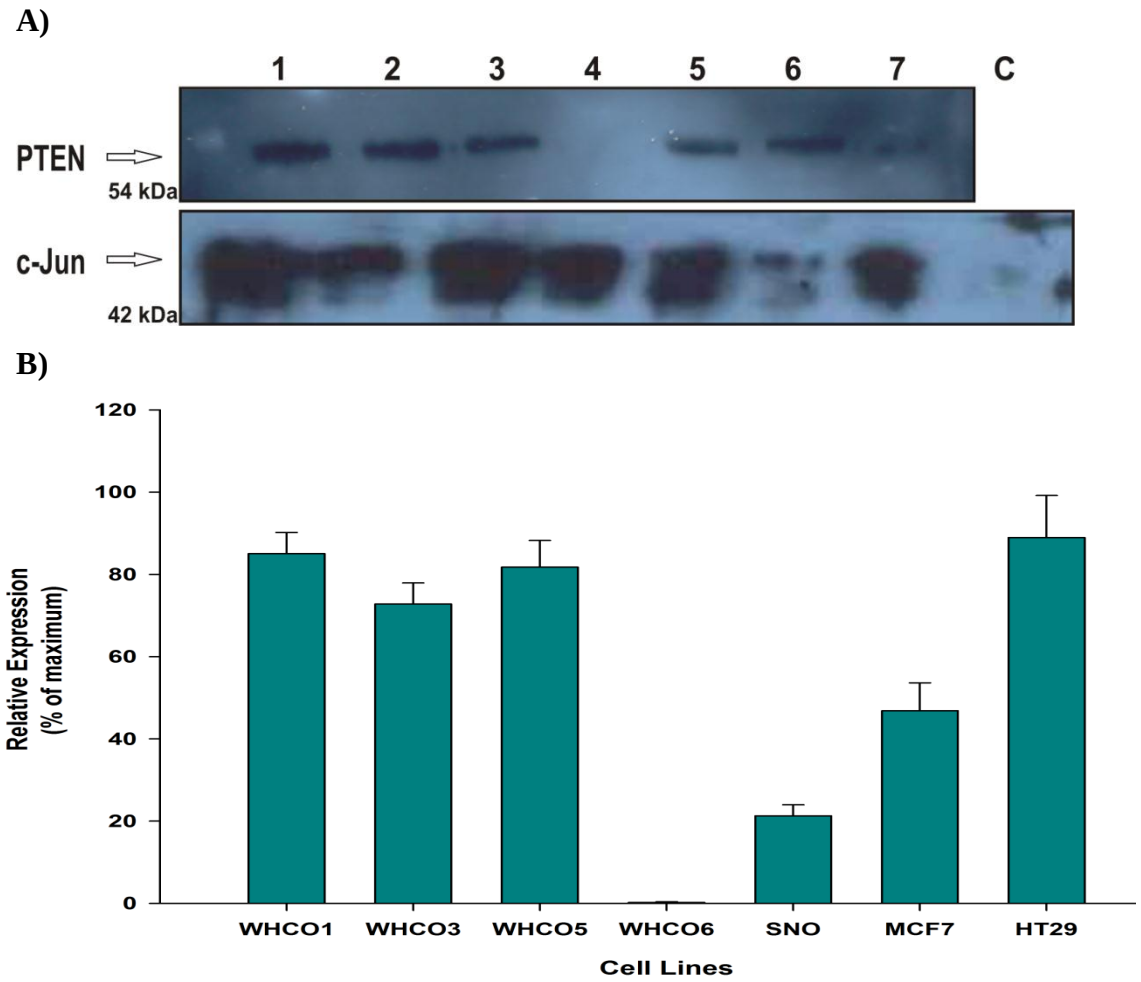


Figure 4. 7: PTEN is highly expressed in the nucleus of HOSCC cells. A) The relative expression of PTEN in the nucleus is shown through western blotting at 54 kDa in the HOSCC, MCF7 and HT29 cell lines (see Appendix A 1.6.6 and 1.7.5 for representative standard curve and 10% SDS-PAGE). The integrity of the nuclear extracts was verified through the positive detection of the c-Jun transcription factor at 42 kDa[352], and the lack thereof in the WHCO6 whole cell protein lysate (C). Lanes 1-8 represent WHCO1, WHCO3, WHCO5, WHCO6, SNO, MCF7, HT29 and WHCO6 whole cell protein extract. **B)** The band representing PTEN was quantified through densitometry (mean ± s.d. of triplicate experiments), showing the highest expression in the WHCO1, and the lowest in the SNO HOSCC cell line. See Appendix C, Table C6 for mean optical density values.

A)

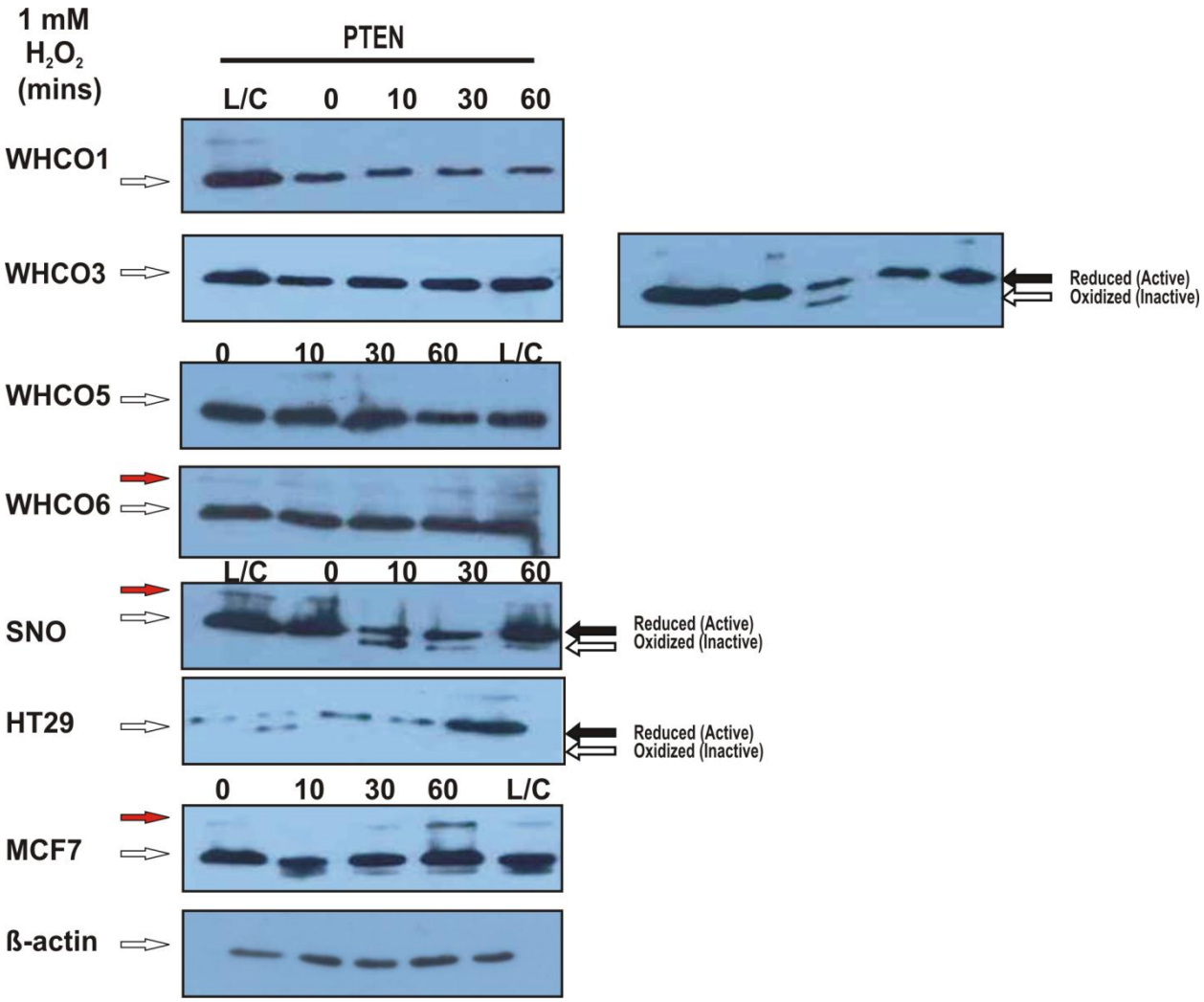


Figure 4. 8 A : Cellular PTEN is inactivated in response to oxidative stress by exposure to H_2O_2. The 5 HOSCC cell lines, HT29 and MCF7 cell lines were treated for 10, 30 and 60 mins with and without 1 mM of H_2O_2. Western blot analysis was used to determine the reduced (active) and oxidized (inactive) state of PTEN, indicated by the white arrows (see Appendix A 1.6.6 and 1.7.5 for representative standard curve and 10% SDS-PAGE). The red arrow indicates possible PTEN ubiquitination, suggested by previous studies[599]. The method used to detect the reduced and oxidized form of PTEN is described in detail under Materials and Methods. β-actin was used as an internal control, and L/C represents a WHCO6 whole cell lysate used as an loading control for comparison between the respective blots.

B)

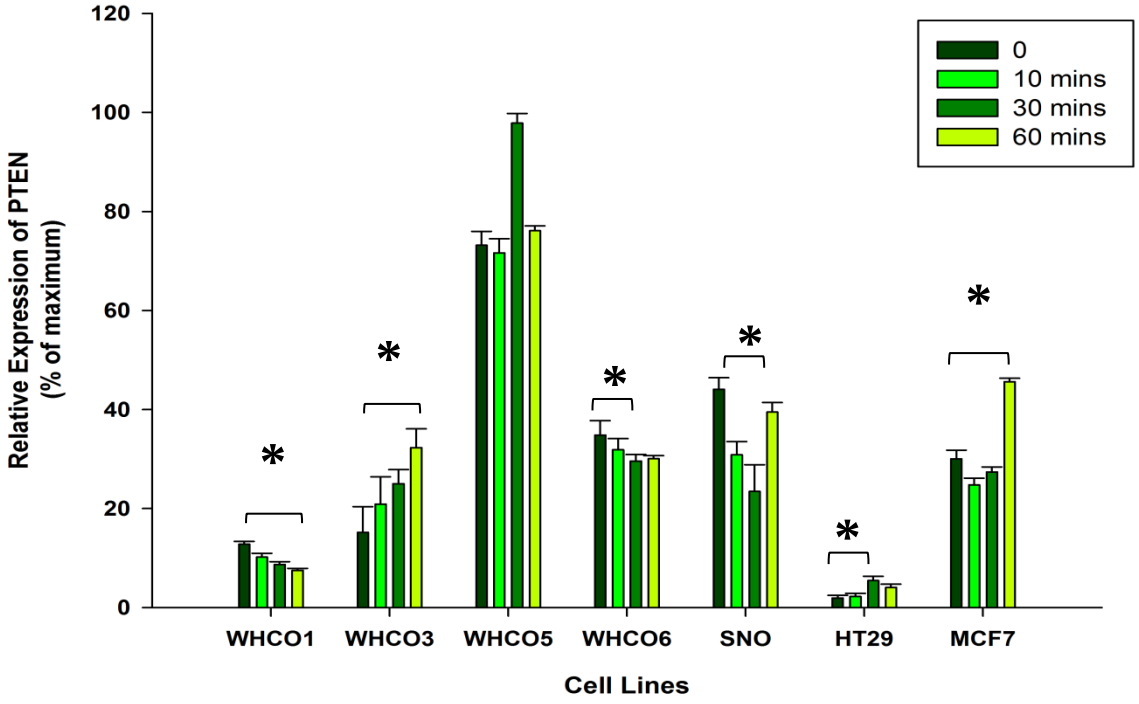


Figure 4.8 B: The experiment was performed in triplicate and the levels of PTEN expression following H_2O_2 exposure were quantified by densitometric analysis and represented in a bar graph (mean ± s.d. of triplicate experiments). Results show a significant decline in PTEN levels in the WHCO1 ($P<0.001$), WHCO6 ($P=0.001$ and 0.005), SNO ($P=0.002$ and <0.0001), and MCF7 ($P=0.001$ and 0.027) cell lines accordingly. On the contrary, a significant increase in PTEN levels was evident in the WHCO3 ($P<0.001$), WHCO5 ($P<0.001$), and MCF7 ($P<0.001$) cell lines respectively. See Appendix C, Table C7 for statistical analysis. *Significantly different from the control, $P<0.05$.

Based on the clear oxidized and inhibited state of PTEN, it became essential to analyse what effect this would have on its intracellular downstream targets described previously; pPKB, pGSK3β, PI3K (p85α), and β-catenin[572]. Levels of pPKB increased significantly in four of the HOSCC cell lines, with the WHCO1 cell line being the exception (see Fig. 4.9A and B). Strikingly, the concentration of pPKB was significantly ($P<0.001$) induced by 38% in the WHCO3 cell line following a 60 min exposure to H_2O_2 (see Fig.4.9A). Even though PTEN was inhibited (Fig. 4.8A), its protein expression was not inversely correlated to pPKB (see Appendix C, Table C9). No inverse relationship between PTEN and pPKB was demonstrated in the positive HT29 and MCF7 controls, but instead their levels correlated at significantly at 60 mins in the MCF7 control respectively (see Appendix C, Table C9).

pGSK3β was also significantly affected in the 5 HOSCC cell lines by H_2O_2 (Fig. 4.9A, and C). It is clear from the above that the increase in PKB activity (pPKB) in Fig. 4.9A did not correlate to the changes in pGSK3β in Fig. 4.10B (see Appendix C, Table C9). A positive correlation between pPKB and pGSK3β levels was only shown in the MCF7 control (see Table C9 in Appendix C).

It was previously demonstrated that PP2A, and not PTEN, was inhibited when the Caco-2 colon cancer cell line was exposed to 20 µM H_2O_2[600]. We therefore included the Caco-2 cell line in this study to further support the inhibitory effect that the 1 mM H_2O_2 utilized here, has on PTEN. Consistent with these results (Fig. 4.9A), the concentration of pPKB was significantly ($P<0.001$) enhanced at 20 µM H_2O_2 in the Caco-2 cell line (Fig. 4.10). In contrast, no similar changes were apparent at 1 mM H_2O_2. Therefore, the changes in pPKB obtained in the HOSCC cells following 1 mM H_2O_2 above (Fig. 4.9A) are PTEN, and not PP2A dependent. This is in agreement with the results shown following direct inhibition of PP2A in the WHCO and SNO cell lines (see Fig. 4.3).

Assessing the protein expression of PI3K (p85α) and β-catenin following H_2O_2 exposure revealed that their expression was significantly affected in the HOSCC cell lines (see Fig. 4.11). The significant increase in the concentration of β-catenin in the WHCO3 cell line ($P<0.001$) is consistent with the increase in β-catenin observed in the control cell line (HT29).

A)

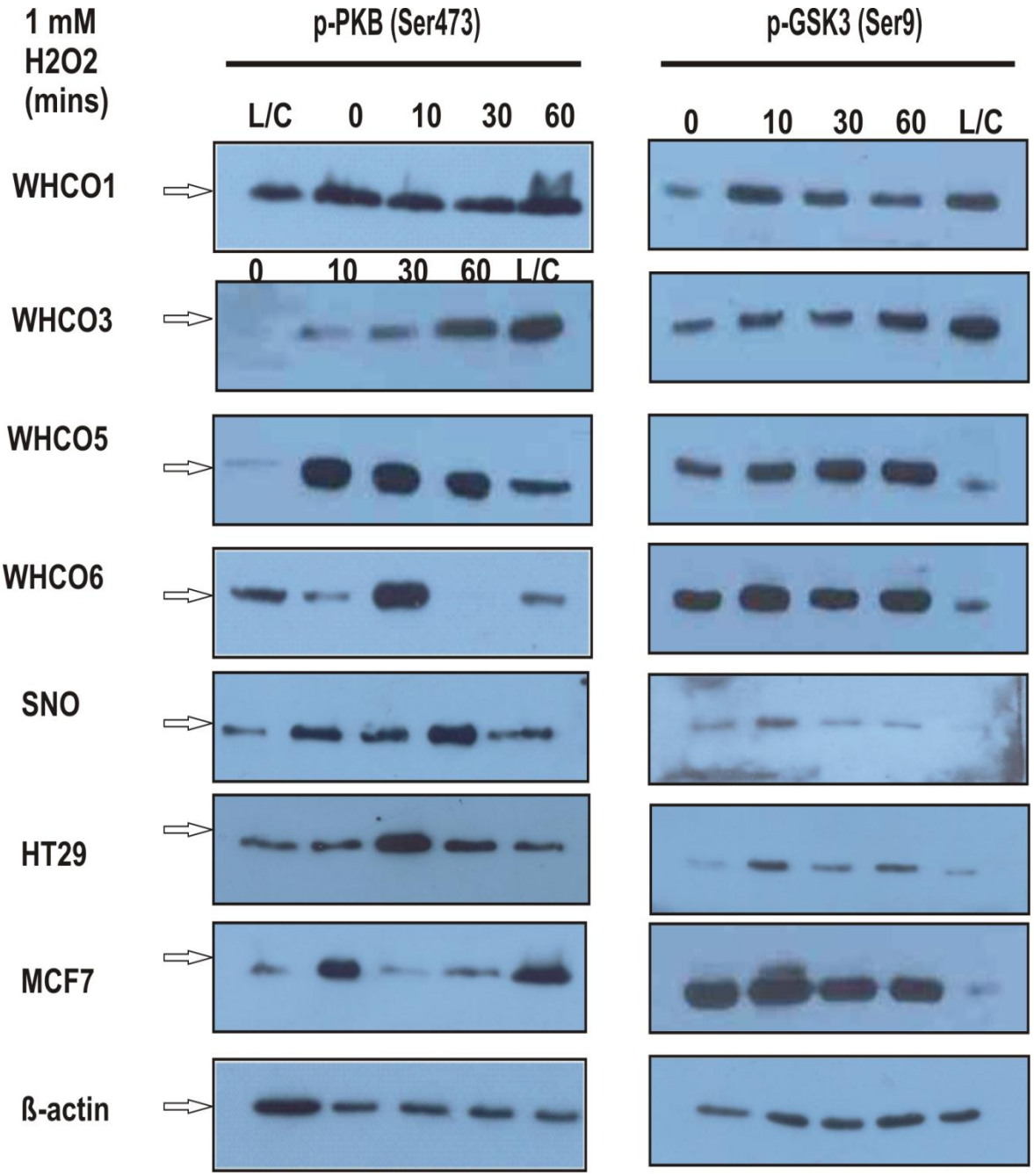
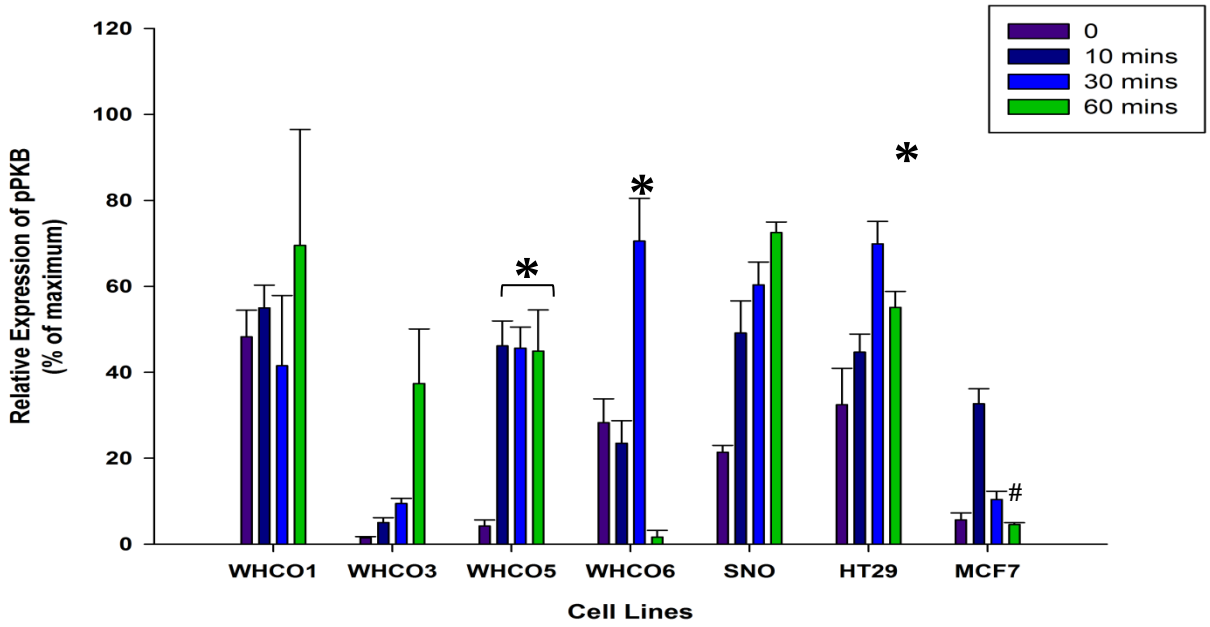


Figure 4. 9 A: The PI3K/PKB pathway is activated in response to PTEN inhibition. Western blot analysis was used to determine the putative active forms of PI3K (p-PKB at Ser473) and PKB (p-GSK3β at Ser9) following exposure to H_2O_2 for 10, 30 and 60 mins in the HOSCC, HT29 and MCF7 cell lines. See Appendix A 1.6.6 and 1.7.5 for representative standard curve and 10% SDS-PAGE. β-actin was used as an internal control, and (L/C) represents a WHCO6 whole cell protein lysate that was used as an loading control for comparison between the different blots.

B)



C)

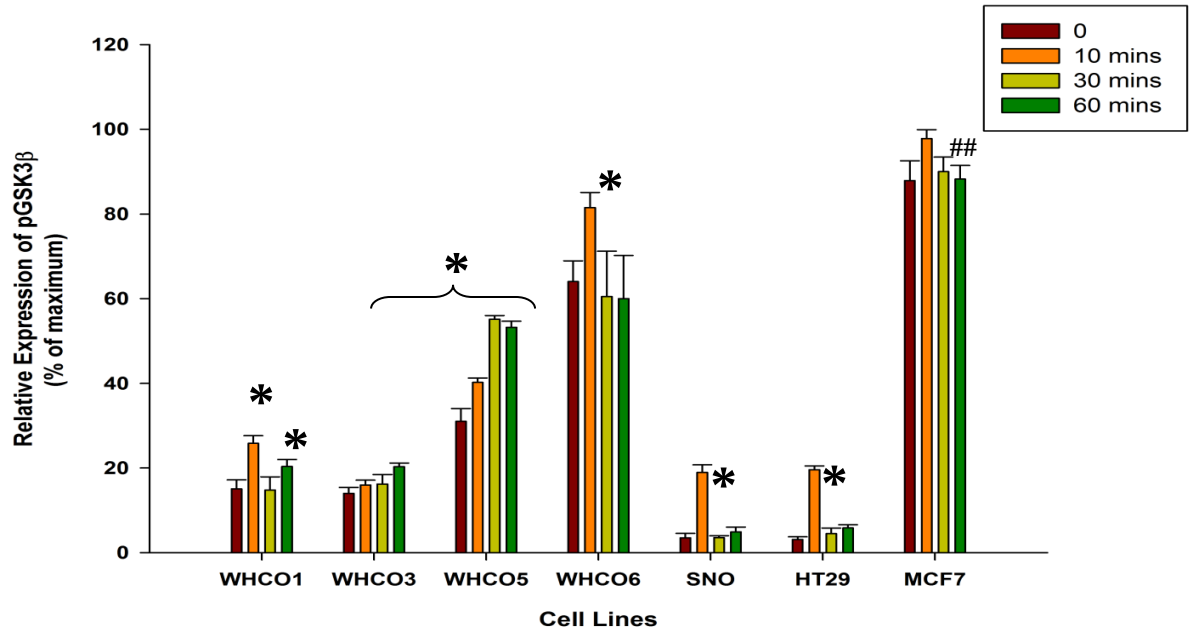


Figure 4.9 B and C: The experiment was performed in triplicate (mean ± s.d.) and the levels of pPKB **(B)** and pGSK3β **(C)** following PTEN inhibition induced through H_2O_2 exposure was quantified by densitometric analysis. Results show a significant (P<0.001) decline in PTEN levels in the WHCO1, WHCO6, SNO, and MCF7 cell lines accordingly. On the contrary, a significant increase in PTEN levels was evident in the WHCO3, WHCO5, and MCF7 cell lines respectively. *P significantly different from control, P<0.05. #, positively correlates with PTEN expression, ##, positively correlates with levels of pPKB. See Appendix C, Table C7 and C10 for the statistical analysis.

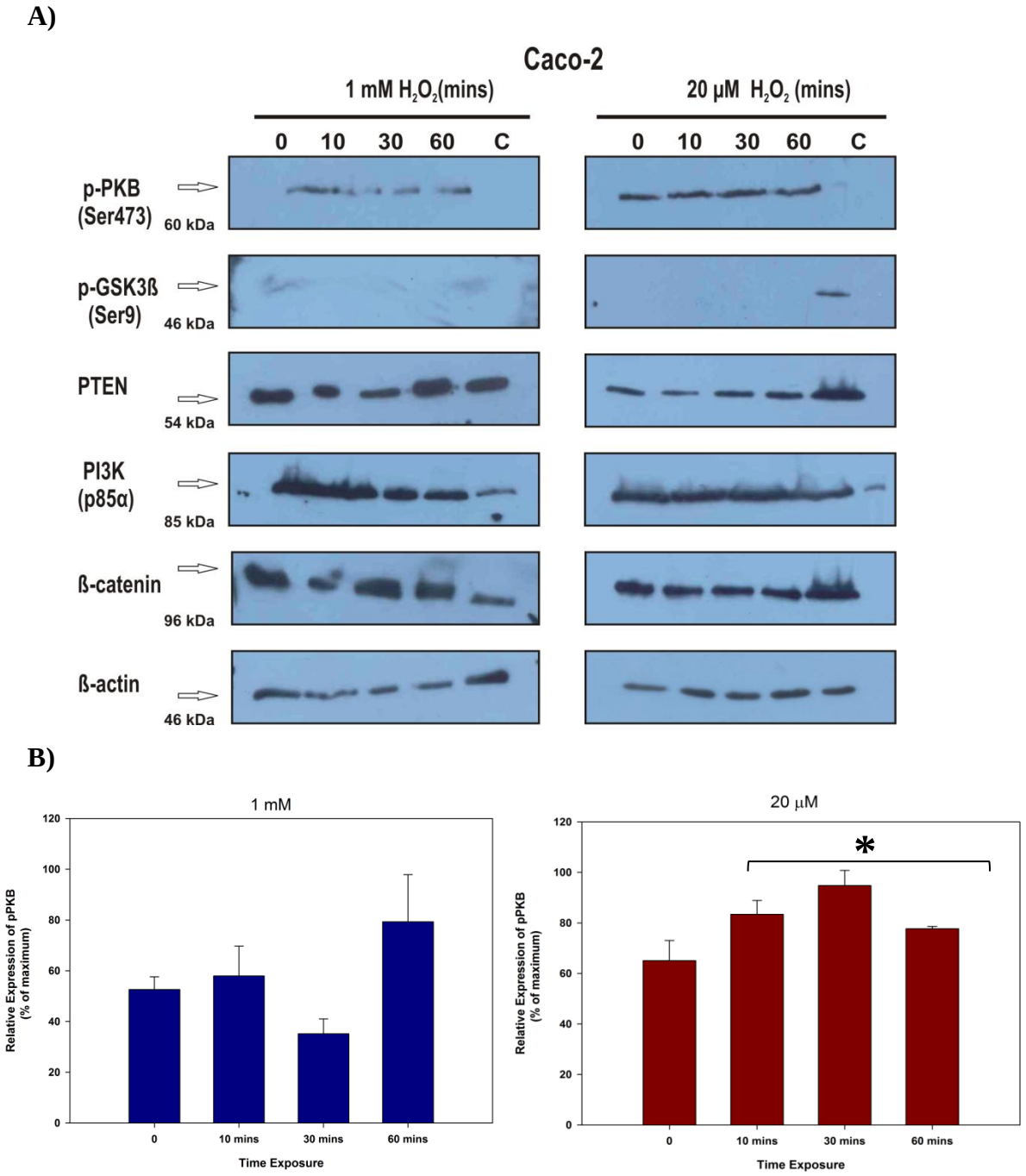


Figure 4. 10 A and B: Caco-2 cells exposed to 20 µM H_2O_2 induces levels of pPKB. A) Caco-2 cells were exposed to 20 µM and 1 mM of H_2O_2 for 10, 30, and 60 mins, and the resultant concentration of p-PKB (Ser473), p-GSKβ (Ser9), total cellular levels of PTEN, PI3K and β-catenin were assessed through western blotting. A standardized loading control (C) was included in blot analysis to allow for comparison between the various immunoblots. β-actin was used as an internal control. **B)** The experiment was repeated three times for pPKB detection and quantified through densitometry showing significant increases in pPKB levels at 20 µM concentrations of H_2O_2 only, see Appendix C, Table C8 for statistical analysis.*P significantly different from control, $P<0.05$.

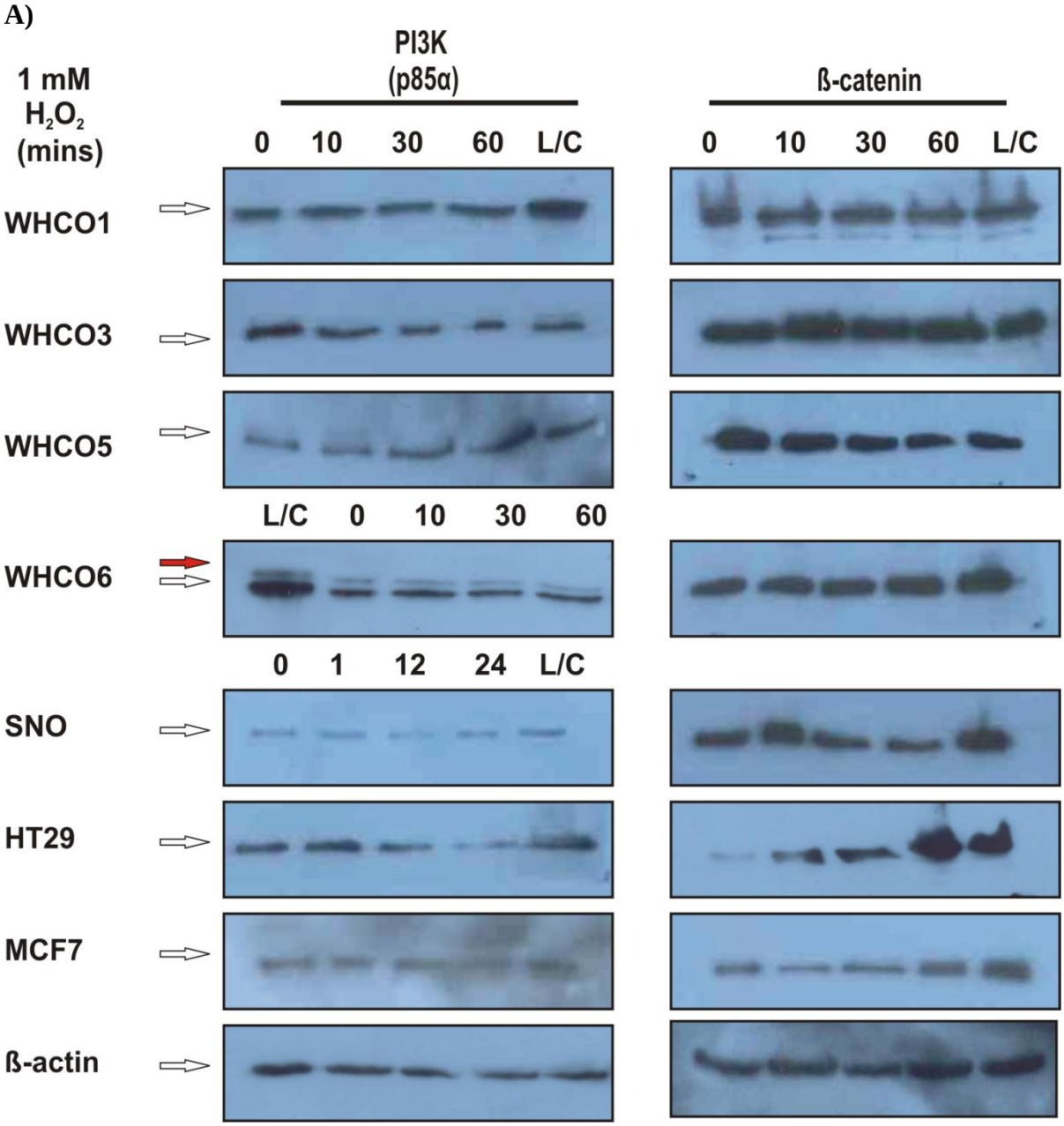
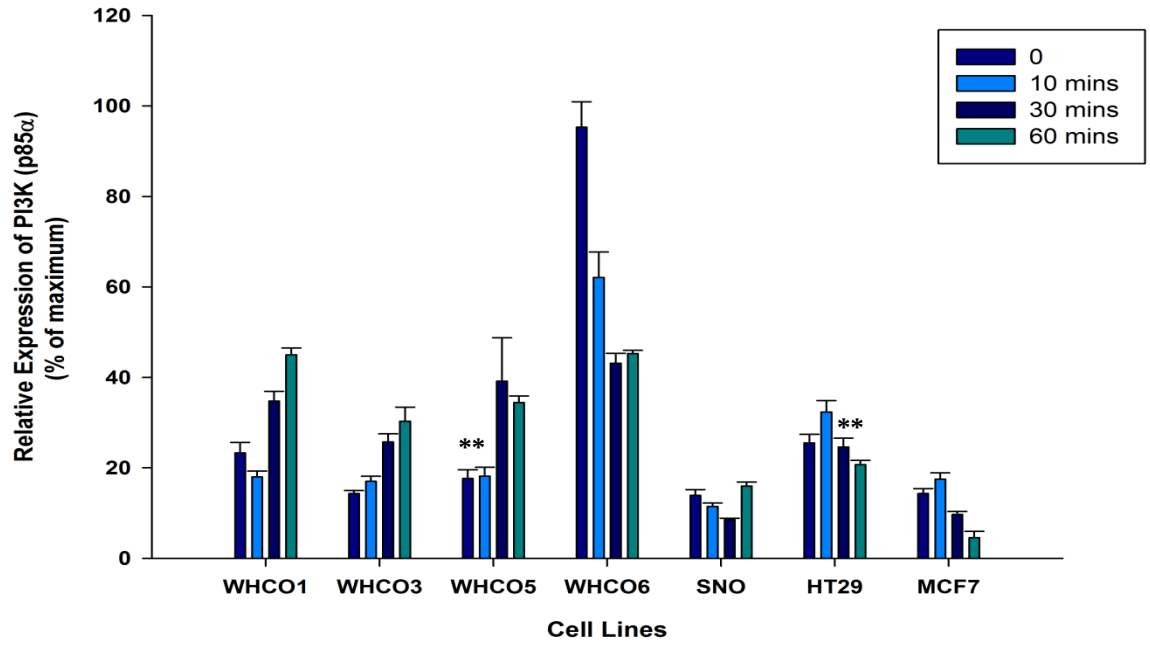


Figure 4. 11 A: The levels of PI3K and β-catenin are not significantly altered in response to H_2O_2 in HOSCC cells. A) HOSCC, HT29 and MCF7 cell lines were treated for 10, 30 and 60 mins with and without 1 mM of H_2O_2. Western blot analysis was used to determine the resultant protein levels of PI3K (p85α) and β-catenin at 86 and 96 kDa respectively (see Appendix A 1.6.6 and 1.7.5 for representative standard curve and 10% SDS-PAGE). β-actin was used as an internal control, and (C) represents a WHCO6 whole cell extract used for comparison between the different blots. The red arrow is indicative of one of the PI3K isoforms, which shares 95% sequence homology to the α isoform of the PI3K (p85α) subunit under evaluation (Upstate Biotechnology, data sheet).

B)



C)

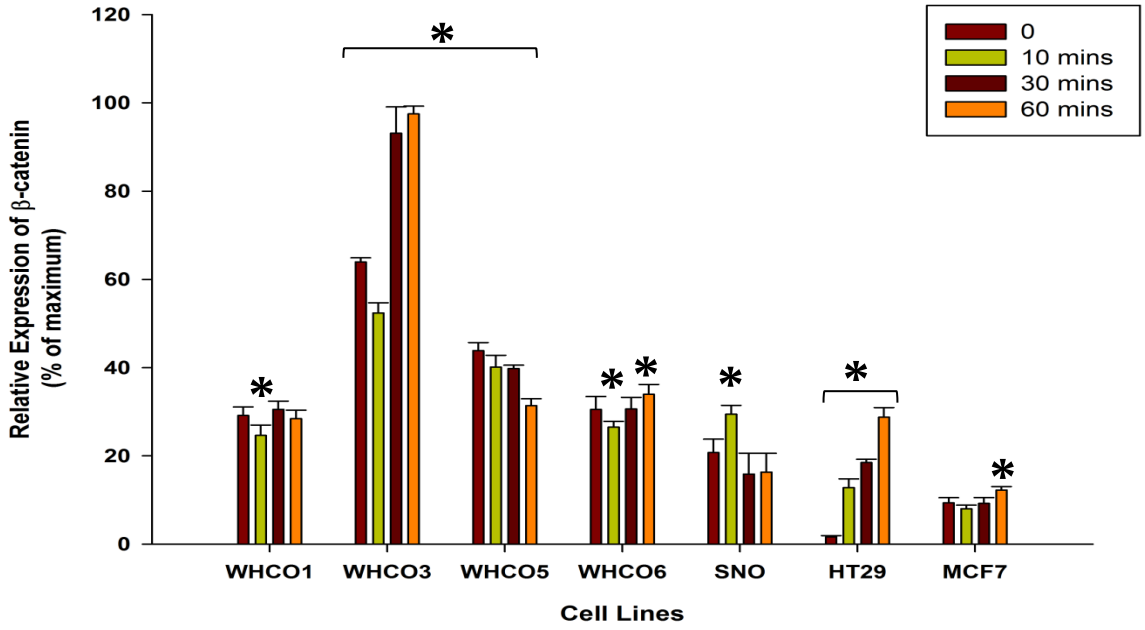


Figure 4.11 B and C: The experiment was performed in triplicate and the levels of PI3K (p85α) **(B)** and β-catenin **(C)** expression following H_2O_2 exposure were quantified by densitometric analysis (mean ± s.d.). Levels of PI3K (p85α) changed significantly for most cell lines ($P<0.05$), **not significantly different from the control, *P significantly different from control, $P<0.05$. See Appendix C, Table C7 for statistical analysis.

4.4 Discussion

Although the antagonistic roles of PTEN and PP2A towards the PI3K/PKB pathway are well established[548, 601], their specific contribution to cancer progression appears to be regulated by the type of cell. Their aberrant expression and tumour suppressive capabilities are frequently associated with the poor prognosis of prostate[602, 603], breast[604, 605], colon[575, 606], and non-small lung cancers[607], whereas similar reports for oesophageal cancer are less common. Furthermore, the preceding chapters point towards the possibility of aberrant PTEN and/or PP2A present within the 5 HOSCC cell lines. The previously established PP2A activity[587, 588] and functional PTEN[589,590], within the HT29 and MCF7 cell lines served as a comparison against the unknown function of PP2A and PTEN in the HOSCC cell lines. In this chapter, we provide evidence that the action of PP2A towards the PI3K/PKB pathway is attenuated and that although weakly expressed, PTEN is indeed active within the WHCO and SNO HOSCC series.

By using the PP2A inhibitor, OA, we verified that PP2A only influences the Ser473 phosphorylation of PKB in the WHCO1 and WHCO6 cell lines, while no significant changes were observed in the remaining HOSCC cell lines (see Fig. 4.3 and 4.4). The specificity of this result was confirmed by the coordinated PP2A inhibition through OA shown in the HT29 and MCF7 control cell lines. Through their regulation of C-ECM adhesion; the integrins are well-recognized for their proficient activation of a variety of intracellular and extracellular signalling pathways[608]. Of interest, the α2β1 integrin has been demonstrated previously to induce PP2A activity, leading to the concomitant dephosphorylation in PKB (Ser473) and GSK3β (Ser9), resulting in their respective inhibition and activation[609, 610]. Since these HOSCC cell lines have reduced levels of both the α2 and β1 integrin subunits[611], may explain why the levels of pPKB in these HOSCC cell lines were unresponsive to PP2A inhibition. These data strongly point to PP2A-independent mechanisms for the dephosphorylation and inhibition of PKB in HOSCC lines. This interpretation is consistent with the 40% reduction or complete loss of PP2A function observed in breast carcinoma cells[612]. In addition to the α2β1 integrins, the activity of PP2A is further attenuated by phosphorylation of its Tyr307 residue mediated by active EGFR[613]. Based on the up-regulated EGFR levels in these HOSCC lines; it seems logical to suggest that the EGFR overexpression status may further contribute to the apparent decreased activity of PP2A observed in this chapter.

The molecular chaperone, Hsp90 and its co-chaperone, Cdc37, are both required for the activity and stability of PKB by preventing PP2A-mediated dephosphorylation[614, 615, 616]. In turn, CK2

phosphorylates and modulates the association between Hsp90 and Cdc37[617, 618]. This opens the possibility for the existence of robust Hsp90-CK2-Cdc37-PKB associations within these HOSCC cell lines; offering PKB protection against PP2A-mediated Ser473 dephosphorylation, thus leading to the lack of responsiveness to PP2A inhibition observed. The notion of robust Hsp90-CK2-Cdc37-PKB associations is supported by evidence demonstrating that the stability of pPKB through its association with CK2 is insensitive to PP2A inhibition through OA treatment[619]. As it is the balanced activity of PDK-1-mediated Thr308 phosphorylation and PP2A-mediated Ser473 dephosphorylation of PKB, that ultimately determines its activational state[180], points to the existence of robust PDK1 activity within these HOSCC cells. Furthermore, these data also clearly indicate that PP2A-independent mechanisms are the cause for the undetectable pPKB levels within the WHCO3 cell line. Certain reports have linked this reduced role for PP2A on PKB to the fact that PP2A is a reluctant or lazy TSP[620, 621, 622].

It was also shown that PP2A plays a significant role in the dephosphorylation, and thus activation of GSK3β on its Ser9 residue in the WHCO6 and SNO HOSCC cell lines. This is in agreement with previous studies, showing the direct relationship between PP2A activity and the augmented Ser9 phosphorylation state of GSK3β[623, 624]. A specific study conducted in mice, revealed that knockdown of PP2A up-regulated the Ser9 phosphorylation of GSK3β, but not the Ser473 phosphorylation of PKB[625]. Evidence suggests that PP2A is only able to dephosphorylate GSK3β on Ser9 when it is associated with APC and Axin[626]. Of note, previous studies have indicated that APC and β-catenin are associated in these HOSCC lines[627]. Moreover, it is known that the association between APC and β-catenin can only take place when simultaneously interacting with Axin and GSK3β[624]. Considering that we were unable to demonstrate a direct link between the concentration of pPKB and pGSK3β (Chapter 2, Section 2.3.7), suggests that PP2A may play a more direct role in regulating pGSK3β levels in HOSCC cell lines.

Several substrates for PP2A have been discussed within the literature[628,629], and therefore even though it does not target PKB in HOSCC cells, it was shown to have a significant impact on the protein levels of PTEN, PI3K (p85α) and β-catenin in the WHCO1 (PTEN and β-catenin), WHCO3 (PI3K and β-catenin), WHCO5 (PTEN), WHCO6 (PI3K), and SNO (PTEN) HOSCC cell lines (see Fig. 4.4) Since PP2A is an integral and direct regulator of β-catenin through its B56 subunit[562], it was no surprise that significant changes in its protein expression were induced through PP2A inhibition. As the role for PP2A in regulating β-catenin cellular levels has been previously shown in the HT29 cell line[562], lends additional support for the significant role played by PP2A in the regulation of β-catenin in the WHCO1 and WHCO3 HOSCC cell lines

specifically. Furthermore, PP2A has been shown to directly regulate the expression of c-myc[630]. Therefore, accumulation of c-myc serves as a good indicator for the presence of attenuated PP2A activity[629]. The identification of a c-myc amplification present within the WHCO3 cell line specifically[631], suggests that the activity of PP2A is indeed suppressed; as most clearly shown here with the nonresponsive pPKB levels.

Various studies have linked the presence of low and/or absent levels of PTEN to the carcinogenic state of the cell, such that, a lower expression is consistent with a reduction in its activity [446,574,575,576]. Consistent with these reports, it was shown that the 5 HOSCC cell lines express low PTEN protein levels. This was verified by comparing it to the high expression of PTEN expressed in the MCF7 cell line[589]. The low protein concentration of PTEN shown here is consistent with a study conducted on Japanese-derived oesophageal squamous cell lines, where levels of PTEN were significantly lower when compared to normal oesophageal epithelium[457]. Notwithstanding the significance of low PTEN concentrations in the prognosis of various cancer types[,574,575, 632], the fact that the mere presence of PTEN is sufficient to antagonize the activity of PI3K and PKB[446], strongly highlights the need to fully understand the specific mechanisms used to control these low PTEN levels.

Similar to these low levels, a disrupted balance between the cytoplasmic and nuclear distribution of PTEN is also considered a good marker for cells with aberrant PTEN[577]. The data presented here indicates that PTEN is highly localized to the cytoplasm in the WHCO1, WHCO5, WHCO6, and SNO HOSCC cell lines. These results are consistent with a previous report demonstrating a predominant cytoplasmic PTEN localization in a separate line of oesophageal cell lines[457]; which they linked to an inactive or dysfunctional PTEN. The presence of PTEN in the nucleus of the WHCO1, WHCO3, WHCO5, and SNO cell lines was also verified through western blotting. Whether it is the nuclear or cytoplasmic localization of PTEN that accounts for its aberrancy is a highly controversial matter[577]. According to Das *et al.*[633]and Liu *et al.*[634]; nuclear PTEN is able to actively suppress growth and proliferation by various mechanisms, while cytoplasmic PTEN is inadequate in this regard. In contrast, results reported by Chung *et al.*[635] clearly demonstrate the integral role for the nuclear import of PTEN during carcinogenesis. Previously, it was shown that PTEN contributes to the differentiation state of neurons through its regulation of mitosis in the nucleus[636]. Thus, it would appear that the particular mechanisms used to regulate the nuclear and cytoplasm partitioning of PTEN are influenced by the intra- and extracellular environment, and thus are particularly tissue specific. The nuclear levels of both PI3K and pPKB were established in the 5 HOSCC cell lines (Chapter 2, Section 2.3.3 and

Section 2.3.5). Interestingly, when the cellular distribution of PTEN obtained here (see Fig. 4.6) is compared with the staining pattern of pPKB shown previously (see Fig. 2.10), it seems clear that cellular localization of these two proteins are mutually exclusive in HOSCC cells. This relationship appears to be highly prevalent within the WHCO1, WHCO5, WHCO6, and SNO HOSCC cell lines; where the nuclear levels of pPKB appears to be linked to the nuclear exclusion and highly cytoplasmic staining for PTEN. Since it is still widely accepted that the altered subcellular localization of PTEN is a major signature for its aberrant signalling in cancer cells; it would appear that the nuclear exclusion and cytoplasmic localization of PTEN in HOSCC cells may prove to be indicative of its aberrant state. In accordance with this view, a recent study provided evidence that activation of PTEN leads to the rapid depletion of nuclear pPKB that caused a corresponding stop in the cell cycle, evidenced by rapid cyclinD1 degradation[637]. It thus became necessary to evaluate whether PTEN is active in these HOSCC cell lines.

The reversible inhibition of PTEN by the oxidation of its active cysteine residues is known to occur upon the intracellular production of H_2O_2 by Nox during the activation of the PI3K signalling pathway[581, 638]. Here, through the H_2O_2-mediated oxidation and inhibition of PTEN, we show that PTEN is indeed active in all the 5 HOSCC lines, evidenced by pPKB detection. Perhaps what was outstanding was the finding that the previously undetectable pPKB levels in the WHCO3 cell line, was expressed following inhibition of PTEN (see Fig. 4.9). The elevation in pPKB established here, is on par with work done on PC12[551] and Caco-2[600] cells, where exposure to lower H_2O_2 concentrations (25 μM and 20 μM) caused a significant increase in the concentration of pPKB respectively. In both cases, however, H_2O_2 induced PP2A, and not PTEN inhibition. Thus, in support of our foregoing results that excluded a role for PP2A in HOSCC cells, it was further shown that under our conditions, the effects elicited by H_2O_2 on pPKB were not induced by PP2A (see Fig. 4.10).

The data presented here suggests that, even though H_2O_2-mediated inhibition of PTEN significantly affected the concentration of pPKB, PTEN oxidation was readily reversed, thus pointing to additional mechanisms utilized by H_2O_2 to induce levels of pPKB. There are a number of plausible explanations for these results. It is well-known that, depending on the cell type, the presence of H_2O_2 is short-lived and is more than likely removed from the system within 30 mins of exposure[639, 640,641]. This is primarily achieved by the presence of peroxiredoxin (Prdx), which readily catalyses the conversion of H_2O_2 into water[642]. Research demonstrates that the expression of PTEN exists in a 1:1 molar ratio with the Prdx1, protecting it from H_2O_2-

induced oxidation and inhibition[643,644,645]. Therefore, based on the rapidly reduced PTEN state in the representative WHCO3 and SNO cell lines within 30 and 60 mins of exposure to H_2O_2 (see Fig. 4.8A), it seems logical to assume that this association (PTEN/Prdx1) may be more pronounced in HOSCC cells. This suggestion is supported by a study performed in mice, whereby knock-down experiments on Prdx1 disenabled their ability to scavenge H_2O_2, which lead to their premature death[646]. Furthermore, the rapid reduction of PTEN shown in the MCF7 cell line supports this concept (see Fig. 4.8 and 4.9), as they were shown to overexpress Prdx1[647].

An earlier study suggested that the existence of a robust H_2O_2 scavenging system impairs the cells ability to respond efficiently to EGFR stimulation[648]. This is deduced from the intimate relationship existing between EGFR activation and H_2O_2 production described above[649, 650]. It was shown in the previous chapter that EGFR stimulation had a minimal impact on the activation of the PI3K/PKB pathway (pPKB levels) (Chapter 3, Section 3.3.5). Therefore, it seems clear that this relationship may be lost in HOSCC. Upon EGFR activation, there are two downstream factors that are central to the simultaneous production of H_2O_2 by Nox. Firstly, the membrane recruitment of PI3K was shown to be critical for the H_2O_2 production through Nox[651, 652]. Since the membrane localization of PI3K in the 5 HOSCC cell lines has been demonstrated (Chapter 2, Section 2.3.3), we can exclude this as a contributing factor. Secondly, aquaporin3 (AQP3) was shown to play a central role in the mediation of EGF-stimulated H_2O_2 production by an unknown mechanism[653, 654, 655]. Conveniently, the colon HT29 cell line was shown to overexpress AQP3[656], and therefore it is not surprising that activation of the PI3K/PKB pathway (pPKB levels) was readily induced by EGFR stimulation (Chapter 3, Section 3.3.5). On the hand, EGFR stimulation in HOSCC cells did not have a similar effect on pPKB levels; lending additional support to an aberrant relationship between EGFR stimulation, PI3K/PKB activation and PTEN inhibition in HOSCC cells.

High levels of active PKB (pPKB) have been shown to correspond to H_2O_2 overproduction, and suggested to be insufficient to maintain the pro-survival state[657]. This has been deduced from certain reports demonstrating that PKB aids in the anti-survival status of a cell by its ability to regulate intracellular levels of H_2O_2 [657,658,659]. These reports have likened this anti-survival capability of PKB to the particular cellular environment, suggesting that cancer cells need to overcome or convert these antagonistic properties of PKB to that of a more "favourable" one. The role for H_2O_2 as a pro-survival molecule is becoming a hot-topic within the literature. Hence, the ability of a cell to use H_2O_2 to their growth advantage is largely determined by its ability to dampen the anti-survival capability of PKB[660]. This scenario is further supported by

PKB knockout mice that similarly gave rise to a higher H_2O_2 tolerance[661]. The authors suggested that absence of PKB activity induces compensatory mechanisms for survival. This may shed some light on why these HOSCC cell lines, particularly the WHCO3 cell line, appear to be more sensitive to H_2O_2 exposure. Based on the rapid reduction of PTEN observed here, it can be assumed that HOSCC cells may circumvent the adverse effects of H_2O_2 by maintaining a low PKB activation status.

Certain of the etiological factors of HOSCC; such as acid reflux, mycotoxins, tobacco- and alcohol-derived carcinogens have been shown to stimulate acute accumulation of H_2O_2[662, 663, 664]. The toxic effects induced by these factors forces the cells of the intermediate layers of the oesophageal epithelium to adapt to these high H_2O_2 levels; creating an environment that is conducive for survival amidst the enhanced H_2O_2 concentrations. Most commonly, this results in a robust H_2O_2 effluent system. Interestingly, recent evidence has indicated that Cys296 and Cys310 of PKB are sensitive to H_2O_2-mediated oxidation[665] (see Fig. 4.12), leading to its inactivation following a 30 min exposure to 100 µM H_2O_2. Uniquely, our data indicate that exposure to H_2O_2, augmented PKB activation in HOSCC cells. It is clear from the H_2O_2-responsive pPKB levels and readily reduced PTEN levels that these HOSCC cells have a higher H_2O_2 tolerance, and may use it for their advantage.

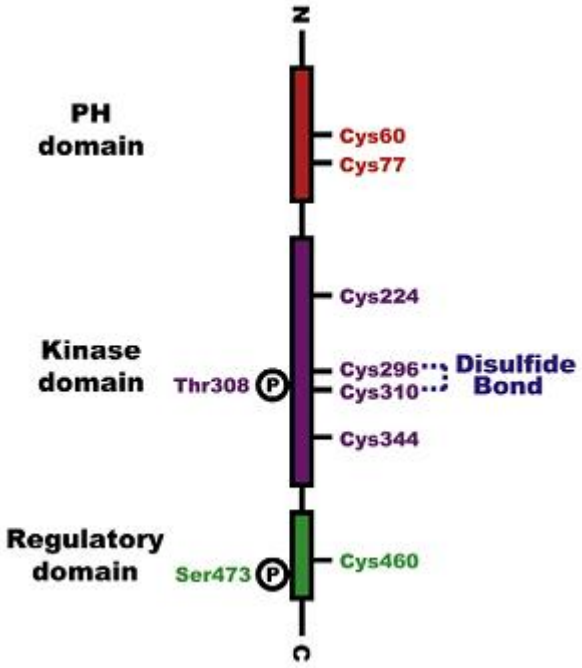


Figure 4. 12: Oxidation of PKB. H_2O_2 induces the oxidation of PKB through disulphide bond formation between its active Cys296 and Cys310 residues, resulting in its reversible inhibition[665]. Additionally, once oxidized, prevents binding to Hsp90, and therefore is susceptible to dephosphorylation by PP2A.

For the first time, we demonstrate that HOSCC cells support the role for H_2O_2 as a pro-survival molecule by activating PKB. Together, our data reveal that unlike the MCF7 and Caco-2 cell lines, PP2A is not a major regulator of PI3K and PKB activity in the HOSCC cell lines. Irrespective of the low PTEN levels in HOSCC cells; these data also indicate that the attenuated levels of pPKB are indeed partially mediated by PTEN. It is clear however, that PTEN is susceptible to oxidation by H_2O_2, and that its expression is very stable in these HOSCC lines. The question thus becomes; what maintains these low and stable levels of PTEN?

Chapter 5
The role of the 26S proteasome in the regulation of PTEN in HOSCC cells

5.1 Introduction

PTEN is one of the key antagonizers of the PI3K/PKB pathway[666], yet its contribution to cancer cells that retain its expression, is still unclear[233,570,596,667]. What is known is that the metastatic potential of cancer cells are exemplified by their ability to lose or reduce cellular levels of PTEN[632, 668,669]. This is substantiated by studies demonstrating the significant impact that overexpression and/or reinstatement of PTEN has on attenuating the migratory and invasive capabilities of cancer cells[670, 671]. With this in mind, it is not surprising that the efficacy of various drugs in cancer therapy have been linked to their ability to preferentially upregulate cellular PTEN levels[672, 673, 674]. Similar to oesophageal cancer, certain breast and lung cancer cells rarely possess PTEN mutations, yet hyperactivation of the PI3K/PKB pathway is still observed[536, 675, 676]. Since these 5 HOSCC cell lines are highly metastatic[333], how do they escape the antagonistic function of PTEN towards the PI3K/PKB pro-survival signalling pathway?

Over the past decade it has become apparent that the molecular intricacies governing the stability and activity of PTEN are extremely complex and largely unknown[677, 678]. A conspicuous finding was that it can be regulated on a transcriptional, translational and post-translational level by several proteins and transcription factors (TFs), that have been shown to be cell-type specific[209]. PTEN is considered to be a haplo-insufficient gene and quasi-sufficient protein[679, 680]. Thus, its expression is directly proportional to its activity, such that, high PTEN levels actively suppress growth, and low levels induce cellular senescence[681]. To date, there are at least 20-30 different proteins (kinases and phosphatases), and TFs, that can regulate the expression, stability, activity and degradation of this TSP[579, 682, 683]. Some of these factors include; CK2[684], early growth regulated transcription factor (EGR-1)[685], transforming growth factorβ (TGFβ)[686], p53[687], DJ-1[688], protein interacting with carboxyl terminus 1 (PICT-1)[689], peroxisome proliferation-activated receptor γ (PPARγ)[690], nuclear factor of kappa light chain gene enhancer in B-cells (NFκB)[691], c-Jun[692], NEDD4-1[693], and the 26S proteasome[694] (some of which are shown in Fig. 5.1). Generally, these proteins affect the expression of PTEN by at least two mechanisms. One such

mechanism is by phosphorylating the C-terminal tail of PTEN, which is thought to enhance its stability while simultaneously masking caspase-3 cleavage sites[695], enabling its escape from degradation via the 26S proteasome (see Fig. 5.1). Secondly, these proteins regulate the transcription and thus expression of PTEN[683]. Therefore, impairment of the tumour suppressive activities of PTEN in cancer is commonly found attributable to abnormalities in the various intermediates that regulate the turnover and activity of PTEN[696, 697, 698]. On the basis of data presented in the former chapters, it is apparent that the protein levels and activity of PTEN are deregulated in the WHCO and SNO HOSCC series. This view is consistent with work performed by Shen-Li *et al.*[699] who demonstrated that a partial reduction in PTEN cellular levels was sufficient to induce the neoplastic state of multiple organs in mice. Therefore, it became necessary to understand the regulation of the protein expression levels of PTEN previously established in HOSCC cells (Chapter 4, Section 4.3.2).

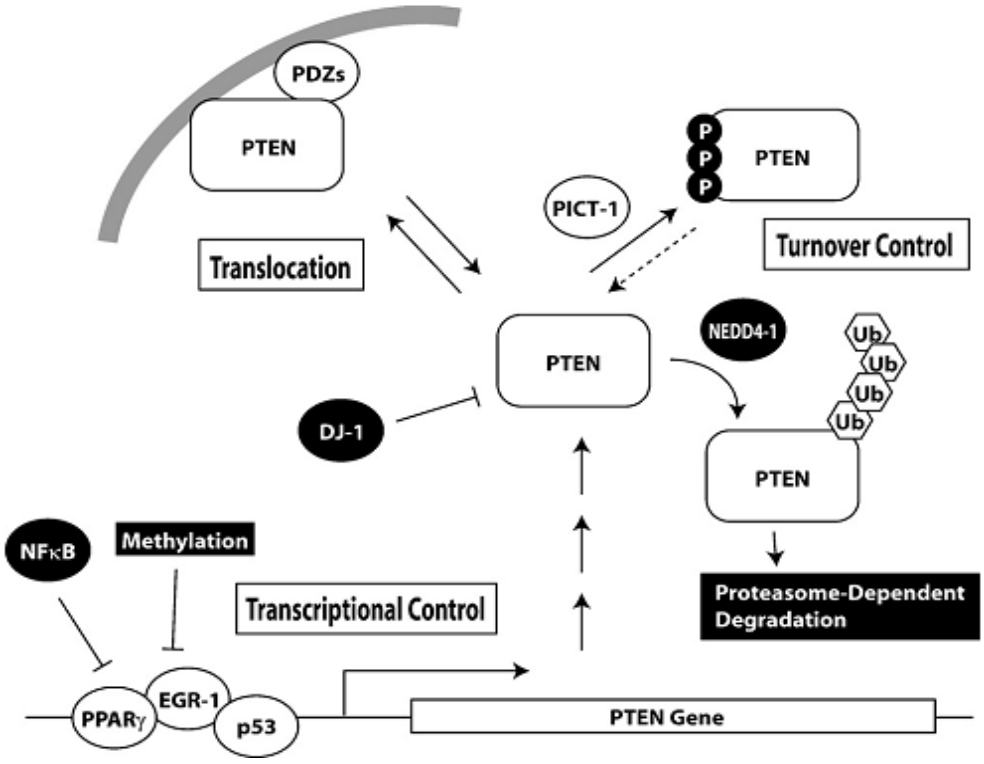


Figure 5. 1: The mechanisms known to regulate PTEN expression[700]. PTEN is regulated at the transcriptional level by EGR-1, p53, PPARγ, NFkB, and methylation. The stability expression and activity of PTEN is regulated by distinct cell-type specific kinases and phosphatases where only a few are illustrated here, namely; DJ-1, PICT-1, and NEDD4-1 that ultimately regulate the cellular localization and turnover of PTEN through 26S proteasome. PDZ: PDZ domain protein, Ub: Ubiquitin.

It is clear from the above that the various intrinsic methods used to regulate PTEN levels are tightly linked to its synthesis and degradation via the protein degradation machinery; the 26S proteasome[701] (see Fig. 5.1). Thus, the degradation of PTEN via the 26S proteasome became an essential component to evaluate in order to understand its regulation in HOSCC.

The 26S proteasome is a large protease that identifies and degrades proteins tagged for destruction by the ubiquitin system[702]. Proteasomal degradation is a highly sophisticated and regulated process that controls the expression of a wide variety of pro-survival and pro-apoptotic proteins and TFs, such as p53, c-Myc, β-catenin, E-cadherin, PTEN, the MAPK pathway, NFkB, the cyclins (i.e. CyclinD1, Cyclin B), and cyclin-dependent kinase inhibitors (i.e. p21)[703, 704, 705]. Bortezomib (formerly known as PS-341, Velcade®) is a dipeptide boronic acid derivative that is a potent and reversible inhibitor specifically targeting the enzymatic activity of the 26S proteasome[706, 707]. Its efficacy has been demonstrated *in vitro* and *in vivo* and is currently being used for the treatment of multiple myeloma[708, 709].

To complicate matters, these proteins and TFs that regulate PTEN (see Fig. 5.1) are in turn, also subject to proteasomal degradation[710, 711]. To address this problem, in addition to the standardized HT29 and MCF7 controls used throughout this study, six additional cell lines were incorporated in this chapter, that have either been exposed to Bortezomib (Bzb) previously, or possess individual molecular characteristics pertaining to the intracellular regulation and degradation of PTEN (see Table 5.1, Materials and Methods). Hence, by using Bzb to specifically inhibit the proteasome, it is shown that relative to another proteasomal target; β-catenin, PTEN is indeed subject to degradation by the 26S proteasome in the five WHCO and SNO HOSCC series. We have discovered the integral role of H_2O_2 in the regulation of PTEN activity in HOSCC (Chapter 4, Section 4.3.4). Since many studies have shown that proteasome inhibition induces the production of H_2O_2[712, 713, 714, 715, 716]; we also report here that the results obtained in the former chapter are independent of the 26S proteasome.

5.2 Materials and Methods

5.2.1 Cell lines and their Culture

In addition to the WHCO, SNO, HT29 and MCF7 cell lines used throughout this study, the COS-7, HEK293, NIH3T3, Caco-2, DLD-1, and Sw480 control cell lines were included (all provided by the ECACC, see Table 5.1). The cells were grown and cultured as previously described; see Chapter 2, Section 2.2.1. **Note:** Any specific references used throughout this chapter pertaining to these control cells can be found in Table 5.1. Where necessary, references are provided.

5.2.2 Antibodies

PI3K (p85α), β-actin, β-catenin, and pro-caspase-3 were specifically detected using rabbit polyclonal antibodies derived from Upstate Biotechnology, Sigma, and Santa Cruz Biotechnology respectively. The Ser473, Ser9, and Ser46 phosphorylation of PKB, GSK3β, and p53 as well as endogenous PTEN and cleaved caspase-3 (Asp175) levels were specifically detected using rabbit polyclonal antibodies obtained from Cell Signalling Technology. The secondary antibody, HRP-bound goat- anti-rabbit IgG (Sigma), was used for the specific detection of all rabbit polyclonal antibodies during immunoblotting.

5.2.3 Whole cell protein extraction

As described in Chapter 2, Section 2.2.5.

5.2.4 Protein Estimation

As detailed in Chapter 2, Section 2.2.8.

5.2.5 Polypeptide Resolution and Western Immunolotting

40 μg of whole cell protein extracts were resolved on a 12% SDS-PAGE (Appendix D 4.1) as detailed in Chapter 2, Section 2.2.9. For optimal detection of total protein expressed, the loading varied between the different proteins under examination, but was kept consistent throughout this study, e.g. 40 μg of protein was loaded for PI3K (p85α) detection. Non-specific binding sites on the nitrocellulose membrane were blocked by incubation in BLOTTO for 1 hour (hr) at RT. Following three 5 min washes in TBS/T, blots were incubated overnight in the primary anti-cleaved-caspase-3 (1:500) and anti-Phospho-p53 (1:500) antibodies diluted in 5% BSA in TBS/T at 4 °C with gentle agitation. Unbound primary from the blots were removed by three 5 min washes in TBS/T that preceded a 1 hr incubation in the

secondary HRP-conjugated goat-anti-rabbit (1:2000) diluted in BLOTTO. For pro-caspase-3 detection, non-specific binding was blocked by 1 hr incubation in BLOTTO. Subsequent to six quick PBS washes, blots were incubated for 2 hrs in anti-pro-caspase-3 (1:500) that was followed by six 5 min PBS washes to remove unbound primary antibody. Blots were incubated in secondary HRP-conjugated goat-anti-rabbit (1:12500) for 1 hr. Thereafter, all membranes were exposed to Supersignal West Pico Chemiluminescent working solution and film as described in Chapter 2, Section 2.2.9. Immunoblot detection for PI3K (p85α), β-actin, β-catenin, pPKB, pGSK3β, and PTEN were carried out as detailed in Chapter 2, Section 2.2.9 and Chapter 4, Section 4.2.8. The experiment was repeated three times. **Note:** All antibodies were diluted in PBS and experiment was conducted at RT, unless otherwise stipulated.

5.2.6 Colorimetric MTT (tetrazolium) assay

The MTT assay was carried out as detailed by Mosmann[717] and Holst-Hansen, *et al*.[718] Briefly, a population of 10 000 cells were plated on 96 well plates for 18 hrs to enable them to adhere under conditions described in Chapter 2, Section 2.2.1. Thereafter, the cell medium was changed, and cells were left to proliferate for a period of 6, 12, and 24 hrs. After the appropriate incubation periods, the medium was discarded from the respective wells and incubated for 3 hrs at 37 °C, 5% CO_2 in 200 µl of the MTT solution (Appendix D 4.2). The resultant formazan crystals were dissolved in 1 hr incubation in DMSO. The colour intensity (absorbance) was measured at a wavelength of 490 nm using the iMarkTM microplate reader (Bio-Rad). The percentage of cell proliferation was calculated relative to the control cells that were not left to proliferate. The experiment was repeated three times. **Note:** Only the WHCO1, MCF7, HEK293, and NIH3T3 cells were selected as representatives for the MTT assay.

5.2.7 Proteasome Inhibition through exposure to Bortezomib (Bzb).

Due to the fact that Bzb is a reversible proteasome inhibitor[719], and based on a series of studies demonstrating a sustained proteasome inhibition for 24 hrs[720, 721], we estimated its duration of action and concentration by exposing cells for a 24 hr period to various Bzb concentrations. Furthermore, according to the literature, concentrations exceeding 200 nM induces apoptosis[722, 723, 724, 725]. Since the purpose of this experiment was not to induce apoptosis, concentrations higher than 200 nM were excluded. Therefore, cells reaching 80% confluence were treated with 1 nM, 5 nM, 10 nM, 25 nM, 50 nM, 100 nM, and 200 nM concentrations of Bzb (Appendix D 4.3) under serum conditions for a period of 24 hrs. An untreated dish containing DMSO served as a control for the experiment. After the 24 hr

incubation, whole cell protein extractions were performed as detailed below and as previously described (see Chapter 2, Section 2.2.5).

5.2.8 Whole cell protein extraction of attached versus detached Bzb-treated cells.

Since Bzb has been reported to adversely affect cell adhesion in epithelial cells[726], we initially collected both attached and detached cells from the WHCO1 and HEK293 cell lines exposed to Bzb described above. These cell lines were specifically chosen based on the significant (WHCO1) and insignificant (HEK293) proliferation rate at 6, 12 and 24 hr periods (see Appendix D 4.4). Briefly, the medium from the Bzb-treated cells was carefully removed into a separate Eppendorf, and spun for 3 mins at 1200 X *g* in the TOMY Capsule HF-120, washed in 1 ml PBS, resuspended and boiled for 5 mins in single lysis buffer. Extraction of protein from the attached cells was carried out as detailed in Chapter 2, Section 2.2.5.

5.2.9 Densitometry

Labworks TM Image Acquisition and Analysis software (Labworks version 4.5) was used for densitometric analysis to semi-quantitatively determine the concentration level of PI3K (p85α), pPKB (Ser473), pGSK3β (Ser9), PTEN, and β-catenin detected through western blotting. **Note:** the densitometric analysis results are an average of 3 separate repeated experiments and represented as a percentage of the maximum concentration.

5.2.10 Image Capturing

All western blot and SDS-PAGE images were captured on a Hewlard Packard Scanjet 4400c series scanner at 300dpi, contrast and brightness of all images were standardised using CorelDRAW version 12®.

5.2.11 Statistical Analysis

Statistical analysis results are inclusive of three independent experiments (mean ± S.D). Statistical analyses were performed using One Way Repeated Measures Analysis of Variance (Holm-Sidak method). All calculations of statistical computations were carried out using the SigmaPlot Release 11.0® statistical software. P-values > 0.05 were considered not to be significant. **Note:** Based on the fact that statistical analysis requires a minimum of three independent experiments, an example of the three blots for the figures in this chapter was chosen (i.e. nothing is gained by showing all three).

5.2.12 Figure Design

All schematic diagrams were designed using the Pathway Builder Tool version 2.0, unless otherwise stipulated.

Table 5. 1: Brief summary of proteins known to interact with and regulate PTEN in the various cell lines used as positive controls for comparative purposes.

Name	Function[682]	HT29	MCF7	COS-7	HEK293	NIH3T3	Caco-2	DLD-1	Sw480
CK2	Generates cas-3 resistant sites on PTEN	high activity[727]	high activity[727]	reg proteasome	low levels[728]	low levels[728]	high activity[727]	high activity[728]	high activity[727]
26S Proteasome	Degrades PTEN	low activity	high activity[729]	Deg PTEN[831]	Deg PTEN	active[730]	high activity	High activity[731]	high activity
Velcade/Bzb	Specifically inhibits catalytic site of 26S proteasome	sensitive[732]	resistant[719]	N.D.	Inhibits ubiquitination[733]	N.D.	resistant	resistant[734]	resistant[735]
c-Jun	Suppresses PTEN mRNA and protein	reg PTEN, high levels[736]	dominant negative[737]	N.D.	high levels, med PTEN	wt[738] and active[739]	high levels, med PTEN	high levels, med PTEN	high levels, med PTEN
EGR-1	Induces PTEN expression in response to H_2O_2	N.D.	absent[740]	N.D.	N.D.	active[741]	active[742]	active	active
DJ-1	Inhibits PTEN during oxidative stress	high levels	active[743]	robust levels[744]	robust levels[745]	wt[746]	N.D.	N.D.	low levels
PTEN	Antagonizes PI3K/PKB pathway	high levels[331]	O.E.[747]	highly acetylated[748]	low levels, activity[749], and acetylation[750]	high levels	high levels[331]	high levels[331]	high levels[331]
MAGI-2	Enhances PTEN membrane association and stability	PTEN interaction[751]		PTEN interaction[831]	PTEN interaction[751]	PTEN interaction[752]	PTEN interaction[751]	PTEN interaction	PTEN interaction
NEDD4-1	Ubiquitinates PTEN	N.D.	low levels[753]	active[754]	high levels[693]	N.D.	N.D.	N.D.	N.D.
p53	Up-and down-regulate PTEN levels	mtR273H[755]	Wt[1112]	N.D.	wt[756]	active, low levels[757]	mtp53[755]	mtR241F[758]	Inactive[755]
PICT-1	Promotes phosphorylation&stabilization of PTEN	N.D.	active[689]	N.D.	N.D.	N.D.			
PPARγ	Protects PTEN from oxidation-induced inactivation	active, high levels	absent[759]	N.D.	wt[760]	N.D.	active[761], high levels	active, high levels[761]	active[761], high levels
XIAP	Regulates PTEN ubiquitination	O.E.[762]	low levels[763]	N.D.	wt[764]	N.D.	O.E.[762]	O.E.	O.E.

Deg: degrades, wt:wild-type, reg:regulates, N.D.:Not Determined,
cas-3: caspase-3, O.E.: Overexpressed, med: mediates, mt: mutant

5.3 Results

5.3.1 Relative expression of PI3K (p85α) levels in the panel of cells used as controls.

It became necessary to develop a set of cell lines displaying individualized characteristics with respect to PI3K (p85α) protein levels, despite having established the levels of PI3K (p85α) in HOSCC cells (Chapter 2, Section 2.3.2). This formed a comparative backdrop for any significant changes in PI3K (p85α) expression as a result of proteasome inhibition (PI). Here, when the known levels of PI3K (p85α) in the 5 HOSCC cell lines (see Fig. 2.7) were compared to its expression in the cells used as controls (Fig. 5.2A); we verify that HOSCC cells express high levels of PI3K (p85α). This was specifically represented in the WHCO5, WHCO6 and SNO cell lines (Fig. 5.2B). With respect to the controls, the expression of PI3K (p85α) was highest in the wtp85α NIH3T3 fibroblasts, which was similar to what was demonstrated previously in this cell line[765]. Consistent with a previous report, levels of PI3K (p85α) were low in the mtPIK3CA Sw480 and DLD-1 colon cell lines[331, 766] , and in the wtp85α COS-7[60] cells (Fig. 5.2). On the other hand, in the wtp85α expressing HEK293[767] cells, levels of PI3K (p85α) were relatively high.

5.3.2 Comparative analysis of PTEN protein levels in HOSCC cells with respect to the control cells.

Similar to PI3K (p85α), it was imperative to compare the protein concentrations of PTEN established in the 5 HOSCC cell lines (Chapter 4, Section 4.3.2) to those previously determined in the cell lines used as controls, in order to fully appreciate any changes that may be induced from PI. Pertaining to the expression of PTEN in the HOSCC cell lines (Chapter 4, Section 4.3.2, Fig. 4.5); it is clear that HOSCC cells, against the known low expressers of PTEN (HEK293, Sw480 and Caco-2 cell lines, see Table 5.1) (Fig. 5.3A), possess low PTEN protein levels (Fig. 5.3B). As determined previously (see Fig. 4.5), levels of PTEN remain highest in the MCF7 control cell line when compared to the cellular milieu used here (Fig. 5.3B). Consistent with a previous report, levels of PTEN were high in the NIH3T3 fibroblasts (see Table 5.1 and Fig. 5.3). Indicative of their stable PTEN levels, the COS-7 and DLD-1 cell line (Table 5.1), demonstrated high levels of PTEN (see Fig. 5.3).

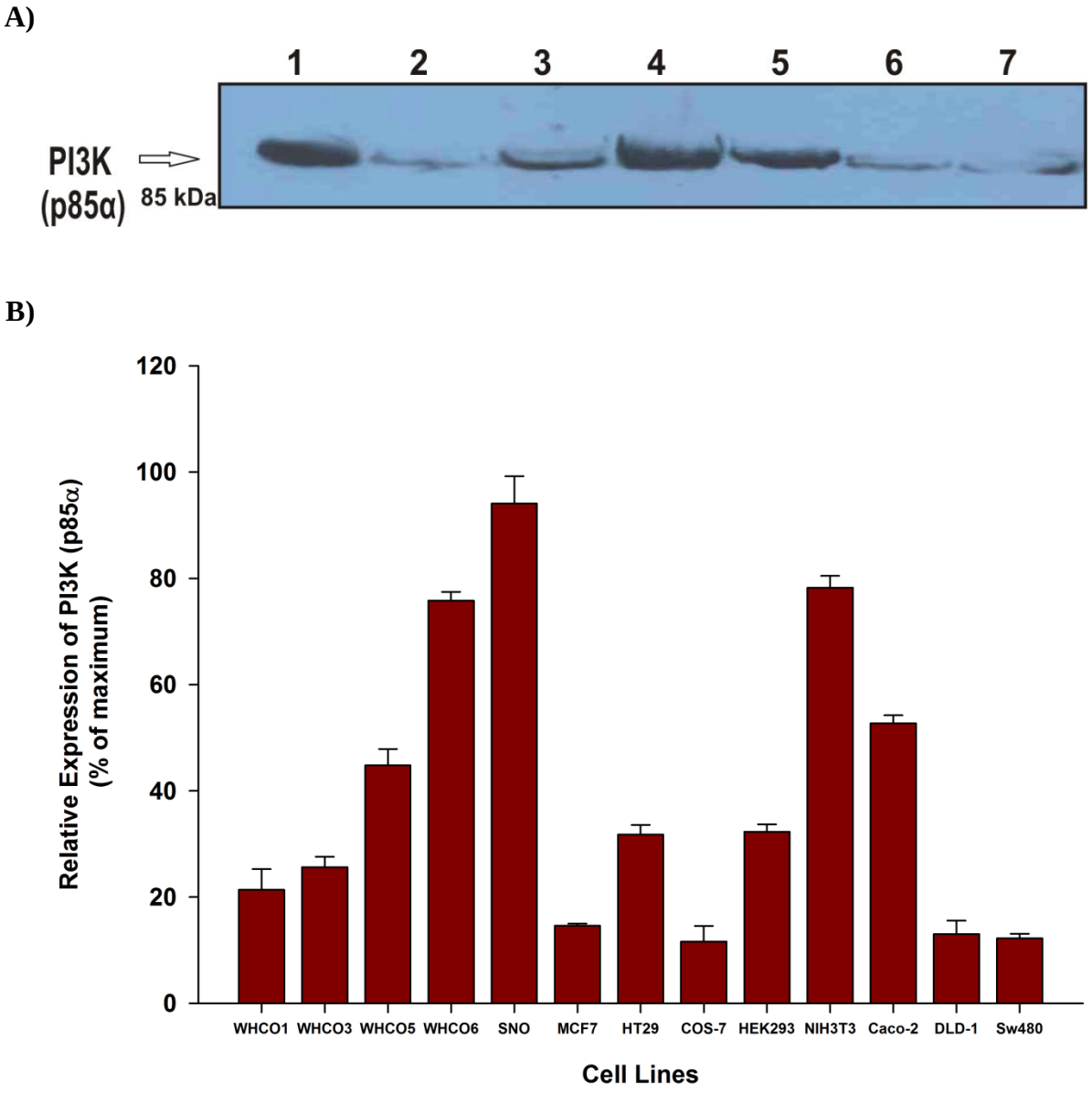


Figure 5. 2: PI3K (p85α) is highly expressed in HOSCC cells in comparison with the control cells. A) PI3K (p85α) western blot analysis of 20 µg of whole cell protein extracts from the COS-7, HEK293, NIH3T3, Caco-2, DLD-1, and Sw480 cell lines (see Appendix A 1.6.6 and 1.7.5 for representative standard curve and 10% SDS-PAGE). Lanes 1-7 represent the WHCO6, COS-7, HEK293, NIH3T3, Caco-2, DLD-1, and Sw480 cell lines respectively. The WHCO6 cell line served as an loading control for comparison against the PI3K (p85α) immunodetection of the HOSCC cell lines in Chapter 2, Section 2.3.2, Fig. 2.5. **B)** Densitometric analysis of PI3K (p85α) detection in the form of a band at 85 kDa. Experiment was repeated three times (mean ± s.d.). See Appendix D, Table D1 for mean optical density values.

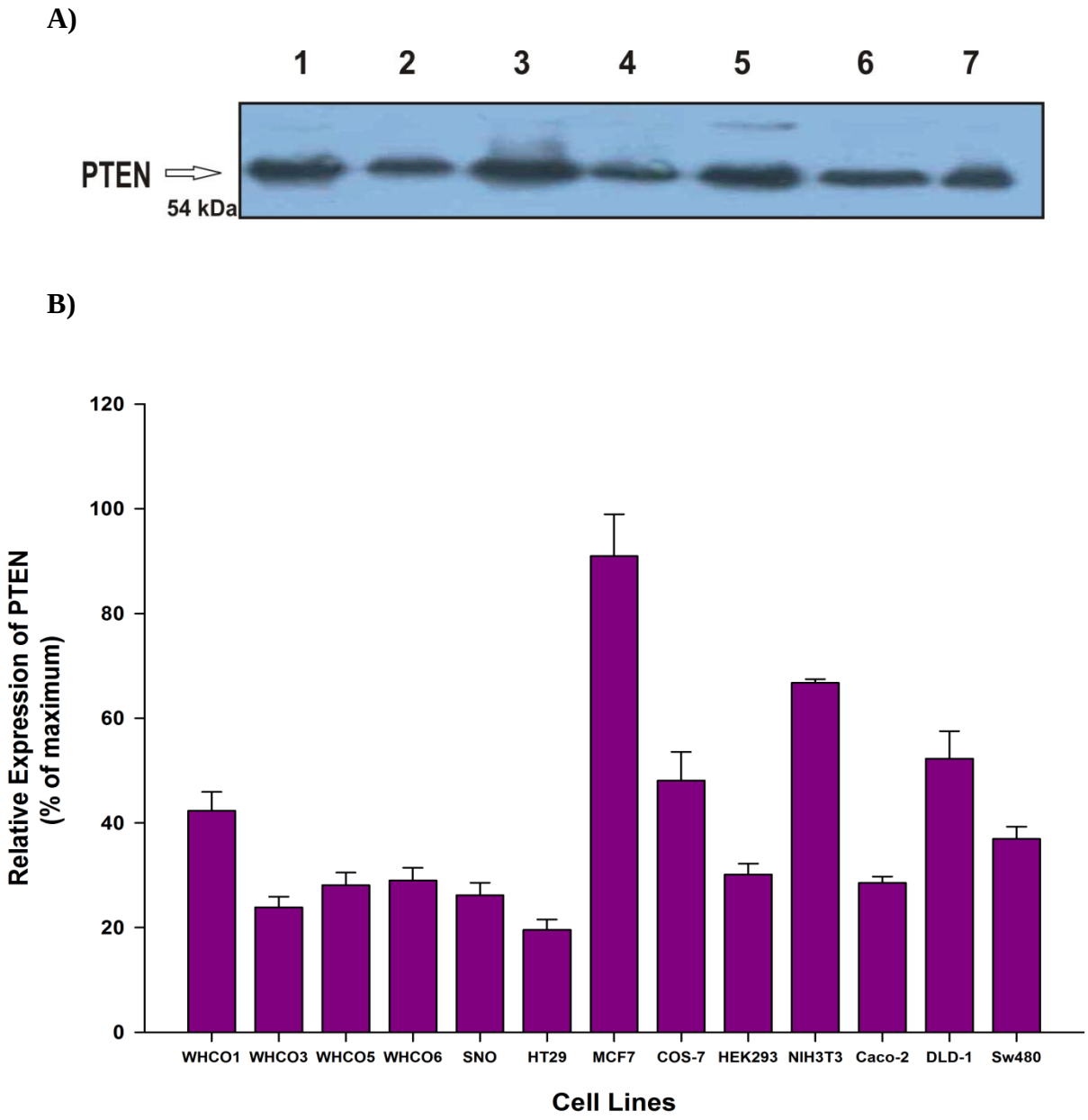


Figure 5. 3: Within a panel of cell lines, HOSCC cells express low levels of PTEN. A) 10 ug of whole cell protein lysates were immunoblotted for the total expression levels of PTEN in the COS-7, HEK293, NIH3T3, Caco-2, DLD-1, and Sw480 cell lines (see Appendix A 1.6.6 and 1.7.5 for representative standard curve and 10% SDS-PAGE). Lanes 1-7 represent the WHCO6, COS-7, HEK293, NIH3T3, Caco-2, DLD-1, and Sw480 cell lines. The WHCO6 cell line served as a control for comparison against the PTEN immunodetection of the HOSCC cell line in Chapter 4, Section 4.3.2; Fig. 4.5. **B)** PTEN detection in the form of a band at 54 kDa was quantified through densitometry. The experiment was repeated three times (mean ± s.d.); see Appendix D, Table D1 for mean optical density values.

5.3.3 Inhibition of the 26S proteasome in HOSCC cells.

Bortezomib (Bzb) is used commonly for the investigation and manipulation of the 26S proteasome in various cellular systems[768, 769, 770]. Recent evidence highlights that proliferating cells are more sensitive to Bzb than quiescent or normal cells[771], and that Bzb reaches its maximum inhibitory potential within the first 24 hours (hrs)[772]. It became mandatory to confirm whether a significant increase in the proliferation rate of the 5 HOSCC cell lines can be detected at 24 hrs.

5.3.3a Evaluation of the proliferation rate of HOSCC cells.

At 24 hrs, a definitive increase in the cell proliferation ($p<0.001$) of the representative HOSCC WHCO1 cell line was exhibited, as measured using the MTT assay (Fig. 5.4). No significant changes were detectable at 6 and 12 hrs (Fig. 5.4). The rise in cell proliferation post 24 hrs in the MCF7 cell line is consistent with its growth rate previously established[773]. As the HEK293 cell line has been previously shown to proliferate within 33 hrs[774], no significant changes in its cell proliferation were observed. In agreement with a previous report[775]; the cellular proliferation was highest in the NIH3T3 fibroblasts and most significant increases were detectable at periods of 6, 12 and 24 hrs (see Fig. 5.4).

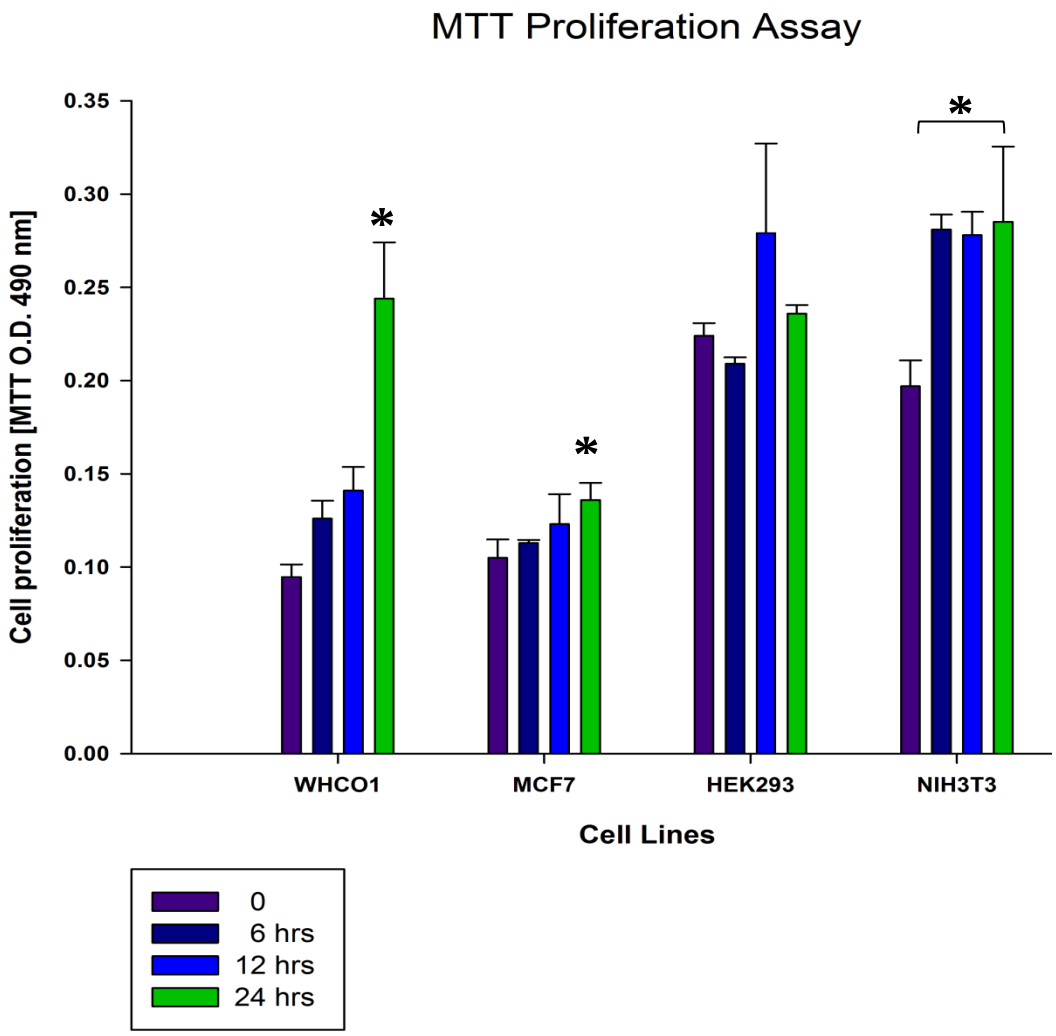


Figure 5. 4: HOSCC cells proliferate within 24 hours. Cells from the WHCO1, MCF7, HEK293 and NIH3T3 were plated on a 96 well plate, and given 6, 12, and 24 hrs to proliferate as described under Materials and Methods. The absorbance readings, representative of the number of proliferating cells were taken at 490 nm. Data are given as an average of triplicate (mean ± s.d.) *, significantly different from the control, $P<0.05$. See Appendix D 4.4 for mean absorbance readings and statistical analysis.

5.3.3b Bortezomib (Bzb) utilizes p53-independent mechanisms in HOSCC cells.

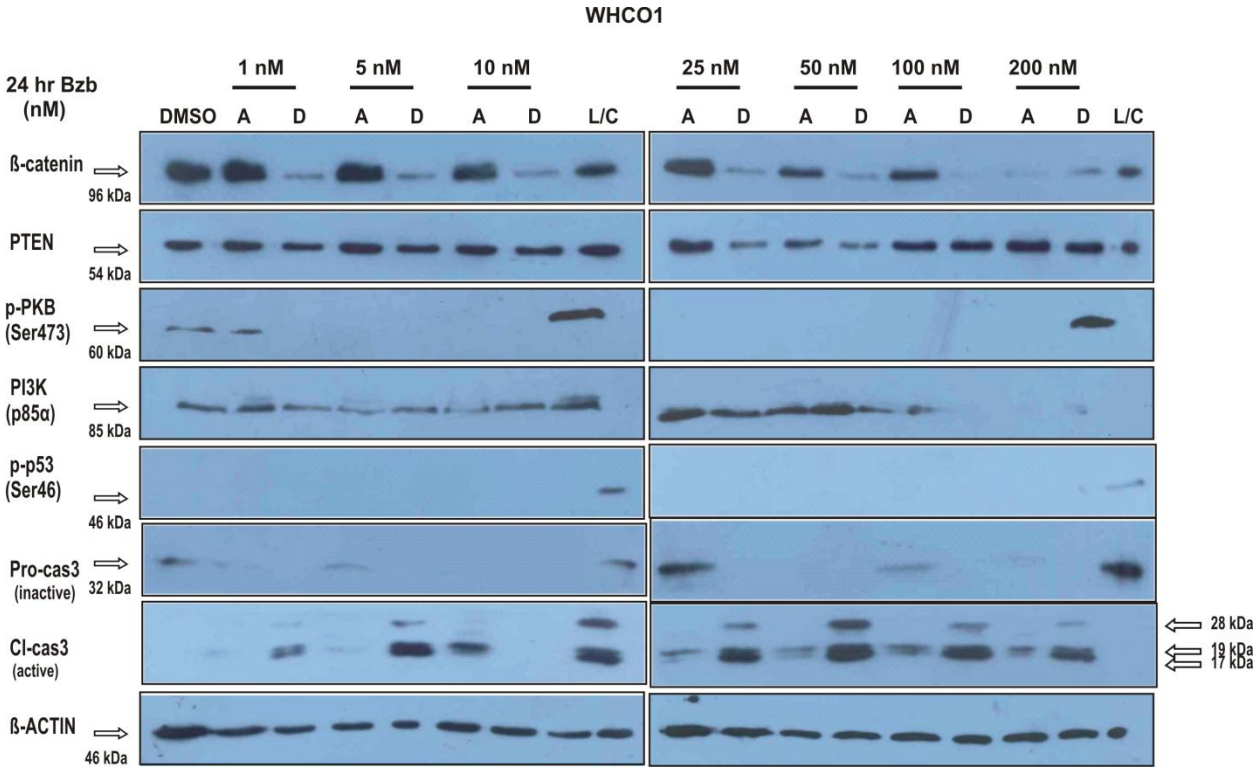
The literature is clear about the ability of Bzb to induce apoptosis at unique IC_{50} values in a wide variety of tumour cells[776, 777]. Bzb-induced apoptosis can be coordinated either through p53-dependent or p53-independent methods[674, 778]. p53-dependent mechanisms include the attenuation of p53 degradation through the up-regulation of its Ser46 phosphorylation leading to the activation of apoptosis[779], while p53-independent mechanisms entail the endoplasmic reticulum (ER)-stress-induced cleavage and activation of pro-caspase-3[780]. Due to the fact that PTEN degradation proceeds in both a caspase-3- and 26S proteasome-dependent manner[695], these factors were included when examining the effect of proteasome inhibition (PI) on PTEN. Since both the Ser46 phosphorylation of p53 and pro-caspase-3 cleavage are used as indicators for this apoptotic induction[781, 750, 725], both were assessed in order to determine which of the two may be a useful marker for apoptosis in this study. With respect to the significant increase in cell proliferation after 24 hrs in the WHCO1 cell line, and the lack thereof in the HEK293 cell line (Fig. 5.4), made them ideal for the initial evaluation of Bzb-induced PI. Moreover, research has demonstrated the negative influence that Bzb has on cell adhesion[726,782,725]. This led us to incorporate the specific effects it may have on attached versus detached cells.

Using expression levels of another proteasomal target; β-catenin[730], as confirmation for PI, we show through western blot analysis that levels of β-catenin are increased upon PI induced in attached WHCO1 and HEK293 cells at low concentrations of Bzb (1-25 nM) (Fig. 5.5A, B, and C). This increase was followed by a consistent decline in β-catenin levels at higher Bzb concentrations (> 25 nM) in the attached cells (Fig. 5.5A, B, and C). The appearance of cleaved-caspase-3 (active) that is simultaneous with a decrease or absence in pro-caspase-3 (inactive) is indicative of apoptotic induction[780]. Therefore, the reduction in β-catenin at these higher concentrations of Bzb may be attributable to the presence of cleaved-caspase-3 (active) in both the attached WHCO1 and HEK293 cells (see in Fig. 5.5A, B, and C). On account of its cell adhesive roles[783], it is no surprise that the expression of β-catenin following PI was reduced in the detached WHCO1 cells (Fig. 5.5A and C). Levels of β-catenin in the detached HEK293 cells were completely absent (Fig. 5.5B and C). Western blot analysis also showed a dose-dependent rise in PTEN up to 25 nM Bzb in the attached WHCO1 cells, whereas levels of PTEN initially declined, followed by a sharp increase at 10 nM Bzb in attached HEK293 cells (see Fig. 5.5A, B, and D). Expression of PTEN was highest following exposure to 200 nM Bzb in the

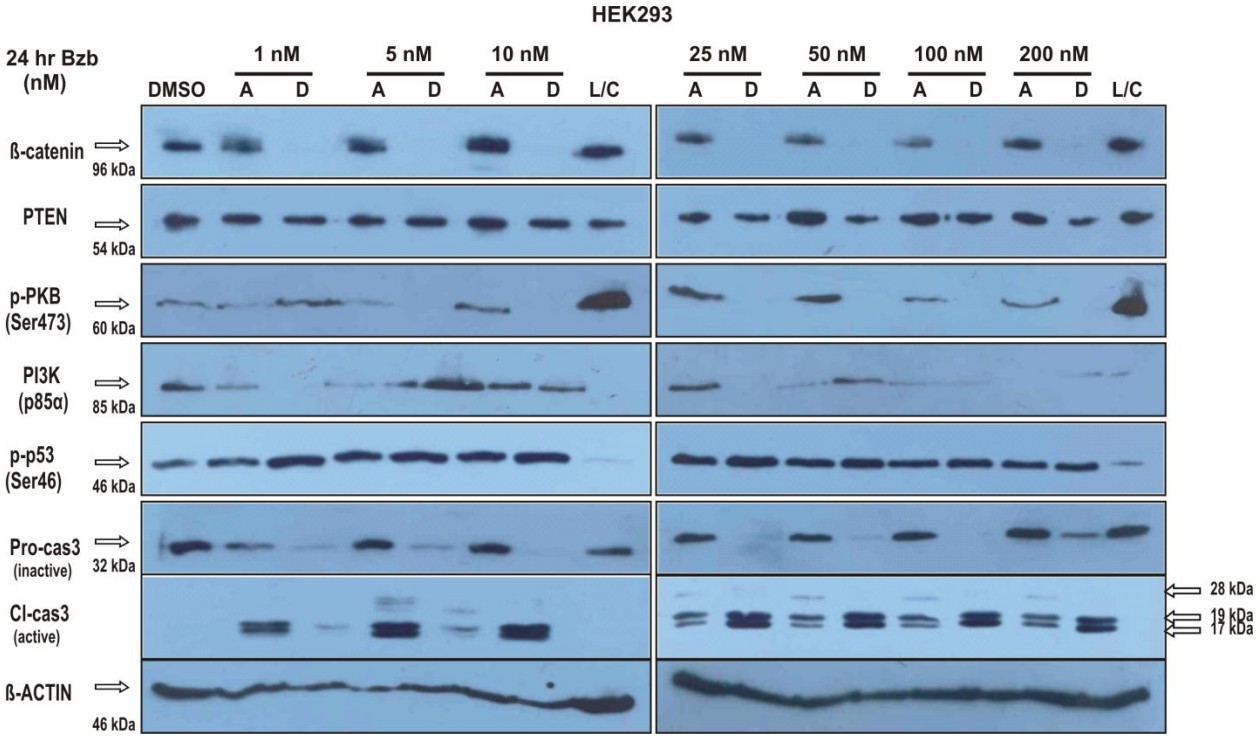
attached WHCO1 cells, despite the distinct fall in PTEN at lower Bzb concentrations (Fig. 5.5A, B and D). The drop in PTEN concentration paralleled the loss of pro-caspase-3 (inactive), and presence of cleaved-caspase-3 (active) in the attached WHCO1 cells at higher Bzb concentrations; indicating the caspase-3-dependent reduction in PTEN protein (see Fig. 5.5A and D). No link between caspase-3 activation and PTEN protein expression was seen in the HEK293 cells.

Proteasome inhibition resulted in an initial drop in pPKB, followed by its immediate absence in the attached WHCO1 cells (as shown in Fig. 5.5A and E). This process appeared to be both PTEN- and caspase-3-dependent, as seen by the simultaneous increase and appearance in PTEN and cleaved-caspase-3 levels respectively (see Fig. 5.5A). However, a similar trend was not observed in the HEK293 cell line. Instead, the concentration of pPKB peaked at 25 nM Bzb, which, relative to the DMSO control, was normalized at higher concentrations of Bzb (Fig. 5.5B and E). This occurred in the presence of sustained pro- and cleaved-caspase-3 (Fig. 5.5B). pPKB was undetectable in both the WHCO1 and HEK293 detached cells (Fig. 5.5A and B). While the Ser46 phosphorylation status of p53 remained unchanged following PI in the HEK293 cell line, no levels were detected in the WHCO1 cell line (Fig. 5.5A), suggesting that Bzb utilizes p53-independent mechanisms. Consistent with the findings by Mayo, *et al*.[779] and Kurihara, *et al*.[784], we show that cleavage, and thus activation of caspase-3 is a more appropriate marker than p-p53 (Ser46) for the apoptotic effects conducted by Bzb in the representative WHCO1 HOSCC cell line (Fig. 5.5A). Based on these results, we inhibited the proteasome using Bzb in the four HOSCC cell lines (WHCO3, WHCO5, WHCO6 and SNO), as well as the additional tumour cell lineages used as controls, but only collected attached cells and used pro- and cleaved-caspase-3 as a marker for Bzb-induced apoptosis.

A)

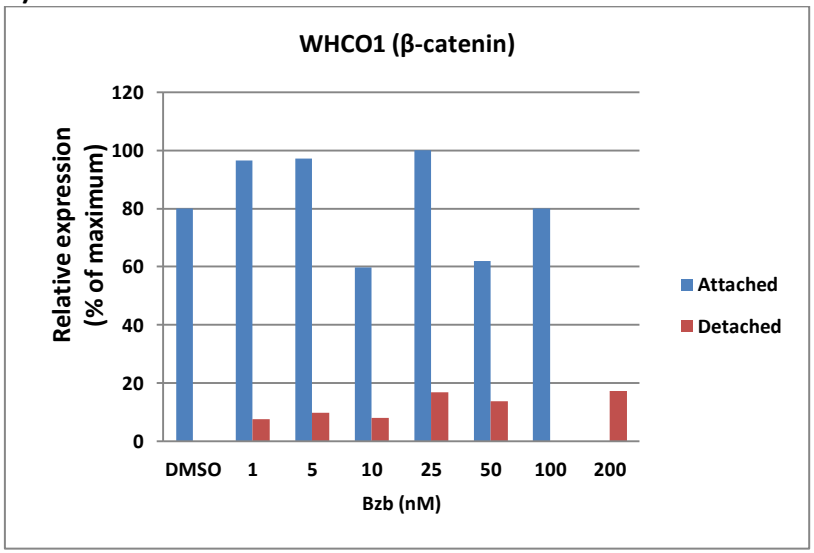


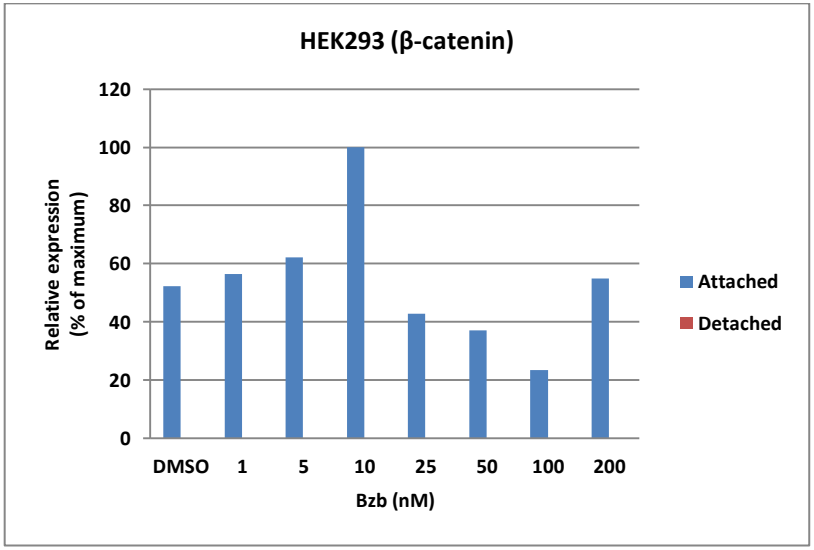
B)



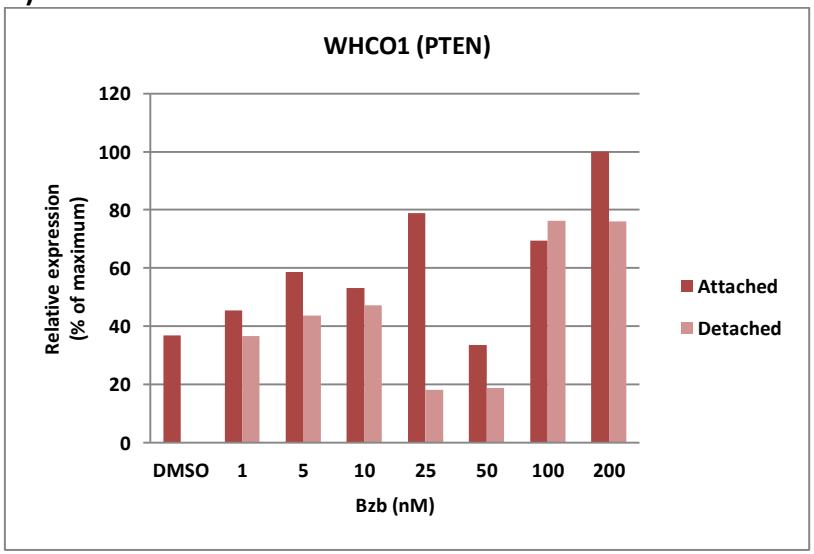
See page 150 for figure legend.

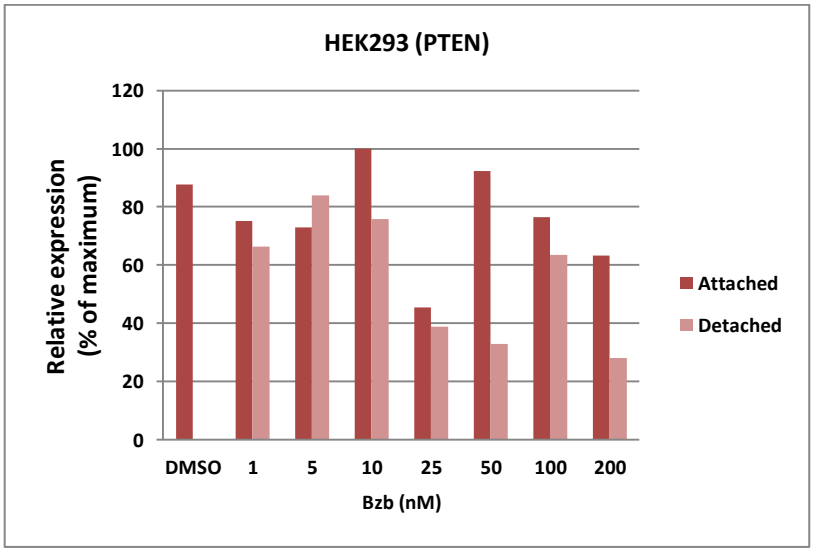
C)





D)





See next page for figure legend.

E)

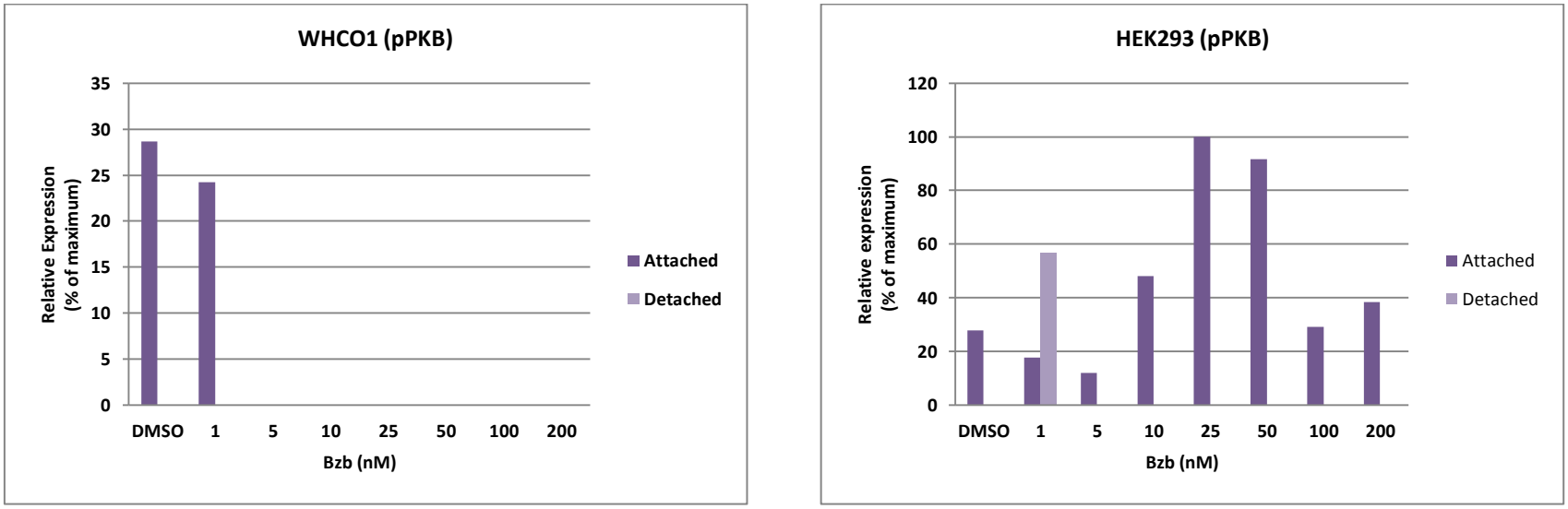


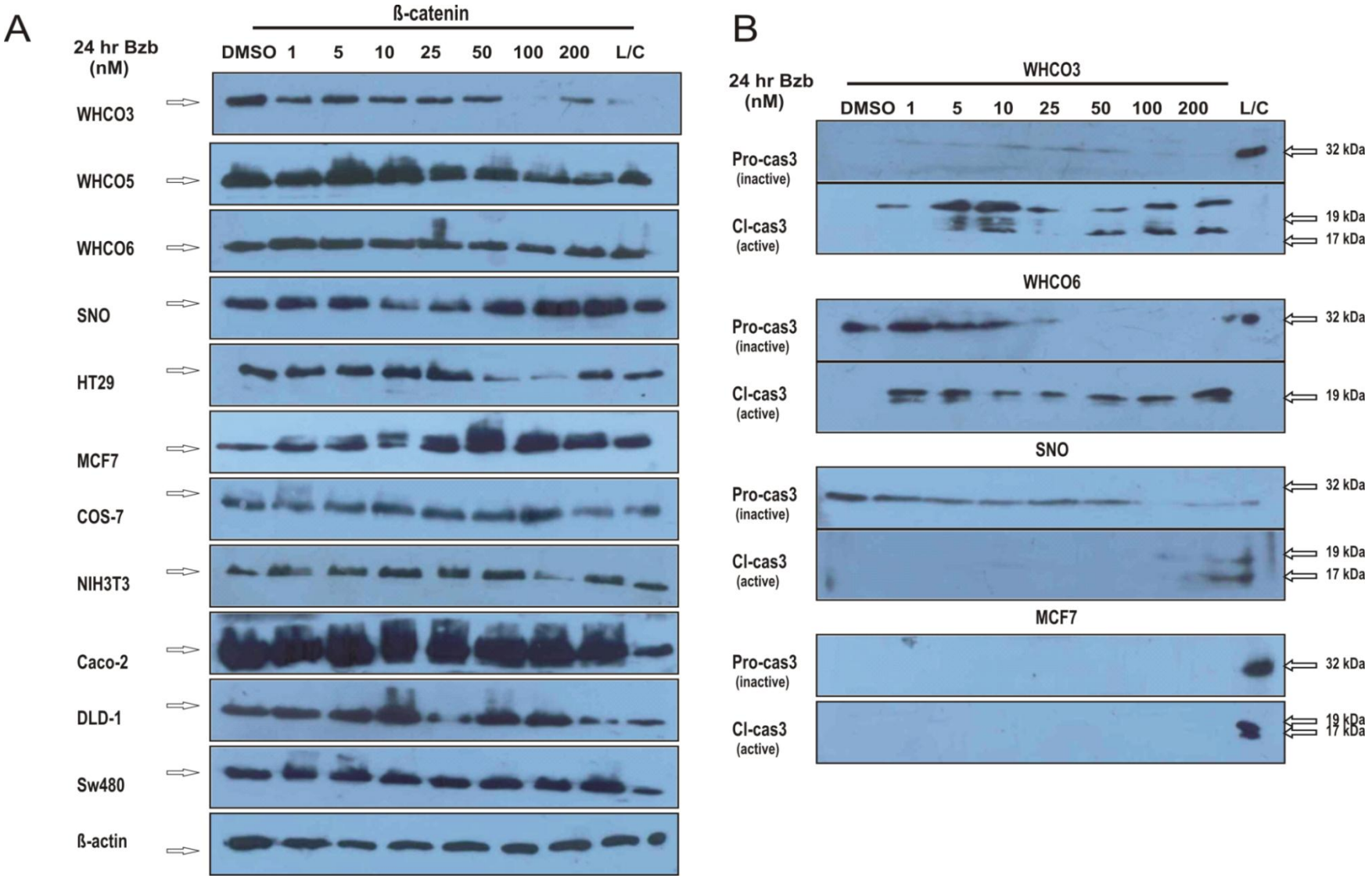
Figure 5. 5: Inhibition of the 26S proteasome attenuates PI3K/PKB signalling, and stabilizes PTEN via caspase-3-dependent mechanisms. WHCO1 **(A)** and HEK293 **(B)** cells were treated for 24 hrs with and without the proteasome inhibitor, Bortezomib (Bzb) at various concentrations (1, 5, 10, 25, 50, 100, and 200 nM). Based on their sensitivity, attached (A) and detached (D) cells were collected. The expressions of β-catenin at 90 kDa, PTEN at 60 kDa, p-PKB (Ser473) at 60 kDa, PI3K (p85α) at 85 kDa were evaluated after Bzb treatment through western blot analysis. Detection of pro-caspase-3 (inactive) and cleaved-caspase-3 (active) (in a range of 28-17 kDa), as well as p-p53 (Ser46) was used to assess the point at which Bzb triggers apoptosis. A standardized loading control (L/C) was included in each western blot analysis to allow for comparison between the various immunoblots. No band was present in the control (C) lane for Cl-cas3, as only cells entering apoptosis would demonstrate such cleavage. All experiments were conducted under serum conditions. β-actin was used as an internal control. The experiment was performed in triplicate, and the band representing β-catenin, PTEN and pPKB were quantified through densitometry and represented in a bar graph in **C)**, **D)**, and **E)** respectively.

5.3.3c The expression of PTEN is upregulated in response to proteasome inhibition.

The 26S proteasome is indeed active in the HOSCC cell lines, as seen by the significant ($P<0.001$) elevation in the concentration of β-catenin in the WHCO5, WHCO6, SNO and including WHCO1 cell lines subsequent to PI in Figs. 5.6 and 5.7. For the sake of clarity two bar graphs are provided. The first allows us to demonstrate the statistical significance of β-catenin levels (Fig. 5.7A), and the second merely mimics the graphical representation of these changes to facilitate visual interpretation (Fig. 5.7B). β-catenin decreased in a dose-dependent manner in the WHCO3 cell line (Fig. 5.6 and 5.7). Similar to the β-catenin response in the WHCO1 cell line, levels of β-catenin in the WHCO5 cell line dropped at higher concentrations of Bzb (Fig. 5.7B). Furthermore, in the representative WHCO3, WHCO6, and SNO cell lines; this increase was indicative of a successful PI evidenced by an increase and decrease in cleaved-caspase-3 (active) and pro-caspase-3 (inactive) (see Fig. 5.6B). Interestingly, expression of β-catenin increased in a dose-dependent manner up to 50 nM Bzb in the MCF7 control, despite it not possessing functional caspase-3[785]. An increase in β-catenin was also detected in the Bzb-resistant controls (Caco-2, DLD-2, and Sw480, see Table 5.1), whereas levels of β-catenin dropped substantially at high Bzb concentrations in the Bzb-sensitive HT29 control (see Fig. 5.6A and Fig. 5.7). PI is further strengthened by the noteworthy up-regulation in levels of β-catenin in the NIH3T3 fibroblasts, which possess full length β-catenin that is subject to degradation by the active 26S proteasome previously established[730]. Distinct from the WHCO3 and WHCO6 cell lines, the SNO cell line tolerated higher concentrations of Bzb, evidenced by the delayed caspase-3 cleavage (activation) as opposed to the caspase-3 cleavage detected at lower Bzb concentrations in the WHCO3 and WHCO6 cell lines (Fig. 5.6B). The extremely high concentration of β-catenin in the Caco-2 cell line, is due to the presence of double β-catenin and APC mutations[786].

On the basis that the activity of the 26S proteasome can easily be manipulated through Bzb (Fig. 5.6 and 5.7), the impact it would have on PTEN protein levels was tested. The total cellular protein concentrations of PTEN in the HOSCC cells were significantly elevated in response to PI ($P<0.05$), albeit to unique degrees (Fig. 5.8). Two graphs are provided for clarity; as described above (Fig. 5.8B and C). As can be seen in Fig. 5.8B and C, this increase is only observed in the WHCO1, WHCO3, WHCO6, and SNO HOSCC cell lines. Irrespective of the cleaved caspase-3 (active) status in the WHCO3 and WHCO6 cell lines specifically, PTEN expression was still up-regulated (Fig. 5.6B and 5.8A). While PTEN

levels continue to rise in a Bzb dose-dependent manner in the WHCO3 cell line, a drop in its levels was observed at higher concentrations of Bzb in the WHCO1, WHCO6, and SNO cell lines (Fig. 5.8B and C). This result was consistent with the increase in PTEN observed in the high expressing PTEN controls; Caco-2 and DLD-1 (see Table 5.1 and Fig. 5.3) (Fig. 5.8B and C). It was interesting to note that the expression of PTEN was reinforced in the WHCO3 and SNO cell line at the strongest concentration of Bzb ($p<0.005$), whereas the WHCO1, WHCO5, and WHCO6 cell lines exhibited down-regulation in PTEN levels at this concentration (see Fig. 5.8). In contrast, a significant ($P<0.05$) decrease in PTEN protein expression was shown in the WHCO5 cell line that was not accompanied by any reinforcement in its protein levels (Fig. 5.8). This was similar to the down-regulated levels of PTEN illustrated in the Bzb-resistant and sensitive MCF7 and HT29 controls respectively (Fig. 5.8 and see Table 5.1, Materials and Methods). Accumulatively these data indicate that cellular levels of PTEN are regulated by the 26S proteasome, but are resistant to caspase-3 cleavage.



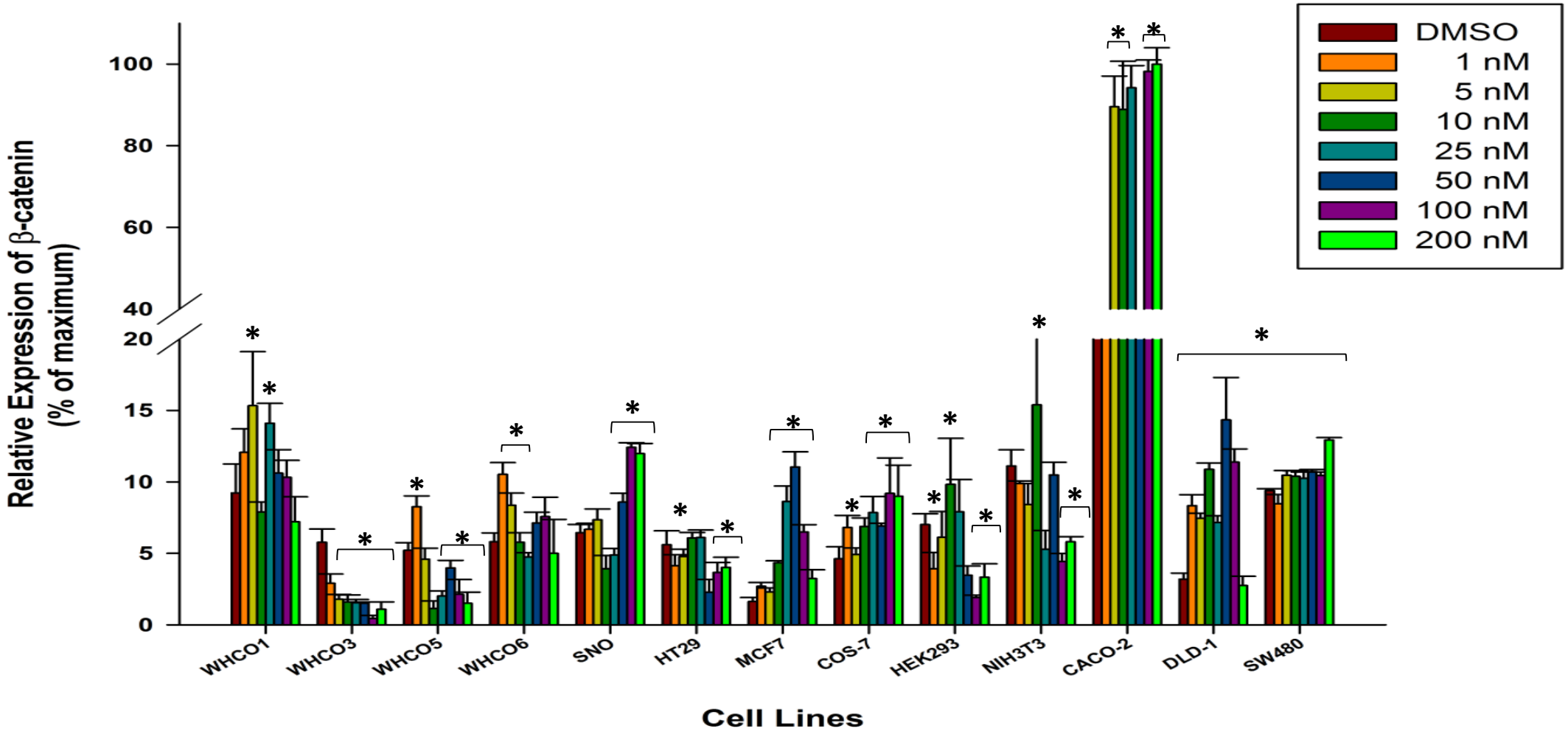
See next page for legend.

Figure 5. 6: Inhibition of the 26S proteasome attenuates the stability of β-catenin in HOSCC cells. A) The 4 HOSCC cell lines (WHCO3, WHCO5, WHCO6, and SNO), in addition to the HT29, MCF7, COS-7, NIH3T3, Caco-2, DLD-1 and Sw480 control cell lines were treated for 24 hrs with and without (DMSO) the proteasome inhibitor, Bzb. The expression of β-catenin at 90 kDa, was evaluated through western blotting (see Appendix A 1.6.6 and 1.7.5 for representative standard curve and 10% SDS-PAGE). The smears are suggested to be indicative of ubiquitin[730, 787]. **B)** To assess the point at which Bzb induces apoptosis, western blot detection of pro-caspase-3 (inactive) and cleaved-caspase-3 in a range of 28-17 kDa (active), was assessed in the WHCO3, WHCO6, SNO and the caspase-3-null cell line, MCF7[788] exclusively. A standardized loading control (C) was included in each western blot analysis to allow for comparison between the various immunoblots. No band was present in the control (C) lane for Cl-cas3, as only cells entering apoptosis would demonstrate such cleavage. Cells treated with DMSO served as a reagent control. All experiments were conducted under serum conditions and performed in triplicate. β-actin was used as an internal control.

5.3.3d Levels of pPKB and PI3K (p85α) are sensitive to PI in HOSCC cell lines.

Any change in the cellular concentrations of PTEN greatly influences its activity[446]. Since significant changes in its expression were obtained as a result of PI (see Fig. 5.8); the effect PI would have on its targets; pPKB and PI3K (p85α) was examined. Additionally, reduced levels of pPKB have been coupled to Bzb sensitivity[789, 790, 791, 792]. Quantification of western blot analysis showed that, similar to what was found above (see Fig. 5.5A and E), PI induced an early induction in pPKB that followed an immediate and strong attenuation in its levels ($P<0.05$) in the WHCO1 and WHCO5 HOSCC cell lines (see Fig. 5.9). No initial increase in pPKB was introduced following PI in the WHCO6 cell line. Levels of pPKB was similarly affected by Bzb in the stable PTEN COS-7 expressing control. The reduction in pPKB levels in WHCO1 and WHCO6 cell lines corresponded with elevated PTEN expression (see Fig. 5.8 and 5.9). These data indicate that the escalation in PTEN levels following Bzb (see Fig. 5.8) also affects its activity.

A)



See next page for legend.

B)

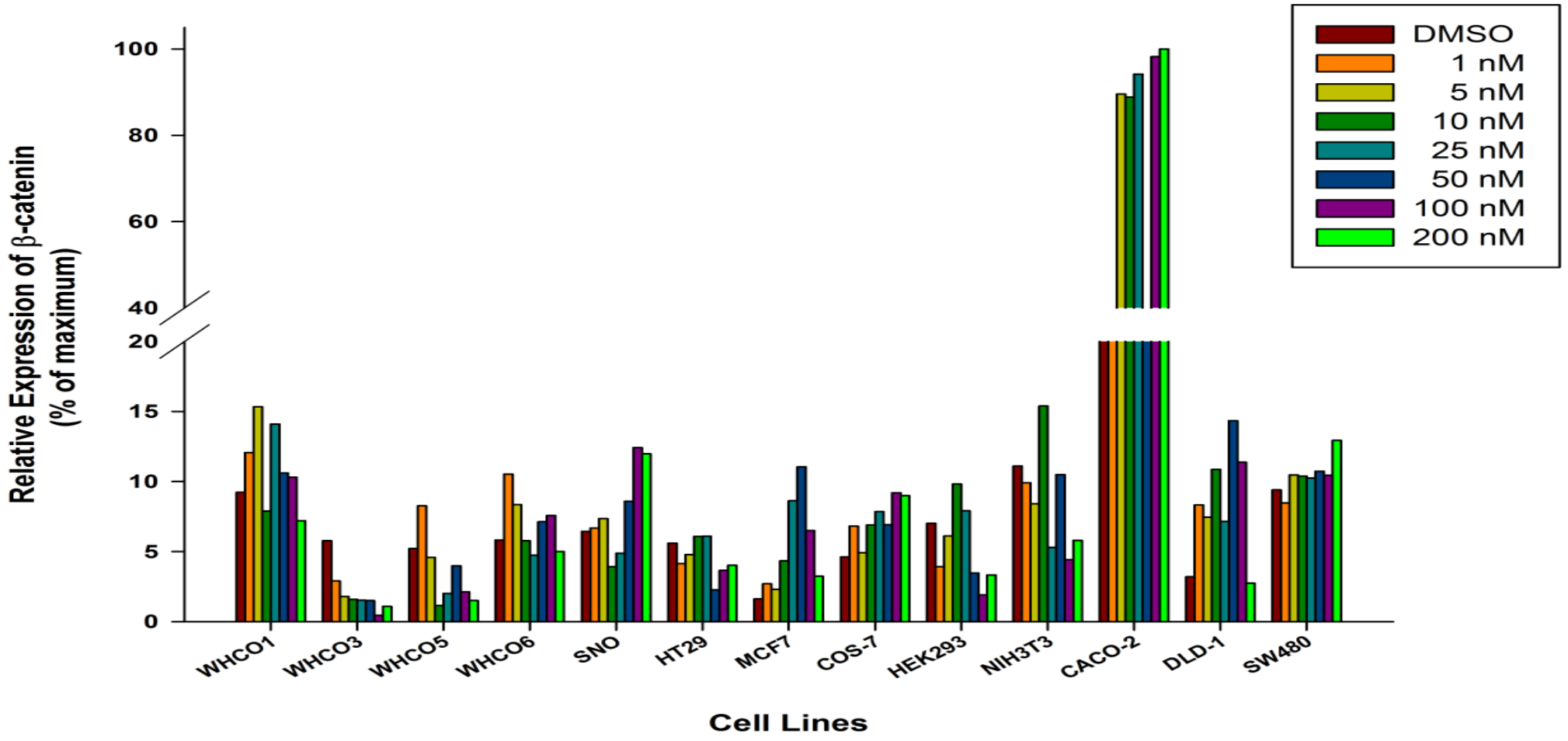
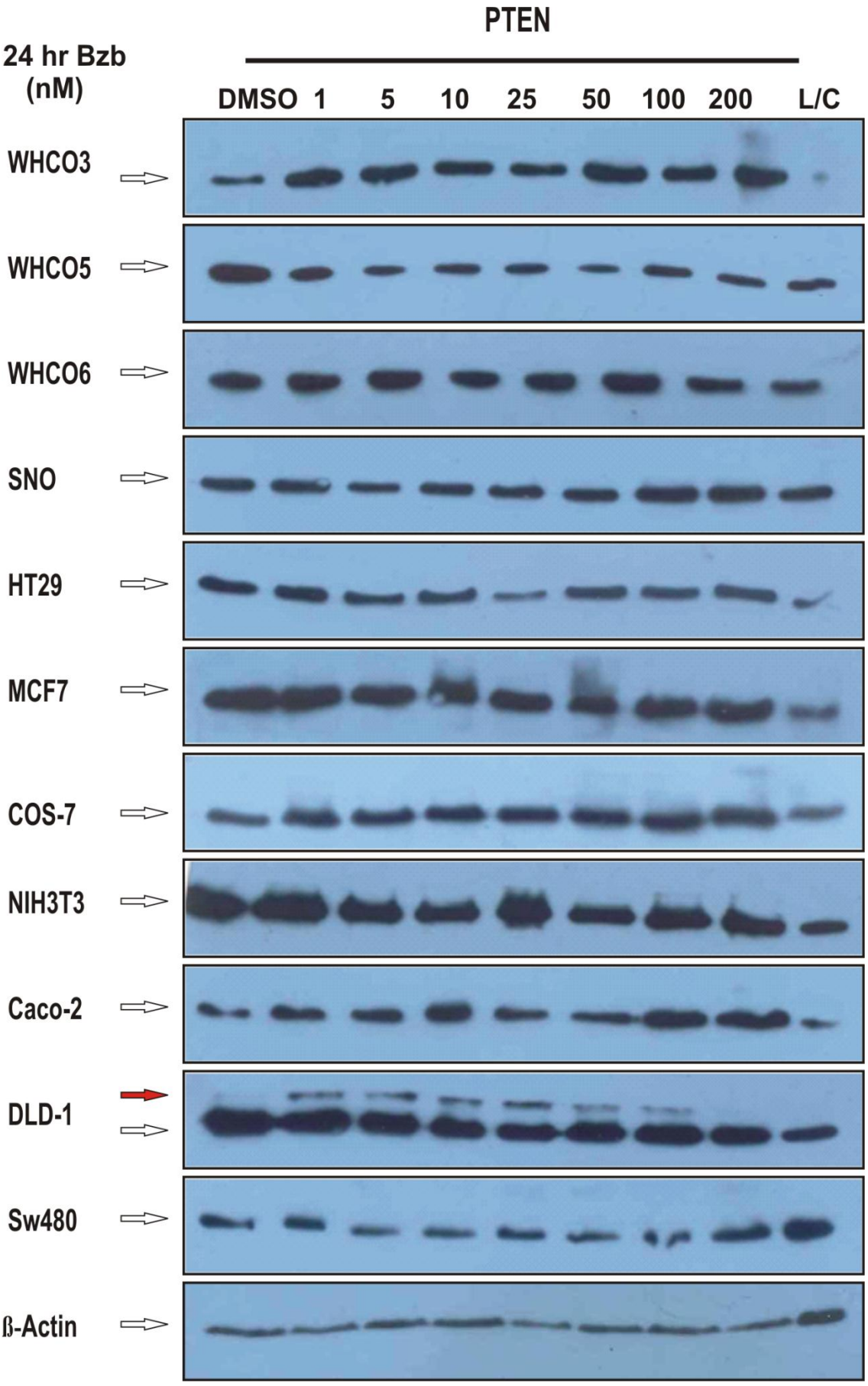


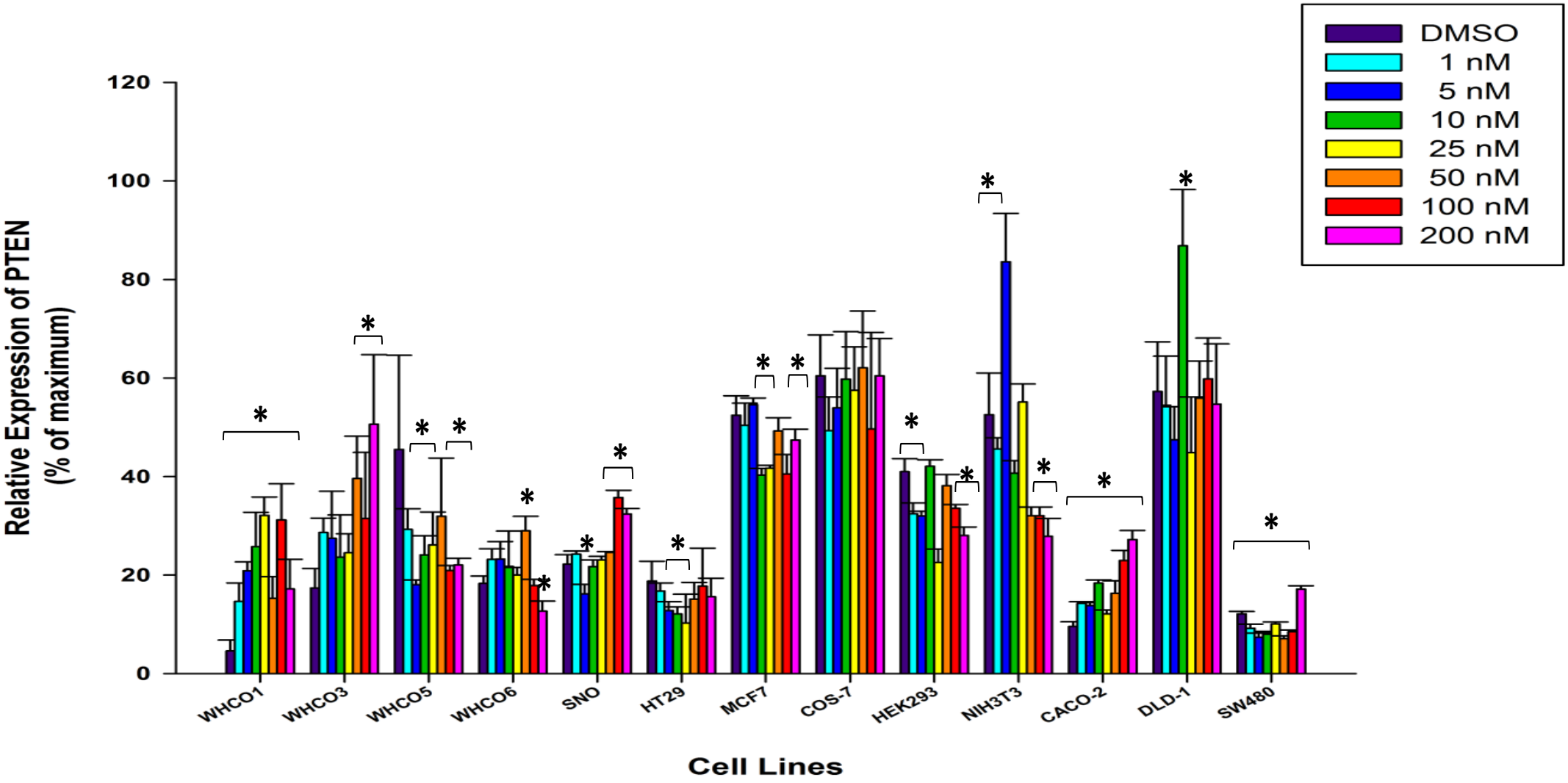
Figure 5. 7: The proteasome is inhibited following exposure to Bzb, evidenced by elevation in β-catenin levels. A) The band representing β-catenin following PI was quantified through densitometry. Data are given as an average of triplicate (mean ± s.d.) *, significantly different from control, P<0.05. Comparison between the various Bzb concentrations against the DMSO control were analysed using the ONE-WAY ANOVA, see Appendix D, Table D2 for statistical analysis. **B)** Simplified bar graph of the changes in β-catenin expression following Bzb exposure mimicking the results displayed in (A).

A)



See next page for legend.

B)



See next page for legend.

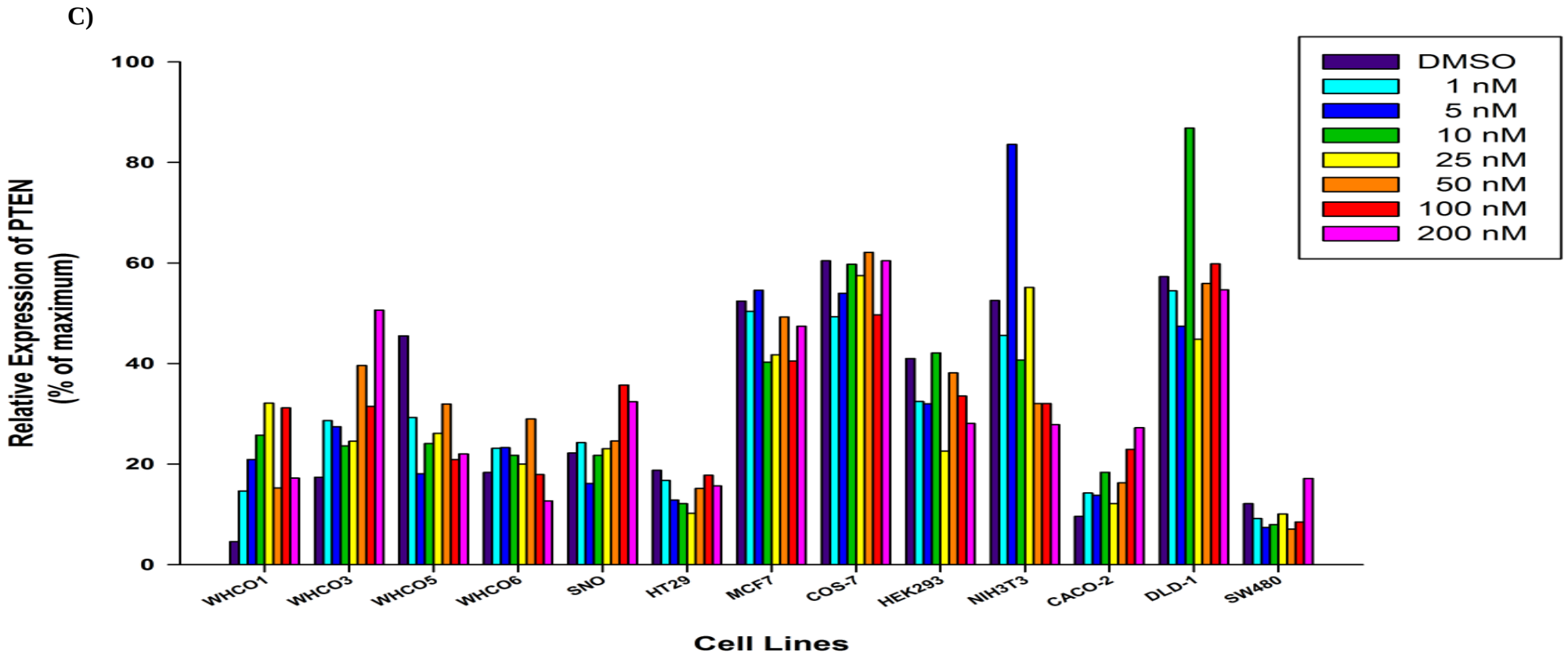
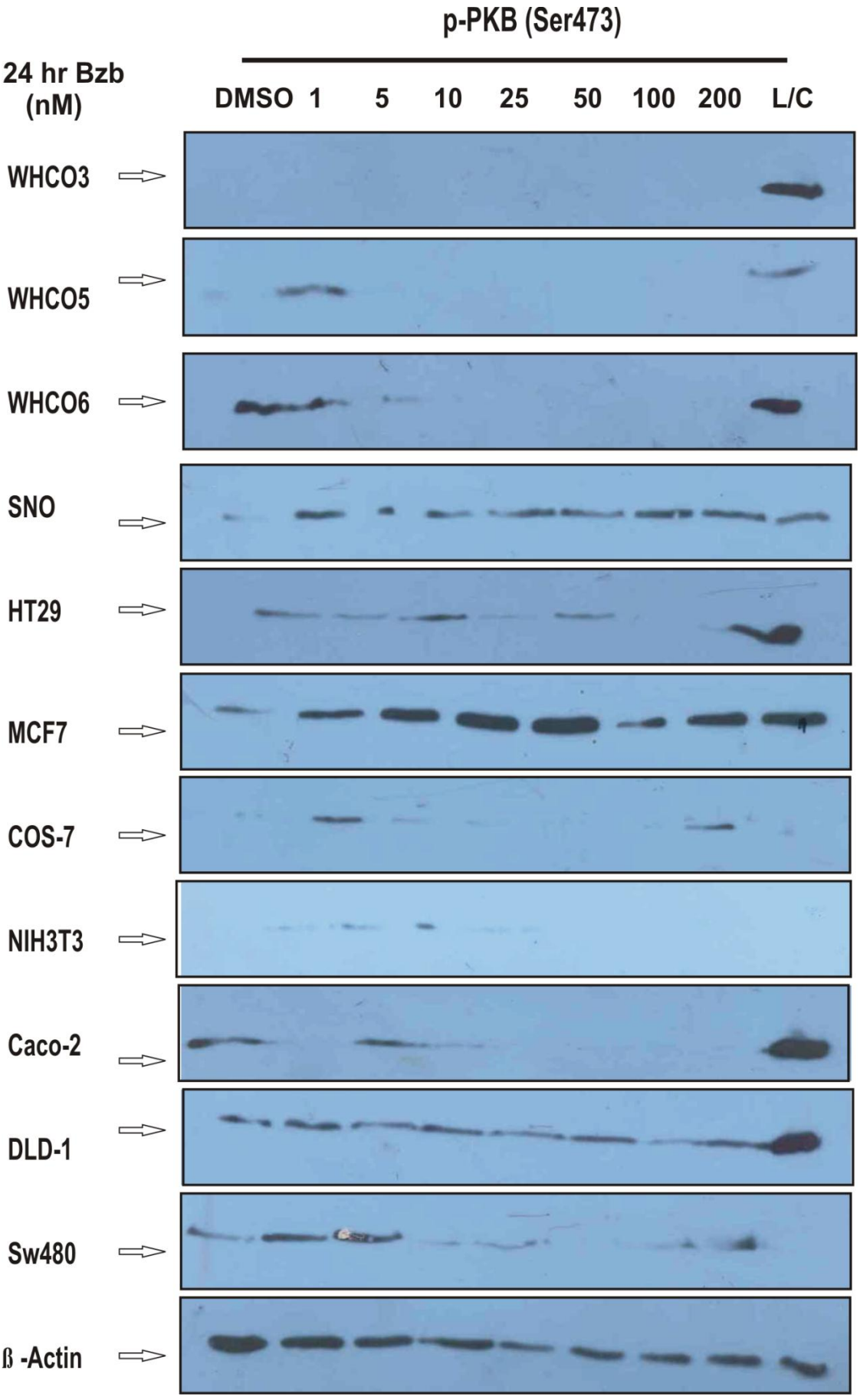


Figure 5.8: The 26S proteasome plays a major role in the degradation of PTEN in HOSCC cells. A) Cells (WHCO3, WHCO5, WHCO6, SNO, HT29, MCF7, Cos-7, NIH3T3, DLD-1 and Sw480) were treated with and without various concentrations of the proteasome inhibitor, Bzb (1-200 nM) for a 24 hr period, and levels of PTEN were subsequently assessed through western blotting (see Appendix A 1.6.6 and 1.7.5 for representative standard curve and 10% SDS-PAGE). A standardized loading control (C) was included in each western blot analysis to allow for comparison between the various immunoblots. DMSO was used as reagent control. All experiments were conducted under serum conditions and in triplicate. β-actin was used as an internal control. Red arrow is considered to be indicative of ubiquitin tags[793]. **B)** The single band detected at 54 kDa representing PTEN was quantified through densitometric analysis. Data are given as an average of three independent experiments (mean ± s.d.) * Significantly different from control, $P< 0.05$. See Appendix D, Table D3 for statistical data. **C)** Simplified bar graph of the changes in PTEN levels following Bzb exposure mimicking the results displayed in (B).

Inhibition of the 26S proteasome did not induce levels of pPKB in the WHCO3 cell line (Fig. 5.9A). Interestingly, a small, yet significant ($P<0.05$) increase in pPKB was observed in the NIH3T3 control, even though the basal levels of pPKB, similar to the WHCO3 cell line, are not detectable (see Fig. 5.9A and B). In contrast, pPKB increased substantially in the SNO HOSCC cell line at higher Bzb concentrations (see Fig. 5.9B). This is consistent with the increase in pPKB levels obtained in the two Bzb-resistant controls (MCF7 and DLD-1). Overall, the HOSCC cell lines, with the WHCO3 and SNO being the exception, displayed an initial increase in pPKB, followed by an immediate deterioration in its levels. However, subsequent to an initial up-regulation in pPKB at distinct Bzb concentrations, levels of pPKB were lowered in both the Bzb-sensitive (HT29) and Bzb-resistant (Sw480) cell lines.

PI lowered PI3K (p85α) protein expression ($P<0.05$) at high Bzb concentrations in the WHCO1, WHCO5, WHCO6, and SNO HOSCC cell lines, albeit to varying degrees (as shown in Fig. 5.10). In the WHCO3 and WHCO5 HOSCC cell lines specifically; this reduction was preceded by an initial increase in PI3K (p85α) expression. This was consistent with the drop attained in PI3K (p85α) levels in the HEK293 control, even though it was at higher concentrations of Bzb (see Fig. 5.10B). Controls possessing mtPIK3CA (MCF7, HT29, DLD-1 and Sw480) demonstrated a dose-dependent decline in PI3K (p85α) levels (Fig. 5.10B), while the expression levels of PI3K (p85α) remained relatively constant in two of the wtPIK3CA control cell lines (NIH3T3 and Caco-2)[794] (see Fig. 5.10).

A)



See next page for legend.

B)

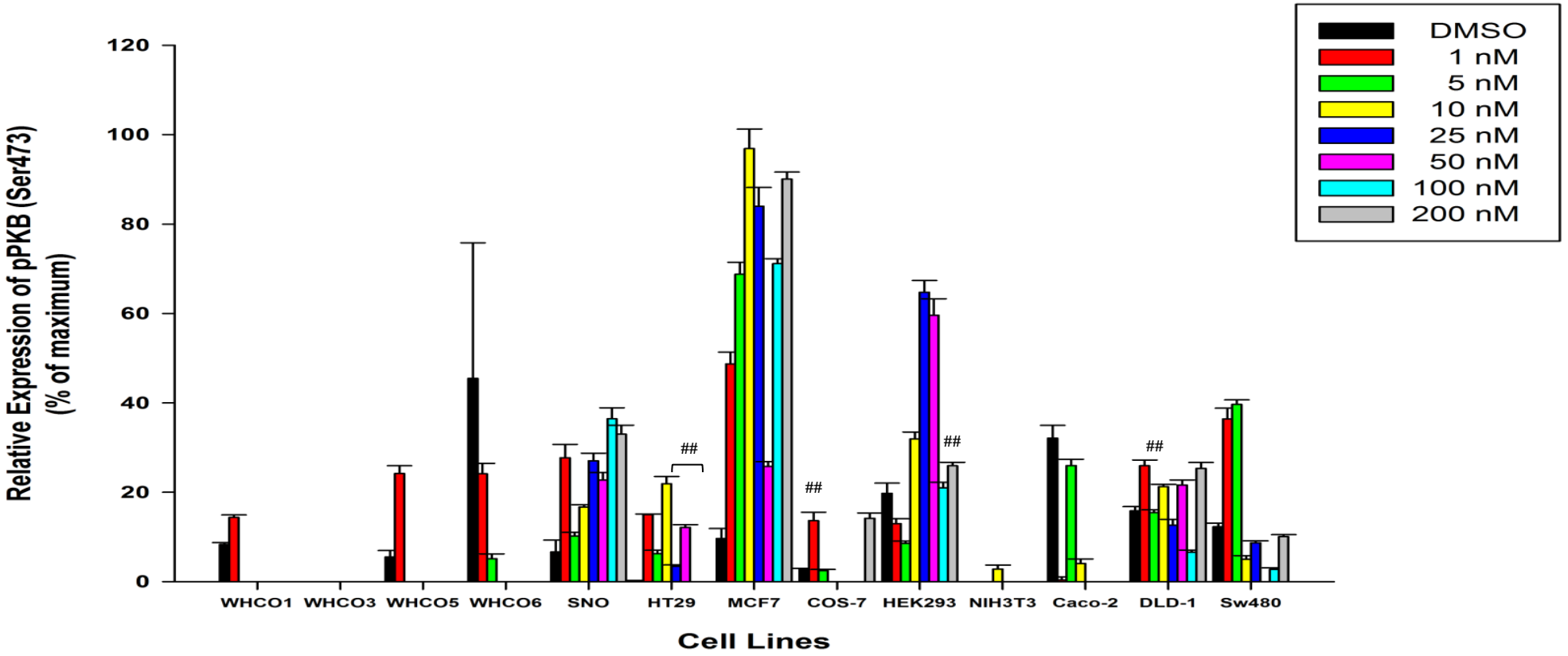
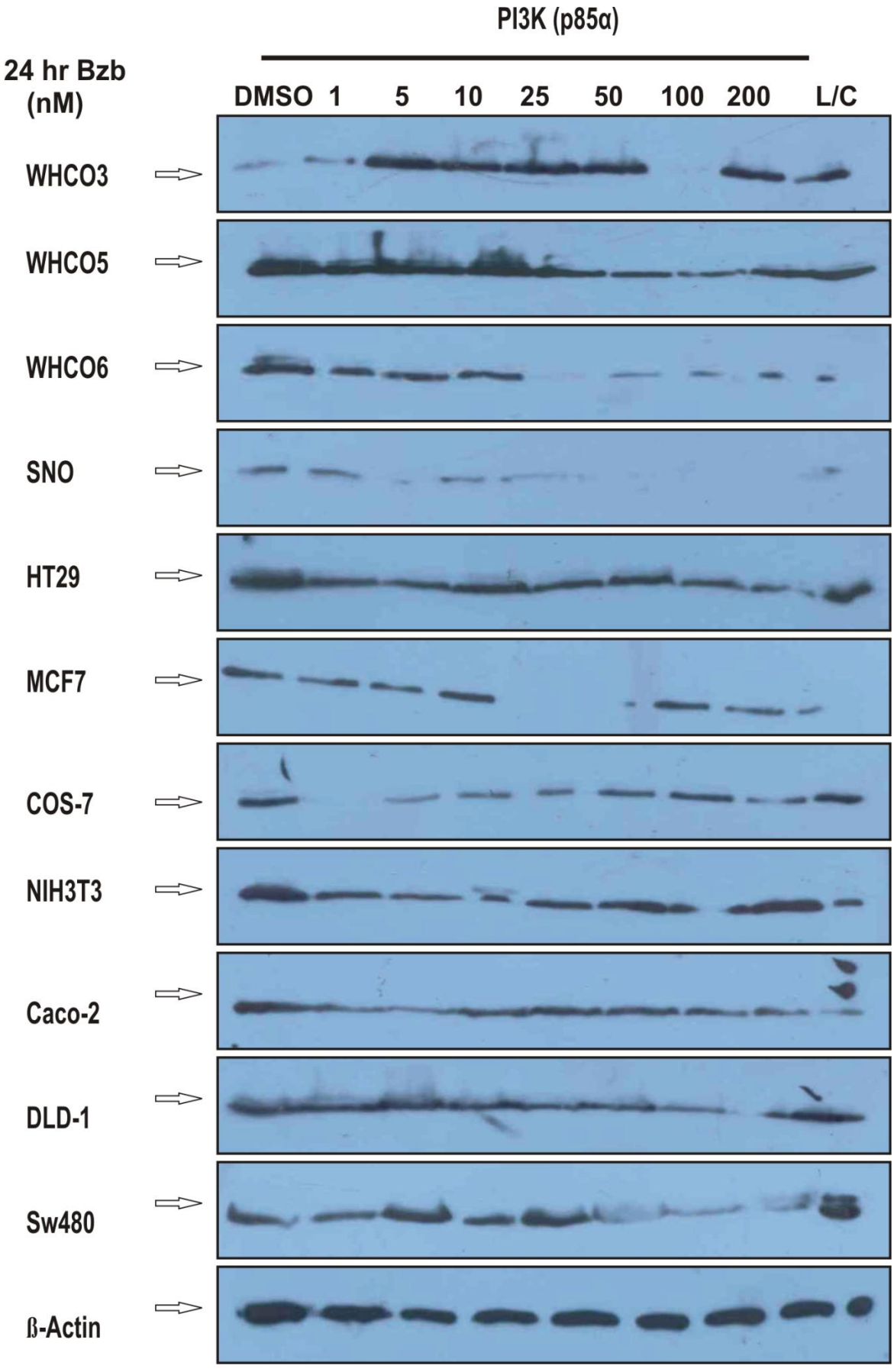


Figure 5. 9: The 26S proteasome playsa major role in the regulation of pPKB levels in HOSCC cells. A) The 4 HOSCC cell lines (WHCO3, WHCO5, WHCO6, and SNO), combined with the various control cell lines (HT29, MCF7, COS-7, NIH3T3, Caco-2, DLD-1, and Sw480) cells were treated for 24 hours with and without Bzb at various concentrations ranging from 1-200 nM. We used western blot analysis to evaluate the effect PI had on the levels of active PI3K and PTEN through the detection of the Ser473 phosphorylation of PKB (pPKB) at 60 kDa (see Appendix A 1.6.6 and 1.7.5 for representative standard curve and 10% SDS-PAGE). A standardized loading control (C) was included in each western blot analysis to allow for comparison between the various immunoblots. All experiments were conducted under serum conditions and in triplicate. β-actin was used as an internal control. **B)** The band at 60 kDa indicative of pPKB levels was quantified using densitometry and represented in a bar graph (mean ± s.d.). For visual simplicity, $^{\#\#}$ indicates that difference is insignificant from the control, P> 0.05. See Appendix D, Table D4 for statistical analysis demonstrating the significant differences.

A)



See next page for legend.

B)

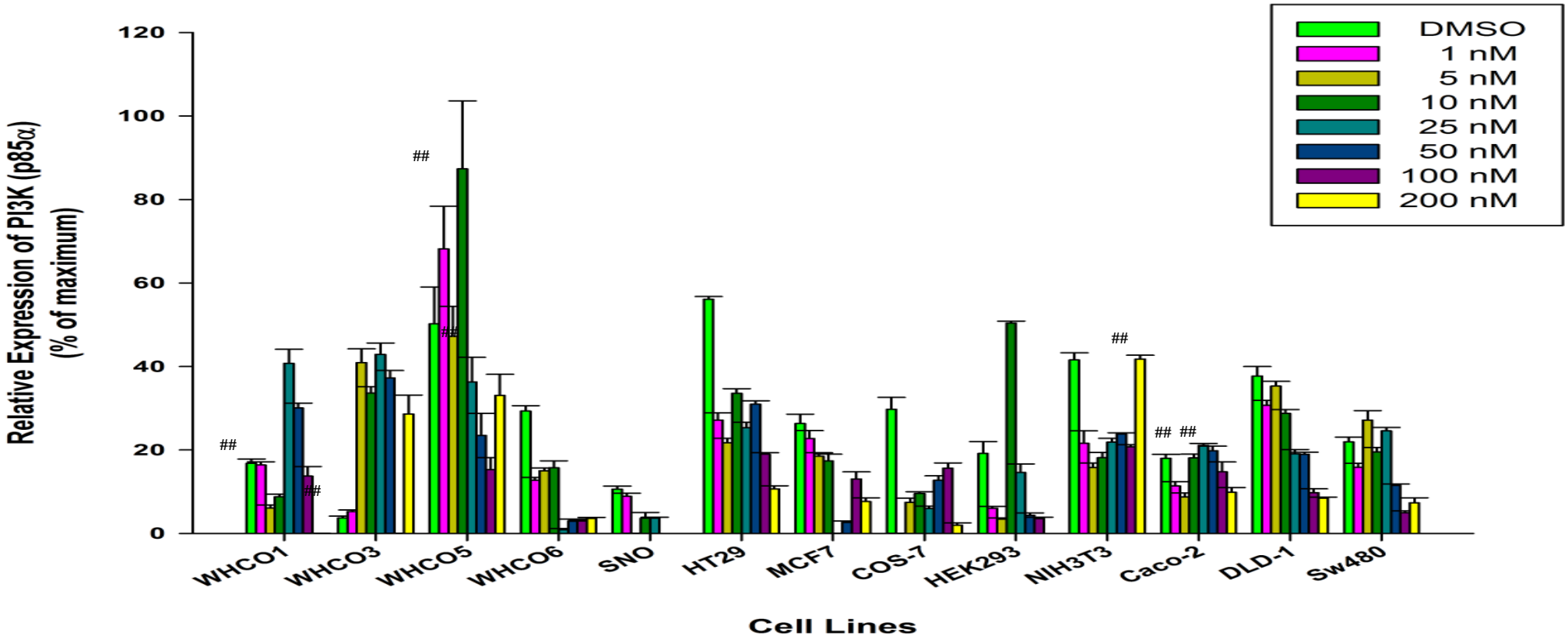


Figure 5. 10: The protein expression of PI3K (p85α) decreases in response to high concentrations of Bzb in HOSCC cells. A) HOSCC cell lines (WHCO3, WHCO5, WHCO6, and SNO), combined with the various control cell lines (HT29, MCF7, COS-7, NIH3T3, Caco-2, DLD-1, and Sw480) were treated for 24 hrs with and without Bzb at 1-200 nM concentrations. Western blot analysis was used to evaluate the effect PI had on the levels of PI3K (85α) at 85 kDa (see Appendix A 1.6.6 and 1.7.5 for representative standard curve and 10% SDS-PAGE). A standardized loading control (C) was included in each western blot analysis to allow for comparison between the various immunoblots. β-actin was used as an internal control. **B)** Densitometric analysis of PI3K (p85α) (mean ± s.d.) confirming that PI3K (p85α) is indeed regulated by the 26S proteasome in HOSCC cells. For visual simplicity, $^{\#\#}$ indicates that difference is insignificant from the control, P> 0.05. See Appendix D, Table D5 for statistical analysis demonstrating the significant differences.

5.4 Discussion

Currently, it is a matter of great interest how particular cancer cells that retain functional PTEN, still manage to uphold their metastatic phenotype[670,795, 796]. Under such circumstances, many studies have shown the need for these cancer cells to maintain low cellular levels of PTEN[797, 798, 799, 800,801, 802, 803], despite the fact that high levels of PTEN appear to be atypical to the metastatic potential of liver cancer[804]. Pertinently, the 5 moderately differentiated HOSCC cell lines were shown to possess low, yet functional PTEN (Chapter 4, Section 4.3.2 and 4.3.4). In this chapter, by focusing on the degradation of PTEN through the 26S proteasome; we provide evidence that manipulation of the 26S proteasome activity using Bzb is able to induce the expression of PTEN in HOSCC. When interpreting the results obtained from proteasome inhibition (PI), it is important to remain cognisant of the dynamic nature of the 26S proteasome[805, 806]. Furthermore, the fact that the degradation of both PKB/PI3K as well as their phosphatase, PTEN was shown to be regulated by the 26S proteasome adds to the complexity of this data interpretation. The various influences that PI had on these respective proteins are discussed below.

5.4.1 HOSCC cells express unique levels of PI3K (p85α) and PTEN.

In order for us to appreciate any changes in the protein levels of PI3K (p85α) and PTEN in the 5 HOSCC cells as a result of PI, we first compared their basal expression status against a range of previously characterized cell lines (see Table 5.1, Materials and Methods). It was revealed here that relative to these controls; levels of PI3K (p85α) were specifically high in the WHCO5, WHCO6, and SNO HOSCC cell lines, with the WHCO1 and WHCO3 cell lines in possession of the least. This implies that unlike the mtPIK3CA controls (MCF7, HT29, and DLD-1)[331] that lose their dependency for p85α, HOSCC cells may be more dependent on these levels for the maintenance of their transformed state, especially since they are all derived from patients with highly metastatic disease[333]. Hence, these data support what was proposed in Chapter 2 (Section 2.4); that elucidation of p85α protein levels may serve as an ideal pathological marker for HOSCC.

The quasi-sufficient nature of PTEN allows for the direct association of its low levels to a correspondingly high level of pPKB[807]; verified in mice[808], and which is strongly linked to the increasing depth of cellular invasion[809]. Importantly, the levels of PTEN protein previously determined in the panel of control cell lines, has been linked to their tumorigenic potential

(see Table 5.1). In this chapter, it was demonstrated, that the protein levels of PTEN are down-regulated in the 5 HOSCC cell lines (see Fig.5.3), similar to the low PTEN expressing HEK293 cell line (see Table 5.1). Consistent with the low PTEN status reported here; lost expression of PTEN, evaluated through immunohistochemistry, significantly correlated to the progression and poor prognosis of Chinese oesophageal cell lines, even though the molecular mechanisms for this loss was not investigated[810]. c-Jun is one of the key suppressors of PTEN transcription and expression[692]. Since the HEK293 cells are known to possess high levels of c-Jun, this strongly implicates a role for c-Jun in the low PTEN levels present within the 5 HOSCC cell lines. Further, the high levels of PTEN in the MCF7 cells (see Fig. 5.3), may be explained by the dominant negative form of c-Jun present within this cell line (see Table 5.1). Altogether, this compliments a role for c-Jun in the down-regulated PTEN protein levels shown in the 5 HOSCC cells. c-Myc, on the other hand, is equally important in attenuating PTEN cellular levels, albeit indirectly by regulating p53 transcriptional activity[811]. Of interest, c-myc is specifically amplified in the WHCO3 cell line[631], and thus may explain the correspondingly low PTEN levels discovered (see Fig. 5.11). Levels of PTEN are considered to be very stable in the HT29 and Caco-2 cell lines; mainly due to the robust interactions that exist between PTEN and MAGI-β-catenin at the plasma membrane[751]. As the expression of PTEN in the 5 HOSCC cells was comparable to the levels of PTEN in these two cell lines (HT29 and Caco-2), it is safe to assume that levels of PTEN, although low, are also stable in HOSCC cells.

5.4.2 The 26S proteasome is active and regulates PTEN protein levels in HOSCC cells.

The expression and degradation of PTEN can be regulated by cellular PIP3 levels via complex mechanisms[218, 812]. Inhibition of PI3K through LY29 exposure (Chapter 2, Section 2.3.8), gave rise to a marked reduction in pPKB levels, which is indicative of dampened PIP3 levels[813] (see Fig. 2.12). Furthermore, no subsequent elevation in PTEN levels was evident, suggesting that the mechanisms controlling PTEN degradation are perturbed in these cells. The function of PTEN, is at least, in part, modulated by its cellular localization[633, 814]. For this reason, the cytoplasmic localization of PTEN (Chapter 4, see Fig. 4.7) has been linked to its enhanced degradation and a hyper Ser473 PKB phosphorylation status[635, 815]. In contrast, the cytoplasmic localization of PTEN in HOSCC cells was associated with low pPKB levels (see Fig. 2.7). It was also demonstrated that the activity of PTEN can be manipulated through exposure to H_2O_2 (Chapter 4, Section 4.3.5) which in turn, has been shown to inhibit the 26S

proteasome[816]. This raised the intriguing question as to whether the 5 HOSCC cell lines are capable of regulating the degradation of PTEN.

Germline mutations in PTEN have been found in a broad range of cancers, such as gastric[817], brain[818], melanoma[819], endometrial[820], prostate[821], colon[257] and breast[452], albeit to independent frequencies. While the mechanisms for low PTEN expression in oesophageal cancer are unknown, mutations within PTEN are considered to be an extremely rare event for HOSCC cells[456,822]. It is acknowledged that the mechanisms regulating the expression, cellular localization, activity and stability of PTEN are not ubiquitous[432]. While the degradation of PTEN is said to proceed in a caspase-3- and 26S proteasome-dependent manner, there are various other proteins, shown to be specific for each cell-type, which regulate this process and are likewise subject to degradation by the 26S proteasome[823, 710] (see Table 5.1, Materials and Methods). In the present study, by exposing the 5 HOSCC cell lines to the reversible 26S proteasome inhibitor, Bortezomib (Bzb), alongside a panel of controls (see Table 5.1), we were able to verify that degradation of PTEN in HOSCC cells is indeed regulated by the 26S proteasome. We further showed that the degradation of PTEN proceeds in a caspase-3-dependent fashion at specific Bzb concentrations. Similar to the results reported by Zhou *et al.*[824], all the cell lines demonstrated significant increases in β-catenin levels subsequent to PI; serving as a good indicator for the presence of an active 26S proteasome. As the existence of an APC truncation in the HT29 cell line supposedly protects β-catenin from degradation[825], it was interesting to note a reduction in the protein levels of β-catenin following PI in this cell line (see Fig 5.7). Notably, two studies have demonstrated that although the specific truncation of the APC gene (position 1555) present in the HT29 cell line[826, 827] predominantly attenuates β-catenin degradation, it is still able to phosphorylate and degrade β-catenin, but at a lower rate. This further supports the presence of an active 26S proteasome in the 5 HOSCC cell lines.

Of interest, was the finding that at high concentrations of Bzb (>50 nM), β-catenin concentrations were significantly reduced in the majority (WHCO1, WHCO3, WHCO6, and WHCO6) of the HOSCC cell lines examined, yet the protein levels of PTEN in all the 5 HOSCC cell lines increased instead. It has been shown that while modest levels of axin accelerate β-catenin degradation, high concentrations tend to inhibit its degradation[828]. In this regard, it would appear that at higher Bzb concentrations (> 50 nM); the concentration of axin would be increased, perpetuating the degradation of β-catenin. Intriguingly, the degree to which β-catenin was stabilized in response to Bzb in myeloma cells was shown to depend

upon the basal levels of "free" β-catenin prior to PI[829]. This suggests that perhaps the basal levels of PTEN in HOSCC cells are similarly "free", contributing to the recovery in PTEN protein levels observed at higher Bzb concentrations. Moreover, recent evidence has revealed that the 26S proteasome is activated by caspase-3[830]. Due to the fact that caspase-3 was indeed activated in this study (see Fig. 5.5 and 5.6B), points to the reactivation of the 26S proteasome by caspase-3 as a convincing alternative explanation for the apparent down-regulation in β-catenin levels at higher Bzb concentrations amidst an inhibited proteasome. It seems clear however, that despite the caspase-3-dependent degradation of PTEN observed at higher Bzb concentrations, the extent to which this took place, relative to the down-regulation of β-catenin, was greatly reduced (see Fig. 5.8). This indicates that an additional integral player that specifically regulates PTEN and not β-catenin is responsible for the increase in PTEN expression at higher concentrations of Bzb (see visualization in Fig. 5.11). There are a number of plausible explanations for these data, which are discussed below.

Post-translationally, many proteins are, and can be, acetylated leading to an increase in its DNA-binding capabilities, stronger interactions with other proteins, and enhanced protein stability leading to extended half-lives[831]. PTEN is highly acetylated in the COS-7 cell line (Table 5.1), which explains its relatively stable expression following PI (see Fig. 5.8). Based on the similarity between the expression of PTEN in the COS-7 and HOSCC cells, would suggest that acetylation of PTEN could account for its stability following PI in HOSCC. This view is further supported by the relatively unstable PTEN in the HEK293 cells in response to PI (see Fig. 5.8), which are known to possess low PTEN acetylation[748].

To complicate matters further, the expression of PTEN can be both attenuated and augmented by p53. When p53 associates with the early growth response gene-1/EGR-1[832], the transcription of PTEN is activated. Research demonstrates that while the wtp53 suppresses the transcription of PTEN, the R175Hp53 mutant is unable to suppress PTEN[755]. Hence, this provides further insight into the stable PTEN expression at higher concentrations of Bzb in the R175Hp53 SNO cell line specifically (see Fig. 5.12 for demonstration).

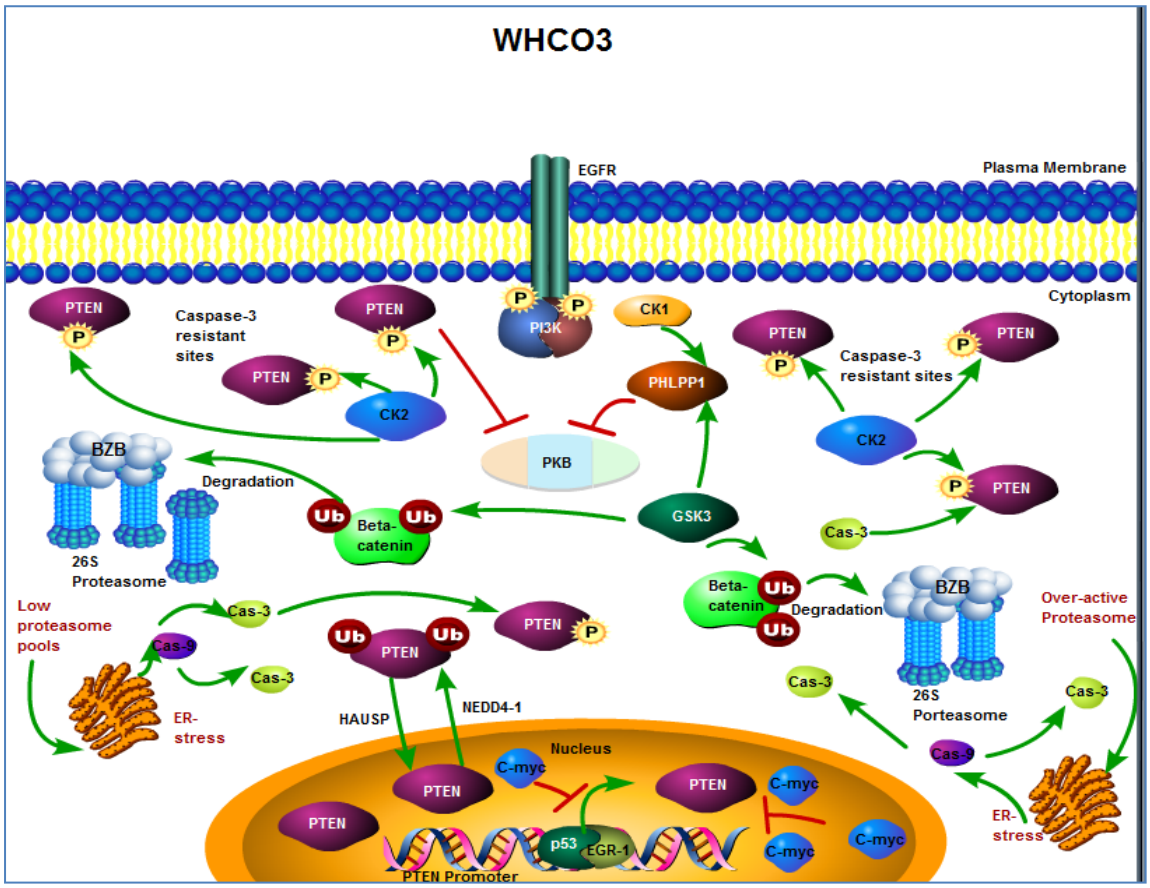


Figure 5. 11: Diagram illustrating the molecular mechanisms underlying the effects of Bzb in the WHCO3 HOSCC cell line. See text for details. Figure generated using Pathway Builder Tool version 2.

A prevailing concept in the literature is that most proteins are stable unless poly-ubiquitinated and labelled for degradation by the 26S proteasome[833]. The literature also suggests that it is the balance between ubiquitination and deubiquitination that ultimately determines a cell's response to PI[834, 835]. HAUSP7 or USP7 is one of the major deubiquitinizing enzymes shown to target PTEN, which leads to its cytosplasmic translocation and stabilization[836, 837]. Although less appears to be known about the activity of HAUSP7 on PTEN in cells, a role for HAUSP7 for the stable PTEN observed here is highly favourable considering its stable cytoplasmic localization established (see Fig. 4.6). Notably, Bzb increases the cellular concentration of ubiquitinated proteins[838]. In addition to HAUSP7, the cellular localization, degradation and thus stability of PTEN is also under the regulation of the E3 ubiquitin ligase, NEDD4-1[839]. The effect that PI has on the levels and activity of NEDD4-1 are undetermined, but their cellular levels have been reported to be inversely proportional to PTEN[753]. Importantly, the levels of NEDD4-1 were shown to be low in the MCF7[747], and high in the

HEK293[693] controls used here (see Table 5.1). Since the levels of PTEN were correspondingly high (MCF7) and low (HEK293) (see Fig. 5.3), suggests that the low levels of PTEN may, in part, be a result of high NEDD4-1 levels (see illustration in Fig. 5.11). Furthermore, polyubiquitination of PTEN through NEDD4-1 maintains PTEN within the cytoplasm, shown to be essential for tumour progression[599]. With respect to the highly cytoplasmic expression of PTEN illustrated within HOSCC cells; it seems clear that its deregulated degradation is highly associated with its cytoplasmic localization and may be influenced by NEDD4-1.

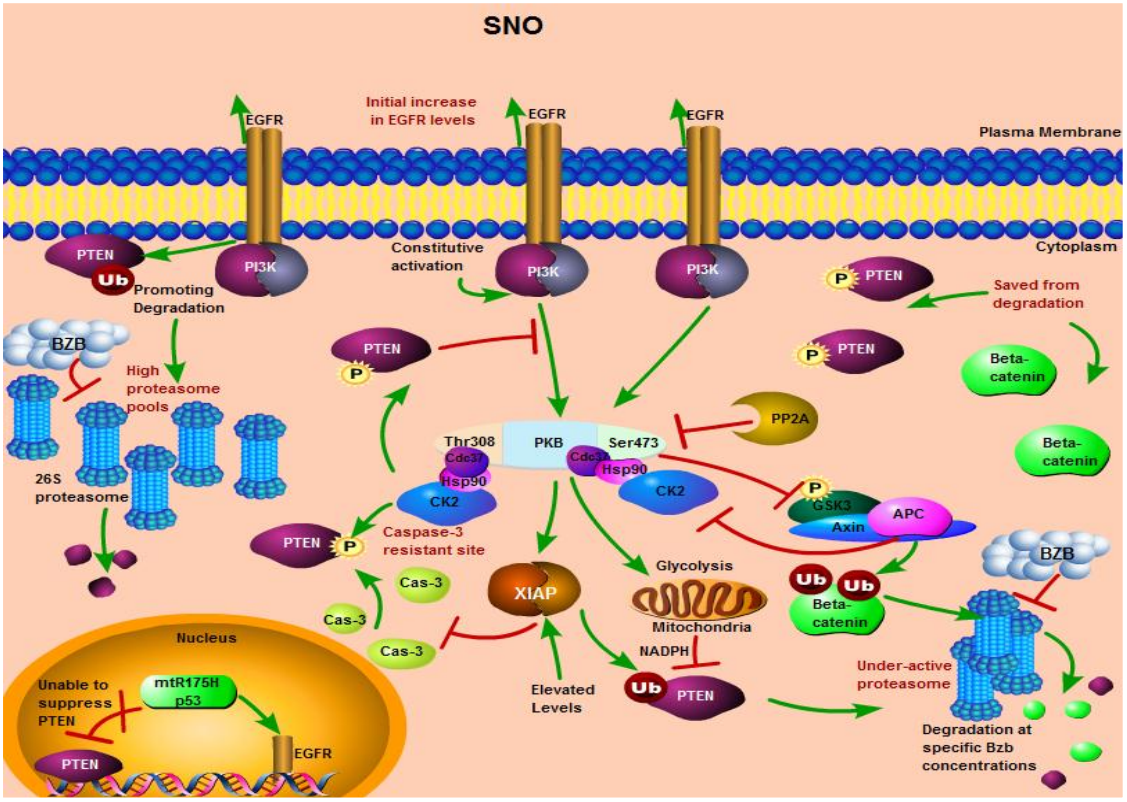


Figure 5. 12: Diagram illustrating the molecular mechanisms underlying the effects of Bzb in the SNO HOSCC cell line.

It is clear from the above that a role for PTEN acetylation and the concerted action of HAUSP7 and NEDD4-1 may be essential for upregulating the expression of PTEN in response to PI. These effects are more than likely induced by protecting PTEN from degradation through polyubiquitination and maintaining its cytoplasmic localization. Since the degradation of PTEN is caspase-3 dependent[695], and we clearly demonstrated caspase-3 activation (see Fig. 5.5 and 5.6B), the question becomes; how was PTEN degradation circumvented? The ubiquitious and constitutively active kinase, CK2 is renowned for creating

caspase-resistant sites in PTEN by phosphorylating its C-terminal[684]. This explanation is further supported by a recent report illustrating that the presence of PTEN in cancer cells is often, if not all the time, accompanied by high CK2 levels, that causes a reduction its phosphatase activity[840]. Thus, it can be assumed that the protection of PTEN to caspase-3 mediated degradation shown here, is obtained from the caspase-3-resistant sites created by CK2 (see demonstration in Figs. 5.11-5.13).

5.4.3 Is the increase in PTEN following PI linked to its action?

Several studies associate the down-regulation in PKB Ser473 phosphorylation to sensitivity to PI induced by Bzb[791, 841, 842]. In this study, we found that exposure of the 5 HOSCC cell lines to Bzb completely abrogated the Ser473 phosphorylation, and thus activation of PKB, in three (WHCO1, WHCO5 and WHCO6) of the HOSCC cell lines. In accordance with its quasi-sufficient nature[446], small changes in the expression levels of PTEN (<10%) was proficient in obstructing PKB Ser473 phosphorylation in the WHCO1 and WHCO6 cell line exclusively at lower Bzb concentrations (see Fig. 5.8 and Fig. 5.9). This result is in line with several reports indicating that relatively small decreases in the protein levels of PTEN significantly perpetuates PKB Ser473 phosphorylation[843, 844, 845, 846]. This is further substantiated by the results depicted in the WHCO3 cell line; where protein levels of PTEN were significantly augmented by PI, and thus no up-regulation in pPKB levels were evident.

Importantly, even though levels of pPKB were abolished, an initial increase in its levels was observed at the lowest concentration of Bzb (1 nM) in the WHCO1 and WHCO5 cell lines (see Fig. 5.9), despite the presence of a simultaneous increase in PTEN protein levels (see Fig. 5.8). These data may point to PTEN-independent mechanisms for the suppression in pPKB levels obtained. This is supported by the consistent decline in PTEN expression seen in the WHCO5 cell line which was not associated with a corresponding escalation in the Ser473 phosphorylation levels of PKB. Likewise, the rise and fall in PTEN levels subsequent to PI at higher concentrations of Bzb in the WHCO1 and WHCO6 cell lines, do not correspondingly impact pPKB levels. Altogether, the data presented here indicate that in addition to PTEN, another key regulator of pPKB levels may be simultaneously up-regulated in response to PI. This is of particular relevance to the results from the SNO cell line; where levels of pPKB were sustained in spite of the clear induction in PTEN levels (see Fig. 5.8 and Fig. 5.9).

In accordance with the initial increase in pPKB levels, Yan *et al.*[847] similarly demonstrated an elevation in the concentration of pPKB following PI. They were able to indicate that its degradation was directly proportional to its phosphorylation state. Although extensive research has been performed on the various ways in which the phosphorylation and dephosphorylation of PKB can be regulated [179, 848] less is known regarding its degradation. What is known, is that its degradation is regulated by its phosphorylation state and can be mediated in both a caspase-dependent and caspase-independent manner[849, 850, 851]. In support of a role for caspase-3 in PKB degradation, down-regulation in pPKB levels was not detectable in the caspase-3-deficient MCF7 cell line[785]. By the same token, pPKB levels were up-regulated in the SNO cell line where caspase-3 cleavage was lacking (see Fig. 5.6B and Fig. 5.9); whereas pPKB was down-regulated in the presence of active caspase-3 in the WHCO1, WHCO5, and WHCO6 cell lines (see Fig. 5.13 for a demonstration). Consistent with Fanucchi and Veale[429], the SNO cell line demonstrated resistance to caspase-3 activation (see Fig. 5.6B). Since the degradation of PTEN proceeds in a caspase-3-dependent manner, may explain why PI did not induce PTEN or pPKB degradation at high concentrations of Bzb in the SNO cell line. The activation of caspase-3 is inhibited by the major caspase inhibitor; X-linked inhibitor of apoptosis (XIAP)[852, 853]. XIAP has been shown to play a role in the acquisition of resistance to chemotherapy in oesophageal cancer[854]. Interestingly, pPKB levels were maintained in cells previously shown to overexpress XIAP (HT29, DLD-1 and Sw480, see Table 5.1). Since PI was shown to greatly influence XIAP levels[711,855], it seems a likely candidate for the increase in pPKB levels and lack of caspase-3 activation in the SNO cell line (see Fig. 5.12 for a graphic representation).

In contrast to the usual pattern of PTEN and pPKB levels (see above), both PTEN and pPKB increased following PI in the SNO cell line, which was similar to that observed in the HEK293 cells. In addition to the reduced PTEN acetylation within the HEK293 cells (see Table 5.1), they have been reported to rely on elevated NADPH levels caused by increased glycolysis known as the "Warburg effect"[749]. In these cells, PKB activation is constitutive based on the high levels of ROS induced via Nox that inhibits PTEN through oxidation and prevents its reduction via thioredoxin[856, 857, 858]. This may provide insight to the sustained pPKB obtained in the SNO cell line, as depicted in Fig. 5.12.

In addition to creating caspase-3 resistant sites for PTEN, CK2 also protects PKB from PP2A-mediated dephosphorylation of its Ser473 residue[619], and sustains PKB in an active state by phosphorylating its Ser129 residue[439]. Of relevance, certain of the controls (HT29, Sw480,

MCF7 and DLD1, see Table 5.1) have been shown to rely on high CK2 levels for their survival[727]. Consistently, all these cell lines maintained PKB Ser473 phosphorylation and PTEN levels in response to PI (see Fig. 5.8 and Fig. 5.9). CK2 is negatively regulated by APC and GSK3β[859]. Hence, the truncated APC status in the colon cells explains their reliance on CK2 levels and the strong Ser9 phosphorylation (inhibition) status of GSK3β in the MCF7 cell line (see Fig. 2.11) may clarify its dependence on CK2. Notably, GSK3β was shown to be severely inhibited (Ser9 phosphorylated) in the SNO cell line (Chapter 2, Section 2.3.6, see Fig. 2.11), and may shed some light on the maintained levels of pPKB obtained through CK2 activity. In contrast, the WHCO6 cell line expressed a similar basal GSK3β Ser9 phosphorylation (see Fig. 2.11), and yet no maintenance in pPKB was evident (see Fig. 5.9). Consistently, the HEK293 and NIH3T3 controls were reported to possess low endogenous levels of CK2[860], yet only the HEK293 maintained pPKB levels. The Hsp90-Cdc37-CK2 complex plays a significant role in the preservation of active pPKB pools[861,614]. Relevantly, and as highlighted in Chapter 2, wtp53 actively suppresses the activity of CK2[441], whereas this function is lost in cells with mtp53[862]. By implication, this may explain why pPKB levels are maintained in the mtp53 SNO cell line (see visualization in Fig. 5.12), whereas in the wtp53 WHCO1, WHCO5, and WHCO6 cell lines, CK2 should be appropriately regulated, thus contributing to the attenuation in pPKB observed (see visualization in Fig. 5.13). Based on the undetectable pPKB levels before and after PI in the WHCO3 cell line, a role for the Hsp90-Cdc37-CK2 complex is assumed to be similarly absent (see visualization in Fig. 5.11).

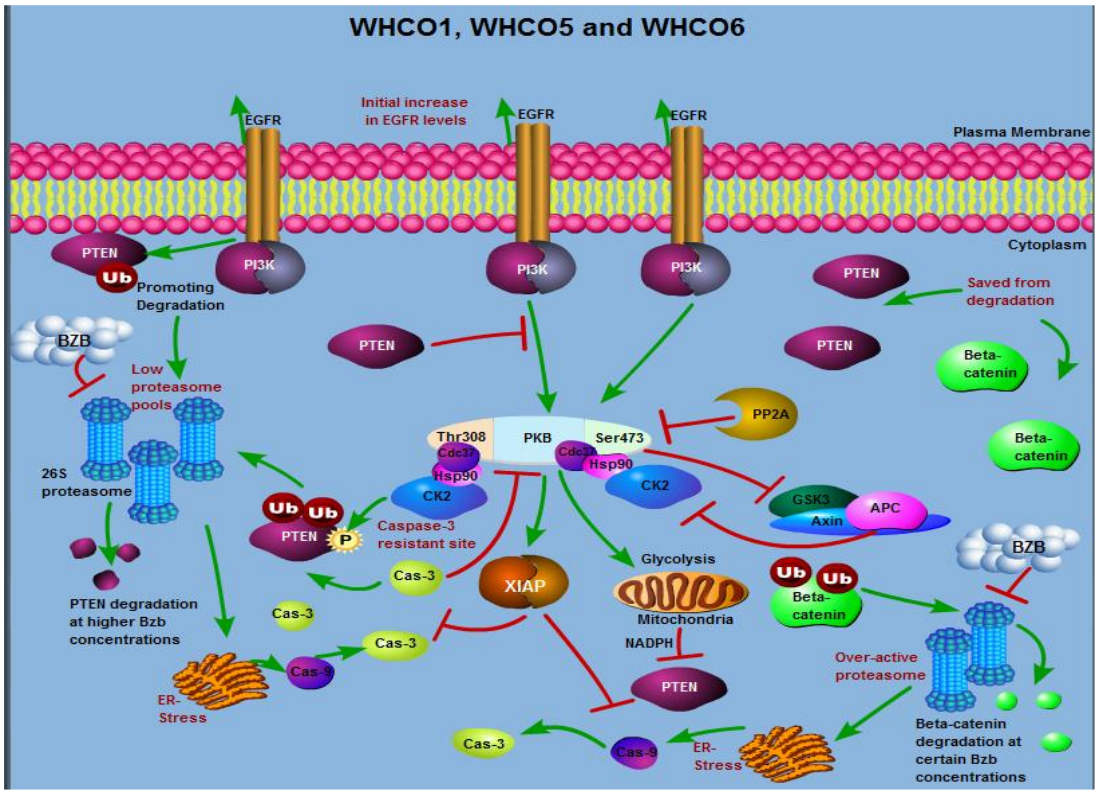


Figure 5. 13: Diagram illustrating the molecular mechanisms underlying the effects of Bzb in the WHCO1, WHCO5, and WHCO6 HOSCC cell lines.

5.4.4 HOSCC cells are highly susceptible to proteasome inhibition mediated by Bzb.

These results strongly suggest that the 26S proteasome is indispensible for the activation of PKB in the WHCO1, WHCO3, WHCO5, and WHCO6 HOSCC cell lines. In fact, the Ser473 phosphorylation levels in these cell lines were completely depleted from Bzb concentrations of as little as 5 nM and higher, indicative of Bzb-sensitivity. This is consistent with a previous report showing that cells responding to low Bzb concentrations (4.9-19 nM) were considered extremely susceptible to PI[863]. The high susceptibility to Bzb in these cell lines is substantiated by other studies only showing caspase-3 cleavage and/or pPKB elimination at higher Bzb concentrations (>50 nM)[791,786,841]. Of relevance, sensitivity to Bzb was predominantly observed from incubations longer than the 24 hrs used in this study; further highlighting Bzb sensitivity in these HOSCC cells. Furthermore, certain hepatocellular carcinoma cells treated for 24 hrs and longer with 1000 nM concentrations of Bzb, displayed prominent resistance[864]. Hence, it is clear that the four HOSCC cell lines (WHCO1, WHCO3, WHCO5, and WHCO6) are highly sensitive to PI through exposure to Bzb (see Figs. 5.11 and 5.13 for visualization).

One of the characteristic cellular responses to PI is the accumulation of unfolded proteins that induce ER-stress[865,735]. Research has demonstrated that, in p53-deficient or mutant cells, ER-stress mediated apoptosis is partially suppressed[866, 867]. Hence, the wtp53 status in the WHCO1, WHCO3, WHCO5, and WHCO6 cell lines contributes to their sensitivity towards PI, whereas the mtp53 status in the SNO cell lines confers resistance to ER-stress induced by PI. Additionally, several studies have indicated that the concentration of 20S proteasome is inversely related to Bzb sensitivity, such that; the lower the concentration, the higher the resistance[782, 868, 869]. With reference to these reports and the data presented in this chapter, it would suggest that the SNO line has a higher proteasomal activity than the WHCO1, WHCO3, WHCO5, and WHCO6 cell lines (as illustrated in Figs. 5.11- 5.13).

5.4.5 Concluding Remarks

The present study reveals an active 26S proteasome present in the 5 HOSCC cell lines. We have also shown that proteasomal-dependent and caspase-3-dependent mechanisms are the preferred method used for PKB degradation in HOSCC. We also provide evidence that the increase in PTEN expression is directly linked to diminished Ser473 phosphorylation levels of PKB in four of the cell lines, with the SNO as the exception. Hence, the sensitivity to PI obtained in the WHCO1, WHCO3, WHCO5, and WHCO6 HOSCC cell lines opens the door to explore the effectiveness of Bzb in the treatment of HOSCC cells that harbour similar molecular characteristics as those disclosed in this chapter. These features are clearly visualized in Figs. 11, 12 and 13.

Chapter 6
Crosstalk between the PI3K and Wnt signalling pathways in HOSCC cells

6.1 Introduction

Quiescent cells are known to express very low levels of β-catenin within the cytoplasm and the nucleus[870]. This is primarily due to the contribution of β-catenin in the architecture of epithelial cells[871]. It does this by forming plasma membrane complexes with E-cadherin and α-catenin in the cell-cell adhesion junctions[872, 873,88]. The membrane localization of β-catenin and exclusion from the cytoplasm/nucleus is enabled through its rapid degradation by the β-catenin destruction complex[874] comprising of PP2A, Axin, APC, and GSK3β that constitutively phosphorylate and label β-catenin for degradation by the 26S proteasome[783] (see Fig. 6.1, left panel). However, in the presence of a Wnt signal, the frizzled family of receptors, along with the co-activator; the low-density lipoprotein receptor-related protein (LRP), become activated, triggering the downstream stimulation of dishevelled (Dvl)[875, 876]. Once active, Dvl phosphorylates GSK3β on its Ser21 residue, causing dissociation and inhibition of the destruction complex, giving rise to the cytoplasmic accumulation of β-catenin[877]. High levels of cytoplasmic β-catenin results in its nuclear translocation, where it interacts with the leukocyte enhance factor-1/T cell factors (LEF-1/TCF) family of transcription factors to upregulate the expression of their target genes, predominantly; cyclinD1, c-myc, c-jun, and the matrix matalloproteinases-7 (MMP-7)[878, 879] (see Fig. 6.1, right panel).

Cong *et al.*[880] and Willert *et al.*[881] linked effective canonical Wnt signalling to the nuclear roles of β-catenin. Consequentially, the oncogenic potential of Wnt signalling in many cancers is directly linked to the accumulation of β-catenin in the nucleus, and as such, acts as a prognostic marker for various forms of cancer, including cancer of the oesophagus[882, 883, 884, 885]. Since the β-catenin destruction complex (PP2A/Axin/APC/GSK3β) is the primary regulator for the nuclear sequestration of β-catenin, inappropriate accumulation of β-catenin in the nucleus is frequently attributable to mutations within APC or β-catenin[886, 887, 888, 889]. Inactivating mutations in APC have been found in over 90% of colon cancers[890, 891, 892]. In contrast to colorectal cancer, where the molecular mechanisms governing the deregulated nuclear levels of β-catenin have been

explored in great detail; these molecular mechanisms still need to be identified in HOSCC[893]. Earlier investigations have shown that canonical Wnt signalling is indeed active within the WHCO and SNO series, and is not attributable to mutations in APC or β-catenin[627,894, 895]. Further, it was found that β-catenin is complexed with the LEF-1/TCF/ transcriptional complex, hinting at the possibility of being active in all the 5 HOSCC cell lines[896]. This led us to question whether there are Wnt-independent mechanisms behind the nuclear sequestration of β-catenin in the WHCO and SNO cells.

Furthermore, the well-known p53 mutations and EGFR overexpression status commonly associated with this disease[897], is considered insufficient to drive the transformation state, and instead, they serve as paramount contributors[268]. The increasing effort in the literature to investigate the potential of crosstalk in the regulation of β-catenin highlights the importance of unveiling and understanding a role for interplay[898, 899]. It should be noted, that although a role for PI3K in the Wnt signalling pathway has been demonstrated by separate studies in various epithelial cancers[327,900, 901], the specific focal point for this interplay and downstream effects are unknown. Thus examination of crosstalk between the PI3K and Wnt signalling pathways in HOSCC allowed us to better understand the regulation of nuclear β-catenin levels. In order to explore this relationship, the nuclear concentration of β-catenin had to be confirmed.

More recently, cancer research is beginning to discover the essential link that exists between the EGFR and Wnt signalling pathways in the initiation and progression of cancers[902]. As such, there have been concerted efforts to disclose the fundamental mediator for this crosstalk, and therefore a number of convergence points have been suggested. These are the NFκB, cyclooxygenase-2 (COX-2), extracellular signal-regulated kinase (ERK) or mitogen-activated protein kinase (MAPK), and the NKD1/NKD2 signal transduction pathways[903, 904, 905]. As an addition to these pathways, a key role for the PI3K signalling pathway was also proposed. A previous study by Woodfield *et al.* [100]revealed an essential contribution made by the p85α regulatory subunit of PI3K in the modulation of cellular β-catenin levels through its association with the E-cadherin membrane adhesion complex. More importantly, previous research on the WHCO and SNO HOSCC cell lines found that the nuclear sequestration of β-catenin was more responsive to EGFR activation than to Wnt signalling[894]. The demonstration that EGFR activates PI3K (Chapter 3, Section 3.3.5) would suggest that PI3K may be implicated in this regulation.

In the previous chapters, while it was clear that we were able to manipulate the activity of PI3K through LY29; PI3K-dependent, and PKB-independent mechanisms are used to regulate the Ser9

phosphorylation, and thus inhibition of GSK3β (Chapter 2, Section 2.3.7). Significantly, attenuation in the Ser9 phosphorylation of GSK3β was still evident, despite the lack of correlation it had to pPKB levels (see Chapter 2, Section 2.3.7). Therefore, in the present study, we explore the possible relationship between Wnt signalling and the overexpression status of EGFR through the PI3K pathway in these HOSCC cells. With respect to the high nuclear levels of β-catenin previously established in the mtAPC and wtAPC HT29 and MCF7 cell lines[906, 894], we first show that β-catenin is present within the nucleus of the 5 HOSCC cell lines whilst maintaining its cell membrane adhesive roles. Uniquely, we also show that although Wnt signalling does regulate the concentration of GSK3β Ser9 phosphorylation, the PI3K pathway is able to directly influence the nuclear accumulation of β-catenin in the WHCO and SNO HOSCC cells.

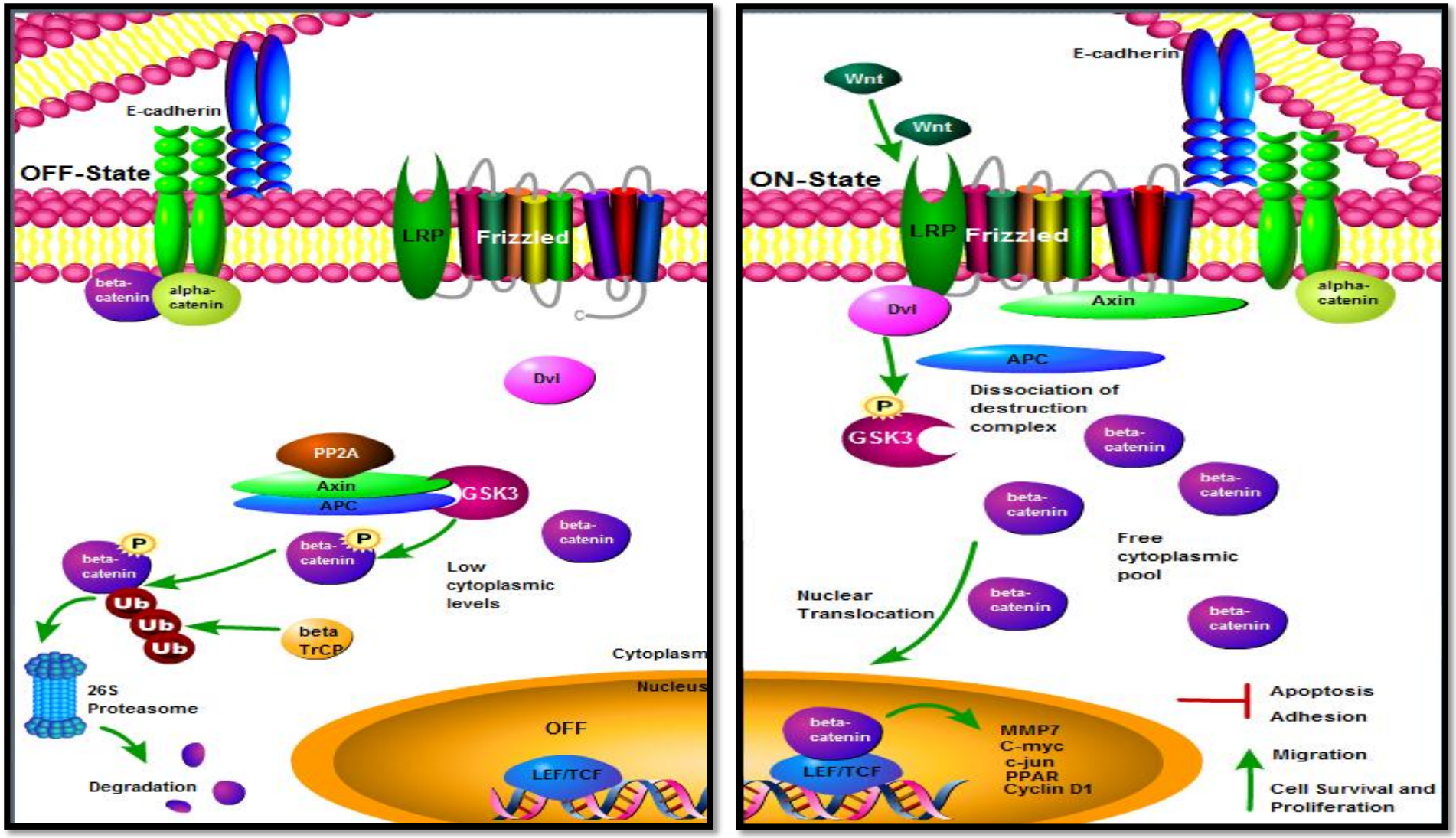


Figure 6. 1: Canonical Wnt signalling pathway. The cytoplasmic localization and nuclear sequestration of β-catenin is under the regulation of the β-catenin destruction complex (PP2A/Axin/APC/GSK3β), see text for more details. Figure generated using the Pathway Builder Tool.2.0.

6.2 Materials and Methods

6.2.1 Cell lines and Culture

As previously described, see Chapter 2, Section 2.2.1.

6.2.2 Antibodies

Rabbit polyclonal antibodies used for immunoblot analysis; anti-β-catenin (Sigma), anti-MMP-7 (Sigma), anti-α-catenin (Sigma), anti-c-Jun (Santa Cruz Biotechnology), anti-PI3 Kinase (p85α) (Upstate Biotechnology), anti-α-Tubulin (Santa Cruz Biotechnology), and anti-β-Actin (Sigma). E-cadherin was specifically detected using the mouse monoclonal anti-E-cadherin antibody (RD science), and hnRNP (A2/B1) was specifically detected using the goat polyclonal anti-hnRNP I (N-20) (Santa Cruz Biotechnology). The rabbit polyclonal anti-Phospho-Akt (Ser473) and anti-Phospho-GSK3β (Ser9) were from Cell Signalling Technology, and was used to explicitly detect PKB/AKT and GSK3β when phosphorylated at Ser473 and Ser9. The secondary antibody, HRP-bound goat- anti-rabbit IgG (Sigma), was used for the specific detection of all rabbit polyclonal antibodies for immunoblotting, whereas detection of all mouse monoclonal and goat polyclonal primary antibodies were specifically detected using the anti-mouse IgG (Fab Specific) and the donkey anti-goat (Santa Cruz Biotechnology) horseradish peroxidase conjugate secondary antibodies.

6.2.3 Nuclear Extraction

As previously described, see Chapter2, Section 2.2.6.

6.2.4 Protein Estimation

As previously described, see Chapter 2, Section 2.2.8.

6.2.5 Polypeptide Resolution and Western Immunolotting

40 μg of protein from each cell line obtained from the various extractions (whole cell, nuclear, and plasma membrane) were prepared and separated by 10% SDS-PAGE, and immunoblotted for β-catenin, PI3K (p85α), β-actin, c-Jun, E-cadherin, pGSK3 and pPKB as detailed in Chapter 2 (Section 2.2.9), and Chapter 3 (Section 3.2.9).

Following the procedure as described in Chapter 2, Section 2.2.9, the respective extracts were immunoblotted with the rabbit polyclonal anti-hnRNP (A2/B1) (1:1000), anti-MMP-7 (1:750), anti-α-catenin (1:1000), and anti-α-tubulin (1:250) antibodies for 2 hrs. This

succeeded six 5 min PBS washes, followed by 1 hr incubation in the HRP-bound goat-anti-rabbit IgG antibody for the specific detection of MMP-7 (1:30000), α-catenin (1:3000), and α-tubulin (1:15000). HRP-bound donkey anti-goat IgG antibody was used for the specific detection of hnRNP (A2/B1) (1:3000). Thereafter, the membranes were incubated for 5 mins in the SuperSignal West Pico Chemiluminescent (Piece, USA), and exposed to film and developed as described in Chapter 2, Section 2.2.9.

6.2.6 Whole Cell protein extraction

As previously detailed see Chapter 2, Section 2.2.5.

6.2.7 Plasma membrane enriched extraction used for Immunoprecipitation reactions

As previously described, see Chapter 3, Section 3.2.7.

6.2.8 Co-immunoprecipitation analysis of β-catenin and its cell adhesive counterparts

200 μg (from each HOSCC cell line) of plasma-membrane-associated protein extracts were incubated on a rotor at 4 °C overnight in 1 μl of the rabbit polyclonal anti-β-catenin antibody (Sigma) diluted in 500 μl IP buffer (Appendix B 2.1.2). Thereafter the protocol was carried out as detailed in Chapter 3 (Section 3.2.11), and immunoblotted for E-cadherin, α-catenin and PI3K (p85α) detection described above (Section 6.2.5). **Note:** All co-immunoprecipitation reactions were performed three times.

6.2.9 Activation of Wnt Signalling through Lithium Chloride (LiCl) Exposure

The Wnt signalling pathway was activated by exposing 80% confluent HOSCC and control cell lines (HT29 and MCF7) under serum conditions to 10 mM LiCl (see Appendix E 5.1) for periods of 3, 12, and 24 hrs. This concentration of LiCl and time exposures used were previously shown to effectively inhibit GSK3β, and thus activate Wnt signalling in the 5 HOSCC cell lines[894]. The constitutively active Wnt signalling status in the mtAPCHT29[907] cell line and the lack thereof in the wtAPCMCF7[908] cell line were used as controls. Consequent to LiCl exposure, whole cell protein extractions were performed as detailed in Chapter 2, Section 2.2.6.

6.2.10 Inhibition of PI3K through LY294002 (LY29) Exposure

Both nuclear and whole cell protein extractions were performed following exposure to LY29 as previously described, see Chapter 2, Section 2.2.11. **Note:** All untreated cells were exposed to the LY29 vehicle control, DMSO, and all treatments were repeated three times.

6.2.11 Densitometry

Labworks TM Image Acquisition and Analysis software (Labworks version 4.5) was used for densitometric analysis to semi-quantitatively determine the concentration levels of β-catenin, MMP-7, c-jun, pPKB (Ser473), pGSK3β (Ser9), and PTEN PI3K (p85α), and pPKB detected through western blotting. **Note:** The densitometric results are an average of three independent experiments (mean ±s.d.) and expressed as a percentage relative to the maximum.

6.2.12 Image Capturing

All western blot and SDS-PAGE images were captured on a Hewlard Packard Scanjet 4400c series scanner at 300dpi, contrast and brightness of all images were standardised using CorelDRAW version 12®.

6.2.13 Statistical Analysis

Statistical analyses were performed using Student's paired *t* test and One Way Repeated Measures Analysis of Variance (One Way RM Anova1) according to the Holm-Sidak method. Statistical analysis results are inclusive of three independent experiments (mean ± S.D). P-values are given in the figure legends, and values of $P > 0.05$ were considered not to be significant. All calculations of statistical computations were carried out using the SigmaPlot Release 11.0® statistical software. **Note:** Based on the fact that statistical analysis requires a minimum of three independent experiments, an example of the three blots for the figures in this chapter was chosen (i.e. nothing is gained by showing all three).

6.2.14 Figure Design

All schematic diagrams were designed using the Pathway Builder Tool version 2.0, unless otherwise stipulated.

6.3 Results

6.3.1 β-catenin is present at high levels in the nucleus of HOSCC cells.

In order to understand the relationship between the canonical Wnt and PI3K signalling pathways, it became crucial to first obtain an accurate measure of the levels of β-catenin in the nucleus of the 5 HOSCC cell lines. Western blot analysis of nuclear-specific extracts showed that the expression of β-catenin in the 5 HOSCC cell lines is high (60%), relative to the mtAPC HT29 and wtAPC MCF7 control cell lines (shown in Fig. 6.2). The WHCO3 cell line possessed significantly ($P<0.05$) higher nuclear levels of β-catenin compared to the WHCO1, WHCO5, WHCO6, and SNO HOSCC cell lines. The integrity of the nuclear extract was confirmed by the western blot detection of the abundant nuclear polypeptides[909]; the heterogenous nuclear ribonucleoproteins (hnRNPs) (Fig. 6.2).

6.3.2 Nuclear β-catenin is transcriptionally active in HOSCC cells.

One of the common mechanisms used to affirm the presence of a transcriptionally active nuclear β-catenin, is through the assessment of one of its numerous gene targets (i.e. cyclin-D1, c-Jun, c-myc, MMP-7)[910, 911, 912,878]. In order to link the nuclear expression of β-catenin determined above (Fig. 6.2) to its activities therein, it became clear that the expression levels of these nuclear targets needed to be elucidated. Here, we investigate the respective protein levels of two of these nuclear targets; MMP-7 and c-Jun. As can be seen by the presence of MMP-7 through western blotting in Fig. 6.3, the nuclear localization of β-catenin is indeed associated to its nuclear gene activation of MMP-7. Based on the lower levels of MMP-7 in the WHCO1 and WHCO6 cell lines (see Fig. 6.3), it would appear that the nuclear gene activation of MMP-7 through β-catenin occurs to a lesser degree. Western blot analysis indicated that the 5 HOSCC cell lines all express high levels of the c-Jun protein (> 60%), indicative of its nuclear gene activation by β-catenin (see Fig. 6.4). The protein levels of c-Jun shown in the HT29 (high) and MCF7 (low) controls (see Fig. 6.4), is consistent with the active state of the β-catenin/LEF-1/TCF transcriptional complex in the HT29 cell line[913] and the low c-Jun levels in the MCF7 cell line[914] previously established.

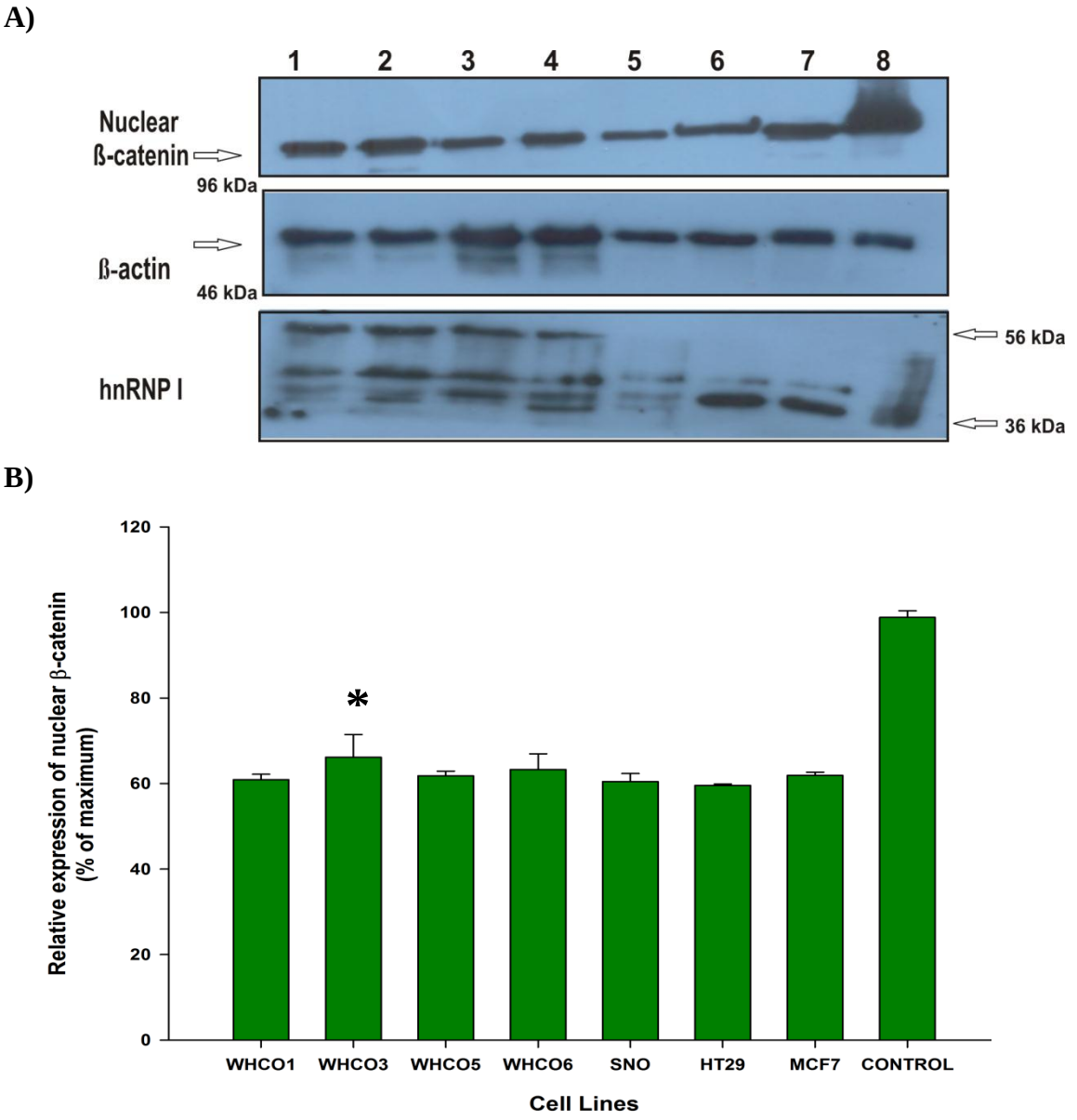
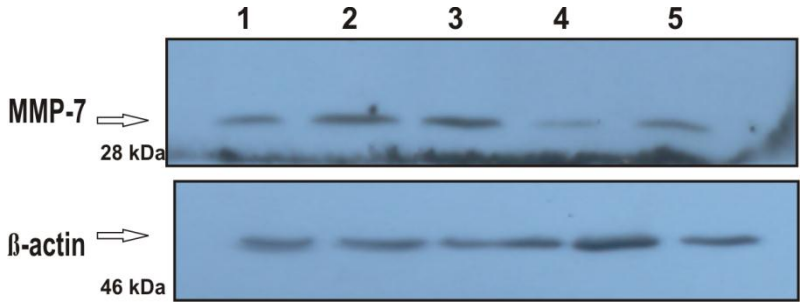


Figure 6. 2: HOSCC cells express high levels of β-catenin in the nucleus. A) Nuclear extracts subjected to western blotting for β-catenin detection from HOSCC, HT29 and MCF7 cells (see Appendix A 1.6.6 and 1.7.5 for representative standard curve and 10% SDS-PAGE). Lanes: 1-WHCO1, 2-WHCO3, 3-WHCO5, 4-WHCO6, 5-SNO, 6-HT29, 7-MCF7, 8-WHCO6 whole cell lysate control. The integrity of the nuclear extract was assessed through the western blot detection of the hnRNPs, type A2/B1 which is an abundant nuclear polypeptide. There are approximately 20 types of hnRNPs, uniquely expressed in specific cell types[909], here we were able to detect at least 2 different types, the prominent 36 kDa and a 56 kDa polypeptide. No clear detection of the hnRNP polypeptides were detected in the whole cell lysate (lane C), further strengthening the integrity of the extract. **B)** Representation of the densitometric analysis of the nuclear expression of β-catenin, showing high levels in all the HOSCC cell lines, with the WHCO3 cell line possessing 10% more. * significantly different from the high levels in the HT29 control, P*<0.05. Note: mean ±s.d. of triplicate experiments; see Appendix E 5.2 for mean optical density values and statistical analysis.

A)



B)

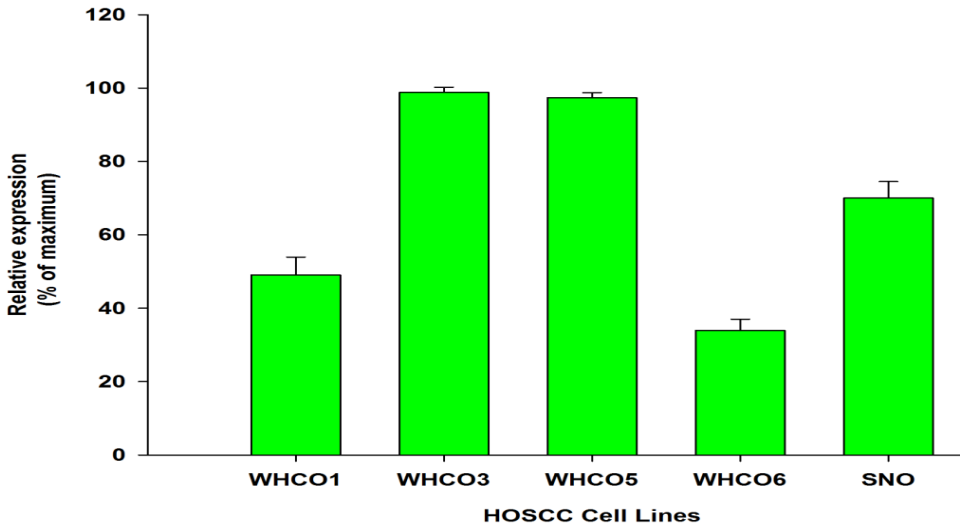


Figure 6. 3: Nuclear B-catenin is active in HOSCC cell lines. A) HOSCC cell lines were immunoblotted for MMP-7 detection at 19 kDa (see Appendix A 1.6.6 and 1.7.5 for representative standard curve and 10% SDS-PAGE). Numbers 1-5 represent the WHCO1, WHCO3, WHCO5, WHCO6, and SNO cell lines respectively. **B)** Quantitative analysis of the band representing MMP-7 reveals high levels in the WHCO3 and WHCO5 cell lines, and modest levels in the WHCO1, WHCO6 and SNO cell lines. Note: mean ±s.d. of triplicate experiments; see Appendix E, Table E1 for mean optical density values.

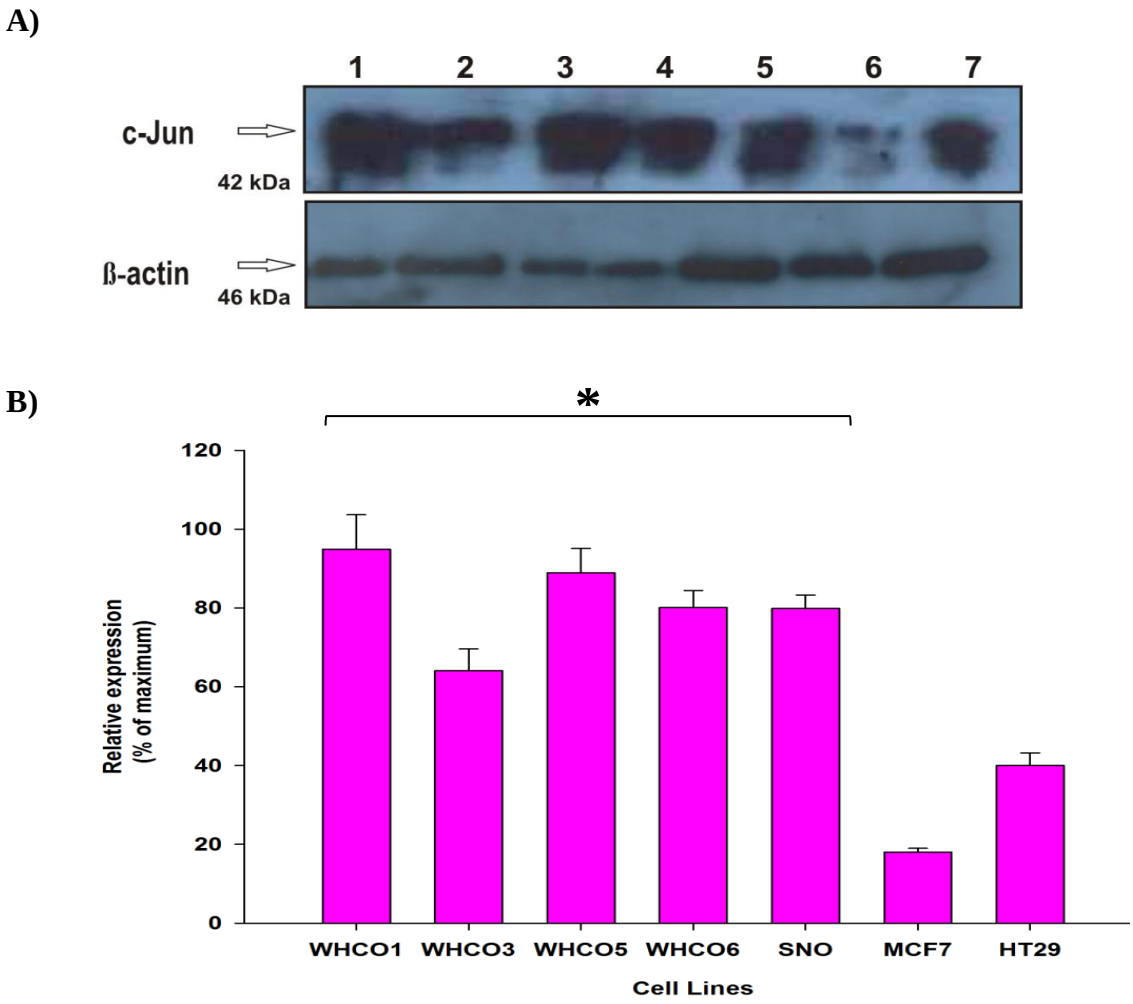


Figure 6. 4: c-Jun is highly expressed in HOSCC cell lines. A) Western blot detection of c-jun at 42 kDa from nuclear-specific extracts from the 5 HOSCC and two control (MCF7 and HT29) cell lines (see Appendix A 1.6.6 and 1.7.5 for representative standard curve and 10% SDS-PAGE). Numbers 1-7 represent the WHCO1, WHCO3, WHCO5, WHCO6, SNO, MCF7 and HT29 cell lines respectively. **B)** Densitometric analysis of the c-Jun western blot detection, revealing significantly stronger c-jun levels in the 5 HOSCC cell lines compared to the MCF7 (low) and HT29 (high) control cell lines. Note: mean ±s.d. of triplicate experiments; * significantly different from the HT29 cell line, P*<0.001. See Appendix E 5.3 for mean optical density values and statistical analysis.

6.3.3 The transcriptionally active β-catenin in relation to its cell adhesive roles in HOSCC cells.

Potentially, the presence of β-catenin in the nucleus is coordinated with a reduction in its cell adhesive associations at the plasma membrane[915]. In contrast, an association between β-catenin and its cell adhesive partners, E-cadherin and α-catenin was established at the plasma membrane of all the HOSCC cell lines (see Fig. 6.5). The WHCO1 cell line showed the weakest association thereof. The specificity of this reaction was verified through the undetectable and detectable E-cadherin/β-catenin/α-catenin associations in the negative (lane 6) and positive (lane 7) controls respectively. The strongest association between β-catenin and E-cadherin was displayed in the WHCO3, WHCO5, and WHCO6 cell lines (see Fig. 6.5). Interestingly, while the WHCO5, WHCO6, and SNO cell lines possessed relatively similar concentrations of β-catenin/α-catenin, this association was particularly strong in the WHCO3 cell line. The SNO HOSCC cell line was the only cell line where PI3K (p85α) was detected in the E-cadherin/β-catenin/α-catenin adhesive complex (Fig. 6.5).

6.3.4 The PI3K/PKB and Wnt signalling pathway in HOSCC cells.

Inhibition of GSK3β is the chief method by which cellular levels of β-catenin are controlled[916]. While the canonical Wnt signalling pathway is the preferential regulator of cellular β-catenin levels through its Ser21 phosphorylation, and inhibition of GSK3β[917, 880], GSK3β can also be inhibited through phosphorylation of its Ser9 residue by the PI3K/PKB pathway[416]. In order to appreciate the part played by the PI3K/PKB pathway on cellular β-catenin levels, it was necessary to first examine the effect that the Wnt signalling pathway has on the PI3K/PKB pathway and the Ser9 phosphorylation state of GSK3β. As seen by the induction of pPKB, activation of Wnt signalling through exposure to LiCl significantly ($P<0.001$) activated PI3K in the WHCO1, WHCO5 and WHCO6 HOSCC cell lines (see Fig. 6.6). This effect was consistent with the increase in pPKB levels shown in the mtAPC (HT29) and wtAPC (MCF7) controls, albeit to unique degrees. Furthermore, evidenced by its up-regulated Ser9 phosphorylation levels, activation of Wnt signalling inhibited GSK3β in all of the HOSCC cell lines ($P<0.001$), with the SNO cell line displaying the least inhibition (Fig. 6.6). In contrast, the pPKB levels were unaffected in the WHCO3 cell line following activation of Wnt signalling (Fig. 6.6A and B), but levels of pGSK3β were significantly augmented (Fig. 6.6A and C).

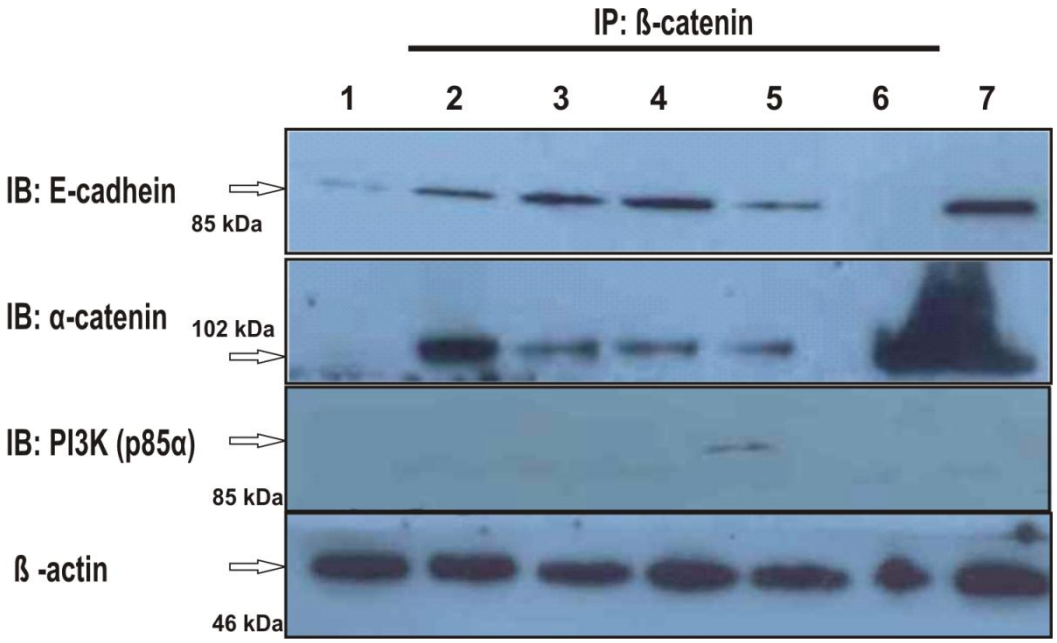


Figure 6. 5: β-catenin interacts with E-cadherin and α-catenin at the plasma membrane in the HOSCC cell lines. β-catenin was detected in complex with its cell adhesive counterparts, E-cadherin and α-catenin through western blotting. PI3K (p85α) was also found in the complex in the SNO cell line. Lanes: 1-WHCO1, 2-WHCO3, 3-WHCO5, 4-WHCO6, 5-SNO, 6-negative control, and 7-positive control. The negative control consists of beads and no antibody, whereas the positive control represents a WHCO6 whole cell lysate. These experiments were executed purely for the detection and not strength of associations between β-catenin/E-cadherin/α-catenin/PI3K (p85α), and therefore no quantifiable data was required. β-actin was used a loading control.

Recent evidence highlights the central role played by PTEN in the levels of β-catenin at the cell-cell adhesion junctions[918]. Next, we analysed cellular PTEN levels following activation of the Wnt signalling pathway. After the Wnt signalling pathway was activated for 24 hrs, significant changes in cellular PTEN levels were observed in the WHCO5 and SNO HOSCC cell lines specifically ($P<0.05$) (Fig. 6.7A and B). The expression of PTEN increased in the WHCO5 cell line, while levels of PTEN dropped substantially in the SNO HOSCC cell line. The decreased concentration of PTEN in the SNO cell line was consistent with the decrease in PTEN observed in the constitutively active Wnt signalling mtAPC HT29 control, albeit at unique time intervals (Fig. 6.7A and B). No significant changes in the PTEN protein levels in response to Wnt signalling were detected in the WHCO1, WHCO3, and WHCO6 HOSCC cell lines, which was consistent with the result portrayed in the wtAPC MCF7 control (Fig. 6.7).

The effect of Wnt signalling on cellular levels of β-catenin was next examined. Activation of Wnt signalling led to an appreciable increase ($P<0.05$) in the expression of β-catenin in the WHCO3 and WHCO6 HOSCC cell lines (see Fig. 6.7). In the WHCO1 and WHCO5 HOSCC cell lines, Wnt signalling induced a reduction in β-catenin levels (Fig. 6.7A and C). Subsequent to activation of Wnt signalling in the WHCO3 and WHCO6 cell lines, the increased levels of pGSK3β (inhibited) (Fig. 6.6B) corresponded to a simultaneous increase in β-catenin expression (Fig. 6.7). This was also the case in the mtAPC HT29 control. No significant changes in the expression of β-catenin were detected in the SNO cell line (Fig. 6.7).

6.3.5 PI3K variously influences the nuclear translocation of β-catenin.

Inhibition of the PI3K pathway caused a significant ($P<0.05$) decline in the nuclear levels of β-catenin in the WHCO1, WHCO6, and the SNO HOSCC cell lines respectively (Fig. 6.8A and C). The diminished concentration of nuclear β-catenin was consistent with the significant ($P<0.05$) drop in the Ser9 phophorylation, and thus activation of GSK3β (Fig. 6.8B). This result was comparable to that observed in the controls (MCF7 and HT29), and supports an involvement of PI3K in the nuclear translocation of β-catenin. A noticeable, yet non-significant drop in the nuclear levels of β-catenin was observed in the WHCO5 HOSCC cell line. No significant changes in the levels of nuclear β-catenin were detected in the WHCO3 cell line, despite the clear decrease shown in the Ser9 phosphorylation of GSK3β (Fig. 6.8C). The total cellular levels of β-catenin, as a result of PI3K inhibition, were included as an additional control for the changes observed in its nuclear localization (Fig. 6.9). Therefore, the influence of PI3K on the nuclear levels of β-catenin (see Fig. 6.8) are dissimilar to the changes detected in its total cellular expression as a result of PI3K inhibition (see Fig. 6.9). The corresponding decrease in the nuclear levels of β-catenin reflected in the total cellular levels exclusively in the WHCO6 cell line (Fig. 6.9).

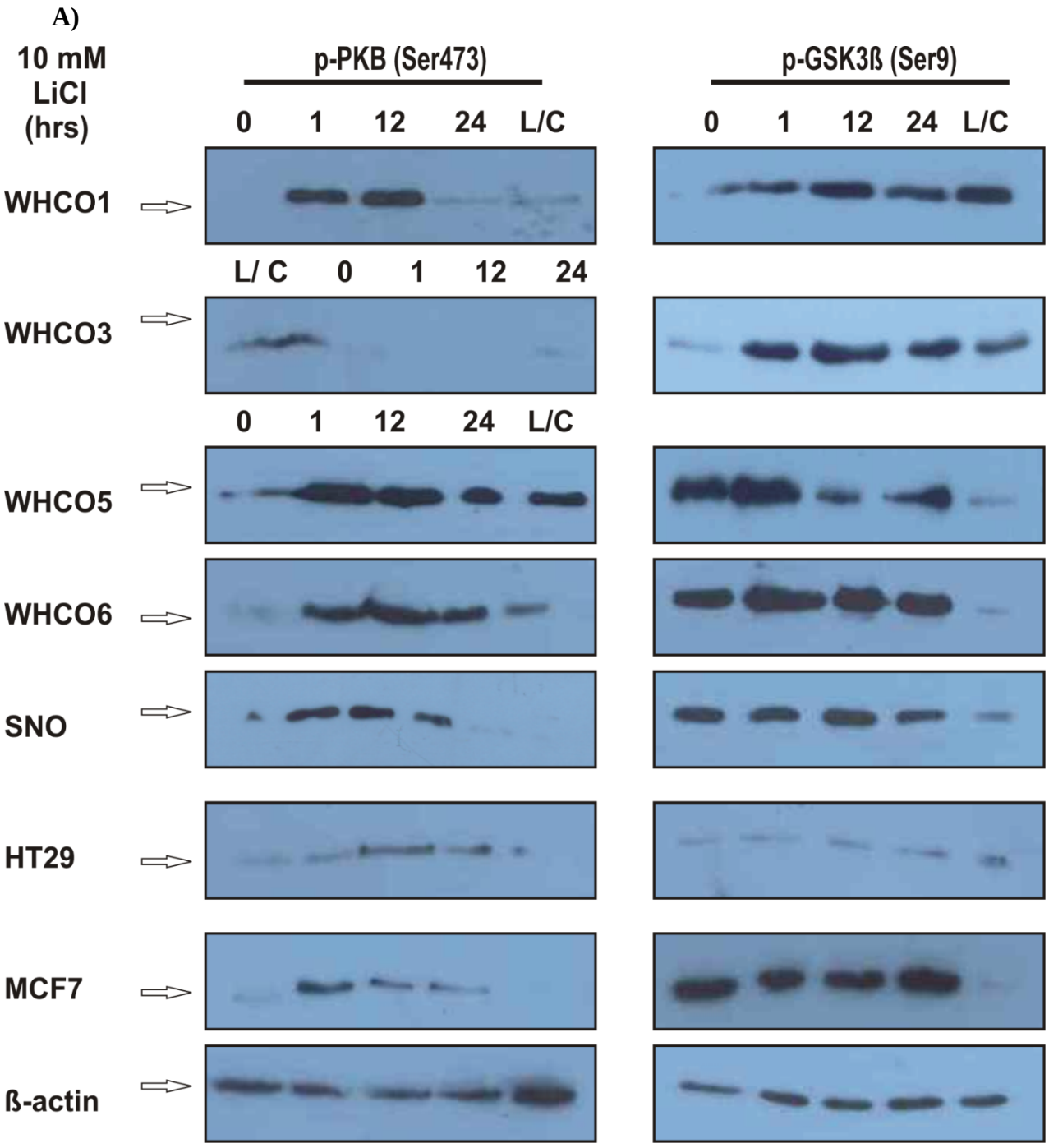
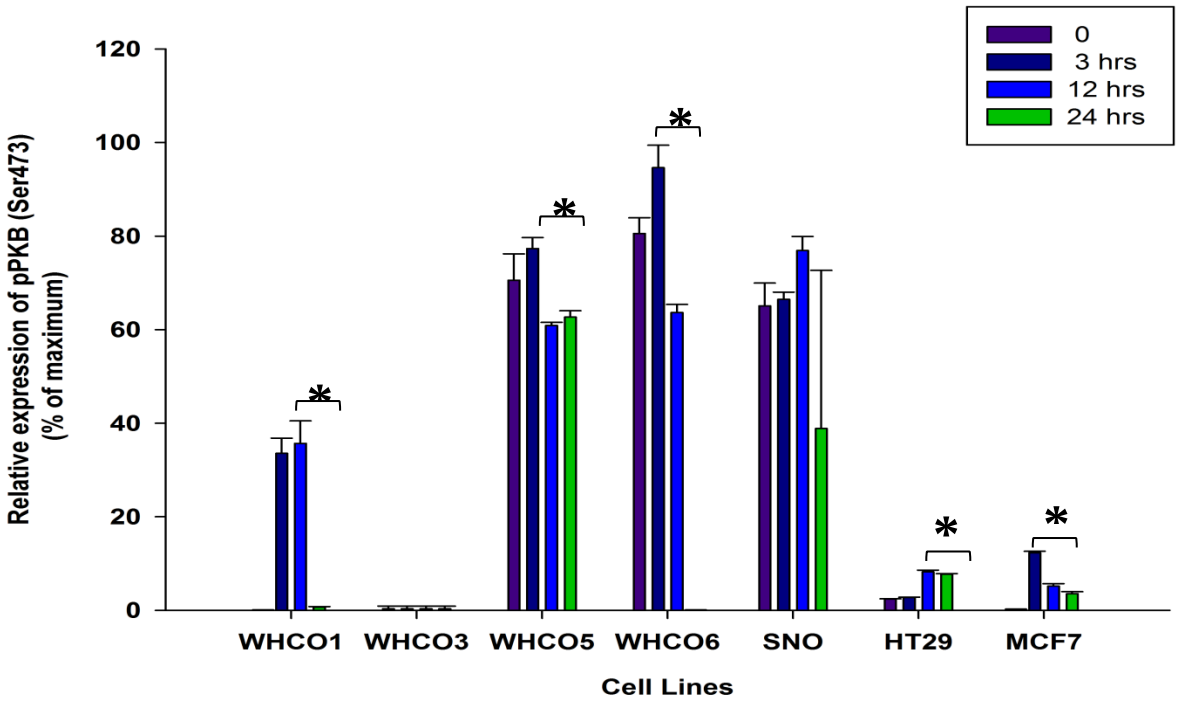


Figure 6. 6A: The Wnt signalling pathway selectively inhibits GSK3β in HOSCC cells. The Wnt signalling pathway was activated in the HOSCC, HT29 and MCF7 cells and immunoblotted for p-PKB (Ser473) and p-GSK3β (Ser9) detection (see Appendix A 1.6.6 and 1.7.5 for representative standard curve and 10% SDS-PAGE). β-actin levels were determined as a loading control, and WHCO6 whole cell lysate served as a loading control (L/C).

B)



C)

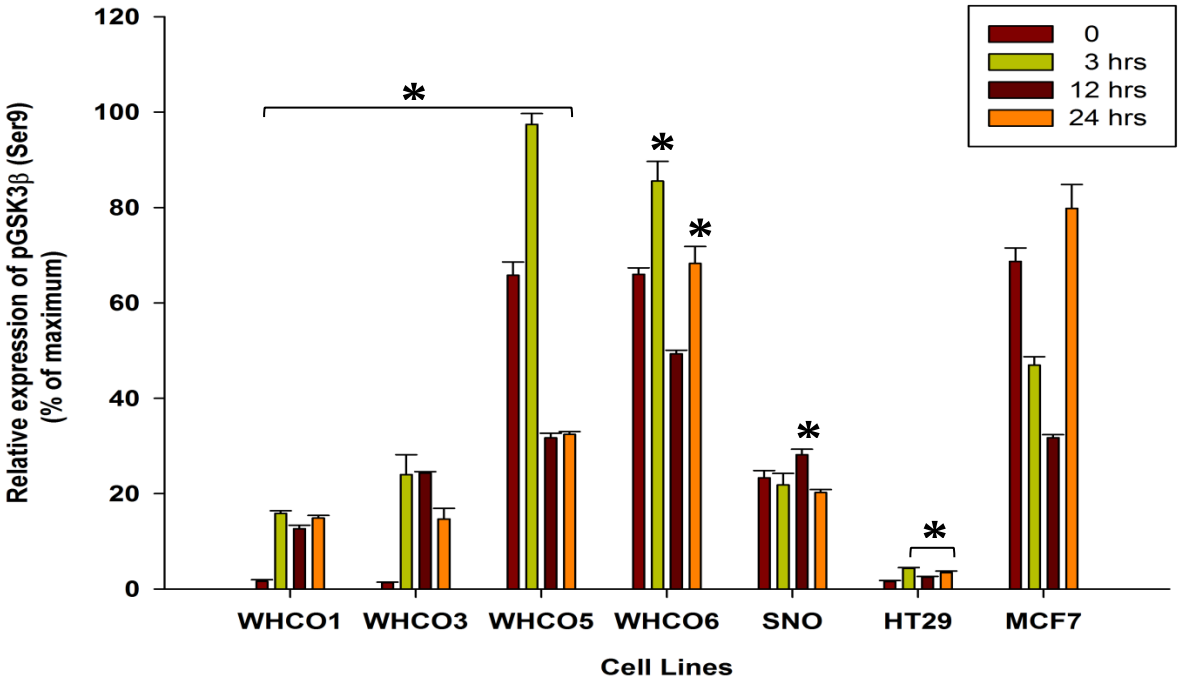


Figure 6.6 B and C: The band representing pPKB **(B)** and pGSK3β **(C)** were quantified through densitometry, showing that Wnt signalling plays a prominent role in the inhibition, and thus Ser9 phosphorylation of GSK3β (p-GSK3β) in four of the HOSCC cell lines, which appears to be independent of their Ser473 phosphorylation status of PKB (p-PKB). Note: these results are mean ±s.d. of triplicate experiments; * significantly different from the control, *P<0.05. See Appendix E, Table E2 for statistical analysis.

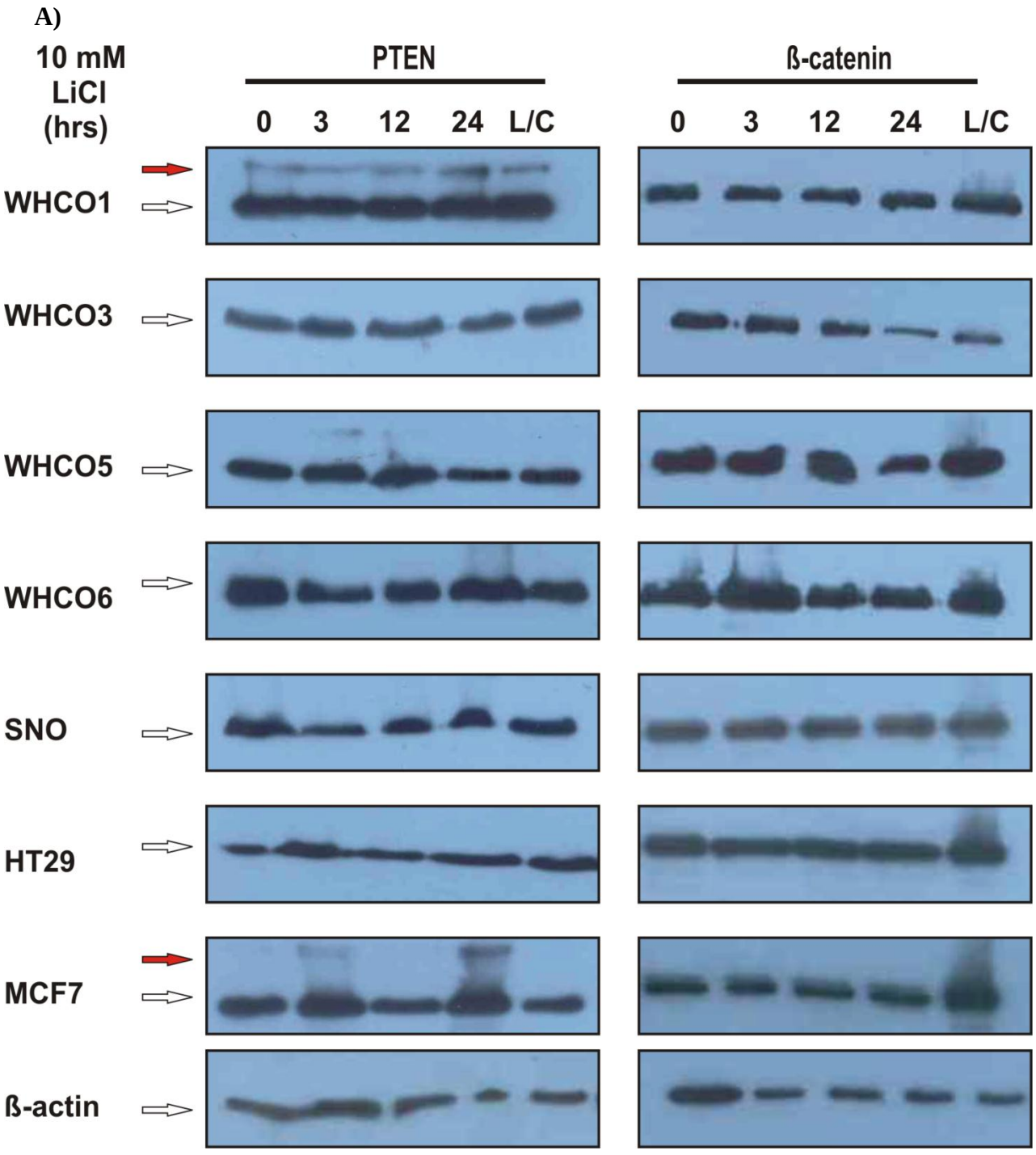
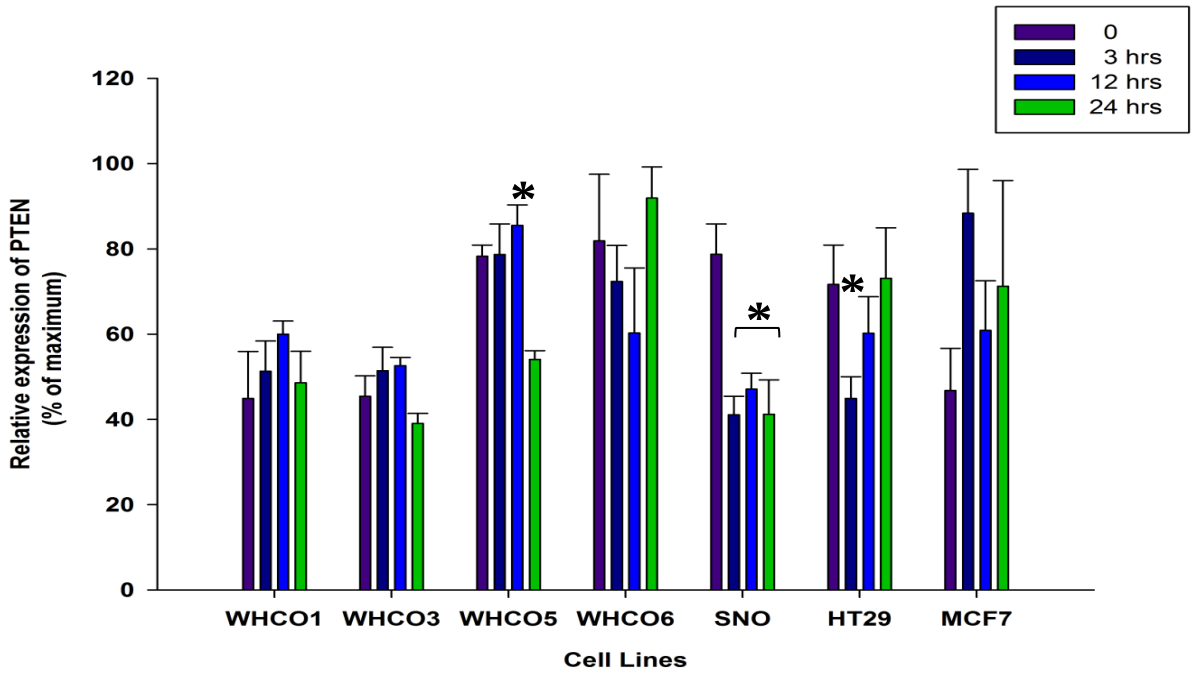


Figure 6. 7A: Activation of the Wnt signalling pathway has a negligible impact on the total cellular levels of PTEN and β-catenin. Wnt signalling was activated in the HOSCC, HT29 and MCF7 cells for periods of 3, 12, and 24 hrs (see Appendix A 1.5.6 and 1.6.5 for representative standard curve and 10% SDS-PAGE). Western blot analysis revealed that Wnt signalling activation did not induce any noticeable changes in the protein levels of PTEN (54 kDa) or β-catenin (89 kDa). Red arrows indicate possible ubiquitinated PTEN^{753}. β-actin levels were determined as a loading control, and the WHCO6 whole cell lysate served as a loading control (L/C).

B)



C)

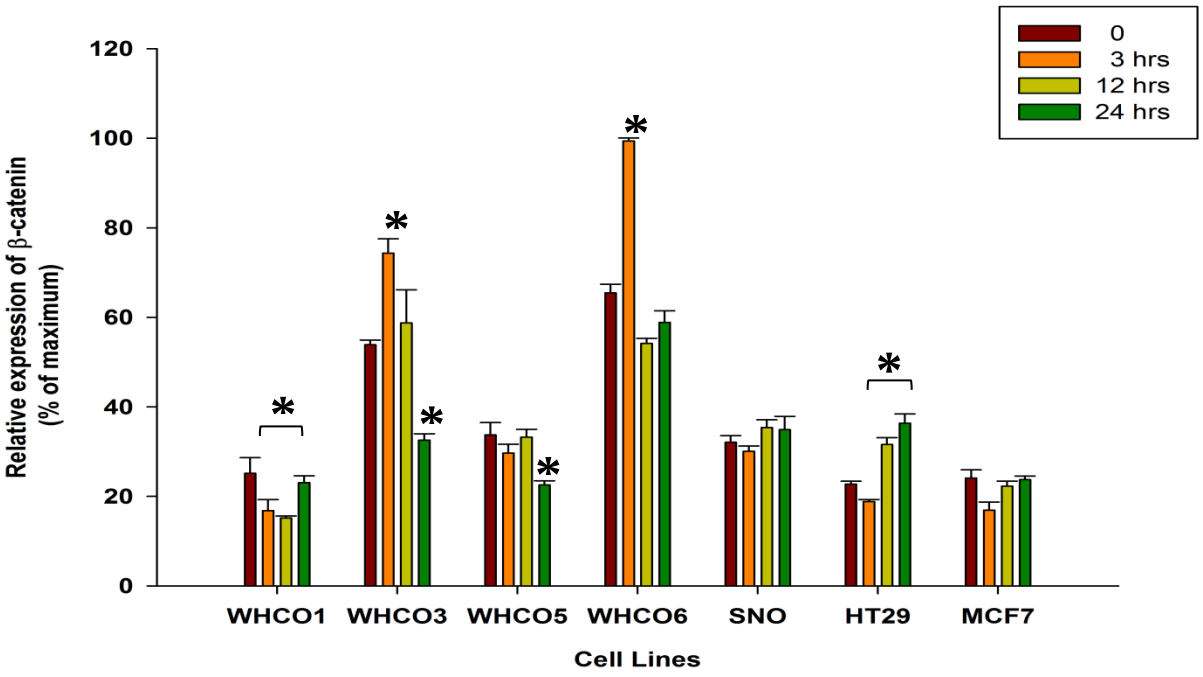


Figure 6.7 B and C: The bands representing PTEN and β-catenin were quantified through densitometry and demonstrated relatively constant PTEN levels **(B)** and significant changes in β-catenin levels in the WHCO1, WHCO3, WHCO5 and WHCO6 HOSCC cell lines **(C)**. Note: these results are mean ±s.d. of triplicate experiments, *significantly different from the control, *P<0.05; see Appendix E, Table E2 for statistical data.

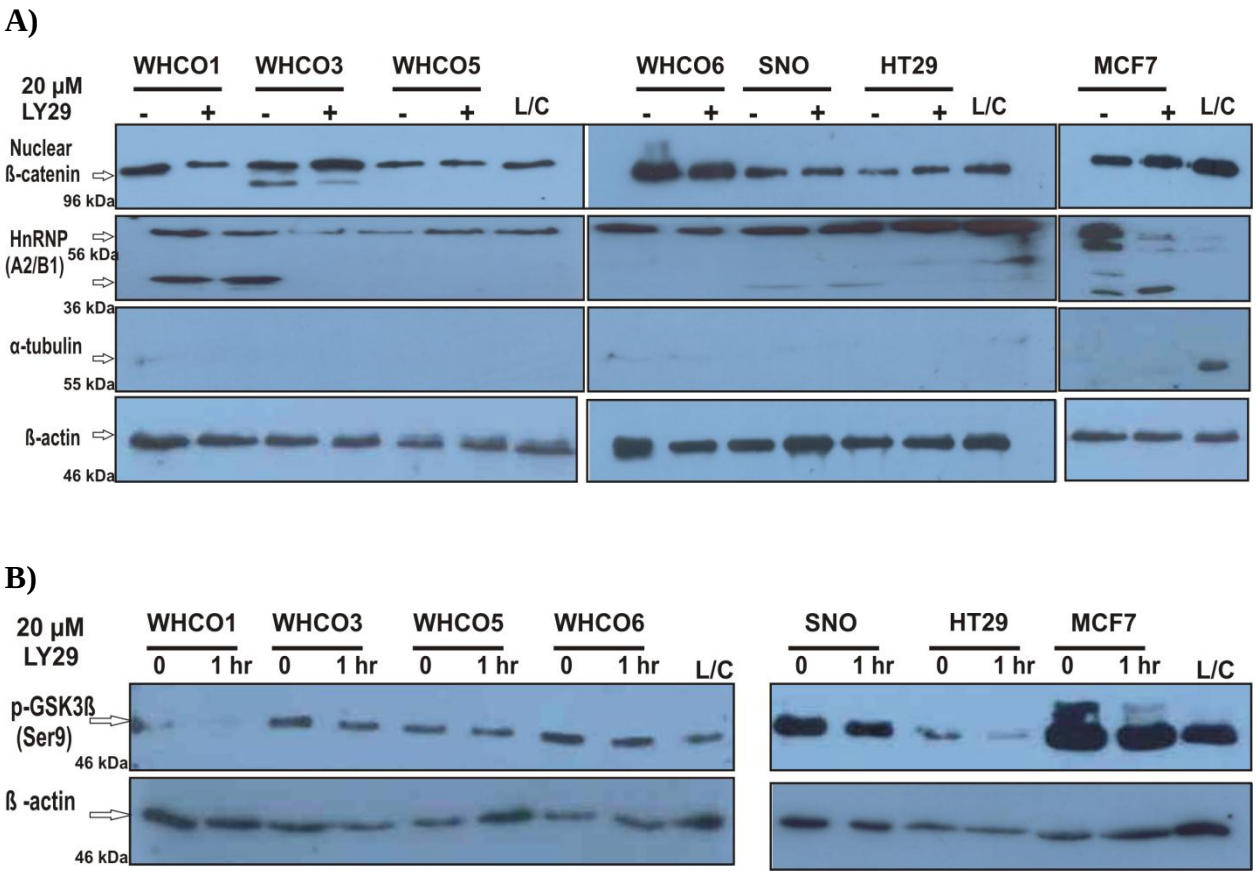


Figure 6. 8 A and B: PI3K modulates the nuclear expression of β-catenin in three HOSCC cell lines. A) PI3K was inhibited in the HOSCC, HT29 and MCF7 cells by exposing them for 1 hour to LY29, and thereafter immunoblotted for β-catenin from nuclear-specific extracts (see Appendix A 1.6.6 and 1.7.5 for representative standard curve and 10% SDS-PAGE). A band at 80 kDa (red arrow) has been presumed to be a partial degradation product[919, 920]. The integrity of the nuclear extract was assessed through the western blot detection of the type A2/B1 hnRNPs, possessing a 56 kDa and 36 kDa polypeptide. The weak or absent western blot detection of the cytoplasmic marker, α-tubulin, further confirmed the integrity of the nuclear extract. C is representative of the WHCO6 whole cell lysate used for comparison between the different blots. **B)** The effect of PI3K inhibition on the Ser9 phosphorylation and thus inhibitory state of GSK3β as per Fig. 2.12 (see Chapter 2, Section 2.3.7). β-actin levels were determined as a loading control.

C)

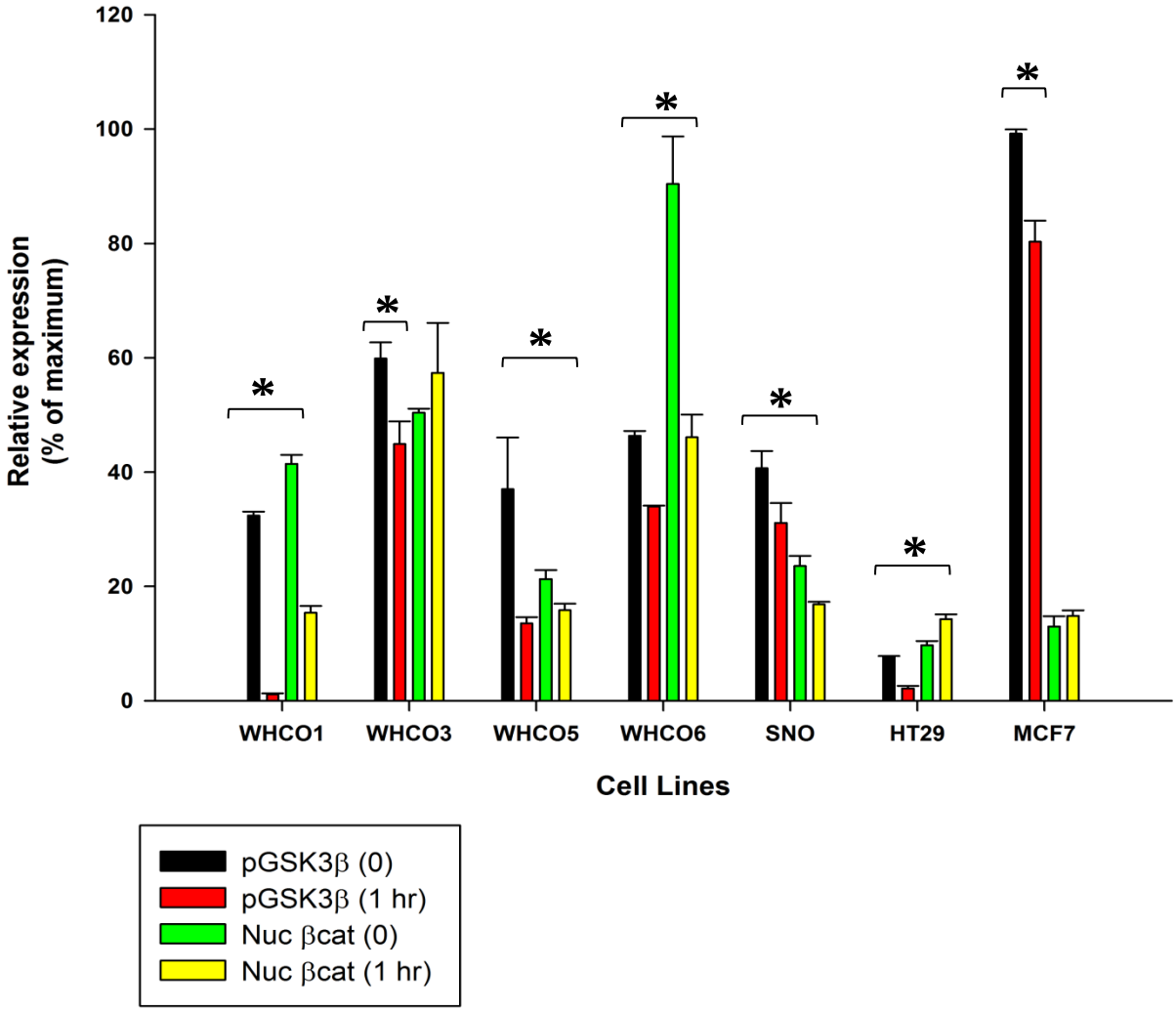


Figure 6.8 C: The densitometric analysis of the nuclear detection of β-catenin in comparison to the Ser9 phosphorylation levels of GSK3β following PI3K inhibition. Based on the significant reduction in β-catenin levels, these results show a positive role played by PI3K in the nuclear accumulation of β-catenin in the WHCO1, WHCO6, and SNO cell line, albeit to a lesser degree in the WHCO5 cell line respectively. No significant role is played by PI3K in the nuclear accumulation of β-catenin in the WHCO3 cell line. Graph also highlights the relationship between pGSK3β and nuclear β-catenin in the WHCO1, WHCO6 and SNO HOSCC cell lines. Note: these results are mean ±s.d. of triplicate experiments, * significantly different from control, *P<0.05; see Appendix E (Table E3) for statistical analysis. Nuc βcat: Nuclear β-catenin.

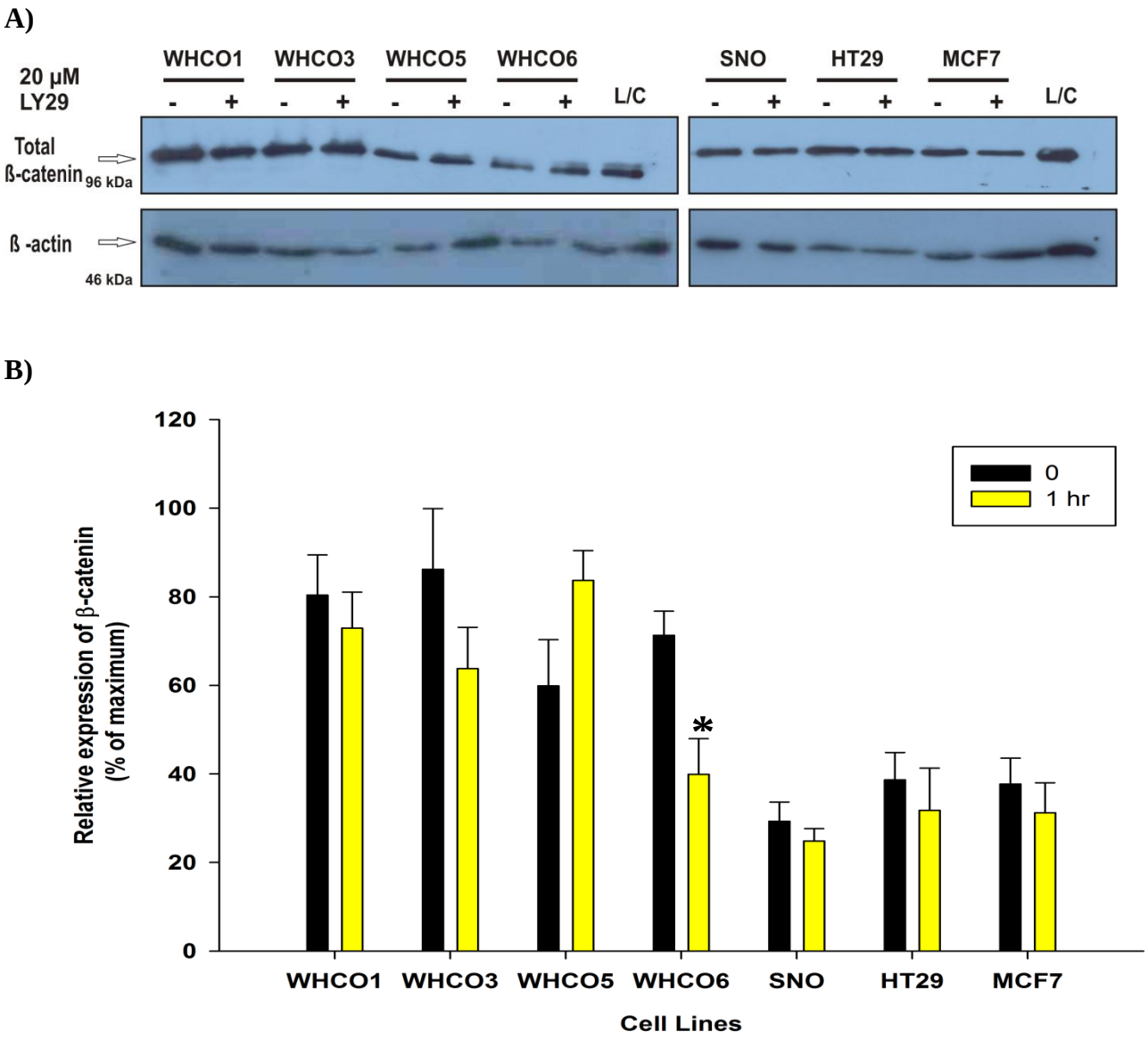


Figure 6. 9: Total cellular levels of β-catenin consequent to to PI3K inhibition. A) HOSCC, HT29 and MCF7 cells were exposed to the PI3K inhibitor and immunoblotted for total cellular levels of β-catenin from whole cell protein extracts (see Appendix A 1.6.6 and 1.7.5 for representative standard curve and 10% SDS-PAGE). C is representative of the WHCO6 whole cell lysate used for comparison between the different blots. Equal loading of treated versus untreated proteins was detected with β-actin. **B)** The densitometric analysis of cellular levels of β-catenin demonstrated a significant change in the total cellular levels of β-catenin in the WHCO6 cell line exclusively. Note: these results are mean ±s.d. of triplicate experiments, * significantly different from control, *P<0.05. See Appendix E, Table E3 for statistical analysis.

6.4 Discussion

Cancer is a dynamic multi-step, multi-mechanism disease that involves complex interactive pathways[921, 922, 923]. Furthermore, it is well-known that these pathways are not propagated in a linear fashion, but instead, comprise of multiple interactive complex networks including both negative and positive inputs from diverse signalling pathways[924, 925, 926, 927, 928], commonly referred to as crosstalk[23]. Inappropriate interaction between intracellular pathways is often found associated with the pathological state of different cancer types by conferring a significant growth and proliferation advantage[929, 930, 931, 932]. In fact, the importance of understanding the critical controlling mechanisms underlying the manipulation of this crosstalk will provide the understanding needed for better therapeutics[22, 933, 934, 935,936, 937]. HOSCC is a highly metastatic disease[492], and in particular the WHCO and SNO series[333]. The molecular characteristics and complexities that govern the maintenance of the transformed state of HOSCC are still a major focus. In this chapter, we provide evidence that interplay between the canonical Wnt and PI3K signalling pathways exist within the 5 HOSCC cell lines.

Over the years, stable nuclear β-catenin levels are repeatedly found in HOSCC and associated with its poor prognosis[294,883, 938, 939]. Lessons learned from various studies in colorectal cancer specifically, has related this trait to the presence of β-catenin and/or APC mutations[363, 826 ,940,941]. Consequentially, little is known regarding the underlying mechanisms for the nuclear sequestration of β-catenin in cancers that have not acquired these mutations. Pertinently, no mutations were found in β-catenin in the WHCO and SNO HOSCC series[942], and accumulative data on these lines have not hinted at the possibility of mutations within APC and Axin[627,943, 944]. The data presented in this chapter provides evidence that nuclear levels of β-catenin are exceptionally high in the 5 HOSCC cell lines. Our data also reveal that these levels were significantly comparable to the overexpressed nuclear β-catenin levels previously established in the mtAPC HT29 colon control cell line[945]. Pertinently, it was shown that the nuclear levels of β-catenin are particularly high in the WHCO3 HOSCC cell line. Similar to what was demonstrated in this chapter, a recent report by Geyer, *et al.*[946] were able to link the elevated nuclear β-catenin levels to the incessant activation of Wnt signalling in a subset of invasive breast cancer cells. Corresponding to the wtβ-catenin status in these HOSCC cell lines, the high nuclear β-catenin levels were not consequent to β-catenin mutations.

Moreover, these high nuclear levels of β-catenin in the 5 HOSCC cell lines were positively coupled to its nuclear gene targeting. This was demonstrated in the protein expression of two of its nuclear target genes; c-Jun and MMP-7. Similar to the conclusion drawn here, the expression of two other transcriptional targets of β-catenin; STAT3 and cyclinD1, were also used to couple the nuclear expression of β-catenin to its nuclear gene activation[947,882]. These data have a number of implications. Firstly, based on the robust nuclear β-catenin levels established, these data inform us that cellular levels of β-catenin are deregulated in the 5 HOSCC cells. Secondly, the protein expression of c-Jun and MMP-7 provide good evidence for an active nuclear β-catenin in the 5 HOSCC cells. Since MMP-7 is known to be expressed during cellular migration and invasion[948], its expression also points to the capability that these HOSCC cells have to degrade components of the ECM. This explanation is supported by evidence demonstrating no immunostaining for MMP-7 in non-cancerous oesophageal mucosa[949]. Strikingly, the expression of c-Jun was stronger in the 5 HOSCC cell lines in comparison to the c-Jun expressed in the constitutively active Wnt signalling mtAPC HT29 control[945]. Hence, this exemplifies that the nuclear β-catenin within these HOSCC cells is significantly linked to its active state.

There is a fine balance that exists between the cell adhesive and nuclear transcriptional activities of β-catenin, such that, a reduction in its cell adhesive function is coupled to its liberated cytoplasmic concentration and subsequent nuclear translocation[783]. In fact, it is this inverse relationship between E-cadherin and β-catenin expression that enable cancer cells to invade and metastasize, a process that is referred to as the epithelial-to-mesenchymal transition (EMT)[88]. Remarkably, despite its obvious nuclear activities, the results shown here reveal that β-catenin is still found complexed with its cell adhesive counterparts; E-cadherin and α-catenin. This result is consistent with the plasma membrane localization of β-catenin demonstrated previously by Jones and Veale[894]. Work performed by McCutcheon[950] demonstrated the strong influence EGFR activation had on the tyrosine phosphorylation of β-catenin in the 5 HOSCC cell lines. A recent study illustrated the adverse effects EGFR activation has on the association between β-catenin and E-cadherin/α-catenin[882]. Thus, what makes this result even more intriguing is that the EGFR overexpression status in these cells is thought to contribute to the attenuated cell adhesive capabilities of β-catenin. One of the mechanisms used by the EGFR to destabilize these interactions is by phosphorylating certain Tyr residues on β-catenin[951, 952, 953]. According to Howard, *et al.*[954], E-cadherin may actually contribute to the nuclear transcriptional activities of β-catenin by an unknown mechanism. This view is supported by E-cadherin knockdown experiments in mice that demonstrated the dependence cellular β-catenin levels had on the presence of E-cadherin[955]. Altogether, our data shows that the nuclear levels of β-catenin are

significantly elevated in the WHCO and SNO series, which are coupled with its cell adhesive and nuclear transcriptional activities.

Through inhibition of PI3K (Chapter 2, Section 2.3.8) we were able to show a marked decrease in the activity of PI3K, evidenced by the detection of the Ser473 phosphorylation of PKB. Moreover, this reduction was particularly symptomatic of an increase in the Ser9 dephosphorylated GSK3β (active form) in all the HOSCC cell lines examined. Since the nuclear translocation of β-catenin is regulated by GSK3β, and the phosphorylation status (activity) of PKB and GSK3β were significantly affected by PI3K inhibition, the downstream effect on the nuclear localization of β-catenin was assessed. Interruption of the PI3K/PKB signalling pathway caused a significant decrease in the nuclear levels of β-catenin in 3 of the HOSCC lines (WHCO1, WHCO6 and SNO). These findings thus identify a positive role played by PI3K, via its downstream effector PKB, in the cellular localization of β-catenin in HOSCC cells. Accordingly, experiments from PI3K knockout mice demonstrated an impaired ability to regulate cellular β-catenin levels through the Wnt signalling pathway[956]. Although interplay has been indicated to occur between the MAPK and PI3K pathways at the levels of Ras and ERK in oesophageal adenocarcinomas[957], this would be the first report to identify the existence of crosstalk between the PI3K and Wnt signalling pathways in HOSCC cells. The importance of crosstalk between signalling pathways is becoming a pertinent aspect of therapeutic research, as many cancers confer drug resistance in the presence of such intracellular crosstalk[481,899,958, 959]. Potentially, this crosstalk indicates that targeting more than one signal transduction pathway may be required for effective therapy in HOSCC.

The non-responsive nuclear β-catenin levels in the WHCO3 and WHCO5 cell line subsequent to PI3K inhibition, indicates that signalling is not confined to the GSK3β pathway. This result was surprising, especially since levels of pGSK3β (inactive) dropped substantially following PI3K inhibition in both of these cell lines. Interestingly, the Wnt and PI3K/PKB regulated pools of GSK-3β are considered to be different, in that, Wnt-regulated GSK-3β is still able to regulate cellular β-catenin levels irrespective of its Ser9 phosphorylation state regulated by PI3K/PKB[960]. We were also able to show the significant contribution made by the Wnt signalling pathway in the Ser9 phosphorylation and thus inhibition of GSK3β. Hence, this may suggest that this influence of the Wnt signalling pathway may be counteracting the effects on GSK3β elicited by PI3K inhibition in this study; further supporting the existence of convergence between the PI3K and Wnt signalling pathways in HOSCC cells. This explanation is highly conceivable especially since it was shown in Chapter 2 (Section 2.3.7) that levels of pPKB were unrelated to levels of

pGSK3β. The data presented for the WHCO3 cell line also suggest that the ability of the PI3K pathway to regulate the nuclear translocation of β-catenin is largely dependent on the presence of pPKB. The involvement of pPKB is substantiated by the fact that no changes in the nuclear levels of β-catenin were evident in the WHCO3 cell line known to possess undetectable pPKB levels, despite the clear influence PI3K inhibition had on pGSK3β (Chapter 2, Section 2.3.7, see Fig. 2.13).

Relatively little is known about the regulation of GSK3β[200, 961]. The general view is that Wnt signalling preferentially targets the Ser21 residue of GSK3β[961], and thus the ability of the Wnt signalling pathway to regulate the Ser9 phosphorylation of GSK3β is a contentious issue. In addition to PKB, regulation of the Ser9 phosphorylation of GSK3β has been ascribed to many other kinases such as ILK, protein kinase A (PKA), S6K, and PP2A, and the specificity of which, has been attributed to the cell type[519,962, 963]. Here, it is clear that in the WHCO and SNO series, the Ser9 phosphorylation of GSK3β is under the regulation of the Wnt signalling pathway.

Uniquely, the data presented here point to Wnt-dependent mechanisms in the regulation of the Ser9 phosphorylation of GSK3β in HOSCC cells. The profound involvement of the Wnt signalling pathway in this regulation is highlighted in the WHCO3 cell line, where levels of pGSK3β significantly increased following activation of Wnt signalling, despite the presence of undetectable pPKB levels. It is quite clear from this chapter that pGSK3β forms a crucial point of convergence for the Wnt and PI3K signalling pathway in HOSCC. However, based on the highly confusing role that each pathway plays in the regulation of GSK3β (see above), there is a definite need for a better understanding of the unique role played by these complex pathways in the nuclear accumulation of β-catenin. This places HOSCC as a prime model for studying the underlining Wnt-independent routes taken for the nuclear translocation of β-catenin. Moreover, our data has unveiled bi-directional interplay between two highly oncogenic signalling pathways, the Wnt and PI3K signalling pathway within the WHCO and SNO HOSCC series.

Chapter 7
General Discussion and Conclusion

The induction and survival of cancer cells are highly dependent on specific aberrations in particular genes and/or proteins, which ultimately appropriate various signalling pathways, that provide the environment needed to maintain the diseased state[26, 964, 965,966, 967, 968]. As a result, most cancer cells develop a dependency on these particular abnormalities for their survival, a phenomenon described as "oncogene addiction"[30]. The PI3K/PKB/PTEN signalling pathway reportedly contributes to the progression of a variety of cancers[36,225, 969]. HOSCC is an obvious omission from this spectrum. Specific characterization of abnormalities in cancer cells provides better insight into their tumorigenic state, and reveals more appropriate candidates for therapeutic targets. This study has focused on understanding the role of the PI3K/PKB signalling network in both HOSCC and as it applies to cancer in general and unveils novel mechanisms in its regulation. Therefore, this thesis forms part of an on-going and current effort in research to characterize the specific role played by this pathway in cancer transformation.

7.1 The significance of p85α expression in HOSCC.

One of the most critical regulatory mechanisms of the PI3K/PKB signalling pathway is elicited through the ClassI_A p85α regulatory subunit[970]. Recently it was shown that mice lacking the gene transcribing this subunit (PIK3R1) display potentiated cell proliferation through increased PKB Ser473 phosphorylation[323]. Furthermore, the important role of p85α as a tumour suppressor has become apparent, yet the mechanisms used to regulate the activation of PI3K by p85α are complex. For this reason, the protein levels of p85α are found reduced in a number of tumour lineages, such as colon, ovarian and endometrial cancers[318, 331, 971,972]. Counter to these epithelial cancers, was the finding that the protein concentration of p85α was significantly high in HOSCC (Chapter 2, Section 2.3.2, and Chapter 5, Section 5.3.1). Fascinatingly, even though p85α was shown localized to the membrane in the absence of exogenous stimulation, which is indicative of its constitutive activation[246], no activating mutations within the iSH2 domain of p85α (PIK3R1) were found in the 5 HOSCC cell lines (Chapter 2, Section 2.3.1). The salient feature of these data, is that unlike other stratified epithelial cancers (see above); this would be the first report to show a membrane localization of p85α that is not accompanied by mutations in the main functional domains in HOSCC.

Independent of its regulation of the p110α catalytic subunit, it has recently been discovered that the p85α regulatory subunit can further antagonize the activation of PI3K by at least two additional mechanisms. One such mechanism is through free or unbound p85α that competes with p110α for binding to the EGFR, reducing the activation of PI3K[973]. A second mechanism is through the novel mutually exclusive interaction between p85α and PTEN, which was shown to stabilize PTEN by preventing its ubiquitination, thus leading to diminished activation of the PI3K/PKB pathway[974, 975, 976]. Therefore, p85α knockdown experiments in mice also illustrate lower and unstable PTEN that potentiates activation of the PI3K/PKB pathway[973]. In the 5 HOSCC lines, high expression of p85α was associated with low and stable PTEN protein levels (Chapter 4, Section 4.3.2, and Chapter 5, Section 5.3.2). Furthermore, p85α was found weakly associated to the EGFR, even under conditions of exogenous stimulation (Chapter 3, Section 3.3.4). Moreover, the concentration of PTEN was shown to be significantly less susceptible to degradation by the 26S proteasome (Chapter 5, Section 5.3.3c). Taken together, these data suggest that the level of free p85α may be high in HOSCC cells and linked to the reduced association observed between p85α and the EGFR, as well as the stable PTEN expression. It may be interesting in the future to evaluate the impact that loss of the PIK3R1 allele may have on the levels of PTEN in the WHCO and SNO series.

According to the literature, poorly differentiated tumours have a higher proliferation rate and tumorigenic potential[977, 978, 979]. The role of PI3K in tumour differentiation is rather contentious, in that both previous and current research shows the positive contribution made by PI3K in the differentiation state of gastric cancer[328], whereas others have established the negative involvement in colon cancer[980]. With respect to the 5 metastatic HOSCC cell lines, they have been classified as both borderline poorly- and well-differentiated tumours, evidenced by their histopathological reports[333] and poor keratinizing capabilities[329]. Therefore, the 5 HOSCC cell lines are considered as “moderately differentiated”. In view of their moderately differentiated state, no distinct relationship between the level of p85α protein expression and their differentiated state was evident. This is substantiated by the low p85α protein levels detected in the WHCO1 and WHCO3 cell lines, and the higher levels present within the WHCO5, WHCO6, and SNO cell lines (see Chapter 2, Section 2.3.2). Hence, a valuable addition to the results presented here, is that unlike the positive link between the up-regulated expression of p85α in the glandular elements of colorectal cancers at all stages[378], levels of p85α in HOSCC cells are not directly associated with their moderately differentiated state.

Fundamentally, the protein expression of p85α in the 5 HOSCC cell lines proved to be extremely stable, despite modifying inputs from EGFR activation (Chapter 3, Section 3.3.1), PP2A inhibition (Chapter 4, Section 4.3.1), or oxidative stress/PTEN inhibition (Chapter 4, Section 4.3.5). Notwithstanding the down-regulation in the protein levels of p85α at higher concentrations of Bzb observed in Chapter 5 (Section 5.5.3c), these data still strongly suggest that unlike the colon cancer cells described above, HOSCC is most compatible with the model wherein levels of p85α may be required for the maintenance of their transformed state. This forms a firm basis to our understanding of the impact of p85α protein expression in HOSCC.

7.2 Activation of PI3K in the WHCO and SNO HOSCC series.

The PI3K/PKB signalling pathway is distinguished for its proficiency in initiating and maintaining cancer cell proliferation, migration and invasion[981, 982, 983]. However, despite the fact that activation of the PI3K/PKB pathway was shown to adversely affect the clinical outcomes of oesophageal cancer patients, its contribution to the transformed state in HOSCC remains poorly defined[295]. Even though it is clear from the literature that the primary effects used by EGFR overexpression to induce transformation are poorly understood, and largely cell-type specific[234, 984, 985, 986], EGFR overexpression or amplification is often endorsed by high pPKB levels[140, 987]. Despite the overexpressed state of EGFR in the 5 HOSCC cell lines, the data presented here shows that levels of active PI3K (pPKB) are low in three of the HOSCC cell lines (WHCO1, WHCO5, and SNO), high in the WHCO6 cell line and below levels of detection in the WHCO3 cell line (see Chapter 2, Section 2.3.5). By utilizing the physiological PI3K inhibitor, LY29 (Chapter 2, Section 2.3.8), and through EGFR activation (Chapter 3, Section 3.3.5), it was demonstrated that while PKB Ser473 phosphorylation is indeed reliant upon PI3K activity in the HOSCC cell lines, the EGFR overexpression status does not have a significant impact on this activity. Specifically, the WHCO3 cell line was shown to possess the highest level of EGF receptors[329], yet this study showed no corresponding pPKB response to EGFR activation.

Somatic mutations within the gene transcribing the catalytic subunit of PI3K (PIK3CA) predominantly induce hyperactivation of the PI3K/PKB pathway, evidenced by augmented pPKB levels[140, 248,988]. However, it is now evident that the presence of PIK3CA mutations in cancer cells may instead, cause a reduced dependency on PKB for their survival, and thus exhibit minimal Ser473 phosphorylation levels[542,543]. This was specifically demonstrated in certain of the mtPIK3CA controls used in this study; MCF7, DLD-1 and HT29 cell lines[330]. Uniquely, the

data presented in this study (see Chapter 2, Section 2.3.4), indicates that, similar to these mtPIK3CA controls, the low and absent pPKB in four of the HOSCC cell lines (WHCO1, WHCO3, WHCO5, and SNO) is symptomatic of a reduced dependency on PKB for their survival and maintenance of the transformed state. Distinctively, these low concentrations of pPKB in the WHCO and SNO HOSCC series were not associated to mtPIK3CA (see Chapter 3, Section 3.3.6).

The importance of mutations within PKB in the induction and maintenance of cancer transformation has become apparent[989]. Although much remains to be determined regarding the specific and relevant perturbations within PKB, many studies in epithelial-derived cancers, have likened its oncogenicity to an activating E17K mutation present within its PH domain, that gives rise to its constitutive membrane translocation[250,254,990]. Recently, it was demonstrated that by inducing activating mutations within the Thr308 and Ser473 residues of PKB, transformation was potentiated through its enhanced membrane binding. Relevantly, given the strong membrane pPKB localization established in the WHCO1, WHCO5 and WHCO6 cell lines (see Chapter 2, Section 2.3.5), combined with a non-mutated PIK3CA within the 5 HOSCC cell lines, the likelihood that PKB mutations within HOSCC may exist was considered. Sequence analysis of the activation-associated PH, linker, catalytic and regulatory domains of PKB[991], showed that the 5 HOSCC cell lines do not possess activating mutations in any of these PKB domains (see Chapter 3, Section 3.3.7). Therefore, mutations within PKB do not account for the low and undetectable pPKB within the WHCO1, WHCO3, WHCO5, and SNO cell lines, or the high pPKB levels in the WHCO6 HOSCC cell line. Consistent with these findings, mutations within PKB were also reported absent in other epithelial based cancers such as epidermal skin cancer[531], breast[533], and non-small lung cancer[32], even though the activating E17K mutation was only explored. In order to further understand the effects of the various intermediates of the PI3K/PKB pro-survival signalling pathway in HOSCC, reassurance of the mutational influences within PIK3CA and PKB was important to exclude.

It has been demonstrated previously, that high activation levels of PI3K (pPKB) can become chronic to tumour cell survival[657]. Hence, these low pPKB levels are suggested to serve as a form of protection from the PKB-mediated attenuation of invasion and metastasis[543]. Evidence emanating from various laboratories has shown that one such mechanism is through its ability to activate the E3 ubiquitin ligase, HDM2/MDM2, which in addition to p53[992], ubiquitinates an invasion-promoting factor, the NFAT (nuclear factor of activated cells)[993, 994, 995]. NFAT contributes to the invasive capabilities of the epithelial breast and colon cancer cells through the

up-regulation of the cyclooxygenase-2 (COX-2) genes responsible for the inflammatory response[996, 997]. Furthermore, the NFAT is known to be activated specifically during α6β4 integrin-induced carcinoma invasion[998]. Even though it is the αv integrin that showed *de novo* overexpression in HOSCC[611], it is well established that the αv integrin potentiates a large repertoire of integrin heterodimer formation during invasion, including the α6β4 integrin[999, 1000]. Furthermore, the role for COX-2 in the invasive and metastatic potential of numerous epithelial cancers, especially oesophageal cancer, is also well recognized[1001, 1002, 1003, 1004, 1005]. Thus, it is conceivable that the low levels of pPKB in the WHCO and SNO series are somewhat deliberate in order to circumvent the PKB-mediated attenuation in invasion and metastasis.

Almost all cancer cells reported to possess activated PI3K and PKB, have accelerated proliferation that gives rise to transformation[1006, 1007, 1008]. Thus, PKB-mediated inhibition of invasion and metastasis is greatly cell-type specific. This cellular specificity is substantiated by Liu *et al.*[1009], who demonstrated that while PKB activation induced proliferation, it simultaneously and adversely affected the motility and invasive potential of breast cancer cells. As Blagosklonny suggested[1010], this paradoxical role of PKB in cellular signalling strongly implies that this pathway primarily operates in a three-dimensional manner and the activation or inhibition of cellular survival is largely dependent upon the cellular context.

Of relevance, Hutchinson, *et al.*[1006] indicated that cancer cells co-expressing activated PKB and ErbB2 possess a lower invasive capability than those expressing activated ErbB2 alone. Therefore, a plausible explanation for the existence of low pPKB in HOSCC, despite their EGFR overexpression status, could be highly suggestive of a mechanism used to counteract the anti-invasive properties of PKB outlined above. Since the activation of PI3K is augmented by the αvβ1 integrin mediated GF-independent activation of EGFR[1011], it was surprising to observe such low pPKB levels. Hence, it can be assumed that the overexpressed state of EGFR and αvβ1 integrins in HOSCC is insufficient to infer constitutive activation of PI3K. This view is verified by the results obtained in the WHCO3 cell line throughout this study. The WHCO3 cell line has the strongest EGFR and β1 integrin overexpression status[332,611], yet levels of pPKB were consistently undetectable and only induced in response to H_2O_2 (see Chapter 4, Section 4.3.4).

Contrary to the general understanding, a recent study demonstrated that as a cancer cell loses its epithelial characteristics by becoming more mesenchymal-like (EMT), under conditions such as tumour cell chemotaxis, it loses its dependence on the EGFR signalling pathway[1012]. The authors also highlighted the significant association between elevated ROS levels, the mesenchymal

phenotype and resistance to chemotherapy. Furthermore, Bar *et al.*[1013] also confirmed that upon transition to the mesenchymal phenotype, cancer cells lose their dependency on the EGFR signal for their continual survival, and instead, become reliant upon alternative pathways, like those triggered by the PDGFR. This may explain why a strong association between the EGFR and PI3K was not found in the 5 HOSCC cell lines (see Chapter 3, Section 3.3.4). One of the methods in which EGFR induces cellular proliferation is through the activation of the ERK (extracellular-signal-regulated kinase) signal transduction pathway[1014]. Moreover, this pathway also regulates the transcription of the EGFR through the early growth response-1 (EGR-1) transcription factor[1015]. Notably, this EGFR-ERK-EGR-1 signalling loop was shown to attenuate the activation of the PI3K/PKB signalling pathway through Gab1[1016]. Pertinently, the indispensability of the EGFR-ERK-EGR-1 pathway in the pathogenesis of the WHCO1, WHCO5, and WHCO6 cell lines was previously shown[1017]. Thus, a plausible explanation for the low activation status of the PI3K/PKB pathway in HOSCC could be attributable to the activation of this EGFR-ERK-EGR-1 signalling pathway loop. It would appear that the PI3K/PKB pathway in the 5 wtPIK3CA HOSCC cell lines, dissimilar to most cancer cell lines[524,1018, 1019, 1020, 1021], is dispensable for the maintenance of their transformed state. Consequently, it seems clear that alternative mechanisms in the regulation of the PI3K/PKB pathway in HOSCC must be sought.

The production of H_2O_2 is imperative for effective signal propagation in response to EGFR activation, and equally essential for the specific activation of the PI3K/PKB signalling pathway[1022, 1023]. Consistently, studies have indicated that specific inhibition of this orchestrated H_2O_2 generation through EGFR and PI3K impedes PDGF- and EGF-mediated signalling[1024, 1025, 1026]. Here, stimulation of EGFR did not provoke activation of the PI3K/PKB pathway, specifically in the WHCO3 cell line, to the same extent as that observed following PTEN oxidation (inhibition) through exposure to H_2O_2 (see Fig. 3.8 and Fig. 4.10B). Given that the membrane localization of PI3K is deemed sufficient to induce the production of H_2O_2 required for PTEN oxidation (inhibition), it was surprising to notice the inconsistency between EGFR activation and pPKB levels occurred despite the obvious increase in the PI3K membrane localization (see Fig. 3.2 and Fig. 3.5). Henceforth, our data indicate that H_2O_2 plays an essential role in the activation of the PI3K/PKB pathway in the WHCO and SNO HOSCC series, but the communication between EGFR activation and H_2O_2 production is somewhat diminished. Indeed, the manner in which exogenous H_2O_2 transmits signals from the EGFR and the strength thereof is highly controversial[1027, 1028, 1029]. Various studies have shown that in addition to permeating and regulating the PI3K/PKB pathway through PTEN, H_2O_2 aids in maintaining the EGFR in an active state by preventing its internalization and degradation[650, 1030, 1031]. Tyrosine

phosphorylation of EGFR is one of the mechanisms that confirm its activational state[985]. Of relevance, it was recently demonstrated that activation of the EGFR substantially resulted in the overall increase of its tyrosine phosphorylation in HOSCC (unpublished data). Therefore, the clear loss of communication between EGFR-mediated PI3K activation and H_2O_2 production in HOSCC cells is not due to the deregulated activation of EGFR.

As noted above, PKB plays an integral role in the regulation of anti-survival. One such mechanism is by regulating intracellular H_2O_2 levels via the forkhead box O (Foxo) transcription factors[660, 1032]. Under conditions where PKB is highly active (pPKB), the production of anti-oxidants through the Foxo transcription factors is constitutively prohibited through PKB, making these cells extremely sensitive to increases in the levels of H_2O_2; and thus suggested to be insufficient to maintain the pro-survival state[660,657, 1033]. The literature indicates that in order for cancer cells to invade and metastasize, they need to overcome these antagonistic properties of PKB through H_2O_2, by maintaining a low concentration of pPKB[657,658,659]. Relevantly, prolonged exposure of the epithelial lining of the oesophagus to either one of its etiological factors such as bile acid, mycotoxins, nicotine, or alcohol, was shown to result in chronic inflammation and H_2O_2 generation[1034, 1035, 1036, 1037]. Moreover, recent evidence has revealed the critical role played by the altered production and clearance of H_2O_2 in the metastatic potential of bladder[1038], breast[1039] and colon cancers[1040]. Ultimately, it would appear that HOSCC cells may have circumvented the adverse effects of H_2O_2 by maintaining a low PKB activation status that aids in the up-regulation of anti-oxidants; that would otherwise be attenuated by PKB. This understanding is consistent with Vaezi *et al.* [280]and Tan *et al.* [1041], who showed the importance of H_2O_2 in the development of oesophageal cancer.

It seems logical to question how the WHCO and SNO HOSCC series may use H_2O_2 for their advantage ascribed, and manage to escape its adverse effects. Research has linked this escape mechanism to the presence of the cell surface mucin, MUC1, which is able to suppress the apoptotic effects induced by intracellular H_2O_2 levels[1042]. This was confirmed by two independent studies demonstrating MUC1 is an oncogene that blocked oxidative stress-induced apoptosis[1043, 1044]. These authors were able to link this activity to the MUC1-dependent up-regulation of catalase, suggested to occur through its association with β-catenin in the nucleus. Catalase is one of the major H_2O_2-eliminating enzymes within a cell. Appropriately, prior research on the 5 HOSCC cells revealed that MUC1 is indeed expressed and associates with β-catenin which was suggested to play a major role in the attenuation of H_2O_2-induced apoptosis[1045]. Furthermore, we were able to demonstrate the elevated nuclear expression of β-

catenin the 5 HOSCC cell lines (see Fig. 6.3). Therefore, it can be assumed that the clear impact H_2O_2 has on the activation of the PI3K/PKB pathway may have been obtained from the initiation of the transformation of the WHCO and SNO HOSCC series, and as such, is a key mechanism that enables these cells to maintain a low PI3K/PKB activation status.

7.3 PTEN - a significant player in PI3K/PKB signalling in HOSCC.

A notable feature of PTEN influence in cells is its antagonism on the PI3K/PKB pathway[537,1046]. Therefore it is not surprising that complete loss of PTEN protein is frequently reported in cancer, and strongly linked to transformation through high pPKB levels[632, 1047,1048, 1049, 1050, 1051, 1052]. As a result, emphasis is placed on the inversely correlated expression of PTEN and pPKB in a number of cancer cells, such that high concentrations of PTEN correspond to low pPKB levels and vice versa[538,1053]. In the WHCO and SNO HOSCC series, for the first time, we show that low levels of PTEN are associated with low concentrations of pPKB (see Fig. 4.6 and Fig. 5.3). Consistent with these attenuated PTEN levels shown here, diminished expression of PTEN was positively linked to the differentiated state of Chinese oesophageal cell lines[457], and thus suggested to serve as a prognostic marker. Pertinently, recent evidence has underpinned the decreased expression of PTEN protein to the inefficacy of cancer prevention and therapy[596, 1054, 1055]. Based on the quasi-sufficient nature of PTEN[565, 681], it is an on-going challenge to understand how certain cancers are able to successfully transform in the presence of PTEN[566, 1056]. Thus, characterising the role of PTEN in the WHCO and SNO HOSCC series is imperative, as it reveals the mechanisms used in these cells to maintain low pPKB. The function and expression of PTEN, on the other hand, is extensively regulated by several genetic, epigenetic, transcriptional and post-translational mechanisms which emphasize its importance as a tumour suppressor[1057]. As a result, multiple mechanisms are likely to converge on the regulation of the expression and function of PTEN in HOSCC.

The tumour suppressive function of PTEN is largely dependent on its cellular localization[1058]. Although it is the cytoplasmic PTEN that inhibits the PI3K/PKB pathway, it has become accepted that PTEN can directly influence the stability, cell-cycle arrest and apoptotic events of a cell through its nuclear translocation[577, 1059]. Thus, it is the balance between these cytoplasmic and nuclear roles of PTEN that ultimately determines the neoplastic state of a cell[635,677,1060]. In this study, we provide evidence that although present within the nucleus of the WHCO1, WHCO3, WHCO5, and SNO cell lines; the cellular localization of PTEN is predominantly expressed within the cytoplasm of HOSCC (see Fig. 4.7 and Fig. 4.8). This was exemplified by

the fact that, the concentration of PTEN in HOSCC was largely excluded from the nucleus, demonstrated through immunoflourescent staining (see Fig. 4.7), and confirmed by the high nuclear PTEN within the colon HT29 control[578]. Recent evidence has revealed that, although the nuclear PTEN levels are high in colorectal cancers, they gradually decrease after malignant transformation[597]. As these HOSCC cells are metastatic, suggests that the loss of nuclear PTEN, similar to colon cancers, may be associated to the maintenance of their transformed state. Evidence to the contrary, performed on the KYSE series of oesophageal cancer[1061], showed that, similar to normal oesophageal epithelium, the expression of PTEN was high in the cytoplasm of 42 surgically resected oesophageal tumours[1062]. Subsequently however, one of the authors reported that results obtained from the KYSE series oesophageal cancer lines should be interpreted with great caution, due to the high level of cross-contamination within these cell lines[1063]. Conversely, research has previously linked the cytoplasmic PTEN to its instability and enhanced activity[398]. Substantially, the cytoplasmic PTEN in the WHCO and SNO HOSCC series was shown, throughout this study, to be relatively stable in spite of its cellular localization.

EGFR-mediated activation of the PI3K/PKB pathway simultaneously leads to the membrane translocation of PTEN, which results in its dephosphorylation by an unknown mechanism[1064]. Dephosphorylation of PTEN diminishes its stability and subsequently aids in its degradation by the 26S proteasome[1065]. As a result, an increase in PTEN activity is strongly associated to its degradation, such that, rapid degradation of PTEN is induced upon its dephosphorylation following PI3K/PKB activation[1066, 1067]. Keeping this in mind, the frequency of PTEN expression was not significantly affected in response to PI3K inhibition (see Fig. 2.13C) or exposure to H_2O_2 (Chapter 4, Section 4.3.4, Fig. 4.9B), despite the obvious activation in the PI3K/PKB pathway. For this reason, the constant, yet low concentration of PTEN in HOSCC was thought to be a product of the degradation process[684,1068]. Here, it was shown that PTEN is indeed subject to degradation by the 26S proteasome in HOSCC (see Fig. 5.7 and Fig. 5.8). Based on the fact that PTEN degradation proceeds in a caspase-3 dependent manner[695], it was surprising to note that levels of PTEN were relatively stable in the WHCO5 and WHCO6 cell lines and elevated in WHCO1, WHCO3, and SNO cell lines despite the active caspase-3 present (see Fig. 5.7). Significantly, these data affirm that PTEN in HOSCC cells are stable. This strongly points to the existence of caspase-3 resistant sites on PTEN in the WHCO and SNO HOSCC series. Since CK2 is responsible for creating these caspase-3 resistant locations on PTEN through phosphorylation of it Ser370 and Ser385 residues[1069, 1070], provides a convincing role for CK2 in the observed stability in PTEN. Consistent with a role for CK2 in the WHCO and SNO HOSCC series, levels of PTEN were also found relatively stable in the MCF7 and HT29 controls that

were previously shown to rely on CK2 activity for their survival[728,906] (see Fig. 5.8). The data presented in this study provides the first evidence for a stable PTEN expression in HOSCC that is predominantly localized to the cytoplasm. The captivating question is how might this attenuated, yet constant expression of PTEN be maintained and retained in the cytoplasm of the WHCO and SNO HOSCC series?

The stability and activity of PTEN are intimately linked[210]. Thus, based on the fact that over 79 proteins are known to interact with and regulate PTEN[1071, 1072], there are multiple mechanisms by which it can contribute to the maintenance of the transformed state[579,1073]. As indicated by the proteasome inhibition experiments, by using various cell lines as controls, we provide evidence for the putative regulators of the low and constant levels of cytoplasmic PTEN in HOSCC. p53 is regarded as a major regulator for the expression and stability of PTEN[1074]. Relevantly, our data indicated that p53 does not seem necessary for the regulation of PTEN protein levels in HOSCC. This was based on the finding that the protein expression of PTEN subsequent to PI was similar across both the wtp53 (WHCO1, WHCO3, WHCO5, WHCO6), the mtp53SNO and mtp53 controls (DLD-1, Sw480, HT29) (see Fig. 5.7 and Fig. 5.8). Pertinently, as c-Jun and c-Myc considerably attenuate PTEN expression,[692,914] the low PTEN levels in HOSCC appear to be highly indicative of the significantly high c-Jun levels established in this study (see Fig. 6.4). Of interest, using locus specific FISH, the amplification of c-Myc was recently confirmed in the 5 HOSCC cell lines[1075], therefore c-Myc is likely to further contribute to low PTEN expression. This is exemplified by the low and high PTEN expressing HEK293 and MCF7 used as controls (see Fig. 5.3) that have been shown to inherently possess stronger and weaker c-Jun levels respectively[692,914].

Furthermore, by identifying similarities and disparities in the stability of PTEN in the WHCO and SNO HOSCC series subsequent to PI, to those displayed within the cell lines used as controls, we were able to provide a view on the intracellular assessment of PTEN regulation. Polyubiquitination of PTEN by NEDD4-1 leads to its cytoplasmic translocation and consequent degradation, whereas monoubiquitination results in its nuclear sequestration, where it is saved from degradation[599]. It is clear, however, that cytoplasmic PTEN is stable and largely excluded from the nucleus within HOSCC, yet it is simultaneously resistant to degradation by the proteasome. Since it is the fine balance between NEDD4-1-mediated polyubiquitination, and HAUSP7-mediated deubiquitination of PTEN that determines both its cytoplasmic and nuclear localization and hence degradation, strongly points to the existence of a deregulated relationship between these proteins in the WHCO and SNO series giving rise to the stable cytoplasmic

PTEN. This viewpoint is supported by recent evidence demonstrating the complete nuclear exclusion of PTEN in cells overexpressing HAUSP7[1076]. As the molecular characterization of HAUSP7 and NEDD4-1 in the 5 HOSCC cell lines was not assessed as part of this study, their specific contribution to PTEN levels is unknown, but highly plausible. Thus, an exciting future prospect would be to explore the relationship between NEDD4-1, HAUSP7 and PTEN in the HOSCC cells.

Based on the undetectable pPKB in the WHCO3 cell line and the low pPKB in the WHCO1, WHCO5 and SNO cell lines, it was believed to be attributable to elevated PTEN expression and activity. However, as outlined above, levels of PTEN are consistently low in all HOSCC cell lines. Thus a major departure from the "norm" in this study was the lack of inverse correlation between PTEN and pPKB (see Chapter 2, Section 2.3.7). Under normal conditions, H_2O_2 is produced by the membrane-bound NADPH oxidase (Nox) as an immediate response to the EGFR-mediated activation of PI3K[1077], leading to the concomitant Cys124 oxidation and reversible inhibition of PTEN[1078]. Remarkably, this study revealed that the activity of PTEN towards the PI3K/PKB pathway in the WHCO and SNO HOSCC series is intact and reliant upon regulation by H_2O_2 (see Chapter 4, Section 4.3.4). The involvement of PTEN in the up-regulated pPKB levels observed in response to H_2O_2 was indicated by its oxidized and thus inhibited state (see Fig. 4.9A). Hence, these data demonstrate that PTEN is functional in HOSCC. A salient feature of these data is that the membrane localized PI3K was established (see Fig. 2.6 and Fig. 2.8), yet the levels of pPKB were not similarly affected in response to EGFR activation (see Fig. 3.8). Thus, with respect to the EGFR overexpression status, it seems clear that the relationship between EGFR-mediated PI3K activation and H_2O_2 production is lost in HOSCC. Although this point holds true for all the HOSCC cell lines, the robust pPKB levels obtained in the WHCO3 cell line following PTEN oxidation (inhibition) by H_2O_2 is of particular relevance (see Fig. 4.9A). Importantly, the literature is very clear about the oxidative inactivation of PTEN via H_2O_2 as an integral mechanism for the activation of the PI3K/PKB pathway[650,1079, 1078, 1080, 1081]. This suggests that the activity of PTEN in HOSCC is not controlled and H_2O_2 plays a significant part in this deregulation.

In the presence of high catalase expression, EGFR-mediated H_2O_2 production is revoked[650]. Catalase, in addition to peroxiredoxin (Prx), and glutathione peroxide (GPx) are H_2O_2-eliminating enzymes that convert H_2O_2 to water and O_2[1082]. Ostensibly, research indicates that cells with robust activity in either one of these H_2O_2-eliminating enzymes, display enhanced H_2O_2 clearance following exogenous stimulation[646,648]. Based on the ability of the HOSCC cells

to readily reduce and thus activate PTEN following exposure to H_2O_2 (see Fig. 4.9A), is tantamount to the presence of a similar sophisticated H_2O_2-eliminating system. Multiple studies reveal that the concentration of H_2O_2 used in this study, enables H_2O_2 to be a representative oxidant, and as such, is considered a strong inducer of oxidative stress[1083, 1084, 1085, 1086, 1087, 1088]. Hence, the cellular response to oxidative stress by H_2O_2 is considered a good indicator of their cellular environment[1033]. Therefore, cells in an aerobic environment are regarded more sensitive to the DNA damage induced by the low oxygen levels, whereas cells that contain an anaerobic environment are highly tolerant of H_2O_2[1089]. This tolerant H_2O_2 environment, in turn, leads to the concomitant up-regulation of anti-oxidants needed to dampen the toxic effects of H_2O_2[1090]. A recent study also revealed the intimate relationship that exists between high cellular H_2O_2 levels, and the propensity to become metastatic[1091]. The same study, along with those reported by Landriscina *et al.*[1092], also showed, that this led to a compensatory increase in antioxidant levels to survive the harsh oxidative environment. In addition to suppressing PTEN levels, c-Myc reduces the intracellular concentration of H_2O_2 by up-regulating the expression of Prdx1[644, 1093,1094]. Since c-Myc is amplified in HOSCC, provides more supporting evidence for the existence of H_2O_2 compatibility mechanisms within this disease. Thus, as suggested above, the cellular environment in the WHCO and SNO HOSCC series appears to be conducive to oxidative stress, thus readily reducing the oxidative state of PTEN observed. Altogether, the obvious heightened tolerance HOSCC has acquired towards H_2O_2-induced oxidative stress has been shown to only occur in cells that are conditioned to such oxidative stress[1095], and as such, provides compelling evidence for the existence of aberrant PTEN oxidation in the WHCO and SNO HOSCC series.

This investigation has clearly demonstrated that the expression of PTEN is indeed suppressed and inappropriately regulated in HOSCC. However, since PTEN can also exert similar tumour suppressive functions independent of its phosphatase activity, through cellular migration and invasion[751, 1096, 1097], may explain why these HOSCC cell lines have not lost all PTEN levels. During migration and invasion, the expression of TGF-β is induced, diminishing PTEN activity and expression[1098, 1099]. In contrast, previous investigations on the WHCO and SNO HOSCC series demonstrated an up-regulation in PTEN expression following exposure to TGF-β[1100]. Therefore it would seem reasonable to suggest that HOSCC cells retain their expression of PTEN, so as direct its function towards migration. Nonetheless, the significantly attenuated and constant PTEN expression in HOSCC, implicates the acquisition for diminished PTEN levels and phosphatase activity as an important event in the maintenance of HOSCC transformation.

7.4 Degradation of PKB by the 26S proteasome.

Exposure to H_2O_2 stimulated the Ser473 phosphorylation of PKB in the PTEN-null Jurkat cell line[1101], suggesting that H_2O_2-mediated inhibition of PTEN may not be the only mechanism for activation of PI3K (pPKB) observed in this study. As noted throughout this investigation, the relative changes in pPKB obtained from PI3K inhibition (see Fig. 2.12), H_2O_2 exposure (see Fig. 4.10) and PI (see Fig. 5.9) respectively, were not inversely proportional to PTEN protein expression; indicating that the down-regulation in the concentration of pPKB in HOSCC is not entirely attributable to PTEN.

In this thesis, evidence was provided demonstrating that PKB is highly resistant to H_2O_2-mediated inactivation in HOSCC (see Fig. 4.10). This is borne out by the fact that a recent report showed that H_2O_2 was able to directly attenuate the Ser473 phosphorylation of PKB through conformational changes that disrupts binding to Hsp90[650]. Here, H_2O_2 seemed necessary for the induction of pPKB levels in HOSCC. Limited data are available regarding the degradation of PKB, but it is known to be tightly linked to dephosphorylation of its Ser473 residue shortly after activation by EGFR[220,850]. The concentration of pPKB was found to be particularly sensitive to PI in the WHCO1, WHCO5, and the WHCO6 cell lines (see Fig. 5.9). These data thus highlight the importance of the 26S proteasome in the regulation of the activation status of the PI3K/PKB pathway in HOSCC. It was interesting to note, that levels of pPKB were not induced in the WHCO3 cell line as a result of PI. Recently, it was shown that the mTORC2-mediated Ser473 phosphorylation and activation of PKB, directly leads to its Lys48 polyubiquitination and degradation of PKB via the 26S proteasome[1102]. The direct degradation of PKB following its activation is suggested to prevent hyperactivation of the PI3K/PKB pathway. It seems clear that the mechanisms used by the WHCO and SNO HOSCC series to maintain a low pPKB status are linked to the 26S proteasome.

To date, Bortezomib (Bzb) represents one of the best characterized and most specific methods used to inhibit the 26S proteasome[772,1103, 1104]. Even though the efficacy of Bzb has been demonstrated in melanomas[1105] and certain epithelial cancers[1106, 1107], its usefulness, and thus mechanism of action in HOSCC is largely unexplored. Various studies have linked the elevation in PTEN, and corresponding down-regulation in PKB Ser473 phosphorylation, as a measure for cellular sensitivity to Bzb[791,1073,1108, 1109]. The data presented in this study indicated that although pPKB was severely down-regulated in the WHCO1, WHCO3, WHCO5, and WHCO6 HOSCC cell lines, PTEN played only a partial role. The exclusion for a role for PTEN was evident by the

unrelated levels of PTEN and pPKB at higher Bzb concentrations (see Fig. 5.9). There are presumably proteasomal-dependent and proteasomal-independent methods used for PKB degradation[849]. Our data show that caspase-3 activation is needed to down-regulate pPKB in the WHCO and SNO HOSCC series (see Fig. 5.6 and Fig. 5.9). The dependence on caspase-3 was made clear by the maintained levels of pPKB in the SNO cell line, where caspase-3 was not activated (see Fig. 5.6 and Fig. 5.9).

It has been reported that the presence of wt or mtp53 in cancer cells dramatically influences their sensitivity to PI induced by Bzb, such that, wtp53 cells are considered more sensitive[1110, 1111]. It seems clear in this investigation, however, that the mtp53 status does not contribute to Bzb resistance. Here, both the R175Hmtp53 SNO cell line[429], and the wtp53 breast MCF7 control used in this study[1112], conferred resistance to Bzb (see Fig. 5.9). Resistance to Bzb established here, is consistent with the resistance to Bzb confirmed previously in the MCF7 control[719]. Of interest, it was shown that p53 is indeed active in the WHCO and SNO HOSCC series, indicated by its Ser46 phosphorylation levels[429]. Although future work would be required to pinpoint the precise mechanism for the acquired resistance to Bzb in the mtp53 SNO HOSCC cell line, it is evident from these findings, that the mtp53 status does not play a role.

H_2O_2 has been shown by previous reports to abrogate 26S proteasomal activity at sub-lethal concentrations (100 μM)[1084, 1113, 1114]. Moreover, the H_2O_2 concentration used in this study (1 mM) was illustrated to induce homologous intracellular protein damage similar to that incurred during incubation with proteasome inhibitors[1115]. In this analysis, the concentration of pPKB was ameliorated in response to H_2O_2 exposure and diminished following PI (see Fig. 4.10 and Fig. 5.9). Of interest, these data may suggest that the 26S proteasome in HOSCC has a higher tolerance for oxidative stress, and that the methods used by H_2O_2 and the 26S proteasome to regulate the PI3K/PKB pathway are distinct. Taken together, the results of this study have clearly demonstrated that the 26S proteasome plays an important role in regulating PI3K activity through PKB Ser473 phosphorylation. These data also strongly implicate that Bzb utilizes H_2O_2-independent mechanisms to induce its apoptotic effects in HOSCC. This would be the first study to focus primarily on the effects of Bzb on the PI3K/PKB pro-survival pathway in HOSCC. As the efficacy of most drug targets are linked to elevation in H_2O_2 levels[1116], the disconnection between H_2O_2 and PI illustrated here may prove to be a double-edged sword when targeting HOSCC.

7.5 Has the importance of PP2A been overlooked in the PI3K/PKB pathway?

It is well established that the PP2A phosphatase is a negative regulator of the PI3K/PKB pro-survival pathway[220,620, 1117, 1118]. The precise mechanisms are unknown, but PP2A can attenuate PKB activation by dephosphorylation of its Thr308 and/or Ser473 residue[179,1119]. PP2A is typically viewed as a "reluctant" or "lazy TSP"[621], and therefore its contribution to transformation is restricted to the tumour lineage[36,1120, 1121, 1122, 1123]. Moreover, the tumour suppressive roles of PP2A are largely dependent on its suppression on the PI3K/PKB pathway through PKB Ser473 dephosphorylation[1124]. Here it was demonstrated that, even though the Ser473 phosphorylation levels of PKB (pPKB) are low in HOSCC (see Fig. 2.9), depletion of PP2A activity through OA did not augment pPKB (see Fig. 4.4A). Therefore the activity of PP2A towards the PI3K/PKB pathway is suppressed in the WHCO and SNO HOSCC series. This deduction is substantiated by other studies that, likewise demonstrated unaffected pPKB levels following PP2A inhibition[551,1125, 1126].

Importantly, these data have presented strong, yet circumstantial evidence for the existence of diminished PP2A activity in the WHCO and SNO HOSCC series. There are several ways in which the activity of PP2A can be suppressed. In normal epithelial cells, PP2A facilitates the degradation of c-Myc[1127]. Therefore, the presence of a c-Myc amplification is persistently viewed as a marker for lost PP2A activity[629, 1122,1128, 1129]. Pertinently, the c-Myc amplification present within the WHCO and SNO HOSCC series further strengthens the existence of lost PP2A activity. The cancerous inhibitor of protein phosphatase 2A (CIP2A) has recently been identified as a novel inhibitor of c-Myc degradation via direct inactivation of PP2A. Consequentially, the aggressiveness of many metastatic tumours, and recently including oesophageal cancer[1130], has been associated to the increased expression of CIP2A through its specific ability to attenuate the tumour suppressive function of PP2A[1131, 1132]. Most recently, inhibition of the proteasome using Bzb was shown to sensitize tumour cells to radiation through the inhibition of CIP2A[1133]. Thus, future evaluation of CIP2A is warranted and may serve useful in the on-going characterization of the PP2A-mediated effects on the PI3K/PKB pathway in HOSCC.

Uniquely, the concentration of pPKB in the WHCO6 cell line increased in response to PP2A inhibition and thus shows that the Ser473 phosphorylation state of PKB in this cell line is in part, regulated by PP2A. The activity of PP2A is induced via the α2β1 integrin[609, 1134]. Importantly, α2 and β1 integrin subunits are down-regulated in the WHCO and SNO HOSCC series[611]. On the

other hand, the activity of PP2A is suppressed by the β1 integrins[1117, 1135]. Possibly, it may be that, the ability to activate PP2A via the integrins is attenuated as a result of the down-regulated α2β1 integrin levels, giving rise to the negligible influence PP2A has on PKB, clearly indicated by OA exposure (see Fig. 4.4A).

Although the apparent down-regulated PP2A activity in HOSCC may be attributable to the α2β1 integrin, the up-regulated levels of EGFR could also contribute to this suppression as previously alluded[613] (see Chapter 4, Section 4.4). It is therefore highly conceivable that the attenuated activity of PP2A in HOSCC is a consequence of the concerted inhibitory influences of EGFR and α2β1 integrin. Furthermore, previous evidence has demonstrated that the mechanism used by one of the initiating factors of HOSCC, the common FB_1 mycotoxin found in grain, was through attenuation of the activity of PP2A by an unknown mechanism[558]. Despite the fact that it is unknown whether FB_1 was responsible for the transformation of the 5 HOSCC cell lines, with respect to the high intake of maize-based foods at the time these cell lines were established[1136, 1137, 1138, 1139], it seems logical to suggest this may be the reason for the reduced PP2A activity on the PI3K/PKB pathway, as most clearly shown in this study. Moreover, various studies have confirmed the importance of FB_1 in the aetiology of the WHCO1, WHCO3, and SNO HOSCC cell lines specifically[1140, 1141, 1142].

These data provide insight into the molecular mechanisms of the PI3K/PKB pathway in HOSCC, in that, the activity of PP2A does not appear to play a predominant role in the attenuation of active PI3K (pPKB) ascribed to the WHCO1, WHCO3, WHCO5 and SNO HOSCC cells. Moreover, arising out of these data and the characteristics previously shown to be present within these HOSCC cells (EGFR overexpression, c-Myc amplification, and α2β1 integrin down-regulation) suggests that these factors may lead to the abrogated activity of PP2A observed in this study. From the identification of suppressed PP2A activity in the WHCO and SNO HOSCC series, our data raises the hypothesis that attenuated PP2A activity plays a role in the maintenance of the transformed state and therefore by introducing treatments that augment PP2A activity, may serve as an ideal means of future therapy for HOSCC.

7.6 The WHCO and SNO HOSCC series – a model for crosstalk between the Wnt and PI3K pathways.

Nuclear accumulation of β-catenin is one of the hallmarks for active canonical Wnt signalling in cancer[941]. In most instances, this nuclear accumulation is found associated to its reduced degradation, caused by mutations within β-catenin and/or mutations in one of the major components of the β-catenin destruction complex (APC/Axin/GSK3β), APC. Of note, the nuclear accumulation of β-catenin is most commonly found attributable to the aggressiveness of oesophageal cancer. However, unlike other epithelial cancers such as those found in colon[940, 1143], mutations within APC or β-catenin appear to be very rare in HOSCC [943,1144,1145, 1146]. Therefore, a better understanding of the factors that govern these nuclear β-catenin levels is essential. Here, we found elevated nuclear β-catenin expression that was strongly affiliated with the protein expression of two of its nuclear gene targets; c-Jun and MMP-7 in HOSCC (see Fig. 6.2-Fig. 6.4). Most recently, it was discovered that knockdown of β-catenin in the Sw480 colon cell line, down-regulated Fas ligand (FasL) expression[1147], which is a type II membrane protein responsible for triggering apoptosis[1148]. Appropriately, the WHCO and SNO HOSCC series were recently shown to express high levels of FasL[1149]. As a result, the expression of FasL, c-Jun, and MMP-7 all point to the presence of an active β-catenin within the nucleus of the HOSCC lines. In non-cancerous cells, there are two distinct pools of β-catenin; the membrane localized β-catenin pool that plays a role in C-C adhesion through its association with E-cadherin and α-catenin, and the nuclear pool that plays a role in gene regulation in response to Wnt signalling[1150, 1151]. Reduced C-C adhesion is one of the major features of metastatic epithelial cancers like HOSCC[1152, 1153]. Therefore, decreased β-catenin/E-cadherin/α-catenin associations are often used as prognostic markers in prostate, breast, lung, stomach, colon, head and neck cancers[1154, 1155, 1156, 1157, 1158]. Corresponding to its dual functions in the nucleus and at the plasma membrane cell adhesion junctions, the data presented in this investigation show that, in spite of its robust nuclear levels, β-catenin was still found complexed with E-cadherin/α-catenin at the plasma membrane (see Fig. 6.5). Therefore, this study highlights that the nuclear accumulation of β-catenin may be a better marker than the decreased β-catenin/E-cadherin/α-catenin associations for the transformed state of HOSCC.

A combination of studies have questioned the relevance of crosstalk between the PI3K and Wnt signalling pathway in the transformation process[1159, 1160, 1161,1048]. Here, it was found that inhibition of PI3K by LY29 substantially increased the nuclear accumulation of β-catenin in the

WHCO1, WHCO6 and SNO HOSCC cell lines specifically (see Fig. 6.8). As indicated by the considerable impact PI3K inhibition had on the Ser9 dephosphorylation levels, and thus activation of GSK3β in HOSCC (see Fig. 2.13B), it was clear that the reduction in the nuclear sequestration of β-catenin was instigated via activation of GSK3β (Fig. 6.8). Uniquely, it was also shown that although the Ser9 phosphorylation of GSK3β was regulated by PI3K, it was only, in part, mediated by PKB (see Fig. 2.12 and Fig. 2.13). Despite the observation that GSK3β was dephosphorylated (inhibited) on its Ser9 residue through PI3K inhibition in the WHCO3 cell line, no corresponding down-regulation in nuclear concentration of β-catenin was observed (see Fig. 6.8). As pPKB is undetectable in this cell line (see Fig. 2.9), the importance of PKB in the crosstalk between the Wnt and PI3K pathway is exemplified. The significance of this finding in HOSCC is further supported by a recent study that was unable to induce the Ser9 phosphorylation of GSK3β as a result of PI3K inhibition[916]. This is the first report to demonstrate the crucial contribution made by the PI3K pathway in the nuclear levels of β-catenin in HOSCC, and show that in addition to GSK3β, PKB plays a significant role during this interplay. The impact of PKB in this relationship is further strengthened by the significant induction in pPKB attained following activation of Wnt signalling in the WHCO1, WHCO5, WHCO6, and SNO cell lines specifically (see Fig. 6.6). These data are in contrast with Ng *et al.*[1162] and Ding *et al.*[1163] , who demonstrated no significant influence of the PI3K/PKB pathway on the nuclear accumulation of β-catenin. Furthermore, a previous report by Sun and Jin[1164], demonstrated interplay between the PI3K and Wnt signalling pathway in intestinal cells, but was shown to be PKB-independent. Most recently, the PI3K-dependent Ser9 phosphorylation of GSK3β was shown to play an essential role in the intestinal-wound healing response by accumulating nuclear β-catenin[1165]. The studies described here reveal that the PI3K pathway is able to significantly impinge upon the canonical Wnt signalling pathway in HOSCC, by regulating the nuclear accumulation of β-catenin via a PKB-dependent mechanism.

The literature refers to two distinct groups of GSK3β in cells; the Wnt-regulated and PKB-regulated GSK3β intracellular pools respectively[200,877, 1166]. As such, the Ser9 phosphorylation status of GSK3β has become a widely accepted marker for active PKB in a wide variety of cell types[962,1167, 1168, 1169]. Conversely, it was shown here, that activation of Wnt signalling had a substantial influence on the Ser9 phosphorylation of GSK3β (inhibition), especially in the WHCO3 and WHCO5 HOSCC cell lines (see Fig. 6.6). Thus, the Wnt signalling pathway is able to regulate the PKB-regulated pools of GSK3β, which suggests that bi-directional crosstalk between the Wnt and PI3K signalling pathways are operant in the WHCO and SNO HOSCC series. This bi-directional crosstalk in HOSCC is further substantiated by the fact that Wnt

signalling in the HT29 cell line is constitutive[1170], and yet no similar up-regulation in Ser9 GSK3β phosphorylation levels were evident following activation of Wnt signalling (see Fig. 6.6). Pertinently, a key role for the Wnt signalling pathway in the Ser9 phosphorylation of GSK3β is clearly epitomized in the WHCO3 a cell line, where the levels of pPKB is undetectable, yet a significant up-regulation in pGSK3β was shown subsequent to activation of Wnt signalling (see Fig. 6.6). Hence, the non-responsive concentration of nuclear β-catenin obtained in the WHCO3 and WHCO5 following PI3K inhibition (see Fig. 6.8), may be indicative of the major role played by the Wnt signalling pathway in regulating GSK3β phosphorylation and activity, negating the influence of the PI3K pathway.

Recent evidence has shown how Nox1 plays a central role in mediating crosstalk between the PI3K and Wnt signalling pathways in colon cancer via H_2O_2-induced PTEN oxidation and inhibition[1081]. Due to the fact that induction of pPKB in the WHCO3 cell line was only subsequent to H_2O_2-induced PTEN oxidation (see Fig. 4.9 and Fig. 4.10) and not activation of Wnt signalling (see Fig. 6.6), suggests that the molecular mechanisms used to activate PKB through Wnt signalling is not via H_2O_2 in HOSCC. It has long been thought that once phosphorylated, the activity of GSK3β is completely inhibited[200,962,1171, 1172, 1173]. Conversely, Doble *et al*.[1174] has illustrated that although phosphorylated and thus inhibited, GSK3β is still able to discernibly attenuate the sequestration of β-catenin into the nucleus, and that this ability is only perturbed upon inactivation or deletion of three or four of its alleles. Therefore, although we were able to indicate that inhibiting PI3K resulted in ameliorated nuclear β-catenin levels in HOSCC, the low extent to which this took place is likely attributable to the presence of active GSK3β that may negate this effect, contributing to the reduction in this regulation in certain of the HOSCC cell lines. Of interest, recent and previous reports have illustrated that the MUC1 oncoprotein attenuates GSK3β-mediated phosphorylation and degradation of β-catenin[1175, 1176]. As highlighted above, a robust interaction was shown to exist between MUC1 and β-catenin in these HOSCC cells. This MUC1/β-catenin interaction may provide additional insight into the reduced involvement for PI3K in regulating the nuclear levels of β-catenin via GSK3β.

Additionally, high pGSK3β (inhibited) levels are considered a pathological marker in oral[1177] and lung cancers[1178]. In contrast, levels of pGSK3β in the WHCO and SNO HOSCC series were extremely varied (see Fig. 2.11). Thus, unlike the oral and lung cancers, pGSK3β may not serve as a good marker for the transformation state of HOSCC. It is accepted that activation of a single pathway is insufficient to provide the highly aggressive and proliferative state of cancers. Collectively, the data presented here provide convincing evidence for the existence of bi-

directional crosstalk between the Wnt and PI3K pathways in the WHCO and SNO HOSCC series. Therefore, treatments targeting a single one of these pathways in HOSCC may serve an efficient therapy.

7.7 A case for the regulation of the PI3K/PKB pro-survival signalling pathway in HOSCC.

An integrated analysis of the major components of the PI3K/PKB pathway was done in order to examine what roles PI3K, PKB and PTEN may play in the maintenance of the transformed state in the WHCO and SNO HOSCC series. Characteristically, the 5 HOSCC cell lines are known to possess an EGFR overexpression status[332] and active signalling of the canonical Wnt pathway[894]. Even though the functional relevance of these traits are still unknown, they were used to determine the status of the PI3K/PKB signalling network within HOSCC. From a tumour biology perspective, it would appear that HOSCC has evolved by reducing its EGFR-mediated activation of the PI3K/PKB pathway. The clear loss in communication between EGFR-mediated PI3K activation and consequent H_2O_2 production through Nox is suggested to play a major role in this diminished influence (as can be seen in Fig. 7.1). Hence, hypo-activation of the PI3K/PKB pathway plays a role in the maintenance of the transformed state of HOSCC. The clear departure of the tumour suppressor function of PTEN in HOSCC appears to be linked to its stability in the cytoplasm. Based on what was shown here, and what is known about these HOSCC cells, it is believed that the concerted action of the c-Myc amplification and the MUC-1/β-catenin nuclear association maintains a low PTEN status and contributes to the overall protection of HOSCC to oxidative stress (demonstrated in Fig. 7.1). It seems clear from this study that the retention and accumulation of p85α protein levels is important in the reduced impact that EGFR has on the PI3K/PKB pathway (see above), and the stability of PTEN (see Fig. 7.1). Furthermore, it would also appear that the acquisition of lost PP2A activity in HOSCC is crucial in maintaining the deregulated and thus hypo-activated state PI3K/PKB pathway. In view of what was discussed above, the activity of the 26S proteasome and caspase-3 are deemed equally important in regulating the PI3K/PKB pathway in the WHCO and SNO HOSCC series. The mechanisms for the de-regulation of the PI3K/PKB pathway in HOSCC are summarised in Fig. 7.1.

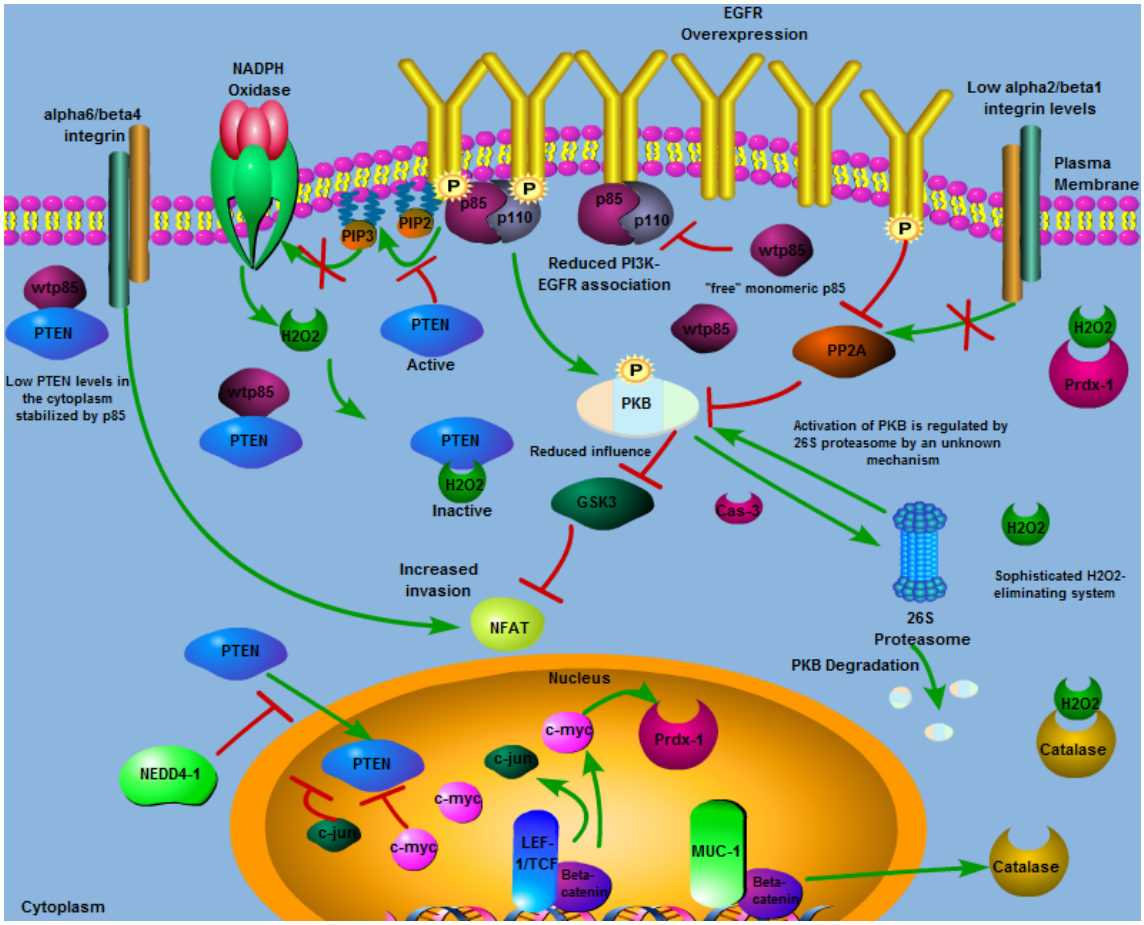


Figure 7. 1: Proposed mechanism for the activation and regulation of the PI3K/PKB pathway in HOSCC. Figure generated using the Pathway Builder Tool. 2.0.

7.8 The PI3K/PKB pathway in HOSCC - novel insights into potential targets for therapy.

This widespread influence and regulation of the PI3K/PKB pathway in HOSCC (see Fig. 7.1) presents a tremendous challenge for therapy. When faced with a non-hereditary cancer such as HOSCC, where the molecular mechanisms involved in the transformation process are multi-faceted[1179], therapeutic targeting becomes more challenging. Currently, surgery and radiation therapy are the only treatments available for patients with oesophageal cancer[1180]. However, these treatments have proven to be mildly successful[1181]. It is well established that the EGFR overexpression and mtp53 status of HOSCC are important components of the transformation process, and are currently the most popular markers to consider when focusing on resistance to therapy[1182]. However, certain reports have demonstrated that mtp53 confers sensitivity to various

therapeutics targeted against HOSCC[1183, 1184], whilst others could not find a significant correlation between the p53 status and the therapeutic response[291, 1185]. Therefore, the acquisition of such resistance remains cryptic and a need for a better understanding is imperative.

The PI3K/PKB pathway is one of the major causes for acquired resistance to therapy in many cancer types[382, 1186, 1187, 1188]. For a long period of time, the LY294002 (LY29) pharmacological inhibitor for PI3K has been extensively used in preclinical studies, and although is not suitable for patient use, its specificity towards PI3K has been exploited for both the design of better PI3K inhibitors and investigating the intracellular functions of PI3K[1189]. Of relevance, the use of LY29 has been shown in oesophageal adenocarcinoma cell lines, and proven to be effective in stopping cell growth[1190]. Importantly, it was demonstrated here that the WHCO5 and SNO HOSCC cell lines conferred resistance to PI3K inhibition through LY29 (see Fig. 2.12 and Fig. 2.13). Furthermore, based on the p53 status in the WHCO5 (wtp53) and SNO (mtp53) cell lines, strongly points away from a potential role for p53 in the resistance observed. The sensitivity to LY29 illustrated in the WHCO1, WHCO3, and WHCO6 cell lines shown here, has been linked to the presence of PI3KCA mutations and high pPKB levels in the Japanese oesophageal cell lines[526, 1191]. In contrast, none of the WHCO and SNO HOSCC series possessed PIK3CA mutations (Chapter 3, Section 3.3.6). Remarkably, the high pPKB levels in WHCO6 cell line demonstrated the greatest sensitivity to LY29-mediated PI3K inhibition; whereas high resistance was obtained in the SNO cell line possessing lower levels of pPKB (see Fig. 2.13). Moreover, *in vitro* and *in vivo* inhibition of PI3K in ovarian and non-small lung cancer cell models selectively induced apoptosis in cells with higher activation levels of PKB (pPKB), and was found less efficient at doing this in cells that possessed lower concentrations of pPKB[1192, 1193]. Prominently, the data presented in this study imply that assessing the pPKB status of HOSCC may serve as a useful marker for efficacy of future treatment. Significantly, these data also suggest that targeting the PI3K/PKB pathway exclusively may not sufficiently reverse the transformation state of HOSCC, based on the tightly linked relationship existing between the Wnt signalling pathway. It has been demonstrated that the efficacy of targeting PI3K in epithelial cancers is largely dependent on the presence of PIK3CA, PTEN and/or HER2 mutations[1194]. Therefore, whereas pPKB may serve as a useful marker for the efficacy of future drugs targeting HOSCC, direct blockage of the PI3K/PKB pathway may not prove effective.

Based on the common EGFR overexpression status in HOSCC, current therapy has focused on targeting the EGFR instead[1195, 1196], but its efficacy is still being explored. Significantly, the fact that the PI3K/PKB pathway in HOSCC cells was more responsive to H_2O_2 (see Fig. 4.10) and

not EGFR activation (see Fig. 3.8), has the potential to explain possible reasons why certain therapies, such as those targeting the EGFR, are ineffective. In support of this, a comparison between pPKB levels before and after chemotherapy in a study of 195 oesophageal patients, demonstrated elevated levels of pPKB during chemotherapy[1197]. Therefore, these low concentrations of pPKB in the WHCO and SNO HOSCC series may aid in the highly drug resistance commonly observed in this disease[1198, 1199]. Considering that H_2O_2 is a common derivative of many therapeutic drugs[1200, 1201, 1202, 1203], proposes that such drugs would be less effective in HOSCC, as most clearly shown here. Taken together, it will prove relevant to take these findings into account when developing new treatment towards HOSCC.

7.9 Conclusion

It is worth noting that knowledge illuminating our understanding and perspective of the molecular and cellular remodelling induced by various oncogenes and tumour suppressor proteins (TSPs) are of critical relevance to our continued search for better cancer therapeutics. Over the past decade there have been a number of genes ascribed to the initiation and maintenance of transformation in oesophageal cancer[1204], yet its metastatic potential and resistance to therapy remains rife. In the case of the South African (SA) moderately differentiated WHCO and SNO HOSCC series, a "model system" has been described for the functional contributions of the major PI3K/PKB pro-survival signalling pathway to the maintenance of their transformed state (see Fig. 7.1). These previously unexplored features of HOSCC may be assessed as candidate response predictors and/or indictors of future therapeutics.

A key prediction from this study is that, like certain breast cancer cells[1205], HOSCC may not fully rely on the PI3K/PKB pathway for its survival. To my knowledge, this is also the first report demonstrating a pro-survival role for H_2O_2 in HOSCC. Based on the wtPIK3CA and wtPKB1 status in HOSCC established here, it would appear that this type of cancer does not fall under the "oncogene addiction" form of carcinogenesis observed in other epithelial-derived tumours. It was also clear that the acquisition of low PTEN levels is an important step in the maintenance of the transformed state in HOSCC. Although the major contributing factors for attenuating PTEN expression and activity are unknown, the concerted functions of p85α, CK2 and HAUSP/ NEDD4-1 were convincingly proposed. A role for CK2 in the initiation and maintenance of HOSCC is very appealing, especially since this non-oncogene addiction state is atypical of CK2-driven cancers[1206].

Based on the fact that the contribution made by PP2A in tumour progression is cell-type specific, this study has clearly highlighted that its multi-faceted functions has been selectively attenuated towards PI3K/PKB signalling in HOSCC. Of interest, would be the future elucidation of the factors determining such suppression, and as such, may present a major tool used for the regulation of the PI3K/PKB pathway in HOSCC. It seems clear that the mechanisms used in HOSCC to maintain low pPKB levels is subject to degradation by the 26S proteasome. Bzb may serve as a good therapy for HOSCC. As it is a known inducer of the ERK pathway, further investigation of the involvement of the ERK pathway in HOSCC will contribute to the understanding of the complex contributors to the transformation of this disease, and in so doing, better therapeutic targeting.

Appendices

Appendix A

1.1 Tissue Culture Medium

1.1.1 DMEM Medium Solution

1.37 %	Dulbecco's Modified Eagle's Medium (DMEM)
0.37 %	Sodium bicarbonate
2 %	Penicillin/Streptomycin solution (Penicillin: 500 U/ml; Streptomycin: 0.5 %)

Make up to final volume with dH_2O.

1.1.2 Hams F12 Medium Solution

1.07 %	Hams F12 medium
0.118 %	Sodium bicarbonate
2 %	Penicillin/Streptomycin solution

Make up to final volume with dH_2O.

Mix:
3 Volumes DMEM medium solutions: 1 volume Hams F12 medium solution
Filter sterilize
Store at 4 °C.

1.1.3 1X Phosphate-buffered saline (PBS)

136.9 mM	NaCl
2.86 mM	KCL
10.1 mM	$Na_2HPO_4 \cdot 12H_2O$
1.76 mM	KH_2PO_4

Make up to 1 L with dH_2O, and adjust the pH to 7.2-7.3.
Sterilize the solution for 20 minutes at 1511bq and store at 4 °C.

1.1.4 Trypsin: EDTA Solution

0.02 %	EDTA in 500 ml PBS
0.1 %	Trypsin in 1 L PBS

Mix EDTA:Trypsin (1:1) to obtain a final concentration:

0.01 %	EDTA
0.05 %	Trypsin

Store at 4 °C.

1.2 Reverse Transcription

1.2.1 MMLV-RT Buffer (5X)

50 mM	Tris-HCL, pH 8.3
75 mM	Potassium Chloride
3 mM	Magnesium Chloride
10 mM	DTT (dithiolthreitol)

1.2.2 Nucleotide Mix (dNTPs)

Each 10 mM dNTP (dATP, dCTP, dGTP, and dTTP) are supplied as sodium salts diluted in dH_2O at a pH of 8.3.

1.2.3 MMLV-RT

This enzyme is supplied in:

20 mM	Tris-HCL, pH7.7
200 mM	Sodium Chloride (NaCl)
0.1 mM	EDTA
1 mM	DTT
0.01 %	Nonidet-P40 (NP-40)
50 %	Glycerol

1.2.4 3 M Sodium Acetate pH 5.2

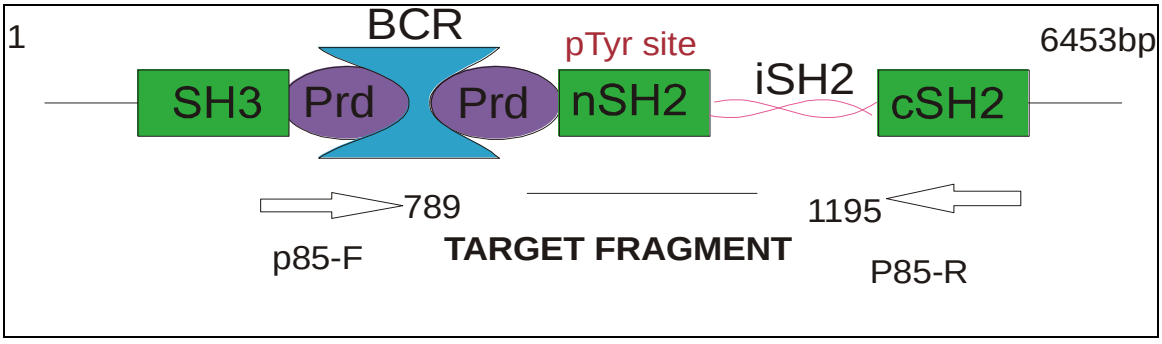
3M Sodium Acetate (anhydrous)
Dissolve in dH_2O.
Adjust the pH to 5.2 using glacial acetic acid.

Make up to final volume with dH_2O.

1.3 PCR

1.3.1 p85α Sequence and Primer Information

The sequence amplifying the region on the gene (PIK3R1) transcribing for the N-terminal domain of the regulatory subunit of PI3K, p85α:



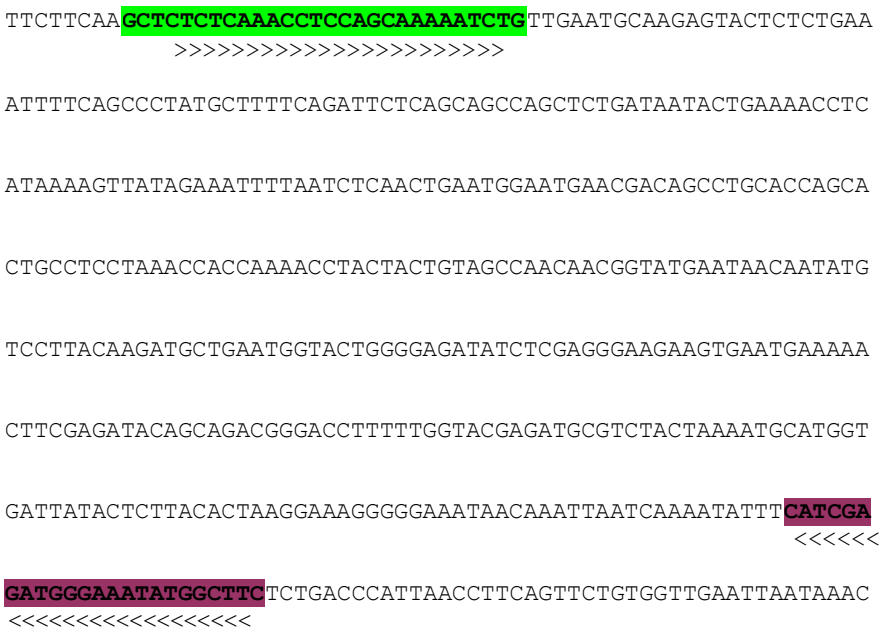


Figure A1: Schematic diagram of the PIK3R1/p85α gene transcript highlighting the region intended to amplify during the PCR reaction that is highlighted by the green (forward primers) and purple (reverse primers) within the sequence.

The primer parameters:

	Primer Length	GC%	Melting Temperature
Forward Primer:	23 bp	47.83	64.18
Reverse Primer:	24 bp	45.83	64.90
PCR Product length:	430 bp		

The hairpin formation and homo-dimer or primer self-dimer was calculated utilizing the OligoAnalyzer (http://www.idtdna.com/analyzer/Applications/OligoAnalyzer):

	Hairpin Formation	Homo-Dimer Formation
Forward Primer:	ΔG=2.44 kcal/mole Melting temperature of 26.1°C	ΔG=-4.74 kcal/mole with 3bp
Reverse Primer:	ΔG=2.13 kcal/mole Melting temperature of 31.5°C	ΔG=-6.76 kcal/mole with 4bp

1.3.2 PCR Reaction Buffer (10X)

20 mM	Tris-HCL, pH 7.5
100 mM	Potassium Chloride (KCl)
1 mM	DTT
0.1 mM	EDTA
0.5%	Tween-20
0.5%	NP40
15M	Magnesium Chloride (MgCl)

1.4 Agarose Gel Electrophoresis

1.4.1 1% Agarose Gel

0.3 g	Agarose
30 ml	TAE Buffer

Heat to dissolve agarose, allow cooling, and then add:

2 µl	10 ng/ml Ethidium bromide (EtBr) diluted in dH2O

Pour mixture into gel casting tanks (Sigma-Aldrich MiniZ33 Horizontal Gel Caster), then add 10-well comb, and leave at RT for 15-20 minutes to set.

1.4.2 1X Tris Acetic Acid EDTA (TAE) Buffer

20 ml	20X TAE buffer
380 ml	dH_2O

TAE Buffer (20X)

1.6 M	Tris
0.8 M	Sodium acetate ($NaAc \cdot 3H_2O$)
40 M	$EDTA \cdot Na_2H_2O$

Adjust the pH to 7.2 using glacial acetic acid.
Make up to a final volume with dH_2O, thereafter, autoclave at 120 °C to sterilize.

1.4.3 Loading Buffer

50 %	2XTAE (10 % of 20XTAE; make up to final volume with dH_2O)
50 %	Glycerol
0.001 %	Coomassie brilliant blue powder

Store at -20 °C

1.5 Sample Preparation

1.5.1 Lysis Buffer

Double Lysis Buffer

4 %	SDS
20 %	Glycerol
10 %	β-mercaptoethanol

Make up solution to a final volume with 0.0625 M Tris-HCL buffer, pH 6.8 (use 1 N HCL to adjust the pH).

Single Lysis Buffer
Dilute double lysis buffer at a ratio of 1:1 using 0.0625 M Tris-HCL buffer, pH 6.8

1.5.2 Nuclear Extraction Buffer

10 mM	Tris-HCL (pH 7.4)
2 mM	$MgCl_2$
0.5 mM	PMSF (Merck, SA)
10 µg/ml	Aprotinin
10 µg/ml	Leupeptin
5 mM	Sodium pyrophosphate
2 mM	β-glycerophosphate

Make up to final volume with dH_2O.

1.5.2.1 Nuclear Wash Buffer

10 mM	Tris-HCL (pH 7.4)

Supplemented with 5 mM $MgCl_2$ and made up to final volume with dH_2O.

1.5.2.2 Sucrose Solution

10 mM	Tris-HCL (pH 7.4)
0.25 M	Sucrose
5 mM	$MgCl_2$

Make up to final volume with dH_2O.

1.5.2.3 Nuclear Lysis Buffer

62.5 mM	Tris-HCL (pH 6.8)
2%	SDS
10%	Glycerol
5%	2-mecaptoethanol

Make up to final volume with dH_2O.

Then add Protease Inhibitors:

5 µl/ml	PMSF (20 mM)
10 µl/ml	Trazylol
1 µl/ml	Pepstatin
0.5 µl/ml	Leupeptin

1.5.3 Plasma Membrane Extraction

1.5.3.1 PBS/PMSF/Trazylol Solution

0.5%	PMSF stock solution (20 mM in Methanol)
1%	Trazylol

Make up to a final volume using PBS

1.5.3.2 Membrane Hypotonic Buffer

20 mM	Tris-HCL (pH7.4)
25 mM	NaF
1 mM	EDTA

Make up to final volume with dH_2O.
Then add Protease Inhibitors:

5 µl/ml	PMSF (20 mM)
10 µl/ml	Trazylol
1 µl/ml	Pepstatin
0.5 µl/ml	Leupeptin

1.6 Protein Estimation

1.6.1 Bovine Serum Albumin (BSA) Solution

0.1 %	BSA (BDH Laboratory reagents)

Make up to final volume with single lysis or nuclear lysis buffer.

1.6.2 7.5% Trichloracetic Acid (TCA)

7.5 %	TCA

Make up to final volume with dH_2O.

1.6.3 Coomassie Brillian Blue Stain

0.25 %	Coomassie blue powder
50 %	Methanol
10 %	Acetic Acid

Make up to final volume with dH_2O.
Store at room temperature

1.6.4 Destain

12 %	Ethanol
10 %	Acetic Acid

Make up to final volume with dH_2O.

1.6.5 Elution Solution

67.35 %	Methanol
31.63 %	dH_2O
1.02 %	Ammonia

Make up to final volume with dH_2O.

1.6.6 Example of Standard curve for protein estimation

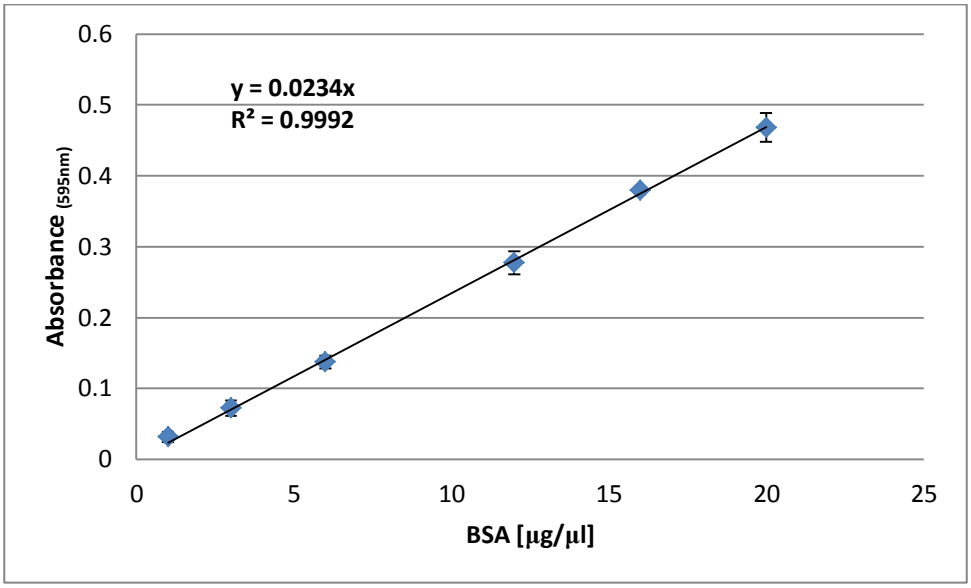


Figure A2: The various absorbance readings (595 nm) of 1, 3, 6, 9, 12, 16, and 20 µg BSA used to construct a standard curve for the protein estimation of various protein extracts. The respective protein concentrations were determined from the standard curve (y = 0.0234x). The standard curve is representative of three independent experiments that was performed for each extraction procedure: mean ± S.D. R^2=linear regression.

1.7 Electrophoresis

1.7.1 Separating Gel (10%)

Seperating Buffer

4.53 g Tris dissolved in dH_2O.
Adjust pH to 8.8 using 1 N HCL.
Make up to 25 ml with dH_2O.

Seperating Gel

0.5 g	Acrylamide
1250 µl	Seperating Buffer
200 µl	SDS (50 mg/ml)
200 µl	Bisacrylamide (25 mg/ml)

Make up to 5 ml with dH_2O.
Add 90 µl of 1.25 % ammonium persulphate (APS) and 12.5 µl of N', N', N', N'-tetramethylene-diamine (TEMED) for gel polymerization.

1.7.2 Stacking Gel

Stacking Buffer

1.51 g Tris dissolved in dH_2O.
Adjust the pH to 6.8 using 1 N HCL
Make up to 25 ml using dH_2O.

Stacking Gel

0.25 g Acrylamide
1250 µl Stacking Buffer
200 µl SDS
200 µl Bisacrylamide
Make up to 5 ml with dH_2O.
Add 90 µl APS and 10 µl TEMED for gel polymerization.

1.7.3 Electrophoresis Running Buffer

0.8 g SDS
11.56 g Glycine
2.42 g Tris
Dissolve in 600 ml dH_2O.
Adjust the pH to 8.3 using 1 N HCL
Make up to final volume of 800 ml using dH_2O.

1.7.4 Destain for SDS-PAGE

10 % Acetic Acid
10 % Methanol
Make up to final volume with dH_2O.

1.7.5 Representation of 10% SDS-PAGE resolution for protein estimation

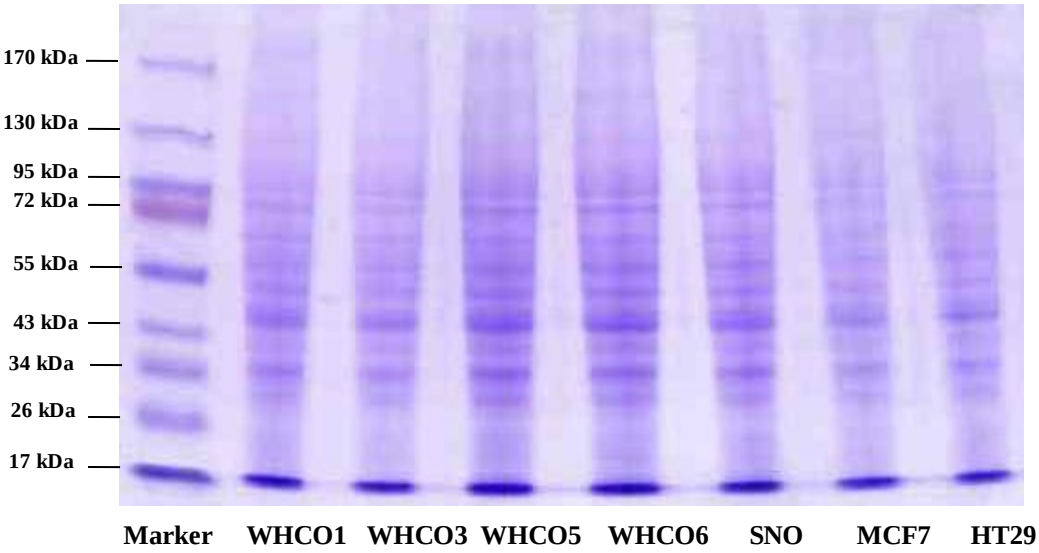


Figure A3: 20 µg of protein lysates from the specific extractions performed were analysed from a separation on a 10 % SDS-PAGE, indicating a successful protein extraction, evidenced by a similar binding pattern of the Coomassie Blue stain in the form of bands.

1.8 Western Blotting

1.8.1 Western Blot Transfer Buffer

0.5 M	Glycine
25 mM	Tris
20 %	Methanol

Make up to final volume with dH_2O.

1.8.2 Blocking Buffer (BLOTTO)

50 mM	Tris-HCL, pH 7.8
2 mM	$CaCl_2 \cdot H_2O$
5 %	Non-fat milk powder
0.01 %	Anti-foam
0.05 %	Triton-X 100

Make up to final volume using dH_2O.
Store at 4 °C.

1.8.3 Developer

6.4 M	Metol
0.6 M	Sodium sulphite
80 mM	Quinol
0.45 M	Sodium carbonate
34 mM	Potassium bromide

Make up to final volume using dH_2O

1.8.4 Fixer

0.8 M Sodium thiosulphate
0.2 M Sodium metabisulphite
Make up to final volume using dH_2O

1.8.5 10X Tris Buffered Saline (TBS)

24.2 g Tris base
80 g NaCl
Dissolve in dH_2O
Adjust the pH to 7.6 using 1 N HCL
Make up to final volume of 1 L using dH_2O.
Store at 4 °C.

1X TBS

10 % 10X TBS
90 % dH_2O

1.8.6 Blocking Buffer

5 % Non-fat milk powder
Make up to final volume using 1X TBS, 0,1 % Tween-20 (TBS/T)

1.8.7 Primary Antibody Dilution Buffer

2.5 % BSA
Make up to final volume using TBS/T

1.9 Indirect Immunoflourescence

1..1 4% Paraformaldehyde Solution

0.2 M Sodium dihydrogen orthophosphate (NaH_2PO_4)/ Solution A
0.6 M Sodium hydroxide (NaOH)/ SolutionB

Mix 166 ml Solution A with 34 ml Solution B
Add 8 g paraformaldehyde
Heat to 80 °C while stirring, until solution becomes clear
Filter and allow cooling, adjust pH to 7.2-7.4
Store at -20 °C

1.9.2 0.25 % Triton-X-100

0.25 % Triton-X-100
Made up to final volume with 1x PBS

1.9.3 Mounting Solution (Elvanol)

0.1 M	Tris
20 %	Polyvinyl Alcohol
50 %	Glycerol

Make up to final volume with dH_2O.

1.10 LY294002 Stock

1 mg	LY294002 (Sigma)

Make up to 500 µl with DMSO (Sigma)
Store at -20 °C

1.11 Optimization of LY294002 exposure in HOSCC cells.

In view of the fact that a fair number of studies using LY294002 (LY29), either do not stipulate the tissue culture conditions used[341,1208,1209], or when mentioned, is frequently performed under low serum (0.1 % or 0.5 %) or normal serum (10 % FCS) conditions[1210-1214]. Furthermore, for the purpose of this study, that is; to manipulate the activity of PI3K, but not to induce apoptosis, most studies use LY29 concentrations > 5 µM[423]. Furthermore, concentrations > 20 µM, LY29 potentially loses its selectivity for PI3K[427]. Therefore, to avoid compromising the potency of PI3K inhibition by LY29, we, like others, initially tested a concentration of 10 µM for 60 mins[1215-1217] in four cell lines (WHCO1, WHCO3, WHCO5 and WHCO6) under serum (10% FCS) and low serum (0.1% FCS) conditions. Since the Ser473 phosphorylation of PKB is highly dependent on PI3K activity[177], we used pPKB levels as an indicator of LY29 efficacy. Under low serum conditions, pPKB (Ser473) was only detectable in WHCO6 without exposure to 10 µM LY29, which was otherwise undetectable in the WHCO1, WHCO3 and WHCO5 (shown in Fig. A4). Therefore, based on these results exposing the cells to LY29 under serum conditions (10% FCS) was used, even though no pPKB was detected in the WHCO3 HOSCC cell line.

Consequently, we sought to ascertain whether a 1 hr exposure to LY29 was sufficient enough to inhibit PI3K. Since induction of cell death is a 24 hr process in the HOSCC cells[429], the cells were not exposed to LY29 for longer than 24 hrs. The 5 HOSCC cell lines, including the MCF7 and HT29 control cell lines were exposed to 10 µM of LY29 for 18 and 24 hrs and western immunoblotted for pPKB detection as a marker for the presence of inhibited PI3K. Excluding the HT29 cell line, no PI3K inhibition was evident in the remaining cell lines following exposure to LY29 for 18 and 24 hrs (see Fig. A4). This is in line with work performed by Levinthal and DeFranco[1218] who demonstrated that the inhibitory action of LY29 is lost after 6 hrs. Therefore, the 5 HOSCC, MCF7 and HT29 cell lines were exposed to 10 µM LY29 for 60 mins supplemented with 10% FCS, the efficacy of LY29 at this concentration, was shown to inhibit PI3K activity'[1219-1222]. Our findings demonstrate that WHCO1, like the MCF7 and HT29 controls [483, 1223], is more sensitive to PI3K inhibition by LY29 at 10 µM, using the noticeable reduction in pPKB as an indicator of this sensitivity (see Fig. A4). Therefore, because PI3K inhibition was not evident in the remaining HOSCC cell lines, we increased the concentration to 20 µM, as this has been demonstrated to be the highest concentration of LY29 at which PI3K specificity is still maintained[424].

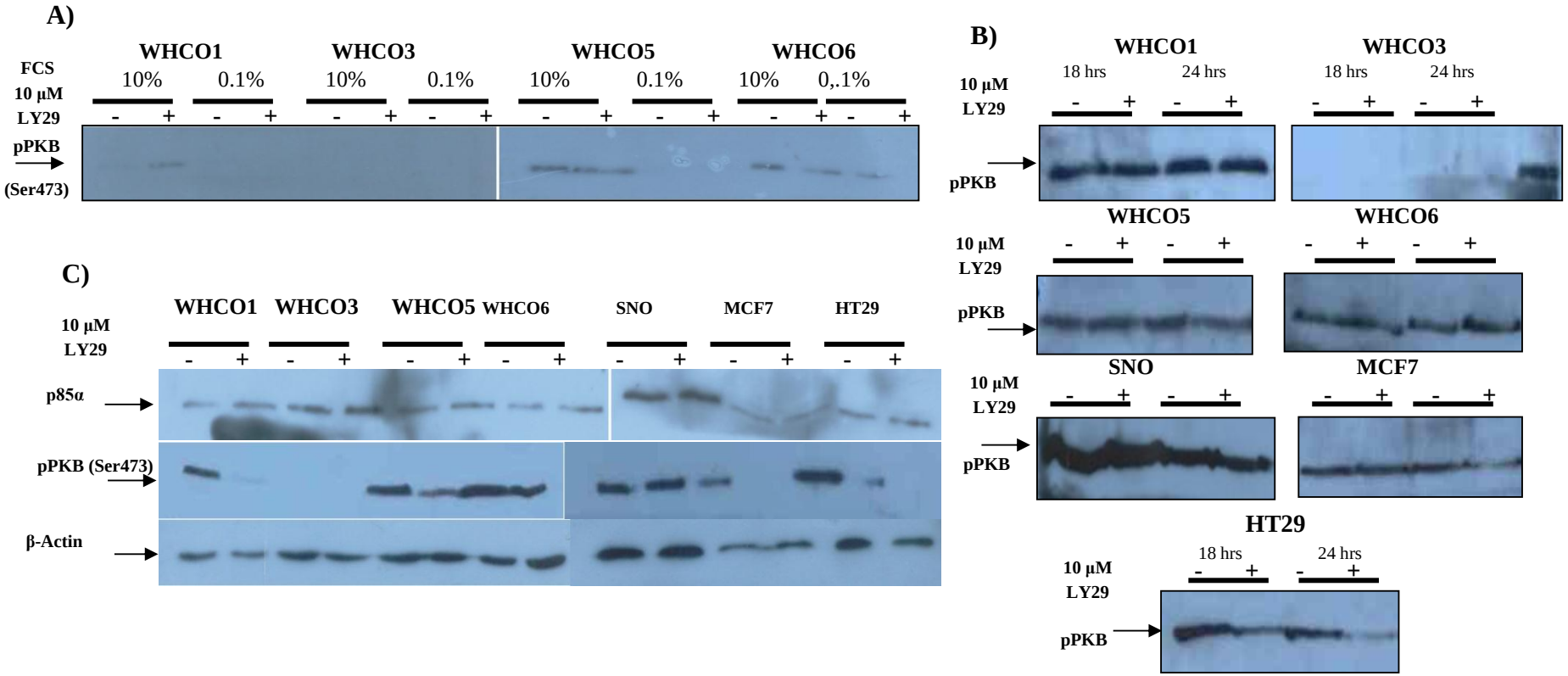
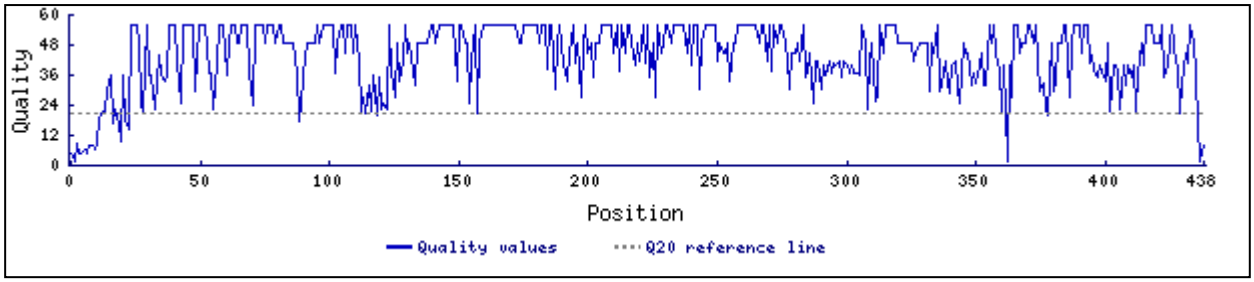


Figure A4: Optimum exposure to LY294002 in HOSCC cells. A) Western blot detection of p-Ser473 in the WHCO1, WHCO3, WHCO5 and WHCO6 HOSCC cell lines treated for 60 mins with 10 µM LY29 (+) supplemented with 10 % FCS and 0.1 % FCS. Controls (-) were untreated but contained the inhibitor vehicle control, DMSO. FCS: Fetal Calf Serum. **B)** 5 HOSCC cells along with the control MCF7 and HT29 cell lines were exposed to for a period of 18 and 24 hrs with (+) and without (-) 10 µM of the PI3K inhibitor, LY29. Thereafter the expression levels of active PI3K (pPKB) was measured through western blotting. As can be seen, long-term exposure to LY29 appears to have no major impact on the active state of PI3K. C=WHCO6 whole cell untreated protein lysate. **C)** Western blot detection of PI3K (p85α) and pPKB prior (-) and subsequent to a 60 min (+) exposure to 10 µM LY29. All untreated (-) were exposed to the LY29 vehicle control, DMSO. Equal loading of treated versus untreated proteins was detected with β-Actin.

1.12 Sequencing results for the PCR amplified N-terminal SH2 domain of the p85α gene transcript.

A)



B)

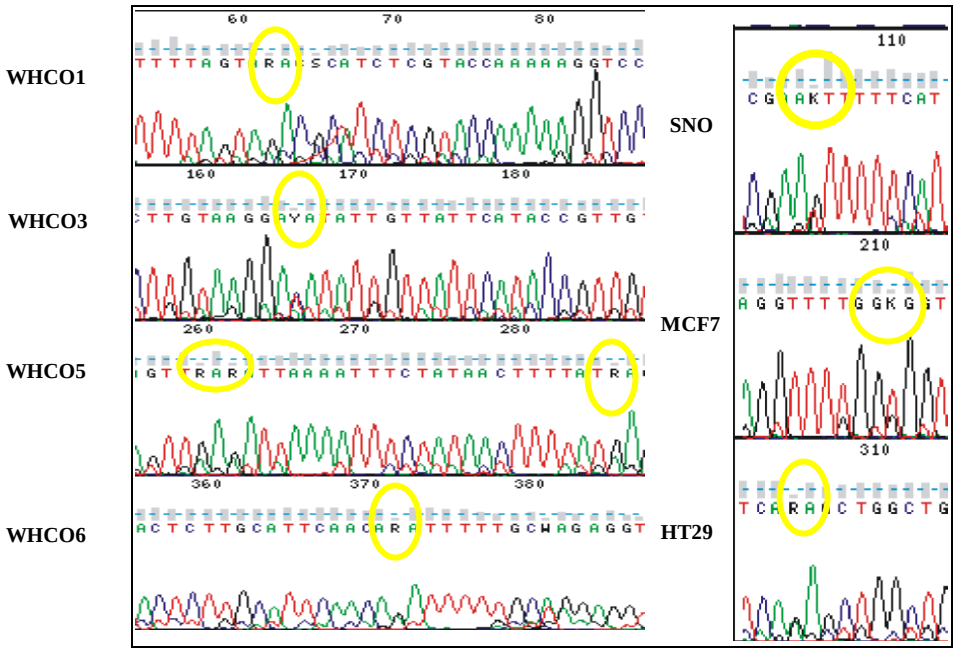


Figure A5: No mutations detected in the nSH2 domain of p85α based on its sequence output and alignment. A) Representative quality graph of the sequencing results. **B)** Representative chromatogram traces. Note: Sequencing was performed in both the forward and reverse direction at Inqaba Biotech SA under the same parameters used during the PCR reactions. The resultant PCR products were evaluated by sequence analysis (Inqaba Biotech) that aligned 97% to the original nucleotide Genbank PIK3R1 cDNA sequence (Accession number: NM_181523) using the BLAST alignment tool, confirming that the band at 430 bp is the nSH2 domain of p85α. No mutations were found in any of the 5 HOSCC cell lines examined. Putative base changes (denoted as Y, K, S, and R in the sequence, highlighted in yellow circles) are negligible. The wild-type (wt) p85α status is confirmed by the wtp85α status in the MCF7 control[1224].

Table A1: Optical density values (mean) of the bands representing whole cell protein expression of PI3K (p85α).

	Whole Cell		Nuclear		Plasma Membrane	
Cell Line	**Mean**	**Mean**	**Mean**	**Std Dev**	**Mean**	**Std Dev**
WHCO1	23.348	23.348	16.499	0.453	38.812	5.901
WHCO3	24.328	24.328	85.627	1.149	22.038	6.399
WHCO5	22.504	22.504	23.237	0.709	59.887	14.301
WHCO6	53.252	53.252	14.736	0.931	78.502	6.999
SNO	82.417	82.417	30.481	2.115	79.41	9.18
MCF7	14.711	14.711	0.047	0.0815	91.471	8.313
HT29	34.078	34.078	13.526	2.168	21.917	6.192

Table A2: Optical density values (mean) of the bands representing total cellular levels of pPKB and pGSK3β.

	pPKB		pGSK3β	
Cell Line	**Mean**	**Std Dev**	**Mean**	**Std Dev**
WHCO1	1.329	1.186	0	0
WHCO3	1	0	5.837	0.497
WHCO5	5.557	0.848	11.134	2.731
WHCO6	26.284	10.053	68.302	1.468
SNO	4.878	0.147	71.444	1.663
HT29	9.305	1.732	0	0
MCF7	7.651	3.973	98.029	1.875

Table A3: Student's *t* test results for pPKB expression following 1 hr exposure to 20 µM of LY29.

	LY29:					
	0		**1Hr**			
Cell Line	**Mean**	**Std Dev**	**Mean**	**Std Dev**	**t**	**P**
WHCO1	67.667	9.38	11.126	14.952	4.358	0.049
WHCO3	0	0	0	0	0	0
WHCO5	94.168	1.021	59.837	0.167	66.873	<0.001
WHCO6	44.759	0.289	11.356	1.53	32.255	<0.001
SNO	63.159	0.527	29.464	6.145	8.887	0.012
HT29	36.439	4.524	1.421	0.496	12.23	0.007
MCF7	99.446	0.518	29.454	0.172	175.661	<0.001

* Indicates levels of significance.

Table A4: Student's *t* test results for pGSK3β expression following 1 hr exposure to 20 µM of LY29.

	LY29:					
	0		**1Hr**			
Cell Line	**Mean**	**Std Dev**	**Mean**	**Std Dev**	**t**	**P**
WHCO1	30.256	0.621	0.837	0.356	54.744	0.001
WHCO3	63.267	12.258	37.922	8.942	7.722	0.016
WHCO5	39.642	17.222	31.72	0.127	0.802	0.507
WHCO6	46.35	0.855	33.977	0.136	24.743	<0.001
SNO	39.436	5.377	29.038	3.226	5.733	0.029
HT29	7.79	0.0323	2.143	0.464	21.024	<0.001
MCF7	99.446	0.518	29.454	0.172	175.661	<0.001

* Indicates levels of significance.

Table A5: Student's *t* test results for PTEN expression following 1 hr exposure to 20 µM of LY29.

	LY29:					
	0		1Hr			
Cell Line	Mean	Std Dev	Mean	Std Dev	t	P
WHCO1	95.117	4.281	38.103	14.759	5.776	0.029
WHCO3	50.466	9.558	20.501	3.2	6.614	0.022
WHCO5	39.272	4.365	61.093	7.28	-11.55	0.007
WHCO6	71.849	0.627	95.108	4.402	-8.365	0.014
SNO	37.32	1.581	26.441	1.108	8.16	0.015
HT29	27.99	0.478	23.44	0.564	7.563	0.017
MCF7	90.7	1.826	58.837	5.82	7.252	0.018

* Indicates levels of significance.

Table A6: Pearson's Correlation Coefficient results for values negatively correlating between pPKB and PTEN expression following 1 hr exposure to 20 µM of LY29.

	Control		20 µM LY29	
	r	P	r	P
WHCO1	-0.453	0.7	-0.682	0.522
WHCO3	0	0	1	0
WHCO5	-0.699	0.507	-0.416	0.965
WHCO6	-0.981	0.125	-0.97	0.156
SNO	0.587	0.601	0.87	0.329
HT29	-0.971	0.154	-0.67	0.533
MCF7	0.285	0.816	-0.00362	0.998

Appendix B

2.1 Co-immunoprecipitation Analysis

2.1.1 Membrane Extraction Buffer

0.5% Triton-X-100
50 mM Tris
150 mM NaCl
1 mM $CaCl_2$
1 mM $MgCl_2$
0.01% Aprotinin
Make up to final volume with dH_2O.
Store at 4 °C

2.1.2 Immunoprecipitation (IP) Buffer

20 mM Tris (pH 8.0)
0.5% NP-40
1.9% NaCl
Make up to 500 ml with dH_2O.
Store at 4 °C

Table B1: One Way RM Anova1 Test results for PI3K (p85α) following EGFR activation.

EGF Expsoure (hours)	WHCO1	WHCO3	WHCO5	WHCO6	SNO	HT29	MCF7
0.5 hrs	0.299	0.133	0.519	0.004	<0.001	0.004	<0.001
1 hr	0.002	0.108	0.967	0.071	<0.001	0.812	0.009
3 hrs	0.155	0.961	0.108	0.222	0.009	0.098	0.009
6 hrs	0.465	0.715	0.05	0.381	<0.001	0.541	0.329
9 hrs	0.092	0.356	0.021	<0.001	<0.001	0.773	0.09
12 hrs	0.002	0.147	<0.001	0.064	<0.001	0.285	0.898

* Indicates levels of significance.

Table B2: Student's t-test for the nuclear and membrane expression of PI3K (p85α) protein following EGFR.

	Nuclear		Membrane	
Cell line	t	P	t	P
WHCO1	8.271	0.014	-14.595	0.005
WHCO3	26.798	0.001	11.448	0.008
WHCO5	-5.119	0.036	-5.215	0.035
WHCO6	2.116	0.169	-3.857	0.061
SNO	31.597	0.001	-5.151	0.036
HT29	-5.942	0.027	-11.653	0.007
MCF7	6.095	0.026	3.886	0.06

*t with 2 degrees freedom. * Indicates levels of significance.

Table B3: P-values obtained from student's t-test for the expression of pPKB following EGFR activation.

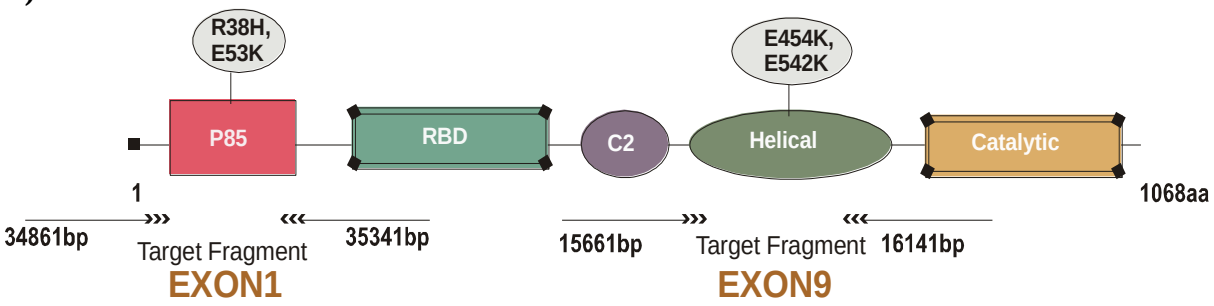
EGF Expsoure	WHCO1	WHCO3	WHCO5	WHCO6	SNO	HT29	MCF7
0 vs 0.5 hrs	0.719	<0.001	0.002	0.001	0.431	<0.001	<0.001
0 vs 1 hr	0.859	<0.001	0.01	0.557	0.024	<0.001	0.783
0 vs 3 hrs	0.001	<0.001	0.002	0.005	0.229	<0.001	0.052
0 vs 6 hrs	<0.001	<0.001	<0.001	0.819	<0.001	0.003	0.164
0 vs 9 hrs	0.059	<0.001	0.002	0.895	0.002	<0.001	0.003
0 vs 12 hrs	0.055	<0.001	0.001	0.261	<0.001	0.018	0.006

*Indicates levels of significance.

2.2 PIK3CA Primer and Sequence Information

2.2.1 Sequence amplifying the p85-binding domain (exon 1) and Helical Domain (exon 9) of the PIK3CA gene:

A)



B)

```
34861 acatactttagatttatgatttttatttagaaagctatttaaGATTACGAAGGTATTGGT
                                               >>>>>>>>>>>>>>>>>>>
34921 TTAGACAGaaatattttagaaagggacaacagttaagctttatggttatttgcattttag
      >>>>>>>>
34981 aataggatattgtatcataccaatttctcgattgaggatcttttcttcacggttgcctac

35041 tggttcaattacttttaaaaagggttgaaaaagccgaaggtcacaaagtcgtcttgtttc

35101 atcaaaaaattcttccctttctgcttcttgagtaacacttacgaaaatgtaagaagattc

35161 atcttgaagaagttgatggaggggtattttcttgcttctttaaatagttcatgctttat

35221 ggttattaatgtagcctcacggaggcattctaaagtcactatcattccatttggtagtaa

35281 acattctactaggattcttgggggcatcaagtggatgccccacagttcaCCTGATGATGG
                                               <<<<<<<<<<<
35341 TCGTGGAGgcat
      <<<<<<<<
```

C)

```
15661 tatgatttCCACAAATATCAATTTACAACCATTGttttaaaaaggcaatgtttatagt
            >>>>>>>>>>>>>>>>>>>>>>>>>>>
15721 ttaaaaatcatgtaaattctgctttatttattccaataggtatggtaaaaacatgctgag
15781 atcagccaaattcagttatttttctgtaataaagaaaaagaaacagagaatctccattt
15841 tagcacttacctgtgactccatagaaaatctttctcctgctcagtgatttcagagagagg
15901 atctcgtgtagaaattgctttgagctgttctttgtcattttcccttaattcattgtctct
15961 agctagtctgttactctgtaaaataaaataatatcttatatagctttctttgtcatattt
16021 ttcccctctggattcacagatgatttacagaaaaagcaaatacattttcaataaatttta
16081 cattgctaattaactgttgtaaaataatttattttcattgcaagactttatttttCAGAGA
                                                        <<<<<<
16141 CAGGAAAGAACCAATC
      <<<<<<<<<<<<<<<<
```

Figure B1:**A)** Schematic diagram of the PIK3CA gene transcript highlighting the p85α-binding (exon 1) and helical domain (exon 9) intended to amplify during the PCR reaction. **B)** Highlighting region to be amplified on exon 1 using published primers[476], highlighted in yellow (reverse primers) and green (forward primers) within the sequence. **C)** Showing the region to be amplified on Exon 9 using published primers (see above), forward primers highlighted in turquoise and reverse primers highlighted in purple.

The primer parameters:

Exon 1:

	Primer Length	GC%	Melting Temperature (°C)
Forward Primer:	19 bp	57.89	62.32
Reverse Primer:	26 bp	38.46	61.44
PCR Product length:	420 bp		

Exon 9:

Forward Primer:	22 bp	45.45	60.81
Reverse Primer:	26 bp	30.77	58.28
PCR Product length:	450 bp		

The hairpin formation and homo-dimer or primer self-dimer was calculated utilizing the OligoAnalyzer (http://www.idtdna.com/analyzer/Applications/OligoAnalyzer):

Exon 1:

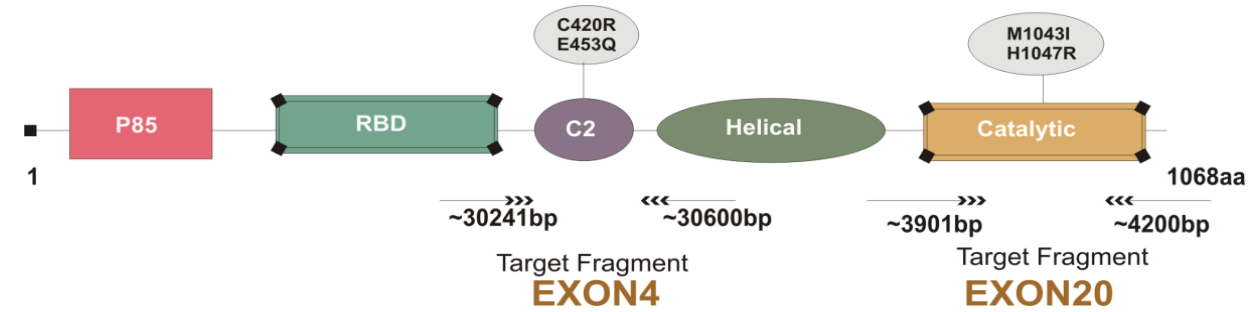
	Hairpin Formation	Homo-Dimer Formation
Forward Primer:	ΔG= 0.31 kcal/mole Melting temperature of 19.9 °C	ΔG= -3.61 kcal/mole with 2 bp
Reverse Primer:	ΔG= -0.12 kcal/mole Melting temperature of 26.4 °C	ΔG= -2.3 kcal/mole with 3 bp

Exon 9:

Forward Primer:	ΔG= -0.15 kcal/mole Melting temperature of 27.5 °C	ΔG= -3.07 kcal/mole with 2 bp
Reverse Primer:	ΔG= -0.41 kcal/mole Melting temperature of 30 °C	ΔG= -5.37 kcal/mole with 4 bp

2.2.2 Sequence amplifying the C2 domain (exon 4) and Kinase Domain (exon 20) of the PIK3CA gene:

A)



B)

```
30241 tcttgatatatttttacattCGGAGATTTGGATGTTCTCCtaaccatctgaaaacatact
                         >>>>>>>>>>>>>>>>>>>>
30301 acaggtcaacagattactgtatagttcaagaaaaaggttatctaaaataatttctataaa
30361 ataataagcatcagcatttgactttaccttatcaatgtctcgaatatttacattcacgta
30421 ggttgcacaaagaatttttattctgagtgcactatttataacccaaagggattttgtaga
30481 tgtttctccattcatatatggtgtagctgtggaaatgcgtctggaataagatggcattgt
30541 aaaaCAGTCCATTGGCAGTTGAGAataaaggctttctttagccatcaacatcaaattggg
          <<<<<<<<<<<<<<<<<<
```

C)

```
 3901 aaccaaatttttttcttcttgtgatccaaaaagtgtccaaaatctatatgaaacagctttc
 3961 aaaaataagaaattatgttatagtttgatatatgcagatacaaaatgtcttgaataaatt
 4021 aagaacaccaaaacattttaaacagagaaaaccattacttgtccatcgtctttcaccatg
 4081 atgttactattgtgacgatctccaattcccaaaatgaaggtagctacacagtatccagca
 4141 catgaacgtgtaaacaggtcaatggctgcatcatatctacaaagaataaacacctcatga
 4201 gtagtatggaaatatagtgattcaggccaacttgagaaaagaaaacagggtgcaagtttc
```

Figure B2: A) Schematic diagram of the PIK3CA gene transcript highlighting the C2 domain (exon 4) and kinase domain (exon 20) intended to amplify during the PCR reaction. **B)** Highlighting region to be amplified on exon 4 using published primers (see above), highlighted in yellow (reverse primers) and green (forward primers) within the sequence. **C)** Showing the region to be amplified on exon209 using published primers forward primers highlighted in turquoise and reverse primers highlighted in purple.

The primer parameters:

Exon 4A:

	Primer Length	GC%	Melting Temperature (°C)
Forward Primer:	22 bp	40.91	58.95
Reverse Primer:	20 bp	50	60.4
PCR Product length:	550 bp		

Exon 4B:

Forward Primer:	20 bp	50	60.4
Reverse Primer:	20 bp	50	60.4
PCR Product length:	350 bp		

Exon 20:

Forward Primer:	21 bp	42.86	58.66
Reverse Primer:	20 bp	50	60.4
PCR Product length:	500 bp		

The hairpin formation and homo-dimer or primer self-dimer was calculated utilizing the OligoAnalyzer (http://www.idtdna.com/analyzer/Applications/OligoAnalyzer):

Exon 4A:

	Hairpin Formation	Homo-Dimer Formation
Forward Primer:	ΔG= -0.14 kcal/mole Melting temperature of 26.8 °C	ΔG= -6.3 kcal/mole with 4 bp
Reverse Primer:	ΔG= -2.09 kcal/mole Melting temperature of 42.1°C	ΔG= -7.82 kcal/mole with 5 bp

Exon 4B:

Forward Primer: ΔG= 0.09 kcal/mole ΔG= -5.02 kcal/mole with 3 bp

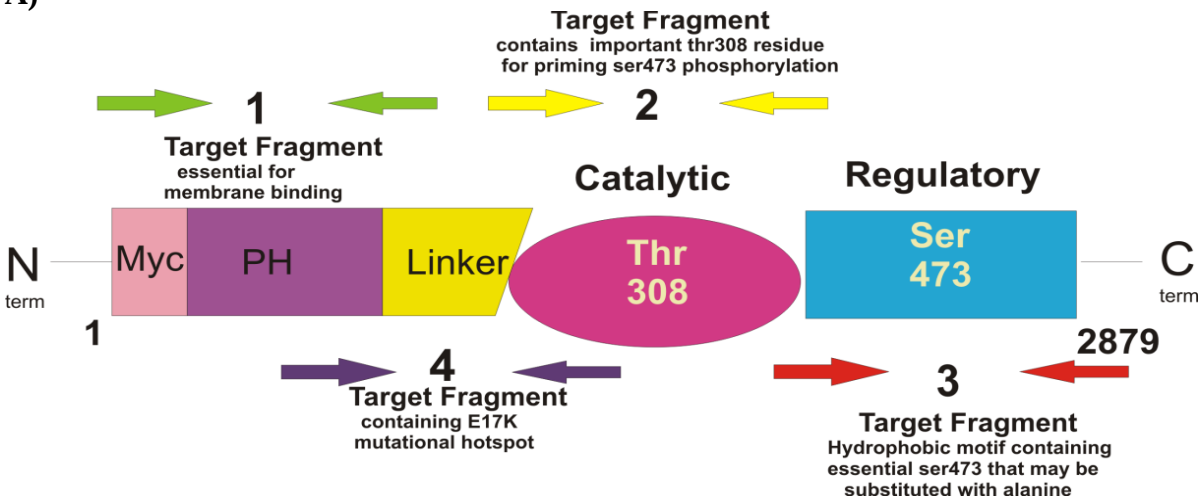
Melting temperature of 23.3 °C
Reverse Primer: ΔG= -2.09 kcal/mole ΔG= -7.82 kcal/mole with 5 bp
Melting temperature of 42.1 °C

Exon 20:

Forward Primer: ΔG= 0.87 kcal/mole ΔG= -1.95 kcal/mole with 2 bp
Melting temperature of 6.7 °C
Reverse Primer: ΔG= -1.49 kcal/mole ΔG= -7.05 kcal/mole with 4 bp
Melting temperature of 38.9 °C

2.3 PKB1 Primer and Sequence Information

A)



B) PH Domain (1):

```
181 ggggtttctcccaggaggtttttgggcttgcgctggagGGCTCTGGACTCCCGTTTgcgc
                                          >>>>>>>>>>>>>>>>
241 cagtggcctgcatcctggtcctgtcttcctcatgtttgaatttctttgctttcctagtct
301 ggggagcagggaggagccctgtgccctgtcccaggatccatgggtaggaacaccatggac
361 agggagagcaaacggggccatctgtcaccaggggcttagggaaggccgagccagcctggg
421 tcaaagaagtcaaaggggctgcctggaggaggcagcctgtcagctggtgcatcagaggct
481 gtggccaggccagctgggctcggggagcgccagcctgagaggagcgcgtgagcgtcgcgg
541 gagcctcgggcaccatgagcgacgtggctattgtgaaggagggttggctgcacaaacgag
601 gggagtacatcaagacctggcggccacgctacttcctcctcaagaatgatggcaccttca
661 ttggctacaaggagcggccgcaggatgtggaccaacgtgaggctcccctcaacaacttct
721 ctgtggcgcagtgccagctgatgaagacggagcggccccggcccaacaccttcatcatcc
781 gctgcctgcagtggaccACTGTCATCGAACGCACCTtccatgtggagactcctgaggagc
                    <<<<<<<<<<<<<<<<<<
```

C) Thr308 (2):

1201 ctttccagacccacgaccgcctctgctttgtcatggagtacgccaacgggggCGAGCTGT
>>>>>>>>>

1261 TCTTCCACCTGTcccgggagcgtgtgttctccgaggaccgggcccgcttctatggcgctg
>>>>>>>>>>>>

1321 agattgtgtcagccctggactacctgcactcggagaagaacgtggtgtaccgggacctca

1381 agctggagaacctcatgctggacaaggacgggcacattaagatcacagacttcgggctgt

1441 gcaaggaggggatcaaggacggtgccaccatgaagacctttgcggcacacctgagtacc

1501 tggcccccgaggtgctggaggacaatgactacggccgtgcagtggactggtgggggctgg

1561 gcgtggtcatgtacgagatgatgtgcggtcgcctgcccttctacaaccaggaccatgaga

1621 agcttttgagctcatcctcatggaggagatccgcttcccgcgcacgcttggtcccgagg

1681 ccaagtccttgcTTTCAGGGCTGCTCAAGAAGgaccccaagcagaggcttggcgggggct

D) Ser473 (3):

121 ttggccaaatGAATGAACCAGATTCAGACCGGcaggggcgctgtggtttaggaggggcct
>>>>>>>>>>>>>>>>>>>>>>>>>

1261 tcttccacctgtcccgggagcgtgtgttctccgaggaccgggcccgcttctatggcgctg

1321 agattgtgtcagccctggactacctgcactcggagaagaacgtggtgtaccgggacctca

1381 agctggagaacctcatgctggacaaggacgggcacattaagatcacagacttcgggctgt

1441 gcaaggaggggatcaaggacggtgccaccatgaagacctttgcggcacacctgagtacc

1501 tggcccccgaggtgctggaggacaatgactacggccgtgcagtggactggtgggggctgg

1561 gcgtggtcatgtacgagatgatgtgcggtcgcctgcccttctacaaccaggaccatgaga

1621 agcttttgagctcatcctcatggaggagatccgcttcccgcgcacgcttggtcccgagg

1681 ccaagtccttgctttcagggctgctcaagaaggaccccaagcagaggcttggcgggggct

1741 ccgaggacgcCAAGGAGATCATGCAGCATCGcttctttgccggtatcgtgtggcagcacg
<<<<<<<<<<<<<<<<<<<<<<<

E) Linker Domain (4):

841 gggaggagtggacaaccgccATCCAGACTGTGGCTGACGgcctcaagaagcaggaggagg
>>>>>>>>>>>>>>>>>>>>>

901 aggagatggacttccggtcgggctcacccagtgacaactcaggggctgaagagatggagg

961 tgtccctggccaagcccaagcaccgcgtgaccatgaacgagtttgagtacctgaagctgc

1021 tgggcaagggcactttcggcaaggtgatcctggtgaaggagaaggccacaggccgctact

1081 acgccatgaagatcctcaagaaggaagtcatcgtggccaaggacgaggtggcccacacac

1141 tcaccgagaaccgcgtcctgcagaactccaggcacccctcctcacagccctgaagtact

1201 ctttccagacccacgaccgcctctgcTTTGTCATGGAGTACGCCAAcgggggcgagctgt
<<<<<<<<<<<<<<<<<<<<<<

1261 tcttccacctgtcccgggagcgtgtgttctccgaggaccgggcccgcttctatggcgctg

See next page for legend.

Figure B3: A) Schematic representation of the PKBα gene highlighting the four regions to be amplified during the PCR reaction; the PH domain (1), the catalytic domain (2), the hydrophobic motif (3), and the Linker domain (4). Figures B-E show the specific target sequence designed for the PCR amplification of the PH domain **(B)**, the catalytic domain **(C)**, the hydrophobic motif **(D)**, and Linker domain **(E)** respectively. Primers specific for these regions were generated using the web-based interactive primer design program; Primer3.

The primer parameters:

	Primer Length	GC%	Melting Temperature (°C)
PH Domain:			
Forward Primer:	18 bp	61.11	62.18
Reverse Primer:	20 bp	50	60.4
PCR Product length:	650 bp		
Linker Domain:			
Forward Primer:	19 bp	57.89	62.32
Reverse Primer:	20 bp	45	58.35
PCR Product length:	450 bp		
Ser473:			
Forward Primer:	22 bp	50	62.67
Reverse Primer:	20 bp	50	60.4
PCR Product length:	319 bp		
Thr308:			
Forward Primer:	20 bp	55	62.45
Reverse Primer:	20 bp	50	60.4
PCR Product length:	450 bp		

The hairpin formation and homo-dimer or primer self-dimer was calculated utilizing the OligoAnalyzer (http://www.idtdna.com/analyzer/Applications/OligoAnalyzer):

	Hairpin Formation	**Homo-Dimer Formation**
PH Domain:		
Forward Primer:	ΔG= 0.17 kcal/mole Melting temperature of 22.1 °C	ΔG= -4.64 kcal/mole with 4 bp
Reverse Primer:	ΔG= 0.58 kcal/mole Melting temperature of 17.1 °C	ΔG= -6.76 kcal/mole with 5 bp
Linker Domain:		
Forward Primer:	ΔG= -1.01 kcal/mole Melting temperature of 39.2 °C	ΔG= -5.02 kcal/mole with 3 bp
Reverse Primer:	ΔG= -0.16 kcal/mole Melting temperature of 27.7 °C	ΔG= -5.38 kcal/mole with 4 bp
Ser473:		
Forward Primer:	ΔG= -1.36 kcal/mole Melting temperature of 38.4 °C	ΔG= -9.75 kcal/mole with 4 bp
Reverse Primer:	ΔG= 0.45 kcal/mole Melting temperature of 16.9 °C	ΔG= -7.05 kcal/mole with 4 bp
Thr308:		
Forward Primer:	ΔG= 0.49 kcal/mole Melting temperature of 18 °C	ΔG= -1.95 kcal/mole with 2 bp
Reverse Primer:	ΔG= -0.75 kcal/mole Melting temperature of 35.7 °C	ΔG= -3.55 kcal/mole with 4 bp

2.4 PCR amplification of exon 4A, exon 4B and exon 20 of the PIK3CA gene.

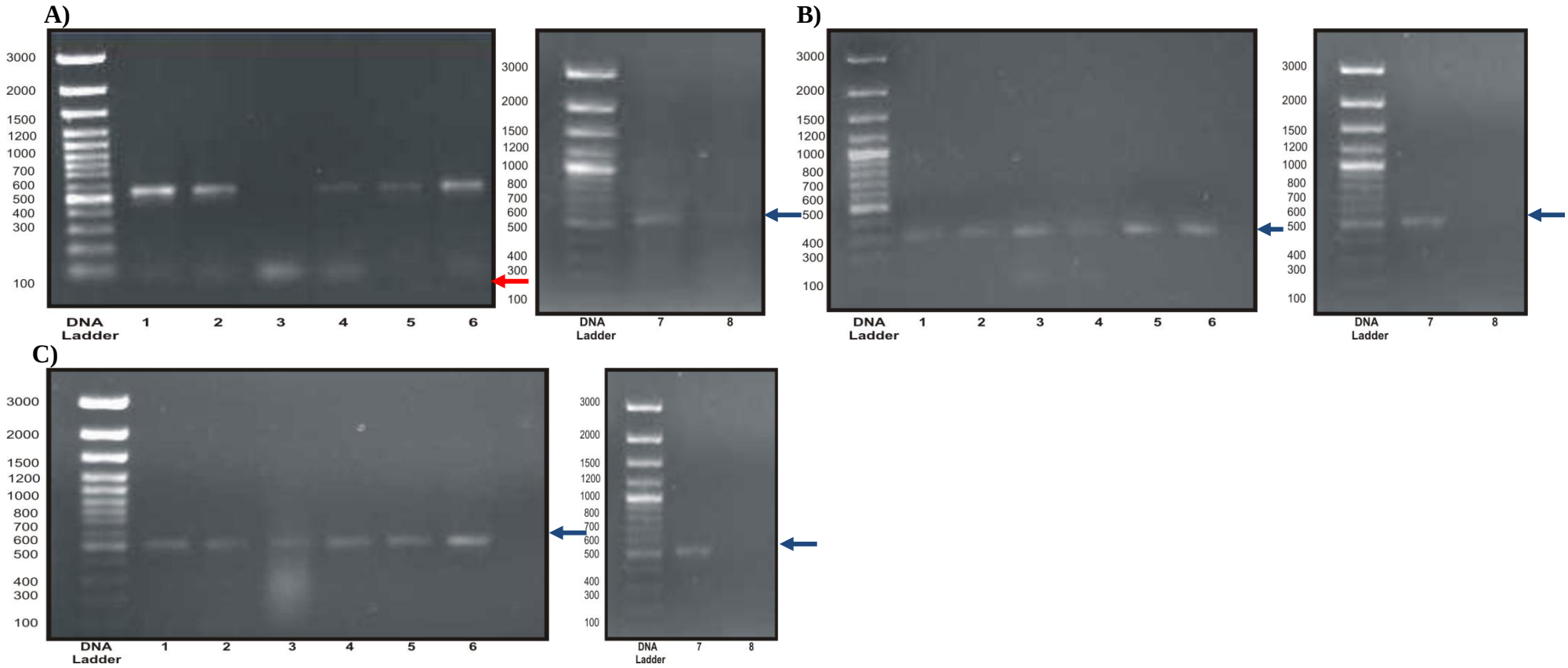
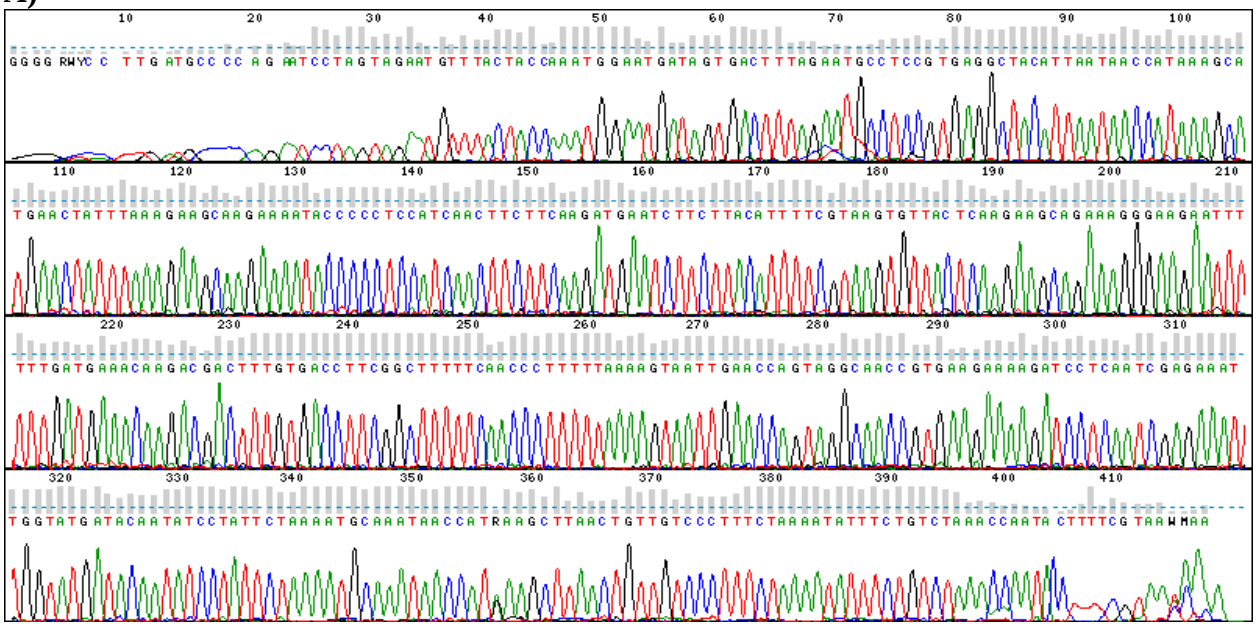


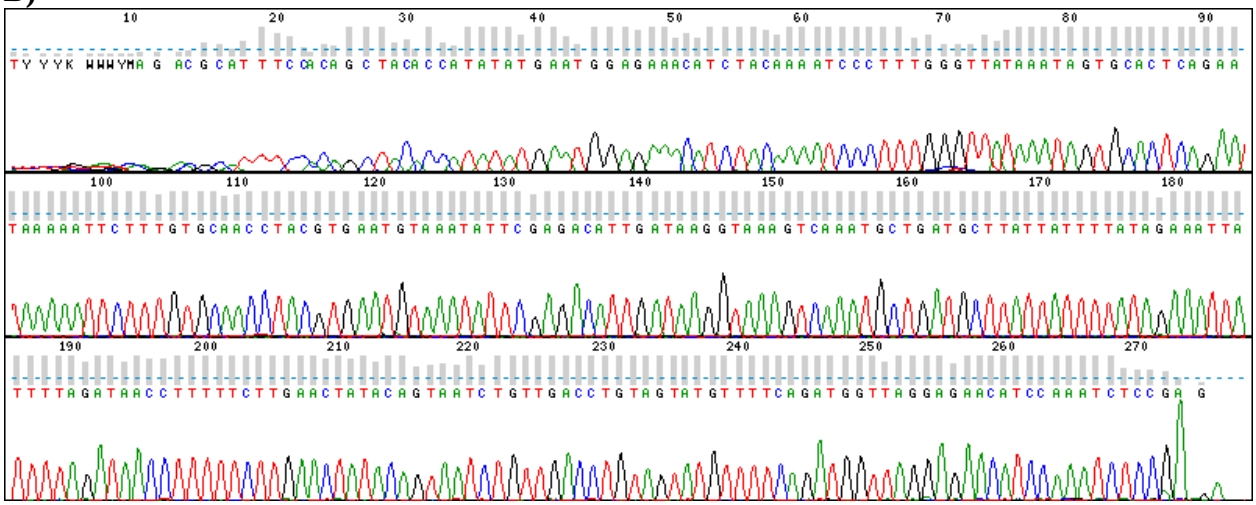
Figure B4: Amplification of Exon 4 (C2 domain) and Exon 20 (kinase domain) of the PIK3CA gene in HOSCC cells. A) The presence of a PCR fragment at 550 bp is indicative of a positive amplification of the larger splice fragment of Exon 4 (Exon 4A), indicated by the blue arrow, and the smaller splice fragment, Exon 4B **(B)**, at 350 bp. The absence of a PCR fragment in lane 8 or the template-free control confirms the specificity of the reaction. Red arrow indicates primer dimer formation. **C)** The presence of a 500 bp PCR amplified fragment is indicative of Exon 20. The absence of a PCR fragment in lane 8 or the template-free control confirms the specificity of the reaction. Lanes 1-8: WHCO1, WHCO3, WHCO5, WHCO6, SNO, MCF7, HT29 and template-free control.

2.5 Representative chromatogram of sequencing results for PIK3CA.

A)



B)



C)

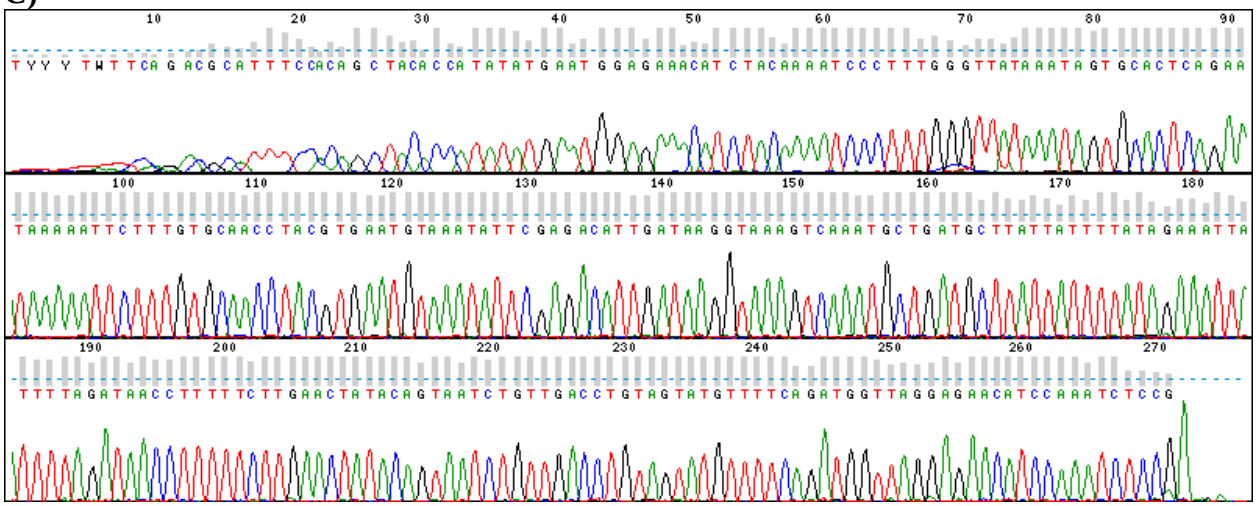


Figure B5: PIK3CA chromatogram traces. A) Exon 1 (p85α-binding domain) **(B)**, Exon 4A and 4B (C2 domain) **(C)**, and Exon 20 (Catalytic domain).

2.6 PCR amplification of PKB1 gene.

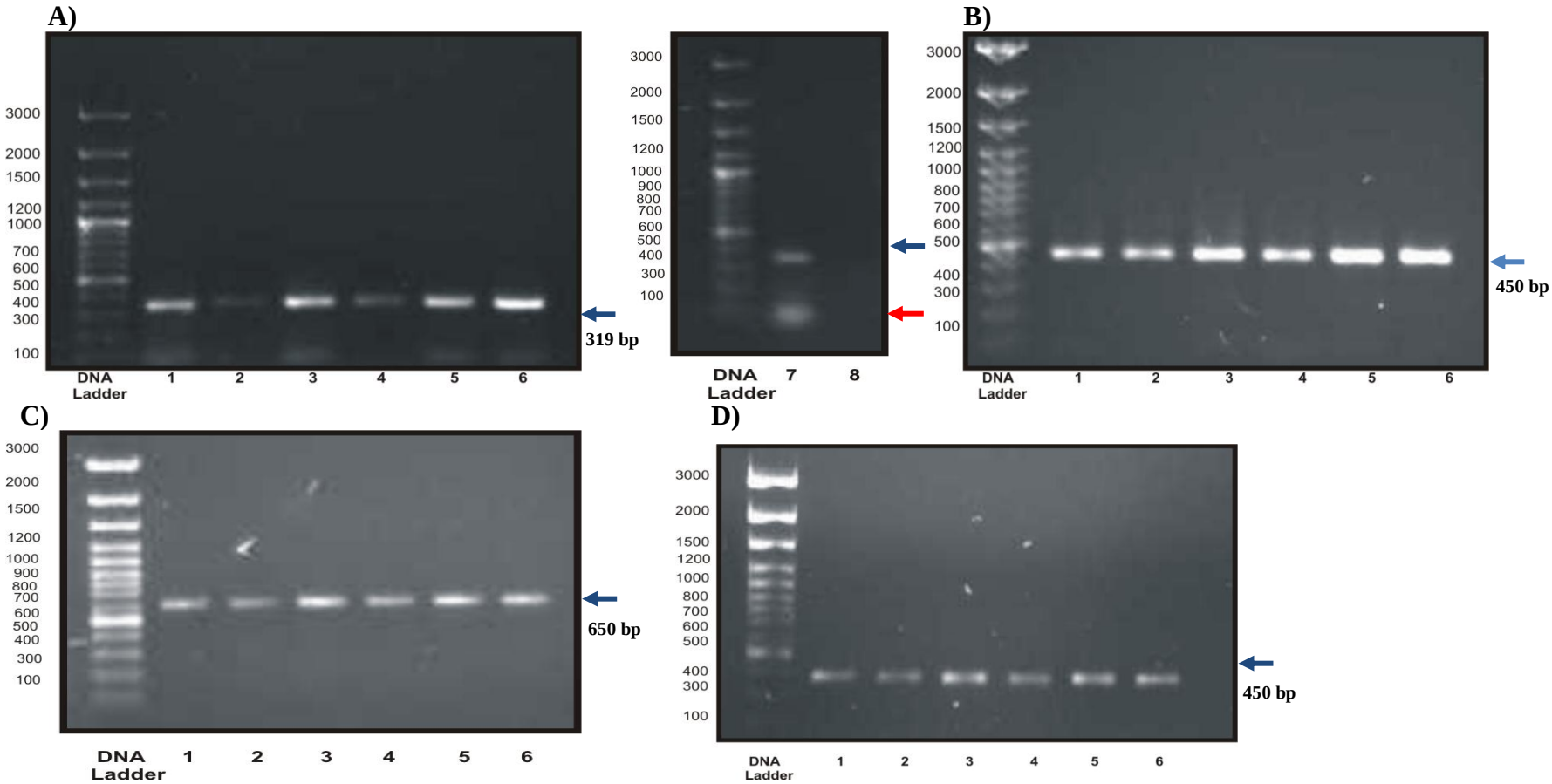
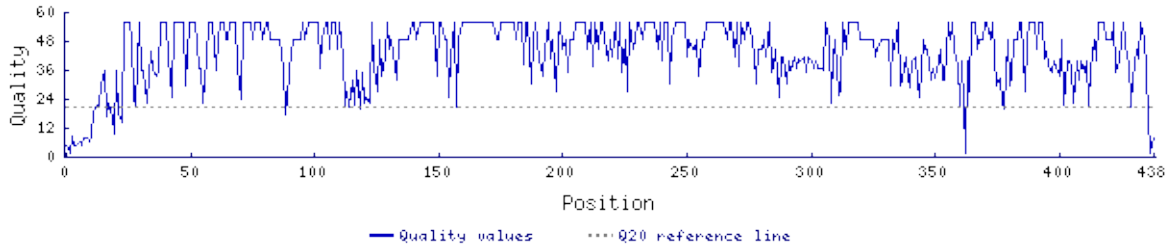


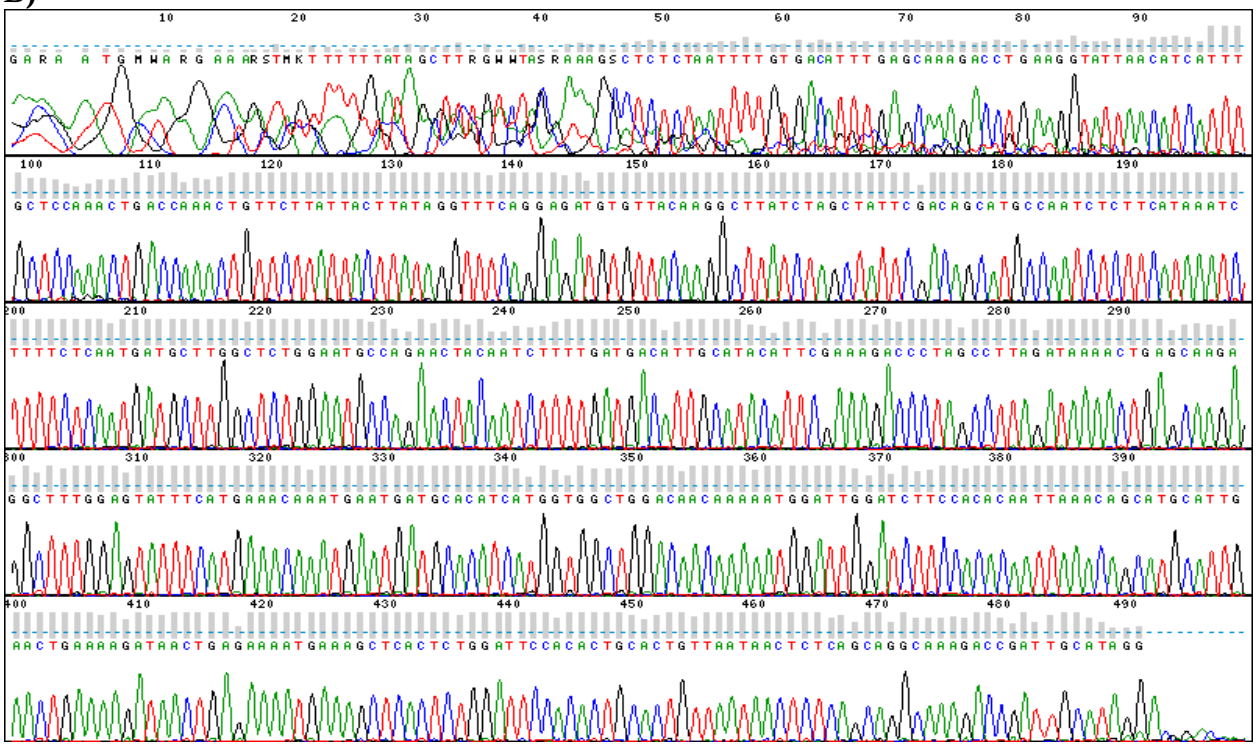
Figure B6: The PKB1 transcript is not impaired in HOSCC cells. A) The presence of a PCR fragment at 319 bp is indicative of the successfully amplified region containing Ser473. **B)** PCR analysis of the region pertaining to Thr308, showing its successful amplification producing a 450 bp fragment. The absence of a band in lane 8 (template-free) confirms the specificity of the PCR reaction. Red arrow is demonstrative of primer-dimer formation. Lanes 1-8: WHCO1, WHCO3, WHCO5, WHCO6, SNO, MCF7, HT29 and template-free control. **C)** PCR fragment at 650 bp is indicative of the successful amplification of the PH domain of the PKB1 transcript. **D)** The presence of a 450 bp fragment reveals that a positive amplification of the Linker domain of the PKB1 transcript.

2.7 Representative chromatogram of sequencing results for PKB1.

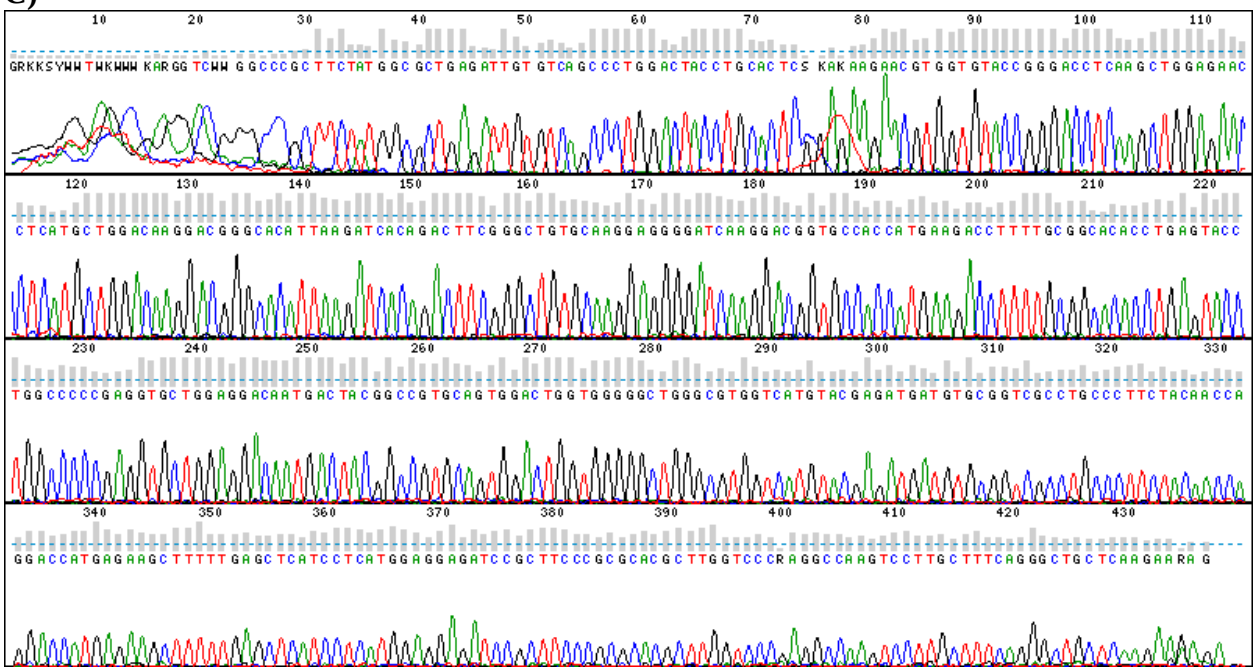
A)



B)

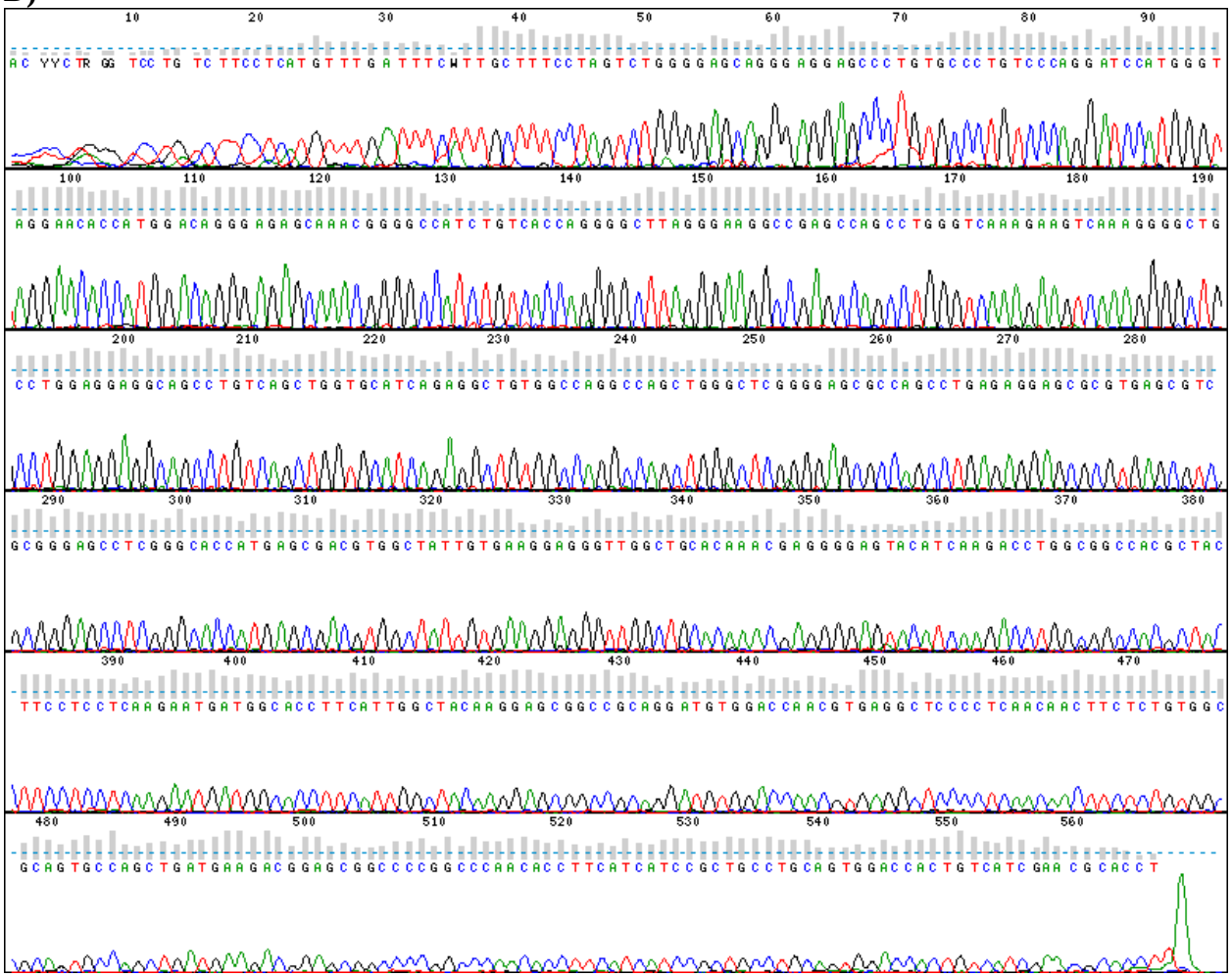


C)



See next page for legend.

D)



E)

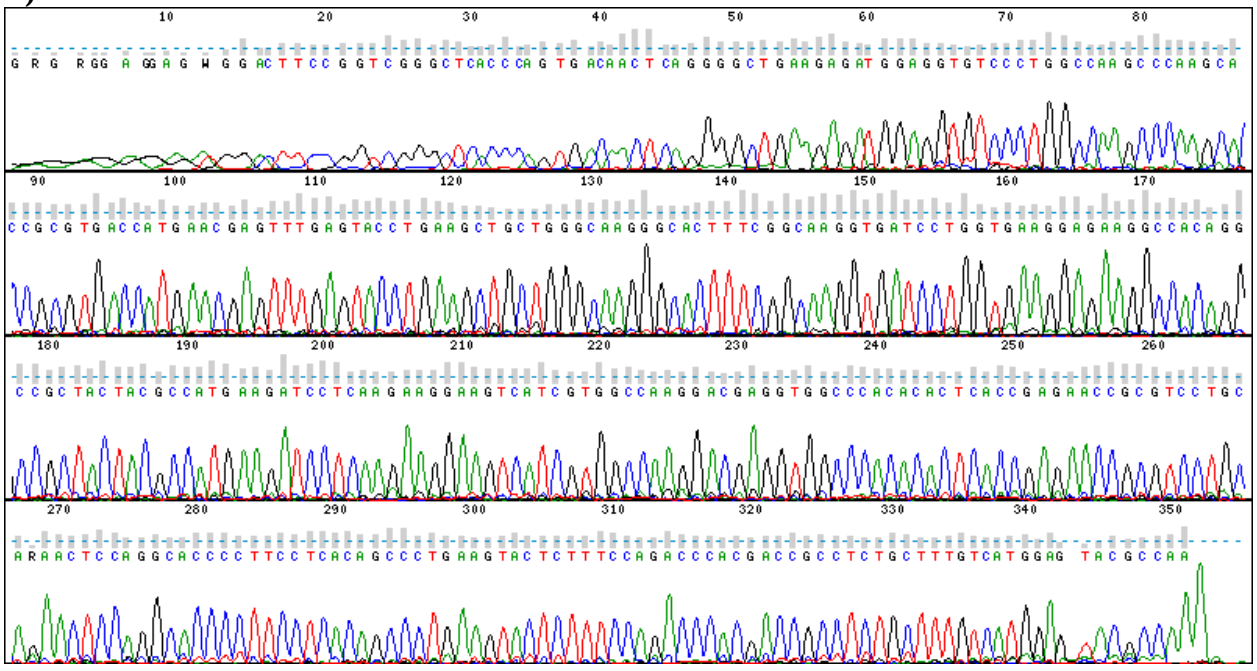


Figure B7: PKB Sequencing Traces. A) Representative quality graph of the sequencing results. Representative sequence chromatogram traces of the region amplifying Ser473 **(B)**, Thr308 **(C)**, PH domain **(D)**, and Linker domain **(E)**. Note: Sequencing was performed in both the forward and reverse direction at Inqaba Biotech SA under the same parameters used during the PCR reactions.

Appendix C

3.1 Optimization for ideal Okadaic Acid (OA) concentration and time exposure.

Diverse concentrations of OA ranging from as little as 2 nM[562] to as high as 10 μM[550] have been used in various cellular systems, each specifically titrated for the respective objectives of the authors[554,1225]. Since PP2A is responsible for dephosphorylating PKB on Ser473, the WHCO6 cell lines was chosen as a representative for the optimization of OA due to their highest pPKB levels (see Chapter 2, Section 2.3.5). Furthermore, the HT29 cell line was included as a control for two reasons; 1) PP2A inhibition was previously established post 1 hr and at 100 nM OA[1226], evidenced by decreased pPKB levels, 2) OA concentrations > 100 nM were shown to reduce HT29 cell viability[1227,1228]. According to our data (Figure C1), 50 nM of OA did not induce pPKB levels in the WHCO6 cell line. Therefore, by increasing the OA concentration to 100 nM, and using the HT29 cell line to control for this, we significantly inhibited PP2A activity following a 1 hr incubation (P=0.001), evidenced by pPKB levels (Figure C1). As our purpose was not to induce apoptosis, we were able to link this inhibition to the presence of pro-caspase-3 (inactive), which was only detected subsequent to a 3 hr exposure to OA (see Figure C1). Therefore, a 1 hr exposure to OA at a concentration of 100 nM deemed sufficient to inhibit PP2A in HOSCC cells.

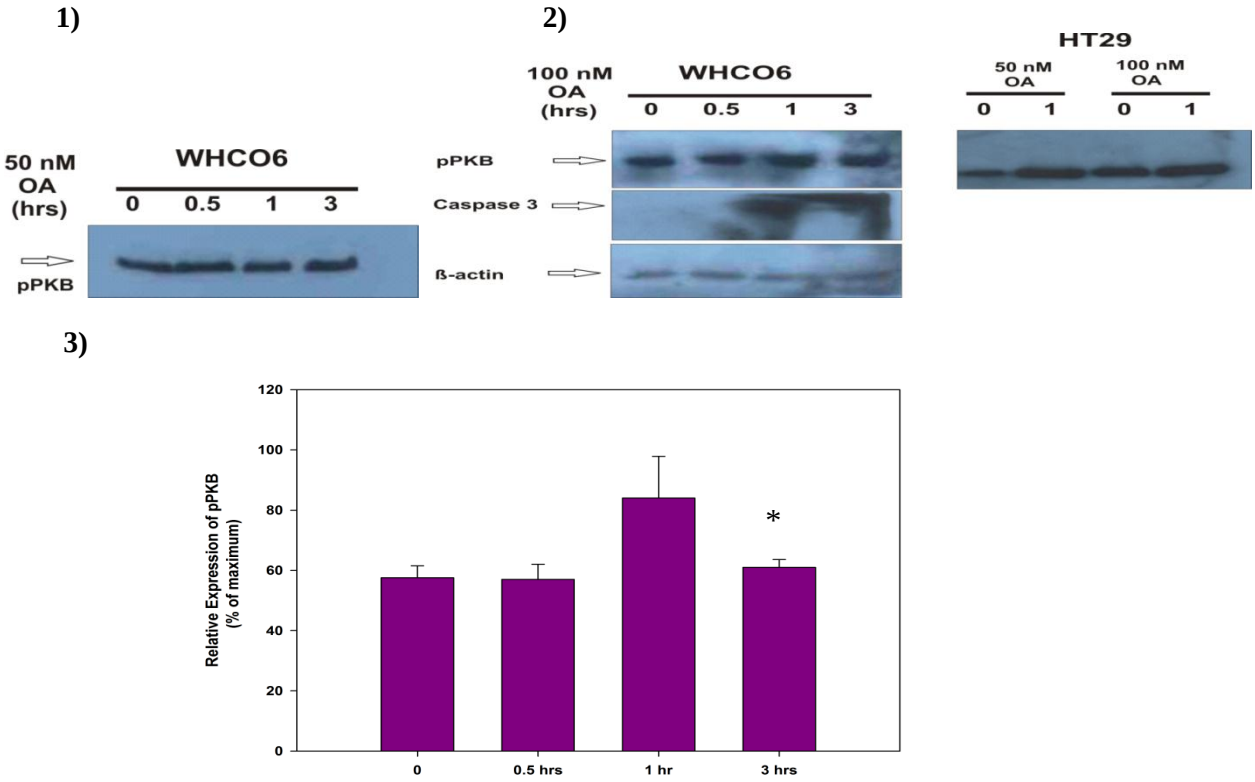


Figure C1: Optimization of exposure to Okadaic Acid (OA) in HOSCC cells. 1) Western blot analysis of pPKB expression in WHCO6 cell line exposed to 50 nM of OA at various intervals (0.5, 1, and 3 hrs). **2)** Protein levels of pPKB and caspase-3 in the WHCO6 cell line subsequent to 100 nM OA exposure at various time intervals (0.5, 1, and 3 hrs), as well as a 1 hr exposure to 50 and 100 nM of OA in the HT29 control. **3)** Three independent treatments of the WHCO6 cell line to 100 nM OA were quantified through densitometry. An increase in pPKB levels was verified following a 1 hr exposure to OA.

3.2 Okadaic Acid (OA) Stock

10 µg Okadaic Acid (Sigma)
Make up to final volume with DMSO
Store at -20 °C

3.3 Non-reducing Buffer

100 mM Tris-HCL (pH 7.0)
150 mM NaCl
1 mM EDTA
50 mM N-Ethylmaleimide (NEM)
4% Triton-X-100
Make up to final volume with dH_2O.

Table C1:Student's *t* test results for pPKB expression following 1 hr exposure to 100 nM of OA.

	OA:					
	0		1Hr			
Cell Line	Mean	Std Dev	Mean	Std Dev	t	P
WHCO1	53.815	9.535	47.399	9.671	28.408	0.001
WHCO3	0.0568	0.0568	0.0568	0.0568	0	1
WHCO5	53.488	8.62	53.13	9.431	0.349	0.761
WHCO6	33.91	5.575	43.301	4.299	-1.705	0.23
SNO	84.691	8.721	89.304	11.402	-2.893	0.102
HT29	36.439	4.524	1.421	0.496	12.23	0.007
MCF7	8.606	0.928	5.972	1.66	5.962	0.027

* Indicates levels of significance. *t with 2 degrees freedom

Table C2: Student's *t* test results for pGSK3β expression following 1 hr exposure to 100 nM of OA.

	OA:					
	0		1Hr			
Cell Line	Mean	Std Dev	Mean	Std Dev	t	P
WHCO1	13.347	3.122	14.238	4.355	-0.447	0.699
WHCO3	6.928	1.443	8.156	1.909	-3.739	0.065
WHCO5	10.845	1.537	14.116	4.35	-1.996	0.184
WHCO6	34.477	4.81	39.076	2.166	-3.008	0.095
SNO	70.869	3.085	94.06	4.166	-5.555	0.031
HT29	0.0484	0.0484	4.401	2.171	-3.457	0.074
MCF7	96.489	3.138	79.919	3.507	5.546	0.031

* Indicates levels of significance. *t with 2 degrees freedom

Table C3: Student's *t* test results for PTEN expression following 1 hr exposure to 100 nM of OA.

	OA:					
	0		1Hr			
Cell Line	Mean	Std Dev	Mean	Std Dev	t	P
WHCO1	54.934	1.219	43.708	2.056	5.939	0.027
WHCO3	46.763	1.611	44.68	4.133	1.389	0.299
WHCO5	42.971	4.165	48.964	4.569	-4.63	0.044
WHCO6	26.092	3.035	35.188	3.048	-2.595	0.122
SNO	36.549	2.185	41.375	0.803	-5.426	0.032
HT29	36.547	0.586	34.209	1.68	3.322	0.08
MCF7	95.022	4.845	42.913	3.523	11.238	0.008

* Indicates levels of significance. *t with 2 degrees freedom.

Table C4: Student's *t* test results for PI3K (p85α) expression following 1 hr exposure to 100 nM of OA.

	OA:					
	0		1Hr			
Cell Line	Mean	Std Dev	Mean	Std Dev	t	P
WHCO1	17.092	2.502	12.415	3.684	3.398	0.077
WHCO3	35.748	1.825	24.231	3.661	7.672	0.017
WHCO5	40.218	4.176	54.702	11.807	-3.09	0.091
WHCO6	46.183	2.878	30.628	6.412	4.906	0.039
SNO	86.171	7.09	97.467	2.865	-2.712	0.113
HT29	74.257	8.28	68.882	13.378	0.431	0.708
MCF7	44.109	7.038	84.426	10.211	-18.394	0.003

* Indicates levels of significance. *t with 2 degrees freedom

Table C5: Student's *t* test results for β-catenin expression following 1 hr exposure to 100 nM of OA.

	OA:					
	0		1Hr			
Cell Line	Mean	Std Dev	Mean	Std Dev	t	P
WHCO1	51.268	4.623	70.488	7.234	-9.728	0.01
WHCO3	95.286	4.277	50.201	6.276	7.439	0.018
WHCO5	59.831	3.963	51.796	5.902	3.759	0.064
WHCO6	32.149	5.307	39.014	2.749	-2.34	0.144
SNO	19.273	2.702	13.956	1.366	3.712	0.066
HT29	11.255	1.585	7.361	1.724	5.447	0.032
MCF7	13.528	3.949	9.303	2.281	4.079	0.055

* Indicates levels of significance. *t with 2 degrees freedom

Table C6: Optical density values (mean) of the bands representing whole cell and nuclear protein expression of PTEN.

	Whole Cell		Nuclear	
Cell Line	**Mean**	**Std Dev**	**Mean**	**Std Dev**
WHCO1	47.057	2.21	85.054	5.133
WHCO3	27.726	2.186	72.799	5.12
WHCO5	30.125	0.562	81.767	6.478
WHCO6	32.946	1.891	0.196	0.196
SNO	28.932	1.312	21.284	2.682
HT29	22.193	2.462	46.809	6.827
MCF7	97.802	2.911	88.966	10.215

Table C7: One Way RM Anova results for PTEN, pPKB, pGSK3β, PI3K (p85α) and β-catenin expression following PTEN oxidation induced by 10, 30, and 60 mins exposure to 1 mM H_2O_2.

PTEN:							
H_2O_2 Exposure	WHCO1	WHCO3	WHCO5	WHCO6	SNO	HT29	MCF7
0 vs. 10 mins	<0.001	0.008	0.482	0.082	0.002	0.403	0.001
0 vs. 30 mins	<0.001	<0.001	<0.001	0.01	<0.001	<0.001	0.027
0 vs. 60 mins	<0.001	<0.001	0.201	0.015	0.131	<0.001	<0.001
pPKB:							
H_2O_2 Exposure	WHCO1	WHCO3	WHCO5	WHCO6	SNO	HT29	MCF7
0 vs. 10 mins	0.178	0.537	<0.001	0.309	<0.001	0.004	<0.001
0 vs. 30 mins	0.178	0.192	<0.001	<0.001	<0.001	<0.001	0.048
0 vs. 60 mins	0.178	<0.001	<0.001	<0.001	<0.001	<0.001	0.586
pGSK3β							
H_2O_2 Exposure	WHCO1	WHCO3	WHCO5	WHCO6	SNO	HT29	MCF7
0 vs. 10 mins	<0.001	0.034	<0.001	0.003	<0.001	<0.001	0.052
0 vs. 30 mins	0.812	0.023	<0.001	0.375	0.98	0.093	0.052
0 vs. 60 mins	0.003	<0.001	<0.001	0.321	0.142	0.008	0.052
PI3K (p85α)							
H_2O_2 Exposure	WHCO1	WHCO3	WHCO5	WHCO6	SNO	HT29	MCF7
0 vs. 10 mins	0.015	0.055	0.901	<0.001	0.021	0.003	0.011
0 vs. 30 mins	<0.001	<0.001	0.003	<0.001	<0.001	0.541	0.002
0 vs. 60 mins	<0.001	<0.001	0.009	<0.001	0.041	0.015	<0.001
β-catenin							
H_2O_2 Exposure	WHCO1	WHCO3	WHCO5	WHCO6	SNO	HT29	MCF7
0 vs. 10 mins	0.005	0.002	0.049	0.001	0.005	<0.001	0.135
0 vs. 30 mins	0.224	<0.001	0.037	0.848	0.055	<0.001	0.887
0 vs. 60 mins	0.518	<0.001	<0.001	0.003	0.073	<0.001	0.01

* Indicates levels of significance.

Table C8: One Way RM Anova results for pPKB expression following PTEN oxidation induced by 10, 30, and 60 mins exposure to 1 mM and 20 µM H_2O_2 in the Caco2 cell line.

H_2O_2 Exposure	1 mM	20 µM
0 vs. 10 mins	0.563	0.004
0 vs. 30 mins	0.092	<0.001
0 vs. 60 mins	0.022	0.022

* Indicates levels of significance.

Table C9: Pearson's correlation coefficient values for the inverse correlation between PTEN and pPKB following PTEN oxidation induced by 10, 30, and 60 mins exposure to 1 mM H_2O_2.

		PTEN and pPKB		pPKB and pGSK3β	
	H_2O_2:	r	P	r	P
WHCO1	0 vs 10 mins	-0.246	0.842	0.979	0.13
	0 vs 30 mins	-0.617	0.576	-0.987	0.104
	0 vs 60 mins	-0.869	0.33	0.679	0.525
WHCO3	0 vs 10 mins	-0.148	0.905	0.975	0.143
	0 vs 30 mins	-0.174	0.888	0.577	0.609
	0 vs 60 mins	0.503	0.665	-0.873	0.324
WHCO5	0 vs 10 mins	0.95	0.202	0.455	0.699
	0 vs 30 mins	0.198	0.873	-0.99	0.088
	0 vs 60 mins	-0.815	0.394	0.936	0.229
WHCO6	0 vs 10 mins	0.32	0.793	-0.0591	0.962
	0 vs 30 mins	-0.989	0.0932	-0.306	0.802
	0 vs 60 mins	-0.845	0.36	0.137	0.912
SNO	0 vs 10 mins	0.198	0.873	-0.3	0.806
	0 vs 30 mins	-0.0929	0.941	0.81	0.399
	0 vs 60 mins	0.542	0.635	0.0724	0.954
HT29	0 vs 10 mins	0.419	0.725	-0.95	0.202
	0 vs 30 mins	0.995	0.0628	-0.598	0.592
	0 vs 60 mins	0.18	0.885	-0.635	0.562
MCF7	0 vs 10 mins	0.214	0.863	-0.936	0.229
	0 vs 30 mins	-0.987	0.104	-0.645	0.554
	0 vs 60 mins	1	0.0166	1	0.0035

* Indicates correlation, levels of significance and possible significance.

Appendix D

4.1 Seperating Gel (12%)

12% Acrylamide
Prepared as described in Appendix A 1.6.

4.2 MTT (3-[4,5-Dimethylthiazol-2-yl]-2,5-diphenyltetrazoliumbromide)

50 mg MTT (Sigma)
Make up to final concentration of 5 mg/ml with 10 ml of PBS.
Store at -20 °C.

4.3 Velcade®/Bortezomib (Bzb)

3.5 mg Bzb powder (Millennium Pharmaceuticals, Inc)
Make up to final concentration with DMSO
Store at -70 °C.

Table D1: Optical density values (mean) of the bands representing whole cell protein expression of PI3K (p85α) and PTEN.

	PI3K (p85α)		PTEN	
CELL LINE	Mean	Std Dev	Mean	Std Dev
WHCO1	21.338	3.902	42.322	3.604
WHCO3	25.615	1.971	23.855	2.05
WHCO5	44.796	3.079	28.089	2.404
WHCO6	75.801	1.655	28.99	2.436
SNO	94.088	5.12	26.191	2.391
MCF7	14.594	0.404	19.564	2.001
HT29	31.745	1.823	90.948	8.017
COS-7	11.627	2.92	48.064	5.493
HEK293	32.287	1.408	30.116	2.113
NIH3T3	78.231	2.219	66.744	0.706
Caco-2	52.716	1.486	28.533	1.208
DLD-1	13.015	2.564	52.27	5.252
Sw480	12.255	0.82	36.951	2.314

4.4 MTT Assay Results

4.4.1 WHCO1

One Way Repeated Measures Analysis of Variance

Normality Test: Passed (P = 0.335)
Equal Variance Test: Passed (P = 0.778)

Treatment Name	N	Missing	Mean	Std Dev	SEM
0	3	0	0.0947	0.00666	0.00384
6hrs	3	0	0.126	0.00961	0.00555
12hrs	3	0	0.141	0.0127	0.00731
24hrs	3	0	0.244	0.0301	0.0174

Source of Variation	DF	SS	MS	F	P
Between Subjects	2	0.000344	0.000172		
Between Treatments	3	0.0378	0.0126	36.719	<0.001
Residual	6	0.00206	0.000343		
Total	11	0.0402			

The differences in the mean values among the treatment groups are greater than would be expected by chance; there is a statistically significant difference (P = <0.001). To isolate the group or groups that differ from the others use a multiple comparison procedure.
Power of performed test with alpha = 0.050: 1.000
All Pairwise Multiple Comparison Procedures (Holm-Sidak method):
Overall significance level = 0.05
Comparisons for factor:

Comparison	Diff of Means	t	Unadjusted P	Critical Level	Significant?
24hrs vs. 0	0.150	9.896	<0.001	0.009	Yes
24hrs vs. 6hrs	0.118	7.802	<0.001	0.010	Yes
24hrs vs. 12hrs	0.104	6.854	<0.001	0.013	Yes
12hrs vs. 0	0.0460	3.041	0.023	0.017	No
6hrs vs. 0	0.0317	2.094	0.081	0.025	No
12hrs vs. 6hrs	0.0143	0.948	0.380	0.050	No

4.4.2 MCF7

One Way Repeated Measures Analysis of Variance

Normality Test: Passed (P = 0.142)
Equal Variance Test: Passed (P = 0.976)

Treatment Name	N	Missing	Mean	Std Dev	SEM
0	3	0	0.105	0.00987	0.00570
6hrs	3	0	0.113	0.00153	0.000882
12hrs	3	0	0.123	0.0161	0.00928
24hrs	3	0	0.136	0.00917	0.00529

Source of Variation	DF	SS	MS	F	P
Between Subjects	2	0.000463	0.000232		
Between Treatments	3	0.00156	0.000521	7.427	0.019
Residual	6	0.000421	0.0000701		
Total	11	0.00245			

The differences in the mean values among the treatment groups are greater than would be expected by chance; there is a statistically significant difference (P = 0.019). To isolate the group or groups that differ from the others use a multiple comparison procedure.
Power of performed test with alpha = 0.050: 0.759
All Pairwise Multiple Comparison Procedures (Holm-Sidak method):
Overall significance level = 0.05
Comparisons for factor:

Comparison	Diff of Means	t	Unadjusted P	Critical Level	Significant?
24hrs vs. 0	0.0307	4.485	0.004	0.009	Yes
24hrs vs. 6hrs	0.0227	3.315	0.016	0.010	No
12hrs vs. 0	0.0173	2.535	0.044	0.013	No
24hrs vs. 12hrs	0.0133	1.950	0.099	0.017	No
12hrs vs. 6hrs	0.00933	1.365	0.221	0.025	No
6hrs vs. 0	0.00800	1.170	0.286	0.050	No

4.4.3 HEK293

One Way Repeated Measures Analysis of Variance

Normality Test: Passed (P = 0.882)

Equal Variance Test: Passed (P = 0.090)

Treatment Name	N	Missing	Mean	Std Dev	SEM
0	3	0	0.224	0.00681	0.00393
6hrs	3	0	0.209	0.00346	0.00200
12hrs	3	0	0.279	0.0480	0.0277
24hrs	3	0	0.236	0.00450	0.00260

Source of Variation	DF	SS	MS	F	P
Between Subjects	2	0.00147	0.000735		
Between Treatments	3	0.00818	0.00273	4.967	0.046
Residual	6	0.00330	0.000549		
Total	11	0.0129			

The differences in the mean values among the treatment groups are greater than would be expected by chance; there is a statistically significant difference (P = 0.046). To isolate the group or groups that differ from the others use a multiple comparison procedure.

Power of performed test with alpha = 0.050: 0.538

All Pairwise Multiple Comparison Procedures (Holm-Sidak method):

Overall significance level = 0.05

Comparisons for factor:

Comparison	Diff of Means	t	Unadjusted P	Critical Level	Significant?
12hrs vs. 6hrs	0.0700	3.658	0.011	0.009	No
12hrs vs. 0	0.0553	2.892	0.028	0.010	No
12hrs vs. 24hrs	0.0435	2.273	0.063	0.013	No
24hrs vs. 6hrs	0.0265	1.385	0.215	0.017	No
0 vs. 6hrs	0.0147	0.767	0.472	0.025	No
24hrs vs. 0	0.0118	0.618	0.559	0.050	No

4.4.4 NIH3T3

One Way Repeated Measures Analysis of Variance

Normality Test: Passed (P = 0.891)

Equal Variance Test: Passed (P = 0.338)

Treatment Name	N	Missing	Mean	Std Dev	SEM
0	3	0	0.197	0.0139	0.00802
6hrs	3	0	0.281	0.00802	0.00463
12hrs	3	0	0.278	0.0125	0.00723
24hrs	3	0	0.285	0.0405	0.0234

Source of Variation	DF	SS	MS	F	P
Between Subjects	2	0.000193	0.0000966		
Between Treatments	3	0.0160	0.00533	8.164	0.015
Residual	6	0.00392	0.000653		
Total	11	0.0201			

The differences in the mean values among the treatment groups are greater than would be expected by chance; there is a statistically significant difference (P = 0.015). To isolate the group or groups that differ from the others use a multiple comparison procedure.

Power of performed test with alpha = 0.050: 0.806

All Pairwise Multiple Comparison Procedures (Holm-Sidak method):

Overall significance level = 0.05

Comparisons for factor:

Comparison	Diff of Means	t	Unadjusted P	Critical Level	Significant?
24hrs vs. 0	0.0877	4.203	0.006	0.009	Yes
6hrs vs. 0	0.0837	4.011	0.007	0.010	Yes
12hrs vs. 0	0.0810	3.883	0.008	0.013	Yes
24hrs vs. 12hrs	0.00667	0.320	0.760	0.017	No
24hrs vs. 6hrs	0.00400	0.192	0.854	0.025	No
6hrs vs. 12hrs	0.00267	0.128	0.902	0.050	No

Table D2: One Way Anova Statistical results for the expression of β-catenin following Bzb exposure.

Bzb Exposure	WHCO1	WHCO3	WHCO5	WHCO6	SNO	HT29	MCF7	COS-7	HEK293	NIH3T3	Caco-2	DLD-1	Sw480
0 vs. 1 nM	0.084	<0.001	<0.001	<0.001	0.647	0.027	0.056	0.038	0.023	0.509	0.118	<0.001	0.005
0 vs. 5 nM	0.001	<0.001	0.211	0.01	0.096	0.185	0.208	0.754	0.477	0.152	<0.001	<0.001	0.002
0 vs. 10 nM	0.397	<0.001	<0.001	0.959	<0.001	0.438	<0.001	0.033	0.037	0.031	<0.001	<0.001	0.003
0. vs. 25 nM	0.007	<0.001	<0.001	0.225	0.008	0.425	<0.001	0.004	0.479	0.005	<0.001	<0.001	0.01
0 vs. 50 nM	0.38	<0.001	0.021	0.148	<0.001	<0.001	<0.001	0.03	0.011	0.733	0.201	<0.001	<0.001
0 vs. 100 nM	0.489	<0.001	<0.001	0.06	<0.001	0.006	<0.001	<0.001	<0.001	0.002	<0.001	<0.001	0.002
0 vs. 200 nM	0.206	<0.001	<0.001	0.354	<0.001	0.018	0.007	<0.001	0.009	0.009	<0.001	0.599	<0.001

* Indicates levels of significance. 0 = DMSO control

Table D3: P values of One Way Anova Statistical results for the expression of PTEN following Bzb exposure

Bzb Exposure	WHCO1	WHCO3	WHCO5	WHCO6	SNO	HT29	MCF7	COS-7	HEK293	NIH3T3	Caco-2	DLD-1	Sw480
0 vs. 1 nM	0.009	0.15	0.035	0.069	0.073	0.362	0.395	0.611	<0.001	<0.001	0.001	0.693	<0.001
0 vs. 5 nM	<0.001	0.194	0.001	0.064	<0.001	0.015	0.381	0.611	<0.001	<0.001	0.003	0.181	<0.001
0 vs. 10 nM	<0.001	0.412	0.008	0.185	0.674	0.008	<0.001	0.611	0.501	0.501	<0.001	<0.001	<0.001
0 vs. 25 nM	<0.001	0.35	0.015	0.507	0.436	0.001	<0.001	0.611	<0.001	<0.001	0.045	0.097	<0.001
0 vs. 50 nM	0.006	0.009	0.072	<0.001	0.039	0.112	0.2	0.611	0.09	0.09	<0.001	0.85	<0.001
0 vs. 100 nM	<0.001	0.077	0.003	0.865	<0.001	0.643	<0.001	0.611	<0.001	<0.001	<0.001	0.723	<0.001
0 vs. 200 nM	0.002	<0.001	0.005	0.037	<0.001	0.167	0.049	0.611	<0.001	<0.001	<0.001	0.716	<0.001

* Indicates levels of significance. 0 = DMSO control

Table D4: P values of One Way Anova Statistical results for the expression of pPKB following Bzb exposure

Bzb Exposure	WHCO1	WHCO3	WHCO5	WHCO6	SNO	HT29	MCF7	COS-7	HEK293	NIH3T3	Caco-2	DLD-1	Sw480
0 vs. 1 nM	<0.001	<0.001	<0.001	0.028	<0.001	<0.001	<0.001	<0.001	<0.001	1	<0.001	<0.001	<0.001
0 vs. 5 nM	<0.001	<0.001	<0.001	<0.001	0.048	<0.001	<0.001	0.714	<0.001	1	<0.001	0.642	<0.001
0 vs. 10 nM	<0.001	<0.001	<0.001	<0.001	<0.001	<0.001	<0.001	<0.001	<0.001	<0.001	<0.001	<0.001	<0.001
0 vs. 25 nM	<0.001	<0.001	<0.001	<0.001	<0.001	<0.001	<0.001	<0.001	<0.001	1	<0.001	0.001	<0.001
0 vs. 50 nM	<0.001	<0.001	<0.001	<0.001	<0.001	<0.001	<0.001	<0.001	<0.001	1	<0.001	<0.001	<0.001
0 vs. 100 nM	<0.001	<0.001	<0.001	<0.001	<0.001	0.711	<0.001	<0.001	0.464	1	<0.001	<0.001	<0.001
0 vs. 200 nM	<0.001	<0.001	<0.001	<0.001	<0.001	0.711	<0.001	<0.001	0.002	1	<0.001	<0.001	0.016

* Indicates levels of significance. 0 = DMSO control

Table D5: P values of One Way Anova Statistical results for the expression of PI3K (p85α) following Bzb exposure

Bzb Exposure	WHCO1	WHCO3	WHCO5	WHCO6	SNO	HT29	MCF7	COS-7	HEK293	NIH3T3	Caco-2	DLD-1	Sw480
0 vs. 1 nM	0.75	0.447	0.021	<0.001	0.003	<0.001	0.006	<0.001	<0.001	<0.001	<0.001	<0.001	<0.001
0 vs. 5 nM	<0.001	<0.001	0.676	<0.001	<0.001	<0.001	<0.001	<0.001	<0.001	<0.001	<0.001	0.023	<0.001
0 vs. 10 nM	<0.001	<0.001	<0.001	<0.001	<0.001	<0.001	<0.001	<0.001	<0.001	<0.001	0.917	<0.001	0.023
0 vs. 25 nM	<0.001	<0.001	0.065	<0.001	<0.001	<0.001	<0.001	<0.001	<0.001	<0.001	0.007	<0.001	0.014
0 vs. 50 nM	<0.001	<0.001	0.002	<0.001	<0.001	<0.001	<0.001	<0.001	<0.001	<0.001	0.096	<0.001	<0.001
0 vs. 100 nM	0.03	0.072	<0.001	<0.001	<0.001	<0.001	<0.001	<0.001	<0.001	<0.001	0.005	<0.001	<0.001
0 vs. 200 nM	<0.001	<0.001	0.027	<0.001	<0.001	<0.001	<0.001	<0.001	<0.001	0.868	<0.001	<0.001	<0.001

* Indicates levels of significance. 0 = DMSO control

Appendix E

5.1 Lithium Chloride (LiCl)

0.04239 g LiCl (Merck)
Make up to 1 ml in tissue culture medium (see Appendix A 1.1).

5.2 Nuclear levels of β-catenin in HOSCC and the significance thereof:

One Way Repeated Measures Analysis of Variance
Data source: Nuclear β-atenin
Normality Test: Passed (P = 0.160)
Equal Variance Test: Passed (P = 0.420)

Treatment Name	N	Missing	Mean	Std Dev	SEM
WHCO1	3	0	60.903	1.249	0.721
WHCO3	3	0	66.177	5.285	3.052
WHCO5	3	0	61.810	1.080	0.624
WHCO6	3	0	63.274	3.685	2.127
SNO	3	0	60.448	1.889	1.090
HT29	3	0	59.550	0.358	0.207
MCF7	3	0	61.897	0.748	0.432
CONTROL	3	0	98.855	1.544	0.891

Source of Variation	DF	SS	MS	F	P
Between Subjects	2	8.388	4.194		
Between Treatments	7	3650.075	521.439	78.188	<0.001
Residual	14	93.367	6.669		
Total	23	3751.831			

The differences in the mean values among the treatment groups are greater than would be expected by chance; there is a statistically significant difference (P = <0.001). To isolate the group or groups that differ from the others use a multiple comparison procedure.
Power of performed test with alpha = 0.050: 1.000
Multiple Comparisons versus Control Group (Holm-Sidak method):
Overall significance level = 0.05
Comparisons for factor:

Comparison	Diff of Means	t	Unadjusted P	Critical Level	Significant?
HT29 vs. CONTROL	39.305	18.641	<0.001	0.007	Yes
HT29 vs. WHCO3	6.627	3.143	0.007	0.009	Yes
HT29 vs. WHCO6	3.724	1.766	0.099	0.010	No
HT29 vs. MCF7	2.347	1.113	0.285	0.013	No
HT29 vs. WHCO5	2.260	1.072	0.302	0.017	No
HT29 vs. WHCO1	1.353	0.642	0.531	0.025	No
HT29 vs. SNO	0.898	0.426	0.677	0.050	No

Table E1: Optical density values (mean) of the bands representing the western blot detection of MMP7.

Cell Line	Mean	Std Dev
WHCO1	49.1	4.841
WHCO3	98.768	1.426
WHCO5	97.389	1.37
WHCO6	33.941	3.05
SNO	69.994	4.541

5.3 The mean optical density values and statistical analysis of c-Jun levels in HOSCC:

One Way Repeated Measures Analysis of Variance
Data source: c-Jun Whole Cell Protein Expression
Normality Test: Passed (P = 0.775)
Equal Variance Test: Passed (P = 0.849)

Treatment Name	N	Missing	Mean	Std Dev	SEM
WHCO1	3	0	94.888	8.769	5.063
WHCO3	3	0	64.053	5.535	3.196
WHCO5	3	0	88.881	6.216	3.589
WHCO6	3	0	80.131	4.288	2.475
SNO	3	0	79.842	3.397	1.961
MCF7	3	0	18.046	0.934	0.539
HT29	3	0	39.987	3.210	1.854

Source of Variation	DF	SS	MS	F	P
Between Subjects	2	102.384	51.192		
Between Treatments	6	14181.662	2363.610	104.221	<0.001
Residual	12	272.147	22.679		
Total	20	14556.193			

The differences in the mean values among the treatment groups are greater than would be expected by chance; there is a statistically significant difference (P = <0.001). To isolate the group or groups that differ from the others use a multiple comparison procedure.
Power of performed test with alpha = 0.050: 1.000
Multiple Comparisons versus Control Group (Holm-Sidak method):
Overall significance level = 0.05
Comparisons for factor:

Comparison	Diff of Means	t	Unadjusted P	Critical Level	Significant?
HT29 vs. WHCO1	54.901	14.119	<0.001	0.009	Yes
HT29 vs. WHCO5	48.894	12.574	<0.001	0.010	Yes
HT29 vs. WHCO6	40.144	10.324	<0.001	0.013	Yes
HT29 vs. SNO	39.855	10.250	<0.001	0.017	Yes
HT29 vs. WHCO3	24.066	6.189	<0.001	0.025	Yes
HT29 vs. MCF7	21.941	5.643	<0.001	0.050	Yes

Table E2: Statistical (P values) results of the bands representing the western blot detection of pPKB (Ser473), pGSK3, PTEN, and β-catenin following LiCl exposure.

pPKB:							
LiCl Exposure:	WHCO1	WHCO3	WHCO5	WHCO6	SNO	HT29	MCF7
0 vs 3hrs	<0.001	<0.001	0.032	<0.001	0.137	0.051	<0.001
0 vs 12hrs	<0.001	<0.001	0.007	<0.001	0.137	<0.001	<0.001
0 vs 24hrs	0.779	<0.001	0.018	<0.001	0.137	<0.001	<0.001
pGSK3β							
0 vs 3hrs	<0.001	<0.001	<0.001	<0.001	0.298	<0.001	<0.001
0 vs 12hrs	<0.001	<0.001	<0.001	<0.001	0.01	0.004	<0.001
0 vs 24hrs	<0.001	<0.001	<0.001	0.35	0.058	<0.001	0.004
PTEN							
0 vs 3hrs	0.162	0.111	0.856	0.127	<0.001	0.002	0.096
0 vs 12hrs	0.162	0.66	0.02	0.127	<0.001	0.068	0.096
0 vs 24hrs	0.162	0.093	<0.001	0.127	<0.001	0.787	0.096
β-catenin							
0 vs 3hrs	0.004	<0.001	0.034	<0.001	0.222	0.021	0.002
0 vs 12hrs	0.002	0.172	0.74	<0.001	0.222	<0.001	0.233
0 vs 24hrs	0.304	<0.001	<0.001	<0.001	0.222	<0.001	0.797

* Indicates levels of significance.

Table E3: Statistical (P values) results of the bands representing the western blot detection of nuclear and total β-catenin concentration following PI3K inhibition.

		Nuclear β-catenin				
	Control		LY29 (1 hr)			
	Mean	Std Dev	Mean	Std Dev	t	P
WHCO1	41.43	1.577	15.381	1.215	22.66	<0.001
WHCO3	50.38	0.702	57.342	8.753	-1.373	0.242
WHCO5	21.275	1.58	15.826	1.132	4.855	0.008
WHCO6	90.421	8.3	46.092	3.934	8.359	0.001
SNO	23.573	1.744	16.86	0.419	6.481	0.003
HT29	9.716	0.739	14.269	0.856	-6.971	0.002
MCF7	12.981	1.819	14.838	0.972	-1.559	0.194
		Total β-catenin				
WHCO1	80.37	9.067	72.901	8.118	1.063	0.348
WHCO3	86.19	13.714	63.803	9.29	2.341	0.079
WHCO5	59.871	10.44	83.663	6.736	-3.317	0.029
WHCO6	71.281	5.452	39.892	8.056	5.589	0.005
SNO	29.289	4.357	24.838	2.793	1.49	0.211
HT29	38.65	6.19	31.769	9.525	1.049	0.353
MCF7	37.725	5.824	31.201	6.779	1.264	0.275

* Indicates levels of significance.

References:

1 Hackel, P., Zwick, E., Prenzel, N., Ullrich, A. (1999). Epidermal growth factor receptors: critical mediators of multiple receptor pathways. *Curr. Op. Biol*, **11**: 184-189.

2 Schwartz, M., Baron, V. (1999). Interactions between mitogenic stimuli, or, a thousand and one connections. *Curr. Op. Cell Biol*, **11**: 197-202.

3 Breslin, T. Krogh, M., Peterson, C., Troein, C. (2005). Signal transduction pathway profiling of individual tumour samples. *BMC Bioinformatics*, **6**: 163-174.

4 James, A., Swann, K., And Recce, M. (1999). Cell Behaviour as a Dynamic Attractor in the Intracellular Signalling System. *J. theor. Biol*., **196**: 269-88.

5 Hunter, T. (2000). Signalling—2000 and Beyond. *Cell*, **100**: 113–127.

6 Alroy, I., and Yarden, Y. (1997). The ErbB signalling network in embryogenesis and oncogenesis: signal diversification through combinatorial ligand–receptor interactions. *FEBS Letters*, **410**: 83–86.

7 Yarden, Y., and Sliwkowski, M. (2001). Untangling the ErbB signalling network. *Nat. Rev*, **2**: 127-137.

8 Liebmann, C., and Böhmerb, F.-D. (2000). Signal Transduction Pathways of G Protein-coupled Receptors and Their Cross-Talk with Receptor Tyrosine Kinases: Lessons from Bradykinin Signalling. *Current Medicinal Chemistry*, **7**: 911-943.

9 Aplin, A. E., Howe, A., Alahari, S. K., Juliano, R. L. (1998). Signal Transduction and Signal Modulation by Cell Adhesion Receptors: The Role of Integrins, Cadherins, Immunoglobulin-Cell Adhesion Molecules, and Selectins. *Pharmacological Reviews*, **50**: 197-264.

10 Fisher, M. J., Paton, R. C., and Matsuno, K. (1999). Intracellular signalling proteins as 'smart' agents in parallel distributed processes. *BioSystems*, **50**: 159 –171.

11 Hurley, J. H., and Meyer, T. (2001). Subcellular targeting by membrane lipids. *Current Opinion in Cell Biology*, **13**: 146–152.

12 Doughman, R. L., Firestone, A. J., Anderson, R. A. (2003). Phosphatidylinositol Phosphate Kinases Put PI4,5P2 in Its Place. *J.Membrane Biol.*, **194:** 77–89.

13 Anderson, R. A., Boronenkov, I. V., Doughman, S. D., Kunz, J., Loijens, J. C. (1999). Phosphatidylinositol Phosphate Kinases, a Multifaceted Family of Signalling Enzymes. *J. Biol. Chem*., **274**: 9907–9910.

14 Hanahan, D., and Weinberg, R., A. (2000). The Hallmarks of Cancer. *Cell*, **100**: 57-70

15 Flynn, D. C. (2001). Adaptor proteins. *Oncogene*, **20**: 6270 -6272.

16 Gschwind, A., Zwick, E., Prenzel, N., Leserer, M., Ullrich, A. (2001). Cell communication networks: Epidermal growth factor receptor transactivation as the paradigm for interreceptor signal transmission. *Oncogene*, **20**: 1594-1600.

17 Holbro, T., Civenni, G., Hynes, N. (2003). The ErbB receptors and their role in cancer progression. *Exp. Cell Res*., **284**: 99-110.

18 Hornberg, J., Bruggeman, F., Westerhoff, H., Lankelma, J. (2006). Cancer: A systems biology disease. *BioSystems*, **83**: 81-90.

19 Lauffenburger, D. A. (2000). Cell signalling pathways as control modules: Complexity for simplicity? *PNAS*, **97**: 5031–5033.

20 Tucker, C. L., Gera, J. F., and Uetz, P. (2001). Towards an understanding of complex protein networks. *Trends in Cell Biology*, **11**: 102-106.

21 Barabási, A.-L., and Oltvai, Z. N. (2004). Network Biology: Understanding the cell's functional organization. *Nature Rev*., **5**: 101-113.

22 Kholodenko, B.N. (2006). Cell signalling dynamics in time and space. *Nat Rev Mol Cell Biol*., **7**: 165–176.
23 Mundy, J., Nielson, H., Broderson, P. (2006). Crosstalk. *Trends in Plant Sciences*, **11**: 63-64.
24 Morales, C. P., Souza, R. F., and Spechler, S. J. (2002). Hallmarks of cancer progression in Barrett's oesophagus. *Lancet*, **360**: 1587–89.
25 Rowinsky, E. K. (2003). Signal Events: Cell signal transduction and its inhibition in cancer. *The Oncologist*, **8**: 5-17.
26 Hanahan, D., and Weinberg, R. A. (2011). Hallmarks of Cancer: The Next Generation. *Cell*, **144**: 646-74.
27 Vogelstein, B., and Kinzler, K. W. (1993). The multistep nature of Cancer. *TIG*, **9**: 138-41.
28 Bronchud, M. H. (2002). Is cancer really a 'local' cellular clonal disease? *Medical Hypotheses*, **59**: 560–565
29 Barrett, J. C. (1993). Mechanisms of Multistep Carcinogenesis and Carcinogen Risk Assessment. *Environmental Health Perspectives*, **100**: 9-20.
30 Weinstein, I. B., and Joe, A. (2008). Oncogene Addiction. *Cancer Res.*, **68:** 3077–80.
31 Weinstein, I. B., and Joe, A. K. (2006). Mechanisms of Disease: oncogene addiction—a rationale for molecular targeting in cancer therapy. *Nature Clinical Clinical Practice*, **3**: 448-457.
32 Garber, K. (2007). The Fragile Tumor. New Insights Into Oncogene Addiction Found. *JNCI J Natl Cancer Inst*., **99**: 264-269.
33 Sharma, S. V., Fischbach, M. A., Haber, D. A., Settleman, J. (2006). 'Oncogenic Shock'': Explaining Oncogene Addiction through Differential Signal Attenuation. *Clin. Cancer Res*., **12**: 4392-4395.
34 Luo, J., Solimini, N. L., and Elledge, S. J. (2009). Principles of Cancer Therapy: Oncogene and Non-oncogene Addiction. *Cell*, **136**: 823–837.
35 Pao, W., and Girard, N. (2011). New driver mutations in non-small-cell lung cancer. *Lancet Oncol*., **12**: 175–80.
36 Yuan, T. L., and Cantley, L. C. (2008). PI3K pathway alterations in cancer: variations on a theme. *Oncogene*, **27**: 5497–5510.
37 Yan , W., Zhang, W., Jiang, T. (2011). Oncogene addiction in gliomas: Implications for molecular targeted therapy. *Journal of Experimental & Clinical Cancer Research*, **30**: 58
38 Campone, M., Noël, B., Couriaud, C., Grau, M., Guillemin, Y., Gautier, F., Gouraud, W., Charbonnel, C., Campion, L., Jézéquel, P., Braun, F., Barré, B., Coqueret, O., Barillé-Nion, S., Juin, P. (2011). c-Myc dependent expression of pro-apoptotic Bim renders HER2-overexpressing breast cancer cells dependent on anti-apoptotic Mcl-1. *Molecular Cancer*, **10**: 110
39 Yin, L., Ahmad, R., Kosugi, M., Kufe, T., Vasir, B., Avigan, D., Kharbanda, S., Kufe, D. (2010). Survival of Human Multiple Myeloma Cells Is Dependent on MUC1 C-Terminal Transmembrane Subunit Oncoprotein Function. *Mol Pharmacol*., **78**: 166–174.
40 Vivanco, I., Sawyers, C. (2002). The phosphatidylinositol 3-kinase-akt pathway in human cancer. *Nat. Rev*., **2**: 489-501.
41 Sharma, S. V., Gajowniczek, P., Way, I. P., Lee, D. Y., Jiang, J., Yuza, Y., Classon, M., Haber, D. A., Settleman, J. (2006). A common signalling cascade may underlie "addiction" to the Src, BCR-ABL, and EGF receptor oncogenes. *Cancer Cell*, **10**: 425–435.
42 She, Q.-B., Chandar lapaty, S., Chandarlapaty, S., Ye, Q., Lobo, J., Haskell, K. M., Leander, K. R., De Feo-Jones, D., Huber, H. E., Rosen, N. (2008). Breast Tumor Cells with PI3K Mutation or HER2 Amplification Are Selectively Addicted to Akt Signalling. *PLoS ONE*, **3**: e3065. doi: 10.1371/jou rnal.pone.0003 065.

43 Choo, A. Y., and Blenis, J. (2006). TORgeting oncogene addiction for cancer therapy. *Cancer Cell*, 77-9. doi 10.1016/j.ccr.2006.01.021.
44 Whitman, M., et. al. (1985). Association of phosphatidylinositol kinase activity with polyoma middle-T competent for transformation. *Nature,* **315**: 239-242.
45 Tolias, K. F., and Cantley, L. C. (1999). Pathways for phosphoinositide synthesis. *Chemistry and Physics of Lipids*, **98**: 69 – 77.
46 Vanhaesebroeck, B., Waterfield, M. (1999). Signalling by distinct classes of Phosphoinositide 3-kinases. *Exp.Cell Res*., **253**: 239-254.
47 Stein, R., Waterfield, M. (2000). PI3-kinase inhibition: a target for drug development? *Mol. Med. Today*, **6**: 347-357.
48 Mazza, S., and Maffucci, T. (2011). Class II phosphoinositide 3-kinase C2alpha: what we learned so far. *Int J Biochem Mol Biol*., **2**: 168-182.
49 Arcaro, A., Zvelebil, M. J.,Wallasch, C., Ullrich, A., Waterfield, M. D., Domin, J. (2000). Class II Phosphoinositide 3-Kinases Are Downstream Targets of Activated Polypeptide Growth Factor Receptors. *Mol. Cell. Biol*., **20**: 3817–3830.
50 Backer, J. M. (2008). The regulation and function of Class III PI3Ks: novel roles for Vps34. *Biochem. J*., **410**: 1–17.
51 Kennedy, A. D., and DeLeo, F. R. (2008). PI3K and NADPH oxidase: a class act. *Blood*, **112**: 4788-4789.
52 Cantley, L. C. (2002). The Phosphoinositide 3-Kinase Pathway. *Science*, **296**: 1655-6.
53 Osaki, M., Oshimura, M., and Ito, H. (2004). PI3K-Akt pathway: Its functions and alterations in human cancer. *Apoptosis*, **9**: 667-676.
54 Koyasu, S. (2003). The role of PI3K in immune cells. *Nature Immunology*, **4**: 313-19.
55 Stein, R., Waterfield, M. (2000). PI3-kinase inhibition: a target for drug development? *Mol. Med. Today*, **6***: 347*-357.
56 Anderson, K., E., Jackson, S., P. (2003). Class Ì phosphoinositide-3-kinases. *IJBCB*. **35**: 1028-1033.
57 Carpenter Duckworth, B. C., Auger, K. R., Cohen, B., Schaffhausen, B. S., Cantley, L. C. (1990). Purification and Characterization of Phosphoinositide 3-Kinase from Rat Liver. *J.Biol.Chem*., **265**:19704-19711.
58 Gout, I., Dhand, R., Panayotou, G., Fry, M., J., Hiles, I., Otsu, M., Waterfield, M., D. (1992). Expression and characterization of the p85 subunit of the phosphatidylinositol 3-kinase complex and a related p85β protein by using the baculovirus expression system. *Biochem.J.,* **288**: 395-405.
59 Lefai, E., Roques, M., Vega, N., Laville, M., Vidal, H. (2001). Expression of the splice variants of the p85α regulatory subunit of phosphoinositide 3-kinase in muscle and adipose tissue of healthy subjects and type 2 diabetic patients. *Biochem. J.,* **360**: 117-125.
60 Klippel, A., Escobedo, J., A., Hu, Q., Williams, L., T. (1993). A region of the 85-Kilodalton (kDa) subunit of Phosphatidylinositol 3-kinase binds the 110-kDa catalytic subunit in vivo. *Mol. Cell. Biol.,* **13**: 5560-5566.
61 Dhand, R., Hara, K., Hiles, I., Bax, B., Gout, I., Panayotou, G., Fry, M., J., Yonezawa, K., Kasuga, M., Waterfield, M., D. (1994). PI 3-kinase: structural and functional analysis of intersubunit interactions. *EMBO J.,* **13**: 511-521.
62 Hiles, I., D., Otsu, M., Volinia, S., Fry, M. J., Gout, I., Dhand, R., Panayotou, G., Ruiz-Larrea, F., Thompson, A. Totty, N. F. (1992). Phosphatidylinositol 3-kinase: structure and expression of the 110 kd catalytic subunit. *Cell,* **70**: 419-429.
63 Beeton, C. A., Chance, E. M., Foukas, L. C., Shepherd, P. R. (2000). Comparison of the kinetic properties of the lipid- and protein-kinase activities of the p110a and p110b catalytic subunits of class-Ia phosphoinositide 3-kinases. *Biochem. J*., **350**: 353-359.

64 Foukas, L. C., Beeton, C. A., Jensen, J., Phillips, W. A., Shepherd, P. R. (2004). Regulation of Phosphoinositide 3-Kinase by Its Intrinsic Serine Kinase Activity In Vivo. *Mol. Cell. Biol*., **24**: 966–975.
65 Yu, J., Zhang, Y., McIlroy, J., Rordorf-Nikolic, T., Orr, G., A., Backer, J., M. (1998). Regulation of the p85/p110 Phosphatidylinositol 3'-kinase: Stabilization and inhibition of the p110α catalytic subunit by the p85 regulatory subunit. *Mol. Cell. Biol.,* **18**: 1379-1387.
66 Klippel, A., Escobedo, J., A., Hirano, M., and Williams, L., T. (1994). The interaction of small domains between the subunits of phosphatidylinositol 3-kinase determines enzyme activity. *Mol. Cell. Biol.,* **14**: 2675-2685.
67 Ueki, K., Fruman, D., A., Brachmann, S., M., Tseng, Y-H., Cantley, L., C., Kahn, C., R. (2002). Molecular balance between the Regulatory and Catalytic subunits of Phosphoinositide 3-kinase regulates cell signalling and survival. *Mol. Cell. Biol.,* **22**: 965-977.
68 Geering, B., Cutillas, P., R., and Vanhaesebroeck, B. (2007). Regulation of class 1A PI3Ks: is there a role for monomeric PI3K subunits? *Biochem. Soc. Trans.,* **35**: 199-203.
69 Holt, K., H., Olson, L., Moye-Rowley, W., S., Pessin, J., E. (1994). Phosphatidylinositol 3-kinase activation is mediated by high-affinity interactions between distinct domains within the p110 and p85 subunits. *Mol. Cell. Biol.,* **14**: 42-49.
70 Jiménez, C., Hernández, C., Pimentel, B., and Carrera, A., C. (2002). The p85 Regulatory subunit controls sequential activation of phosphoinositide 3-kinase by Tyr kinases and Ras. *J. Biol. Chem.,* **277**: 41556-41562.
71 Woscholski, R., Dhand, R., Fry, M., J., Waterfield, M., D., Parker, P., J. (1994). Biochemical characterization of the free catalytic p110α and the complexed heterodimeric p110α·p85α forms of the mammalian phosphatidylinositol 3-kinase. *J. Biol. Chem.,* **269**: 25067-25072.
72 Kazlauskas, A., and Cooper, J., A. (1990). Phosphorylation of the PDGF receptor β subunit creates a tight binding site for phoaphatidylinositol 3 kinase. *EMBO J.,* **9**: 3279-3286.
73 Czech, M., P. (2000). PIP2 and PIP3: Complex roles at the cell surface. *Cell,* **100**: 603-606.
74 Cantrell, D., A. (1994). Phosphoinositide 3-kinase signalling pathways. *J. Cell Sci.,* **114**: 1439-1445.
75 Leevers, S. J., Vanhaesebroeck, B., Waterfield, M. D. (1999). Signalling through phosphoinositide 3-kinases: the lipids take centre stage. *Current Opinion in Cell Biology*, **11**: 219–225.
76 Brazil, D.P., Hemmings, B.A., (2001). Ten years of protein kinase B signalling: a hard Akt to follow, *Trends Biochem. Sci.,* **26**: 657-664.
77 Welch, H., Eguinoa, A., Stephens, L. R., Hawkins, P. T. (1998). Protein Kinase B and Rac Are Activated in Parallel within a Phosphatidylinositide 3OH-kinase-controlled Signalling Pathway. *J. Biol. Chem*., **273**: 11248 –11256.
78 Sansal, I., and Sellers, W. R. (2004). The Biology and Clinical Relevance of the PTEN Tumor Suppressor Pathway. *J Clin Oncol*., **22**: 2954-2963.
79 Takeichi, M. (1990). Cadherins: a molecular family important in selective cell-cell adhesion. *Annu. Rev. Biochem*., **59**: 237–252.
80 Cavallaro, U., Scaffhauser, B., Christofori, G. (2002). Cadherins and the tumour progression: is it all in a switch? *Cancer Lett*, **176**: 123-128.
81 Halbleib, J. M., and Nelson, W. J. (2006). Cadherins in development: cell adhesion, sorting, and tissue morphogenesis. *Genes&Development*, **20**: 3199–3214.
82 Ivanov, D. B., Philippova, M. P., and Tkachu, V. A. (2001). Structure and Functions of Classical Cadherins. *Biochemistry (Moscow)*, **66:** 1174-1186.

83 Young, P., Boussadia, O., Halfter, H., Grose, R., Berger, P., Leone, D. P., Robenek, H., Charnay, P., Kemler, R., Suter, U. (2003). E-cadherin controls adherens junctions in the epidermis and the renewal of hair follicles. *The EMBO Journal*, **22**: 5723-5733.

84 Baum, B., and Georgiou, M. (2011). Dynamics of adherens junctions in epithelial establishment, maintenance, and remodelling. *J. Cell Biol*., **192**: 907–917.

85 Choi, Y.-S., and Gumbiner, B. (1989). Expression of Cell Adhesion Molecule E-Cadherin in Xenopus Embryos Begins at Gastrulation and Predominates in the Ectoderm. *The Journal of Cell Biology*, **108**: 2449-2458.

86 Barui, A., Banerjee, P., Das, R. K., Basu, S. K., Dhara, S., Chatterjee, J. (2011). Immunohistochemical Evaluat ion of p63, E-Cadherin, Collagen I and III Expression in Lower Limb Wound Healing under Honey. *Evidence -Based Complementary and Alternative Medicine*, doi:10.1155/2011/239864.

87 Greenburg, G., and Hay, E. D. (1982). Epithelia Suspended in Collagen Gels Can Lose Characteristics of Migrating Mesenchymal Cells Polarity and Express. *J. Cell Biol*., **95**: 333-339.

88 Heuberger, J., and Birchmeier, W. (2010). Interplay of Cadherin-Mediated Cell Adhesion and Canonical Wnt Signalling. *Cold Spring Harb Perspect Biol*; **2**: a002915.

89 Christofori, G., Semb, H. (1999). The role of the cell-adhesion molecule E-cadherin as a tumour suppressor gene. *TIBS*, **24**: 73-76.

90 Van Aken, E., De Wever, O., Correia da Rocha, A. S., Mareel, M. (2001). Defective E-cadherin/catenin complexes in human cancer. *Virchows Arch*., **439**: 725–751.

91 Pang, J., Kraemer, A., Stehbens, S., Frame, M., Yap, A. (2005). Recruitment of Phosphoinositide 3-kinase defines a positive contribution of tyrosine kinase signalling to E-cadherin function. *J.Biol.Chem*. **280**: 3043-3050.

92 Yap, A. S., Niessen, C. M., and Gumbiner, B. M. (1998). The Juxtamembrane Region of the Cadherin Cytoplasmic Tail Supports Lateral Clustering, Adhesive Strengthening, and Interaction with p21 ctn. *The Journal of Cell Biology*, **141**: 779-789.

93 Reddy, P., Liu, L., Ren, C., Lindgren, P., Boman, K., Shen, Y., Lundin, E., Ottander, U., Rytinki, M., Li, K. (2005). Formation of E-Cadherin-Mediated Cell-Cell Adhesion Activates Akt and Mitogen Activated Protein Kinase via Phosphatidylinositol 3 Kinase and Ligand-Independent Activation of Epidermal Growth Factor Receptor in Ovarian Cancer Cells. *Molecular Endocrinology*, **19**: 2564–2578

94 Rivard, N. (2009). Phosphatidylinositol 3-kinase: a key regulator in adherens junction formation and function. *Frontiers in Bioscience*, **14**: 510-522.

95 Pece, S., Chiariello, M., Murga, C., Gutkind, J. S. (1999). Activation of the Protein Kinase Akt/PKB by the Formation of E-cadherin-mediated Cell-Cell Junctions. Evidence for the association of phosphatidylinositol 3-kinase with the E-cadherin adhesion complex. *J. Biol. Chem*., **274**: 19347–19351.

96 Laprise, P., Chailler, P., Houde, M., Beaulieu, J. F., Boucher, M. J., Rivard, N. (2002). Phosphatidylinositol 3-kinase controls human intestinal epithelial cell differentiation by promoting adherens junction assembly and p38 MAPK activation. *J.Biol.Chem*, **277**: 8226-8234.

97 Kovacs, E. M., Ali, R. G., McCormack, A. J., Yap, A. S. (2002). E-cadherin Homophilic Ligation Directly Signals through Rac and Phosphatidylinositol 3-Kinase to Regulate Adhesive Contacts. *J. Biol. Chem*., **277**: 6708 –6718.

98 Nakagawaa, T., Murakami, A., Barwe, S. P., D'Ambrosio, J., Gopal, J., Lu, K., Ryazantsev, S., Rajasekaran, S. A., Rajasekaran, A. K. (2007). E-cadherin increases squamous cell carcinoma antigen expression through phosphatidylinositol-3 kinase-Akt pathway in squamous cell carcinoma cell lines. *Oncology Reports*, **18**: 175-179.

99 Vogelmann, R., Nguyen-tat, M.-D., Giehl, K., Adler, G., Wedlich, D., Menke, A. (2005). TGFβ-induced down-regulation of E-cadherin-based cell-cell adhesion depends on PI3-kinase and PTEN. *Journal of Cell Science*, **118**: 4901-4912.
100 Woodfield, R., Hodgkin, M., Akhtar, N., Morse, M., Fuller, K., Saqib, K., Thompson, N., Wakelam, M. (2001). The p85 subunit of phosphoinositide 3-kinase is associated with β-catenin in the cadherin-based adhesion complex. *Biochem J.*, **360**: 335-344.
101 Inge, L. J., Barwe, S. P., D'Ambrosio, J., Gopal, J., Lu, K., Ryazantsev, S., Rajasekaran, S. A., Rajasekaran, A. K. (2011). Soluble E-cadherin promotes cell survival by activating epidermal growth factor receptor. Exp. Cell. Res., **317**: 838–848.
102 Qian, X., Karpova, T., Sheppard, A. M., McNally, J., Lowy, D. R. (2004). E-cadherin-mediated adhesion inhibits ligand-dependent activation of diverse receptor tyrosine kinases. *The EMBO Journal*, **23**: 1739–1748.
103 Kim, S., Schein, A. J., and Nadel, J. A. (2005). E-cadherin promotes EGFR-mediated cell differentiation and MUC5AC mucin expression in cultured human airway epithelial cells. *Am J Physiol Lung Cell Mol Physiol.*, **289**: 1049 –1060.
104 Wang, D., Su, L., Huang, D., Zhang, H., Shin, D. M., Chen, Z. G. (2011). Down-regulation of E-Cadherin enhances proliferation of head and neck cancer through transcriptional regulation of EGFR. *Molecular Cancer*, **10**: 116
105 Friedl, P., Wolf, K. (2003). Tumor-cell invasion and migration: diversity and escape mechanisms. *Nature Rev.*, **3**: 362-373.
106 Alberts A. B., Johnson, A., Lewis, J., Raff, M., Roberts, K., and Walter, P. (2002). Mol Biol Cell, 4th edition. Garland Inc.New York., pg. 1113-1118.
107 Huttenlocher, A., Ginsberg, M. H., Horwitz, A. F. (1996). Modulation of Cell Migration by Integrin-mediated Cytoskeletal Linkages and Ligand-binding Affinity. *The Journal of Cell Biology*, **134**: 1551-1562.
108 Juliano, R., L., Haskill, S. (1993). Signal Transduction from the Extracellular Matrix. *J. Cell Biol*, **120**: 577-585.
109 Hood, J. D., and Cheresh, D. A. (2002). Role of integrins in cell invasion and migration. *Nature Reviews Cancer*, **2**: 91-100.
110 Vicente-Manzanares, M., Choi, C. K., and Horwitz, A. R. (2009). Integrins in cell migration – the actin connection. *Journal of Cell Science*, **122**: 199-206.
111 Friedl, P., Wolf, K. (2003). Tumor-cell invasion and migration: diversity and escape mechanisms. *Nature Rev.*, **3**: 362-373.
112 Hynes, R. O. (2002). Integrins: Bidirectional, Allosteric Signalling Machines. *Cell*, **110**: 673–687.
113 Danen, E. H. J., Sonneveld, P., Brakebusch, C., Fassler, R., Sonnenberg, A. (2002). The fibronectin-binding integrins α5β1 and αvβ3differentially modulate RhoA–GTP loading, organization of cell matrix adhesions, and fibronectin fibrillogenesis. *The Journal of Cell Biology*, **159**: 1071–1086.
114 Schwimmer, R., and Ojakian, G. K. (1995). The α2β1 integrin regulates collagen-mediated MDCK epithelial membrane remodeling and tubule formation. *Journal of Cell Science*, **108**: 2487-2498.
115 Fujiwara, H., Honda, T., Ueda, M., Nakamura, K., Yamada, S., Maeda, M., Mori, T. (1997). Laminin suppresses progesterone production by human luteinizing granulosa cells via interaction with integrin α6β1. *Journal of Clinical Endocrinology and Metabolism*, **82**: 2122–2128.
116 Harburger, D. S., and Calderwood, D. A. (2009). Integrin signalling at a Glance. *Journal of Cell Science*, **122**: 159-163.
117 Boudreau, N. J., and Jones, P. L. (1999). Extracellular matrix and integrin signalling: the shape of things to come. *Biochem. J.*, **339**: 481-488.

118 Vachon, P. H. (2011). Integrin Signalling, Cell Survival, and Anoikis: Distinctions, Differences, and Differentiation. *Journal of Signal Transduction*, doi:10.1155/2011/738137.
119 Guan, J.-L. (1997). Focal Adhesion Kinase in Integrin Signalling. *Matrix Biology*, **16**: 195-200.
120 Schlaepfer, D. D., and Hunter, T. (1998). Integrin signalling and tyrosine phosphorylation: just the FAKs? *trends in Cell Biology*, **8**: 151-7.
121 Dedhar, S., Williams, B., Hannigan, G. (1999). Integrin-linked kinase (ILK): a regulator of integrin and growth-factor signalling. *Trends Cell Biol*., **9**: 319-322.
122 Mitra, S. K., and Schlaepfer, D. D. (2006). Integrin-regulated FAK–Src signalling in normal and cancer cells. *Current Opinion in Cell Biology*, **18**: 516–523.
123 Veevers-Lowe, J., Ball, S. G., Shuttleworth, A., Kielty, C. M. (2010). Mesenchymal stem cell migration is regulated by fibronectin through a5b1-integrin-mediated activation of PDGFR-b and potentiation of growth factor signals. *Journal of Cell Science*, **124**: 1288-1300.
124 Rabinovitz, I., Mercurio, A., M. (1997). The integrin α6β4 functions in carcinoma cell migration on laminin-1 by mediating the formation and stabilization of actin-containing motility structures. *J Cell Biol.*, **139**: 1873-1884.
125 Parise, L., V., Lee, J., W., Juliano, R., L. (2000). New aspects of integrin signalling in cancer. *Sem Cancer Biol*., **10**: 407-414.
126 Hehlgans, S., Haase, M., Cordes, N. (2007). Signalling via the integrins: Implications for cell survival and anticancer strategies. *Biophys. Acta.*, **1775**: 163-180.
127 Tamura, M., Gu, J., Tran, H., Yamada, K. (1999). PTEN gene and integrin signalling in cancer. *J Natl Cancer Inst*, **91**: 1820-1828.
128 Eliceiri, B. P. (2001). Integrin and Growth Factor Receptor Crosstalk. *Circ Res.*, **89**: 1104-1110.
129 Cabodi, S., Moro, L. Bergatto, E., Boeri Erba, E., Di Stefano, P., Turco, E., Tarone, G., Defilippi, P. (2004). Integrin regulation of epidermal growth factor (EGF) receptor and of EGF-dependent responses. *Biochemical Society Transactions*, **32**: 438-42.
130 Demers, M.-J., Thibodeau, S., Noël, D., Fujita, N., Tsuruo, T., Gauthier, R., Arguin, M., Vachon, P. H. (2009). Intestinal Epithelial Cancer Cell Anoikis Resistance: EGFR-Mediated Sustained Activation of Src Overrides Fak-Dependent Signalling to MEK/Erk and/or PI3-K/Akt-1. *Journal of Cellular Biochemistry*, **107**: 639–654.
131 Cybulsky, A. V. (1999). Extracellular matrix as a determinant of signalling responses in glomerular epithelial cells. *Kidney International* , **56**: 1242–1246.
132 Cybulsky, A. V., McTavish, A. J., and Cyr, M.-D. (1994). Extracellular Matrix Modulates Epidermal Growth Factor Receptor Activation in Rat Glomerular Epithelial Cells. *J. Clin. Invest*., **94**: 68-78.
133 Soung, Y. H., Clifford, J. L., and Chung, J. (2010). Crosstalk between integrin and receptor tyrosine kinase signalling in breast carcinoma progression. *BMB reports*, **43**: 311-318.
134 Liu, Y., Pixley, R., Fusaro, M., Godoy, G., Kim, E., Bromberg, M. E., Colman, R. W. (2009). Cleaved high molecular weight kininogen and its domain 5 inhibit migration and invasion of human prostate cancer cells via the epidermal growth factor receptor pathway. *Oncogene*. **28**: 2756–2765.
135 Holbro, T., Civenni, G., Hynes, N., E. (2003). The ErbB receptors and their role in cancer progression. *Exp. Cell Res.*, **284**: 99-110.
136 Jorissen, R., N., Walker, F., Pouliot, N., Garrett, T., P., J., Ward, C., W., Burgess, A., W. (2003). Epidermal growth factor receptor:mechanisms of activation and signalling. *Exp. Cell Res.*, **284**: 31-53.

137 Valverde, C., M., Macarulla, T., Casado, E., Ramos, F., J., Martinelli, E., Tabernero, J. (2006). Novel targets in gastric and esophageal cancer. *Crit. Rev. Oncol.,***59**: 128-138.
138 Yarden, Y. (2001). The EGFR family and its ligands in human cancer: signalling mechanisms and therapeutic opportunities. *European Journal of Cancer,* **37**: S3–S8.
139 Olayioye, M., A., Neve, R. M., Lane, H. A., Hynes, N. E. (2000). The ErbB signalling network: receptor heterodimerization in development and cancer. *EMBO J.,* **19**: 3159-3167.
140 Klein, S., and Levitzki, A. (2009). Targeting the EGFR and the PKB pathway in cancer. *Current Opinion in Cell Biology*, **21**: 185–193.
141 Harris, R., C., Chung, E., and Coffey, R., J. (2003). EGF receptor ligands. *Exp. Cell Res.,* **284**: 2-13.
142 Graus-Porta, D., Beerli, R., R., Daly, J., M., Hynes, N., E. (1997). ErbB-2, the preferred heterodimerization partner of all ErbB receptors is a mediator of lateral signalling. *EMBO J.,* **16**: 1647-1655.
143 Citri, A., Skaria, K. B., and Yarden, Y. (2003). The deaf and the dumb: the biology of ErbB-2 and ErbB-3. *Exp. Cell Res.,* **284**: 54–65.
144 Fischer, O., M., Hart, S., Gschwind, A., Ullrich, A. (2003). EGFR signal transduction in cancer cells. *Biochem. Soc. Trans.,* **31**: 1203-1208.
145 King, C., R., Borrello, I., Porter, L., Comoglio, P., Schlessinger, J. (1989). Ligand-independent tyrosine phosphorylation of EGF receptor and the *erbB-2/neu* proto-oncogene product is induced by hyperosmotic shock. *Oncogene,* **4**: 13-18.
146 Coffer, P., J., Burgering, B., M., Peppelenbosch, M., P., Bos, J., L., Kruijer, W. (1995). UV activation of receptor tyrosine kinase activity. *Oncogene,* **11**: 561-569.
147 Ye, Y., N., Liu, E., S., L., Shin, V., Y., Wu, W., K., K., Luo, J., C., Cho, C., H. (2004). Nicotine promoted colon cancer growth via Epidermal growth factor receptor, c-Src and 5-Lipoxygenase-mediated signal pathway. *JPET*, **308**: 66-72.
148 Bogdan, S., and Klämbt, C. (2002). Epidermal growth factor receptor signalling. *Curr. Biol.,* **10**: 292-295.
149 Shoelson, S., E. (1997). SH2 and PTB domain interactions in tyrosine kinase signal transduction. *Curr. Opin. Chem. Biol.,* **1**: 227-234.
150 Rodrigues, G. A., Falasca, M., Zhang, Z., Ong, S. H., Schlessinger, J. (2000). A Novel Positive Feedback Loop Mediated by the Docking Protein Gab1 and Phosphatidylinositol 3-Kinase in Epidermal Growth Factor Receptor Signalling. *Mol. Cell. Biol.,* **20**: 1448–1459.
151 Mattoon, D. R., Lamothe, B., Lax, I., and Schlessinger, J. (2004). The docking protein Gab1 is the primary mediator of EGF-stimulated activation of the PI-3K/Akt cell survival pathway. *BMC Biology*, **2**: 24
152 Lemmon, M., A., Bu, Z., Ladbury, J. E., Zhou, M., Pinchasi, D., Lax, I., Engelman, D. M., Schlessinger, J. (1997). Two EGF molecules contribute additively to stabilization of the EGFR dimmer. *EMBO J.,* **16**: 281-294.
153 Fergusan, K., M. (2004). Active and inactive conformations of the epidermal growth factor receptor. *Biochem. Soc. Trans.,* **32**: 742-745.
154 Hurwitz, D., R., Emanuel, S. L., Nathan, M. H., Sarver, N., Ullrich, A., Felder, S., Lax, I., Schlessinger, J. (1991). EGF induces increased ligand binding affinity and dimerization of soluble epidermal growth factor (EGF) receptor extracellular domain. *J. Biol. Chem.,* **266**: 22035-22043.
155 Defize, L. H. K., Boonstra, J., Meisenhelder, J., Kruijer, W., Tertoolen, L. G., Tilly, B. C., Hunter, T., van Bergen en Henegouwen, P. M., Moolenaar, W. H., de Laat, S. W. (1989). Signal Transduction by Epidermal Growth Factor Occurs Through the Subclass of High Affinity Receptors. *The Journal of Cell Biology*, **109**: 2495-2507.

156 Őzcan, F., Klein, P., Lemmon, M. A., Lax, I., Schlessinger, J. (2006). On the nature of low- and high-affinity EGF receptors on living cells. *PNAS*, **103**: 5735–5740.
157 Krall, J. A., Beyer, E. M., and MacBeath, G. (2011). High- and Low-Affinity Epidermal Growth Factor Receptor-Ligand Interactions Activate Distinct Signalling Pathways. *PLoS ONE*, **6**: e15945. doi:10.1371/journal.pone.0015945.
158 Escobedo, J. A., Kaplan, D.R. (1991). A Phosphatidylinositol-3 Kinase Binds to Platelet-Derived Growth Factor Receptors through a Specific Receptor Sequence Containing Phosphotyrosine. *Mol. Cell. Biol*., **11:** 1125-113.
159 Savir, A., and Kass, D. (2010). Inhibition Of PI3K/AKT Blocks PDGF-Stimulated Induction Of Twist-1 In Rat Lung Fibroblasts. *Am J Respir Crit Care Med*., **181**: A3535.
160 Pickett, E. A., Olsen, G. S., and Tallquist, M. D. (2008). Disruption of PDGFR-initiated PI3K activation and migration of somite derivatives leads to spina bifida. *Development*, **135**: 589-598.
161 John, C., Johansen, T., and Gibb, A. J. (2010). Textbook of Receptor Pharmacology,3rd edition, CRC Press, Taylor&Francis Group, New York, Chapter 2, Fig.8.4, p 231.
162 Newton, A. C. (2009). Lipid activation of protein kinases. *J. Lipid Res*., **50**: 266–271.
163 Hurley, J. H. (2006). Membrane binding domains. *Biochim Biophys Acta*, **1761**: 805–811.
164 Hurley, J. H., and Misra, S. (2000). Signalling and subcellular targeting by membrane-binding domains. *Annu. Rev. Biophys. Biomol. Struct*., **29**: 49–79.
165 Kavran, J. M., Klein, D. E., Lee, A., Falasca, M., Isakoff, S. J., Skolnik, E. Y., Lemmon, M. A. (1998). Specificity and Promiscuity in Phosphoinositide Binding by Pleckstrin Homology Domains. *J. Biol. Chem*., **273**: 30497–30508.
166 Insall, R. H., and Weiner, O. D. (2001). PIP3, PIP2, and Cell Movement Similar Messages, Different Meanings? *Developmental Cell*, **1**: 743–747.
167 Rameh, L. E., Chen, C.-S., and Cantley, L. C. (1995). Phosphatidylinositol (3,4,5)P3 Interacts with SH2 Domains and Modulates PI 3-Kinase Association with Tyrosine-Phosphorylated Proteins. *Cell*, **83**: 821-830.
168 Coffer, P. J., Jin, J., and Woodgett, J. R. (1998). Protein kinase B (c-Akt): a multifunctional mediator of phosphatidylinositol 3-kinase activation. *Biochem. J*., **335**: 1-13.
169 Staal, S. P., Hartley, J. W., Rowe, W. P. (1977). Isolation of transforming murine leukemia viruses from mice with a high incidence of spontaneous lymphoma. *Proc. Nati. Acad. Sci. USA*, **74**: 3065-3067.
170 Ruan, G.-X., Kazlauskas, A. (2010). Focus on Molecules: Akt (PKB). *Exp. Eye. Res.* doi: 10.1016/j.exer.2010.0 6 .016.
171 Altomare, D. A., Guo, K., Cheng, J. Q., Sonoda, G., Walsh, K., and Testa, J. R. (1995). Cloning, chromosomal localization and expression analysis of the mouse Akt2 oncogene. *Oncogene*, **11**: 1055–1060.
172 Nakatani, K., Sakaue, H., Thompson, D. A., Weigel, R. J., and Roth, R. A. (1999). Identification of a human Akt3 (protein kinase B γ) which contains the regulatory serine phosphorylation site. *Biochem. Biophys. Res. Commun*., **257**: 906 –910.
173 Webster, M. K., Goya, L., Ge, Y., Maiyar, A. C., Firestone, G. L. (1993). Characterization of sgk, a Novel Member of the Serine/Threonine Protein Kinase Gene Family Which Is Transcriptionally Induced by Glucocorticoids and Serum. *Mol. Cell. Biol*., **13**: 2031-2040.
174 Hanada, M., Feng, J., and Hemmings, B. A. (2004). Structure, regulation and function of PKB/AKT—a major therapeutic target. *Biochimica et Biophysica Acta*, **1697**: 3–16.
175 Dummler, B., Tschopp. O., Hynx, D., Yang, Z. Z., Dirnhofer, S., Hemmings, B. A. (2006). Life with a Single Isoform of Akt: Mice Lacking Akt2 and Akt3 Are Viable but

Display Impaired Glucose Homeostasis and Growth Deficiencies. *Mol. Cell. Biol.*, **26:** 8042–8051.
176 Buzzi, F., Xu, L., Zuellig, R. A., Boller, S. B., Spinas, G. A., Hynx, D., Chang, Z., Yang, Z., Hemmings, B. A., Tschopp, O., Niessen, M. (2010). Differential Effects of Protein Kinase B/Akt Isoforms on Glucose Homeostasis and Islet Mass. *Mol. Cell. Biol.*, **30**: 601–612.
177 Ma, K., Cheung, S. M., Marshall, A. J., Duronio, V. (2008). PI(3,4,5)P 3 and PI(3,4)P 2 levels correlate with PKB/akt phosphorylation at Thr308 and Ser473, respectively; PI(3,4)P 2 levels determine PKB activity. *Cellular Signalling*, **20**: 684–694.
178 Calleja, V., Laguerre, M., Parker, P. J., and Larijani, B. (2009). Role of a novel PH-kinase domain interface in PKB/Akt regulation: Structural mechanism for allosteric inhibition. *PLoS Biol* , **7**: e1000017. doi:10.1371/journal.pbio.1000017.
179 Liao, Y., Hung, M.-C. (2010). Physiological regulation of Akt activity and stability. *Am J Transl Res.*, **2**: 19-42
180 Vanhaesebroeck, B., and Alessi, D. R. (2000). The PI3K–PDK1 connection: more than just a road to PKB. *Biochem. J.*, **346**: 561-576.
181 Toker, A., and Newton, A. C. (2000). Cellular Signalling: Pivoting around PDK-1. *Cell*, **103**: 185–188.
182 Ananthanarayanan, B., Fosbrink, M., Rahdar, M., and Zhang, J. (2007). Live-cell Molecular Analysis of Akt Activation Reveals Roles for Activation Loop Phosphorylation. *J. Biol. Chem.*, **282**: 36634 –36641.
183 Park, J., Feng, J., Li, Y., Hammarsten, O., Brazil, D. P., Hemmings, B. A. (2009). DNA-dependent Protein Kinase-mediated Phosphorylation of Protein Kinase B Requires a Specific Recognition Sequence in the C-terminal Hydrophobic Motif. *J. Biol. Chem.*, **284**: 6169 –6174.
184 Feng, J., Park, J., Cron, P., Hess, D., and Hemmings, B. A. (2004). Identification of a PKB/Akt Hydrophobic Motif Ser-473 Kinase as DNA-dependent Protein Kinase. *J. Biol. Chem.*, **279**: 41189 –41196.
185 Persad, S., Attwell, S., Gray, V., Mawji, N., Deng, J. T., Leung, D., Yan, J., Sanghera, J., Walsh, M. P., Dedhar, S. (2001). Regulation of Protein Kinase B/Akt-Serine 473 Phosphorylation by Integrin-linked Kinase. Critical roles for kinase activity and amino acids Arginine 211 and Serine 343. *J. Biol. Chem.*, **276**: 27462–2746.
186 Hresko, R. C., and Mueckler, M. (2005). mTOR-RICTOR Is the Ser473 Kinase for Akt/ Protein Kinase B in 3T3-L1 Adipocytes. *J. Biol. Chem.*, **280**: 40406 –40416.
187 Laplante, M., and Sabatini, D. M. (2009). mTOR signalling at aGlance. *Journal of Cell Science*, **122**:3589-3594.
188 Proud, C. G. (2009). Dynamic Balancing: DEPTOR Tips the Scales. *Journal of Molecular Cell Biology*, **1**: 61–63.
189 Sarbassov, D. D., Guertin, D. A. Ali, S. M., and Sabatini, D. M. (2005). Phosphorylation and Regulation of Akt/PKB by the Rictor-mTOR Complex. *Science*, **307:** 1098-1101.
190 Frias, M. A., Thoreen, C. C., Jaffe, J. D., Schroder, W., Sculley, T., Carr, S. A., Sabatini, D. M. (2006). mSin1 Is Necessary for Akt/PKB Phosphorylation, and Its Isoforms Define Three Distinct mTORC2s. *Current Biology*, **16**: 1865–1870.
191 Newton, A. C. (2009). Lipid activation of protein kinases. *J. Lipid Res.*, **50**: S266–S271.
192 PIK3CA GenBank Accesion Number: NC_000003.11.
193 Bi, L., Okabe, I., Bernard, D. J., Wynshaw-Boris, A., Nussbaum, R. L. (1999). Proliferative Defect and Embryonic Lethality in Mice Homozygous for a Deletion in the p110a Subunit of Phosphoinositide 3-Kinase. *J. Biol. Chem.*, **274**: 10963–10968.
194 Blume-Jensen, P., and Hunter, T. (2001). Oncogenic kinase signalling. *Nature*, **411**: 355-65.

195 Ruan, G.-X., and Kazlauskas, A. (2010). Focus on Molecules: Akt (PKB). *Exp. Eye. Res.* doi:10.1016/j.exer.2010.0 6 .016.
196 Summers, S. A., Kao, A. W., Kohn, A. D., Backus, G. S., Roth, R. A., Pessin, J. E., Birnbaum, M. J. (1999). The Role of Glycogen Synthase Kinase 3β in Insulin-stimulated Glucose Metabolism. *J. Biol. Chem*., **274**: 17934 –17940.
197 Cross, D. A. E., Alessi, D. R., Cohen, P., Andjelkovich, M., and Hemmings, B. A. (1995). Inhibition of glycogen synthase kinase-3 by insulin mediated by protein kinase B. *Nature*, **378**: 785-789.
198 Hoeflich, K. P., Luo, J., Rubie, E. A., Tsao, M. S., Jin, O., Woodgett, J. R. (2000). Requirement for glycogen synthase kinase-3beta in cell survival and NF-kappaB activation. *Nature*, **406**: 86–90.
199 MacAulay, K., Doble, B. W., Patel, S., Hansotia, T., Sinclair, E. M., Drucker, D. J., Nagy, A., Woodgett, J. R. (2007). Glycogen synthase kinase 3alpha-specific regulation of murine hepatic glycogen metabolism. *Cell Metab.*, **6**: 329–337.
200 Harwood, A. J. (2001). Regulation of GSK-3: A Cellular Multiprocessor. *Cell*, **105**: 821–824.
201 Wu, D., and Pan, W. (2009). GSK3: a multifaceted kinase in Wnt Signalling. *Trends in Biochemical Sciences*, **35**: 161-8.
202 Cadigan, K. M., and Liu, Y. I. (2005). Wnt signalling: complexity at the surface. *Journal of Cell Science*, **119**: 395-402.
203 Zhurinsky, J., Shtutman, M., and Ben-ze'ev, A. (2000). Differential Mechanisms of LEF/TCF Family-Dependent Transcriptional Activation by β-Catenin and Plakoglobin. *Mol. Cell. Biol*., **20**: 4238–4252.
204 Downes, C., P., Bennett, D., McConnachie, G., Leslie, N. R., Pass, I., MacPhee, C., Patel, L., Gray, A. (2001). Antagonism of PI 3-kinase-dependent signalling pathways by the tumour suppressor protein, PTEN. *Biochem. Soc. Trans.*, **29**: 846-851.
205 Li, J., Yen, C., Liaw, D., Podsypanina, K., Bose, S., Wang, S. I., Puc, J., Miliaresis, C., Rodgers, L., McCombie, R., Bigner, S. H., Giovanella, B. C., Ittmann, M., Tycko, B., Hibshoosh, H., Wigler, M. H., Parsons, R. (1997). PTEN, a putative protein tyrosine phosphatase gene mutated in human brain, breast, and prostate cancer. *Science*, **275**: 1943–1947.
206 Steck, P. A., Pershouse, M. A., Jasser S. A., Yung, W. K., Lin, H., Ligon, A. H., Langford, L. A., Baumgard, M. L., Hattier, T., Davis, T., Frye, C., Hu, R., Swedlund, B., Teng, D. H., Tavtigian, S. V. (1997). Identification of a candidate tumour suppressor gene, MMAC1, at chromosome 10q23.3 that is mutated in multiple advanced cancers, *Nat. Genet*., **15**: 356–362.
207 Omerovic, J., Clague, M. J., and Prior, I. A. (2010). Phosphatome profiling reveals P TPN2, P TPRJ and PTEN as potent negative regulators of PKB/Akt activation i n Ras-mutated cancer cells. *Biochem. J*., **426**: 65–72.
208 Leslie, N. R., Maccario, H., Spinelli, L., and Davidson, L (2009). The significance of PTEN's protein phosphatase activity. *Advances in Enzyme Regulation*, **49**: 190–196.
209 Chow, L. M. L., and Baker, S. J. (2006). PTEN function in normal and neoplastic growth. *Cancer Letters*, **241**: 184–196.
210 Li, L., and Ross, A. H. (2007). Why Is PTEN an Important Tumor Suppressor? *Journal of Cellular Biochemistry*, **102**: 1368 – 1374.
211 Taylor, V., Wong, M., Brandts, C., Reilly, L., Dean, N. M., Cowsert, L. M., Moodie, S., Stokoe, D. (2000). 5' Phospholipid Phosphatase SHIP-2 causes Protein Kinase B inactivation and cell cycle arrest in Glioblastoma cells. *Mol. Cell. Biol.*, **120**: 6860-6871.
212 Decker, S. J., and Saltiel, A. R. (2005). Staying in SHIP shape. *Nat. Med.*, **11**: 123-4.

213 Backers, K., Blero, D., Paternotte, N., Zhang, J., Erneux, C. (2003). The termination ofPI3K signalling by SHIP1 and SHIP2 inositol 5-phosphatases. *Advan. Enzyme Regul*., **43**: 15–28.
214 Sasaki, J., Kofuji, S., Itoh, R., Momiyama, T., Takayama, K., Murakami, H., Chida, S., Tsuya, Y., Takasuga, S., Eguchi, S., Asanuma, K., Horie, Y., Miura, K., Davies, E. M., Mitchell, C., Yamazaki, M., Hirai, H., Takenawa, T., Suzuki, A., Sasaki, T. (2010). The PtdIns(3,4)P 2 phosphatase INPP4A is a suppressor of excitotoxic neuronal death. *Nature*, **465**: 497-501.
215 Gewinner, C., Wang, Z. C., Richardson, A., Teruya-Feldstein, J., Etemadmoghadam, D., Bowtell, D., Barretina, J., Lin, W. M., Rameh, L., Salmena, L., Pandolfi, P. P., Cantley, L. C. (2009). Evidence that Inositol Polyphosphate 4-Phosphatase Type II Is a Tumor Suppressor that Inhibits PI3K Signalling. *Cancer Cell*, **16**: 115–12.
216 Rameh, L., E., Chen, C-C., and Cantley, L., C. (1995). Phosphatidylinositol (3,4,5)P3 Interacts with SH2 domains and modulates PI 3-Kinase association with tyrosine-phosphorylated proteins. *Cell*, **83**: 821-830.
217 Zhu, Z., He, X., Johnson, C., Stoops, J., Eaker, A., E., Stoffer, D., S., Bell, A., Zarnegar, R., DeFrances, M., C. (2007). Negative regulation of PI3K by PIK3IP1, a novel p110 interacting protein. *Biochem. Biophys. Res. Commun.*, **358**: 66-72.
218 Leslie, N. R., Dixon, M. J., Schenning, M., Gray, A., Batty, I. H. (2011). Distinct inactivation of PI3K signalling by PTEN and 5-phosphatases. *Advances in Enzyme Regulation*, doi:10.1016/j.advenzreg.2011.09.010.
219 Bayascas, J. R., and Alessi, D. R. (2005). Regulation of Akt/PKB Ser473 Phosphorylation. *Molecular Cell*, **18**: 143-5.
220 Meier, R., Thelen, M., and Hemmings, B. A. (1998). Inactivation and dephosphorylation of protein kinase Ba (PKBa) promoted by hyperosmotic stress. *The EMBO Journal*, **17**: 7294–7303.
221 Maira, S.M., Galetic, I., Brazil, D. P., Kaech, S., Ingley, E., Thelen, M., Hemmings, B. A. (2001). Carboxyl-terminal modulator protein (CTMP), a negative regu-lator of PKB/Akt and v-Akt at the plasma membrane. *Science*, **294**: 374 – 80.
222 Gao, T., Furnari, F., and Newton, A. C. (2005). PHLPP: A Phosphatase that Directly Dephosphorylates Akt , Promotes Apoptosis, an d Suppresses Tumor Growth. *Molecular Cell*, **18**: 13–24.
223 Cully, M., You , H., Levine, A. J., and Mak, T. W. (2006). Beyond PTEN mutations: the PI3K pathway as an integrator of multiple inputs during tumorigenesis. *Nature Reviews Cancer* , **6**: 184–192.
224 van der Heijden, M. S., and Bernards, R. (2010). Inhibition of the PI3K Pathway: Hope We Can Believe in? *Clin Cancer Res*; **16**: 30 94–9.
225 Courtney, K. D., Corcoran, R. B., and Engelman, J. A. (2010). The PI3K Pathway As Drug Target in Human Cancer. *J Clin Oncol*., **28**: 1075-1083.
226 Wymann, M. P., and Marone, R. (2005). Phosphoinositide 3-kinase in disease: timing, location, and scaffolding. *Curr Opin Cell Biol*., **17:** 141-9.
227 Osaki, M., Oshimuram, M., and Ito, H. (2004). PI3K-Akt pathway: Its functions and alterations in human cancer. *Apoptosis*, **9**: 667–676.
228 Klippel, A., Reinhard, C., Kavanaugh, M., Apell, G., Escobedo, M-A., Williams, L., T. (1996). Membrane localization of phosphatidylinositol 3-kinase is sufficient to activate multiple signal-transducing kinase pathways. *Mol. Cell. Biol.*, **16**: 4117-4127.
229 Sebastian, S., Settleman, J., Reshkin, S. J., Azzariti, A., Bellizzi, A., Paradiso, A. (2006). The complexity of targeting EGFR signalling in cancer: From expression to turnover. *Biochimica et Biophysica Acta*, **1766**: 120 –139.
230 Scaltriti, M., and Baselga, J. (2006). The Epidermal Growth Factor Receptor Pathway: A Model for Targeted Therapy. *Clin. Cancer Res*., **12**: 5268-5272.

231 Salomon, D., S., Brandt, R., Ciardiello, F., Normanno, N. (1995). Epidermal growth factor-related peptides and their receptors in human malignancies. *Crit. Rev. Oncology,* **19**: 183-232.
232 Shi, W., Zhang, X., Pintilie, M., Ma, N., Miller, N., Banerjee, D., Tsao, M. S., Mak, T., Fyles, A., Liu, F. F. (2003). Dysregulated Pten-Pkb And Negative Receptor Status In Human Breast Cancer. *Int. J. Cancer*, **104**: 195–203.
233 Heinemann, V., Stintzing, S., Kirchner, T., Boeck, S., Jung, A. (2009). Clinical relevance of EGFR- and KRAS-status in colorectal cancer patients treated with monoclonal antibodies directed against the EGFR. *Cancer Treatment Reviews*, **35**: 262–271.
234 Schrevel, M., Gorter, A., Kolkman-Uljee, S. M., Trimbos, J. B., Fleuren, G. J., Jordanova, E. S. (2011). Molecular mechanisms of epidermal growth factor receptor overexpression in patients with cervical cancer. *Modern Pathology*, **24**: 720 –728.
235 Limas, C., Bair, R., Bernhart, P., Reddy, P. (1993). Proliferative activity of normal and neoplastic urothelium and its relation to epidermal growth factor and transferrin receptors. *JClin Pathol*., **46**: 810-816.
236 Giamas, G., Man, Y. L., Hirner, H., Bischof, J., Kramer, K., Khan, K., Ahmed, S. S., Stebbing, J., Knippschild, U. (2010). Kinases as targets in the treatment of solid tumors. *Cellular Signalling*, **22**: 984 –1002.
237 Bader, A., G., Kang, S., and Vogt, P., K. (2005). Cancer-specific mutations in PIK3CA are oncogenic *in vivo. PNAS*, **103**: 1475-1479.
238 Li, V., S., W., Wong, C., W., Chan, T., L., Chan, A., S., W., Zhao, W., Chu, K-M., So, S., Chen, X., Yuen, S., T., Leung, S., Y. (2005). Mutations of PIK3CA in gastric adenocarcinoma. *BMC Cancer*, **5**: 29-35.
239 Isakoff, S., J., Engelman, J., A., Irie, H., Y., Luo, J., Brachmann, S., M., Pearline, R., V., Cantley, L., C., Brugge, J., S. (2005). Breast cancer-associated PIK3CA mutations are oncogenic in mammary epithelial cells. *Cancer Res.,* **65**: 10992-11000.
240 Campbell, I., G., Russell, S., E., Choong, D., Y., H., Montgomery, K., G., Ciavarella, M., L., Hooi, C., S., F., Cristiano, B., E., Pearson, R., B., Phillips, W., A. (2004). Mutation of the PIK3CA gene in ovarian and breast cancer. *Cancer Res.,* **64**: 7678-7681.
241 Zhao, J., J., Liu, Z., Wang, L., Shin, E., Loda, M., F., Roberts, T., M. (2005). The oncogenic properties of mutant p110α and p110β phosphatidylinositol 3-kinases in human mammary epithelial cells. *PNAS*, **102**: 18443-18448.
242 Pedrero, J., M., G., Carracedo, D., G., Pinto, C., M., Zapatero, A., H., Rodrigo, J., P., Nieto, C., S., Gonzalez, M., V. (2004). Frequent genetic and biochemical alterations of the PI3-/AKT/PTEN pathway in head and neck squamous cell carcinoma. *Int. J. Cancer*, **114**: 242-248.
243 Ma, Y-Y., Wei, S-J., Lin, Y-C., Lung, J-C., Chang, T-C., Whang-Peng, J., Liu, J., M., Yang, D-M., Yang, W., K., Shen, C-Y. (2000). PIK3CA as an oncogene in cervival cancer. *Oncogene*, **19**: 2739-2744.
244 Markman, B., Atzori, F., Pe´rez-Garcı´a, J., Tabernero, J., and Baselga, J. (2010). Status of PI3K inhibition and biomarker development in cancer therapeutics. *Annals of Oncology*, **21**: 683–691.
245 Shekar, S., C., Wu, H., Fu, Z., Yip, S-C., Nagajyothi, Cahill, S., M., Girvin, M., E., Backer, J., M. (2005). Mechanism of constitutive phosphoinositide 3-kinase activation by oncogenic mutants of the p85 regulatory subunit. *J. Biol. Chem.,* **280**: 27850-27855.
246 Sun, M., Hillmann, P., Hofmann, B. T., Hart, J. R., Vogt, P. K. (2010). Cancer-derived mutations in the regulatory subunit p85 α of phosphoinositide 3-kinase function through the catalytic subunit p110 α. *PNAS*, **107**: 15547–15552.
247 Staal, S. P. (1987). Molecular cloning of the akt oncogene and its human homologuesAKTI and AKT2: Amplification of AKTI in a primary humangastric adenocarcinoma. *Proc. Natl. Acad. Sci. USA*, **84**:5034-5037.

248 Altomare, D. A., and Testa, J. R. (2005). Perturbations of the AKT signalling pathway in human cancer. *Oncogene*, **24**: 7455–7464.
249 Dunlap, J., Le, C., Le, C., Shukla, A., Patterson, J., Presnell, A., Heinrich, M. C., Corless, C. L., Troxell, M. L. (2010). Phosphatidylinositol-3-kinase and AKT1 mutations occur early in breast carcinoma. *Breast Cancer Res Treat*., **120**: 409–418.
250 Malanga, D., Scrima, M., De Marco, C., Fabiani, F., De Rosa, N., De Gisi, S., Malara, N., Savino, R., Rocco, G., Chiappetta, G., Franco, R., Tirino, V., Pirozzi, G., Viglietto, G. (2008). Activating E17K mutation in the gene encoding the protein kinase AKT1 in a subset of squamous cell carcinoma of the lung. *Cell Cycle*, **7**: 665-669.
251 Askham, J. M., Platt, F., Chambers, P. A., Snowden, H., Taylor, C. F., Knowles, M. A. (2010). AKT1 mutations in bladder cancer: identification of a novel oncogenic mutation that can cooperate with E17K. *Oncogene*, **29**: 150–155.
252 Renner, O., Blanco-Aparicio, C., and Carnero, A. (2008). Genetic modelling of the PTEN/AKT pathway in cancer research. *Clin Transl Oncol*., **10**: 618-627.
253 Falke, J. J. (2007). Membrane Recruitment as a Cancer Mechanism: A Case Study of Akt PH Domain. *Cellscience*, **4**: 25–30.
254 Carpten, J.D., Faber, A. L, Horn, C., Donoho, G. P., Briggs, S. L., Robbins, C. M., Hostetter, G., Boguslawski, S., Moses, T. Y., Savage, S., Uhlik, M., Lin, A., Du, J., Qian, Y. W., Zeckner, D. J., Tucker-Kellogg, G., Touchman, J., Patel, K., Mousses, S., Bittner, M., Schevitz, R., Lai, M. H., Blanchard, K. L., Thomas, J. E. (2007). A transforming mutation in the pleckstrin homology domain of AKT1 in cancer. *Nature*, **448**: 439–444.
255 Brugge, J., Hung, M.-C., and Mills, G. B. (2007). A New Mutational aktivation in the PI3K Pathway. *Cancer Cell*, **12**: 104-107.
256 Jin, G., Kim, M. J., Jeon, H. S., Choi, J. E., Kim, D. S., Lee, E. B., Cha, S. I., Yoon, G. S., Kim, C. H,. Jung, T. H., Park, J. Y. (2010). PTEN mutations and relationship to EGFR , ERBB2 , KRAS , and TP53 mutations in non-small cell lung cancers. *Lung Cancer* , **69**: 279–283.
257 Dicuonzo, G., Angeletti, S., Garcia-Foncillas, J., Brugarolas, A., Okrouzhnov, Y., Santini, D., Tonini, G., Lorino, G., De Cesaris, M., Baldi, A. (2001). Colorectal Carcinomas and PTEN/MMAC1 Gene Mutations. *Clin. Cancer Res*., **7**: 4049 – 4053
258 Berger, M. F., Lawrence, M. S., Demichelis, F., Drier, Y., Cibulskis, K., Sivachenko, A. Y., Sboner, A., Esgueva, R., Pflueger, D., Sougnez, C., Onofrio, R., Carter, S. L., Par,k K., Habegger, L., Ambrogio, L., Fennell, T., Parkin, M., Saksena, G., Voet, D., Ramos, A. H., Pugh, T. J., Wilkinson, J., Fisher, S., Winckler, W., Mahan, S., Ardlie, K., Baldwin, J., Simons, J. W., Kitabayashi, N., MacDonald, T. Y., Kantoff, P. W., Chin, L., Gabriel, S. B., Gerstein, M. B., Golub, T. R., Meyerson, M., Tewari, A., Lander, E. S., Getz, G., Rubin, M. A., Garraway, L. A. (2011). The genomic complexity of primary human prostate cancer. *Nature*, **470**: 214-20.
259 Feilotter, H., E., Coulon, V., McVeigh, J., L., Boag, A., H., Dorion-Bonnet, F., Duboue, B., Latham, W., C., Eng, C., Mulligan, L., M., Longy, M. (1999). Analysis of the 10q23 chromosomal region and the PTEN gene in human sporadic breast carcinoma. *Br. J. Cancer*, **79**: 718-723.
260 Garcia, J., M., Silva, J., M., Dominguez, G., Gonzalez, R., Navarro, A., Carretero, L., Provencio, M., Espana, P., Bonilla, F. (1999). Allelic loss of the PTEN region (10q23) in breast carcinomas of poor pathophenotype. *Breast Cancer Res. Treat.*, **57**: 237-243.
261 Tokunaya, E., Oki, E., Kimura, Y., Yamanaka, T., Egashira, A., Nishida, K., Koga, T., Morita, M., Kakeji, Y., Maehara, Y. (2006). Coexistence of the loss of heterozygosity at the PTEN locus and HER2 overexpression enhances the Akt activity thus leading to a negative progesterone receptor expression in breast carcinoma. *Breast Cancer Res. Treat.*, **101**: 249-257.

262 Zhang, S., and Yu, D. (2010). PI(3)King Apart PTEN's Role in Cancer. *Clin. Cancer Res*., **16**: 4325-4330.
263 Jemal, A., Siegel, R., Xu, J., Ward, E. (2010). Cancer Statistics, 2010. *CA Cancer J Clin*., **60**: 277–300.
264 Kamangar, F., Dores, G. M., and Anderson, W. F. (2006). Patterns of Cancer Incidence, Mortality, and revalence Across Five Continents: Defining Priorities to Reduce Cancer Disparities in Different Geographic Regions of the World. *J Clin Oncol.*, **24**: 2137-2150.
265 Dandara, C., Ballo, R., Parker, M., I. (2005) CYP3A5 genotypes and risk of oesophageal cancer in two South African populations. Cancer Lett. *225*:275-282.
266 Hendricks, D., Parker, I., M. (2002). Oesophageal Cancer in Africa. IUBMB Life. *53*, 263-268.
267 O'Donovan, T. R., O'Sullivan, G. C., and McKenna, S. L. (2011). Induction of autophagy by drug-resistant esophageal cancer cells promotes their survival and recovery following treatment with chemotherapeutics. *Autophagy*. **7**: 509–524.
268 Syrigos, K. N., Zalonis, A., Kotteas, E., Saif, M. W. (2008). Targeted therapy for oesophage al cancer: an overview. *Cancer Metastasis Rev*., **27**: 273 –288.
269 Jin, J.,Liao, Z., Zhang, Z., Ajani, J., Swisher, S., Chang, J.Y, Jeter, M., Guerrero, T., Stevens, C. W., Vaporciyan, A., Putnam, J. Jr., Walsh, G., Smythe, R., Roth, J., Yao, J., Allen, P., Cox, J. D., Komaki, R. (2004). Induction chemotherapy improved outcomes of patients with resectable esophageal cancer who received chemoradiotherapy followed by surgery. *Int. J. Radiation Oncology Biol. Phys*., **60**: 427– 436.
270 Ancona, E., Rampado, S., Cassaro, M., Battaglia, G., Ruol, A., Castoro, C., Portale, G., Cavallin, F., Rugge, M. (2008). Prediction of Lymph Node Status in Superficial Esophageal Carcinoma. *Annals of Surgical Oncology*, **15**: 3278 –3288.
271 Kulwinder S. (2003). New Approach to Malignant Strictures of the Esophagus. *Current Gastroenterology Reports*, **5**: 198–205.
272 Stoner, G., D., Gupta, A. (2001). Etiology and chemoprevention of oesophageal squamous cell. Carcinogenesis. *22*:1737-1746.
273 Kamangar, F., Chow, W. H., Abnet, C. C., Dawsey, S. M. (2009). Environmental Causes of Esophageal Cancer. *Gastroenterol Clin North Am*., **38**: 27–vii. doi:10.1016/j.gtc.2009.01.004.
274 Vaughan, T. L., Davis, S., Kristal, A., and Thomas, D. B. (1995). Obesity, Alcohol, and Tobacco as Risk Factors for Cancers of the Esophagus and Gastric Cardia: Adenocarcinoma versus Squamous Cell Carcinoma. *Cancer Epidemiol Biomarkers Prev*., **4**: 85-92.
275 Brown, L., M. (2005). Epidemiology of alcohol-associated cancers. Alcohol. *35*:161-168.
276 Lee, C.-H., Wu, D.-C., Lee, J. M., Wu, I. C., Goan, Y. G,. Kao, E. L., Huang, H. L., Chan, T. F., Chou, S. H., Chou, Y. P., Lee, C. Y., Chen, P. S., Ho, C. K., He, J., Wu, M. T. (2007). Carcinogenetic impact of alcohol intake on squamous cell carcinoma risk of the oesophagus in relation to tobacco smoking. *European J. Cancer*, **43**: 1188 –1199.
277 Islami, F., Boffetta, P., Ren, J. S., Pedoeim, L., Khatib, D., Kamangar, F. (2009). High-temperature beverages and Foods and Esophageal Cancer Risk -- A Systematic Review. *Int J Cancer*, **125**: 491–524.
278 Wiseman, E. F., and Ang, Y. S. (2011). Risk factors for neoplastic progression in Barrett's esophagus. *World J Gastroenterol*., **17**: 3672-3683.
279 Zhang, R., Gong, J., Wang, H., and Wang, L. (2005). Bile salts inhibit growth and induce apoptosis of human esophageal cancer cell line. *World J Gastroenterol*, **11**: 5109-5116.
280 Vaezi, M.F., and Richter, J. E. (1997). Contribution of acid and duodenogastro-oesophageal reflux to esophageal mucosal injury and symptoms in partial gastrectomy patients. *Gut*, **41**: 297–302.

281 Jakszyn, P., and González, C. A. (2006). Nitrosamine and related food intake and gastric and oesophageal cancer risk: A systematic review of the epidemiological evidence. *World J Gastroenterol*., **12**: 4296-4303.
282 Syrjänen, K. J. (2002). HPV infections and oesophageal cancer. *J Clin Pathol*., **55**: 721–728.
283 Stein, H. J., Kauer, W. K., Feussner, H., Siewert, J. R. (1999). Bile acids as components of the duodenogastric refluxate: detection, relationship to bilirubin, mechanism of injury, and clinical relevance. *Hepatogastroenterology*, **46**: 66-73.
284 Shankar, S., vanSonnenberg, E., Silverman, S. G., Tuncali, K., Banks, P. A. (2004). Imaging and Percutaneous Management of Acute Complicated Pancreatitis. *Cardiovasc Intervent Radiol* ., **27**: 567–580.
285 Shigemitsu, K., Naomoto, Y., Shirakawa, Y., Haisa, M., Gunduz, M., Tanaka, N. (2002). A case of advanced esophageal cancer with extensive lymph node metastase successfully treated with multidomain therapy. *Jpn. J. Clin. Oncol*., **32**: 310-314.
286 Syme-Grant, N., Walsh, S. V. (2006). Pathology of oesophageal Tumours. *Surgery*, **24**: 85-6.
287 Grace, M.P., Kim, K.H., True, L.D. and Fuchs, E. (1985) Keratin Expression in Normal Esophageal Epithelium and Squamous Cell Carcinoma of the Esophagus. *Cancer Res*., **45**: 841-46.
288 McCabe, M., L., Dlamini, Z. (2005). The molecular mechanisms of oesophageal cancer. Int. Immuno Phar., *5:1113*-1130.
289 Mandard, A.-M., Hainaut, P., and Hollstein, M. (2000). Genetic steps in the development of squamous cell carcinoma of the esophagus. *Mutation Research*, **462**: 335–342.
290 Nishihira, T., Hashimoto, Y., Katayama, M., Mori, S., Kuroki, T. (1993). Molecular and cellular features of esophageal cancer cells. *J Cancer Res Clin Oncol.*, **119**: 441-449.
291 Sarbia, M., Ott, N., Puhringer-Oppermann, F., and Brucher, B. L. D. M. (2007). The predictive value of molecular markers (p53, EGFR, ATM,CHK2) in multimodally treated squamous cell carcinoma of the Oesophagus. *British Journal of Cancer*, **97**: 1404 – 1408.
292 Mathew,R.,Arora,S.,Khanna,R.,Mathur,M.,Shukla,N.,K.,Ralhan,R. (2002). Alteration in p53 and pRb pathways and their prognostic significance in oesophageal cancer. *Euro J Cancer.*, **38**:832-841.
293 Yamashita, K., Mori, M., Kataoka, A., Inoue, H., and Sugimachi, K. (2001). The clinical significance of MMP-1 expression in oesophageal carcinoma. *British Journal of Cancer*, **84**: 276–282.
294 Lv, J., Cao, X.-F., Ji, L., Zhu, B., Wang, D. D., Tao, L., Li, S. Q. (2011). Association of β-catenin, Wnt1, Smad4, Hoxa9, and Bmi-1 with the prognosis of esophageal squamous cell carcinoma. *Med Oncol*., doi 10.1007/s12032-010-9816-5.
295 Hildebrandt, M. A. T., Yang, H., Hung, M. C., Izzo, J. G., Huang, M., Lin, J., Ajani, J. A., Wu, X. (2009). Genetic Variations in the PI3K/PTEN/AKT/mTOR Pathway Are Associated With Clinical Outcomes in Esophageal Cancer Patients Treated With Chemoradiotherapy. *J Clin Oncol*, **27**: 857-871.
296 Hamano, R., Miyata, H., Yamasaki, M., Kurokawa, Y., Hara, J., Moon, J. H., Nakajima, K., Takiguchi, S., Fujiwara, Y., Mori, M., Doki, Y. (2011). Overexpression of miR-200c Induces Chemoresistance in Esophageal Cancers Mediated Through Activation of the Akt Signalling Pathway. *Cancer Res.*, **17**: 3029–38.
297 Ramljak, D., Calvert, R., J., Wieserfeld, P., W., Diwan, B., A., Catipovic, B., Marasus, W., F., O., Victor, T., C., Anderson, L., M., Gelderblom, W., C., A. (2000). A potential mechanism for fumonisin B1-mediated hepatocarcinogenesis: cyclin D1 stabilization association with activation of Akt and inhibition of GSK-3β activity. *Carcinogenesis*, **21**:1537-1546.

298 West, K., A., Linnoila, H., R., Belinsky, S., S., Harris, C., C., Dennis, P., A. (2004). Tobacco carcinogen-induced cellular transformation increases activation of the phosphatidylinositol 3'-kinase/Akt pathway *in Vitro*. *Cancer Res.*,**64**: 446-451.
299 West, K., A., Brognard, J., Clark, A., S., Linnoila, I., R., Yang, X., Swain, S., M., Harris, C., Belinsky, S., Dennis, P., A. (2003). Rapid Akt activation by nicotine and a tobacco carcinogen modulate the phenotype of normal human airway epithelial cells. *J. Clin. Invest.*, **111**:81-90.
300 Aklilu, M., and Ilson, D. H. (2006). Targeted Agents and Esophageal Cancer—The Next Step? *Semin Radiat Oncol*., **17**:62-69.
301 Dragovich, T., and Campen, C. (2009). Anti-EGFR-Targeted Therapy for Esophageal and Gastric Cancers: An Evolving Concept. *Journal of Oncology*, doi:10.1155/2009/804108.
302 Zhao, L., and Vogt, P. K. (2008). Class I PI3K in oncogenic cellular transformation PI3K in oncogenic cellular transformation. *Oncogene*, **27**: 5486-5496.
303 Gu, J., and Iyer, V. R. (2006). PI3K signalling and miRNA expression during the response of quiescent human fibroblasts to distinct proliferative stimuli. *Genome Biology*, **7**: R42 (doi:10.1186/gb-2006-7-5-r42).
304 Kapeller, R., and L. C. Cantley. (1994). Phosphatidylinositol 3-kinase. *Bio-Essays*, **16**: 565–576.
305 Krymskaya, V. P., Ammit, A. J., Hoffman, R. K., Eszterhas, A. J., Panettieri, R. A. Jr. (2001). Activation of class IA PI3K stimulates DNA synthesis in human airway smooth muscle cells. *Am J Physiol Lung Cell Mol Physiol*., **280**: 1009–1018.
306 Maurer, M., Su, T., Saal, L. H., Koujak, S., Hopkins, B. D., Barkley, C. R., Wu, J., Nandula, S., Dutta, B., Xie, Y., Chin, Y. R., Kim, D. I., Ferris, J. S., Gruvberger-Saal, S. K., Laakso, M., Wang, X., Memeo, L., Rojtman, A., Matos, T., Yu, J. S., Cordon-Cardo, C., Isola, J., Terry, M. B., Toker, A., Mills, G. B., Zhao, J. J., Murty, V. V., Hibshoosh, H., Parsons, R. (2009). 3-Phosphoinositide–Dependent Kinase 1 Potentiates Upstream Lesions on the Phosphatidylinositol 3-Kinase Pathway in Breast Carcinoma. *Cancer Res*., **69**: 6299–306.
307 Bos, J. L. (1995). A target for phosphoinositide 3-kinase: Akt/PKB. *TIBS*, **20**: 441-2.
308 Dario, R. Alessi, D. R., Deak, M., Casamayor, A., Caudwell, F. B., Morrice, N., Norman, D. G., Gaffney, P., Reese, C. B., MacDougall, C. N., Harbison, D., Ashworth, A., Bownes, M. (1997). 3-Phosphoinositide-dependent protein kinase-1 (PDK1): structural and functional homology with the Drosophila DSTPK61 kinase. *Current Biology*, **7**: 776–789.
309 Piguet, A.-C., and Dufour, J.-F. (2011). PI(3)K/PTEN/AKT pathway. *Journal of Hepatology*, **54**: 1317–1319.
310 Carnero, A. (2010). The PKB/AKT Pathway in Cancer. *Current Pharmaceutical Design*, **16**: 34-44.
311 Ekstrand, A. I., Jönsson, M., Lindblom, A., Borg, A., Nilbert, M. (2010). Frequent alterations of the PI3K/AKT/mTOR pathways in hereditary nonpolyposis colorectal cancer. *Familial Cancer*, **9**: 125–129.
312 Link, W., Rosado, A., Fominaya, J., Thomas, J. E., Carnero, A. (2005). Membrane Localization of all Class I PI 3-Kinase Isoforms Suppresses c-Myc-Induced Apoptosis in Rat1 Fibroblasts via Akt. *Journal of Cellular Biochemistry*, **95**: 979–989.
313 Holt, K., H., Olson, L., Moye-Rowley, W., S., Pessin, J., E. (1994). Phosphatidylinositol 3-kinase activation is mediated by high-affinity interactions between distinct domains within the p110 and p85 subunits. *Mol. Cell. Biol.*, **14**: 42-49.
314 Williams, R., Berndt, A., Miller, S., Hon, W. C., Zhang, X. (2009). Form and flexibility in phosphoinositide 3-kinases. *Biochem Soc Trans*., **37**: 615-26.

315 Woscholski, R., Dhand, R., Fry, M., J., Waterfield, M., D., Parker, P., J. (1994). Biochemical characterization of the free catalytic p110α and the complexed heterodimeric p110α·p85α forms of the mammalian phosphatidylinositol 3-kinase. *J. Biol. Chem.,* **269**: 25067-25072.
316 Yip, S.-C., El-Sibai, M., Hill, K. M., Wu, H., Fu, Z., Condeelis, J. S., Backer, J. M. (2004). Over-Expression of the p110β But Not p110α Isoform of PI 3-Kinase Inhibits Motility in Breast Cancer Cells. *Cell Motility and the Cytoskeleton*, **59**: 180–188.
317 Jamshidi, Y., Snieder, H., Wang, X., Pavitt, M. J., Spector, T. D., Carter, N. D., O'Dell, S. D. (2006). Phosphatidylinositol 3-kinase p85 alpha regulatory subunit gene PIK3R1 haplotype is associated with body fat and serum leptin in a female twin population. *Diabetologia*, **49**: 2659–2667.
318 Philp, A. J., Campbell, I. G., Leet, C., Vincan, E., Rockman, S. P., Whitehead, R. H., Thomas, R. J., Phillips, W. A. (2001). The Phosphatidylinositol 3-kinase p85αGene is an Oncogene in Human Ovarian and Colon Tumors. *Cancer Res.*, **61**: 7426–7429.
319 Jücker, M., Südel, K., Horn, S., Sickel, M., Wegner, W., Fiedler, W., Feldman, R., A. (2002). Expression of a mutated form of the p85α regulatory subunit of phosphatidylinositol 3-kinase in a Hodgkin's lymphoma-derived cell line (CO). *Leukemia,* **16**: 894-901.
320 Dbouka, H. A., Panga, H., Fiser, A., and Backer, J. M. (2010). A biochemical mechanism for the oncogenic potential of the p110β catalytic subunit of phosphoinositide 3-kinase. *PNAS*, **107**: 19897–19902.
321 Liu, Y., Liu, H., Bai, X., Ye, Z., Sun, H., Bai, R., Wang, D. (2011). Differentiation of metastatic from non-metastatic lymph nodes in patients with uterine cervical cancer using diffusion-weighted imaging. *Gynecologic Oncology*, **122**: 19–24.
322 Sunayama, J., Sato, A., Matsuda, K., Tachibana, K., Suzuki, K., Narita, Y., Shibui, S., Sakurada, K., Kayama, T., Tomiyama, A., Kitanaka, C. (2010). Dual blocking of mTor and PI3K elicits a pro-differentiation effect on glioblastoma stem-like cells. *Neuro Oncol.*, **12**: 1205-1219.
323 Wu, X., Chen, S., Orlando, S. A., Yuan, J., Kim, E. T., Munugalavadla, V., Mali, R. S., Kapur, R., Yang, F. C. (2011). p85alpha regulates osteoblast differentiation by cross-talking with the MAPK pathway. *J. Biol. Chem.*, **286**: 13512-21.
324 Brachmann, S. M., Yballe, C. M., Innocenti, M., Deane, J. A., Fruman, D. A., Thomas, S. M., Cantley, L. C. (2005). Role of Phosphoinositide 3-Kinase Regulatory Isoforms in Development and Actin Rearrangement. *Mol. Cell. Biol.*, **25**: 2593–2606.
325 Munugalavadla, V., Vemula, S., Sims, E. C., Krishnan, S., Chen, S., Yan, J., Li, H., Niziolek, P. J., Takemoto, C., Robling, A. G., Yang, F. C., Kapur, R. (2008). The p85α Subunit of Class IA Phosphatidylinositol 3-Kinase Regulates the Expression of Multiple Genes Involved in Osteoclast Maturation and Migration. *Mol. Cell. Biol.*, **28**: 7182–7198.
326 Ptasznik, A., Vemula, S., Sims, E. C., Krishnan, S., Chen, S., Yan, J., Li, H., Niziolek, P. J., Takemoto, C., Robling, A. G., Yang, F. C., Kapur, R. (1997). Phosphatidylinositol 3-Kinase Is a Negative Regulator of Cellular Differentiation. *The Journal of Cell Biology*, **137**: 1127–1136.
327 Peng, Y., Jiang, B. H., Yang, P. H., Cao, Z., Shi, X., Lin, M. C., He, M. L., Kung, H. F. (2004). Phosphatidylinositol 3-Kinase Signalling Is Involved in Neurogenesis during Xenopus Embryonic Development. *J. Biol. Chem.*, **279**: 28509–28514.
328 Bai, Z., Zhang, Z., Ye, Y., and Wang, S. (2010). Sodium butyrate induces differentiation of gastric cancer cells to intestinal cells via the PTEN/phosphoinositide 3-kinase pathway. *Cell Biol. Int.*, **34**: 1141–1145.
329 Veale, R. B., and Thornley, A. L. (1984). Atypical cytokeratins synthesized by Human oesophageal Carcinoma Cells in culture. *South African Journal of Science,* **80**: 260-7.

330 Ikediobi, O. N., Davies, H., H., Bignell, G., Edkins, S., Stevens, C., O'Meara, S., Santarius, T., Avis T, Barthorpe S, Brackenbury, L., Buck, G., Butler, A., Clements, J., Cole, J., Dicks, E., Forbes, S., Gray, K., Halliday, K., Harrison, R., Hills, K., Hinton, J., Hunter, C., Jenkinson, A., Jones, D., Kosmidou, V., Lugg, R., Menzies, A., Mironenko, T., Parker, A., Perry, J., Raine, K., Richardson, D., Shepherd, R., Small, A., Smith, R., Solomon, H., Stephens, P., Teague, J., Tofts, C., Varian, J., Webb, T., West, S., Widaa, S., Yates, A., Reinhold, W., Weinstein, J. N., Stratton, M. R., Futreal, P. A., Wooster, R. (2006). Mutation analysis of 24 known cancer genes in the NCI-60 cell line set. *Mol. Cancer Ther.*, **5**: 2606–2612.

331 Morrowa, C. J., Gray, A., and Dive, C. (2005). Comparison of phosphatidylinositol-3-kinase signalling within a panel of human colorectal cancer cell lines with mutant or wild-type PIK3CA. *FEBS Letters*, **579**: 5123–5128.

332 Veale, R.B., Thornley, A.L. (1989). Increased single class low-affinity EGF receptors expressed by human oesophageal squamous carcinoma cell lines. *S. Afri. J. Sci.*, **85**:375-379.

333 Bey E., Alexander, J., Whitcutt, J. M., Hunt, J. A., Gear, J. H. (1976). Carcinoma of the oesophagus in Africans: Establishment of a continuously growing cell line from a tumor specimen. *In Vitro*. **12**: 107-114.

334 Kawasaki, E.S., and Wang, A.M. (1989). Detection of gene expression, In: Erlich HA ed. PCR technology: Principles and applications for DNA amplification. *Stockton Press, New York*: 89-97.

335 Laemmli, U.K. (1970). Cleavage of structural proteins during the assembly of the head of bacteriophage T4. *Nature*, **227**:680-685.

336 Chartier, N. T., Laine, M., Gout, S., Pawlak, G., Marie, C. A., Matos, P., Block, M. R., Jacquier-Sarlin, M. R. (2006). Laminin-5-integrin interaction signals through PI 3-kinase and Rac1b to promote assembly of adherins junctions in HT-29 cells. *J. Cell Sci.*, **119**:31-46.

337 Dignam, J. D., Lebovitz, M. R., and Roeder, R. G. (1983). Accurate transcription initiation by RNA polymerase II in a soluble extract from isolated mammalian nuclei. *Nucleic Acids Research*, **11**: 1475-89.

338 Chen, R., Ding, W.V., McCormick, F. (2000). Wnt Signalling to β-catenin involved Two Interactive components. *J. Biol. Chem.*, **275**: 17894-17899.

339 Bradford, M.M. (1976). A rapid and sensitive method for the quantification of microgram quantities of protein utilizing the principle of protein-dye binding. *Anal. BioChem.*, **72**:248-254.

340 Bramhall S, Noack N, Wu M, and Loewenberg JR, (1969). A simple colorimetric method for determination of protein. *Analytical Biochemistry*, **31**: 146-8.

341 Blommaart, E., F., C., Krause, U., Schellens, J. P., Vreeling-Sindelárová, H., Meijer, A. J. (1997). The phosphatidylinositol 3-kinase inhibitors wortmannin and LY294002 inhibit autophagy in isolated rat hepatocytes. *Eur. J. Biochem*, **243**: 240-246.

342 Vlahos, C., J., Matter, W., F., Hui, K., Y., Brown, R., F. (1994). A specific inhibitor of Phosphatiduylinositol 3-kinase, 2-(4-morpholinyl)-8-phenyl-4H-1benzopyran-4-one (LY294002). *J. Biol. Chem.*, **269**: 5241-5248.

343 Walker, E., H., Pacold, M., E., Perisic, O., Stephens, L., Hawkins, P., T., Wymann, M., P., Williams, R., L. (2000). Structural determinants of Phosphoinositide 3-kinase inhibition by Wortmannin, LY294002, Quercetin, Myricetin, and Staurosporine. *Mol. Cell*, **6**: 909-919.

344 Ryu, K. H., Choi, S. H., and Lee, J. S. (2000). Restriction Primers as Short as 6-mers for PCR Amplification of Bacterial and Plant Genomic DNA and Plant Viral RNA. *Molecular Biotechnology*, **14**: 1073–6085.

345 Szymański, M., Baraiszewska, M., Z., Erdmann, V., A., and Baraiszewski, J. (2003). 5 S rRNA: structure and interactions. *Biochem J.*, **371**: 641-651.
346 Habib, A., Hognason, T., Ren, J., Stefansson, K., Ratan, R. (1998). The epidermal growth factor receptor associates with and recruits phosphatidylinositol 3-kinase to the platelet-derived growth factor β receptor. *J. Biol.Chem*, **273**: 6885-6891.
347 Zhao, J., Cheng, H., Jia, S., Wang, L., Gjoerup, O. V., Mikami, A., Roberts, T. M. (2006). The p110α isoform of PI3K is essential for proper growth factor signalling and oncogenic transformation. *PNAS*, **103**: 16296-16300.
348 Kingsbury, S.,R., Gout, I.,T. (2003). Phosphoinositide 3-kinases and Cancer. *Exp. Onc.*, **25**: 3-15.
349 Martin-Fernandez, C., Bales, J., Bales, J., Hodgkinson, C., Welman, A., Welham, M. J., Dive, C., and Morrow, C. J. (2009). Blocking PI3-Kinase Activity in Colorectal Cancer Cells Reduces Proliferation but does not Increase Apoptosis Alone or in Combination with Cytotoxic Drugs. *Mol. Cancer Res.*, **7**: 955–965.
350 Ozawa, M., and Kemler, R. (1998). The membrane proximal region of the E-cadherin cytoplasmic domain prevents dimerization and negatively regulates adhesion activity. *J. Cell. Biol.*, **142**: 1605-1613.
351 Torres, V., A., Tapia, J., C., Rodriguez, D. A., Lladser, A., Arredondo, C., Leyton, L., Quest, A. F. (2007). E-cadherin is required for caveolin-1-mediated down-regulation of the inhibitor of apoptosis protein surviving via reduced β-catenin-Tcf/Lef-dependent transcription. *Mol. Cell. Biol.*, **27**: 7707-7717.
352 Wisdom, R., Johnson, R. S., and Moore, C. (1999). c-Jun regulates cell cycle progression and apoptosis by distinct mechanisms. *The EMBO Journal*, **18**: 188–197.
353 Garcon, F., Patton, D. T., Emery, J. L., Hirsch, E., Rottapel, R., Sasaki, T., Okkenhaug, K. (2008). CD28 provides T-cell costimulation and enhances PI3K activity at the immune synapse independently of its capacity to interact with the p85/p110 heterodimer. *Blood*, **111**: 1464-1471.
354 Ciaraldi, T. P., Kong, A. P., Chu, N. V., Kim, D. D., Baxi, S., Loviscach, M., Plodkowski, R., Reitz, R., Caulfield, M., Mudaliar, S., Henry, R. R. (2002). Regulation of Glucose Transport and Insulin Signalling by Troglitazone or Metformin in Adipose Tissue of Type 2 Diabetic Subjects. *Diabetes*, **51**: 30–36.
355 Chan, T. O., Rittenhouse, S. E., and Tsichlis, P. N. (1999). Akt/PKB and other D3 phosphoinositide-regulated kinases:kinase activation by phosphoinositide-dependent phosphorylation. *Annu. Rev. Biochem*, **68**: 965–1014.
356 Lawlor, M. A., and Alessi, D. R. (2001). PKB/Akt: a key mediator of cell proliferation, survival and insulin responses*? Journal of Cell Science*, **114**: 2903-2910.
357 Duronio, V. (2008). The life of a cell: apoptosis regulation by the PI3K/PKB pathway. *Biochem. J.*, **415**: 333–344.
358 Freeburn, R. W., Wright, K. L., Burgess, S. J., Astoul, E., Cantrell, D. A., Ward, S. G. (2002). Evidence That SHIP-1 Contributes to Phosphatidylinositol 3,4,5-Trisphosphate Metabolism in T Lymphocytes and Can Regulate Novel Phosphoinositide 3-Kinase Effectors. *The Journal of Immunology*, **169**: 5441–5450.
359 Maiuri, T., Ho, J., and Stambolic, V. (2010). Regulation of Adipocyte Differentiation by Distinct Subcellular Pools of Protein Kinase B (PKB/Akt). *J. Biol. Chem.*, **285**: 15038–15047.
360 Ohori, K., Miura, T., Tanno, M., Miki, T., Sato, T., Ishikawa, S., Horio, Y., Shimamoto, K. (2008). Ser9 phosphorylation of mitochondrial GSK-3β is a primary mechanism of cardiomyocyte protection by erythropoietin against oxidant-induced apoptosis. *Am J Physiol Heart Circ Physiol.*, **295**: 2079–2086.

361 Zhang, H. H., Lipovsky, A. I., Dibble, C. C., Sahin, M., Manning, B. D. (2006). S6K1 Regulates GSK3 under Conditions of mTOR-Dependent Feedback Inhibition of Akt. *Molecular Cell*, **24**: 185–197.
362 Stuenæs, J. T., Bolling, A., Ingvaldsen, A., Rommundstad, C., Sudar, E., Lin, F. C., Lai, Y.C., Jensen, J. (2010). β-Adrenoceptor stimulation potentiates insulin-stimulated PKB phosphorylation in rat cardiomyocytes via cAMP and PKA. *British Journal of Pharmacology*, **160**: 116–129.
363 Shakoori, A., Ougolkov, A., Yu, Z. W., Zhang, B., Modarressi, M. H., Billadeau, D. D., Mai, M., Takahashi, Y., Minamoto, T. (2005). Deregulated GSK3b activity in colorectal cancer: Its association with tumor cell survival and proliferation. *BBRC*, **334**: 1365–1373.
364 Alao, J. P., Stavropoulou, A. V., Lam, E. W., Coombes, R. C. (2006). Role of glycogen synthase kinase 3 beta (GSK3β) in mediating the cytotoxic effects of the histone deacetylase inhibitor trichostatin A (TSA) in MCF-7 breast cancer cells. *Molecular Cancer*, **5**: 40-45.
365 Martelli, A. M., Tazzari, P. L., Tabellini, G., Bortul, R., Billi, A. M., Manzoli, L., Ruggeri, A., Conte, R., Cocco, L. (2003). A new selective AKT pharmacological inhibitor reduces resistance to chemotherapeutic drugs, TRAIL, all-trans-retinoic acid, and ionizing radiation of human leukemia cells. *Leukemia*, **17**: 1794–1805.
366 Li, X. H., Zheng, H. C., Takahashi, H., Masuda, S., Yang, X. H., Takano, Y. (2009). PTEN expression and mutation in colorectal carcinomas. *Oncol Rep.*, **22**: 757-64.
367 Fine, B., Hodakoski, C., Koujak, S., Su, T., Saal, L. H., Maurer, M., Hopkins, B., Keniry, M., Sulis, M. L., Mense, S., Hibshoosh, H., Parsons, R. (2009). Activation of the PI3K Pathway in Cancer through inhibition of PTEN by exchange factor P-REX2a. *Science*, **325**: 1261-5.
368 Campbell,R., B., Liu, F., and Ross, A. H. (2003). Allosteric Activation of PTEN Phosphatase by Phosphatidylinositol 4,5-Bisphosphate. *J. Biol. Chem.*, **278**: 33617–33620.
369 Dahia, P., Aguiar, R. C., Alberta, J., Kum, J. B., Caron, S., Sill, H., Marsh, D. J., Ritz, J., Freedman, A., Stiles, C., Eng, C. (1999). PTEN is inversely correlated with the cell survival factor Akt/PKB and is inactivated via multiple mechanismsin haematological malignancies. *Human Molecular Genetics*, **8**: 185-193.
370 Wan, X., and Helman, L. J. (2003). Levels of PTEN protein modulate Akt phosphorylation on serine 473, but not on threonine 308, in IGF-II-overexpressing rhabdomyosarcomas cells. *Oncogene*, **22**: 8205-11.
371 Yang, Z., Yi, J., Li, X., Long, W. (2005). Correlation between loss of PTEN expression and PKB/AKT phosphorylation in hepatocellular carcinoma. *J Huazhong Univ Sci Technolog Med Sci.*, **25**: 45-7..
372 Ermoian, R. P., Furniss, C. S., Lamborn, K. R., Basila, D., Berger, M. S., Gottschalk, A. R., Nicholas, M. K., Stokoe, D., Haas-Kogan, D. A. (2002). Dysregulation of PTEN and Protein Kinase B Is Associated with Glioma Histology and Patient Survival. *Clin. Cancer Res.*, **8**: 1100-1106.
373 Munugalavadla, V., Sims, E. C., Borneo, J., Chan, R. J., and Kapur, R. (2007). Genetic and pharmacologic evidence implicating the p85α, but not p85β, regulatory subunit of PI3K and Rac2 GTPase in regulating oncogenic KIT-induced transformation in acute myeloid leukemia and systemic mastocytosis. *Blood*, **110**: 1612–1620.
374 Hellwinkel, O. J. C., Rogmann, J. P., Asong, L. E., Luebke, A. M., Eichelberg, C., Ahyai, S., Isbarn, H., Graefen, M., Huland, H., Schlomm, T. (2007). A comprehensive analysis of transcript signatures of the phosphatidylinositol-3 kinase/protein kinase B signal-transduction pathway in prostate cancer. *BJU International*, **101**: 1454–1460.
375 Cheung, L. W. T., Hennessy, B. T., Li, J., Yu, S., Myers, A. P., Djordjevic, B., Lu, Y., Stemke-Hale, K., Zhang, F., Ju, Z., Cantley, L. C., Scherer, S. E., Liang, H., Lu, K. H.,

Broaddus, R. R., Mills, G. B. (2011). High Frequency of PIK3R1 and PIK3R2 Mutations in endometrial cancer elucidates a Novel Mechanism for regulation of PTEN Protein stability. *Cancer Discovery*, doi: 10.1158/2159-8290.CD-11-0039.

376 Sunpaweravong, P., Suwiwat, S., Sunpaweravong, S., Puttawibul, P., Mitarnun, W. (2009). Correlation of Epidermal Growth Factor Receptor Mutation, Immunohistochemistry, and Fluorescence in Situ Hybridization in Esophageal Squamous Cell Carcinoma. *J Med Assoc Thai*., **92**: 1-7.

377 Yamamoto, H., Shigematsu, H., Nomura, M., Lockwood, W. W., Sato, M., Okumura, N., Soh, J., Suzuki, M., Wistuba, I. I., Fong, K. M., Lee, H., Toyooka, S., Date, H., Lam, W. L., Minna, J. D., Gazdar, A.F. (2008). PIK3CA Mutations and Copy Number Gains in Human Lung Cancers. *Cancer Res*., **68**: 6913–6921.

378 Rychahou, P. G., Jackson, L. N., Silva, S. R., Rajaraman, S., Evers, B. M. (2006). Targeted Molecular Therapy of the PI3K Pathway Therapeutic Significance of PI3K Subunit Targeting in Colorectal Carcinoma. *Ann Surg*., **243**: 833–844.

379 Fry, M., J., Panayotou, G., Dhand, R., Ruiz-Larrea, F., Gout, I., Nguyen, O., Courtneidge, S. A., Waterfield, M. D. (1992). Purification and characterization of a phosphatidylinositol 3-kinase complex from bovine brain by using phosphopeptide affinity columns. *Biochem. J.,* **288**: 383-393.

380 Stephens, L., R., Jackson, T., R., and Hawkins, P., T. (1993). Agonist-stimulated synthesis of phosphatidylinositol (3,4,5)-triphosphate: a new intracellular signalling system? *Biochem et Biophys. Acta.,* **1179**: 27-75.

381 Lee, J., Y., Engelman, J., A., and Cantley, L., C. (2007). PI3K Charges Ahead. *Biochemistry,* **317**: 206-207.

382 Vara, J., A., Casado, E., de Castro, J., Cejas, P., Belda-Iniesta, C., González-Barón, M. (2004). PI3K/Akt signalling pathway and cancer. *Cancer Treat. Rev.*, **30**: 193-204.

383 Sasaki, A. T., Janetopoulos, C., Lee, S., Charest, P. G., Takeda, K., Sundheimer, L. W., Meili, R., Devreotes, P. N., Firtel, R. A. (2007). G protein–independent Ras/PI3K/F-actin circuit regulates basic cell motility. *The Journal of Cell Biology*, **178**: 185–191.

384 Yuan, T.L., Wulf, G., Burga, L., and Cantley, L.C. (2011) Cell-to-cell variability in PI3K protein regulates PI3K-AKT pathway activity in cell populations. *Curr Biol*., **21**: 173-183.

385 Kamikura, D. M., Khoury, H., Maroun, C., Naujokas, M. A., Park, M. (2000). Enhanced Transformation by a Plasma Membrane-Associated Met Oncoprotein: Activation of a Phosphoinositide 3'-Kinase-Dependent Autocrine Loop Involving Hyaluronic Acid and CD44. *Mol. Cell. Biol.*, **20**: 3482–3496.

386 Funamoto, S., Meili, R., Lee, S., Parry, L., Firtel, R. A. (2002). Spatial and Temporal Regulation of 3-Phosphoinositides by PI 3-Kinase and PTEN Mediates Chemotaxis. *Cell*, **109**: 611–623.

387 Franca-Koh, J., and Devreotes, P. N. (2004). Moving Forward: Mechanisms of Chemo-attractant Gradient Sensing. *Physiology*, **19**: 300–308.

388 Maddika, S., Ande, S., R., Panigrahi, S., Paranjothy, T., Weglarczyk, K., Zuse, A., Eshraghi, M., Manda, K. D., Wiechec, E., Los, M. (2007). Cell survival, cell death and cell cycle pathways interconnected: Implications for cancer therapy. *Drug Resist. Updat.*, **10**: 1016-1034.

389 Krasilnikov, M.,A. (2000). Phosphoinositol-3 Kinase Dependent Pathways: the Role in Control of Cell Growth, Survival, and Malignant Transformation. *Biochem (Mosc).*, **65**:59-67.

390 Ledden, R., W., and Wu, G. (2004). Nuclear lipids: Key signalling effectors in the nervous system and other tissues. *J. Lipid Res.,* **45**: 1-8.

391 Cocco, L., Martelli, A., M., Barnabei, O., Manzoli, F., A. (2001). Nuclear inositol lipid signalling. *Advan. Enzyme Regul.,* **41**: 361-384.

392 Martelli, A., M., Manzoli, L., Faenza, I., Bortul, R., Billi, A., Cocco, L. (2002). Nuclear inositol lipid signalling and its potential involvement in malignant transformation. *Biochem. Biophys. Acta,* **1603**: 11-17.
393 Neri, L., M., Borgatti, P., Capitani, S., and Martelli, A., M. (2002). The nuclear phosphoinositide 3-kinase/AKT pathway: a new second messenger system. *Biochem. Biophys. Acta.* **1584**: 73-80.
394 Lu, P-J., Hsu, A-L., Wang, D. S., Yan, H. Y., Yin, H. L., Chen, C. S. (1998). Phosphoinositide 3-kinase in rat liver nuclei. *Biochemistry,* **37**: 5738-5745.
395 Neri, L., M., Milani, D., Bertolaso, L., Stroscio, M., Bertagnolo, V., Capitani, S. (1994). Nuclear translocation of phosphatidylinositol 3-kinase in rat pheochromocytoma PC12 cells after treatment with nerve growth factor. *Cell. Mol. Biol.,* **40**: 619-626.
396 Marchisio, M., Bertagnolo, V., Colamussi, M., L., Capitani, S., Neri, L., M. (1998). Phosphatidylinositol 3-kinase in HL-60 nucleai is bound to the nuclear matrix and increases during granulocytic differentiation. *Biochem. Biophys. Res. Comm.,* **253**: 346-351.
397 Zini, N., Ognibene, A., Bavelloni, A., Santi, S., Sabatelli, P., Baldini, N., Scotlandi, K., Serra, M., Maraldi, N. M. (1996). Cytoplasmic and nuclear localization sites of phosphatidylinositol 3-kinase in human osteosarcama sensitive and multidrug-resistant Saos-2 cells. *Histochem. Cell. .Biol.,* **106**: 457-464.
398 Liu, J-L., Mao, Z., LaFortune, T. A., Alonso, M. M., Gallick, G. E., Fueyo, J., Yung, W. K. (2007). Cell cycle-dependent nuclear export of phosphatase and tensin homologue tumor suppressor is regulated by the phophoinositide-3 kinase sigaling cascade. *Cancer Res.,* **67**: 11054-11063.
399 Martelli, A., M., Faenza, I., Billi, A. M., Manzoli, L., Evangelisti, C., Falà, F., Cocco, L. (2006). Intranuclear 3'-phosphoinositide metabolism and Akt signalling: New mechanisms for tumorigenesis and protection against apoptosis? *Cell. Sig.,* **18**: 1101-1107.
400 Kim, S., J. (1998). Insulin rapidly induces nuclear translocation of PI3-kinase in HepG2 cells. *Biochem. Mol. Biol. Int.,* **46**: 187-196.
401 Bavelloni, A., ., Santi, S., Sirri, A., Riccio, M., Faenza, I., Zini, N., Cecchi, S., Ferri, A., Auron, P., Maraldi, N. M., Marmiroli, S. (1999). Phosphatidylinositol 3-kinase translocation to the nucleus is induced by interleukin 1 and prevented by mutation of interleukin 1 receptor in human oesteosarcoma Saos-2 cells. *J. Cell Sci.,* **112**: 631-640.
402 Martelli, A., Faenza, I., Bortul, R., Billi, A., Cocco, L. (2000). Phosphatidylinositol 3-kinase translocates to the nucleus of osteoblast-like MC3T3-E1 ccells in response to insulin-like growth factor I and platelet-derived growth factor but not to the proapoptotic cytokine tumor necrosis factor α. *J. Bone Miner. Res.,* **15**: 1716-1730.
403 Toker, A. (2008). Akt signalling: a damaging interaction makes good. *Trends Biochem. Sci.,* **33**: 356-359.
404 Sun, H., Lesche, Lesche, R., Li, D. M., Liliental, J., Zhang, H., Gao, J., Gavrilova, N., Mueller, B., Liu, X., Wu, H. (1999). PTEN modulates cell cycle progression and cell survival by regulating phophatidylinositol 3,4,5-triphosphate and Akt/protein kinase B signalling pathway. *Proc. Natl. Acad. Sci. USA,* **96**: 6199-6204.
405 Haas-Kogan, D., Shalev, N., Wong, M., Mills, G., Yount, G., Stokoe, D. (1998). Protein kinase B (PKB/Akt) activity is elevated in glioblastoma cells due to mutation of the tumor suppressor PTEN/MMAC. *Current Biology*, **8**: 1195–1198.
406 Woodgett, J., R. (2005). Recent advances in the protein kinase B signalling pathway. *Curr. Op. Cell Biol.,* **17**: 150-157.
407 Downward, J. (1998). Mechanisms and consequences of activation of protein kinase B/Akt. *Curr. Op. Cell Biol.*, **10**: 262-267.

408 Scheid, M., P., Marignani, P., A., Woodgett, J., R. (2002). Multiple phosphoinositide 3-kinase-dependent steps in activation of protein kinase B. *Mol. Cell. Biol.*, **22**: 6247-6260.
409 Sun, M., Wang, G., Paciga, J. E., Feldman, R. I., Yuan, Z. Q., Ma, X. L., Shelley, S. A., Jove, R., Tsichlis, P. N., Nicosia, S. V., Cheng, J. Q. (2001). AKT1/PKB Kinase Is Frequently Elevated in Human Cancers and Its Constitutive Activation Is Required for Oncogenic Transformation in NIH3T3 Cells. *Am J Pathol* ., **159**: 431–437.
410 Oehler-Jänne, C., von Bueren, A. O., Vuong, V., Hollenstein, A., Grotzer, M. A., Pruschy, M. (2008). Temperature sensitivity of phospho-Ser473-PKB/AKT. *Biochem. Biophys. Res. Comm.*, **375**: 399-404.
411 Missiroli, S., Etro, D., Buontempo, F., Ye, K., Capitani, S., Neri, L., M. (2009). Nuclear translocation of active AKT is required for erythroid differentiation in erythropoietin treated K562 erythroleukemia cells. *Int. J. Biochem. Cell Biol.*, **41**: 570-577.
412 Kim, E., Y., Tucker, D. F., Yun, S. J., Do, K. H., Kim, M. S., Kim, J. H., Kim, C. D., Birnbaum, M. J., Bae, S. S. (2008). Linker region of Alt1/protein kinase Bα mediates platelet-derived growth factor-induced translocation and cell migration. *Cell Sig.*, **20**: 2030-2037.
413 Hutchinson J, Jin, J., Cardiff, R. D., Woodgett, J. R., Muller, W. J. (2001). Activation of Akt (protein kinase B) in mammary epithelium provides a critical cell survival signal required for tumor progression. *Mol Cell Biol*., **21**: 2203–2212.
414 Polakiewicz, R. D., Schieferl, S. M., Gingras, A. C., Sonenberg, N., Comb, M. J. (1998). μ-Opioid Receptor Activates Signalling Pathways Implicated in Cell Survival and Translational Control. *J. Biol. Chem*., **273**: 23534–23541.
415 Hundsrucker, C., Skroblin, P., Christian, F., Zenn, H. M., Popara, V., Joshi, M., Eichhorst, J., Wiesner, B., Herberg, F. W., Reif, B., Rosenthal, W., Klussmann, E. (2010). Glycogen Synthase Kinase 3β Interaction Protein Functions as an A-kinase Anchoring Protein. *J. Biol. Chem*., **285**: 5507–5521.
416 Jensen, J., Brennesvik, E. O., Lai, Y-C., and Shepherd, P. R. (2007). GSK-3β regulation in skeletal muscles by adrenaline and insulin: Evidence that PKA and PKB regulate different pools of GSK-3. *Cellular Signalling*, **19**: 204–210.
417 Anai, M., Shojima, N., Katagiri, H., Ogihara, T., Sakoda, H., Onishi, Y., Ono, H., Fujishiro, M., Fukushima, Y., Horike, N., Viana, A., Kikuchi, M., Noguchi, N., Takahashi, S., Takata, K., Oka, Y., Uchijima, Y., Kurihara, H., Asano, T. (2005). A Novel Protein Kinase B (PKB)/AKT-binding Protein Enhances PKB Kinase Activity and Regulates DNA Synthesis. *J. Biol. Chem*., **280**: 18525–18535.
418 Cybulski, N., and Hall, M. N. (2009). TOR complex 2: a signalling pathway of its own. *Trends in Biochemical Sciences*, **34**: 620-7.
419 Cho, J. Y., and Park, J. (2008). Contribution of Natural Inhibitors to the Understanding of the PI3K/PDK1/PKB Pathway in the Insulin-mediated Intracellular Signalling Cascade. *Int. J. Mol. Sci*., **9**: 2217-2230.
420 Wymann, M. P., Zvelebil, M., and Laffargue, M. (2003). Phosphoinositide 3-kinase signalling – which way to target? *Trends in Pharmacological Sciences*, **24**: 366-76.
421 Gharbi, S. I., Zvelebil, M. J., Shuttleworth, S. J., Hancox, T., Saghir, N., Timms, J. F., Waterfield, M. D. (2007). Exploring the specificity of the PI3K family inhibitor LY294002. *Biochem. J*., **404**: 15–21.
422 Tolloczko, B., Turkewitsch, P., Al-Chalabi, M., Martin, J. G. (2004). LY-294002 [2-(4-Morpholinyl)-8-phenyl-4H-1-benzopyran-4-one] Affects Calcium Signalling in Airway Smooth Muscle Cells Independently of Phosphoinositide 3-Kinase Inhibition. *JPET*, **311**: 787–793.
423 Liu, P., Xu, B., Li, J., and Lu, H. (2008). LY294002 inhibits leukemia cell invasion and migration through early growth response gene 1 induction independent of phosphatidylinositol 3-kinase-Akt pathway. *BBRC.*, **277**: 187-190.

424 Davies, S., P., Reddy, H., Caivano, M., Cohen, P. (2000). Specificity and mechanism of action of some commonly used protein kinase inhibitors. *Biochem. J.*, **351**: 95-105.
425 Kim, S., Domon-Dell, C., Kang, J., Chung, D. H., Freund, J. N., Evers, B. M. (2004). Down-regulation of the Tumor Suppressor PTEN by the Tumor Necrosis Factor-α/Nuclear Factor-κB (NF-κB)-inducing Kinase/NF-κB Pathway Is Linked to a Default IκB- Autoregulatory Loop. *J. Biol. Chem*., **279**: 4285–4291.
426 DeGraffenried, L., A., Fulcher, L., Friedrichs, W. E., Grünwald, V., Ray, R. B., Hidalgo, M. (2004). Reduced PTEN expression in breast cancer cells confers susceptibility to inhibitors of the PI3 kinase/Akt pathway. *Ann. Oncol.*, **15**: 1510-1516.
427 Neshat, M., S., Mellinghoff, I., K., Tran, C., Stiles, B., Thomas, G., Petersen, R., Frost, P., Gibbons, J. J., Wu, H., Sawyers, C. L. (2001). Enhanced sensitivity of PTEN-deficient tumors to inhibition of FRAP/mTOR. *Proc. Natl. Acad. Sci. USA.*, **98**: 10314-10319.
428 Bar, J., Lukaschuk, N., Zalcenstein, A., Wilder, S., Seger, R., Oren, M. (2005). The PI3K inhibitor LY294002 prevents p53 induction by DNA damage and attenuates chemotherapy-induced apoptosis. *Cell Death and Diff.*, **12**: 1578-1587.
429 Fanucchi, S., and Veale, R.B. (2009). Role of p53/FAK association and p53Ser46 phosphorylation in staurosporine-mediated apoptosis: Wild type versus mutant p53-R175H. *FEBS Letters*, **583**: 3557–3562.
430 Matsumoto, J., Kaneda, M., Tada, M., Hamada, J., Okushiba, S., Kondo, S., Katoh, H., Moriuchi, T. (2002). Differential mechanisms of constitutive Akt/PKB activation and its influence on gene expression in pancreatic cancer cells. *Jpn. J. Cancer Res.*, **93**: 1317-1326.
431 Voet, D., and Voet, J., G. (1995). Biochemistry, 2nd Edition. *John Wiley&Sons, Inc.*,**P**: 356-357.
432 Lobo, G., P., Waite, K., A., Planchon, S., M., Romigh, T., Houghton, J., A., Eng, C. (2008). ATP modulates PTEN subcellular localization in multiple cancer cell lines. *Human Mol. Gen.*, **17**: 2877-2885.
433 Ignatoski, K., M., W., Maehama, T., Markwart, S., M., DiXon, J., E., Livant, D., L., Ethier, S., P. (2000). ErbB-2 overexpression confers PI 3'kinase-dependent invasion capacity on human mammary epithelial cells. *Br. J. Cancer*, **82**: 666-674.
434 Clark, A., S., West, K., Streicher, S., and Dennis, P., A. (2002). Constitutive and inducible Akt activity promotes resistance to chemotherapy, Trastazumab, or Tamoxifen in breast cancer cells. *Mol. Cancer Therap.*, **1**: 707-717.
435 Knuefermann, C., Lu, Y., Liu, B., Jin, W., Liang, K., Wu, L., Schmidt, M., Mills, G., B., Mendelsohn, J., Fan, Z. (2003). HER2/PI-3K/Akt activation leads to a multidrug resistance in human breast adenocarcinoma cells. *Oncogene*, **22**: 3205-3212.
436 Dong, P., Xu, Z., Jia, N., Li, D., and Feng, Y. (2009). Elevated eXpression of p53 gain-of-function mutation R175H in endometrial cancer cells can increase the invasive phenotypes by activation of the EGFR/PI3K/AKT pathway. *Molecular Cancer*, **8**: 103-110.
437 Ludes-Meyers, J. H., Subler, M. A., Shivakumar, C. V., Munoz, R. M., Jiang, P., Bigger, J. E., Brown, D. R., Deb, S. P., Deb, S. (1996). Transcriptional Activation of the Human Epidermal Growth Factor Receptor Promoter by Human p53. *Mol. Cell. Biol*., **16**: 6009–6019.
438 Silva, A., Yunes, J. A., Cardoso, B. A., Martins, L. R., Jotta, P. Y., Abecasis, M., Nowill, A. E., Leslie, N. R., Cardoso, A. A., Barata, J. T. (2008). PTEN posttranslational inactivation and hyper-activation of the PI3K/Akt pathway sustain primary T cell leukemia viability. *J. Clin. Invest*. **118**: 3762–3774.
439 Di Maira, G., Salvi, M., Arrigoni, G., Marin, O., Sarno, S., Brustolon, F., Pinna, L. A., Ruzzene, M. (2005). Protein kinase CK2 phosphorylates and up-regulates Akt/PKB. *Cell Death and Differentiation*, **12**: 668–677.

440 Guerra, B. (2006). Protein kinase CK2 subunits are positive regulators of AKT kinase. *Int. J. Oncology*, **28**: 685-693.
441 Schuster, N., Götz, C., Faust, M., Schneider, E., Prowald A., Jungbluth, A., Montenarh, M. (2001). Wild-Type p53 Inhibits Protein Kinase CK2 Activity. *Journal of Cellular Biochemistry*, **81**: 172-183.
442 Maher, M. T., Mo, R., Flozak, A. S., Peled, O. N., Gottardi, C. J. (2010). β-Catenin Phosphorylated at Serine 45 Is Spatially Uncoupled from β-Catenin Phosphorylated in the GSK3 Domain: Implications for Signalling. *PLoS ONE*, **5**(4): e10184. doi:10.1371/journal.pone.0010184.
443 Wu, C., and Dedhar, S. (2001). Integrin-linked kinase (ILK) and its interactors: a new paradigm for the coupling of extracellular matrix to actin cytoskeleton and signalling complexes. *J. Cell Biol*., **155**: 505–510.
444 Petrocelli, T., and Slingerland, J. M. (2001). PTEN deficiency: a role in mammary carcinogenesis. *Breast Cancer Res*, **3**:356-360.
445 Stambolic, V. (2002). PTEN: a new twist on β-catenin? *Trends in Pharmacological Sciences*, **23**: 104-106.
446 Alimonti, A., Carracedo, A., Clohessy, J. G., Trotman, L. C., Nardella, C., Egia, A., Salmena, L., Sampieri, K., Haveman, W. J., Brogi, E., Richardson, A. L., Zhang, J., Pandolfi, P. P.. (2010). Subtle variations in Pten dose determine cancer Susceptibility. *Nature Genetics*, **42**: 454-8.
447 Dumont, J. E. (2002). PTEN: countdown to understanding PIP3 signalling. *Trends in Cell Biology*, **12**: 321.
448 Campbell, R. B., Liu, F., and Ross, A. H. (2003). Allosteric Activation of PTEN Phosphatase by Phosphatidylinositol 4,5-Bisphosphate. *J. Biol. Chem*., **278**: 33617–33620.
449 Adams, J. R., Schachter, N. F., Liu, J. C., Zacksenhaus, E., Egan, S. E. (2011). Elevated PI3K signalling drives multiple breast cancer subtypes. *Oncotarget*, **2**: 435–447.
450 Wang, Q., and Greene, M. I. (2005). EGFR enhances Survivin expression through the phosphoinositide 3 (PI-3) kinase signalling pathway. *Experimental and Molecular Pathology*, **79**: 100–107.
451 Vazquez, F., and Seller, W.R. (2000). The PTEN tumor suppressor protein: an antagonist of phosphoinositide 3-kinase signalling. *Biochem Biophys Acta*., **1470**: M21-M35.
452 She, Q-B., Chandarlapaty, S., Ye, Q., Lobo, J., Haskell, K. M., Leander, K. R., De Feo-Jones, D., Huber, H. E., Rosen, N. (2008). Breast Tumor Cells with PI3K Mutation or HER2 Amplification Are Selectively Addicted to Akt Signalling. *PLoS ONE*, **3**: e3065. doi:10.1371/journal.pone.0003065
453 Jina, G., Kim, M. J., Jeon, H. S., Choi, J. E., Kim, D. S., Lee, E. B., Cha, S. I., Yoon, G. S., Kim, C. H., Jung, T. H., Park, J. Y. (2010). PTEN mutations and relationship to EGFR, ERBB2, KRAS, and TP53 mutations in non-small cell lung cancers. *Lung Cancer*, **69**: 279–283.
454 Guanti, G., Resta, N., Simone, C., Cariola, F., Demma, I., Fiorente, P., and Gentile, M. (2000). Involvement of PTEN mutations in the genetic pathways of colorectal carcinogenesis. *Human Molecular Genetics*, **9**: 283-287.
455 Serra, V., Markman, B., Scaltriti, M., Eichhorn, P. J. A., Valero, V., Guzman, M., Botero, M. L., Llonch, E., Atzori, F., Di Cosimo, S., Maira, M., Garcia-Echeverria, C., Parra, J. L., Arribas, J., and Baselga, J. (2008). NVP-BEZ235, a Dual PI3K/mTOR Inhibitor, Prevents PI3K Signalling and Inhibits the Growth of Cancer Cells with Activating PI3K Mutations. *Cancer Res*., **68**: 8022–30.
456 Hu, Y. C., Lam, K. Y. L., Tang, J. C. O., and Srivastava, G. (1999). Mutational analysis of the PTEN/MMAC1 gene in primary oesophageal squamous cell carcinomas. *J. Clin. Pathol: Mol Pathol*., **52**: 353–356.

457 Hou, G., Lu, Z., Liu, M., Liu, H., Xue, L. (2011). Mutational analysis of the PTEN gene and its effects in esophageal squamous cell carcinoma. Dig Dis Sci., 56: 1315-22.
458 Wang, S. E., Narasanna, A., Perez-Torres, M., Xiang, B., Wu, F. Y., Yang, S., Carpenter, G., Gazdar, A. F., Muthuswamy, S. K., Arteaga, C. L. (2006). HER2 kinase domain mutation results in constitutive phosphorylation and activation of HER2 and EGFR and resistance to EGFR tyrosine kinase inhibitors. *Cancer Cell*, **10**: 25–38.
459 Bianco, R., Gelardi, T., Damiano, V., Ciardiello, F., Tortora, G. (2007). Rational bases for the development of EGFR inhibitors for cancer treatment. *The International Journal of Biochemistry & Cell Biology*, **39**: 1416–1431.
460 Ekman, S., Bergqvist, M., Heldin, C-H., Lennartsson, J. (2007). Activation of Growth factor Receptors in Esophageal Cancer-Implications for Therapy. *The Oncologist*, **12**: 1165-1177.
461 Hanawa, M., Suzuki, S., Dobashi, Y., Yamane, T., Kono, K., Enomoto, N., Ooi, A. (2006). EGFR protein overexpression and gene amplification in squamous cell carcinomas of the esophagus. *Int. J. Cancer*, **118**: 1173–1180.
462 Gabelli, S. B., Mandelker, D., Schmidt-Kittler, O., Vogelstein, B., Amzel, L. M. (2010). Somatic mutations in PI3Kα: structural basis for the enzyme activation and drug design. *Biochim Biophys Acta*., **1804**: 533. doi:10.1016/j.bbapap.2009.11.020.
463 van Eijk, R., Licht J, Schrumpf, M., Talebian Yazdi, M., Ruano, D., Forte, G. I., Nederlof, P. M., Veselic, M., Rabe, K. F., Annema, J. T., Smit, V., Morreau, H., van Wezel, T. (2011). Rapid KRAS, EGFR, BRAF and PIK3CA Mutation Analysis of Fine Needle Aspirates from Non-Small-Cell Lung Cancer Using Allele-Specific qPCR. *PLoS ONE*, **6**(3): e17791. doi:10.1371/journal.pone.0017791
464 Loi, S., Haibe-Kains, B., Majjaj, S., Lallemand, F., Durbecq, V., Larsimont, D.,Gonzalez-Angulo, A. M., Pusztai, L., Symmans, W. F., Bardelli, A., Ellis, P., Tutt, A. N.,Gillett, C. E., Hennessy, B. T., Mills, G. B., Phillips, W. A., Piccart, M. J., Speed, T. P., McArthur, G. A., Sotiriou, C. (2010). PIK3CA mutations associated with gene signature of low mTORC1 signalling and better outcomes in estrogen receptor–positive breast cancer. *PNAS*, **107**: 10208–10213.
465 Samuels, Y., Wang, Z., Bardelli, A., Silliman, N., Ptak, J., Szabo, S., Yan, H., Gazdar, A., Powell, S. M., Riggins, G. J., Willson, J. K., Markowitz, S., Kinzler, K. W., Vogelstein, B.,Velculescu, V. E. (2004). High Frequency of Mutations of the PIK3CA Gene in Human Cancers. *Science*, **204**: 554.
466 Lin, Y., Jiang, X., Shen, Y., Li, M., Ma, H., Xing, M., Lu, Y. (2009). Frequent mutations and amplifications of the PIK3CA gene in pituitary tumors. *Endocrine-Related Cancer*, **16**: 301–310.
467 Peles, E., Lamprecht, R., Ben-Levy, R., Tzahar, E., Yarden, Y. (1992). Regulated coupling of the *Neu* Receptor to phosphatidylinositol 3'-kinase and its release by oncogenic activation. *J. Biol. Chem.*, **267**: 12266-12274.
468 Cheng, J. Q., Godwin, A. K., Bellacosa, A., Taguchi, T., Franke, T. F., Hamilton, T. C., Tsichlis, P. N., Testa, J. R. (1992). AKT2, a putative oncogene encoding a member of a subfamily of protein-serine/threonine kinases, is amplified in human ovarian carcinomas. *Proc Natl Acad Sci USA*, **89**: 267–71.
469 Scheid, M. P., and Woodgett, J. R. (2001). PKB/AKT: functional insights from genetic models. *Nature Reviews Molecular Cell Biology*, **2**: 760-768.
470 Brugge, J., Hung, M. C., and Mills, G. B. (2007). A new mutational AKTivation in the PI3K pathway. *Cancer Cell*, **12**: 104-107.
471 Fujita, T., Doihara, H., Kawasaki, K., Takabatake, D., Takahashi, H., Washio, K., Tsukuda, K., Ogasawara, Y., Shimizu, N. (2006). PTEN activity could be a predictive marker of trastuzumab efficacy in the treatment of ErbB2-overexpressing breast cancer. *British Journal of Cancer*, **94**: 247–252.

472 Li, Y., Wang, H., Tu, C., Shiverick, K. T., Silverman, D. N., Frost, S. C. (2011). Role of hypoxia and EGF on expression, activity, localization and phosphorylation of carbonic anhydrase IX in MDA-MB-231 breast cancer cells. *Biochimica et Biophysica Acta*, **1813**: 159 –167.

473 Shen, X., and Kramer, R. H. (2004). Adhesion-Mediated Squamous Cell Carcinoma Survival through Ligand-Independent Activation of Epidermal Growth Factor Receptor. *Am J Pathol*., **165**: 1315–1329.

474 Sorkin, A., and Duex, J. E. (2010). Quantitative Analysis of Endocytosis and Turnover of Epidermal Growth Factor (EGF) and EGF Receptor. *Curr Protoc Cell Biol*., Chapter: Unit–15.14. doi:10.1002/0471143030.cb1514s46.

475 Giancotti FG, and Ruoslahti E. (1990). Elevated levels of the α5β1 fibronectin receptor suppress the transformed phenotype of Chinese hamster ovary cells. *Cell*, **60**: 849-59.

476 Wu, G., Xing, M., Mambo, E., Huang, X., Liu, J., Guo, Z., Chatterjee, A., Goldenberg, D., Gollin, S. M., Sukumar, S., Trink, B., Sidransky, D. (2005). Somatic mutation and gain of copy number of PIK3CA in human breast cancer. *Breast Cancer Research*, **7**: 609-616.

477 Bublil, E. M., and Yarden, Y. Yarden, Y. (2007). The EGF receptor family: spearheading a merger of signalling and therapeutics. *Current Opinion in Cell Biology*, **19**: 124–134

478 Karunagaran, D., Tzahar, E., Beerli, R., R., Chen, X., Graus-Porta, D., Ratzkin, B., J., Seger, R., Hynes, N., E., Yarden, Y. (1996). ErbB-2 is a common auxiliary subunit of NDF and EGF receptors: implications for breast cancer. *EMBO J*., **15**: 254-264.

479 Azemar, M., Schmidt, M., Arlt, F., Kennel, P., Brandt, B., Papadimitriou, A., Groner, B., Wels, W. 2000). Recombinant antibody toxins specific for ErbB2 and EGF Receptor inhibit the *In Vitro* growth of human Head and Neck cancer cells and cause rapid tumor regression *In Vivo*. *Int. J. Cancer*, **86**: 269-275.

480 Davidson, N. E., Gelmann, E. P., Lippman, M. E., and Dickson, R. B. (1987). Epidermal growth factor receptor gene expression in estrogen receptor-positive and negative human breast cancer cell lines. *Mol. Endocrinol*., **1**: 216–223.

481 Loeffler-Ragg, J., J, Skvortsov, S., Sarg, B., Skvortsova, I., Witsch-Baumgartner, M., Mueller, D., Lindner, H., Zwierzina, H. (2005). Gefitinib-responsive EGFR-positive colorectal cancers have different proteome profiles from non-responsive cell lines. *European Journal of Cancer*, **41**: 2338–2346.

482 Huang, C-H., Mandelker, D., Schmidt-Kittler, O., Samuels, Y., Velculescu, V. E., Kinzler, K. W., Vogelstein, B., Gabelli, S. B., Amzel, L. M. (2007). The structure of a human p110α/p85α complex elucidates the effects of oncogenic PI3Kα mutations. *Science*, **318**: 1744-1748.

483 Cheng, J. Q., Lindsley, C. W.,, Cheng, G. Z.,Yang, H.,and Nicosia, S. V. (2005). The Akt/PKB pathway: molecular target for cancer drug discovery. *Oncogene*, **24**: 7482–7492.

484 Blanco-Aparicio, C., Cañamero, M., Cecilia, Y., Pequeño, B., Renner, O., Ferrer, I., Carnero, A. (2010). Exploring the Gain of Function Contribution of AKT to Mammary Tumorigenesis in Mouse Models. *PLoS ONE*, **5**: e9305. doi:10.1371/journal.pone.0009305.

485 Lauring, J., Cosgrove, D. P., Fontana, S., Gustin, J. P., Konishi, H., Abukhdeir, A. M., Garay, J. P., Mohseni, M., Wang, G. M., Higgins, M. J., Gorkin, D., Reis, M., Vogelstein, B., Polyak, K., Cowherd, M., Buckhaults, P. J., Park, B. H. (2010). Knock in of the AKT1 E17K mutation in human breast epithelial cells does not recapitulate oncogenic PIK3CA mutations. *Oncogene*, **29**: 2337–2345.

486 Wang, Q., Somwar, R., Bilan, P. J., Liu, Z., Jin, J., Woodgett, J. R., Klip, A. (1999). Protein Kinase B/Akt Participates in GLUT4 Translocation by Insulin in L6 Myoblasts. *Mol. Cell. Biol*., **19**: 4008–4018.

487 Yim, E-K., Peng, G., Dai, H., Hu, R., Li, K., Lu, Y., Mills, G. B., Meric-Bernstam, F., Hennessy, B. T., Craven, R. J., Lin, S. Y. (2009). Rak Functions as a Tumor Suppressor by Regulating PTEN Protein Stability and Function. *Cancer Cell*, **15**: 304–314.
488 Cantley, L. C., Auger, K. R., Carpenter, C., Buckworth, B., Graziani, A., Kapeller, R., and Soltoff, S. (1991). Oncogenes and Signal Transduction. *Cell*, **64**: 261-302.
489 Marshall, C., and Vousden, K. (2011). Genetic and cellular mechanisms of oncogenesis. *Current Opinion in Genetics & Development*, **21**: 1–3.
490 Friess, H., Fukuda, A., Tang, W. H., Eichenberger, A., Furlan, N., Zimmermann, A., Korc, M., Büchler, M. W. (1999). Concomitant Analysis of the Epidermal Growth Factor Receptor Family in Esophageal Cancer: Overexpression of Epidermal Growth Factor Receptor mRNA but Not of c-erbB-2 and c-erbB-3. *World J. Surg*., **23**: 1010–1018.
491 Sudo, T., Mimori, K., Nagahara, H., Utsunomiya, T., Fujita, H., Tanaka, Y., Shirouzu, K., Inoue, H., Mori, M. (2007). Identification of EGFR mutations in esophageal cancer. *EJSO*, **33**: 44-48.
492 Tew, W. P., Kelsen, D. P., and Ilson, D. H. (2005). Targeted Therapies for Esophageal Cancer. *The Oncologist*, **10**: 590–601.
493 Park, J. C., and Moon, C. (2008). Gene therapy for esophageal cancer. *Cancer Therapy*, **6**: 35-46.
494 Mitsudomi, T., and Yatabe, Y. (2010). Epidermal growth factor receptor in relation to tumor development: EGFR gene and cancer. *FEBS Journal*, **277**: 301–308.
495 Citri, A., and Yarden, Y. (2003). EGF–ERBB signalling: towards the systems level. *Nature Reviews Molecular Cell Biology*, **7**: 505-516.
496 Roskoski Jr., R. (2004). The ErbB/HER receptor protein-tyrosine kinases and cancer. *Biochemical and Biophysical Research Communications*, **319**: 1–11.
497 Erjala, K., Sundvall, M., Junttila, T. T., Zhang, N., Savisalo, M., Mali, P., Kulmala, J., Pulkkinen, J., Grenman, R., Elenius, K. (2006). Signalling via ErbB2 and ErbB3 Associates with Resistance and Epidermal Growth Factor Receptor (EGFR) Amplification with Sensitivity to EGFR Inhibitor Gefitinib in Head and Neck Squamous Cell Carcinoma Cells. *Clin. Cancer. Res*., **12**: 4103-4111.
498 Jathal, M. K., Chen, L., Mudryj, M., Ghosh, P. M. (2011). Targeting ErbB3: the New RTK(id) on the Prostate Cancer Block. *Immunol Endocr Metab Agents Med Chem*., **11**: 131–149.
499 Zhou, B. P, Liao, Y., Xia, W., Spohn, B., Lee, M. H., Hung, M. C. (2001). Cytoplasmic localization of p21Cip1/WAF1 by Akt-induced phos-phorylation in HER-2/neu-overexpressing cells. *Nat Cell Biol*., **3**: 245–252.
500 Neri, L. M., Stehlik, C., Medan, D., Huang, C., Hu, S., Chen, F., Shi, X., Rojanasakul, Y. (2003). The Phosphoinositide 3-Kinase/AKT1 Pathway Involvement in Drug and All-Trans-Retinoic Acid Resistance of Leukemia Cells. *Molecular Cancer Research*, **1**: 234–246.
501 Richter, P., Böhmer, F. D., Hindermann, W., Borsi, L., Hyckel, P., Schleier, P., Katenkamp, D., Kosmehl, H., Berndt, A. (2005). Analysis of activated EGFR signalling pathways and their relation to laminin-5 γ2 chain expression in oral squamous cell carcinoma (OSCC). *Histochem Cell Biol*., **124**: 151–160.
502 Lu, B., Wang, L., Stehlik, C., Medan, D., Huang, C., Hu, S., Chen, F., Shi, X., Rojanasakul, Y. (2006). Phosphatidylinositol 3-Kinase/Akt Positively Regulates Fas (CD95)-Mediated Apoptosis in Epidermal Cl41 Cells. *The Journal of Immunology*, **176**: 6785– 6793.
503 Yang, S., Raymond-Stintz, M. A., Ying, W., Zhang, J., Lidke, D. S., Steinberg, S. L., Williams, L., Oliver, J. M., Wilson, B. S. (2007). Mapping ErbB receptors on breast cancer cell membrane during signal transduction. *J. Cell Science*, **120**: 2763-2773.

504 Shibasaki, F., Fukami, K., Fukui, Y., Takenawa, T. (1994). Phosphatidylinositol 3-kinase binds to α-actinin through the p85 subunit. *Biochem. J*., **302**: 551-557.
505 De Santis, G., Miotti, S., Mazzi, M., Canevari, S., Tomassetti, A. (2009). E-cadherin directly contributes to PI3K/AKT activation by engaging the PI3K-p85 regulatory subunit to adherens junctions of ovarian carcinoma cellsE-cadherin in PI3K/AKT activation in ovary cancer. *Oncogene*, **28**: 1206-1217.
506 Laprise, P., Langlois, M. J., Boucher, M. J., Jobin C., Rivard, N. (2004). Down-Regulation of MEK/ERK Signalling by E-Cadherin-Dependent PI3K/Akt Pathway in Differentiating Intestinal Epithelial Cells. *Journal of Cellular Physiology*, **199**: 32–39.
507 Farias, E., Lu, M., Li, X., and Schnapp, L. M. (2005). Integrin a 8b 1–fibronectin interactions promote cell survival via PI3 kinase pathway. *Biochemical and Biophysical Research Communications*, **329**: 305–311.
508 Ning, S., Chen, Z., Dirks, A., Husbeck, B., Hsu, M., Bedogni, B., O'Neill, M., Powell, M. B., Knox, S. J. (2007). Targeting Integrins and PI3K/Akt-Mediated Signal Transduction Pathways Enhances Radiation-Induced Anti-angiogenesis. *Radiation Res*., **168**: 125–133.
509 Chen, H.-C., Appeddu, P. A., Isoda, H., Guan, J. L. (1996). Phosphorylation of Tyrosine 397 in Focal Adhesion Kinase Is Required for Binding Phosphatidylinositol 3-Kinase. *J. Biol. Chem*., **271**: 26329–26334.
510 Fanucchi, S. (2011). The interaction of focal adhesion kinase with apoptotic regulators underpins anoikis resistance in human oesophageal carcinoma. PhD Dissertation, University of the Witwatersrand, http://www.wits.ac.za.
511 Neri, L. M., Marchisio, M., Colamussi, M. L., Bertagnolo, V. (1999). Monocytic Differentiation of HL-60 Cells Is Characterized by the Nuclear Translocation of Phosphatidylinositol 3-Kinase and of Definite Phosphatidylinositol-Specific Phospholipase C Isoforms. *Biochemical and Biophysical Research Communications*, **259**: 314 –320.
512 Rubio, M., Avitabile D, Fischer, K., Emmanuel, G., Gude, N., Miyamoto, S., Mishra, S., Schaefer, E. M., Brown, J. H., Sussman, M. A. (2009). Cardioprotective stimuli mediate phosphoinositide 3-kinase and phosphoinositide dependent kinase 1 nuclear accumulation in cardiomyocytes. *Journal of Molecular and Cellular Cardiology*, **47**: 96 –103.
513 Martellia, A. M., Manzolia, L., and Cocco, L. (2004). Nuclear inositides: facts and perspectives. *Pharmacology & Therapeutics*, **101**: 47-64.
514 Pele, E., Lamprecht, R., Ben-Levy, R., Tzahar, E., Yarden, Y. (1992). Regulated Coupling of the Neu Receptor to Phosphatidylinositol 3'Kinase and Its Release by Oncogenic Activation. *J. Biol. Chem*., **267**: 12266-12274.
515 Cuevas, B. D., Lu, Y., Mao, M., Zhang, J., LaPushin, R., Siminovitch, K., Mills, G. B. (2001). Tyrosine Phosphorylation of p85 Relieves Its Inhibitory Activity on Phosphatidylinositol 3-Kinase. *J. Biol. Chem*., **276**: 27455–27461.
516 Reif, K., Gout I, Waterfield, M. D., and Cantrell, D. A. (1993). Divergent Regulation of Phosphatidylinositol 3-Kinase p85α and p85β Isoforms upon T Cell Activation. *J. Biol. Chem*., **268**: 10780-10788.
517 Kobayashi, M., Iwamatsu, A., Shinohara-Kanda, A., Ihara, S., Fukui, Y. (2003). Activation of ErbB3–PI3-kinase pathway is correlated with malignant phenotypes of adenocarcinomas. *Oncogene*, **22**: 1294–1301.
518 Okano, J., Gaslightwala, I., Birnbaum, M. J., Rustgi, A. K., Nakagawa, H. (2000). Akt/Protein Kinase B Isoforms Are Differentially Regulated by Epidermal Growth Factor Stimulation. *J. Biol. Chem*., **275**: 30934 –30942.
519 Delcommenne, M., Tan, C., Gray, V., Rue, L., Woodgett, J., Dedhar, S. (1998). Phosphoinositide-3-OH kinase-dependent regulation of glycogen synthase kinase 3 and protein kinase B/AKT by the integrin-linked kinase. *Proc Natl Acad Sci USA*. **95**: 11211-11216.

520 Driver, G. A., and Veale, R. B. (2006). Modulation of integrin-linked kinase (ILK) expression in human oesophageal squamous cell carcinoma cell lines by the EGF and TGFβ1 growth factors. *Cancer Cell International* , **6**: 12

521 Cohen, Y., Merhavi-Shoham, E., Avraham-Lubin, B. C., Savetsky, M., Frenkel, S., Pe'er, J., Goldenberg-Cohen, N. (2009). PI3K/Akt pathway mutations in retinoblastoma. *Invest Ophthalmol Vis Sci*., **50**: 5054-6.

522 Karakas, B., Bachman, K. E., and Park, B. H. (2006). Mutation of the PIK3CA oncogene in human cancers. *British Journal of Cancer*, **94**: 455–459.

523 Ligresti, G., Militello, L., Steelman, L. S., Cavallaro, A., Basile, F., Nicoletti, F., Stivala, F., McCubrey, J. A., Libra, M. (2009). PIK3CA mutations in human solid tumors. Role in sensitivity to various therapeutic approaches. *Cell Cycle*, **8**: 1352-1358.

524 Hayes, M. P., Douglas, W., and Ellenson, L. H. (2009). Molecular alterations of EGFR and PIK3CA in uterine serous carcinoma. *Gynecol Oncol*., **113**: 370–373.

525 Phillips, W. A., Russell, S., E., Ciavarella, M. L., Choong, D. Y., Montgomery, K. G., Smith, K., Pearson, R. B., Thomas, R. J., Campbell, I. G. (2006). Mutation analysis of PIK3CA and PIK3CB in esophageal cancer and Barrett's esophagus. *Int. J. Cancer*, **118**: 2644–2646.

526 Mori, R., Ishiguro, H., Kimura, M., Mitsui, A., Sasaki, H., Tomoda, K., Mori, Y., Ogawa, R., Katada, T., Kawano, O., Harada, K., Fujii, Y., Kuwabara, Y. (2008). PIK3CA mutation status in Japanese Esophageal squamous cell carcinoma. *J. Surg. Res.*, **145**: 320-326.

527 Qiu, W., Tong, G. X., Manolidis, S., Close, L. G., Assaad, A. M., Su, G. H. (2008). Novel mutant-enriched sequencing identified high frequency of PIK3CA mutations in pharyngeal cancer. *Int. J. Cancer*: **122**: 1189–1194.

528 Aleskandarany, M. A., Rakha, E. A., Ahmed, M. A., Powe, D. G., Ellis, I. O., Green, A. R. (2010). Clinicopathologic and molecular significance of phospho-Akt expression in early invasive breast cancer. *Breast Cancer Res Treat*., doi 10.1007/s10549-010-1012-y.

529 Roy, H. K., Olusola, B. F., Clemens, D. L., Karolski, W. J., Ratashak, A., Lynch, H. T., Smyrk, T. C. (2002). AKT proto-oncogene overexpression is an early event during sporadic colon carcinogenesis. *Carcinogenesis*, **23**: 201-205.

530 Tanga, J-M.,, Hea, Q-Y., Guob,R-X., and Chang, X-J. (2006). Phosphorylated Akt overexpression and loss of PTEN expression in non-small cell lung cancer confers poor prognosis. *Lung Cancer*, **51**: 181-191.

531 Waldmann, V., Wacker, J., and Deichmann, M. (2001). Mutations of the activation-associated phosphorylation sites at codons 308 and 473 of protein kinase B are absent in human melanoma. *Arch Dermatol Res*., **293** :368–372.

532 Tibes, R. Kornblau, S. M., Qiu, Y., Mousses, S. M., Robbins, C., Moses, T., Carpten, J. D. (2007). PI3K/AKT pathway activation in acute myeloid leukaemias is not associated with AKT1 pleckstrin homology domain mutation. *British Journal of Haematology*, **140**: 344–347.

533 Shoji, K., Oda, K., Nakagawa, S., Hosokawa, S., Nagae, G., Uehara, Y., Sone, K., Miyamoto, Y., Hiraike, H., Hiraike-Wada, O., Nei, T., Kawana, K., Kuramoto, H., Aburatani, H., Yano, T., Taketani, Y. (2009). The oncogenic mutation in the pleckstrin homology domain of AKT1 in endometrial carcinomas. *Br J Cancer*.**101**: 145-8.

534 Rychahoua, P. G., Kang, J., Gulhati, P., Doan, H. Q., Chen, L. A., Xiao, S. Y., Chung, D. H., Evers, B. M. (2008). Akt2 overexpression plays a critical role in the establishment of colorectal cancer metastasis. *PNAS*, **105**: 20315–20320.

535 Matsutani, T., Nagai, Y., Mine, S., Murai , H., Saeki, N., Iwadate, Y. (2009). Akt/protein kinase B overexpression as an accurate prognostic marker in adult diffuse astrocytoma. *Acta Neurochir*., **151**: 263–268.

536 David, O., Jett, J., LeBeau, H., Dy,G., Hughes, J., Friedman, M., Brody, A. R. (2004). Phospho-Akt Overexpression in Non–Small Cell Lung Cancer Confers Significant Stage-Independent Survival Disadvantage. *Clin. Cancer Res.*, **10**: 6865–6871.
537 Maehama, T., and Dixon, J., E. (1998). The tumor suppressor, PTEN/MMAC1, de-phosphorylates the lipid second messenger, phosphatidylinositol 3,4,5-trisphosphate. *J Biol Chem*., **273**: 13375–13378.
538 Georgescu, M.-M. (2011). PTEN Tumor Suppressor Network in PI3K-Akt Pathway Control. *Genes & Cancer*, **1**: 1170 –1177.
539 Chin, Y. R., and Toker, A. (2009). Function Of Akt/Pkb Signalling To Cell Motility, Invasion And The Tumor Stroma In Cancer. *Cell Signal*., **21**: 470–476.
540 Capodanno, A., Camerini, A., Orlandini, C., Baldini, E.,, Resta, M. L., Bevilacqua, G., Collecchi, P. (2009). Dysregulated PI3K/Akt/PTEN pathway is a marker of a short disease-free survival in node-negative breast carcinoma. *Human Pathology*, **40**: 1408 – 1417.
541 Sasaki, T., Nakashiro, K.-I., Tanaka, H., Azuma, K., Goda, H., Hara, S., Onodera, J., Fujimoto, I., Tanji, N., Yokoyama, M., Hamakawa, H. (2010). Knockdown of Akt isoforms by RNA silencing suppresses the growth of human prostate cancer cells in vitro and in vivo. *Biochemical and biophysical research communications*, **399***:* 79-83.
542 Stemke-Hale, K., Gonzalez-Angulo, A. M., Lluch, A., Neve, R. M., Kuo, W.-L., Davies, M., Carey, M., Hu, Z., Guan, Y., Sahin, A., Symmans, W. F., Pusztai, L., Nolden, L. K., Horlings, H., Berns, K., Hung, M.-C., van de Vijver, M. J., Valero, V., Gray, J. W., Bernards, R., Mills, G. B., Hennessy, B. T. (2008). An Integrative Genomic and Proteomic Analysis of PIK3CA, PTEN, and AKT Mutations in Breast Cancer. *Cancer Res*., **68**: 6084–6091.
543 Vasudevan, K. M., Barbie, D. A., Davies, M. D., Rabinovsky, R., McNear, C. J., Kim, J. J., Hennessy, B. T., Tseng, H., Pochanard, P., Kim, S. Y., Dunn, I. F., Schinzel, A. C., Sandy, P., Hoersch, S., Sheng, Q., Gupta, P. B., Boehm, J. S., Reiling, J. H., Silver, S., Lu, Y., Stemke-Hale, K., Dutta, B., Joy, C., Sahin, A. A., Gonzalez-Angulo, A. M., Lluch, A., Rameh, L. E., Jacks, T., Root, D. E., Lander, E. S., Mills, G. B., Hahn, W. C., Sellers, W. R., Garraway, L. A. (2009). AKT-Independent Signalling Downstream of Oncogenic PIK3CA Mutations in Human Cancer. *Cancer Cell*, **16**: 21–32.
544 Vazquez, F., and Devreotes, P. (2006). Regulation of PTEN Function as a PIP3 Gatekeeper Through Membrane Interaction. *Cell Cycle*, **5**: 1523-1527.
545 Downes, C. P., et. al. (2007). Stimulation of PI 3-kinase signalling via inhibition of the tumor suppressor phosphatase, PTEN. *Advan. Enzyme Regul*., **47**: 184–194.
546 Janssens,V., and Goris, J. (2001). Protein phosphatase 2A: a highly regulated family of serine/threonine phosphatases implicated in cell growth and signalling. *Biochem. J*., **353**: 417-439.
547 Yang, J., and Phiel, C. (2010). Functions of B56-containing PP2As in major developmental and cancer signalling pathways. *Life sciences*, **87**: 659-66.
548 Sablina, A. A., and Hahn, W. C. (2007). The Role of PP2A A Subunits in Tumor Suppression. *Cell Adhesion & Migration*, **1**: 140-141.
549 Perrotti, D., and Neviani, P. (2008). Protein phosphatase 2A (PP2A), a drugable tumor suppressor in Ph1(+) leukemias. *Cancer Metastasis Rev*., **27**: 159–168.
550 Bialojan, C., and Takai, A. (1988). Inhibitory effect of a marine-sponge toxin, okadaic acid, on protein phosphatases. *Biochem. J.*, **256**: 283-290.
551 Finnegan, S., Mackey, A. M., and Cotter, T. G. (2010). A stress survival response in retinal cells mediated through inhibition of the serine/threonine phosphatase PP2A. *The European journal of neuroscience*, **32**: 322-34.
552 Lim, Y.-W., Yoon, S.-Y., Choi, J.-E., Kim, S.-M., Lee, H.-S., Choe, H., Lee, S.-C., Choe, H., Lee, S.-C., Kim, D.-H. (2010). Maintained activity of glycogen synthase kinase-3beta

despite of its phosphorylation at serine-9 in okadaic acid-induced neurodegenerative model. *Biochemical and biophysical research communications*, **395**: 207-12.

553 Singh, A., Ye, M., Bucur, O., Zhu, S., Santos, M. T., Rabinovitz, I., Wei, W., Gao, D., Hahn, W. C., and Khosravi-Far, R. (2010). Protein Phosphatase 2A Reactivates FOXO3a through a Dynamic Interplay with 14-3-3 and AKT. *Molecular Biology of the Cell*, **21**: 1140 -1152.

554 Fernández, J. J., Candenas, M. L., Souto, M. L., Trujillo, M. M., and Norte, M. (2002). Okadaic acid, useful tool for studying cellular processes. *Current medicinal chemistry*, **9***:* 229-62.

555 Götz, J., Probst, A., Mistl, C., Nitsch, R., M., Ehler, E. (2000). Distinct role of protein phosphatase 2A subunit Cα in the regulation of E-cadherin and β-catenin during development. *Mech. Develop.*, **93**: 83-93.

556 Götz, J., Probst, A., Ehler, E., Hemmings, B., Kues, W. (1998). Delayed embryonic lethality in mice lacking protein phosphatase 2A catalytic subunit C alpha. *Proc. Natl. Acad. Sci. USA*, **95**: 12370-12375.

557 Götz, J., and Kues, W. (1999). The role of protein phosphatase 2A catalytic subunit Cα in embryogenesis: Evidence from sequence analysis and localization studies. *Biol. Chem.*, **380**: 1117-1120.

558 Fukuda, H., Shima, H., Vesonder, R., F., Tokuda, H., Nishino, H., Katoh, S., Tamura, S., Sugimura, T., Nagao, M. (1996). Inhibition of protein serine/threonine phophatases by Fumonisin B1, a mycotoxin. *Biochem. Biophys. Res. Commun.*, **220**: 160-165.

559 Pim, D., Massimi, P., Dilworth, S. M., and Banks, L. (2004). Activation of the protein kinase B pathway by the HPV-16 E7 oncoprotein occurs through a mechanism involving interaction with PP2A. *Oncogene*, **24**: 7830–7838.

560 Tan, J., Lee, P. L., Li, Z., Jiang, X., Lim, Y. C., Hooi, S. C., and Yu, Q. (2010). B55β-Associated PP2A Complex Controls PDK1-Directed Myc Signalling a nd Modulates Rapamycin S ensitivity in Colorectal Cancer. *Cancer Cell*, **18**: 459–471.

561 Yung, H. W., Charnock-Jones, D. S., and Burton, G. J. (2011). Regulation of AKT Phosphorylation at Ser473 and Thr308 by End oplasmic Reticulum Stress Modulates Substrate Specificity in a Severity Dependent Manner. *PLoS ONE*, **6**(3): e17894. doi:10.1371/jo urnal.pone.0017 894.

562 Seeling, J. M., Miller, J. R., Gil, R., Moon, R. T., White, R., and Virshup, D. M. (1999). Regulation of beta-catenin signalling by the B56 subunit of protein phosphatase 2A. *Science*, **283**: 2089-91.

563 Verheyen, E. M., and Gottardi, C. J. (2010). Regulation of Wnt/beta-catenin signalling by protein kinases. *Developmental dynamics*, **239**: 34-44.

564 Maehama, T., Taylor, G. S. and Dixon, J. E. (2001). PTEN and myotubularin: novel phosphoinositide phosphatases. *Annu. Rev. Biochem.*, **70**: 247-279.

565 Kwon, C-H., Zhao, D., Chen, J., Alcantara, S., Li, Y., Burns, D. K., Mason, R. P., Lee, E. Y.-H. P., Wu, H., and Parada, L. F. (2008). Pten Haploinsufficiency Accelerates Formation of High-Grade Astrocytomas. *Cancer Res.*, **68**: 3286–94.

566 Trotman, L. C. Niki, M., Dotan, Z. A., Koutcher, J. A., Di Cristofano, A., Xiao, A., Khoo, A. S., Roy-Burman, P., Greenberg, N. M., Van Dyke, T., Cordon-Cardo, C., Pandolfi, P. P. (2003). Pten dose dictates cancer progression in the prostate. *PLoS Biol*. **1**, E59.

567 Fang, J., Ding, M., Yang, L., Liu, L. Z., Jiang, B. H. (2007). PI3K/PTEN/AKT Signalling Regulates Prostate Tumor Angiogenesis. *Cell. Signal.*, **19**: 2487–2497.

568 Chalhoub, N. and Baker, S. J. (2009). PTEN and the PI3-Kinase Pathway in Cancer. *Annu Rev Pathol*; **4**: 127–150.

569 Parsons, R. (2004). Human cancer, PTEN and the PI-3 kinase pathway. *Seminars in Cell & Developmental Biology*, **15**: 171–176.

570 Jiang, B.-H., and Liu, L.-Z. (2008). PI3K/PTEN signalling in tumorigenesis and angiogenesis. *Biochimica et Biophysica Acta*, **1784**: 150 – 158.
571 Mulholland, D. J., Jiao, J., and Wu, H. (2008). Hormone Refractory Prostate Cancer: Lessons Learned from the PTEN Prostate Cancer Model. *Hormonal Carcinogenesis*,**5**: 87-95.
572 Yoo, L. I., Liu, D. W., Le Vu, S., Bronson, R. T., Wu, H., Yuan, J. (2006). Pten Deficiency Activates Distinct Downstream Signalling Pathways in a Tissue-Specific Manner. *Cancer Res*., **66**: 1929-39.
573 Wu, H., Goel, V., and Haluska, F. G., (2003). PTEN signalling pathways in melanoma. *Oncogene*, **22**: 3113–3122.
574 Saal, L. H., Johanssonc, P., Holm, K., Gruvberger-Saal, S. K., She, Q.-B., Maurer, M., Koujak, S., Ferrando, A. A., Malmstrὸm, P., Memeo, L., Isolai, J., Bendahl, P., Rosend, N., Hibshoosh, H., Ringnérc, M., Borg, A., and Parsons, R. (2007). Poor prognosis in carcinoma is associated with a gene expression signature of aberrant PTEN tumor suppressor pathway activity. *PNAS*, **108**: 7564–7569.
575 Mao, C., Liao, R-Y., and Chen, Q. (2010). Loss of PTEN expression predicts resistance to EGFR-targeted monoclonal antibodies in patients with metastatic colorectal cancer. *British Journal of Cancer*, **102**, 940. doi:10.1038/sj.bjc.6605575.
576 Rodrigues de Amorim, M. A., Garcia-Segura, L. M., Goya, R. G., Portiansky, E. L. (2010). Decrease in PTEN and increase in Akt expression and neuron size in aged rat spinal cord. *Experimental Gerontology*, **45**: 457–463.
577 Planchon, S., M., Waite, K., A., and Eng, C. (2007). The nuclear affairs of PTEN. *J. Cell Science,* **121**: 249-253.
578 Jang, K-S., Song, Y. S., Jang, S.-H., Min, K.-W., Na, W., Jang,S. M., Jun, J.Y., Lee, K. H., Choi, D., Paik, S. S. (2010). Clinicopathological significance of nuclear PTEN expression in colon cancer. *Histopathology*, **56**: 229–239.
579 Gericke, A., Munson, M., and Ross, A. H. (2006). Regulation of the PTEN phosphatase. *Gene*, **374**: 1-9.
580 Lee, S. R., Yang, K. S., Kwon, J., Lee, C., Jeong, W. and Rhee ,S. G. (2002) Reversible inactivation of the tumor suppressor PTEN by H2O2. *J Biol Chem*., **277**: 20336-20342.
581 Leslie, N. R., Bennett, D., Lindsay, Y. E., Stewart, H., Gray, A., and Downes, C. P. (2003). Redox regulation of PI 3-kinase signalling via inactivation of PTEN. *The EMBO Journal*, ***22***: 5501-10.
582 Lee, S-R. (2005). Reversible Oxidation and Inactivation of the Tumor Suppressor PTEN in Neutrophils Stimulated with f MLP. *Kor J Gerontol*., **15**: 29-32.
583 Saunders, J. A., Rogers, L. C., Klomsiri, C., Poole, L. B., Daniel, L. W. (2010). Reactive oxygen species mediate lysophosphatidic acid induced signalling in ovarian cancer cells. *Free Radical Biology & Medicine*, **49**: 2058– 2067.
584 Szypowska, A. A., and Burgering, M. T. B. (2011). The Peroxide Dilemma: Opposing and Mediating Insulin Action. *Anti oxid. Redox Signal* . **15**: doi: 10.1089/ars.2010.3794.
585 Boudreau, R. T. M., and Hoskin, D. W. (2005). The use of okadaic acid to elucidate the intracellular role(s) of protein phosphatase 2A: Lessons from the mast cell model system. *International Immunopharmacology*, **5**: 1507–1518.
586 Xing, Y., Xu, Y., Chen, Y., Jeffrey, P. D., Chao, Y., Lin, Z., Li, Z., Strack, S., Stock, J. B., Shi, Y. (2006). Structure of Protein Phosphatase 2A Core Enzyme Bound to Tumor-Inducing Toxins. *Cell*, **127**: 341–353.
587 Tao, G-Z., Toivola, D. M., Zhou, Q., Strnad, P., Xu, B., Michie, S. A., Omary, M. B. (2006). Protein phosphatase-2A associates with and dephosphorylates keratin 8 after hyposmotic stress in a site- and cell-specific manner. *J. Cell Science*, **119**: 1425-1432.

588 Favre, B., Turowski, P., and Hemmings, B. A. (1997). Differential Inhibition and Posttranslational Modification of Protein Phosphatase 1 and 2A in MCF7 Cells Treated with Calyculin-A, Okadaic Acid, and Tautomycin. *J. Biol. Chem*., **272**: 13856–13863.
589 Ghosh, A., K., Grigorieva, I., Steele, R., Hoover, R., G., Ray, R., B. (1999). PTEN transcriptionally modulates c-myc gene expression in human breast carcinoma cells and is involved in cell growth regulation. *Gene*, **235**: 85-91.
590 Weng, L-P., Smith, W., M., Dahia, P., L., M., Ziebold, U., Gil, E., Lees, J., A., Eng, C. (1999). PTEN suppresses breast cancer cell growth by phosphatase activity-dependent G1 arrest followed by cell death. *Cancer Res.*, **59**: 5808-5814.
591 Nick R.Leslie, Deborah Bennett,Yvonne E.Lindsay, Hazel Stewart, Alex Gray and C.Peter Downes. (2003). Redox regulation of PI 3-kinase signalling via inactivation of PTEN. *EMBO J*., **22**: 5501-5510.
592 Meng, T-C., Fukada, T., and Tonks, N. K. (2002). Reversible Oxidation and Inactivation of Protein Tyrosine Phosphatases In Vivo. *Molecular Cell*, **9**: 387–399.
593 Martin, L., Magnaudeix, A., Esclaire, F., Yardin, C., and Terro, F. (2009). Inhibition of glycogen synthase kinase-3beta downregulates total tau proteins in cultured neurons and its reversal by the blockade of protein phosphatase-2A. *Brain research*, **1252**: 66-75.
594 Ratcliffe, M. J., Itoh, K., and Sokol, S. Y. (2000). A Positive Role for the PP2A Catalytic Subunit in Wnt Signal Transduction. *J. Biol. Chem*., **275**: 35680–35683.
595 Sparks, A. B., Morin, P. J., Vogelstein, B., and Kinzler, K. W. (1998). Mutational Analysis of the APC//3-Catenin/Tcf Pathway in Colorectal Cancer. *Cancer Res*., **58**: 1130-1134.
596 Carracedo, A., Alimonti, A., and Pandolfi, P. P. (2011). PTEN Level in Tumor Suppression: How Much Is Too Little? *Cancer Res*., **71**: 629–33.
597 Hsu, C. P., Kao, T. Y., Chang, W. L., Nieh, S., Wang, H. L., Chung, Y. C (2011). Clinical significance of tumor suppressor PTEN in colorectal carcinoma. *EJSO*, **37**: 140-147.
598 Liu, J-L., Sheng, X., Hortobagyi, Z., K., Mao, Z., Gallick, G., E., Yung, W., K., A. (2005). Nuclear PTEN-mediated growth suppression is independent of Akt down-regulation. *Mol. Cell. Biol.*, **25**: 6211-6224.
599 Trotman, L.C., Wang, X., Alimonti, A., Chen, Z., Teruya-Feldstein, J., Yang, H., Pavletich, N. P., Carver, B. S., Cordon-Cardo, C., Erdjument-Bromage, H., Tempst, P., Chi, S. G., Kim, H. J., Misteli, T., Jiang, X., Pandolfi, P. P. (2007). Ubiquitination Regulates PTEN Nuclear Import and Tumor Suppression. *Cell*, **128**: 141–156.
600 Rao, R., K., and Clayton, L., W. (2002). Regulation of protein phosphatase 2A by hydrogen peroxide and Glutathionylation. *BBRC*, **293**:610–616.
601 Goberdhan, D. C. I., and Wilson, C. (2003). PTEN: tumour suppressor, multifunctional growth regulator and more. *Human Molecular Genetics*, **12**: 239–248.
602 Vlietstra, R. J., van Alewijk, D. C., Hermans, K. G. L., van Steenbrugge, G. J.,and Trapman, J. (1998). Frequent inactivation of PTEN in prostate cancer cell lines and xenografts. *Cancer Res*., **58**: 2720-3.
603 Bhardwaj, A., Singh S., SSrivastava, S. K., Honkanen, R. E., Reed, E., and Singh , A. P. (2011). Modulation of protein phosphatase 2A activity alters androgen-independent growth of prostate cancer cells: therapeutic implications. *Mol Cancer Ther*., **10**: 720-31.
604 Saal, L. H., Gruvberger-Saal, S. K., Persson, C., Lövgren, K., Jumppanen, M., Staaf, J., Jönsson, G., Pires, G. M., Maurer, M., Holm, K., Koujak, S., Subramaniyam, S., Vallon-Christersson, J., Olsson, H., Su, T., Memeo, L., Ludwig, T., Ethier, S. P., Krogh, M., Szabolcs, M., Murty, V.V.V.S., Isola, J., Hibshoosh, H., Parsons, R., and Borg, A. (2008). Recurrent gross mutations of the PTEN tumor suppressor gene in breast cancers with deficient DSB repair. *Nature genetics*, **40**: 102-7.

605 Vazquez, A., Kulkarni, D., Grochola, L. F., Bond, G. B., Barnard, N., Toppmeyer, D., Levine, A. J., and Hirshfield, K. M. (2011). A genetic variant in a PP2A regulatory subunit encoded by the PPP2R2B gene associates with altered breast cancer risk and recurrence. *Int. J. Cancer*, **128**: 2335–2343.
606 Wang, S. S., Esplin, E. D., Li, J. L., Huang, L., Gazdar, A., Minna, J., Evans, G. A. (1998). Alterations of the PPP2R1B Gene in Human Lung and Colon Cancer. *Science*, **282**: 284-7.
607 Tang, J.-M., He, Q.-Y., Guo, R.-X., and Chang, X.-J. (2006). Phosphorylated Akt overexpression and loss of PTEN expression in non-small cell lung cancer confers poor prognosis. *Lung cancer*, **51**: 81-91.
608 Anthis, N. J., and Campbell, I. D. (2011). The tail of integrin activation. *Trends in Biochemical Sciences*, **819**: 1–8.
609 Ivaska, J., Nissinen, L., Immonen, N., Eriksson, J. E., Kähäri, V-M., and Heino, J. (2001). Integrin α2β1 Promotes Activation of Protein Phosphatase 2A and Dephosphorylation of Akt and Glycogen Synthase Kinase 3β. *Mol. Cell. Biol.*, **22**: 1352–1359.
610 Pankov, R., Cukierman, E., Clark, K., Matsumoto, K., Hahn, C., Poulin, B., Yamada, K., M. (2003). Integrin site selectively regulates Akt/PKB signalling Signalling via Local Activation of Protein Phosphatase 2A. *J. Biol. Chem*., **278**: 18671–18681.
611 Miller, S., E., and Veale, R., B. (2001). Environmental modulation of αv, α2 and β1 integrin subunit expression in human oesophageal squamous cell carcinomas. *Cell. Biol. Int.*, **25**: 61-69.
612 Suzuki, K., and Takahashi, K. (2006). Induction of E-cadherin endocytosis by loss of protein phosphates 2A expression in human breast cancers. *Biochem. Biophys. Res. Commun.*, **349**: 255-260.
613 Wong, L. L., Chang, C. F., Koay, E. S. C., and Zhang, D. (2009). Tyrosine phosphorylation of PP2A is regulated by HER-2 signalling and correlates with breast cancer progression. I*nt. J. Oncology*, **34**: 1291-1301.
614 Sato, S., Fujita, N., and Tsuruo, T. (2000). Modulation of Akt kinase activity by binding to Hsp90. *PNAS*, **97**: 10832–10837.
615 Terasawa, K., Yoshimatsu, K., Iemura, S., Natsume, T., Tanaka, K., and Minami, Y. (2006). Cdc37 Interacts with the Glycine-Rich Loop of Hsp90 Client Kinases. *Mol. Cell. Biol*., **26**: 3378–3389.
616 Theodoraki, M.A., and Caplan, A.J. (2011). Quality control and fate determination of Hsp90 client proteins, *Biochim. Biophys. Acta*, doi:10.1016/j.bbamcr.2011.08.006.
617 Miyata, Y. (2009). CK2: The kinase controlling the Hsp90 chaperone machinery. *Cell.Mol.Life Sci*., **66**: 1840–1849.
618 Vaughan, C. K., Mollapour, M., Smith, J. R., Truman, A., Hu, B., Good, V. M., Panaretou, B., Neckers, L., Clarke, P. A., Workman, P., Piper, P. W., Prodromou, C., and Pearl, L. H. (2008). Hsp90-Dependent Activation of Protein Kinases Is Regulated by Chaperone-Targeted Dephosphorylation of Cdc37. *Mol Cell.*, **31**: 886–895.
619 Di Maira, G., Brustolon, F., Pinna, L. A., Ruzzene, M. (2009). Dephosphorylation and inactivation of Akt/PKB is counteracted by protein kinase CK2 in HEK 293T cells. *Cell. Mol. Life Sci.*, **66**: 3363–3373.
620 Sontag, E. (2001). Protein phosphatase 2A: the Trojan Horse of cellular signalling. *Cellular Signalling*, **13**: 7-16.
621 Mumby, M. (2007). PP2A: Unveiling a Reluctant Tumor Suppressor. *Cell*, **130**: 21-4.
622 Janssens, V., Goris, J., and Van Hoof, C. (2005). PP2A: the expected tumor suppressor. *Current Opinion in Genetics & Development*, **15**: 34–41.
623 Lima, Y-W., Yoon, S-Y., Choi, J-E., Kima, S-M., Lee, H-S., Choe, H., Lee, S-C., Kima, D-H. (2010). Maintained activity of glycogen synthase kinase-3b despite of its

phosphorylation at serine-9 in okadaic acid-induced neurodegenerative model. *BBRC*, **395**: 207–212.

624 Verheyen, E. M., and Gottardi, C. J. (2010). Regulation of Wnt/β-Catenin Signalling by Protein Kinases. *Developmental Dynamics*, **239**: 34–44.

625 Zhou, X.W., Winblad, B., Guan, Z., and Pei, J.J. (2009). Interactions between glycogen synthase kinase 3beta, protein kinase B, and protein phosphatase 2A in tau phosphorylation in mouse N2a neuroblastoma cells. *J Alzheimers Dis*., **17**: 929-37.

626 Hernańdez, F., Langa, E., Cuadros, R., Avila, J., Villanueva, N. (2010). Regulation of GSK3 isoforms by phosphatases PP1 and PP2A. *Mol Cell Biochem*, **344**: 211–215.

627 Bezuidenhout, B., C. (2008). The role of axin in the degradation of β-catenin in human oesophageal squamous cell carcinoma. MSc Dissertation, University of the Witwatersrand, http://www.wits.ac.za.

628 Saraf, A., Oberg, E. A., and Strack, S. (2010). Molecular Determinants for PP2A Substrate Specificity: Charged Residues Mediate Dephosphorylation of Tyrosine Hydroxylase by the PP2A/B′ Regulatory Subunit. *Biochemistry*, **49**: 986–995.

629 Arnold, H. K., and Sears, R. C. (2008). A tumor suppressor role for PP2A-B5 6α through negative regulation of c-Myc and other key oncoproteins. *Cancer Metastasis Rev*., **27**: 147 –158.

630 Sears, R. C. (2004). The life cycle of c-myc. *Cell Cycle*, **3**: 1133-1137.

631 Jones, G. J., Heiss, N.S., Veale, R. B., and Thornley, A. L. (1993). Amplification and Expression of the TGF-α, EGF Receptor and c-myc Genes in Four Human Oesophageal Squamous Cell Carcinoma Lines. *Bioscience Reports*, **13**: 303-312.

632 Squire, J. A. (2009). TMPRss2-eRG and PTen loss in prostate cancer. *Nat. Gen*., **41**: 509-10.

633 Das, S., Dixon, J. E., and Cho, W. (2002). Membrane-binding and activation mechanism of PTEN. *PNAS*, **100**: 7491–7496.

634 Liu, J-L., Sheng, X., Hortobagyi, Z., K., Mao, Z., Gallick, G., E., Yung, W., K., A. (2005). Nuclear PTEN-mediated growth suppression is independent of Akt down-regulation. *Mol. Cell. Biol.*, **25**: 6211-6224.

635 Chung, J.-H., and Eng, C. (2005). Nuclear-Cytoplasmic Partitioning of Phosphatase and Tensin Homologue Deleted on Chromosome 10 (PTEN) Differentially Regulates the Cell Cycle and Apoptosis. *Cancer Res*., **65**: 8096-100.

636 Lachyankar,M. B., Sultana, N., Schonhoff, C. M., Mitra, P., Poluha, W., Lambert, S., Quesenberry, P. J., Litofsky, S. N., Recht, L. D., Nabi, R., Miller, S. J., Ohta, S., Neel, B. G., and Ross, A H. (2000). A Role for Nuclear PTEN in Neuronal Differentiation. *The Journal of Neuroscience*, **20**: 1404–1413.

637 Mistafa, O., Ghalali, A., Kadekar, S., Högberg, J., and Stenius, U. (2010). Purinergic Receptor-mediated Rapid Depletion of Nuclear Phosphorylated Akt Depends on Pleckstrin Homology Domain Leucine-rich Repeat Phosphatase, Calcineurin, Protein Phosphatase 2A, and PTEN Phosphatases. *J. Biol. Chem*., **285**: 27900 –27910.

638 Rhee, S.G., Chang, T. S., Bae, Y. S., Lee, S. R., Kang, S., W. (2003). Cellular Regulation by Hydrogen Peroxide. *J Am Soc Nephrol*, **14**: 211–215.

639 Ji, A.-R., Ku, S.-Y., Cho, M. S., Kim, Y. Y., Kim, Y. J., Oh, S. K., Kim, S. H., Ku, S.-Y., Cho, M. S., Moon, S. Y., Choi, Y. M. (2010). Reactive oxygen species enhance differentiation of human embryonic stem cells into mesendodermal lineage. *Experimental and Molecular Medicine*, **42**: 175-86.

640 Li, M., Zhao, L., Liu, J., Liu, A., Jia, C., Ma, D., Jiang, Y., Bai, X. (2010). Multi-mechanisms are involved in reactive oxygen species regulation of mTORC1 signalling. *Cellular Signalling*, **22**: 1469-76.

641 Fabiani, R., Rosignoli, P., De Bartolomeo, A., Fuccelli, R., Servili, M., & Morozzi, G. (2011). The production of hydrogen peroxide is not a common mechanism by which olive oil phenols induce apoptosis on HL60 cells. Food Chemistry, 125: 1249-1255.
642 Brigelius-Flohé, R., and Kipp, A. (2009). Glutathione peroxidases in different stages of carcinogenesis. *Biochimica et Biophysica Acta*, **1790**: 1555–1568.
643 Graves, J. A., Metukuri, M., Scott, D., Rothermund, K., and Prochownik, E. V. (2009). Regulation of Reactive Oxygen Species Homeostasis by Peroxiredoxins and c-Myc. *J Biol Chem.*, **284**: 6520–6529.
644 Egler, R. A., Fernandes, E., Rothermund, K., Sereika, S., de Souza-Pinto, N., Jaruga, P., Dizdaroglu, M., Prochownik, E. V. (2005). Regulation of reactive oxygen species, DNA damage, and c-Myc function by peroxiredoxin 1. *Oncogene*, **24**: 8038–8050.
645 Cao, J., Schulte, J., Knight, A., Leslie, N. R., Zagozdzon, A., Bronson, R., Manevich, Y., Beeson, C., Neumann, C. A. (2009). Prdx1 inhibits tumorigenesis via regulating PTEN/AKT activity. *The EMBO Journal*, **28**: 1505–1517.
646 Ho, Y. S., Magnenat, J. L., Bronsoni, R. T., Cao, J., Gargano, M., Sugawara, M., Funk, C. D. (1997). Mice Deficient in Cellular Glutathione Peroxidase Develop Normally and Show No Increased Sensitivity to Hyperoxia. *J. Biol. Chem.*, **272**: 16644–16651.
647 Cha, M-K., Suh, K-H., and Kim, I-K. (2009). Overexpression of peroxiredoxin I and thioredoxin1 in human breast carcinoma. *Journal of Experimental & Clinical Cancer Research*, **28**: 93-105.
648 Li, Q., Harraz, M. M., Zhou, W., Zhang, L. N., Ding, W., Zhang, Y., Eggleston, T., Yeaman, C., Banfi, B., and Engelhardt, J. F. (2006). Nox2 and Rac1 Regulate H2O2-Dependent Recruitment of TRAF6 to Endosomal Interleukin-1 Receptor Complexes. *Mol. Cell. Biol.*, **26**: 140–154.
649 Peus, D., and Vasa, R. A. (1998). H2O2 is an important mediator of UVB-induced EGF-Receptor Phosphorylation in Cultured Keratinocytes. *J. Invest. Dermatol.*, **110**: 966-971.
650 DeYulia, Jr., G. J., Cãrcamo, J. M., Bórquez-Ojeda, O., Shelton, C. C., and Golde, D. W. (2005). Hydrogen peroxide generated extracellularly by receptor–ligand interaction facilitates cell signalling. *PNAS*, **102**: 5044–5049.
651 Matheny Jr., R. W., and Adamo, M.L. (2010). PI3K p110α and p110β have differential effects on Akt activation and protection against oxidative stress-induced apoptosis in myoblasts. *Cell Death Differ.*, **17**: 677–688.
652 Qin, S., and Chock, P.B. (2003). Implication of Phosphatidylinositol 3-Kinase Membrane Recruitment inHydrogen Peroxide-Induced Activation of PI3K and Akt. *Biochemistry*, **42**: 2995-3003.
653 Verkman, A. S. (2009). Knock-out models reveal new aquaporin functions. *Handb. Exp. Pharmacol.*, **190**: 359-81.
654 Shankardas, J., Patil, R. V., and Vishwanatha, J. K. (2010). Effect of down-regulation of aquaporins in human corneal endothelial and epithelial cell lines. *Molecular Vision*, **16**: 1538-1548.
655 Roudier, N., Ripoche, P., Gane, P., Le Pennec, P. Y., Daniels, G., Cartron, J. P., Bailly, P. (2002). AQP3 Deficiency in Humans and the Molecular Basis of a Novel Blood Group System, GIL. *J. Biol. Chem.*, **277**: 45854–45859.
656 Itoh, A., Tsujikawa, T., Fujiyama, Y., and Bamba, T. (2003). Enhancement of aquaporin-3 by vasoactive intestinal polypeptide in a human colonic epithelial cell line. *Journal of Gastroenterology and Hepatology*, **18**: 203–210.
657 van Gorp, A. G. M., Pomeranz, K. M., Birkenkamp, K. U., Hui, R. C-H., Lam, E. W-F., Coffer, P. J. (2005). Chronic Protein Kinase B (PKB/c-akt) Activation

Leads to Apoptosis Induced by Oxidative Stress–Mediated Foxo3a Transcriptional Up-regulation. *Cancer Res*, **66**: 10760-9.

658 Los, M., Maddika, S., Erb, B., and Schulze-Osthoff, K. (2009). Switching Akt: from survival signalling to deadly response. *Bioessays*, **31**: 492–495.

659 Kops, G. J. P. L., Dansen, T. B., Polderman, P. E., Saarloos, I., Wirtz, K. W., Coffer, P. J., Huang, T. T., Bos, J. L., Medema, R. H., and Burgering, B. M. (2002). Forkhead transcription factor FOXO3a protects quiescent cells from oxidative stress. *Nature*, **419**: 316-21.

660 Dolado, I., and Nebreda, A. R. (2008). AKT and Oxidative Stress Team Up to Kill Cancer Cells. *Cancer Cell*, **14**: 427-9.

661 Yuan, Y., Zu, L., Becker, L. C., and Cai, Z. P. (2009). Myocardial Injury is Attenuated in Akt Knockout Mice After Ischemia-Reperfusion. *Circulation*, **120**: S783.

662 Minervini, F., Lacalandra, G. M., Filannino, A., Garbetta, A., Nicassio, M., Dell'aquila, M. E., Visconti, A. (2010). Toxic effects induced by mycotoxin fumonisin B1 on equine spermatozoa: Assessment of viability, sperm chromatin structure stability, ROS production and motility. *Toxicology in Vitro*, **24**: 2072–2078.

663 Huang, M-F., Lin, W-L., and Ma, Y-C. (2005). A study of reactive oxygen species in mainstream of cigarette. *Indoor Air*, **15**: 135–140.

664 González, A., Pariente, J. A., and Salido, G. M. (2007). Ethanol stimulates ROS generation by mitochondria through Ca2+ mobilization and increases GFAP content in rat hippocampal astrocytes. *Brain Research*, **1178**: 28 – 37.

665 Cao, J., Xu, D., Wang, D., Wu, R., Zhang, L., Zhu, H., He, Q., and Yang, B. (2009). ROS-driven Akt dephosphorylation at Ser-473 is involved in 4-HPR-mediated apoptosis in NB4 cells. *Free Radical Biology & Medicine*, **47**: 536– 547.

666 Stambolic V, Suzuki A, de la Pompa JL, Brothers GM, Mirtsos C, Sasaki T, Ruland J, Penninger JM, Siderovski DP, Mak TW (1998). Negative regulation of PKB/AKT-dependent cell survival by tumor suppressor PTEN. *Cell*, **95**: 29-39.

667 Rodríguez-Escudero, I., Oliver, M. D., Andrés-Pons, A., Molina, M., Cid, V. J., Pulido, R. (2011). A comprehensive functional analysis of PTEN mutations: implications in tumor- and autism-related syndromes. *Hum Mol Genet*., **20**: 4132-42.

668 Sze, K., M-F., Wong KL, Chu GK, Lee JM, Yau TO, Oi-Lin Ng, I. (2011). Loss of Phosphatase and Tensin Homolog Enhances Cell Invasion and Migration Through AKT/Sp-1 Transcription Factor/Matrix Metalloproteinase 2 Activation in Hepatocellular Carcinoma and Has Clinicopathologic Significance. *Hepatology*, **53**: 1558-1569.

669 Depowski, P. L., Rosenthal, S. I., and Ross, J. S. (2001). Loss of Expression of the PTEN Gene Protein Product Is Associated with Poor Outcome in Breast Cancer. *Mod Pathol*., **14**: 672–676.

670 Chen, H., Mei, L, Zhou, L., Shen, X., Guo, C., Zheng, Y., Zhu, H., Zhu, Y., Huang, L. (2011). PTEN restoration and PIK3CB knockdown synergistically suppress glioblastoma growth in vitro and in xenografts. *J Neurooncol*., **104**: 155–167.

671 Chen, H., Shen, X., Guo, C., Zhu, H., Zhou, L., Zhu, Y., Wang, H., Zheng, Y., Huang, L. (2010). Phosphatase and Tensin Homolog Reconstruction and Vascular Endothelial Growth Factor Knockdown Synergistically Inhibit the Growth of Glioblastoma. *Cancer Biotherapy And Radiopharmaceuticals*, **25**: 713-21.

672 Pan, L., Matloob, A. F., Du, J., Pan, H., Dong, Z., Zhao, J., Feng, Y., Zhong, Y., Huang, B., Lu, J. (2010). Vitamin D stimulates apoptosis in gastric cancer cells in synergy with trichostatin A/sodium butyrate-induced and 5-aza-2' -deoxycytidine-induced PTEN up-regulation. *FEBS Journal*, **277**: 989–999.

673 Zhao, M. (2007). PTEN: a promising pharmacological target to enhance epithelial wound healing. *British Journal of Pharmacology*, **152**: 1141–1144.

674 Naumann, R. W. (2011). The role of the phosphatidylinositol 3-kinase (PI3K) pathway in the development and treatment of uterine cancer. *Gynecol Oncol*., doi:10.1016/j.ygyno. 2011.08.002.
675 Akca, H., Demiray, A., Tokgun, O., and Yokota, J. (2011). Invasiveness and anchorage independent growth ability augmented by PTEN inactivation through the PI3K/AKT/NFkB pathway in lung cancer cells. *Lung Cancer* , **73**: 302– 309.
676 Ma, Y., Hu, C., Riegel, A. T., Fan, S., and Rosen, E. M. (2007). Growth Factor Signalling Pathways Modulate BRCA1 Repression of Estrogen Receptor-Activity. *Molecular Endocrinology*, **21**: 1905–1923.
677 Leslie, N. R., and Downes, C. P. (2004). PTEN function: how normal cells control it and tumour cells lose it. *Biochem. J*., **382**: 1–11.
678 Stiles, B. L. (2009). Phosphatase and Tensin Homologue deleted on Chromosome 10: Extending its PTENtacles. *Int J Biochem Cell Biol*., **41**: 757–761.
679 Fodde, R., and Smits, R. (2002). Cancer Biology: A Matter of Dosage. *Science*, **298**: 761-2.
680 Bignell, G. R., et. al. (2010). Signatures of mutation and selection in the cancer genome. *Nature*, **463**: 893–898.
681 Berger, A. H., Knudson, A. G., and Pandolfi, P. P. (2011). A continuum model for tumour suppression. *Nature*, **476**: 163-69.
682 Bonifant, C. L., Kim, J-S., and Waldman, T. (2007). NHERFs, NEP, MAGUKs, and More: Interactions That Regulate PTEN. *J. Cellular Biochemistry*, **102**: 878–885.
683 Salmena, L., Carracedo, A., and Pandolfi, P. P. (2008). Tenets of PTEN Tumor Suppression. *Cell*, **133**: 403-414.
684 Torres, J. and Pulido, R. (2001). The tumor suppressor pten is phosphorylated by the protein kinase CK2 at Its C terminus. Implications for PTEN stability to proteasome-mediated degradation. *J. Biol. Chem*., **276**: 993–998.
685 Virolle T, Adamson ED, Baron V, Birle, D., Mercola, D., Mustelin, T., de Belle, I. (2001). The Egr-1 transcription factor directly activates PTEN during irradiation-induced signalling. *Nat Cell Biol*., **3**: 1124–8.
686 Li, D. M, Sun, H. (1997). TEP1, encoded by a candidate tumor suppressor locus, is a novel protein tyrosine phosphatase regulated by transforming growth factor beta. *Cancer Res*., **57**: 2124–9.
687 Stambolic, V., MacPherson, D., Sas, D., Lin, Y., Snow, B., Jang, Y., Benchimol, S., Mak, T. W. (2001). Regulation of PTEN transcription by p53. *Mol Cell*., **8**: 317-25.
688 Kim, R. H. Peters, M., Jang, Y., Shi, W., Pintilie, M., Fletcher, G. C., DeLuca, C., Liepa, J., Zhou, L., Snow, B., Binari, R. C., Manoukian, A. S., Bray, M. R., Liu, F. F., Tsao, M. S., Mak, T. W. (2005). DJ-1, a novel regulator of the tumor suppressor PTEN. *Cancer Cell*, **7**: 263–273.
689 Okahara, F., Ikawa, H., Kanaho, Y., Maehama, T. (2004). Regulation of PTEN Phosphorylation and Stability by a Tumor Suppressor Candidate Protein. *J. Biol. Chem*., **279**: 45300–45303.
690 Patel, L., Pass, I., Coxon, P., Downes, C. P., Smith, S. A., Macphee, C. H. (2001). Tumor suppressor and anti-inflammatory actions of PPARγ agonists are mediated via up-regulation of PTEN. *Curr Biol*., **11**: 764– 8.
691 Xia, D., Srinivas, H., Ahn, Y. H., Sethi, G., Sheng, X., Yung, W. K., Xia, Q., Chiao, P. J., Kim, H., Brown, P. H., Wistuba, I. I., Aggarwal, B. B., Kurie, J. M. (2007). Mitogen-activated protein kinase kinase-4 promotes cell survival by decreasing PTEN expression through an NF κ B-dependent pathway. *J Biol Chem*., **282**: 3507–19.
692 Hettinger, K., Vikhanskaya, F., Poh, M. K., Lee, M. K., de Belle, I., Zhang, J. T., Reddy, S. A., Sabapathy, K. (2007). c-Jun promotes cellular survival by suppression of PTEN. *Cell Death and Differentiation*, **14**: 218–229.

693 Wang, X., Trotman, L. C., Koppie, T., Alimonti, A., Chen, Z., Gao, Z., Wang, J., Erdjument-Bromage, H., Tempst, P., Cordon-Cardo, C., Pandolfi, P. P., Jiang, X. (2007). NEDD4–1 is a proto-oncogenic ubiquitin ligase for PTEN. *Cell*, **128**: 129–39.
694 Wu, W., Wang, X., Zhang, W., Reed, W., Samet, J. M., Whang, Y. E. and Ghio, A. J. (2003). Zinc-induced PTEN protein degradation through the proteasome pathway in human airway epithelial cells. *J. Biol. Chem*., **278**: 28258–28263.
695 Torres, J., Rodriguez, J., Myers, M. P., Valiente, M., Graves, J. D., Tonks, N. K., Pulido, R. (2003). Phosphorylation-regulated Cleavage of the Tumor Suppressor PTEN by Caspase-3. *J. Biol. Chem*., **278**: 30652–30660.
696 Leslie, N. R., Spinelli, L., Tibarewal, P., Zilidis, G., Weerasinghe, N., Lim, J. C., Maccario, H., Downes, C. P. (2009). Advances in Enzyme Regulation Indirect mechanisms of carcinogenesis via down-regulation of PTEN function. *Advances in Enzyme Regulation*, **3**: 1-7.
697 Fournier, M. V., Fata, J., Martin, K., Yaswen, P., Bissell, M. J. (2009). Interaction of E-cadherin and PTEN regulates morphogenesis and growth arrest in human mammary epithelial cells. *Cancer Res*., **69**: 4545-52.
698 Chalhoub, N., and Baker, S. J. (2009). PTEN and the PI3-kinase pathway in cancer. *Annual review of pathology*, **4**: 127-50.
699 Shen-Li, H., Koujak, S., Szablocs, M., and Parsons, R. (2011). Reduction of Pten dose leads to neoplastic development in multiple organs of PtenshRNA mice. *Cancer Biol Ther*., **10**: 1194–1200.
700 Maehama, T. (2007). PTEN: Its Deregulation and Tumorigenesis. *Biol. Pharm. Bull*., **30**: 1624—1627.
701 Peters, J. M. (1994). Proteasomes: protein degradation machines of the cell. *Trends Biochem Sci*., **19**: 377-82.
702 Ciechanover, A. (1994). The Ubiquitin-Proteasome Proteolytic Pathway. *Cell*, **79**: 13-21.
703 Kwak, J., Workman, J. L., and Lee, D. (2011). The proteasome and its regulatory roles in gene expression. *Biochimica et Biophysica Acta*, **1809**: 88 –96.
704 Lecker, S. H., Goldberg, A. L., and Mitch, W. E. (2006). Protein Degradation by the Ubiquitin–Proteasome Pathway in Normal and Disease States. *J Am Soc Nephrol*., **17**: 1807–1819.
705 Jung, T., Catalgol, B., and Grune, T. (2009). The proteasomal system. *Molecular Aspects of Medicine*, **30**: 191–296.
706 Adams, J., Palombella, V. J. (1999). Proteasome Inhibitors: A Novel Class of Potent and Effective Antitumor Agents. *Cancer Res*., **59**: 2615–2622.
707 Adams J, Elliott PJ. (2000). New agents in cancer clinical trials. *Oncogene*, **19**: 6687–6692.
708 Chauhan, D., Hideshima, T., Mitsiades, C., Richardson, P., Anderson, K. C. (2005). Proteasome inhibitor therapy in multiple myeloma. *Mol Cancer Ther*., **4**: 686 – 92.
709 Shahshahan, M. A., Beckley, M. N., and Jazirehi, A. R. (2011). Potential usage of proteasome inhibitor bortezomib (Velcade, PS-341) in the treatment of metastatic melanoma: basic and clinical aspects. *Am J Cancer Res*., **1**: 913-924.
710 Kwak, J., Workman, J. L., and Lee, D. (2010). The proteasome and its regulatory roles in gene expression. *Biochimica et Biophysica Acta*, doi:10.1016/j.bbagrm.2010.08.001.
711 Hoeller, D., and Dikic, I. (2009). Targeting the ubiquitin system in cancer therapy. *Nature*, **458**: 438-44.
712 Wu, W. K. K., Cho, C. H., Lee, C. W., Wu, K., Fan, D., Yu, J., Sung, J. J. Y. (2010). Proteasome inhibition: A new therapeutic strategy to cancer treatment. *Cancer Letters*, **293**: 15–22.

713 Han, Y. H., and Park, W. H. (2010). MG132, a proteasome inhibitor decreased the growth of Calu-6 lung cancer cells via apoptosis and GSH depletion. *Toxicology in Vitro*, **24**: 1237–1242.
714 Ebert, B., Kisiela, M., Wsól, V., and Maser, E. (2011). Proteasome inhibitors MG-132 and bortezomib induce AKR1C1, AKR1C3, AKR1B1, and AKR1B10 in human colon cancer cell lines SW-480 and HT-29. *Chemico-Biological Interactions*, **191:** 239–249.
715 Mi, L., Gan, N., and Chung, F. L. (2010). Isothiocyanates inhibit proteasome activity and proliferation of multiple myeloma cells. *Carcinogenesis*, **32**: 216–223.
716 Ling, Y.-H., Liebes, L., Zou, Y., and Perez-Soler, R. (2003). Reactive Oxygen Species Generation and Mitochondrial Dysfunction in the Apoptotic Response to Bortezomib, a Novel Proteasome Inhibitor, in Human H460 Non-small Cell Lung Cancer Cells. *J. Biol. Chem.*, **278**: 33714–33723.
717 Mosmann, T. (1983). Rapid Colorimetric Assay for Cellular Growth and Survival: Application to Proliferation and Cytotoxicity Assays. *Journal of lmmunological Methods*, **65**: 55-63.
718 Holst-Hansen, C., and Brunner, N. (1998). Cell and Tissue Culture and Associated Techniques. Cell Biology: A laboratory Handbook, Second Edition, Vol 1, pages 16-18.
719 Mimnaugh, E. G., Xu, W., Vos, M., Yuan, X., Isaacs, J. S., Bisht, K. S., Gius, D., Neckers, L. (2004). Simultaneous inhibition of hsp 90 and the proteasome promotes protein ubiquitination, causes endoplasmic reticulum-derived cytosolic vacuolization, and enhances antitumor activity. *Mol Cancer Ther.*, **3**: 551–66.
720 Fribley, A., Zeng, Q., and Wang, C-Y. (2004). Proteasome Inhibitor PS-341 Induces Apoptosis through Induction of Endoplasmic Reticulum Stress-Reactive Oxygen Species in Head and Neck Squamous Cell Carcinoma Cells. *Mol. Cell. Biol.*, **24**: 9695–9704.
721 Strauss, S. J., Higginbottom, K., Jüliger, S., Maharaj, L., Allen, P., Schenkein, D., Lister, T. A., Joel, S. P. (2007). The Proteasome Inhibitor Bortezomib Acts Independently of p53 and Induces Cell Death via Apoptosis and Mitotic Catastrophe in B-Cell Lymphoma Cell Lines. *Cancer Res.*, **67** :2783–90.
722 Canestraro, M., Galimberti, S., Savli, H., Palumbo, G. A., Tibullo, D., Nagy, B., Guerrini, F., Piaggi, S., Cine, N., Metelli, M. R., Petrini, M. (2010). Synergistic antiproliferative effect of arsenic trioxide combined with bortezomib in HL60 cell line and primary blasts from patients affected by myeloproliferative disorders. *Cancer Genetics and Cytogenetics*, **199**: 110-120.
723 Shah, M. S., Power, D. G., Kindler, H. L., Holen, K. D., Kemeny, M. M., Ilson, D. H., Tang, L., Capanu, M., Wright, J. J., Kelsen, D. P. (2010). A multicenter, phase II study of Bortezomib (PS-341) in patients with unresectable or metastatic gastric and gastroesophageal junction adenocarcinoma. *Invest New Drugs*, DOI 10.1007/s10637-010-9474-7.
724 Bardag-Gorce, F., Oliva, J., Lin, A., Li, J., French, B. A., French, S. W. (2011). Proteasome inhibitor up regulates liver antioxidative enzymes in rat model of alcoholic liver disease. *Experimental and Molecular Pathology*, **90**: 123–130.
725 Ko, B-S., et. al. (2010). Bortezomib suppresses focal adhesion kinase expression via interrupting nuclear factor-kappa B. *Life Sciences*, **86**: 199–206.
726 Lorch, J. H., Thomas, T. O., and Schmoll, H-J. (2007). Bortezomib Inhibits Cell-Cell Adhesion and Cell Migration and Enhances Epidermal Growth Factor Receptor Inhibitor–Induced Cell Death in Squamous Cell Cancer. *Cancer Res.*, **67**: 727–34.
727 Ruzzene, M., Pinna, L. A. (2010). Addiction to protein kinase CK2: A common denominator of diverse cancer cells? *Biochimica et Biophysica Acta*, **1804**: 499–504.
728 Tapia, J. C., Torres, V. A., Rodriguez, D. A., Leyton, L., and Quest, A. F. G. (2006). Casein kinase 2 (CK2) increases survivin expression via enhanced β-catenin–T cell

factorlymphoid enhancer binding factor-dependent transcription. *PNAS*, **103**: 15079–15084.

729 Barnes, C. J., Li, F., Talukder, A. H., and Kumar, R. (2005). Growth Factor Regulation of a 26S Proteasomal Subunit in Breast Cancer. *Clin. Cancer Res.*, **11**: 2868-2874.

730 Aberle, H., Bauer, A., Stappert, J., Kispert, A., Kemler, R. (1997). β-catenin is a target for the ubiquitin–proteasome pathway. *The EMBO Journal*, **16**: 3797–3804.

731 Vandenberghe I, Créancier L, Vispé S, Annereau JP, Barret JM, Pouny I, Samson A, Aussagues Y, Massiot G, Ausseil F, Bailly C, Kruczynski A. (2008). Physalin B, a novel inhibitor of the ubiquitin-proteasome pathway, triggers NOXA-associated apoptosis. *Biochem Pharmacol*., **76**: 453-62.

732 Aghajanian, C., Soignet, S., Dizon, D. S., Pien, C. S., Adams, J., Elliott, P. J., Sabbatini, P., Miller, V., Hensley, M. L., Pezzulli, S,, Canales, C., Daud, A., Spriggs, D. R. (2002). A Phase I Trial of the Novel Proteasome Inhibitor PS341 in Advanced Solid Tumor Malignancies. *Clin. Cancer Res*., **8**: 2505–2511.

733 Williamson MJ, Blank JL, Bruzzese FJ, Cao Y, Daniels JS, Dick LR, Labutti J, Mazzola AM, Patil AD, Reimer CL, Solomon MS, Stirling M, Tian Y, Tsu CA, Weatherhead GS, Zhang JX, Rolfe M. (2006). Comparison of biochemical and biological effects of ML858 (salinosporamide A) and bortezomib. *Mol Cancer Ther*., **5**: 3052-61.

734 Plattner, R., Gupta S, Khosravi-Far, R., Sato, K. Y., Perucho, M., Der, C. J., Stanbridge, E. J. (1999). Differential contribution of the ERK and JNK mitogen-activated protein kinase cascades to Ras transformation of HT1080 ribrosarcoma and DLD-1 colon carcinoma cells. *Oncogene*, **18**: 1807-1817.

735 Hill, D. S., Martin, S., Armstrong, J. L., Flockhart, R., Tonison, J. J., Simpson, D. G., Birch-Machin, M. A., Redfern, C. P., Lovat, P. E. (2009). Combining the ER-stress inducing agents bortezomib and fenretinide as a novel therapeutic strategy for metastatic melanoma. *Clin Cancer Res*., **15**: 1192–1198.

736 Abreu-Martin, M. T., Palladino, A. A., Faris, M., Carramanzana, N. M., Nel, A. E., Targan, S. R. (1999). Fas activates the JNK pathway in human colonic epithelial cells: lack of a direct role in apoptosis. *Am J Physiol Gastrointest Liver Physiol*., **276**: 599-605.

737 Duan, L., Sterba, K., Kolomeichuk, S., Kim, H., Brown, P. H., and Chambers, T. C. (2007). Inducible overexpression of c-Jun in MCF7 cells causes resistance to vinblastine via inhibition of drug-induced apoptosis and senescence at a step subsequent to mitotic arrest. *Biochem Pharmacol*., **73**: 481–490.

738 Chen, S.-L., Tsao, L.-T., and Tsao, Y.-P. (1994). Antisense oligodeoxynucleotides to c-jun inhibits proliferation of transformed NIH 3T3 cells induced by E5a of HPV-11. *Cancer Letters*, **85**: 119-123.

739 Saníger ML, Oya R, Macías D, Domínguez JN, Aránega A, Luque F. (2006). c-Jun kinase mediates expression of VEGF induced at transcriptional level by Rac1 and Cdc42Hs but not by RhoA. *J Cell Biochem*., **98**: 650-60.

740 Mitchell, A., Dass, C. R., Sun, L-Q., and Khachigian, L. M. (2004). Inhibition of human breast carcinoma proliferation, migration, chemoinvasion and solid tumour growth by DNAzymes targeting the zinc finger transcriptionfactor EGR-1. *Nucleic Acids Research*, **32**: 3065-3069.

741 Jain, N., Mahendran, R., Philp, R., Guy, G. R., Tan, Y. H., Cao, X. (1996). Casein Kinase II Associates with Egr-1 and Acts as a Negative Modulator of Its DNA Binding and Transcription Activities in NIH 3T3 Cells. *J. Biol. Chem*., **271**: 13530–13536.

742 Van Erk, M. J., Teuling, E., Staal, Y. C., Huybers, S., Van Bladeren, P. J., Aarts, J. M., Van Ommen, B. (2004). Time- and dose-dependent effects of curcumin on gene expression in human colon cancer cells. *J Carcinog*., **3**: 8.

743 Sala, G. L., Bellocci, M., and Rossini, G. P. (2009). The Cytotoxic Pathway Triggered by Palytoxin Involves a Change in the Cellular Pool of Stress Response Proteins. *Chem. Res. Toxicol*., **22**: 2009–2016.
744 Junn, E., Taniguchi, H., Jeong, B. S., Zhao, X., Ichijo, H., and Mouradian, M. M. (2005). Interaction of DJ-1 with Daxx inhibits apoptosis signal-regulating kinase 1 activity and cell death. *PNAS*, **102**: 9691–9696.
745 Mo , J-S., Kim , M-Y., Ann , E-J., Hong, J-A., and Park, H-S. (2008). DJ-1 modulates UV-induced oxidative stress signalling through the suppression of MEKK1 and cell death. *Cell Death and Differentiation*, **15**: 1030–1041.
746 Taira, T., Saito, Y., Niki, T., Iguchi-Ariga, S. M, Takahashi, K., Ariga, H. (2004). DJ-1 has a role in antioxidative stress to prevent cell death. *EMBO Rep*., **5**: 213-8.
747 Ginn-Pease, M. E., and Eng, C. (2003). Increased Nuclear Phosphatase and Tensin Homologue Deleted on Chromosome 10 Is Associated with G0-G1 in MCF-7 Cells. *Cancer Res*., **63**: 282–286.
748 Ikenoue, T., Inoki, K., Zhao, B., and Guan, K. L. (2008). PTEN Acetylation Modulates Its Interaction with PDZ Domain. *Cancer Res*., **68**: 6908–12.
749 Almeida, A., Bolaños, J. P., and Moncada, S. (2009). E3 ubiquitin ligase APC/C-Cdh1 accounts for the Warburg effect by linking glycolysis to cell proliferation. *PNAS*, **107**: 738–741.
750 Morgillo F, D'Aiuto, E., Troiani, T., Martinelli, E., Cascone, T., De Palma, R., Orditura, M., De Vita, F., Ciardiello, F. (2010). Antitumor activity of bortezomib in human cancer cells with acquired resistance to anti-epidermal growth factor receptor tyrosine kinase inhibitors. *Lung Cancer*, doi:10.1016/j.lungcan. 2010.06.005.
751 Kotelevets, L., van Hengel, J., Bruyneel, E., Mareel, M., van Roy, F., Chastre, E. (2005). Implication of the MAGI-1b/PTEN signalosome in stabilization of adherens junctions and suppression of invasiveness. *Faseb J*., **19**: 115-117.
752 Tolkacheva, T., Boddapati, M., Sanfiz, A., Tsuchida, K., Kimmelman, A. C., and Chan, A. M.-L. (2001). Regulation of PTEN Binding to MAGI-2 by Two Putative Phosphorylation Sites at Threonine 382 and 383. *Cancer Res*., **61**: 4985-4989.
753 Fouladkou, F., Landry, T., Kawabe, H., Neeb, A., Lu, C., Brose, N., Stambolic, V., Rotin, D. (2008). The ubiquitin ligase Nedd4-1 is dispensable for the regulation of PTEN stability and localization. *PNAS*, **105**: 8585–8590.
754 Yasuda, J., Hunter, E., Nakao, M., Shida, H. (2002). Functional involvement of a novel Nedd4-like ubiquitin ligase on retrovirus budding. *EMBO Rep*., **3**: 636-40.
755 Bossi, G., Lapi, E., Strano, S., Rinaldo, C., Blandino, G. and Sacchi, A. (2006) Mutant p53 gain of function: reduction of tumor malignancy of human cancer cell lines through abrogation of mutant p53 expression. *Oncogene*, **25**: 304-309.
756 Sun, L., Shen, X., Liu, Y., Zhang , G., Wei, J., Zhang, H., Zhang, E., and Ma, F. (2010). The location of endogenous wild-type p53 protein in 293T and HEK293 cells expressing low-risk HPV-6E6 fusion protein with GFP. *Acta Biochim Biophys Sin*., **42**: 230–235.
757 Meek, D. W., and Eckhart, W. (1988). Phosphorylation of p53 in Normal and Simian Virus 40-Transformed NIH 3T3 Cells. *Mol. Cell. Biol*., **8**: 461-465.
758 Gu, S., Liu Z., Pan, S., Jiang, Z., Lu, H., Amit, O., Bradbury, E. M., Hu, C. A., Chen, X. (2004). Global Investigation of p53-induced Apoptosis Through Quantitative Proteomic Profiling Using Comparative Amino Acid-coded Tagging. *Molecular & Cellular Proteomics*, **3**: 998–1008.
759 Bocca, C., Bozzo, F., Francica, S., Colombatto, S., and Miglietta, A. (2002). Involvement of PPARγ and E-cadherin/β-catenin pathway in the antiproliferative effect of conjugated linoleic acid in MCF-7 cells. *Int. J. Cancer*, **121**: 248–256.

760 Lu, D., Cottam, H. B., Corr, M., and Carson, D. A. (2005). Repression of β-catenin function in malignant cells by nonsteroidal antiinflammatory drugs. *PNAS*, **102**: 18567–18571.
761 Seed, B. (1998). PPARγ and colorectal carcinoma: Conflicts in a nuclear family. *Nat. Med*., **104:** 1004-5.
762 Qiao, L., Li, G. H., Dai, Y., Wang, J., Li, Z., Zou, B., Gu, Q., Ma, J., Pang, R., Lan, H. Y., Wong, B. C. (2009). Gene expression profile in colon cancer cells with respect to XIAP expression status. *Int J Colorectal Dis*., **24**: 245–260.
763 Chawla-Sarkar, M., Bae, S. I., Reu, F. J., Jacobs, B. S., Lindner, D. J., and Borden, E. C. (2004). Downregulation of Bcl-2, FLIP or IAPs (XIAP and survivin) by siRNAs sensitizes resistant melanoma cells to Apo2L/TRAIL-induced apoptosis. *Cell Death and Differentiation*, **11**: 915–923.
764 Mufti, A. R., Burstein, E., Csomos, R. A., Graf, P. C. F., Wilkinson, J. C., Dick, R. D., Challa, M., Son, J.-K., Bratton, S. B., Su, G. L., Brewer, G. J., Jakob, U., and Ducket, C. S. (2006). XIAP Is a Copper Binding Protein Deregulated in Wilson's Disease and Other Copper Toxicosis Disorders. *Molecular Cell*, **21**: 775–785.
765 Roche, S., Dhand, R., Waterfield, M. D., Courtneidge, S. A. (1994). The catalytic subunit of phosphatidylinositol 3-kinase is a substrate for the activated platelet-derived growth factor receptor, but not for middle-T antigen-pp6O-src complexes. *Biochem. J*., **301**: 703-711.
766 Samuels, Y., Diaz L. A. Jr, Schmidt-Kittler, O., Cummins, J. M., Delong, L., Cheong, I., Rago, C., Huso, D. L., Lengauer, C., Kinzler, K. W., Vogelstein, B., Velculescu, V. E. (2005). Mutant PIK3CA promotes cell growth and invasion of human cancer cells. *Cancer Cell*., **7**: 561-73.
767 James, M. J., and Zomerdijk, J. C. B. M. (2004). Phosphatidylinositol 3-Kinase and mTOR Signalling Pathways Regulate RNA Polymerase I Transcription in Response to IGF-1 and Nutrients. *J. Biol. Chem*., **279:** 8911–8918.
768 Landowski, T. H., Megli, C. J., Nullmeyer, K. D., Lynch, R. M., Dorr, R. T. (2005). Mitochondrial-Mediated Disregulation of Ca2+ Is a Critical Determinant of Velcade (PS-341/Bortezomib) Cytotoxicity in Myeloma Cell Lines. *Cancer Res*., **65**: 3828-36.
769 Shin, D. H., Chun, Y. S., Lee, D. S., Huang, L. E., Park, J. W. (2008). Bortezomib inhibits tumor adaptation to hypoxia by stimulating the FIH-mediated repression of hypoxia-inducible factor-1. *Blood*, **111**: 3131-3136.
770 Mitsiades, C. S., McMillin, D., Kotoula, V., Poulaki, V., McMullan, C., Negri, J., Fanourakis, G., Tseleni-Balafouta, S., Ain, K. B., Mitsiades, N. (2006). Antitumor Effects of the Proteasome Inhibitor Bortezomib in Medullary and Anaplastic Thyroid Carcinoma Cells in Vitro. *J Clin Endocrinol Metab*., **91**: 4013– 4021.
771 Belloni, D., Veschini, L., Foglieni, C., Dell'Antonio, G., Caligaris-Cappio, F., Ferrarini, M., Ferrero, E. (2010). Bortezomib induces autophagic death in proliferating human endothelial cells. *Exp Cell Res*., **316**: 1010-8.
772 Papandreou, C. N., and Logothetis, C. J. (2004). Bortezomib as a Potential Treatment for Prostate Cancer. *Cancer Res*., **64**: 5036–5043.
773 Osborne, C. K., Hobbs, K., and Trent, J. M. (1987). Biological differences among MCF-7 human breast cancer cell lines from different laboratories. *Breast Cancer Research and Treatment*, **9**: 111-12.
774 Sahni, M., Wilcox, S., Mettner, P., Reiss, C., Gilliland, S. L., Purtle, D. R., Etchberger, K. J. (2006). HEK 293 Cell Growth and Virus Production in EX-CELL™ 293 Serum-Free Medium. SAFC Biosciences, Inc.
775 Todaro, G. J., and Green,H. (1963). Quantitative Studies Of The Growth Of Mouse Embryo Cells In Culture And Their Development Into Established Lines. *J. Cell Biol*., **17**: 299-313.

776 Adams, J. (2002). Development of the Proteasome Inhibitor PS-341. *The Oncologist*, **7**: 9-16.
777 Lauricella, M., Emanuele, S., D'Anneo, A., Calvaruso, G., Vassallo, B., Carlisi, D., Portanova, P., Vento, R., Tesoriere, G. (2006). JNK and AP-1 mediate apoptosis induced by bortezomib in HepG2 cells via FasL/caspase-8 and mitochondria-dependent pathways. *Apoptosis*, **11**: 607–625.
778 Poulaki, V., Mitsiades, C. S., Kotoula, V., Negri, J., McMillin, D., Miller, J. W., Mitsiades, N. (2007). The Proteasome Inhibitor Bortezomib Induces Apoptosis in Human Retinoblastoma Cell Lines In Vitro. *Invest Ophthalmol Vis Sci*., **48**: 4706 – 4719.
779 Mayo, L. D., Seo, Y. R., Jackson, M. W., Smith, M. L., Rivera Guzman, J., Korgaonkar, C. K., Donner, D. B. (2005). Phosphorylation of Human p53 at Serine 46 Determines Promoter Selection and whether Apoptosis Is Attenuated or Amplified. *J. Biol. Chem*., **280**: 25953–25959.
780 Porter, A. G., and JaÈnicke, R. U. (1999). Emerging roles of caspase-3 in apoptosis. *Cell Death and Differentiation*, **6**: 99-104.
781 Zang, C-L., Y., Zang, Y., Sen, M., Leeman-Neill, R. J., Man, D. S., Grandis, J. R., Johnson, D. E. (2009). Bortezomib up-regulates activated signal transducer and activator of transcription-3 and synergizes with inhibitors of signal transducer and activator of transcription-3 to promote head and neck squamous cell carcinoma cell death. *Mol. Cancer Ther*., **8:** 2211–20.
782 Di Raimondo, F., Conticello, C. (2009). Captivating Bortezomib: An active but still mysterious drug. *Leuk Res*; **34**:411-2.
783 Brembeck, F. H., Manni, S., Tubi, L. Q., Montini, B., Pavan, L., Colpo, A., Gnoato, M., Cabrelle, A., Adami, F., Zambello, R., Trentin, L., Gurrieri, C., Semenzato, G. (2006). Balancing cell adhesion and Wnt signalling, the key role of β-catenin. *Current Opinion in Genetics & Development*, **16**: 51–59.
784 Kurihara, A., Nagoshi, H., Yabuki, M., Okuyama, R., Obinata, M., and Shuntaro Ikawa, S. (2007). Ser46 phosphorylation of p53 is not always sufficient to induce apoptosis: multiple mechanisms of regulation of p53-dependent apoptosis. *Genes to Cells*, **12**: 853–861.
785 JaÈ nicke RU, Sprengart ML, Wati MR and Porter AG (1998) Caspase-3 is required for DNA fragmentation and morphological changes associated with apoptosis. *J.Biol. Chem.,* **273**: 9357-9360.
786 Voutsadakis, I. A., Patrikidou, A., Tsapakidis, K., Karagiannaki, A., Hatzidaki, E., Stathakis, N. E., Papandreou, C. N. (2010). Additive inhibition of colorectal cancer cell lines by aspirin and bortezomib. *Int J Colorectal Dis*., **25**: 795–804.
787 Naito, M., Katayama, R., Katayama R, Ishioka, T., Suga, A., Takubo, K., Nanjo, M, Hashimoto, C., Taira, M., Takada, S., Takada, R., Kitagawa, M., Matsuzawa, S., Reed, J. C., Tsuruo, T. (2004). Cellular FLIP Inhibits β-Catenin Ubiquitylation and Enhances Wnt Signalling. *Mol. Cell. Biol*., **24**: 8418–8427.
788 Kagawa, S., Gu, J., Honda, T., McDonnell, T. J., Swisher, S. G., Roth, J. A., Fang, B. (2001). Deficiency of Caspase-3 in MCF7 Cells Blocks Bax-mediated Nuclear Fragmentation but not Cell Death. *Clin. Cancer Res*., **7**: 1474–1480.
789 Sarkòzi, R., Perco, P., Hochegger, K., Enrich, J., Wiesinger, M., Pirklbauer, M., Eder, S., Rudnicki, M., Rosenkranz, A. R., Mayer, B., Mayer, G., Schramek, H. (2008). Bortezomib-Induced Survival Signals and Genes in Human Proximal Tubular Cells. *JPET*, **327**:645–656.
790 Archer, C. R., Koomoa, D.-L. T., Mitsunaga, E. M., Clerc, J., Shimizu, M., Kaiser, M., Schellenberg, B., Dudler, R., Bachmann, A. S. (2010). Syrbactin class proteasome inhibitor-induced apoptosis and autophagy occurs in association with p53 accumulation and Akt/PKB activation in neuroblastoma. *Biochemical pharmacology*, **80**: 170-8.

791 Chen, K.-feng, Yeh, P.-yen, Yeh, K.-huei, Lu, Y.-shen, and Huang, S.-yi. (2008). Down-regulation of Phospho-Akt Is a Major Molecular Determinant of Bortezomib-Induced Apoptosis in Hepatocellular Carcinoma Cells. *Cancer Research*, **15**: 6698-6707.

792 Ikeda, H., Hideshima, T., Fulciniti, M., Perrone, G., Miura, N., Yasui, H., Okawa, Y., Kiziltepe, T., Santo, L., Vallet, S., Cristea, D., Calabrese, E., Gorgun, G., Raje, N. S., Richardson, P., Munshi, N. C., Lannutti, B. J., Puri, K. D., Giese, N. A., Anderson, K. C. (2010). PI3K / p110 { delta } is a novel therapeutic target in multiple myeloma. *Blood*, **166**: 1460-1468.

793 Kwak, Y. D., Wang, B., Pan, W., Xu, H., Jiang, X., Liao, F. F. (2010). Functional interaction of phosphatase and tensin homologue (PTEN) with the E3 ligase NEDD4-1 during neuronal response to zinc. *J Biol Chem*., **285**: 9847-57.

794 Ikenoue, T., Kanai, F., Hikiba, Y., Obata, T., Tanaka, Y., Imamura, J., Ohta, M., Jazag, A., Guleng, B., Tateishi, K., Asaoka, Y., Matsumura, M., Kawabe, T., and Omata, M. (2005). Functional Analysis of PIK3CA Gene Mutations in Human Colorectal Cancer. *Cancer Res*., **65**: 4562-7.

795 Dan, S., Okamura, M., Seki, M., Yamazaki, K., Sugita, H., Okui, M., Mukai, Y., Nishimura, H., Asaka, R., Nomura, K., Ishikawa, Y., Yamori, T. (2010). Correlating phosphatidylinositol 3-kinase inhibitor efficacy with signalling pathway status: in silico and biological evaluations. *Cancer research*, **70**: 4982-94.

796 Goltsov, A., Faratian, D., Langdon, S. P., Mullen, P., Harrison, D. J., Bown, J. (2011). Features of the reversible sensitivity-resistance transition in PI3K/PTEN/AKT signalling network after HER2 inhibition. *Cell. Signal*., doi:10.1016/j.cellsig.2011.09.030.

797 Leslie, N. R., Spinelli L., Tibarewal, P., Zilidis, G., Weerasinghe, N., Lim, J. C., Maccario, H., Downes, C. P. (2010). Indirect mechanisms of carcinogenesis via down-regulation of PTEN function. *Advances in Enzyme Regulation*, **50**: 112–118.

798 Stahl, J. M., Cheung, M., Sharma, A., Trivedi, N. R., Shanmugam, S., Robertson, G. P. (2003). Loss of PTEN Promotes Tumor Development in Malignant Melanoma. *Cancer Res*., **63**: 2881–2890.

799 Mutter, G. L., Lin, M. C., Fitzgerald, J. T., Kum, J. B., Baak, J. P., Lees, J. A., Weng, L. P., Eng, C. (2000). Altered PTEN Expression as a Diagnostic Marker for the Earliest Endometrial Precancers. *J Natl Cancer Inst*., **92**: 924–31.

800 Bose S, Crane A, Hibshoosh H, Mansukhani M, Sandweis L, Parsons R (2002). Reduced expression of PTEN correlates with breast can-cer progression. *Hum Pathol*., **33**: 405-9.

801 Sarmadi, S., Izadi-Mood, N., Sotoudeh, K., Tavangar, S. M. (2009). Altered PTEN expression; a diagnostic marker for differentiating normal, hyperplastic and neoplastic endometrium. *Diagnostic Pathology*, **4**: 41 doi:10.1186/1746-1596-4-41.

802 Alyasiri, N. S., Mehdi, S. J., Alam, M. S., Ali, A., Mandal, A. K., Gupta, S., Singh, I., Rizvi, M. M. (2011). PTEN-mediated AKT activation contributes to the reduced apoptosis among Indian oral squamous cell carcinoma patients. *J Cancer Res Clin Oncol*., DOI 10.1007/s00432-011-1077-y.

803 Wan, X.-W., Jiang, M., Cao, H. F., He, Y. Q., Liu, S. Q., Qiu, X. H., Wu, M. C., Wang, H. Y. (2003). The alteration of PTEN tumor suppressor expression and its association with the histopathological features of human primary hepatocellular carcinoma. *J Cancer Res Clin Oncol*., **129**: 100–106.

804 Feng, C., Yao, R., Huang, F., Liu, X., Nie, W. (2011). High Level of PTEN Expression and Its Association with Low-grade Liver Metastases and Satisfactory Patient Survival in Pancreatic Cancer. *Archives of Medical Research*, doi:10.1016/j.arcmed.2011.10.008.

805 Robert, J., and Hochstrasser, M. (2011). Order of the Proteasomal ATPases and Eukaryotic Proteasome Assembly. *Cell Biochem Biophys*., **60**: 13–20.

806 Xie, Y. (2010). Structure, Assembly and Homeostatic Regulation of the 26S Proteasome. *Journal of Molecular Cell Biology*: doi:10. 1093/jmcb /mjq030.

807 Panigrahi, A. R., Pinder, S. E., Chan, S. Y., Paish E. C., Robertson, J. F., Ellis, I. O. (2004). The role of PTEN and its signalling pathways, including AKT, in breast cancer; an assessment of relationships with other prognostic factors and with outcome. *J Pathol*., **204**: 93–100.

808 Lam, J. B. B., Chow, K. H., Xu, A., Lam, K. S., Liu, J., Wong, N. S., Moon, R. T., Shepherd, P. R., Cooper, G. J., Wang, Y. (2009) Adiponectin Haploinsufficiency Promotes Mammary Tumor Development in MMTV-PyVT Mice by Modulation of Phosphatase and Tensin Homolog Activities. *PLoS ONE*, **4**: e496 8. doi:10.1 371/journal.p one.000496.

809 Chung, J-Y., Hong S. M., Choi, B. Y., Cho, H., Yu, E., Hewitt, S. M. (2009). The Expression of Phospho-AKT, Phospho-mTOR, and PTEN in Extrahepatic Cholangiocarcinoma. *Clin Cancer Res*., **15**: 660-7.

810 Chang, D., Wang, T-Y., Li, H. C., Wei, J. C., Song, J. X. (2007). Prognostic significance of PTEN expression in esophageal squamous cell carcinoma from Linzhou City, a high incidence area of northern China. *Diseases of the Esophagus*, **20**: 491–496.

811 Kim, J., Eltoum, I-E. A., Roh, M., Wang, J., Abdulkadir, S. A. (2009). Interactions between Cells with Distinct Mutations in c-MYC and Pten in Prostate Cancer. *PLoS Genet*, **5**: e1000542. doi:10.1371/journal.pgen.1000542.

812 Redfern, R. E., Redfern, D., Furgason, M. L., Munson, M., Ross A. H., Gericke, A. (2008). PTEN Phosphatase Selectively Binds Phosphoinositides and Undergoes Structural Change. *Biochemistry*, **47**: 2162-2171

813 Furumoto, Y., Brooks, S., Olivera, A., Takagi, Y., Miyagishi, M., Taira, K., Casellas, R, Beaven, M. A., Gilfillan, A. M., Rivera, J. (2006). Cutting Edge: Lentiviral Short Hairpin RNA Silencing of PTEN in Human Mast Cells Reveals Constitutive Signals That Promote Cytokine Secretion and Cell Survival. *The Journal of Immunology*, **176**: 5167–5171.

814 Vazquez, F., Ramaswamy, S., Nakamura, N. and Sellers, W. R. (2000) Phosphorylation of the PTEN tail regulates protein stability and function. *Mol. Cell. Biol*., **20**: 5010–5018.

815 Slipicevic, A., Holm, R., Nguyen, M. T., Bøhler, P. J., Davidson, B., Flørenes, V. A. (2005). Expression of Activated Akt and PTEN in Malignant Melanomas. *Am J Clin Pathol*., **124**: 528-536.

816 Livnat-levanon, N., and Glickman, M. H. (2011). Ubiquitin–Proteasome System and mitochondria—Reciprocity. *Biochimica et Biophysica Acta*, **1809**: 80-87.

817 Sato, K., Tamura, G., Tsuchiya, T., Endoh, Y., Sakata, K., Motoyama, T., Usuba, O., Kimura, W., Terashima, M., Nishizuka, S., Zou, T., Meltzer, S. J. (2002). Analysis of genetic and epigenetic alterations of the PTEN gene in gastric cancer. *Virchows Arch*, **440**: 160-165.

818 Li, J. (1997). PTEN, a Putative Protein Tyrosine Phosphatase Gene Mutated in Human Brain, Breast, and Prostate Cancer. *Science*, **275**: 1943-1947.

819 Mirmohammadsadegh, A., Marini, A., Nambiar, S., Hassan, M., Tannapfel, A., Ruzicka, T., and Hengge, U. R. (2006). Epigenetic Silencing of the PTEN Gene in Melanoma. *Cancer Res*., **66**: 6546-6552.

820 Minaguchi, T., Yoshikawa, H., and Oda, K. (2001). PTEN Mutation Located Only Outside Exons 5, 6, and 7 Is an Independent Predictor of Favorable Survival in Endometrial Carcinomas. Clinical *Cancer Research*, **7**: 2636-2642.

821 Gray I.C., Stewart LM, Phillips, S. M., Hamilton, J. A., Gray, N. E., Watson, G. J., Spurr, N. K., Snary, D. (1998). Mutation and expres-sion analysis of the putative prostate tumour-suppressor gene PTEN. *Br J Cancer*, **78**: 1296–1300.

822 Tachibana M, Shibakito, M., Ohno, S. Shibakita, M., Ohno, S., Kinugasa, S., Yoshimura, H., Ueda, S., Fujii, T., Rahman, M. A., Dhar, D. K., Nagasue, N. (2005) Expression and

prognostic significance of PTEN product protein in patient with esophageal squamous cell carcinoma. *Cancer*, **94**: 1955–1960.

823 Maehama, T., Okahara, F., and Kanaho, Y. (2004). The tumour suppressor PTEN: involvement of a tumour suppressor candidate protein in PTEN turnover. *Biochemical Society Transactions* **32**: 343-347.

824 Zhou, L., Hou, J., Fu, W., Wang, D., Yuan, Z., Jiang, H. (2007). Arsenic trioxide and 2-methoxyestradiol reduce β-catenin accumulation after proteasome inhibition and enhance the sensitivity of myeloma cells to Bortezomib. *Leukemia Res.*, **32**: 1674–1683.

825 Rowan, A. J., Lamlum, H., Ilyas, M., Wheeler, J., Straub, J., Papadopoulou, A., Bicknell, D., Bodmer, W. F., Tomlinson, I. P. (1999). APC mutations in sporadic colorectal tumors: A mutational ‘‘hotspot’’ and interdependence of the ‘‘two hits’’. *PNAS*, **97**: 3352–3357.

826 Yang, J., Zhang, W., P. M., Chen, X., He, X., Liu, C. (2006). Adenomatous Polyposis Coli (APC) Differentially Regulates β-Catenin Phosphorylation and Ubiquitination in Colon Cancer Cells. *J. Biol. Chem.*, **281**: 17751–17757.

827 Sadot, E., Conacci-Sorrell, M., Zhurinsky, J., Shnizer, D., Lando, Z., Zharhary, D., Kam, Z., Ben-Ze'ev, A., Geiger, B. (2002). Regulation of S33/S37 phosphorylated β-catenin in normal and transformed cells. *J. Cell Science*, **115**: 2771-2780.

828 Lee, E., Salic, A., Krüger, R., Heinrich, R., and Kirschner, M. W. (2003). The Roles of APC and Axin Derived from Experimental and Theoretical Analysis of the Wnt Pathway. *PLoS Biology*, **1**: 116-132.

829 Zhou, L. L., Fu, W. J., Yuan, Z. G., Wang, D. X., Hou, J. (2008). Study on the relationship of beta-catenin level and sensitivity to Bortezomib of myeloma cell lines. *Zhonghua Xue Ye Xue Za Zhi*., **29**: 234-7.

830 Wang, X. H., Zhang, L., Mitch, W. E., LeDoux, J. M., Hu, J., Du, J. (2010). Caspase-3 Cleaves Specific 19 S Proteasome Subunits in Skeletal Muscle Stimulating Proteasome Activity. *J. Biol. Chem.*, **285**: 21249–21257.

831 Kouzarides, T. (2000). Acetylation: a regulatory modification to rival phosphorylation? *The EMBO Journal*, **19**: 1176–1179.

832 Ferraro, B., Bepler, G., Sharma, S., Cantor, A., and Haura, E. B. (2005). EGR1 Predicts PTEN and Survival in Patients With Non–Small-Cell Lung Cancer. *J. Clin. Oncol.*, **23**: 1921-1926.

833 Asher, G., and Shaul, Y. (2005). p53 Proteasomal Degradation. *Cell Cycle*, **4**: 1015-1018.

834 Ramakrishna, S., Suresh, B., Baek, K-H. (2010). The role of deubiquitinating enzymes in apoptosis. *Cell. Mol. Life Sci.*, doi 10.1007/s00018-010-0504-6.

835 Marques, C., Guo, W., Pereira, P., Taylor, A., Patterson, C., Evans, P. C., Shang, F. (2006). The triage of damaged proteins: degradation by the ubiquitin-proteasome pathway or repair by molecular chaperones. *FASEB J.*, **20**: 741-3.

836 Sacco, J. J., Coulson, J. M., Clague, M. J., and Urbe’, S. (2010). Emerging Roles of Deubiquitinases in Cancer-Associated Pathways. *Life*, **62**: 140–157.

837 Song, M. S., Salmena, L., Carracedo, A., Egia, A., Lo-Coco, F., Teruya-Feldstein, J., Pandolfi, P. P. (2008). The deubiquitinylation and localization of PTEN are regulated by a HAUSP –PML network. *Nature*, **455**: 813-7.

838 Carrier, L. (2010). Too much of a good thing is bad: proteasome inhibition induces stressed hearts to fail. *Cardiovascular Research*, **88**: 389–390.

839 Tamguney, T., and Stokoe, D. (2007). New insights into PTEN. *J. Cell Science*, **120**: 4071-4079.

840 Barata, J. T. (2011). The impact of PTEN regulation by CK2 on PI3K-dependent signalling and leukemia cell survival. *Adv Enzyme Regul.*, **51**: 37-49.

841 Chen, K-F., Yeh, P. Y., Hsu, C., Hsu, C. H., Lu, Y. S., Hsieh, H. P., Chen, P. J., Cheng, A. L. (2009). Bortezomib Overcomes Tumor Necrosis Factor-related Apoptosis-inducing

Ligand Resistance in Hepatocellular Carcinoma Cells in Part through the Inhibition of the Phosphatidylinositol 3-Kinase/Akt Pathway. *J. Biol. Chem.*, **284**: 11121–11133.

842 Que, W., Chen, J., Chuang, M., and Jiang, D. (2011). Knockdown of c-Met enhances sensitivity to bortezomib in human multiple myeloma U266 cells via inhibiting Akt/ mTOR activity. *APMIS*, DOI 10.1111/j.16 00-0463.2011.02 836.x.

843 Roccaro, A. M., Sacco, A., Husu, E. N., Pitsillides, C., Vesole, S., Azab, A. K., Azab, F., Melhem, M., Ngo, H. T., Quang, P., Maiso, P., Runnels, J., Liang, M. C., Wong, K. K., Lin, C., Ghobrial, I. M. (2010). Dual targeting of the PI3K/Akt/mTOR pathway as an antitumor strategy in Waldenstrom macroglobulinemia. *Blood*, **115**: 559-569.

844 Zhu, Y., Wloch, A., Wu, Q., Peters, C., Pagenstecher, A., Bertalanffy, H., Sure, U. (2009). Involvement of PTEN Promoter Methylation in Cerebral Cavernous Malformations. *Stroke*, **40**: 820-826.

845 Manning, B. D., Logsdon M. N., Lipovsky, A. I., Abbott, D., Kwiatkowski, D. J., Cantley, L. C. (2005). Tsc2 lacking Feedback inhibition of Akt signalling limits the growth of tumors. *Genes Dev.*, **19**: 1773-1778.

846 de Amorim, M. A. R., Garcia-Segura, L. M., Goya, R. G., Portiansky, E. L. (2010). Decrease in PTEN and increase in Akt expression and neuron size in aged rat spinal cord. *Experimental Gerontology*, **45**: 457–463.

847 Yan, D., Guo, L., and Wang, Y. (2006). Requirement of dendritic Akt degradation by the ubiquitin–proteasome system for neuronal polarity. *J. Cell Biology*, **174**: 415–424.

848 Coloff, J. L., and Rathmell, J. C. (2006). Metabolic regulation of Akt: roles reversed. *The Journal of Cell Biology*, **175**: 845–847.

849 Lu, Z., and Hunter, T. (2009). Degradation of Activated Protein Kinases by Ubiquitination. *Annu Rev Biochem.*, **78**: 435–475.

850 Riesterer, O., Zingg, D., Hummerjohann, J., Bodis, S., Pruschy, M. (2004). Degradation of PKB/Akt protein by inhibition of the VEGF receptor/mTOR pathway in endothelial cells. *Oncogene*, **23**: 4624–4635

851 Liu, J., Netherland, C., Pickle, T., Sinensky, M. S., Thewke, D. P. (2009). Stimulation of Akt poly-ubiquitination and proteasomal degradation in P388D1 cells by 7-ketocholesterol and 25-hydroxycholesterol. *Arch Biochem Biophys.*, **487**: 54-8.

852 Wei, Y., Fan, T., and Yu, M. (2008). Inhibitor of apoptosis proteins and apoptosis. *Acta Biochim Biophys Sin.*, **40**: 278-288.

853 Yamaguchi, K., Nagai, S., Ninomiya-Tsuji, J., Nishita, M., Tamai, K., Irie, K., Ueno, N., Nishida, E., Shibuya, H., Matsumoto, K. (1999). XIAP, a cellular member of the inhibitor of apoptosis protein family, links the receptors to TAB1–TAK1 in the BMP signalling pathway. *The EMBO Journal*, **18**: 179–187.

854 Zhang, S., Ding, F., Luo, A., Chen, A., Yu, Z., Ren, S., Liu, Z., Zhang, L. (2007). XIAP is Highly Expressed in Esophageal Cancer and Its Down-regulation by RNAi Sensitizes Esophageal Carcinoma Cell Lines to Chemotherapeutics. *Cancer Biology & Therapy*, **6**: 973-980.

855 Galbán, S., and Duckett, C. S. (2010). XIAP as a ubiquitin ligase in cellular signalling. *Cell Death and Differentiation*, **17**: 54–60.

856 Kim, J., and Dang, C. V. (2006). Cancer's Molecular Sweet Tooth and the Warburg Effect. *Cancer Res.*, **66**: 8927-30.

857 Hui, S. T. Y., Andres, A. M., Miller, A. K., Spann, N. J., Potter, D. W., Post, N. M., Chen ,A. Z., Sachithanantham, S., Jung, D. Y., Kim, J. K., Davis, R. A. (2007). Txnip balances metabolic and growth signalling via PTEN disulfide reduction. *PNAS*, **105**: 3921–3926.

858 Vander Heiden, M. G., Cantley, L. C., and Thompson, C. B. (2009). Understanding the Warburg Effect: The Metabolic Requirements of Cell Proliferation. *Science*, **324**: 1029-1033.

859 Meggio, F., and Pinna, L. A. (2003). One-thousand-and-one substrates of protein kinase CK2? *FASEB J.*, **17**: 349–368.
860 Romieu-Mourez, R., Landesman-Bollag, E., Seldin, D. C., and Sonenshein, G. E. (2002). Protein Kinase CK2 Promotes Aberrant Activation of Nuclear Factor-κB, Transformed Phenotype, and Survival of Breast Cancer Cells. *Cancer Res.*, **62**: 6770–6778.
861 Pearl, L. H. (2005). Hsp90 and Cdc37 – a chaperone cancer conspiracy. *Current Opinion in Genetics & Development*, **15**: 55–61.
862 Dominguez, I., Sonenshein, G. E., and Seldin, D. C. (2009). CK2 and its role in Wnt and NF-kB signalling: Linking development and cancer. *Cell.Mol.Life Sci.*, **66**: 1850–1857.
863 Constantine S., McMillin, D., Kotoula, V., Poulaki, V., McMullan, C., Negri, J., Fanourakis, G., Tseleni-Balafouta, S., Ain, K. B., Mitsiades, N. (2006). Antitumor Effects of the Proteasome Inhibitor Bortezomib in Medullary and Anaplastic Thyroid Carcinoma Cells in Vitro. *The Journal of Clinical Endocrinology & Metabolism*, **91** :4013–4021.
864 Chen, K-F., Yu, H. C., Liu, T. H., Lee, S. S., Chen, P. J., Cheng, A. L. (2010). Synergistic interactions between sorafenib and bortezomib in hepatocellular carcinoma involve PP2A-dependent Akt inactivation. *Journal of Hepatology*, **52**: 88–95.
865 Mani, A., and Gelmann, E. P. (2005). The Ubiquitin-Proteasome Pathway and Its Role in Cancer. *J Clin Oncol.*, **23**: 4776-4789.
866 Li, J., Lee, B., and Lee, A. S. (2006). Endoplasmic Reticulumstress-Induced Apoptosis Multiple Pathways And Activation Of P53-Up Regulatedmodulator Of Apoptosis (Puma) And Noxa By P53. *J. Biol. Chem.*, **281**: 7260–7270.
867 Breckenridge, D. G., Germain, M., Mathai, J. P., Nguyen, M., Shore, G. C. (2003). Regulation of apoptosis by endoplasmic reticulum pathways. *Oncogene*, **22**: 8608–8618.
868 Kumar, S., and Rajkumar, S. V. (2008). Many facets of bortezomib resistance/ susceptibility. *Blood*, **112**: 2177-8.
869 Bianchi, G., Oliva L, Cascio P, Pengo N, Fontana F, Cerruti F, Orsi A, Pasqualetto E, Mezghrani, A., Calbi, V., Palladini, G., Giuliani, N., Anderson, K. C., Sitia, R., Cenci, S. (2009). The proteasome load versus capacity balance determines apoptotic sensitivity of multiple myeloma cells to proteasome inhibition. *Blood*, **113**: 3040-3049.
870 Ougolkov, A., Zhang, B., Yamashita, K., Bilim, V., Mai, M., Fuchs, S. Y., Minamoto, T. (2004). Associations Among β-TrCP, an E3 Ubiquitin Ligase Receptor, β-Catenin, and NF-κB in Colorectal Cancer. *J Natl Cancer Inst.*, **96**: 1161–70.
871 Hartsock, A., and Nelson, W. J. (2008). Adherens and Tight Junctions: Structure, Function and Connections to the Actin Cytoskeleton. *Biochim Biophys Acta.*, **1778**: 660–669.
872 Shapiro, L. (2001). β-catenin and its multiple partners: promiscuity explained. *Nature Structural Biology*, **8**: 484-7.
873 Gottardi, C. J., and Gumbiner, B. M. (2001). Adhesion signalling: How β-catenin interacts with its partners. *Current Biology*, **11**: 792–794.
874 Kimelman, D., and Xu, W. (2006). β-Catenin destruction complex: insights and questions from a structural Perspective. *Oncogene*, **25**: 7482–7491.
875 Mao, J., Wang, J., Liu, B., Pan, W., Farr, G. H., Flynn, C., Yuan, H., Takada, S., Kimelman, D., Li, L., Wu, D. (2001). Low-Density Lipoprotein Receptor-Related Protein-5 Binds to Axin and Regulates the Canonical Wnt Signalling Pathway. *Molecular Cell*, **7**: 801–809.
876 Peifer, M., and Polakis, P. (2000). Wnt Signalling in Oncogenesis and Embryogenesis--a Look Outside the Nucleus. *Science*, **287**: 1606-1609.

877 Hongisto, V., Vainio, J. C., Thompson, R., Courtney, M. J., Coffey, E. T. (2008). The Wnt Pool of Glycogen Synthase Kinase 3β Is Critical for Trophic-Deprivation-Induced Neuronal Death. *Mol. Cell. Biol*., **28**: 1515–1527.
878 Brabletz, T., Jung, A., Dag, S., Hlubek, F., Kirchner, T. (1999). β-Catenin Regulates the Expression of the Matrix Metalloproteinase-7 in Human Colorectal Cancer. *Am J Pathol*., **155**: 1033–1038.
879 Hoogeboom, D., and Burgering, B. M. T. (2009). Should I stay or should I go: β -catenin decides under stress. *Biochim. Biophys. Acta*, doi:10.1016/j.bbcan.20 09.02.0 02.
880 Cong, F., Schweizer, L., Chamorro, M., Varmus, H. (2003). Requirement for a Nuclear Function of β-Catenin in Wnt Signalling. *Mol. Cell. Biol*., **23**: 8462–8470.
881 Willert, K., and Jones, K. A. (2006). Wnt signalling: is the party in the nucleus? *Genes & Development*, **20**: 1394–1404.
882 Lee, C-H., Hung, H-W., Hung, P-H., and Shieh, Y-S. (2010). Epidermal growth factor receptor regulates β-catenin location, stability, and transcriptional activity in oral cancer. *Molecular Cancer*, **9** :64
883 Ji, L., Cao, X-F., Hung, P. H., Shieh, Y. S. (2007). Expression level of beta-catenin is associated with prognosis of esophageal carcinoma. *World J Gastroenterol*, **13**: 2622-2625.
884 Aamodt, R., Bondi, J., Andersen, S. N., Bakka, A., Bukholm, G., and Bukholm, I. R. K. (2010). The Prognostic Impact of Protein Expression of E-Cadherin-Catenin Complexes Differs between Rectal and Colon Carcinoma. *Gastroenterology research and practice*, doi:10.1155/2010/616023
885 Takemaru, K.-I., Ohmitsu, M., and Li, F. Q. (2008). An Oncogenic Hub: β-Catenin as a Molecular Target for Cancer Therapeutics. *Handbook of Experimental Pharmacology*, **186**: pp. 261-84.© Springer-Verlag Berlin Heidelberg 200.
886 Schneikert, J., and Behrens, J. (2007). The Canonical Wnt Signalling Pathway And Its Apc Partner In Colon Cancer Development. *Gut*, **56**: 417–425.
887 Svedlund, J., Aurén, M., Sundström, M., Dralle, H., Akerström, G., Björklund, P., Westin, G. (2010). Aberrant WNT/β-catenin signalling in parathyroid Carcinoma. *Molecular Cancer*, **9**: 294
888 Ilyas, M. (2005). Wnt signalling and the mechanistic basis of tumour Development. *J Pathol*., **205:** 130–144.
889 Priyadarsini, R. V., Murugan, R. S., and Nagini, S. (2011). Aberrant activation of Wnt/β-catenin signalling pathway contributes to the sequential progression of DMBA-induced HBP carcinomas. *Oral Oncol*, doi: 10.1 016/j.oral oncology.20 11.08.008.
890 Cottrell S, Bicknell D, Kaklamanis L, Bodmer WF. (1992). Molecular analysis of APC mutations in familial adenomatous polyposis and sporadic colon carcinomas. *Lancet*, **340**: 626-630.
891 Powell, S. M., Zilz, N., Beazer-Barclay, Y., Bryan, T. M., Hamilton, S. R., Thibodeau, S. N., Vogelstein B, Kinzler, K. W. (1992). APC mutations occur early during colorectal tumorigenesis. *Nature*, **359**: 235-237.
892 Morin PJ, Sparks AB, Korinek V, Barker N, Clevers H, Vogelstein B, Kinzler KW (1997). Activation of β-catenin-Tcf signalling in colon cancer by mutations in β-catenin or APC. *Science*, **275**: 1787-1790.
893 Zhao, X.-J., Li, H., Chen, H., Liu, Y.-X., Zhang, L.-H., Liu, S.-X., and Feng, Q.-L. (2003). Expression of e-cadherin and beta-catenin in human esophageal squamous cell carcinoma: relationships with prognosis. *World journal of gastroenterology*, **9**: 225-32.
894 Jones, L. J. G., and Veale, R. B. (2003). Redistribution of β-catenin in response to EGF and lithium signalling in human oesophageal squamous carcinoma cell lines. *Cancer Cell International*, **3**:13

895 Schnugh, J. (2005). Modification of β-catenins adenomatous polyposis coli binding site in oesophageal carcinoma and its role in metastasis. *Honours dissertation, University of the Witwatersrand, School of Molecular and Cell Biology, Johannesburg.*

896 Thomson, B. M. (2010). β-catenin interaction with, and regulation of, integrin-linked kinase-1 in human oesophageal squamous cell carcinoma. *MSc Dissertation, University of the Witwatersrand,* **http://www.wits.ac.za.**

897 Boonstra, J. J., van Marion, R., Beer, D. G., Lin, L., Chaves, P., Ribeiro, C., Pereira, A. D, Roque, L., Darnton, S. J., Altorki, N. K., Schrump, D. S., Klimstra, D. S., Tang, L. H., Eshleman, J. R., Alvarez, H., Shimada, Y., van Dekken, H., Tilanus, H. W., Dinjens, W. N. (2010). Verification and unmasking of Widely used Human esophageal adenocarcinoma Cell Lines. *J Natl Cancer Inst*., **102**: 271–274.

898 Case, N., and Rubin, J. (2010). β-Catenin—A Supporting Role in the Skeleton. *Journal of Cellular Biochemistry*, **110**: 545–553.

899 Cizkova M., Cizeron-Clairac, G., Vacher, S., Susini, A., Andrieu, C., Lidereau, R., Bièche, I. (2010). Gene Expression Profiling Reveals New Aspects of PIK3CA Mutation in ERalpha-Positive Breast Cancer: Major Implication of the Wnt Signalling Pathway. *PLoS ONE*, **5**: e15647. doi: 10.1371/journal.p one.0015647

900 Cox, S. N., Sallustio, F., Serino, G., Pontrelli, P., Verrienti, R., Pesce, F., Torres, D. D., Ancona, N., Stifanelli, P., Zaza, G., Schena, F. P. (2010). Altered modulation of WNT–β-catenin and PI3K/Akt pathways in IgA nephropathy. *Kidney International*, **78**: 396–407.

901 Saif, M. W., and Chu, E. (2010). Biology of Colorectal Cancer. *Cancer J*., **16**: 196–201.

902 Hu, T., and Li, C. (2010). Convergence between Wnt-b-catenin and EGFR signalling in cancer. *Molecular Cancer*, **9**:236-43.

903 Suh, Y., Afaq, F., Johnson, J. J., Mukhtar, H. (2009). A plant flavonoid fisetin induces apoptosis in colon cancer cells by inhibition of COX2 and Wnt/EGFR/NF-κB signalling pathways. *Carcinogenesis*, **30**: 300–307.

904 Faivre E. J., and Lange, C. A. (2007). Progesterone receptors upregulate Wnt-1 to induce epidermal growth factor receptor transactivation and c-Src-dependent sustained activation of Erk1/2 mitogen-activated protein kinase in breast cancer cells. *Mol Cell Biol*., **27**: 466-480.

905 Agarwal A, Das K, Lerner N, Sathe S, Cicek M, Casey G, Sizemore N. (2005). The AKT/I kappa B kinase pathway promotes angiogenic/metastatic gene expression in colorectal cancer by activating nuclear factor-kappa B and beta-catenin. *Oncogene*, **24**: 1021-1031.

906 Seldin, D. C., Landesman-Bollag, E., Farago, M., Currier, N., Lou, D., Dominguez ,I. (2005). CK2 as a positive regulator of Wnt signalling and tumourigenesis. *Molecular and Cellular Biochemistry*, **274**: 63–67.

907 Ilyas, M., Tomlinson, I. P., Rowan, A., Pignatelli, M., Bodmer, W. F. (1997). β-Catenin mutations in cell lines established from human colorectal cancers. *Proc. Natl. Acad. Sci. USA*, **94**: 10330–10334.

908 Schlosshauer, P. N., Brown, S. A., Eisinger, K., Yan, Q., Guglielminetti, E. R., Parsons, R., Ellenson, L. H., Kitajewski, J. (2000). APC truncation and increased β–catenin levels in a human breast cancer cell line. *Carcinogenesis*, **21**: 1453-56.

909 Kamma, H., Horiguchi, H., Wan, L., Matsui, M., Fujiwara, M., Fujimoto, M., Yazawa, T., Dreyfuss, G. (1999). Molecular Characterization of the hnRNP A2/B1 Proteins: Tissue-Specific Expression and Novel Isoforms. *Experimental Cell Research*, **246**: 399–411.

910 Fang, Y. J., Lu, Z. H., Wang, G. Q., Pan, Z. Z., Zhou, Z. W., Yun, J. P., Zhang, M. F., Wan, D. S. (2009). Elevated expressions of MMP-7, TROP2, and surviving are associated with survival, disease recurrence, and liver metastasis of colon cancer. *Int J Colorectal Dis*., **24**: 875–884.

911 Nateri , A. S., Spencer-Dene, B., and Behrens, A. (2005). Interaction of phosphorylated c-Jun with TCF4 regulates intestinal cancer development. *Nature Lett*., **437**: 281-5.
912 Dydensborg, A. B., Teller, I. C., Groulx, J. F., Basora, N., Paré, F., Herring, E., Gauthier, R., Jean, D., Beaulieu, J. F. (2009). Integrin α6Bβ4 inhibits colon cancer cell proliferation and c-Myc Activity. *BMC Cancer*, **9**:223-36.
913 Snoeks, L., Weber, C. R., Turner, J. R., Bhattacharyya, M., Wasland, K., Savkovic, S. D. (2008). Tumor Suppressor Foxo3a Is Involved in the Regulation of Lipopolysaccharide-Induced Interleukin-8 in Intestinal HT-29 Cells. *Infection And Immunity*, **76**: 4677–4685.
914 Smith, L. M., Wise, S. C., Hendricks, D. T., Sabichi, A. L., Bos, T., Reddy, P., Brown, P. H., Birrer, M. J. (1999). cJun overexpression in MCF-7 breast cancer cells produces a tumorigenic, invasive and hormone resistant phenotype. *Oncogene*, **18**: 6063-6070.
915 Wu, X., Tu, X., Joeng, K. S., Hilton, M. J., Williams, D. A., Long, F. (2008). Rac1 Activation Controls Nuclear Localization of β-catenin during Canonical Wnt Signalling. *Cell*, **133**: 340–353.
916 Mishra, P., Senthivinayagam, S., Rana, A., and Rana, B. (2010). Glycogen Synthase Kinase-3beta regulates Snail and beta-catenin during gastrin-induced migration of gastric cancer cells. *Journal of Molecular Signalling*, **5**: 9.
917 Fodde, R., and Tomlinson, I. (2010). Nuclear β-catenin expression and Wnt signalling: in defence of the dogma. *J Pathol*., **221**: 239–241.
918 Langlois, M-J., Bergeron, S., Bernatchez, G., Boudreau, F., Saucier, C., Perreault, N., Carrier, J. C., Rivard, N. (2010). The PTEN Phosphatase Controls Intestinal Epithelial Cell Polarity and Barrier Function: Role in Colorectal Cancer Progression. *PLoS ONE*, **5**: e15742. doi:10.1371/jo urnal.pone.0015 742.
919 Takahashi, M., Fukuda, K., Sugimura, T., and Wakabayashi, K. (1998). β-Catenin Is Frequently Mutated and Demonstrates Altered Cellular Location in Azoxymethane-induced Rat Colon Tumors. *Cancer Res*., **58**: 42-46.
920 Ninomiya, I., Endo, Y., Fushida, S., Sasagawa, T., Miyashita, T., Fujimura, T., Nishimura, G., Tani, T., Hashimoto, T., Yagi, M., Shimizu, K., Ohta, T., Yonemura, Y., Inoue, M., Sasaki, T., Miwa, K. (2000). Alteration of β-Catenin Expression In Esophageal Squamous-Cell Carcinoma. *Int. J. Cancer*, **85**: 757–761.
921 Qu, K., Haidar, A. A., Fan, J., Ensman, L., Tuncay, K., Jolly, M., Ortoleva, P. (2007). Cancer onset and progression: A genome-wide, nonlinear dynamical systems perspective on onconetworks. *Journal of Theoretical Biology*, **246**: 234–244.
922 Sonnenschein, C., and Soto, A.M. (2008). Theories Of Carcinogenesis: An Emerging Perspective. *Semin Cancer Biol*., **18**: 372–377.
923 Prehn, R. T. (1994). Cancers Beget Mutations versus Mutations Beget Cancers. *Cancer Res*., **54**: 5296-5300.
924 Ferrell Jr, J. E. (2002). Self-perpetuating states in signal transduction: positive feedback, double-negative feedback and bistability. *Current Opinion in Chemical Biology*, **6**: 140–148.
925 Ferrell, Jr, J. E. (1996). Tripping the switch fantastic: how a protein kinase cascade can convert graded inputs into switch like outputs. *TIBS*, **21**: 460-466.
926 Eungdamrong, N. J., and Iyengar, R. (2004). Modeling Cell Signalling Networks. *Biology of the Cell*, **96**: 355–362.
927 Hornung, G., and Barkai, N. (2008). Noise Propagation and Signalling Sensitivity in Biological Networks: A Role for Positive Feedback. *PLoS Comput Biol*., **4**: e8. doi:10.1 371/journal.pcbi .0040008.
928 Yeger-Lotem, E., Sattath, S., Kashtan, N., Itzkovitz, S., Milo, R., Pinter, R. Y., Alon, U., Margalit, H. (2004). Network motifs in integrated cellular networks of transcription–regulation and protein–protein interaction. *PNAS*, **101**: 5934 –5939.

929 Rosenfeld, S., and Kapetanovic, I. (2008). Systems Biology and Cancer Prevention: All Options on the Table. *Gene Regulation and Systems Biology*, **2:** 307–319.
930 López-Otín, C., and Hunter, T. (2010). The regulatory crosstalk between kinases and proteases in cancer. *Nature Reviews Cancer*, **10**: 278-292.
931 Margadant, C., and Sonnenberg, A. (2010). Integrin–TGF-β crosstalk in fibrosis, cancer and wound healing. *EMBO reports*, **11**: 97–105.
932 Pietras, K., and Östman, A. (2010). Hallmarks of cancer: Interactions with the tumor stroma. *Experimental Cell Research*, **316**: 1324–1331.
933 Kitano, H. (2002). Tumour tactics. *Nature*, **426**: 125.
934 Araujo, R. P., and Liotta, L. A. (2006). A control theoretic paradigm for cell signalling networks: a simple complexity for a sensitive robustness. *Current Opinion in Chemical Biology*, **10**: 81–87.
935 Endy, D., and Brent, R. (2001). Modelling cellular behaviour. *Nature*, **409**: 391-5.
936 Wang, E., Lenferink, A., and Connor-McCourt, M. O. (2007). Cancer systems biology: exploring cancer-associated genes on cellular networks. *Cell. Mol. Life Sci*., **64**: 1752–1762.
937 Ao, P., Galas, D., Hood, L., and Zhu, X. (2008). Cancer as robust intrinsic state of endogenous molecular-cellular network shaped by evolution. *Medical Hypotheses*, **70**: 678–684.
938 Lv, J., Cao, X-F., Ji, L., Zhu, B., Tao, L., Wang, D. D. (2010). Association of Wnt1/β-Catenin with Clinical Pathological Characteristics and Prognosis of Esophageal Squamous Cell Carcinoma. *Genetic Testing And Molecular Biomarkers*, **14**: 363–369.
939 Jankowski, J. A., Wright, N. A., Meltzer, S. J., Triadafilopoulos, G., Geboes, K., Casson, A. G., Kerr, D., Young, L. S. (1999). Molecular Evolution of the Metaplasia-Dysplasia-Adenocarcinoma Sequence in the Esophagus. *Am J Pathol*., **154**: 965–973.
940 Clevers, H. (2004). Wnt breakers in colon cancer. *Cancer Cell*: 5-6.
941 MacDonald, B. T., Tamai, K., and He, X. (2009). Wnt/β-Catenin Signalling: Components, Mechanisms, and Diseases. *Developmental Cell*, **17**: 9-26.
942 Schnugh, J. (2005). Modification of β-catenins adenomatous polyposis coli binding site in oesophageal carcinoma and its role in metastasis. *Honours dissertation, University of the Witwatersrand, School of Molecular and Cell Biology, Johannesburg.*
943 Kudo, J., Nishiwaki, T., Haruki, N., Ishiguro, H., Shibata, Y., Terashita, Y., Sugiura, H., Shinoda, N., Kimura, M., Kuwabara, Y., Fujii, Y. (2007). Aberrant nuclear localization of β-catenin without genetic alterations in β-catenin or Axin genes in esophageal cancer. *World Journal of Surgical Oncology*, **5:** 21.
944 Wang, Y., Zhou, X. (2005). Overexpression of EB1 in human esophageal squamous cell carcinoma (ESCC) may promote cellular growth by activating β-catenin/TCF Pathway. *Oncogene*, **24**: 6637–6645.
945 Schneikert, J., Grohmann, A., and Behrens, J. (2007). Truncated APC regulates the transcriptional activity of β-catenin in a cell cycle dependent manner. *Human Molecular Genetics* , **16**: 199–209.
946 Geyer, F. C., Lacroix–Triki, M., Savage, K., Arnedos, M., Lambros, M. B., MacKay, A., Natrajan, R., Reis-Filho, J. S. (2011). β-Catenin pathway activation in breast cancer is associated with triple-negative phenotype but not with CTNNB1 mutation. *Modern Pathology*, **24**: 209–231.
947 Yan, S., Zhou, C., Zhang, W., Zhang, G., Zhao, X., Yang, S., Wang, Y., Lu, N., Zhu, H., Xu, N. (2008). β-Catenin/TCF pathway upregulates STAT3 expression in human esophageal squamous cell carcinoma. *Cancer Letters*, **271**: 85–97.
948 Mareel, M., and Leroy, A. (2003). Clinical, Cellular, and Molecular Aspects of Cancer Invasion. *Physiol Rev*., **83**: 337–376.

949 Gu, Z-D., Li, J. Y., Li, M., Gu, J., Shi, X. T., Ke, Y., Chen, K. N. (2005). Matrix Metalloproteinases Expression Correlates with Survival in Patients with Esophageal Squamous Cell Carcinoma. *Am J Gastroenterol*, **100**: 1835–1843.

950 McCutcheon, L. J. G. (2008). β-catenin Expression and Associated Signalling in Moderately Differentiated Human Oesophageal Squamous Carcinoma Cell Lines. *PhD Dissertation, University of the Witwatersrand,* **http://www.wits.ac.za.**

951 Tominaga, J., Fukunaga, Y., Abelardo, E., and Nagafuchi, A. (2008). Defining the function of β-catenin tyrosine phosphorylation in cadherin-mediated cell–cell adhesion. *Genes to Cells*, **13**: 67–77.

952 Hu, P., O'Keefe, E. J., and Rubenstein, D. S. (2001). Tyrosine Phosphorylation of Human Keratinocyte β-Catenin and Plakoglobin Reversibly Regulates their Binding to E-Cadherin and α-Catenin. *J. Invest Dermatol*., **117**: 1059-1067.

953 Piedra, J., Martínez, D., Castano, J., Miravet, S., Dunach, M., de Herreros, A. G. (2001). Regulation of β-Catenin Structure and Activity by Tyrosine Phosphorylation. *J. Biol. Chem*., **276**: 20436–20443.

954 Howard, S., Deroo, T., Fujita, Y., and Itasaki, N. (2011). A Positive Role of Cadherin in Wnt/β-Catenin Signalling during Epithelial-Mesenchymal Transition. *PLoS ONE*, **6**: e238 99. doi:10.1 371/journal.pone. 0023899.

955 Herzig, M., Savarese, F., Novatchkova, M., Semb, H., and Christofori, G. (2007). Tumor progression induced by the loss of E-cadherin independent of β-catenin/Tcf-mediated Wnt signallingE-cadherin, β-catenin and Wnt signalling. *Oncogene*, **26**: 2290-2298.

956 Lee, G., Goretsky, T., Managlia, E., Dirisina, R., Singh, A. P., Brown, J. B., May, R., Yang, G. Y., Ragheb J. W., Evers, B. M., Weber, C. R., Turner, J. R., He, X. C., Katzman, R. B., Li, L., Barrett, T. A. (2010). Phosphoinositide 3-Kinase Signalling Mediates β-Catenin Activation in Intestinal Epithelial Stem and Progenitor Cells in Colitis. *Gastroenterology*, **139**: 869–881.

957 Keld, R. R., and Ang, Y. S. (2011). Targeting key signalling pathways in oesophageal adenocarcinoma: A reality for personalised medicine? *World J Gastroenterol*, **17**: 2781-2790.

958 Berasain, C., Latasa, M. U., Urtasun, R., Goñi, S., Elizalde, M., Garcia-Irigoyen, O., Azcona, M., Prieto, J., and Ávila, M. A. (2011). Epidermal Growth Factor Receptor (EGFR) Crosstalks in Liver Cancer. *Cancers*, **3**: 2444-2461.

959 van der Veeken, J., Oliveira, S., Schiffelers, R. M., Storm, G., van Bergen En Henegouwen, P. M., Roovers, R. C. (2009). Crosstalk between epidermal growth factor receptor- and insulin-like growth factor-1 receptor signalling: implications for cancer therapy. *Curr Cancer Drug Targets*, **9**:748-60.

960 McManus, E. J., Sakamoto, K., Armit, L. J., Ronaldson, L., Shpiro, N., Marquez, R., Alessi, D. R. (2005). Role that phosphorylation of GSK3 plays in insulin and Wnt signalling defined by knockin analysis. *The EMBO Journal*, **24**: 1571–1583.

961 Medina, M., and Wandosell, F. (2011). Deconstructing GSK-3:The Fine Regulation of Its Activity. International *Journal of Alzheimer's Disease*, **2011**: doi:10.4061/2011/479249

962 Fang, X., Yu, S. X., Lu, Y., Bast, R. C. Jr, Woodgett, J. R., Mills, G. B. (2000). Phosphorylation and inactivation of glycogen synthase kinase 3 by protein kinase A. *PNAS*, **97**: 11960 –11965.

963 Hernández, F., Langa, E., Cuadros, R., Avila, J., Villanueva, N. (2010). Regulation of GSK3 isoforms by phosphatases PP1 and PP2A. *Mol Cell Biochem*, **344**: 211–215.

964 Weinstein, I. B., Begemann, M., Zhou, P., Han, E. K., Sgambato, A., Doki, Y., Arber, N., Ciaparrone, M., Yamamoto, H. (1997). Disorders in Cell Circuitry Associated with Multistage Carcinogenesis: Exploitable Targets for Cancer Prevention and Therapy. *Clin. Cancer Res*., **3**: 2696-2702.

965 Shay, J. W., and Roninson, I. B. (2004). Hallmarks of senescence in carcinogenesis and cancer therapy. *Oncogene*, **23**: 2919–2933.
966 Meyerson, M., Gabriel, S., and Getz, G. (2010). Advances in understanding cancer genomes through second-generation sequencing. *Nature Reviews Genetics*, **11**: 685–696.
967 Lisanti, M.P., Martinez-Outschoorn, U. E., Chiavarina, B., Pavlides, S., Whitaker-Menezes, D., Tsirigos, A., Witkiewicz, A., Lin, Z., Balliet, R., Howell A., Sotgia, F. (2010). Understanding the "lethal" drivers of tumor-stroma co-evolution. Emerging role(s) for hypoxia, oxidative stress and autophagy/mitophagy in the tumor microenvironment. *Cancer Biology & Therapy*, **10**: 537-542.
968 Jacks, T., and Weinberg, R. A. (2002). Taking the Study of Cancer Cell Survival to a New Dimension. *Cell*, **111**: 923–925.
969 Hennessy, B. T., Smith, D. L., Ram, P. T., Lu, Y., Mills, G. B. (2005). Exploiting the PI3K/AKT Pathway for Cancer Drug Discovery. *Nature Reviews Drug Discovery*, 4: 988-1004.
970 Terauchi,Y. Tsuji, Y., Satoh, S., Minoura, H., Murakami, K., Okuno, A., Inukai, K., Asano, T., Kaburagi, Y., Ueki, K., Nakajima, H., Hanafusa, T., Matsuzawa, Y., Sekihara, H., Yin, Y., Barrett, J. C., Oda, H., Ishikawa, T., Akanuma, Y., Komuro, I., Suzuki, M., Yamamura, K., Kodama, T., Suzuki, H., Yamamura, K., Kodama, T., Suzuki, H., Koyasu, S., Aizawa, S., Tobe, K., Fukui, Y., Yazaki, Y., Kadowaki, T. (1999). Increased insulin sensitivity and hypoglycaemia in mice lacking the p85α subunit of phosphoinositide 3-kinase. *Nat. Genet.*, **21**: 230–235.
971 Jaiswal, B. S., Janakiraman, V., Kljavin, N. M., Chaudhuri, S., Stern, H. M., Wang, W., Kan, Z., Dbouk, H. A., Peters, B. A., Waring, P., Dela Vega, T., Kenski, D. M., Bowman, K. K., Lorenzo, M., Li, H., Wu, J., Modrusan, Z., Stinson, J., Eby, M., Yue, P., Kaminker, J. S., de Sauvage, F. J., Backer, J. M., Seshagiri, S. (2009). Somatic mutations in p85α promote tumorigenesis through class IA PI3K activation. *Cancer Cell*, **16**: 463–474.
972 Herrero-Gonzalez, S., and Di Cristofano, A. (2011). New Routes to Old Places: PIK3R1 and PIK3R2 Join PIK3CA and PTEN as Endometrial Cancer Genes. *Cancer Discovery*, **1**: 106–7.
973 Taniguchi CM, Winnay. J., Kondo, T., Bronson, R. T., Guimaraes, A. R., Aleman, J. O., Luo, J., Stephanopoulos, G., Weissleder, R., Cantley, L. C., Kahn, C. R. (2010). The phosphoinositide 3-kinase regulator y subunit p85alpha can exert tumor suppressor proper ties through negative regulation of growth factor signalling. *Cancer Res.*, **70**: 5305–15.
974 Chagpara, R. B., Links, P. H., Pastor, M. C., Furber, L. A., Hawrysh, A. D., Chamberlain, M. D., Anderson, D. H. (2010). Direct positive regulation of PTEN by the p85 subunit of phosphatidylinositol 3-kinase. *PNAS*, **107**: 5471–5476.
975 He J, de la Monte S, Wands JR. (2010). The p85beta regulatory subunit of PI3K serves as a substrate for PTEN protein phosphatase activity during insulin mediated signalling. *Biochem Biophys Res Commun*., **397**: 513–9.
976 Rabinovsky, R., Pochanard, P., McNear, C., Brachmann, S. M., Duke-Cohan, J. S., Garraway, L. A., Sellers, W. R. (2009). p85 Associates with unphosphorylated PTEN and the PTEN-associated complex. *Mol Cell Biol*., **29**: 5377–88.
977 Riedel, H. (2007). Models for Tumour Growth and Differentiation. The Cancer Handbook 2nd Edition, John Wiley & Sons, Ltd.
978 Neve, R. M., Chin, K., Fridlyand, J., Yeh, J., Baehner, F. L., Fevr, T., Clark, L., Bayani, N., Coppe, J. P., Tong, F., Speed, T., Spellman, P. T., DeVries, S., Lapuk, A., Wang, N. J., Kuo, W. L., Stilwell, J. L., Pinkel, D., Albertson, D. G., Waldman, F. M., McCormick, F., Dickson, R. B., Johnson, M. D., Lippman, M., Ethier, S., Gazdar, A., Gray, J. W.

(2006). A collection of breast cancer cell lines for the study of functionally distinct cancer subtypes. *Cancer Cell*, **10**: 515–527.
979 Harris, H. (2004). Tumour suppression: putting on the brakes. *Nature*, **427**: 201.
980 de Araújo, W. M., Vidal, F. C., de Souza, W. F., de Freitas, J. C. Jr., de Souza, W., Morgado-Diaz, J. A. (2010). PI3K/Akt and GSK-3β prevents in a differential fashion the malignant phenotype of colorectal cancer cells. *J Cancer Res Clin Oncol.*, **136**: 1773–1782.
981 Shukla, S., Maclennan, G. T., Hartman, D. J., Fu, P., Resnick, M. I., Gupta, S. (2007). Activation of PI3K-Akt signalling pathway promotes prostate cancer cell invasion. *Int. J. Cancer*: **121**, 1424–1432.
982 Ruth, M. C., Xu, Y., Maxwell, I. H., Ahn, N. G., Norris, D. A., Shellman, Y. G. (2006). RhoC Promotes Human Melanoma Invasion in a PI3K/Akt-Dependent Pathway. *Journal of Investigative Dermatology*, **126**: 862–868.
983 Johnson-Holiday, C., Singh, R., Johnson, E. L., Grizzle, W. E., Lillard, J. W. Jr., Singh, S. (2011). CCR9-CCL25 interactions promote cisplatin resistance in breast cancer cell through Akt activation in a PI3K-dependent and FAK-independent fashion. *World Journal of Surgical Oncology*, **9**: 46
984 Selvaggi, G., Novello, S., Torri, V., Leonardo, E., De Giuli, P., Borasio, P., Mossetti, C., Ardissone, F., Lausi, P., Scagliotti, G. V. (2004). Epidermal growth factor receptor overexpression correlates with a poor prognosis in completely resected non-small-cell lung cancer. *Annals of Oncology*, **15**: 28–32.
985 Habib, A. A., Chun, S. J., Neel, B. G., Vartanian, T. (2003). Increased Expression of Epidermal Growth Factor Receptor Induces Sequestration of Extracellular Signal-Related Kinases and Selective Attenuation of Specific Epidermal Growth Factor-Mediated Signal Transduction Pathways. *Mol. Cancer Res*., **1**: 219–233.
986 Spano, J.-P., Lagorce, C., Atlan, D., Milano, G., Domont, J., Benamouzig, R., Attar, A., Benichou, J., Martin, A., Morere, J. F., Raphael, M., Penault-Llorca, F., Breau, J. L., Fagard, R., Khayat, D., Wind, P. (2005). Impact of EGFR expression on colorectal cancer patient prognosis and survival. *Annals of Oncology*, **16:** 102–108.
987 Wallerand, H., Cai, Y., Wainberg, Z. A,. Garraway, I., Lascombe, I., Nicolle, G., Thiery, J. P., Bittard, H., Radvanyi, F., Reiter, R. R. (2010). Phospho-Akt pathway activation and inhibition depends on N-cadherin or phospho-EGFR expression in invasive human bladder cancer cell lines. *Urologic Oncology: Seminars and Original Investigations*, **28**: 180–188.
988 Bononi, A., Agnoletto, C., De Marchi, E., Marchi, S., Patergnani, S., Bonora, M., Giorgi, C., Missiroli, S., Poletti, F., Rimessi, A., Pinton, P. (2011). Protein Kinases and Phosphatases in the Control of Cell Fate. *Enzyme Research*, **2011**: doi:10.4061/2011/329098.
989 Vogiatzi, P., and Giordano, A. (2007). Following the Tracks of AKT1 Gene. *Cancer Biology & Therapy*, **6**: 1521-1524.
990 Ju, X., Katiyar, S., Wang, C., Liu, M., Jiao, X., Li, S., Zhou, J., Turner, J., Lisanti, M. P., Russell, R. G., Mueller, S. C., Ojeifo, J., Chen, W. S., Hay, N., Pestell, R. G. (2007). Akt1 governs breast cancer progression in vivo. *PNAS*, **104**: 7438–7443.
991 Scheid, M. P., and Woodgett, J. R. (2003). Unravelling the activation mechanisms of protein kinase B/Akt. *FEBS Letters*, **546**: 108-112.
992 Fuchs, S. Y.; Adler, V.; Buschmann, T.; Wu, X. W.; Ronai, Z. (1998). Mdm2 association with p53 targets its ubiquitination. *Oncogene*, **17**: 2543-2547.
993 Wyszomierski, S. I., and Yu, D. (2005). A knotty turnabout?: Akt1 as a metastasis suppressor. *Cancer Cell*, 437-9.

994 Yoeli-Lerner, M., Yiu, G. K., Rabinovitz, I., Erhardt, P., Jauliac, S., and Toker, A. (2005). Akt Blocks Breast Cancer Cell Motility and Invasion through the Transcription Factor NFAT. *Molecular Cell*, **20**: 539–550.
995 Yoeli-Lerner, M., Chin, Y. R., Hansen, C. K., Toker, A. (2009). Akt/Protein Kinase B and Glycogen Synthase Kinase-3β Signalling Pathway Regulates Cell Migration through the NFAT1 Transcription Factor. *Mol Cancer Res.*, **7**: 425–32.
996 Duque, J., Fresno, M., and Iñiguez, M. A. (2002). Expression and Function of the Nuclear Factor of Activated T Cells in Colon Carcinoma Cells. Involvement In The Regulation Of Cyclooxygenase-2. *J. Biol. Chem*., **280**: 8686–8693.
997 Yiu, G. K., and Toker, A. (2006). NFAT Induces Breast Cancer Cell Invasion by Promoting the Induction of Cyclooxygenase-2. *J. Biol. Chem*., **281**: 12210–12217.
998 Jauliac, S., López-Rodriguez, C., Shaw, L. M., Brown, L. F., Rao, A., Toker, A. (2002). The role of NFAT transcription factors in integrin-mediated carcinoma invasion. *Nature Cell Biology*, **4**: 540 – 544.
999 Wang, Y., Shenouda, S., Baranwal, S., Rathinam, R., Jain, P., Bao, L., Hazari, S., Dash, S., Alahari, S. K. (2011). Integrin subunits alpha5 and alpha6 regulate cell cycle by modulating the chk1 and Rb/E2F pathways to affect breast cancer metastasis. *Molecular Cancer*, **10**: 84
1000 Dingemans, A. C., van den Boogaart, V., Vosse, B. A., van Suylen, R. J., Griffioen, A. W., Thijssen, V. L. (2010). Integrin expression profiling identifies integrin alpha5 and beta1 as prognostic factors in early stage non-small cell lung cancer. *Molecular Cancer*, **9**: 152
1001 Koki, A. T., Khan, N. K. (2002). Characterization of cyclooxygenase-2 (COX-2) during tumorigenesis in human epithelial cancers: evidence for potential clinical utility of COX-2 inhibitors in epithelial cancers. *Prostglandind, Leokotrienes and Essential Fatty Acids*, **66**: 12-18.
1002 Zhi, H., Wang, L., Zhang, J., Zhou, C., Ding, F., Luo, A., Wu, M., Zhan, Q., Liu, Z. (2006). Significance of COX-2 expression in human esophageal squamous cell carcinoma. *Carcinogenesis*, **27**: 1214–1221.
1003 Bhandari, P., Bateman, A. C., Mehta, R. L., Stacey, B. S., Johnson, P., Cree, I. A., Di Nicolantonio, F., Patel, P. (2006). Prognostic significance of cyclooxygenase-2 (COX-2) expression in patients with surgically resectable adenocarcinoma of the oesophagus. *BMC Cancer*, **6**: doi:10.1186/1471-2407-6-134.
1004 Huang, J.-X., Xiao, W., Chen, W. C., Lin, M. S., Song, Z. X., Chen, P., Zhang, Y. L., Li, F. Y., Qian, R. Y., Salminen, E. (2010). Relationship between COX-2 and cell cycle-regulatory proteins in patients with esophageal squamous cell carcinoma. *World J Gastroenterol*., **16**: 5975-5981.
1005 Li, L., Zhao, J., Wu, Z., Wang, G., and Chen, G. (2009). Meta-analysis: clinicopathological and prognostic significance of cyclooxygenase-2 expression on oesophageal squamous cell carcinoma. *Aliment Pharmacol Ther*., **30**: 589–596.
1006 Hutchinson, J. N., Jin, J., Cardiff, R. D., Woodgett, J. R., Muller, W. J. (2004). Activation of Akt-1 (PKB-) Can Accelerate ErbB-2-Mediated Mammary Tumorigenesis but Suppresses Tumor Invasion. *Cancer Res*., **64**: 3171–3178.
1007 De Laurentiis, A., Pardo, O. E., Palamidessi, A., Jackson, S. P., Schoenwaelder, S. M., Reichmann, E., Scita, G., Arcaro, A. (2011). The catalytic class IA PI3K isoforms play divergent roles in breast cancer cell migration. *Cellular Signalling*, **23**: 529–541.
1008 Madhunapantula, S. V., and Robertson, G. P. (2011). Therapeutic Implications of Targeting AKT Signalling in Melanoma. *Enzyme Research*, **2011**: doi:10.4061/2011/327923.

1009 Liu, H., Radisky, D. C., Nelson, C. M., Zhang, H., Fata, J. E., Roth, R. A., Bissell, M. J. (2006). Mechanism of Akt1 inhibition of breast cancer cell invasion reveals a protumorigenic role for TSC2. *PNAS*, **103**: 4134–4139.
1010 Blagosklonny, M. V. (2003). Apoptosis, proliferation, differentiation: in search of the order. *Seminars in Cancer Biology*, **13**: 97–105.
1011 Lee, J. W., and Juliano, R. L. (2002). The α5β1 integrin selectively enhances epidermal growth factor signalling to the phosphatidylinositol-3-kinase/Akt pathway in intestinal epithelial cells. *Biochimica et Biophysica Acta*, **1542**: 23-31.
1012 Thomson, S., Petti, F., Sujka-Kwok, I., Mercado, P., Bean, J., Monaghan, M., Seymour, S. L., Argast, G. M., Epstein, D. M., Haley, J. D. (2011). A systems view of epithelial–mesenchymal transition signalling states. *Clin Exp Metastasis*, **28**: 137–155.
1013 Barr, S., Thomson, S., Buck, E., Russo, S., Petti, F., Sujka-Kwok, I., Eyzaguirre, A., Rosenfeld-Franklin, M., Gibson, N. W., Miglarese, M., Epstein, D., Iwata, K. K., Haley, J. D. (2008). Bypassing cellular EGF receptor dependence through epithelial-to-mesenchymal-like transitions. *Clin Exp Metastasis*, **25**: 685–693.
1014 Kolch, W. (2000). Meaningful relationships : the regulation of the Ras/Raf/MEK/ERK pathway by protein interactions. *Biochem. J.*, **351**: 289-305.
1015 Chen ,A., Xu, J., and Johnson, A. C. (2006). Curcumin inhibits human colon cancer cell growth by suppressing gene expression of epidermal growth factor receptor through reducing the activity of the transcription factor Egr-1. *Oncogene*, **25**: 278–287.
1016 Buck, E., Eyzaguirre, A., Rosenfeld-Franklin, M., Thomson, S., Mulvihill, M., Barr, S., Brown, E., O'Connor, M., Yao, Y., Pachter, J., Miglarese, M., Epstein, D., Iwata, K. K., Haley, J. D., Gibson, N. W., Ji, Q. S. (2008). Feedback Mechanisms Promote Cooperativity for Small Molecule Inhibitors of Epidermal and Insulin-Like Growth Factor Receptors. *Cancer Res.*, **68**: 8322–32.
1017 Wang, B., Hendricks, D. T., Wamunyokoli, F., Parker, M. I. (2006). A Growth-Related Oncogene/CXC Chemokine Receptor 2 Autocrine Loop Contributes to Cellular Proliferation in Esophageal Cancer. *Cancer Res.*, **66**: 3071-7.
1018 Kwiatkowska, A., Kijewska, M., Lipko, M., Hibner, U., Kaminska, B. (2011). Down-regulation of Akt and FAK phosphorylation reduces invasion of glioblastoma cells by impairment of MT1-MMP shuttling to lamellipodia and downregulates MMPs expression. *Biochim. Biophys. Acta*., doi:10.1016/j.bbamcr.2011.01.020.
1019 Velasco, A., Bussaglia, E., Pallares, J., Dolcet, X., Llobet, D., Encinas, M., Llecha, N., Palacios, J., Prat, J., Matias-Guiu, X. (2006). PIK3CA gene mutations in endometrial carcinoma: correlation with PTEN and K-RAS alterations. *Hum Pathol*., **37**: 1465–72.
1020 Murugan, A. K., Hong, N. T., Fukui, Y., Munirajan, A. K,. Tsuchida, N. (2008). Oncogenic mutations of the PIK3CA gene in head and neck squa-mous cell carcinomas. *Int J Oncol.*, **32**: 101–11.
1021 Rudd, M. L., Price, J. C., Fogoros, S., Godwin, A. K., Sgroi, D. C., Merino, M., Bell, D. W. (2011). A unique spectrum of somatic PIK3CA (p110a) mutations within primary endometrial carcinomas. *Clin Cancer Res.*, **17**: 1331–40.
1022 Rigoulet, M., Yoboue, E. D., and Devin, A. (2011). Mitochondrial ROS Generation and Its Regulation: Mechanisms Involved in H2O2 Signalling. *Antioxid. Redox Signal*., **14:** 459–468.
1023 Leslie, N. R. (2006). The Redox Regulation of PI 3-Kinase–Dependent Signalling. *Antioxid. Redox Signal*., **8**: 1765–1774.
1024 Rhee, S. G. (2006). H2O2, a Necessary Evil for Cell Signalling. *Science*, **312**: 1882-3.
1025 Sundaresan, M., Yu, Z. X., Ferrans, V. J,. Irani, K., Finkel, T. (1995) Requirement for generation of H2O2 for platelet-derived growth factor signal transduction. *Science*, 270: 296–299.

1026 Bae, Y.S. Kang, S. W., Seo, M. S., Baines, I. C., Tekle, E., Chock, P. B., Rhee, S. G. (1997) Epidermal growth factor (EGF)-induced generation of hydrogen peroxide. Role in EGF receptor-mediated tyrosine phosphorylation. *J. Biol. Chem.*, **272**: 217–221.
1027 Magder, S. (2006). Reactive oxygen species: toxic molecules or spark of life? *Critical Care*, **10**: 208 (doi:10.1186/cc3992).
1028 Jones, D. P. (2008). Radical-free biology of oxidative stress. *Am J Physiol Cell Physiol*., **295**: 849-868
1029 Forman, H. J., Fukuto, J. M., and Torres, M. (2004). Redox signalling: thiol chemistry defines which reactive oxygen and nitrogen species can act as second messengers. *Am J Physiol Cell Physiol*., **287**: 246–256.
1030 Gamou, S., and Shimizu, N. (1995). Hydrogen peroxide preferentially enhances the tyrosine phosphorylation of epidermal growth factor receptor. *FEBS Letters*, **357**: 161-164.
1031 de Wit, R., Makkinje, M., Boonstra, J., Verkleij, A. J., and Post, J. A. (2000). Hydrogen peroxide reversibly inhibits epidermal growth factor (EGF) receptor internalization and coincident ubiquitination of the EGF receptor and Eps15. *The FASEB Journal*, **10**.1096/fj.00-0454fje.
1032 Zhang, X., Tang, N., Hadden, T. J., Rishi, A. K. (2011). Akt, FoxO and regulation of apoptosis. *Biochim. Biophys. Acta*., doi: 10.1016/j.bbamcr.2011.03.010
1033 Myatt, S. S., Brosens, J. J., and Lam, E. W. (2011). Sense and Sensitivity: FOXO and ROS in Cancer Development and Treatment. *Anti oxid. Redox Signal*., **14**: 675–687.
1034 Bird-Lieberman, E. L., and Fitzgerald, R. C. (2009). Early diagnosis of oesophageal cancer. *British Journal of Cancer*, **101**: 1–6.
1035 Chen, G., Izzo, J., Demizu, Y., Wang, F., Guha, S., Wu, X., Hung, M. C., Ajani, J. A., Huang, P. (2009). Different Redox States in Malignant and Nonmalignant Esophageal Epithelial Cells and Differential Cytotoxic Responses to Bile Acid and Honokiol. *Antioxid. Redox Signal*., **11**: 1083–1095.
1036 Hu, Y., Zhang, Z., and Yang, C. (2007). The determination of hydrogen peroxide generated from cigarette smoke with an ultrasensitive and highly selective chemiluminescence method. *Analytica Chimica Acta*, **601**: 95–100.
1037 Sun, L., König, I. R., and Homann, N. (2009). Manganese Superoxide Dismutase (MnSOD) Polymorphism, Alcohol, Cigarette Smoking and Risk of Oesophageal Cancer. *Alcohol & Alcoholism*, **44**: 353–357.
1038 Hempel, N., Ye, H., Abessi, B., Mian, B., Melendez, J. A. (2009). Altered redox status accompanies progression to metastatic human bladder cancer. *Free Radical Biology & Medicine*, **46**: 42–50.
1039 Tobar, N., Guerrero, J., Smith, P. C., and Martınez, J. (2010). NOX4-dependent ROS production by stromal mammary cells modulates epithelial MCF-7 cell migration. *British Journal of Cancer*, **103**: 1040–1047.
1040 Gibellini, L., Pinti, M., Pinti, M., Nasi, M., De Biasi, S., Roat, E., Bertoncelli, L., and Cossarizza, A. (2010). Interfering with ROS Metabolism in Cancer Cells: The Potential Role of Quercetin. *Cancers*, **2**: 1288-1311.
1041 Tan, D-J., Chang, J., Liu, L. L., Bai R. K., Wang, Y. F., Yeh, K. T., Wong, L. J. (2006). Significance of somatic mutations and content alteration of mitochondrial DNA in esophageal cancer. *BMC Cancer*, **6**: 93 doi:10.1186/1471-2407-6-93.
1042 Zaretsky, J. Z., Barnea, I., Aylon, Y., Gorivodsky, M., Wreschner, D. H., Keydar, I. (2006). MUC1 gene overexpressed in breast cancer: structure and transcriptional activity of the MUC1 promoter and role of estrogen receptor alpha (ERα) in regulation of the MUC1 gene expression. *Molecular Cancer*, **5**: 57.
1043 Yin, L., Kharbanda, S., and Kufe, D. (2009). MUC1 oncoprotein promotes autophagy in a survival response to glucose deprivation. *Int J Oncol*., **34**: 1691–1699.

1044 Yin, L., Li, Y., Ren, J., Kuwahara, H., Kufe, D. (2003). Human MUC1 Carcinoma Antigen Regulates Intracellular Oxidant Levels and the Apoptotic Response to Oxidative Stress. *J. Biol. Chem*., **278**: 35458–35464.

1045 Metcalfe, C. (2006). MUC1 interacts with Wnt-effector β-catenin in human oesophageal squamous cell carcinoma cell lines. *MSc Dissertation, University of the Witwatersrand,* **http://www.wits.ac.za.**

1046 Myers, M. P., Pass, I., Batty, I. H., Van der Kaay, J., Stolarov, J. P., Hemmings, B. A., Wigler, M. H., Downes, C. P., Tonks, N. K. (1998). The lipid phosphatase activity of PTEN is critical for its tumor supressor function. *Proc. Natl. Acad. Sci. USA*, **95**: 13513–13518.

1047 Li, L., Dutra A., Pak, E., Labrie, J. E. 3rd., Gerstein, R. M., Pandolfi, P. P., Recht, L. D., Ross, A.H. (2009). EGFRvIII expression and PTEN loss synergistically induce chromosomal instability and glial tumors. *Neuro Oncol*.,**11** :9-21.

1048 Ahmad, I., Morton, J. P., Singh, L. B., Radulescu, S. M., Ridgway, R. A., Patel, S., Woodgett, J., Winton, D. J., Taketo, M. M., Wu, X. R., Leung, H. Y., Sansom, O. J. (2011). β-Catenin Activation Synergises with PTEN Loss to Cause Bladder Cancer Formation. *Oncogene*, **30**: 178–189.

1049 Jiang, X., Chen, S., Asara, J. M., and Balk, S. P. (2010). Phosphoinositide 3-Kinase Pathway Activation in Phosphate and Tensin Homolog (PTEN)-deficient Prostate Cancer Cells Is Independent of Receptor Tyrosine Kinases and Mediated by the p110 and p110 Catalytic Subunits. *J. Biol. Chem*., **285**: 14980–14989.

1050 Davies, M. A., Koul, D., Dhesi, H., Berman, R., McDonnell, T. J., McConkey, D., Yung, W. K., Steck, P. A. (1999). Regulation of Akt/PKB Activity, Cellular Growth, and Apoptosis in Prostate Carcinoma Cells by MMAC/PTEN. *Cancer Res*., **59**: 2551–2556.

1051 Kurose, K., Zhou, X.-P., Araki, T., Cannistra, S. A., Maher, E. R., Eng, C. (2001). Frequent Loss of PTEN Expression Is Linked to Elevated Phosphorylated Akt Levels, but Not Associated with p27 and Cyclin D1 Expression, in Primary Epithelial Ovarian Carcinomas. *The American Journal of Pathology*, **158**: 2097-2106.

1052 Colakoglu, T., Yildirim, S., Kayaselcuk, F., Nursal, T. Z., Ezer, A., Noyan, T., Karakayali, H., Haberal, M. (2008). Clinicopathological significance of PTEN loss and the phosphoinositide 3-kinase/Akt pathway in sporadic colorectal neoplasms: is PTEN loss predictor of local recurrence? *The American Journal of Surgery*, **195**: 719–725.

1053 Marone, R., Cmiljanovic, V., Giese, B., Wymann, M. P. (2008). Targeting phosphoinositide 3-kinase—Moving towards therapy. *Biochimica et Biophysica Acta*, **1784**: 159–185.

1054 Zhuang, H-Q., Wang, J., Yuan, Z. Y., Zhao, L. J., Wang, P., Wang, C. L. (2009). The drug-resistance to gefitinib in PTEN low expression cancer cells is reversed by irradiation in vitro. *Journal of Experimental & Clinical Cancer Research*, **28**: 123 doi:10.1186/1756-9966-28-123.

1055 McEllin, B., Camacho, C. V., Mukherjee, B., Hahm, B., Tomimatsu, N., Bachoo, R. M., Burma, S. (2010). PTEN Loss Compromises Homologous Recombination Repair in Astrocytes: Implications for Glioblastoma Therapy with Temozolomide or Poly(ADP-Ribose) Polymerase Inhibitors. *Cancer Res*., **70**: 5457–64.

1056 Blanco-Aparicio, C., Renner, O., Leal, J. F. M., and Carnero, A. (2007). PTEN, more than the AKT pathway. *Carcinogenesis*, **28**: 1379–1386.

1057 Downes, C. P., Perera, N., Ross, S., Leslie, N. R. (2007). Substrate specificity and acute regulation of the tumour suppressor phosphatase, PTEN. *Biochem. Soc. Symp*., **74**: 69–80.

1058 Sulis, M. L., and Parsons, R. (2003). PTEN: from pathology to biology. *TRENDS in Cell Biology*, **13**: 478-83.

1059 Song,M. S., Carracedo, A., Salmena, L., Song, S. J., Egia, A., Malumbres, M., and Pandolfi, P. P. **(**2011). Nuclear PTEN Regulates the APC-CDH1 Tumor-Suppressive Complex in a Phosphatase-Independent Manner. *Cell*, **144**: 187-199.
1060 Carracedo, A., Salmena, L. and Pandolfi, P. P. (2008).SnapShot: PTEN signalling pathways. *Cell*, **133**: 550.
1061 Shimada, Y., lmamura, M., Wagata, T., Yamaguchi, N., Tobe, T. (1992). Characterization of 21 Newly Established Esophageal Cancer Cell Lines. *Cancer*, **69**: 277-284.
1062 Ding, Y., Shimada, Y., Kano, M., Itami, A., Kawabe, A., Maeda, M., Li, Z., Hong, T., Sato, F., Kaganoi, J., Imamura, M. (2000). PTEN/MMAC1 expression in esophageal squamous cell carcinomas. *International Journal of Oncology*, **17**: 695-704.
1063 Shimada, Y. (2005). Researchers Should Have Respect for the Originator of the Cell Lines. *Clin. Cancer Res*., **11**: 4634.
1064 Rossa, A. H., and Gericke, A. (2009). Phosphorylation keeps PTEN phosphatase closed for business. *PNAS*, **106**: 1297–1298.
1065 Vivanco, I., Rohle, D., Versele, M., Iwanami, A., Kuga, D., Oldrini, B., Tanaka, K., Dang, J., Kubek, S., Palaskas, N., Hsueh, T., Evans, M., Mulholland, D., Wolle, D., Rajasekaran, S., Rajasekaran, A., Liau, L. M., Cloughesy, T. F., Dikic, I., Brennan, C., Wu, H., Mischel, P. S., Perera, T., Mellinghoff, I. K. (2010). The phosphatase and tensin homolog regulates epidermal growth factor receptor (EGFR) inhibitor response by targeting EGFR for degradation. PNAS, **107**: 6459–6464.
1066 Mao, J-H., Kim, I. J., Wu, D., Climent, J., Kang, H. C., DelRosario, R., Balmain, A. (2008). FBXW7 Targets mTOR for Degradation and Cooperates with PTEN in Tumor Suppression. *Science*, **321**: 1499-1502.
1067 Maccario, H., Perera, N. M., Gray, A., Downes, C. P., Leslie, N. R. (2010). Ubiquitination of PTEN (Phosphatase and Tensin Homolog) Inhibits Phosphatase Activity and Is Enhanced by Membrane Targeting and Hyperosmotic Stress. *J. Biol. Chem*., **285**: 12620–12628.
1068 Gallastegui, N., and Groll, M. (2010). The 26S proteasome: assembly and function of a destructive machine. *TIBS*, **783**: 1-9.
1069 Al-Khouri AM, Ma Y, Togo SH, Williams S, and Mustelin T. (2005). Cooperative phosphorylation of the tumor suppressor phosphatase and tensin homologue (PTEN) by casein kinases and glycogen synthase kinase 3beta. *J Biol Chem*., **280**: 35195-202.
1070 Miller SJ, Lou DY, Seldin DC, Lane WS, and Neel BG. (2002). Direct identification of PTEN phosphorylation sites. *FEBS Lett*., **528**: 145-53.
1071 Crockett, D. K., Fillmore, G. C., Elenitoba-Johnson, K. S., Lim, M. S. (2005). Analysis of phosphatase and tensin homolog tumor suppressor interacting proteins by in vitro and in silico proteomics. *Proteomics*, **5**: 1250–1262.
1072 Gunaratne, J., Goh, M. X., Swa, H. L., Lee, F. Y., Sanford, E., Wong, L. M., Hogue, K. A., Blackstock, W. P., Okumura, K. (2011). Protein Interactions of Phosphatase and Tensin Homologue (PTEN) and Its Cancer-associated G20E Mutant Compared by Using Stable Isotope Labeling by Amino Acids in Cell Culture-based Parallel Affinity Purification. *J. Biol. Chem*., **286**: 18093–18103.
1073 Kim, R. H., and Mak, T.M. (2006). Tumours and tremors: how PTEN regulation underlies both. *British Journal of Cancer*, **94:** 620–624.
1074 Feng, Z., Hu, W., de Stanchina, E., Teresky, A. K., Jin, S., Lowe, S., Levine, A. J. (2007). The Regulation of AMPK B1, TSC2, and PTEN Expression by p53: Stress, Cell and Tissue Specificity, and the Role of These Gene Products in Modulating the IGF-1-AKT-mTOR Pathways. *Cancer Res*., **67**: 3043–53.

1075 Brown, J., Bothma, H., Veale, R., and Willem, P. (2011). Genomic imbalances in esophageal carcinoma cell lines involve Wnt pathway genes. *World J Gastroenterol*., **17**: 2909-2923.
1076 Nicholson, B., and Kumar, K. G. S. (2011). The Multifaceted Roles of USP7: New Therapeutic Opportunities. *Cell Biochem Biophys,* doi 10.1007/s12013-011-9185-5.
1077 DeCourseya, T. E., and Ligeti, E. (2005). Regulation and termination of NADPH oxidase activity. *Cell. Mol. Life Sci*., **62**: 2173–2193.
1078 Kwon, J., Lee, S.-R., Yang KS, Ahn, Y., Kim, Y. J., Stadtman, E. R., Rhee, S. G. (2004). Reversible oxidation and inactivation of the tumor suppressor PTEN in cells stimulated with peptide growth factors. *PNAS*, **101**: 16419–16424.
1079 Trachootham, D., Lu, W., Ogasawara, M. A., Valle, N. R-D., And Huang, P. (2008). Redox Regulation of Cell Survival. *Antioxid. Redox Signal*., **10**: 1343–1374.
1080 Lee, E. J., Kim, N.-S., Kim, N., Kang, K. H., Kim, J. W. (2011). Phosphorylation/ inactivation of PTEN by Akt-independent PI3K signalling in retinal pigment epithelium. *Biochem. Biophys. Res. Commun*., doi: 10.1016/j.b brc.2011. 09.083.
1081 Coant, N., Mkaddem, S. B., Ben Mkaddem S, Pedruzzi E, Guichard C, Tréton X, Ducroc R, Freund JN, Cazals-Hatem D, Bouhnik Y, Woerther PL, Skurnik D, Grodet A, Fay M, Biard D, Lesuffleur T, Deffert C, Moreau R, Groyer A, Krause KH, Daniel F, Ogier-Denis E. (2010). NADPH Oxidase 1 Modulates WNT and NOTCH1 Signalling To Control the Fate of Proliferative Progenitor Cells in the Colon. *Molecular And Cellular Biology*, **30**: 2636–2650.
1082 Rhee, S. G., Yang, K. S., Kang, S. W., Woo, H. A., Chang, T. S. (2005). Controlled Elimination of Intracellular H2O2: Regulation of Peroxiredoxin, Catalase, and Glutathione Peroxidase via Post-translational Modification. *Antioxid. Redox Signal*., **7**: 619–626.
1083 Scorrano, L., Oakes, S. A., Opferman, J. T., Cheng, E. H., Sorcinelli, M. D., Pozzan, T., Korsmeyer, S. J. (2003). BAX and BAK regulation of endoplasmic reticulum Ca2+: a control point for apoptosis. *Science*, **300**: 135-9.
1084 Gracanin, M., Lam, M. A., Morgan, P. E., Rodgers, K. J., Hawkins, C. L., Davies, M. J. (2011). Amino acid, peptide, and protein hydroperoxides and their decomposition products modify the activity of the 26S proteasome. *Free Radical Biology & Medicine*, **50**: 389–399.
1085 Alexander, A., Cai, S. L., Kim, J., Nanez, A., Sahin, M., MacLean, K. H., Inoki, K., Guan, K. L., Shen, J., Person, M. D., Kusewitt, D., Mills, G. B., Kastan, M. B., Walker, C. L. (2010). ATM signals to TSC2 in the cytoplasm to regulate mTORC1 in response to ROS. *PNAS*, **107**: 4153–4158.
1086 Smith, E. M., Finn, S. G., Tee, A. R., Browne, G. J., Proud, C. G. (2005). The Tuberous Sclerosis Protein TSC2 Is Not Required for the Regulation of the Mammalian Target of Rapamycin by Amino Acids and Certain Cellular Stresses. *J. Biol. Chem*., **280**: 18717–18727.
1087 Shin, S. Y., Chin, B. R., Lee, Y. H., Kim, J. H. (2006). Involvement of glycogen synthase kinase-3β in hydrogen peroxide-induced suppression of Tcf/Lef-dependent transcriptional activity. *Cellular Signalling*, **18**: 601–607.
1088 Duan, I., Duan, J., Zhang, Z., and Tong, T. (2005). Irreversible cellular senescence induced by prolonged exposure to H2O2 involves DNA-damage-and-repair genes and telomere shortening. *The International Journal of Biochemistry & Cell Biology*, **37**: 1407–1420.
1089 Martindale, J. L., And Holbrook, N. J. (2002). Cellular Response to Oxidative Stress: Signalling for Suicide and Survival. *Journal Of Cellular Physiology*, **192**: 1–15.
1090 Jenkins, G. J. S., D'Souza, F. R., Suzen, S. H., Eltahir, Z. S., James, S. A., Parry, J. M., Griffiths, P. A., Baxter, J. N. (2007). Deoxycholic acid at neutral and acid pH, is

genotoxic to oesophageal cells through the induction of ROS: the potential role of anti-oxidants in Barrett's oesophagus. *Carcinogenesis*, **28**: 136–142.
1091 Kloet, D. E. A., and Burgering, B. M. T. (2011). The PKB/FOXO switch in aging and cancer. *Biochimica et Biophysica Acta*, **1813**: 1926–1937.
1092 Landriscina, M., Maddalena, F., Laudiero, G., and Esposito, F. (2009). Adaptation to Oxidative Stress, Chemoresistance, and Cell Survival. *Antioxid. Redox Signal*, **11**: 2701–2716.
1093 Nonn, L., Berggren, M., and Powis, G. (2003). Increased Expression of Mitochondrial Peroxiredoxin-3 (Thioredoxin Peroxidase-2) Protects Cancer Cells Against Hypoxia and Drug-Induced Hydrogen Peroxide-Dependent Apoptosis. *Mol. Cancer Res.*, **1**: 682–689.
1094 Simon, A. R., Rai, U., Fanburg, B. L., and Cochran, B. (1998). Activation of the JAK-STAT pathway by reactive oxygen species. *Am J Physiol Cell Physiol.*, **275**: 1640-1652.
1095 Al-Gubory, K. H., Fowler, P. A., Garrel, C. (2010). The roles of cellular reactive oxygen species, oxidative stress and antioxidants in pregnancy outcomes. *The International Journal of Biochemistry & Cell Biology*, **42**: 1634–1650.
1096 Maier, D., Jones, G., Li, X., Schönthal, A. H., Gratzl, O., Van Meir, E. G., Merlo, A. (1999). The PTEN Lipid Phosphatase Domain Is Not Required to Inhibit Invasion of Glioma Cells. *Cancer Res.*, **59**: 5479-5482.
1097 Raftopoulou, M., Etienne-Manneville, S., Self, A., Nicholls, S., Hall, A. (2004). Regulation of Cell Migration by the C2 Domain of the Tumor Suppressor PTEN. *Science*, **303**: 1179-81.
1098 Giehl, K., and Menke, A. (2006). Moving on: Molecular mechanisms in TGFβ-induced epithelial Cell migration. *Signal Transduction*, **6**: 355–364.
1099 Chow, J. Y. C., Ban, M., Wu, H. L., Nguyen, F., Huang, M., Chung, H., Dong, H., Carethers, J. M. (2010). TGF-β downregulates PTEN via activation of NF-κB in pancreatic cancer Cells. *Am J Physiol Gastrointest Liver Physiol.*, **298**: 275–282.
1100 Driver, G., A. (2006). Integrin-linked Kinase (ILK) Expression in Moderately Differentiated Human Oesophageal Squamous Carcinoma Cell Lines-Growth Factor Modulation, Activity and Link to Adhesion. *PhD Dissertation, University of the Witwatersrand*, **http://www.wits.ac.za.**
1101 LaHair, M. M., Howe, C. J. (2006). Molecular Pathways Leading to Oxidative Stress-Induced Phosphorylation of Akt. *Antioxid. Redox Signal.*, **8**: 1749–1756.
1102 Wu, Y.-T., Ouyang, W., Lazorchak, A. S., Liu, D., Shen, H. M., Su, B. (2011). mTOR Complex 2 Targets Akt for Proteasomal Degradation via Phosphorylation at the Hydrophobic Motif. *J. Biol. Chem.*, doi: 10.1074/jbc.M111.219923
1103 Panischeva, L. A., Kakpakova, E. S., Rybalkina, E. Y., Stavrovskaya, A. A. (2011). Influence of Proteasome Inhibitor Bortezomib on the Expression of Multidrug Resistance Genes and Akt Kinase Activity. *Biochemistry (Moscow)*, **76**: 1009-1016.
1104 Sarosiek, K. A., Cavallin, L. E., Bhatt, S., Toomey, N. L., Natkunam, Y., Blasini, W., Gentles, A. J., Ramos, J. C., Mesri, E. A., Lossos, I. S. (2010). Efficacy of bortezomib in a direct xenograft model of primary effusion lymphoma. *Proc Natl Acad Sci U S A.*, **107**: 13069-74.
1105 Cavo, M. (2007). Current Status of Bortezomib in the Treatment of Multiple Myeloma. *Current Hematologic Malignancy Reports*, **2**: 128–137.
1106 Eberta, B., Kisielaa,M., Wsól, V., and Maser, E. (2011). Proteasome inhibitors MG-132 and bortezomib induce AKR1C1, AKR1C3, AKR1B1, and AKR1B10 in human colon cancer cell lines SW-480 and HT-29. *Chemico-Biological Interactions*, **191**: 239–249.
1107 Yerlikaya, A., and Erin, N. (2008). Differential sensitivity of breast cancer and melanoma cells to proteasome inhibitor Velcade. *International Journal Of Molecular Medicine*, **22**: 817-823.

1108 Marx, C., Yau, C., Banwait, S., Zhou, Y., Scott, G. K., Hann, B., Park, J. W., Benz, C. C. (2007). Proteasome-Regulated ERBB2 and Estrogen Receptor Pathways in Breast Cancer. *Mol Pharmacol*, **71**: 1525–1534.
1109 Sloss, C. M., Wang F., Liu, R., Xia, L., Houston, M., Ljungman, D., Palladino, M. A., Cusack, J. C. Jr. (2008). Proteasome inhibition activates EGFR and EGFR-independent mitogenic kinase signalling pathways in pancreatic cancer cells: Implications for combination therapy. *Clin Cancer Res.*, **14**: 5116–5123.
1110 Jones, R. J., Chen, Q., Voorhees, P. M., Young, K. H., Bruey-Sedano, N., Yang, D., Orlowski, R. Z. (2008). Inhibition of the p53 E3 Ligase HDM-2 Induces Apoptosis and DNA Damage-Independent p53 Phosphorylation in Mantle Cell Lymphoma. *Clin Cancer Res.*, **14**: 5416–5425.
1111 Williams, S. A., and McConkey, D. J. (2003). The Proteasome Inhibitor Bortezomib Stabilizes a Novel Active Form of p53 in Human LNCaP-Pro5 Prostate Cancer Cells. *Cancer Res.*, **63**: 7338–7344.
1112 Blagosklonny, M. V., An, W. G., Romanova, L. Y., Trepel, J., Fojo, T., Neckers, L. (1998). p53 Inhibits Hypoxia-inducible Factor-stimulated Transcription. *J. Biol. Chem.*, **273**: 11995–11998.
1113 Zmijewski, J. W., Zhao, X., Xu, Z., and Abraham, E. (2007). Exposure to hydrogen peroxide diminishes NF-kB activation, IkB-α degradation, and proteasome activity in neutrophils. *Am J Physiol Cell Physiol*, **293**: 255–266.
1114 Zmijewski, J. W., Banerjee, S., Bae, H., Friggeri, A., Lazarowski, E. R., Abraham, E. (2010). Exposure to Hydrogen Peroxide Induces Oxidation and Activation of AMP-activated Protein Kinase. *J. Biol. Chem.*, **285**: 33154–33164.
1115 Demasi, M., and Davies, K. J. A. (2003). Proteasome inhibitors induce intracellular protein aggregation and cell death by an oxygen-dependent mechanism. *FEBS Letters*, **542**: 89-94.
1116 Indran, I. R., Tufo, G., Pervaiz, S., Brenner, C. (2011). Recent advances in apoptosis, mitochondria and drug resistance in cancer cells. *Biochimica et Biophysica Acta*, **1807**: 735–745.
1117 Sontag, J-M., and Sontag, E. (2006). Regulation of cell adhesion by PP2A and SV40 small tumor antigen: An important link to cell transformation. *Cell. Mol. Life Sci.*, **63**: 2979–2991.
1118 Ramel, D., Lagarrigue, F., Dupuis-Coronas, S., Chicanne, G., Leslie, N., Gaits-Iacovoni, F., Payrastre, B., Tronchère, H. (2009). PtdIns5P protects Akt from dephosphorylation through PP2A inhibition. *Biochemical and Biophysical Research Communications*, **387**: 127–131.
1119 Andjelkpvić, M., Jakubowicz, T., Cron, P., Ming, X. F., Han, J. W., Hemmings, B. A. (1996). Activation and phosphorylation of a pleckstrin homology domaincontaining protein kinase (RACPK/PKB) promoted by serum and protein phosphatase inhibitors (signal transduction/mitogenic activation/phosphatase inhibitors. *Proc. Natl. Acad. Sci. USA*, **93**: 5699-5704.
1120 Martin, M., Kettmann, R., and Dequiedt, F. (2010). Recent insights into Protein Phosphatase 2A structure and regulation: the reasons why PP2A is no longer considered as a lazy passive housekeeping enzyme. *Biotechnol. Agron. Soc. Environ.*, **14**: 243-252.
1121 Arroyo, J. D., and Hahn, W. C. (2005). Involvement of PP2A in viral and cellular transformation. *Oncogene*, **24**: 7746–7755.
1122 Sablina, A. A., Hector, M., Colpaert, N., Hahn, W. C. (2010). Identification of PP2A Complexes and Pathways Involved in Cell Transformation. *Cancer Res.*, **70**: 10474–84.
1123 Chen, W., Arroyo, J. D., Timmons, J. C., Possemato, R., Hahn, W. C. (2005). Cancer-Associated PP2A Aα Subunits Induce Functional Haploinsufficiency and Tumorigenicity. *Cancer Res.*, **65**: 8183-92.

1124 Andrabi, S., Gjoerup, O. V., Kean, J. A., Roberts, T. M., Schaffhausen, B. (2007). Protein phosphatase 2A regulates life and death decisions via Akt in a context-dependent manner. *PNAS*, **104**: 19011–19016.
1125 Baoping, Y., Guoyong, H., Jieping, Y., Zongxue, R., Hesheng, L. (2004). Cyclooxygenase-2 Inhibitor Nimesulide Suppresses Telomerase Activity by Blocking Akt/PKB Activation in Gastric Cancer Cell Line. *Digestive Diseases and Sciences*, **49**: 948–953.
1126 Cazzolli, R., Carpenter, L., Biden, T. J., Schmitz-Peiffer, C. (2001). A Role for Protein Phosphatase 2A–Like Activity, but Not Atypical Protein Kinase C, in the Inhibition of Protein Kinase B/Akt and Glycogen Synthesis by Palmitate. *Diabetes*, **50**: 2210 –2218.
1127 Yeh, E., Cunningham, M., Arnold, H., Chasse, D., Monteith, T., Ivaldi, G., Hahn, W. C., Stukenberg, P. T., Shenolikar, S., Uchida, T., Counter, C. M., Nevins, J. R., Means, A. R., Sears, R. (2004). A signalling pathway controlling c-Myc degradation that impacts oncogenic transformation of human cells. *Nat Cell Biol*, **6**: 308–318.
1128 Arnold, H. K., and Sears, R. C. (2008). A tumor suppressor role for PP2A-B56α through negative regulation of c-Myc and other key oncoproteins. *Cancer Metastasis Rev*., **27**: 147–158.
1129 Myant, K., and Sansom, O. J. (2011). Wnt/Myc interactions in intestinal cancer: Partners in crime. *Experimental Cell Research*, **317**: 2725–2731.
1130 Qu, W., Li, W., Li, W., Wei, L., Xing, L., Wang, X., Yu, J. (2010). CIP2A is overexpressed in esophageal squamous cell carcinoma. *Med Onco*l., doi 10.1007/s12032-010-9768-9.
1131 Côme, C., Laine, A., Chanrion, M., Edgren, H., Mattila, E., Liu, X., Jonkers, J., Ivaska, J., Isola, J., Darbon, J. M., Kallioniemi, O., Thézenas, S., Westermarck, J. (2009). CIP2A Is Associated with Human Breast Cancer Aggressivity. *Clin Cancer Res*., **15**: 5092–100.
1132 Liu, J., Wang, X., Zhou, G., Wang, H., Xiang, L., Cheng, Y., Liu, W., Wang, Y., Jia, J., Zhao, W. (2011). Cancerous inhibitor of protein phosphatase 2A is overexpressed in cervical cancer and up-regulated by human papillomavirus 16 E7 oncoprotein. *Gynecol Oncol*., doi:10.1016/j.ygyno.2011.04.031.
1133 Huang, C.-Y., Wei, C. C., Chen, K. C., Chen, H. J., Cheng, A. L., Chen, K. F. (2011). Bortezomib enhances radiation-induced apoptosis in solid tumors by inhibiting CIP2A. *Cancer Letters*, doi: 10.1016/j.canlet.2011.11.005.
1134 Mulrooney, J., Foley, K., Vineberg, S., Barreuther, M., Grabel, L. (2000). Phosphorylation of the β1 Integrin Cytoplasmic Domain: Toward an Understanding of Function and Mechanism. *Exp. Cell Res.*, **258**: 332–341.
1135 Tamura, S., Toriumi, S., Saito, J., Awano, K., Kudo, T. A., Kobayashi, T. (2006). PP2C family members play key roles in regulation of cell survival and apoptosis. *Cancer Sci*., **97**: 563–567.
1136 Sydenham E.W., Gelderblom W.C.A., Thiel P.G. and Marasas W.F.O. (1990). Evidence for the natural occurrence of fumonisin B1, a mycotoxin produced by *Fusarium moniliforme*, in corn. *J. Agric. Food Chem*., **38**: 285–290.
1137 Marasas W.F.O., Wehner F.C., van Rensburg S.J. and van Schalkwyk D.J. (1981). Mycoflora of corn produced in human oesophageal cancer areas in Transkei,South Africa. *Phytopathology*, **71**: 792–796.
1138 Chelule, P. K., Gqaleni, N., Dutton, M. F., Chuturgoon, A. A. (2001). Exposure of Rural and Urban Populations in KwaZulu Natal, South Africa, to Fumonisin B1 in Maize. *Environ Health Perspect*., **109**: 253-256.
1139 Gedlerblom, W. C. A., Jaskiewicz, K., Marasas, W. F., Thiel, P. G., Horak, R. M., Vleggaar, R., Kriek, N. P. (1988). Fumonisins-Novel Mycotoxins with Cancer-Promoting Activity Produced by Fusarium moniliforme. *Applied And Environmental Microbiology*, **54**: 1806-1811.

1140 Myburg, R. B., Dutton, M. F., and Chuturgoon, A. A. (2002). Cytotoxicity of Fumonisin Bv Diethylnitrosamine, and Catechol on the SNO Esophageal Cancer Cell Line. *Environ Health Perspect*, **110**: 813-815.
1141 Seegers, J. C., Joubert, A. M., Panzer, A., Lottering, M. L., Jordan, C. A., Joubert, F., Maree, J. L., Bianchi, P., de Kock, M., Gelderblom, W. C. (2000). Fumonisin B1 influenced the effects of arachidonic acid, prostaglandins E2 and A2 on cell cycle progression, apoptosis induction, tyrosine- and CDC2-kinase activity in oesophageal cancer cells. *Prostaglandins, Leukotrienes and Essential Fatty Acids*, **62**: 75–84.
1142 Myburg, R. B.,Needhi, N., and Chuturgoon, A. A. (2009). The ultrastructural effects and immunolocalization of fumonisin B1 on cultured oesophageal cancer cells (SNO). *South African Journal of Science*, **105**: 217-22.
1143 Anderson, C. B., Neufeld, K. L., and White, R. L. (2002). Subcellular distribution of Wnt pathway proteins in normal and neoplastic colon. *PNAS*, **99**: 8683–8688.
1144 Kim, M. S., Chang, X., LeBron, C., Nagpal, J. K., Lee, J., Huang, Y., Yamashita, K., Trink, B., Ratovitski, E. A., Sidransky, D. (2010). Neurofilament Heavy Polypeptide Regulates the Akt-β-Catenin Pathway in Human Esophageal Squamous Cell Carcinoma. *PLoS ONE* 5(2): e9003. doi:10.1371/journal.pone.0009003.
1145 Osterheld, M.-C., Bian, Y.-S., Bosman, F. T., Benhattar, J., Fontolliet, C. (2002). Beta-Catenin Expression and Its Association With Prognostic Factors in Adenocarcinoma Developed in Barrett Esophagus. *Am J Clin Pathol*., **117**: 451-456.
1146 Choi, Y. W., Heath, E. I., Heitmiller, R., Forastiere, A. A., Wu, T. T. (2000). Mutations in β-Catenin and APC Genes are Uncommon in Esophageal and Esophagogastric Junction Adenocarcinomas. *Mod Pathol*., **13:** 1055–1059.
1147 Wu, J., Richards, M. H., Huang, J., Al-Harthi, L., Xu, X., Lin, R., Xie, F., Gibson, A. W., Edberg, J. C., Kimberly, R. P. (2011). Human FasL Gene Is a Target of β-Catenin/T-Cell Factor Pathway and Complex FasL Haplotypes Alter Promoter Functions. *PLoS ONE*, **6**: e26143. doi:10.1371/jo urnal.pone. 0026143.
1148 Griffith TS, Brunner T, Fletcher SM, Green DR, Ferguson T A. (1995). Fas ligand-induced apoptosis as a mechanism of immune privilege. *Science*, **270**: 1189–1192.
1149 Fanucchi, S., and Veale, R. B. (2011). Delayed caspase-8 activation and enhanced integrin β1-activated FAK underpins anoikis in oesophageal carcinoma cells harbouring mt p53-R175H. *Cell Biol Int*., **35**: 819-26.
1150 Cadigan KM and Nusse R. (1997).Wnt signalling: a common theme in animal development. *Genes Dev*., **11**: 3286–3305.
1151 Smalley MJ and Dale TC. (1999). Wnt signalling in mammalian development and cancer. *Cancer Metastasis Rev*., **18**: 215–230.
1152 Krishnadath KK, Tilanus HW, Van Blankenstein M, Hop, W. C., Kremers, E. D., Dinjens, W. N., Bosman, F. T. (1997). Reduced expression of the cadherin-catenin complex in oesophageal adenocarcinoma correlates with poor prognosis. *J Pathol*., **182**: 331-338.
1153 Bailey, T., Biddlestone, L., Shepherd, N., Barr, H., Warner, P., Jankowski, J. (1998). Altered Cadherin and Catenin Complexes in the Barrett's Esophagus-Dysplasia-Adenocarcinoma Sequence-Correlation with Disease Progression and Dedifferentiation. *AmJPathol*., **152**: 135-144.
1154 Morton, R. A., Ewing, C. M., Nagafuchi, A., Tsukita, S., Isaacs, W. B. (1993). Reduction of E-cadherin levels and deletion of the alpha-catenin gene in human prostate cancer. *Cancer Res*., **53**: 3585-3590.
1155 Rimm DL, Sinard JH, Morrow JS. (1995). Reduced alpha-catenin and E-cadherin expression in breast cancer. *Lab Invest*., **72**: 506-512.

1156 Schipper, J. H., Frixen, U. H., Behrens, J., Unger, A., Jahnke, K., Birchmeier, W. (1991). E-cadherin expression in squamous cell carcinomas of head and neck: inverse correlation with tumor dedifferentiation and lymph node metastasis. *Cancer Res*., **51**: 6328-6337.
1157 Van der Wurff, A. A. M., Vermeulen, S. J. T., Van der Linden, E. P. M., Mareel, M. M., Bosman, F. T., Arends, J. W. (1997). Patterns of alpha- and beta-catenin and E-cadherin expression in colorectal adenomas and carcinomas. *J Pathol.*, **182**: 325-330.
1158 Shimazui T, Schalken, J. A., Giroldi, L. A., Jansen, C. F., Akaza, H., Koiso, K., Debruyne, F. M., Bringuier, P. P. (1996). Prognostic value of cadherin-associated molecules (alpha-, beta-, gamma-catenins and p120cas) in bladder tumors. *Cancer Res*., **56**: 4154-4158.
1159 Voskas, D., Ling, L. S., and Woodgett, J. R. (2010). Does GSK-3 provide a shortcut for PI3K activation of Wnt signalling? *F1000 Biol. Reports*, **2**: 82
1160 Agoulnik, I. U., Hodgson, M. C., Bowden, W. A., Ittmann, M. M. (2011). INPP4B: the New Kid on the PI3K Block. *Oncotarget*, **2**: 321–328.
1161 Mulholland, D. J., Dedhar, S., Wu, H., and Nelson, C. C. (2006). PTEN and GSK3β: key regulators of progression to androgen-independent prostate cancer. *Oncogene*, **25**: 329–337.
1162 Ng, S. S., Mahmoudi, T., Danenberg, E., Bejaoui, I., de Lau, W., Korswagen, H. C., Schutte, M., Clevers, H. (2009). Phosphatidylinositol 3-Kinase Signalling Does Not Activate the Wnt Cascade. *J. Biol. Chem.*, **284**: 35308 –35313.
1163 Ding, V. W., Chen, R. H., McCormick, F. (2000). Differential Regulation of Glycogen Synthase Kinase 3β by Insulin and Wnt Signalling. *J. Biol. Chem*., **275**: 32475–32481.
1164 Sun, J., and Jin, T. (2008). Both Wnt and mTOR signalling pathways are involved in insulin-stimulated proto-oncogene expression in intestinal cells. *Cellular Signalling*, **20**: 219–229.
1165 Karrasch, T., Spaeth, T., Allard, B., and Jobin, C. (2011). PI3K-Dependent GSK3ß (Ser9)-Phosphorylation Is Implicated in the Intestinal Epithelial Cell Wound-Healing Response. *PLoS ONE*, **6**: e263 40. doi:10.1 371/journal.p one.0026340.
1166 Anderson, E. C., and Wong, M. H. (2010). Caught in the Akt: Regulation of Wnt signalling in the intestine. *Gastroenterology*, **139**: 718–722.
1167 Lee, M. Y., Lim, H. W., Lee, S. H., Han, H. J. (2009). Smad, PI3K/Akt, and Wnt-Dependent Signalling Pathways Are Involved in BMP-4-Induced ESC Self-Renewal. *Stem Cells*, **27**:1858–1868.
1168 Ackermann, T. F., Kempe, D. S., Lang, F., Lang, U. E. (2010). Hyperactivity and Enhanced Curiosity of Mice Expressing PKB/SGK-resistant Glycogen Synthase Kinase-3 (GSK-3). *Cell Physiol Biochem*., **25**: 775-786.
1169 Humphrey, R. K., Yu, S. M., Flores, L. E., Jhala, U S. (2010). Glucose Regulates Steady-state Levels of PDX1 via the Reciprocal Actions of GSK3 and AKT Kinases. *J. Biol. Chem*., **285**: 3406–3416.
1170 Anderson, E. C. (2011). The Role of Colorectal Cancer Stem Cells in Metastatic *Disease and Therapeutic Response. Cancers (Basel)*, **3**: 319–339.
1171 Lin, C.-C. (2009). GSKIP, an Inhibitor of GSK3β, Mediates the N-Cadherin/β -Catenin Pool in the Differentiation of SH-SY5Y Cells. *Journal of Cellular Biochemistry*, **108**: 1325–1336.
1172 Piao, S. F., Lee S. H., Kim, H., Yum, S., Stamos, J. L., Xu, Y., Lee, S. J., Lee, J., Oh, S., Han, J. K., Park, B. J., Weis, W. I., Ha, N. C. (2008). Direct Inhibition of GSK3 b by the Phosphorylated Cytoplasmic Domain of LRP6 in Wnt/ β-Catenin Signalling. *PLoS ONE*, **3**: e4046. doi:10.1371/jo urnal.pone. 0004046.
1173 Fang Zhang, F., Phiel, C. J., Spece, L., Gurvich, N., Klein, P. S. (2003). Inhibitory Phosphorylation of Glycogen Synthase Kinase-3 (GSK-3) in Response to Lithium. Evidence for autoregulation of GSK3. *J. Biol. Chem*., **278**: 33067–33077.

1174 Doble, B. W., Patel, S., Wood, G. A., Kockeritz, L. K., and Woodgett, J. R. (2007). Functional Redundancy of GSK-3α and GSK-3β in Wnt/β-Catenin Signalling Shown by Using an Allelic Series of Embryonic Stem Cell Lines. *Developmental Cell*, **12**: 957–971.
1175 Zhang, W., and Qiu, M. (2008). MUC1-β-catenin interaction facilitates epithelial-mesenchymal transition in colorectal carcinoma. *Bioscience Hypotheses*, **1**: 123-124.
1176 Huang, L., Chen, D., Liu, D., Yin, L., Kharbanda, S., Kufe, D. (2005). MUC1 Oncoprotein Blocks Glycogen Synthase Kinase 3β–Mediated Phosphorylation and Degradation of β-Catenin. *Cancer Res.*, **65**: 10413-22.
1177 Mishra, R. (2010). Glycogen synthase kinase 3 beta: can it be a target for oral cancer. *Molecular Cancer*, **9**: 144.
1178 Zheng, H., Saito, H., Masuda, S., Yang, X., Takano, Y. (2007). Phosphorylated GSK3,-ser9 and EGFR are Good Prognostic Factors for Lung Carcinomas. *Anticancer Research*, **27:** 3561-3570.
1179 Koppert, L. B., Wijnhoven, B. P. L., van Dekken, H., Tilanus, H. W., Dinjens, W. N. (2005). The Molecular Biology of Esophageal Adenocarcinoma. *Journal of Surgical Oncology*, **92**: 169–190.
1180 Wolf, M. C., Stahl, M., Krause, B. J., Bonavina, L., Bruns, C., Belka, C., Zehentmayr, F. (2011). Curative treatment of oesophageal carcinoma: current options and future developments. *Radiation Oncology*, **6**: 55
1181 Nguyen, G. H., Murph, M. M., and Chang, J. Y. (2011). Cancer Stem Cell Radioresistance and Enrichment: Where Frontline Radiation Therapy May Fail in Lung and Esophageal Cancers. *Cancers (Basel)*, **3**: 1232–1252.
1182 Fareed, K. R., Kaye, P., Soomro, I. N., Ilyas, M., Martin, S., Parsons, S. L., Madhusudan, S. (2009). Biomarkers of response to therapy in oesophago-gastric cancer. *Gut*, **58:** 127–143.
1183 Bataille F, Rummele, P., Dietmaier, W., Gaag, D., Klebl, F., Reichle, A., Wild, P., Hofstädter, F., Hartmann, A. (2003). Alterations in p53 predict response to preoperative high dose chemotherapy in patients with gastric cancer. *Mol Pathol*., **56**: 286–92.
1184 Okumura H, Natsugoe S., Matsumoto, M., Mataki, Y., Takatori, H., Ishigami, S., Takao, S., Aikou, T. (2005). The predictive value of p53, p53R2, and p21 for the effect of chemoradiation therapy on oesophageal squamous cell carcinoma. *Br J Cancer*, **92**: 284–9.
1185 Akamatsu, M., Matsumoto, T., Oka, K., Yamasaki, S., Sonoue, H., Kajiyama, Y., Tsurumaru, M., Sasai, K. (2003). c-erbB-2 oncoprotein expression related to chemoradioresistance in esophageal squamous cell carcinoma. *Int J Radiat Oncol Biol Phys*., **57**: 1323–7.
1186 Liu, P., Cheng, H., Santiago, S., Raeder, M., Zhang, F., Isabella, A., Yang, J., Semaan, D. J., Chen, C., Fox, E. A., Gray, N. S., Monahan, J., Schlegel, R., Beroukhim, R., Mills, G. B., Zhao, J. J. (2011). Oncogenic PIK3CA-driven mammary tumors frequently recur via PI3K pathway–dependent and PI3K pathway–independent mechanisms. *Nature Med*., **17**: 1116-20.
1187 Wee, S., Jagain, Z., Xiang, K. X., Loo, A., Dorsch, M., Yao, Y. M., Sellers, W. R., Lengauer, C., Stegmeier, F. (2009). PI3K Pathway Activation Mediates Resistance to MEK Inhibitors in KRAS Mutant Cancers. *Cancer Res*., **69**: 4286–93.
1188 Miller, T. W., Rexer B. N., Garrett, J. T., Arteaga, C. L. (2011). Mutations in the phosphatidylinositol 3-kinase pathway: role in tumor progression and therapeutic implications in breast cancer. *Breast Cancer Research*, **13**: 224 doi:10.1186/bcr3039.
1189 Falasca, M. (2010). PI3K/Akt Signalling Pathway Specific Inhibitors: A Novel Strategy to Sensitize Cancer Cells to Anti-Cancer Drugs. *Current Pharmaceutical Design*, **16**: 1410-1416.

1190 Vona-Davis, L., Frankenberry, K., Cunningham, C., Riggs, D. R., Jackson, B. J., Szwerc, M. F., McFadden, D. W. (2005). MAPK and PI3K Inhibition Reduces Proliferation of Barrett's Adenocarcinoma in Vitro. *Journal of Surgical Research*, **127**: 53–58.
1191 Baba, Y., Iyama, K-I., Hirashima, K., Nagai, Y., Yoshida, N., Hayashi, N., Miyanari, N., Baba, H. (2008). Laminin-332 promotes the invasion of oesophageal squamous cell carcinoma via PI3K activation. *Br. J. of Cancer*, **98**: 974–980.
1192 Brognard, J., Clark, A. S., Ni, Y., and Dennis, P. A. (2001). Akt/Protein Kinase B Is Constitutively Active in Non-Small Cell Lung Cancer Cells and Promotes Cellular Survival and Resistance to Chemotherapy and Radiation. *Cancer Res.*, **61**: 3986 –3997.
1193 Altomare, D. A., Wang, H. Q., Skele, K. L., De Rienzo, A., Klein-Szanto, A. J., Godwin, A. K., Testa, J. R. (2004). AKT and mTOR phosphorylation is frequently detected in ovarian cancer and can be targeted to disrupt ovarian tumor cell growth. *Oncogene*, **23**: 5853–5857.
1194 Crowder, R. J., and Ellis, M. J.(2005). Treating breast cancer through novel inhibitors of the phosphatidylinositol 3′-kinase pathway. *Breast Cancer Research*, **7**: 212-214.
1195 Ekman, S., Bergqvist, M., Heldin, C. H., and Lennartsson, J. (2007). Activation of Growth Factor Receptors in Esophageal Cancer—Implications for Therapy. *The Oncologist*, **12:** 1165–1177.
1196 Hu, Y., Bandla, S., Godfrey, T. E., Tan, D., Luketich, J. D., Pennathur, A., Qiu, X., Hicks, D. G., Peters, J. H., Zhou, Z. (2011). HER2 amplification, overexpression and score criteria in esophageal adenocarcinoma. *Mod Pathol*., **24**: 899–907.
1197 Yoshioka, A., Miyata, H., Miyata, H., Doki, Y., Yasuda, T., Yamasaki, M., Motoori, M., Okada, K.,Matsuyama, J., Makari, Y., Sohma, I., Takiguchi, S., Fujiwara, Y., Monden, M. (2008). The activation of Akt during preoperative chemotherapy for esophageal cancer correlates with poor prognosis. *Oncology Reports*, **19**: 1099-1107.
1198 O'Donovan, T. R., O'Sullivan, G. C., McKenna, S. L. (2011). Induction of autophagy by drug-resistant esophageal cancer cells promotes their survival and recovery following treatment with chemotherapeutics. *Autophagy*, **7**: 509-524.
1199 Takashima, N., Ishiguro, H., Kuwabara, Y., Kimura, M., Mitui, A., Mori, Y., Mori, R., Tomoda, K., Hamaguchi, M., Ogawa, R., Katada, T., Harada, K., Fujii, Y. (2008). Gene expression profiling of the response of esophageal carcinoma cells to Cisplatin. *Diseases of the Esophagus*, **21**: 230–235.
1200 Trachootham, D., Alexandre, J., and Huang, P. (2009). Targeting cancer cells by ROS-mediated mechanisms: a radical therapeutic approach? *Nature Reviews Drug Discovery*, **8**: 579-591.
1201 Nebbioso, A., Pereira, R., Khanwalkar, H., Matarese, F., García-Rodríguez, J., Miceli, M., Logie, C., Kedinger, V., Ferrara, F., Stunnenberg, H. G., de Lera, A. R., Gronemeyer, H., Altucci, L. (2011). Death receptor pathway activation and increase of ROS production by the triple epigenetic inhibitor, UVI5008. *Mol. Cancer Ther*., **11**: doi: 10.1158/1535-7163.
1202 Davis, W., Ronai, Z., Tew, K. D. (2001). Cellular Thiols and Reactive Oxygen Species in Drug-Induced Apoptosis. *JPET*, **296**: 1–6.
1203 Efferth, T., Giaisi, M., Merling, A., Krammer, P. H., Li-Weber, M. (2007). Artesunate Induces ROS-Mediated Apoptosis in Doxorubicin-Resistant T Leukemia Cells. *PLoS ONE*, **2**: e693. doi:10.1371/journal.pone.0000693.
1204 Lin, D.-C., Du, X.-L., and Wang, M.-R. (2009). Protein alterations in ESCC and clinical implications: a review. *Diseases of the Esophagus*, **22**: 9–20.
1205 Hsieh, M-J., Chen, K-S., Chiou, H-L., Hsieh, Y-S. (2010). Carbonic anhydrase XII promotes invasion and migration ability of MDA-MB-231 breast cancer cells through the p38 MAPK signalling pathway. *European Journal of Cell Biology*, **89**: 598–606.

1206 Solimini, N. L., Luo, J., and Elledge, S. J. (2007). Non-Oncogene Addiction and the Stress Phenotype of Cancer Cells. *Cell*, **130**: 986-88.